UNIVERSITÀ DEGLI STUDI DELL'AQUILA
DIPARTIMENTO DI SCIENZE FISICHE E CHIMICHE

Dottorato di Ricerca in

Scienze Fisiche e Chimiche

Curriculum Chimica Organica

XXXVIII ciclo

Titolo della tesi

Development of new organocatalytic and organo-photocatalytic asymmetric methodologies, total synthesis of natural compounds and development of computer aided retrosynthesis software

SSD CHEM-05/A

Dottorando

Alessandro Brusa

Coordinatore del corso

Prof. Massimiliano Aschi

Tutor

Prof. Armando Carlone

Co-tutor

Dr. Fabio Pesciaioli

a.a. 2024/2025

“Work hard, party harder” cit. B. List

Summary

Introduction 7
Aim of the thesis 7
Organic chemistry *is* crafting molecules 7
Why make new molecules and old ones better 9
Chapter 1 - Acetaldehyde in the Enders triple cascade reaction via acetaldehyde dimethyl acetal 11
Organocatalysis – historical perspective 11
Nucleophilic catalysis as the first example of organocatalysis 11
Asymmetric organocatalysis 13
The foundation of the asymmetric organocatalysis field 15
Organocatalysis – activation modes 16
Iminium ion activation 16
Enamine activation 18
Hydrogen-bond activation 20
Asymmetric Counterion Direct Catalysis 21
Enders' cascade 22
Use of acetaldehyde in organocatalysis 24
Reaction optimization 26
Scope 30
The origin of poor diastereoselectivity 31
Conclusions 34
Supporting Information 35
General information 35
Instrumentations 35
Materials and Methods 36
Experimental procedures 37
Optimisation reactions 37
General procedure 38
General procedure for racemic compound preparation 39
Bibliography 90
Chapter 2 - Organo-photocatalyzed α-functionalization of carbonyl compounds with aryl-diazo compounds 95
Introduction- photochemistry and photocatalysis 95
Basic principles of photocatalysis 98
Photochemistry aryldiazosulphones: introduction 102
Asymmetric organocatalyzed α – arylation with aryldiazosulphones 105
Other possible α - functionalization paths 106

Experimental 108
Catalyst-aryldiazosulphone compatibility 108
Reactivity test – static conditions 109
Enamine synthesis 110
Direct reaction of enamine with aryldiazosulphones 112
Re-design of reaction: enol chemistry 115
Experimental 116
Conclusions 118
Supporting information 119
Bibliography 124
Chapter 3 – Organosilicon chemistry 128
Introduction 128
Properties of silicon 128
Danheiser cyclopentane annulation 131
Design of an organocatalyzed asymmetric Danheiser cyclopentane annulation 132
Experimental 134
Materials synthesis 134
Screening campaign 136
Computational investigation 140
Cheap calculation 140
Re-design of Danheiser cyclopentane annulation: photocatalysis 142
Experimental – first attempt 143
Alternative photo-activation mode design 144
Experimental – second attempt 145
Low-order Danheiser cyclopentane annulation 148
Experimental – third attempt 149
Conclusions 152
Supporting information 153
Bibliography 172
Chapter 4 – Asymmetric photo-organocatalyzed reductive coupling 176
Mechanistic investigation 176
Literature background 179
Experimental - homocoupling 180
Future work 183
Hetero coupling 184
Future work 187
Conclusions 187

Supporting information 188
Bibliography 196
Chapter 5 – Divergent total synthesis of polycyclic norcembranoid diterpenes 198
Introduction 198
Reported synthetic approaches 199
Stoltz's strategy for Scabrolide A 200
Sarlah's strategy for Scabrolide A and Yanorolide 201
Fürstner's strategy for Scabrolide A 202
Wood's strategy for Ineleganolide and Sinlochmodin C 203
Fürstner's strategy for Scabrolide B, Sinuscalide C, Ineleganolide and Horiolide 204
Zhang strategy for Sinulochmodin C 206
Our synthetic plan 207
Radical cascade 208
Diels-Alder 209
Michael addition-aldol condensation 209
Experimental 210
Radical cyclization 210
Why radical cyclization does not work 215
Diels-Alder strategy 217
Why Diels-Alder cycloaddition does not work 233
Michael addition-intramolecular aldol reaction 237
Best results with Diels-Alder and cut-and-sew strategy 241
Conclusions 243
Supporting information 244
Bibliography 305
Chapter 6 - Scalable, enantioselective total synthesis of (S)-autumnaline 314
Collaboration with Industry 314
Scope of the work 314
Autumnaline synthesis to date 315
Synthetic strategy evaluation 316
Results 318
Intermediate 4 318
Intermediate 6 323
Intermediate 8 – experimental results 323
Intermediate 9 – strategy and asymmetric HAT optimization 324
Intermediate 10 332
Autumnaline 333

Conclusions 335
Supporting information 335
Synthetic procedures 336
Electronic Circular Dichroism 369
Computational procedure for the calculation of the ECD spectrum 370
Bibliography 373
Chapter 7 – Synthonpedia 378
Introduction 378
Retrosynthetic analysis 379
Computer-driven retrosynthesis 379
Filling the gap 380
Software workflow 381
1 – Synthons as query elements 382
2 – Synthons as database elements and encoding rules 383
3 – Searching algorithm 384
4 – Combinatorial disconnection 385
5^{I} – Filtering 387
5^{II} – Ranking 387
Synthetic tree problem 392
Conclusions 393
Supporting information 394
Bibliography and sitography 405
Final remarks 408

Abstract

In this manuscript the development of new organocatalytic asymmetric methodologies and photocatalytic methodologies for application in organic synthesis are discussed (sometimes with project failure). Moreover, an attempt of total synthesis of the norcembranoid diterpenes family extracted from "Sinularia Coral" and other natural sources carried out at the University of Texas at Dallas is discussed. Finally, the development of a sfotware to help program a synthetic sequence from scretch is discussed, with some examples.

Introduction

Aim of the thesis

Organic chemistry is a subfield of chemistry which involves the study of structure, properties and transformations of all the matters containing carbon atoms. This definition is broad and includes the study of small molecules, polymers and nanostructures, involving chemical reactivity, many kinds of spectroscopy, material science, analytical chemistry and uncountable examples of industrial applications. During my PhD studies I focused on conventional organic chemistry, studying methodologies and synthesis of small organic compounds, in the context of the Vitality project.

The Vitality project is an ecosystem for the innovation, digitalization and sustainability for the economy in the center Italy.[1] Vitality project is founded by the Italian PNRR and involves 24 research institutes, including the University of L'Aquila and the group of Professor Armando Carlone, my supervisor.

Following the guidelines given by Vitality, the aim of my PhD studies presented in this thesis is trying to develop new methodologies in organic chemistry and new convenient synthesis for molecules of interest, both for industry and study of bioactive natural products for academic research.

During these 3 years I had the opportunity to work in the group of Professor Armando Carlone and Dr. Fabio Pesciaioli at the University of L'Aquila, and Professor Filippo Romiti at the University of Texas at Dallas. Moreover, I had the opportunity to cooperate with the group of Professor Protti at the University of Pavia and with Indena S.p.A., a multinational pharmaceutical company based in Milan.

Organic chemistry *is* crafting molecules

Organic chemistry was born to study the structure of carbon-based matter, and ultimately to replicate it artificially. The process of making an organic substance is

complex and requires both strategic thinking and the development of catalysis tools. The concept can be extrapolated and compared to the more general crafting of microscopic objects, taking a piece of furniture as an example. Let's say that a famous Swedish furniture seller wants to create a new shelf, that is sold as separated components to assembly at home. Part of the designer work is to create an *assembly process sequence* as smart as possible: easy for the customer to understand, easy to handle (what if during the assembly this heavy object cannot self-standing?), fast and using cheap components (Figure 1). Another part of the work, not less important, is to create *new and better tools* to help the assembly process: an allen key easier to handle for screws in the corners, new wood joints that do not require screws at all (Figure 1) or a new type of glue to merge corner-shaped pieces.

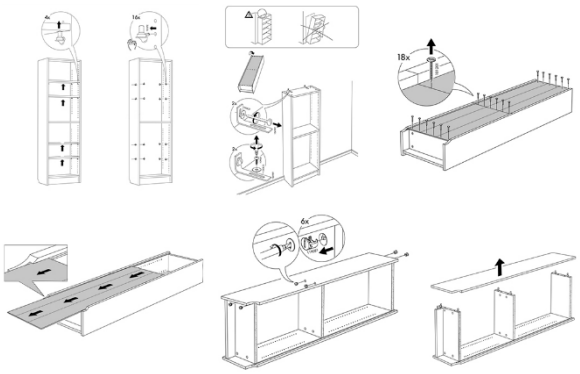

Figure 1 - Shelf assembly sequence

Figure 2 – Screw-free wood joint

The same ground concept is valid both for furniture sellers and chemical companies, the difference is only the target object.

To make a comparison, a recent example of the synthesis strategy helped by new chemical tools can be found in the total synthesis of Nimbolide by Sarlah and coworkers[2] (Figure 3).

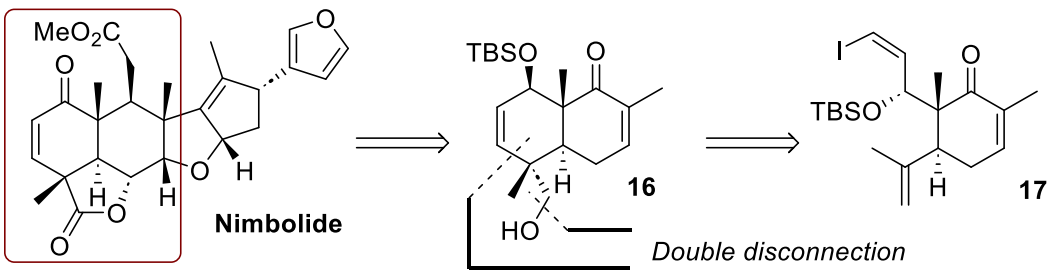

Figure 3 - Total synthesis of Nimbolide - an example of tool/strategy integration

The key bicycle intermediate **16**, if disconnected between the C-O bond and the quaternary C – alkene bond, brings back to intermediate **17**, easily accessible

from carvone. The strategic advantage of this disconnection consists in closing a congested ring, setting up a quaternary stereocenter and making a C-O bond otherwise difficult to introduce without pre-functionalization. Pre-functionalization in this step would be very difficult, since the 2-propenyl group is already contained in the carvone structure. To realize this transformation the chemists decided to adopt the tandem borylative-Heck-oxidation reaction shown in Figure 4.

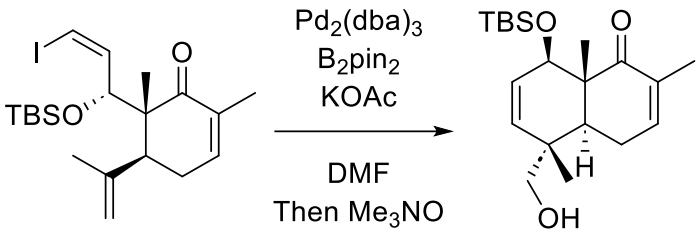

Figure 4 - Tandem borylative Heck - oxidation reaction

This interesting variant of the Heck reaction was previously developed by other research groups.[3,4] This innovative methodology and its application in the total synthesis of nimbolide represent a nice example of new tool development and direct strategic application. Indeed, without that methodology, the construction of such a congested ring would have been very difficult in only 3 steps starting from a feedstock chemical.

Why make new molecules and old ones better

Making new organic molecules is very important in different fields, especially in pharmaceutical industry. Different molecular structures, both of natural origin and artificial, show a different biological activity. Medicinal chemistry studies these aspects, which are essential to find always new drugs. But not only new molecules are important: already known molecules can be important as well. Accessing complicated structures in a smart and fast way can be vital for industry, as the production cost of intricated, but incredibly bioactive molecules can hamper the market access to these APIs. A famous example is the anti-tumoral Vincristine (Figure 5).

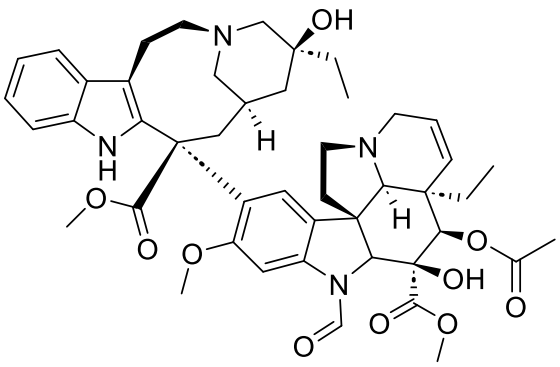

Figure 5 - Vincristine structure

Currentyl, most of it is produced by semi synthesis, extracting the main building blocks from *Catharanthus roseus* and merging them by artificial synthesis. Probably, an efficient total synthesis of this molecule would allow industry to eliminate the tedious extraction process, which is done using tons of vegetable material.

Of course, this is peculiar example, but the same basic principle can be applied to all pharmaceutical production: efficient synthetic methodologies and smart synthetic plans reduce the cost of APIs production, both in energy and materials used.

During these three years I had the opportunity to study different topics in organic chemistry, ranging from total synthesis both in academia and industry, asymmetric organocatalysis, asymmetric organophotoredox catalysis, photochemistry, organometallic chemistry, synergistic organometallic-organocatalysis and computer-aided synthesis. The most significant results and projects encountered on this journey will be exposed into detail in the following chapters.

Bibliography

(1) Https://Vitality.Unipg.It/Il-Progetto/.

(2) Ryffel, D. B.; Ryffel, P. C.; Martinelli, M.; Pillai, V. R.; Sarlah, D. Stereoselective Total Synthesis of Nimbolide. *J Am Chem Soc* 2025. https://doi.org/10.1021/jacs.5c04899.

(3) Yoon, H.; Jang, Y. J.; Lautens, M. Diastereoselective Pd-Catalyzed Domino Heck/Arylborylation Sequence Forming Borylated Chromans. *Synthesis (Germany)* 2016, *48* (10), 1483–1490. https://doi.org/10.1055/s-0035-1561567.

(4) Vachhani, D. D.; Butani, H. H.; Sharma, N.; Bhoya, U. C.; Shah, A. K.; Van Der Eycken, E. V. Domino Heck/Borylation Sequence towards Indolinone-3-Methyl Boronic Esters: Trapping of the σ-Alkylpalladium Intermediate with Boron. *Chemical Communications* 2015, *51* (80), 14862–14865. https://doi.org/10.1039/c5cc05193b.

Chapter 1 - Acetaldehyde in the Enders triple cascade reaction via acetaldehyde dimethyl acetal

Organocatalysis – historical perspective

Nucleophilic catalysis as the first example of organocatalysis

Organocatalysis is the use of small-organic molecules that do not contain inorganic elements to promote chemical reactions.[1] The first examples of organocatalysis can be traced back to the 19th and 20th century organic chemistry: the basic reactivity of nitrogen and phosphorous had already been exploited at the time to accelerate what are now considered well-established chemical processes. The first ever reported example of organocatalysis is the dicyanide hydrolysis promoted by acetaldehyde reported by Von Liebig in 1860.[2] Some other examples of early organocatalysis will be briefly described, despite it was not called by such a name at the time.

An interesting example is the use of N,N-dimethylaminopiridine (DMAP) as a catalyst in the Steglich esterification,[3] which is the coupling of alcohols or thiols and carboxylic acids promoted by a carbodiimide. An example of this reaction is shown in Figure 6.

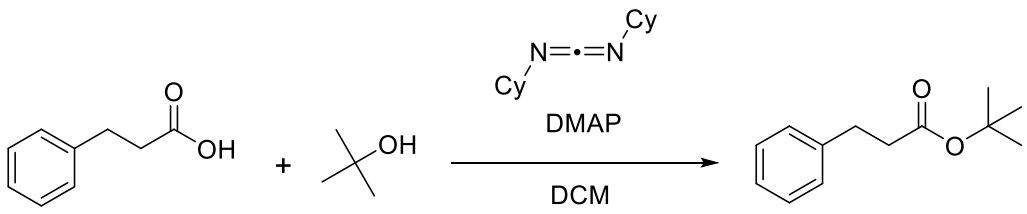

Figure 6 - Example of Steglich condensation reaction

Taking advantage of the already-reported pyridine effect, Steglich and coworkers speculated that the more electron rich, cheap and readily available DMAP could catalyze carbodiimide-promoted condensations with greater efficiency. DMAP acts

as an organocatalyst here, exploiting the nucleophilicity of the sp^2 nitrogen lone pair and its coordinative saturation. The nucleophilic catalysis mechanism key step, which is very well kwon, is shown in Figure 7.

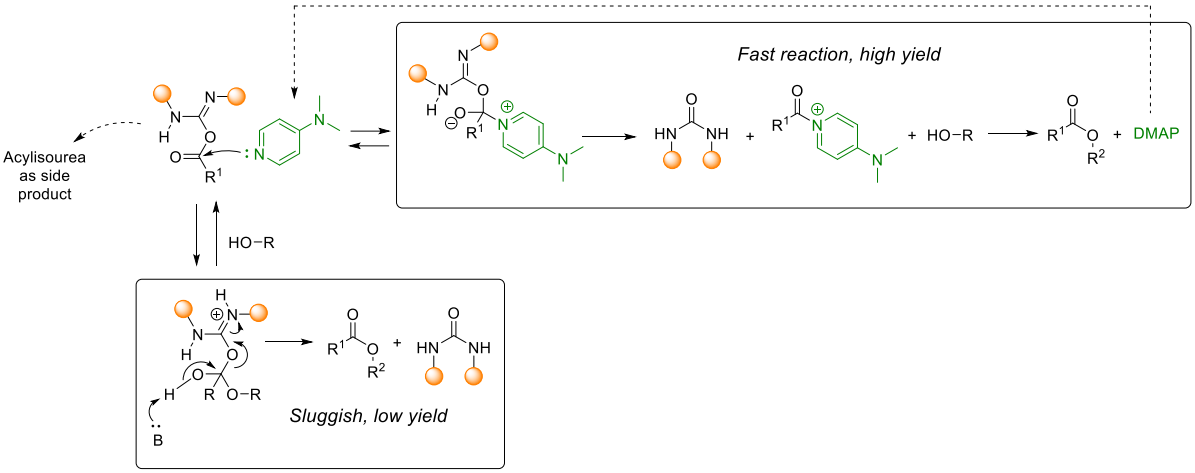

Figure 7 - Key steps of the Steglich condensation

It can be observed that both speed and yield are increased, as the acyl-isourea intermediates in the uncatalyzed version react so sluggish to be by-products themselves. It is a natural consequence that bulky alcohols, such as tert-butanol, can react thanks to the catalytic action of DMAP.

Catalysis speeds up *every* reaction, even transformations at a null rate, unlocking a completely new reactivity. An example of this from the early days of organocatalysis is exemplified by the Morita-Baylis-Hillman (MBH) reaction. MBH is the α-functionalization of α,β-unsaturated carbonyl compounds with carbon electrophiles. There is no possibility for this transformation to proceed just mixing the reagents: a tertiary amine or a phosphine is necessary. The first example of MBH reaction using amine as catalyst with the generally accepted mechanism is shown in Figure 8.[4]

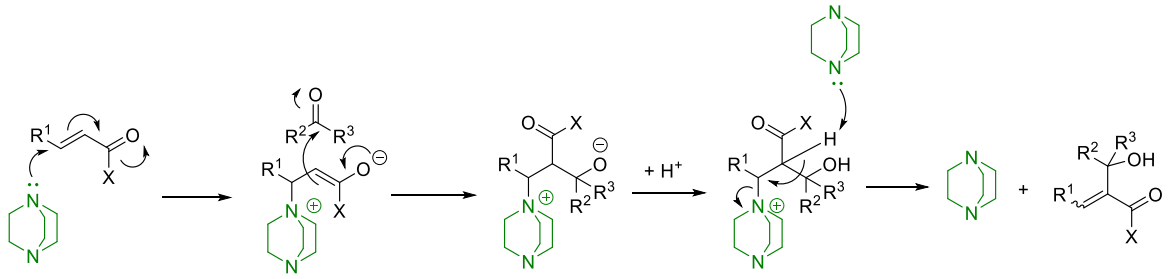

Figure 8 - Example of MBH reaction using DABCO as catalyst

In this transformation the tertiary, nucleophilic amine plays a double role: first, it reacts with the α,β-unsaturated compound in a Michael addition reaction (nucleophilic catalysis), generating an enolate. This enolate is reactive at C2 and

can attack the ketone. After re-protonation and amine-induced enolate elimination the product is generated, freeing the catalyst.

Asymmetric organocatalysis

Once the property of small organic molecules to catalyze chemical transformations through various activation modes was proven, it follows naturally that *asymmetric small organic molecules* can catalyze *enantioselective transformations*. To give historical perspective, the first significant example of an efficient organocatalytic process is the Hajos-Parrish-Eder-Sauer-Wiechert- reaction for the synthesis of the homonymous ketone and the Wieland-Miescher ketone.[5] The synthetic effort comes from the industrial world: bicyclic ketones like these are important chemical intermediates, especially in the total synthesis of steroids. The transformation is shown in Figure 9.

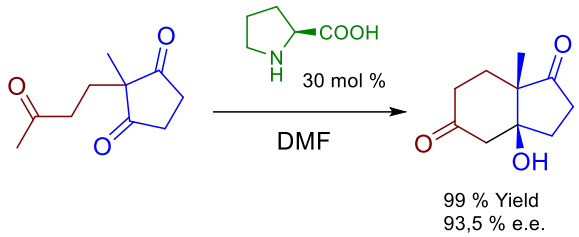

Figure 9 - Hajos-Parrish-Eder-Sauer-Wiechert synthesis of steroid intermediates

Three mechanisms have been proposed here:[4] aldolase type mechanism involving the activation of the carbonyl moiety via H-bond and enol attack[5], cooperative enamine-H bond activation involving two molecules of proline and cooperative enamine-H bond activation involving only one molecule of proline which acts as a double functional catalyst.[6,7] The last mechanism is shown in Figure 10.

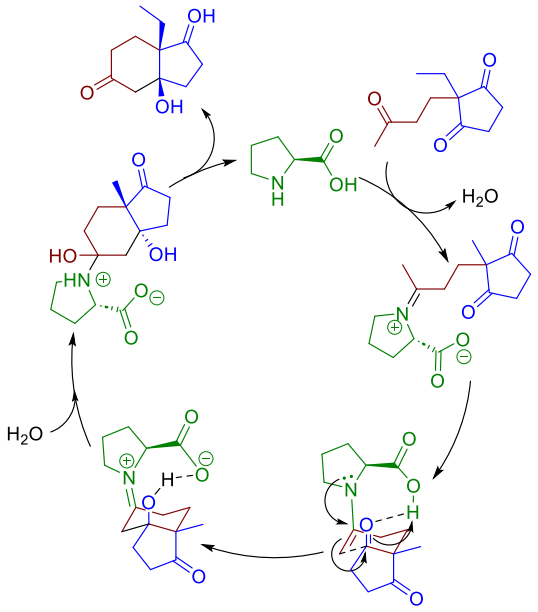

Figure 10 - Houk and coworkers theorized mechanism

It can already be noted a complex series of activation modes expressed by such a simple molecule – proline: enamine and carbonyl H-bond activation in a template fashion. A remarkable example which received due attention in the scientific community after the rush on organocatalysis studies.

Another remarkable ante-litteram example is represented by the Shi epoxidation. It is well known that ketones react with persulphates to produce dioxirane intermediates, which can transfer the oxygen atom to other functional groups, such as olefins. This simple but powerful activation mode can be exploited with ketones derived from the chiral pool – asymmetric organocatalysis is there again. Shi epoxidation uses fructose-derived ketones as asymmetric organocatalysts. Such a template proved very efficient compared to previous methodologies aiming the same target.[8,9]

The generally accepted reaction mechanism is shown in Figure 11.[4,8,10]

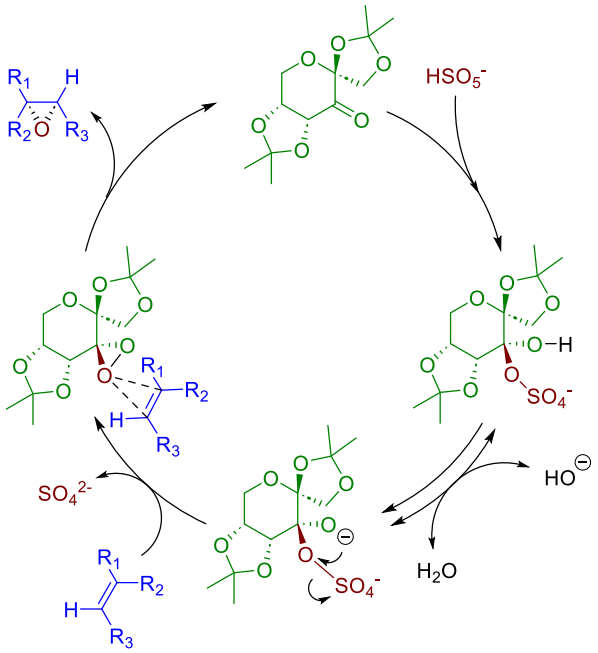
R1
H
R2
O
R3
HSO5-
O
O
O

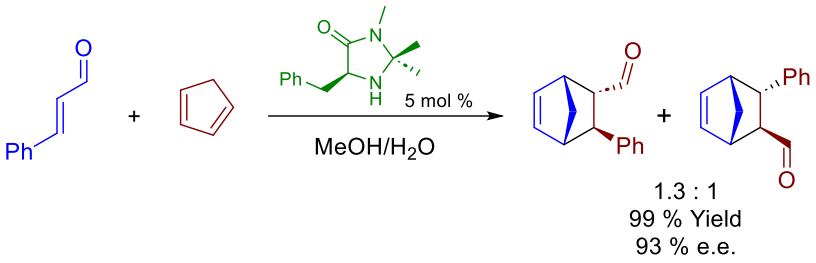

Figure 13 - Imidazolidinone-catalyzed Diels-Alder reaction

Since that moment, it has followed a lot of scientific work to find other organocatalytic activation modes other than amine catalysis, and to exploit these new activation modes in different systems. In 2021 List and MacMillan were awarded the Nobel prize in chemistry for their seminal contribution in organocatalysis. It was recognized that until that moment the only macro-classes of asymmetric methodologies consisted of chiral metal complexes (metal catalysis) and enzymes (biocatalysis). Organocatalysis is the third pillar.[13]

Organocatalysis – activation modes

It follows some of the activation modes typical of organocatalysis: iminium ion, enamine, hydrogen bond activation, asymmetric counter-ion directed catalysis (ACDC). Only the activation modes classes used during the experimental activities will be introduced.

Iminium ion activation

Iminium ions are salts in which the cation has the structure $R^2C{=}N^+R^2$. Thus N-hydronated imines and their N-substituted derivatives.[14] In other words, iminium ions are α-amino carbocations. The lone pair of the nitrogen atom is conjugated with the p orbital of carbon, stabilizing the system. The conjugated π orbital can be extended to 4 atoms (or more) system, giving unsaturated iminium ions (Figure 14).

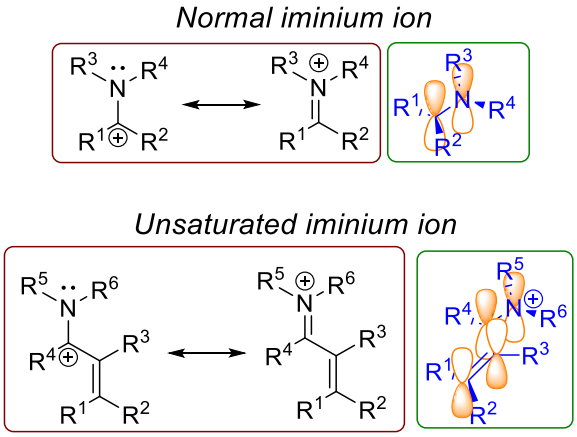

Figure 14 - Iminium ion electronic structure

Thus, iminium ions are stable enough to be readily formed at environmental conditions with common functional groups. At the same time, iminium ions are reactive electrophiles and are involved in many fundamental organic processes, such as Mannich reaction, Pictet-Spengler reaction and Petasis reaction, just to cite a few.

In this context of nucleophilic attack, simple iminium ions are reaction intermediates that are lost after the reaction - once the nucleophile enters the process is finished. Thus, to exploit the electrophilicity of iminium ions to *activate* other functional groups, we have to focus about α,β–unsaturated iminium ions. These are bidentate electrophiles that can undergo 1,2-attack (as normal iminium ions) or 1,4-attack, just as Michael acceptors. In the second case the resulting saturated iminium ion can be hydrolyzed back to a saturated aldehyde, starting a new catalytic cycle. The described activation mode is shown in Figure 15. The 1,2-attack is represented as reversible, but it can be also irreversible, depending on the nucleophile used.

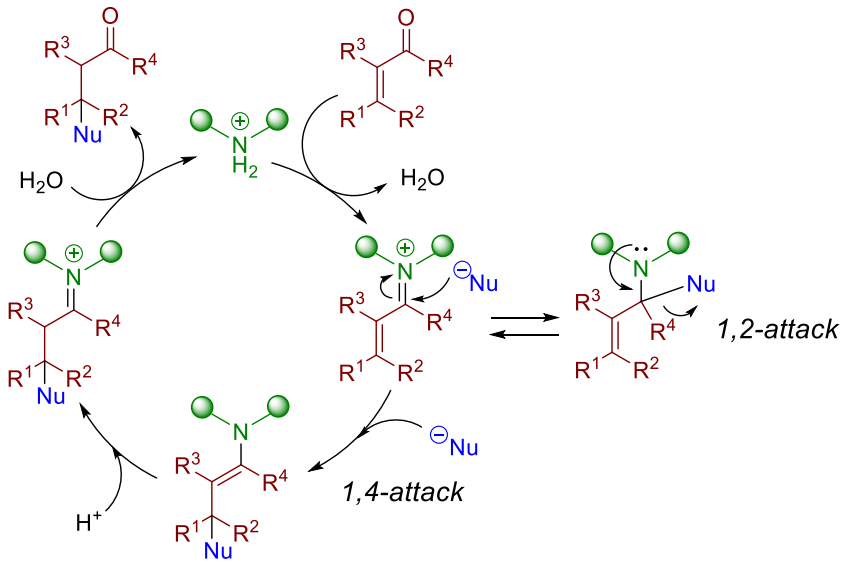

Figure 15 - Iminium ion activation mode

The electrophilicity character of the α,β-unsaturated iminium ion compared to a corresponding aldehyde is orders of magnitude greater. As example, we can compare the reported E values from the Mayr-Patz scale[15] for cinnamaldehyde (E = 19,9[I])[16], its iminium ion made with pyrrolidine (E = - 9,8)[17] and the MacMillan (II) catalyst (E = - 5,52)[18] (Figure 16). It can be observed as the simple pyrrolidine-derived iminium increases the electrophilicity of 10 orders of magnitude.

[I] It is referred to the aldehyde itself, not to the C3 – this site must be even less electrophilic since the test reaction was going on the carbonyl.

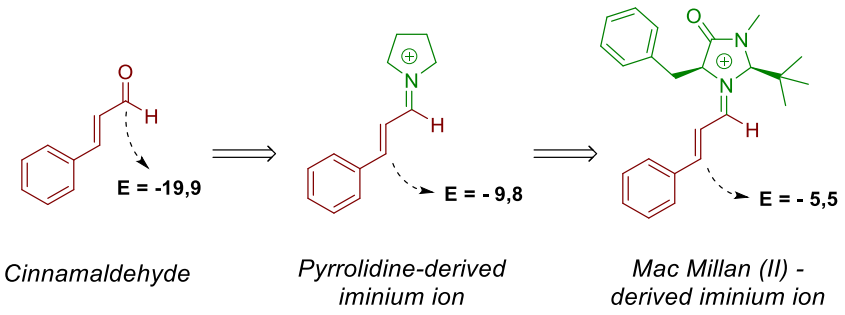

Figure 16 - Example of increased electrophilicity of unsaturated iminium ions

The example of iminium ion made with Mac Millan (II) catalyst introduces two other simple but important concepts which are true for both the iminium ions themselves and for organocatalysis in general. Not only is the asymmetric structure of the catalyst able to induce enantioselectivity, but also it *changes* the reactivity of the intermediate. The constraint imposed by the substituents in the scaffold forces a different aligning of the nitrogen lone pair, tuning the reactivity of the iminium ion. A concurrent tuning effect is given by the electro-withdrawing/donating electronics of the substituents.

Enamine activation

Enamines are vinylic amines with the general structure R2NCR=CR2, usually obtained from the condensation of a carbonyl compound and an amine.[19] Enamines have been studied long as useful synthetic intermediates, but they have lived a second life in the scientific community for the development of organocatalysis. Indeed, thanks to the conjugation of the nitrogen to the vinylic system, the C2 is nucleophilic, as represented in Figure 17.

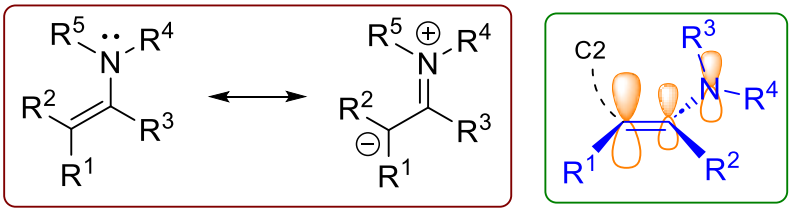

Figure 17 - Enamine electronic structure

The activation mode for enamines is described in Figure 18 and it is analogous to the iminium ion activation mode (Figure 15): the speed and reversibility of iminium ion/enamine formation process is fully exploited.

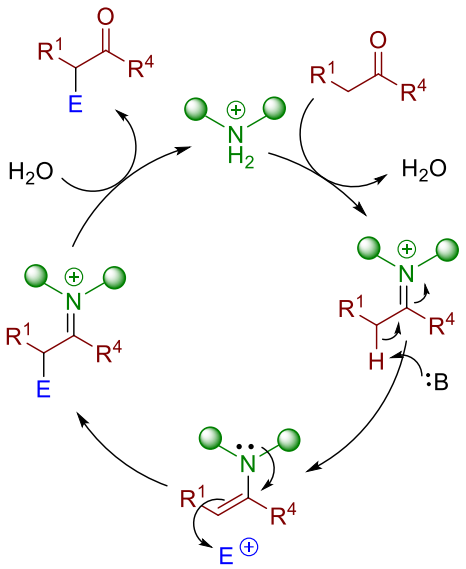

Figure 18 - Enamine activation mode

The predominance of the enamine form or the iminium ion form can be tuned with the amount and/or the strength of the acid. An equimolar amount of strong acid protonates everything, forcing the iminium ion formation. *Viceversa*, a sub-stoichiometric amount of weak acid only helps the enamine formation *through* the iminium ion, but it has an appreciably strong conjugated base, favoring the enamine. Indeed, the acid-catalyzed formation of the enamine is the most common and effective method to activate these types of processes, but the enamine-like reactivity can be expressed even without the presence of an acid. In that case the enamine formation goes through *internal proton exchanges*.

Enamine intermediates generated from carbonyl compounds, show an enolate-like reactivity. The comparison of enol derivatives and enamine reactivity is crucial to understand their synthetic power. The nucleophilicity parameter (N) expresses orders of magnitude of difference across different chemical species, as shown in Figure 19.

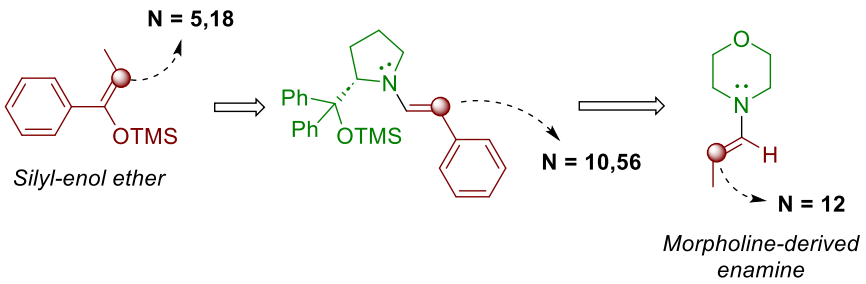

Figure 19 - Example of increased electrophilicity of enamines

Enamines show typically 5 or more orders of magnitude[20,21] of reactivity compared to enol ethers (N = 5,18)[22] – which need to be synthesized and isolated, while enamines are formed *in situ* catalytically. For comparison, metal enolates are

roughly 7 orders of magnitude more reactive than the corresponding enamine,[23] but they need to be synthesized in a separate vessel with harsh conditions, and their tolerance of functional group is lower than enamines.

Iminium ion and enamine activation are among the most important and common activation modes exploited in organocatalysis. These intermediates are formed from the same carbonyl compounds and react with opposite chemical species (electrophiles and nucleophiles). Moreover, after the reaction event one is transformed into the other, and both can be easily interconverted into each-other under mild conditions. This sort of opposite behavior with a reciprocal interdependence can be used for advanced catalytic transformations, involving both electrophiles and nucleophiles additions in sequence to build more complex molecular scaffolds in one step. This complementary behavior has been described allegorically as “ying and yang”.[24]

Hydrogen-bond activation

Hydrogen-bond (HB) activation is another very important activation mode that has found many applications in the activation of poorly reactive electrophiles. The organocatalyst in this case acts as a HB donor, establishing one or two bonds with the substrate and forming an activated complex. The lone pair(s) sharing by the electrophile has two important consequences: first, the formation of the complex helps to orient the substrates, pre-organizing the transition state. This reduces the entropy required, lowering the overall $\Delta G^{\ddagger}$. Second, the electronic density is pulled *away* from the electrophile, somehow lowering its LUMO. Moreover, it is a common feature of this class of catalysts to have a second structural part which has a weak interaction with the target substrate, such as π-stacking interaction or another H-bond.[25] This additional interaction helps to organize even more the transition state and/or enables further electronic shifts which helps the reaction. A representative scheme of this activation mode is shown in Figure 20.

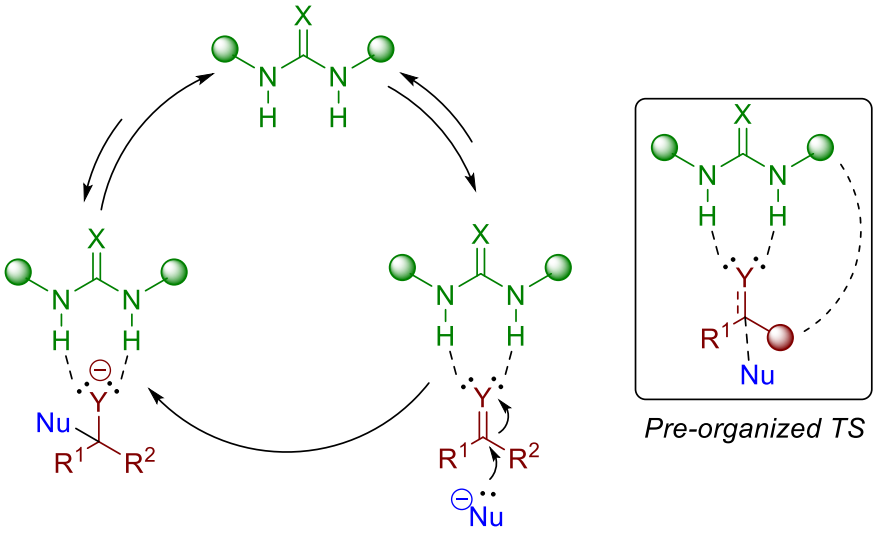

Figure 20 - H-bond activation mode

The Mayr-Patz electrophilicity data are not available for a comparison in this case, because an isolable complex is needed for the measurement. The H-bonded complex forms reversibly and the equilibrium cannot be shifted, unless by changing the temperature.

Asymmetric Counterion Direct Catalysis

Asymmetric Counterion Direct Catalysis (ACDC) is a term which describes an *asymmetric induction mode*.[26,27] Reactions that go through polar intermediates must have a counter-ion around if the solvent does not separate the ionic couple. Thus, if the ionic couple is tight enough the *chiral* counter-ion can induce enantioselectivity. The activation modes presented until now have the common characteristic to have the chiral element *close to* electronically active structure of catalyst-substrate complex that builds the stereocenter. In ACDC the chiral element is just the "spectator" ion, which is actually *not* a spectator. ACDC is thus a very general term which involves both chiral ions and cations, organocatalysis, transition metal catalysis, photoredox[25] catalysis and electrocatalysis[28].

A general reaction scheme is represented in Figure 21.[II]

[II] The catalytic cycle is arbitrary sketched using a positively charge "active catalyst" and a negatively charged chiral counter ion for simplicity. Switching the charges and the electrophile and nucleophile is equivalent for the general concept.

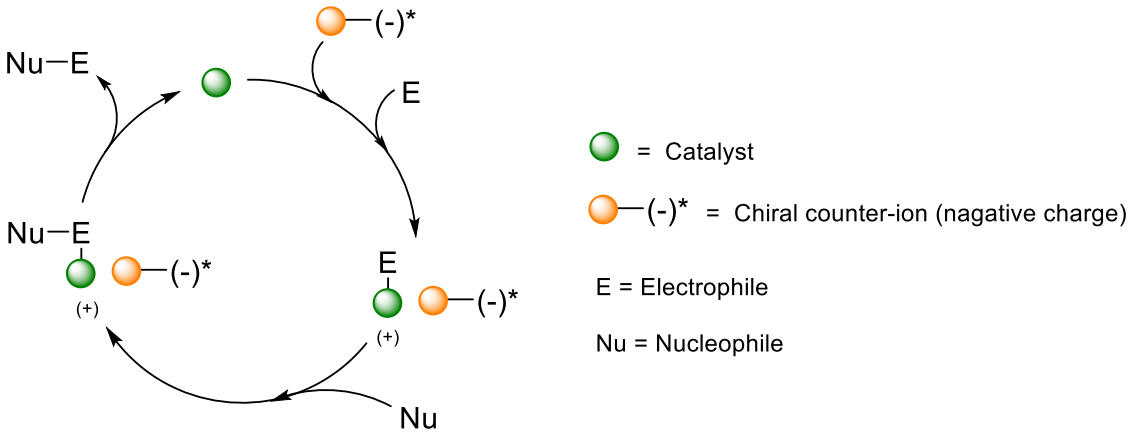

Figure 21 - ACDC activation mode

A straightforward example of ACDC in organocatalysis is the use of BINOL-derived chiral phosphoric acids, for example TRIP, as showed in Figure 22.[29,30]

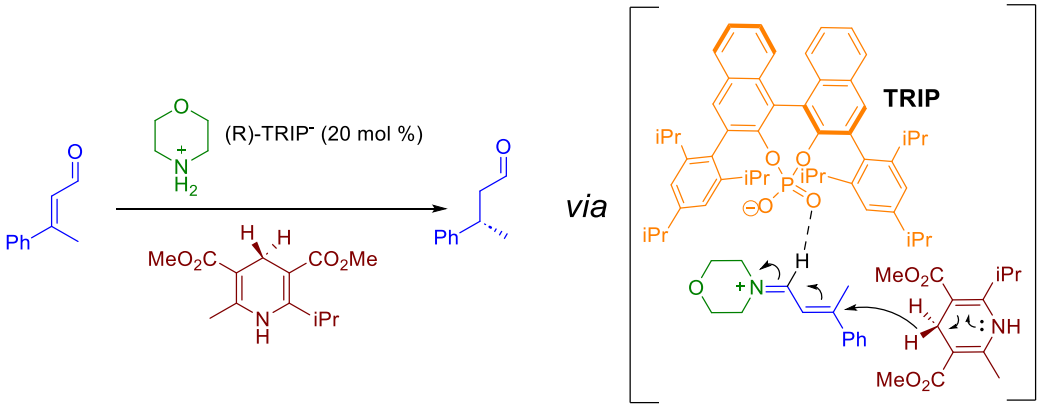

Figure 22 - Example of ACDC catalysis

List and co-workers also considered an H-bond interaction between the phosphate anion and the formyl hydrogen of the iminium ion, which would help to organize the transition state.

Enders' cascade

The "Enders' triple cascade" is an asymmetric organocatalyzed multicomponent reaction developed by Enders and coworkers in 2006.[31] It is the condensation of an aliphatic aldehyde, a β-nitrostryrene and a cinnamaldehyde on its first version, to make an asymmetric cyclohexene-carbaldehyde with four contiguous stereocenters (Figure 23).

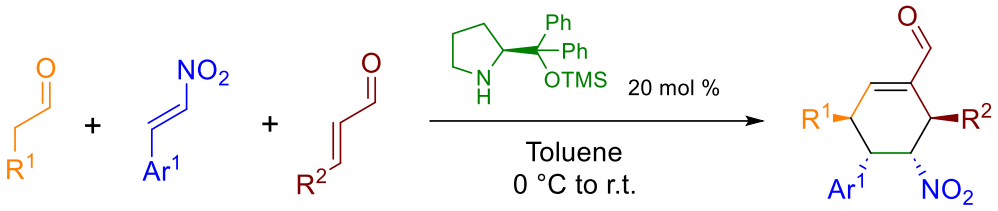

Figure 23 - Enders' cascade - general reaction

This transformation is one of the iconic examples of organocatalysis power; an asymmetric three-component reaction to make a substrate difficult to synthesize with other methodologies with mild conditions, simple reagents and catalyst. The commonly accepted mechanism, proposed by the authors,[31] is a sequence of Michael addition of an enamine to the β-nitrostryrene, followed by Michael addition of a nitro-enolate to an α,β-unsaturated iminium ion, and an intramolecular aldol condensation. The sequence is reported in Figure 24.

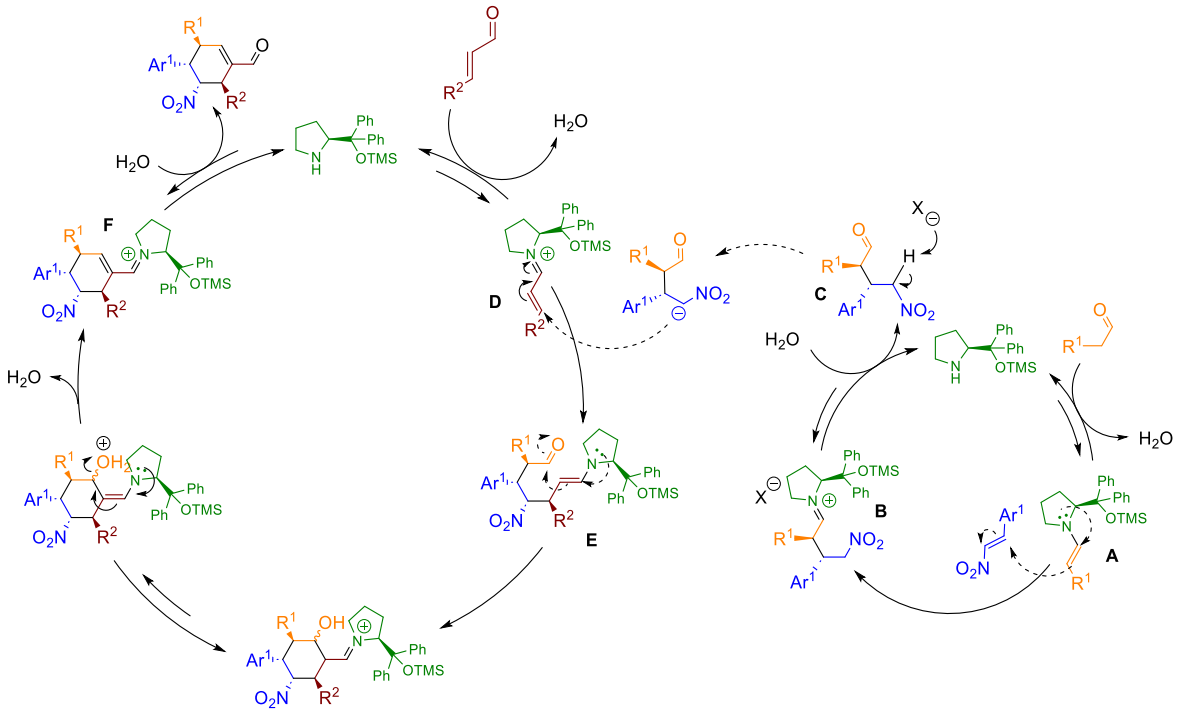

Figure 24 - Enders' cascade accepted cycle

First, the organocatalyst (green) condensates with the aliphatic aldehyde (orange, right side) to yield intermediate enamine **A** at the equilibrium. This then reacts with the β-nitrostryrene (blue) in a Michael fashion, yielding intermediate **B**. This is then hydrolyzed to free the catalyst and the nitroalkane **C**, which can be deprotonated in the reaction environment to give the corresponding nitro-enolate. This step is actually not discussed in the original paper. However, the low pKa of nitroalkanes is well known, as it is their reactivity – for example well exploited in the Henry reaction. Thus, it is reasonable to suppose that the actual reactive species is the nitro-enolate, with the organocatalyst acting as a base. In the meantime, the

Hayashi-Jørgensen organocatalyst can condensate at the equilibrium with the unsaturated aldehyde derivative to yield iminium ion **D**, which can be attacked by **C** in a Michael fashion, yielding **E**. The enamine **E** is probably reactive enough to start an intramolecular aldol reaction with the other aldehyde functionality. There is another possible intramolecular aldol condensation, which would involve the other enamine with α-branched aldehyde. However, the formation of this enamine would be inhibited compared to intermediate **E**, for steric reasons, and this could account for the exclusive formation of the final product.

After a protonation-tautomerization sequence the hydroxyl group can then be eliminated to yield intermediate **F**, thatcan finally be hydrolyzed, freeing the product and the catalyst.

The formation of the chiral centers is established in two different steps (Figure 25).

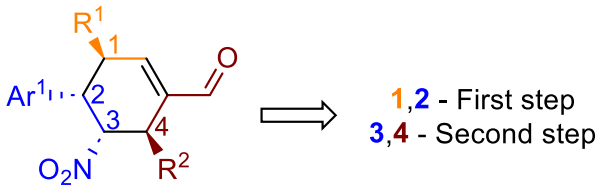

Figure 25 - Chiral centers formation

Chiral centers 1 and 2 are formed during the Michael addition of the catalyst-derived enamine to the β-nitrostyrene (**A** → **B**). Chiral centers 3 and 4 are formed during the Michael addition of nitro-enolate to the unsaturated iminium ion (**C** → **D**). Thus, the absolute stereochemistry of C1, C2 and C4 is strictly correlated to the structure of the organocatalyst, while C3 depends on the nitro-enolate geometry. C3 is the only reported stereocenter which undergoes variations, leading to two diastereomeric products. In the Enders' conditions one major product is obtained, ranging from 3.5:1 to 45:1 diastereomeric ratio.

Use of acetaldehyde in organocatalysis

In the field of organocatalysis the use of aliphatic aldehyde is ubiquitous as they can undergo enamine formation very easily. However, the use of acetaldehyde as a reagent has always been challenging for different reasons. First, the low boiling point (21 °C), the high volatility and the high toxicity of this substance poses a handling problem. Second, the chemical behavior of acetaldehyde is difficult to control for different reasons, lowering both the chemoselectivity and stereoselectivity of the related transformations. From the chemoselectivity perspective, it can perform side reactions at a much higher rate compared to heavier

aldehydes, such as self-condensation, polymerization, Mannich addition with the amine organocatalysts and Tishchenko-type processes, as shown in Figure 26.[32]

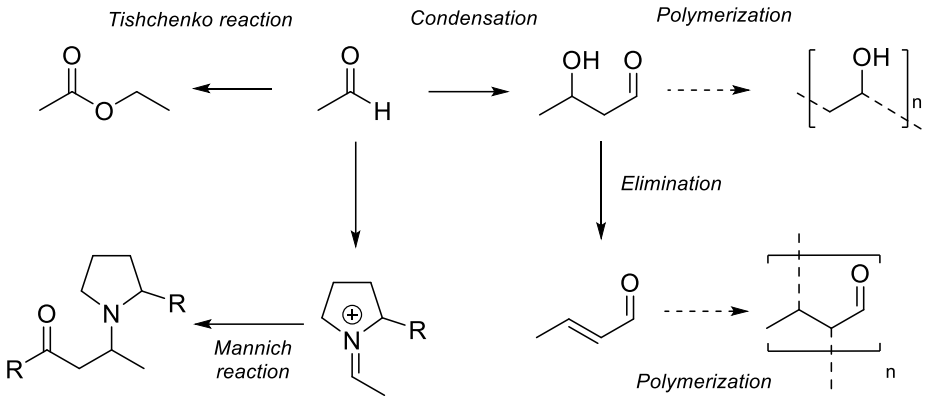

Figure 26 - Acetaldehyde degradation

The presence of these decomposition pathways usually forces the use of a super-stoichiometric amount of acetaldehyde.[33–35]

From the stereoselectivity side, the enamine adduct of acetaldehyde lacks the steric hindrance of more substituted analogues, so the enantio-discrimination process could be more difficult in general.

A possible solution to the chemoselectivity problem is to use acetaldehyde masked agents, that slowly release acetaldehyde *in situ*. This approach in general shuts down the self-reactivity of acetaldehyde. There are various examples with different masked acetaldehyde reagents, such as vinyl acetate,[36] vinyl-silyl ethers,[37] ethanol,[38] pyruvic acid,[38] (E)-3-chloroacrylic acid,[38] 2,4,6-trimethyl-1,3,5-trioxane (paraldehyde)[39] and acetaldehyde dimethyl acetal (ADA), by our group.[40–42]

Interestingly, the Enders' cascade has never been performed using acetaldehyde as aliphatic aldehyde. Thus, we became interested in the use of ADA in the Enders' cascade, as it already proved to be an efficient method to introduce acetaldehyde *in situ* for organocatalyzed processes, as it already demonstrated to lower the amount of organocatalyst and acetaldehyde needed compared to other methods.[42] This variant of the Enders' reaction would yield unprecedented cyclohexane carbaldehydes. Similar cascades have already been reported, as shown in Figure 27.

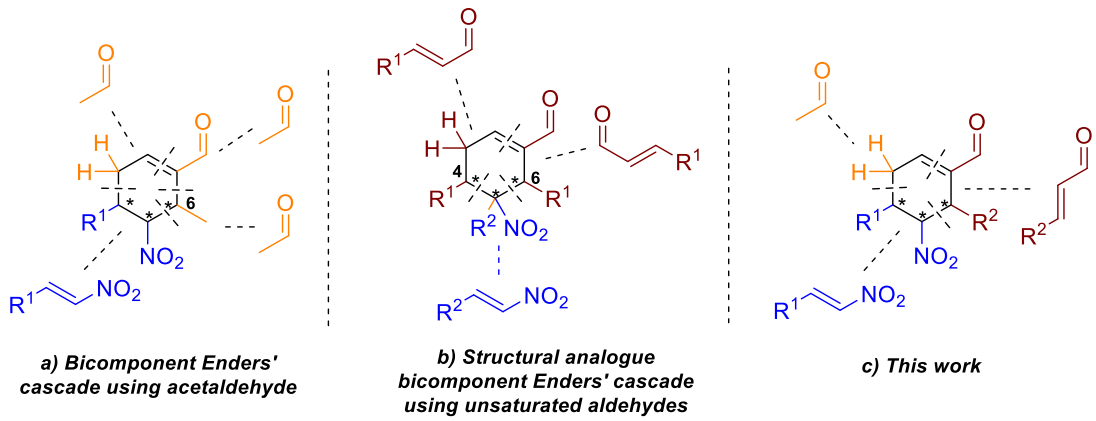

Figure 27 - Comparison with other asymmetric organocatalyzed multicomponent cascades

The first structure from left (Figure 27, a) derives from the multicomponent reaction of 3 equivalents of acetaldehyde and 1 equivalent of β-nitrostyrene.[43] It is structure-limited as the substituent at C6 must be methyl. The second example (Figure 27, b) merges 2 equivalents of an unsaturated aldehyde and 1 equivalent of β-nitrostyrene.[44] Again, the structural variability is limited by the fact that the substituents at C4 and C6 must be the same.

Thus, we reasoned that our group experience in asymmetric organocatalysis with ADA could be used to forge new structures using mild conditions. As shown in Figure 27 c, the introduction of ADA allows to forge a more customizable 6-membered ring, as the nitroalkene and the cinnamaldehyde derivative would introduce different structures in the scaffold.

Reaction optimization

First, we evaluated if the same Enders' carbocyclic aldehyde can be obtained simply using acetaldehyde as aliphatic aldehyde, as showed in Figure 28.

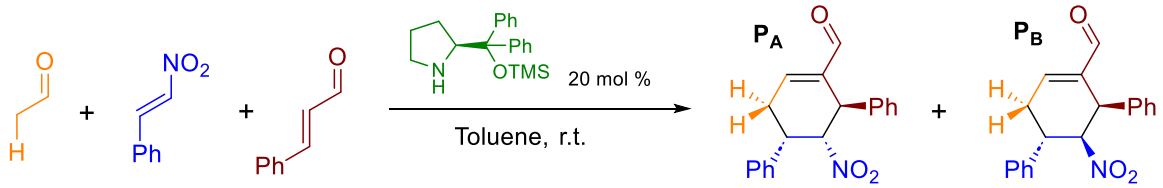

Figure 28 - Enders' cascade with acetaldehyde

The initial tests, sketched in Table 1, immediately showed a decrease both in the diastereomeric ratio and the yield compared to aliphatic substrates.

Table 1 - Initial tests

Entry	Catalyst (eq.)	NMR Yield	d.r.	Conversion[a]	Selectivity[b]

1	20%	43%	1:1.4	91%	47.5
2	10%	33%	1:1.3	95%	34.7

Table 2 - Initial tests

Reaction conditions: β-nitrostyrene (0.5 mmol, 1 eq.), acetaldehyde (0.6 mmol, 1.2 eq.), cinnamaldehyde (0.525 mmol, 1.05 eq.) were added to a solution of Hayashi's catalyst (0.05 mmol, 0.1 eq.) in toluene (0.625 M) and allowed to stir for 24 hours at room temperature. [a] Measured by HNMR, [b] Measured by HNMR

The decrease in the diastereomeric ratio, observed also in the conditions developed with ADA, will be discussed later. The general low yield can be explained by the behavior of acetaldehyde, as described above. Indeed, reacting with itself and/or deactivating the catalyst through Mannich condensation, the other components are partially unreacted. The "selectivity" value is defined here as the ratio converted β-nitrostyrene/product, evaluated with ^{1}HNMR yield using an internal standard. This is because we're dealing with a multistep reaction and β-nitrostyrene, which is one of the two reagents in the first step, is also the limiting reagent. Indeed, the intermediate nitro-alkane can partially react with cinnamaldehyde, and only at that point convert to the final product (Figure 29).

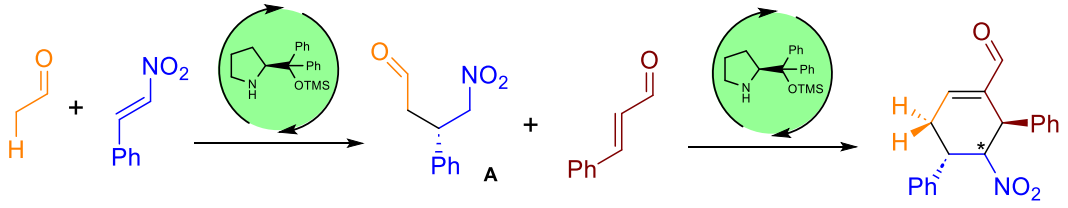

Figure 29 - Low selectivity for β-nitrostyrene

As shown later, the poor selectivity observed in the first tests is improved in the final optimization, but it's still low. This fact is reinforced by the observation of more aldehyde peaks in the ^{1}HNMR spectrum of the crude. These extra aldehyde peaks could be assigned to the mentioned nitro-alkanes, which have never been isolated, as we were more interested in obtaining the final products at the time. In this scenario, we may assume that these nitroalkanes have an alternative fate than the product: maybe direct Henry condensation with acetaldehyde in direct competition with iminium catalyzed Michael addition. Further investigation is needed to prove or disprove this.

Given the poor results obtained with the Enders' conditions, we tackled improving the conditions using ADA, exploiting the expertise of our group in this field.[40,42] To free the aldol group some acid catalysis and the presence of water is needed, and these conditions must be fit with the organocatalytic cycle. Indeed, water drives left the equilibrium of catalyst-substrate bond formation, and the acid catalytic loading must be finely tuned to not shut down the reactivity of these adducts. It was already discovered that the combination of 2 equivalents of ADA, 6 equivalents of water and 0.1 equivalents of Amberlyst-15® are compatible with

catalytic systems. Thus, we decided to start a screening campaign, hoping to find more satisfactory conditions for the inclusion of acetaldehyde as reaction partner. The results[III] are summarized in Table 3

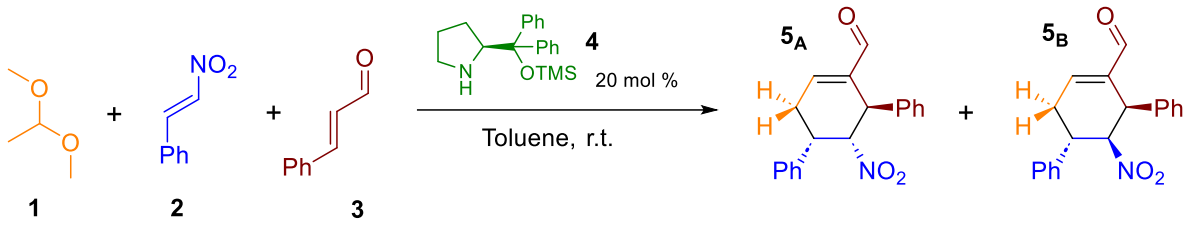

Entry	1 (eq.)	2 (eq.)	4 (eq.)	Solvent	Conversion	NMR Selectivity	NMR Yield	d.r.	e.e.
1	1.2	1.5	0.1	$CHCl_3$	53 %	62 %	33 %	1.4:1	> 99%
2	2	1.05	0.1	CHCl3	54 %	79 %	43 %	1.1:1	> 99%
3	2	1.05	0.2	CHCl3	45 %	44 %	20 %	1.2:1	> 99 %
4	2	1.05	0.1	ACN	43 %	12 %	5 %	1.5:1	\
5	2	1.05	0.1	EtOAc	77 %	23 %	18 %	1.0:1	\
6	2	1.05	0.1	THF	79 %	37 %	29 %	0.8:1	\
7	2	1.05	0.1	PhH	58 %	43 %	25 %	0.8:1	\
8	2	1.05	0.1	PhMe	61 %	66 %	40 %	1.0:1	\
9 [b]	2	1.05	0.1	PhMe	62 %	37 %	23 %	0.8:1	\
10 [c]	2	1.05	0.1	PhMe	59 %	50 %	30 %	0.9:1	\
11	2	2.1	0.1	PhMe	70 %	48 %	33 %	0.8:1	\
12 [d]	2	1.05	0.1	PhMe	72 %	47 %	34 %	0.7:1	\
13 [e]	2	1.05	0.1	PhMe	58 %	45 %	26 %	0.6:1	\
14 [f]	2	1.05	0.1	PhMe	71 %	50 %	36 %	0.8:1	\
15 [g]	2	1.05	0.1	PhMe	75 %	48 %	36 %	0.8:1	\

Table 3 - Enders' cascade with ADA optimization

[a]Reaction conditions: 3 (0.1 mmol, 1 eq.), 1 (indicated equivalents.), 2 (indicated equivalents) and Amberlyst-15 (0.01 mmol, 0.1 eq.,), H_2O (0,6 mmol, 6 eq.) were added to a solution of the catalyst 4 (indicated equivalents) in the indicated solvent (0.1 M) and allowed to stir for the 48 hours at room temperature. [b] 20% Amberlyst-15; [c] 5% Amberlyst-15; [d] Reaction performed at 40 °C; [e] Reaction performed at 60 °C; [f] 10% Alumina added; [g] 10% Amberlite-45 IR added.

From the first tests (entry 1-3) it was immediately clear that with only 10 mol% of catalyst loading we were able to obtain similar yields compared to the Enders conditions that employ 20 mol% of Hayashi chiral amine. Moreover, the enantiomeric excess was immediately optimal, as expected for a sequence of reaction forging more than one stereocenter.[45] The diastereoselectivity was poor, so we tested some common solvents (entry 4-8), observing that the reactivity in toluene was very similar, with no improving in the diastereoselectivity. Heating the reaction (entry 13 and 14) and change the catalyst loading of Amberlyst-15 (entry 10 and 12) did not improve the results. Then, there has been an attempt to improve selectivity. As already mentioned, the potentially difficult step is the nitroalkene

[III] These tests include also some previous exploration by Dr. Giuliana Giorgianni.

intermediate conversion. Thus, in theory the presence of a catalytic amount of base can help. However, it cannot be added directly in solution, as it would quench Amberlyst-15. The idea was to usea basic solid resin additive, in order to have some basic sites at the solution/solid interphase, to help the deprotonation of the nitro-alkane. Normally, the first reaction between an acid and a base added to the same environment would be a simple proton transfer, faster than any other possible catalytic activity on the substrates of interest. However, one must consider that chloroform is an apolar solvent, and the protonation events create ionic couples, usually poorly solvated. Thus, it may be reasonable to speculate that any protonation activity would be very close to the Amberlyst-15 surface. Hoping that chloroform proton shuttle activity is very low, it is possible to have different particles in the same suspension with superficial acid and basic activity. The idea is represented in Figure 30.

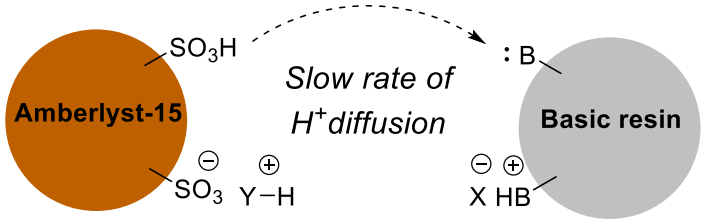

Figure 30 - Representation of solid-state Bronsted catalysis

Both alumina and Amberlite-45-IR were tested as co-resins, but lower conversion and yield were measured. This discouraged us from further investigating new designs of the catalytic systems and we went on for another round of reaction optimization.

Toluene was the solvent of choice, as it gave the best results together with chloroform, but is a more benign solvent. Reaction time and substrate concentration were screened, and the results are shown in Table 4.

Entry	Conversion	Selectivity	Yield	d.r.	$[2]_0$	Time
1	36 %	59 %	21 %	0,8	0.05 M	24 h
2	72 %	48 %	35 %	1,1	0.25 M	24 h
3	93 %	42 %	39 %	1,2	0.5 M	24 h
4	88 %	40 %	35 %	1,3	1 M	24 h
5	63 %	39 %	25 %	0,8	0.05 M	48 h
6	79 %	56 %	44 %	1,1	0.25 M	48 h
7	77 %	48 %	37 %	1,2	0.5 M	48 h
8	93 %	44 %	41 %	1,2	1 M	48 h

Table 4 - Time and concentration optimization

[a] Reaction conditions: 3 (0.1 mmol, 1 eq.), 2' (0.2. mmol, 2 eq.), 4 (0.105 mmol, 1.05 eq.) and Amberlyst-15 (0.01 mmol, 0.1 eq.) were added to a solution of 1 (0.01 mmol, 0.1 eq.) in toluene (indicated concentration) and allowed to stir for the indicated time at room temperature.

The best results during the optimization come from entry 6: 0,25 M and a reaction time of 48 h gave 79 % conversion, 56 % selectivity, 44 % yield and an enantiomeric excess of 98,8 %, calculated as the average of the two diastereoisomers obtained.

Scope

With the best conditions in our hands, we explored the scope of the developed methodology. We included aromatic substrates with both electro-donating and electro-withdrawing groups, alkyl nitroolefin and an α,β-unsaturated aldehyde. Both the diastereoisomers obtained for each reaction were isolated and fully characterized. The enantiomeric excess was determined for each diastereoisomers and expressed as an average as in all cases the results were very similar between each other. So, no relevant information can be easily deduced reporting both enantiomeric excesses. The single enantiomeric excesses are reported into details in the supporting information). The results are shown in Figure 31.

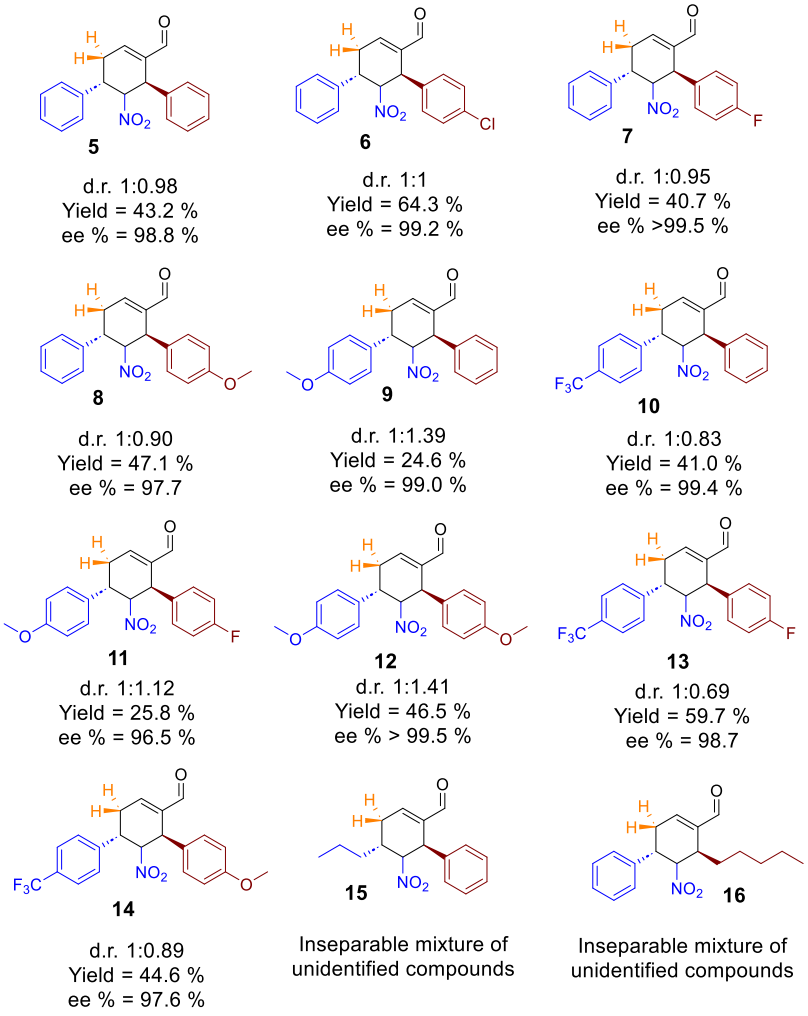

Figure 31 - Reaction scope

The results obtained deserve some comment: the yield is generally between 40 % and 45 %, with some exceptions: **6** and **13** with a higher yield (64.3 % and 59.7 %, respectively) and **9** and **11** with a lower yield (24.6% and 25.8 %, respectively). Apparently, there is no obvious reason why **6** and **13** have a higher yield compared to the model reaction (**5**). Both have an electron-withdrawing group in the para position of the α,β-unsaturated aldehyde, but in that case, **7** should have a higher yield as well: probably it is a peculiar combination of electronic effects, but we did not investigate this further. The low yield found for the substrate **9** and **11** can be attributed to presence of an electron-donating group on the nitroolefin without any α,β-unsaturated aldehyde partner with an electron-withdrawing group. This experimental observation can be justified with a slow attack in the first reaction step, because of the more electron-rich system of the nitroolefin.

Both the diastereomeric ratio and the enantiomeric excess fluctuate slightly with the different substituents (going from 1:1.41 to 1:0.69 and from 95.8 % to more than 99.5 %). As expected, the presence of various substituents in the aromatic ring causes a modification of the relative energies of the paths which generate the different enantiomers and diastereoisomers, but the oscillations are not of such magnitude to make further reasonable observations. Unfortunately, with aliphatic substituents (**15** and **16**), a complex mixture of compound is formed, and it was not possible to characterize the products. Thus, it can be concluded that the developed methodology does not work both for aliphatic α,β-unsaturated aldehydes and nitroalkenes. This differs from the original reported Enders' cascade[31] – the substituent of the α,β-unsaturated aldehyde *can* be aliphatic.

The origin of poor diastereoselectivity

As already described, during the optimization phase the diastereomeric ratio was close to 1:1 without any significant deviations. On contrary, other aldehydes than acetaldehyde have shown higher diastereomeric selectivity, as represented in Figure 32.

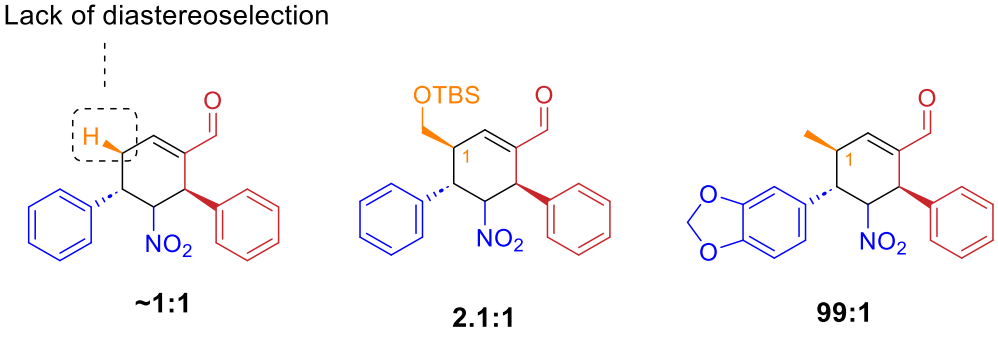

Figure 32 - Comparison of diastereoselection of other Enders' cascade products

Thus, it is straightforward to suppose that the C1 substituent contributes in some way to the diastereoselection of the whole process. The addition on nitro-enolates to unsaturated aldehyde via iminium ion catalysis was computationally studied by Moliner and co-workers[46], furnishing an interpretation model. It was calculated that the approach of the nitronate in the transition state, which determines the formation of the stereocenter, has always oxygen atoms of the nitro group oriented *toward* the organocatalyst residue (Figure 33), both in water and dichloromethane. This means that the *intrinsic* electronic structure of the transition state imposes that the aliphatic chain residue of the nitro-enolate is on the *opposite side* of the organocatalyst: with this geometry it is not easy to control which face of the nitro-enolate approaches the α,β-unsaturated iminium-ion intermediate, simply because there cannot be any strong secondary interaction such as dispersion forces, hydrogen bond or steric hindrance.[47–49] Thus, the sketched **TS1** and **TS2** are probably similar in terms of Gibbs energy. It is *intrinsically* very difficult to find a catalyst which can select one of the two geometries.

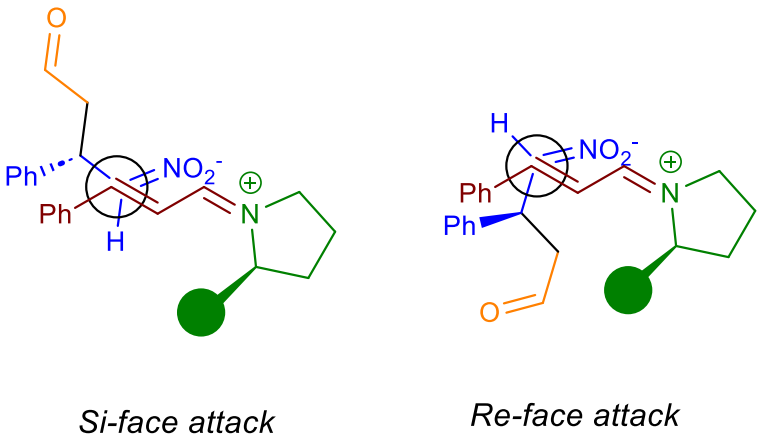

Figure 33 - Different approaches of the nitronate ion in the second reaction step

The scenario could change if a third component takes part to the transition state, coordinating in some way one or both the other molecules in order to control the facial selectivity of the nitro enolate during the reaction event. We evaluated that this approach was too difficult to be attempted.

Trying to enhance the diastereoselectivity of the reaction, we focused on the α-nitro group formation step. [31] If one wants to obtain a decent diastereoselectivity of this reaction, a way to control the organocatalyzed-Micheal-addition of the nitronate to the α,β-unsaturated iminium ion has to be found (Figure 34).

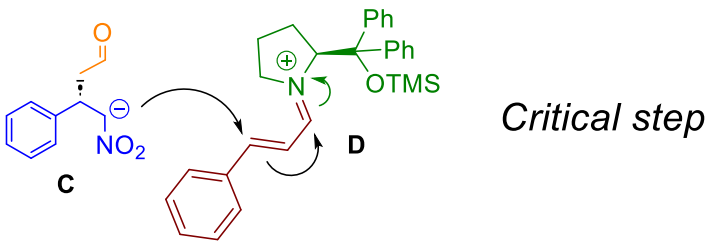

Figure 34 - Critical nitro-enolate Michael addition

We evaluated two different approaches to solve the problem: the first is to find a way to *discriminate* the two faces of the nitro-enolate during the attack to obtain the desired diastereoselectivity. Of course, this could be effective only if during the course of the reaction there are no (or negligible) epimerization phenomena. The second strategy exploits the latter point: if one of the two diastereoisomers is more *thermodynamically* stable than the other, an epimerization can be induced to shift the equilibrium, getting one major product.

First, the possible epimerization phenomena were investigated: the two diastereoisomers obtained in the model reaction were isolated and put in the reaction conditions, but nothing was observed (Figure 35).

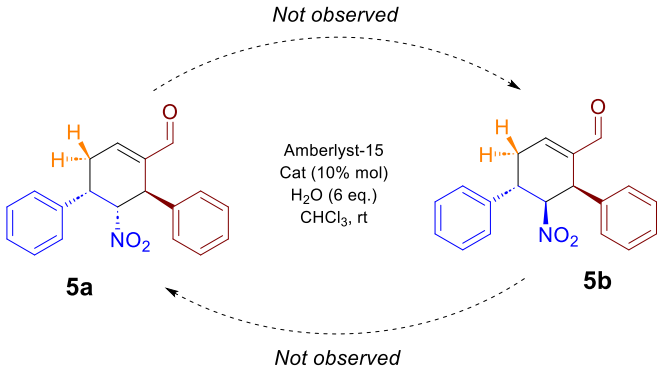

Figure 35 - Epimerization experiment

The epimerization process was further investigated using a strong basic environment, potassium tert-butoxide in methanol, to force the formation of the secondary nitronates (Figure 36). In this way, assuming that there is no kinetic preference during the re-protonation event, the mixture of diastereoisomers will reflect their relative Gibbs formation energy. After the base treatment, an epimerization process was observed on both the compounds with a final diastereomeric ratio of 1.4:1. Not very interesting from a synthetic point of view, and close to the already measured value.

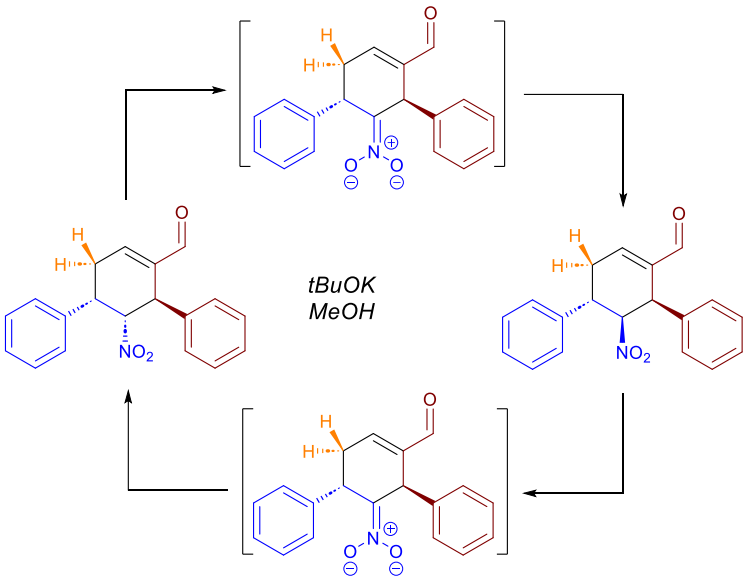

Figure 36 - Strong base-induced epimerization

With these results in our hands, it is now clear that the observed diastereomeric ratio is probably the *direct* result of the reaction with no post-process epimerization. And even if the epimerization is induced, there is no relevant improvement of the diastereomeric ratio, at least in the tested solvent. Thus, excluding low-temperature re-protonation for technical reasons, the only possible way is to obtain a good diastereomeric ratio is to *directly* improve the diastereoselectivity of the reaction between the transient species **C** and **D** (Figure 34). But as already stated above, all our efforts were fruitless.

It was observed that an improved diastereoselectivity was obtained using aliphatic aldehyde instead of acetaldehyde (Figure 32). It was not possible to rationalize this result, as to the best of our knowledge there are no advanced stereo-selection models available. So, in our hands it was not possible to significantly improve the diastereomeric ratio.

Conclusions

An unprecedented methodology for the synthesis of 4,6-disubstituted 5-nitrocyclohexene carbaldehydes with three contiguous chiral centers using acetaldehyde as one of the reaction components of an Enders' cascade reaction has been developed. The acetaldehyde is introduced in the system in the masked form of acetaldehyde dimethyl acetal, which is hydrolyzed in situ using Amberlyst-15 as acid catalyst. This makes this methodology safer, given the intrinsically danger in the handling of acetaldehyde. Using mild reaction conditions, we were able to obtain these functionalized cyclohexene carbaldehyde with a wide variety of substituents on the aromatic rings in good yield and with good enantiomeric

excess. Unfortunately, the developed methodology works only for aromatic substrates and the diastereomeric ratio between the obtained product was always around 1:1, regardless of our efforts. The main data obtained from this work have been published in the Beilstein Journal of Organic Chemistry.[50]

Supporting Information

It follows the experimental data for this project.

General information

Instrumentations

Nuclear magnetic resonance analyses (^{1}H-NMR spectra) were acquired using a Bruker Advance III 400 MHz spectrophotometer. Chemical shifts (δ) are reported in ppm relative to residual solvent signals for ^{1}H-NMR (^{1}H-NMR: 7.26 ppm for $CDCl_3$). Coupling constants are given in Hz. Due to the congestion in the products, in some cases additional peaks and line broadenings are observed due to rotameric species. ^{1}H-NMR yields were measured by analysing the reaction mixture using triphenylmethane as an internal standard. Chromatographic purifications of compound **5a**-**j** were performed using automated Biotage® Isolera LS Systems. HPLC analyses were acquired using an Agilent 1220 Infinity II liquid chromatographer equipped with Phenomenex columns Lux 3µm i-Cellulose 5, 100 X 4.6 mm. HPLC analysis was performed on the aldehyde products and it often revealed a set of two peaks for each enantiomer, probably due to the formation of emiacetal/acetal derivatives. Therefore, the evaluation of the enantiomeric excess was performed by integrating both peaks; the retention time was arbitrarily reported with respect to the first peak of the set for each compound. Reduction to the alcohol with $NaBH_4$ was attempted but it afforded a complex mixture of products, with probably also a likely epimerisation on the carbon α to the nitro group. Optical rotations were measured on a ZUZI 412 Digital Polarimeter (tube length: 100 mm). Exact masses were measured on hybrid quadrupole-TOF high resolution (HRMS) mass spectrometer (Xevo G2 QTOF, Waters, Manchester, UK) using a Z-spray-ESI interface operating in positive ionization mode with resolution of the TOF mass spectrometer about 20,000 at full width half maximum (FWHM).

Materials and Methods

Acetaldehyde dimethyl acetal (**6**), trans-β-nitrostyrene (**3a**), (*S*)/(*R*)-(–)-α,α-Diphenyl-2-pyrrolidinemethanol trimethylsilyl ether (**1**), Amberlyst-15 hydrogen form (Amberlyst-15), *trans*-cinnamaldehyde (**4a**) were purchased from Merck, aldehydes **4b**-**d** were purchased from Fluorochem and used as received unless otherwise stated. Silica Gel 60A (35-70 μ), HPLC solvents and analytical grade solvents were purchased from Merck. Nitroalkenes **3b**-**c** were prepared as previously reported.[1] All nitroalkenes and aldehydes used are shown below.

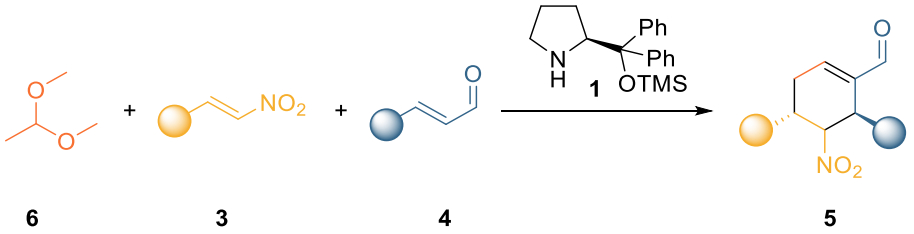

6 **3** **4** **5**

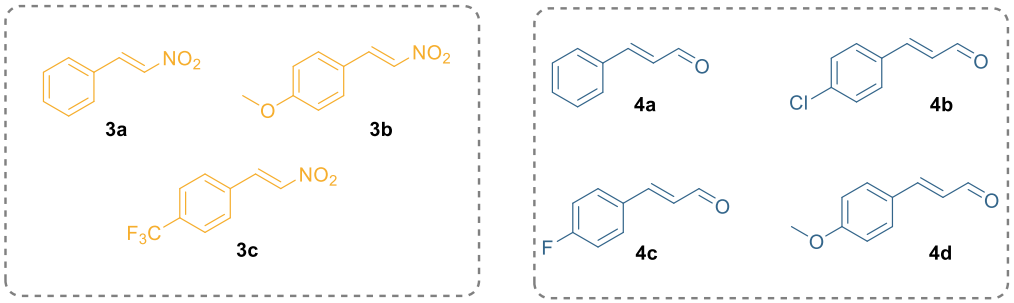

Experimental procedures

Optimisation reactions

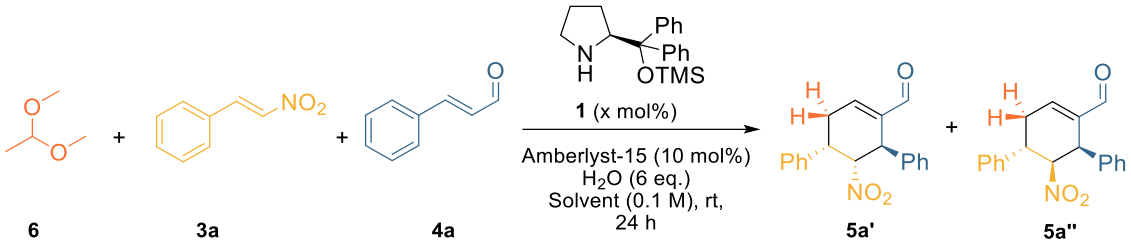

Table 5: Optimisation reactions

Entry	6 (eq.)	4a (eq.)	1 (eq.)	Solvent	Conversion (%)	Selectivity (%)	NMR Yield (%)	*dr* (5a' : 5a'')
1	1.2	1.5	0.1	Chloroform	53	62	33	58:42
2	2	1.05	0.1	Chloroform	54	79	43	52:48
3	2	1.05	0.2	Chloroform	45	44	20	60:40
4	2	1.05	0.1	Acetonitrile	43	12	5	50:50
5	2	1.05	0.1	Ethyl acetate	77	23	18	50:50
6	2	1.05	0.1	Tetrahydrofuran	79	37	29	44:56
7	2	1.05	0.1	Cyclohexane	58	43	25	44:56
8	**2**	**1.05**	**0.1**	**Toluene**	**61**	**66**	**40**	**50:50**
9 [a]	2	1.05	0.1	Toluene	62	37	23	44:56
10 [b]	2	1.05	0.1	Toluene	59	50	30	47:53
11	2	2.1	0.1	Toluene	70	48	33	44:56
12 [c]	2	1.05	0.1	Toluene	72	47	34	41:59
13 [d]	2	1.05	0.1	Toluene	58	45	26	37:63
14 [e]	2	1.05	0.1	Toluene	71	50	36	44:56
15 [f]	2	1.05	0.1	Toluene	75	48	36	44:56

[a] 20% Amberlyst-15; [b] 5% Amberlyst-15; [c] Reaction performed at 40 °C; [d] Reaction performed at 60 °C; [e] 10% Alumina added; [f] 10% Amberlite-45 IR added.

Entry 1, *2* and *3* demonstrated that **6** performs similarly to acetaldehyde in this reaction. As expected, all reactions gave high enantiomeric excesses since the process involves two consecutive enantioselective steps. Therefore, different solvents have been screened and toluene gave the best results in terms of selectivity and conversion (*entry 8*). Additionally, different acidic resins, temperatures, and additives were screened. Nevertheless, the best results were given by *entry 8* and a further concentration-time optimisation of these conditions has been carried out, as shown in Table 2.

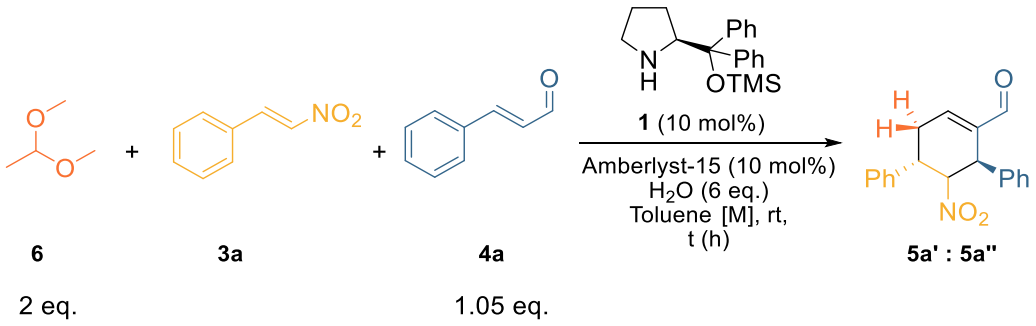

Table 6: Concentration-time optimisation

Entry	Concentration (M)	Time (h)	Conversion (%)	Selectivity (%)	NMR Yield (%)	*dr* (5a' : 5a'')
1	0.05	24	36	59	21	44:56
2	0.25	24	72	48	35	52:48
3	0.5	24	93	42	39	55:45
4	1	24	88	40	35	57:43
5	0.05	48	63	39	25	44:56
6[a]	**0.25**	**48**	**79**	**56**	**44**	**52:48**
7	0.5	48	77	48	37	55:45
8	1	48	93	44	41	55:45

[a] *Enantiomeric excess 99%, measured as the average of the two diastereomers*

Starting from the good outcomes obtained from entry 8 (Table 1), different concentrations and reaction times have been screened. *Entry 6* gave the best results in terms of yield and selectivity and these conditions were employed to perform the reaction scope.

General procedure

Acetaldehyde dimethyl acetal (**6**) (2 eq.) and a *trans*-cinnamaldehyde derivative (**4**) (0.525 mmol 1.05 eq.) were added to a 4 mL scintillation vial equipped with a magnetic bar containing a solution of (S)-diphenyltrimethylsiloxymethylpyrrolidine (**1**) (16.3 mg, 0.05 mmol, 0.1 eq.), nitroalkene (**3**) (0.5 mmol, 1 eq.), Amberlyst-15 (10.6 mg, 4.7 mmol/g, 0.1 eq), water (54 µL, 3 mmol, 6 eq.) and toluene (2 mL). The reaction mixture was left stirring at room temperature for 48h. Amberlyst-15 resin was filtered off using a cotton plug and the solvent was evaporated under reduced pressure. The crude was purified by flash chromatography on SiO_2 using a mixture of petroleum ether/ethyl acetate to yield the desired products. The absolute configuration of **5a** was assigned by comparison with the literature.[2] The absolute configuration of other products was assigned by analogy, considering a uniform mechanism of stereoinduction.

General procedure for racemic compound preparation

The racemic mixture used for the measurement of the enantiomeric excess were prepared “artificially”, setting-up a parallel reaction with the other enantiomer of the catalyst. The corresponding products were purified and used as they were for the HPLC analysis.

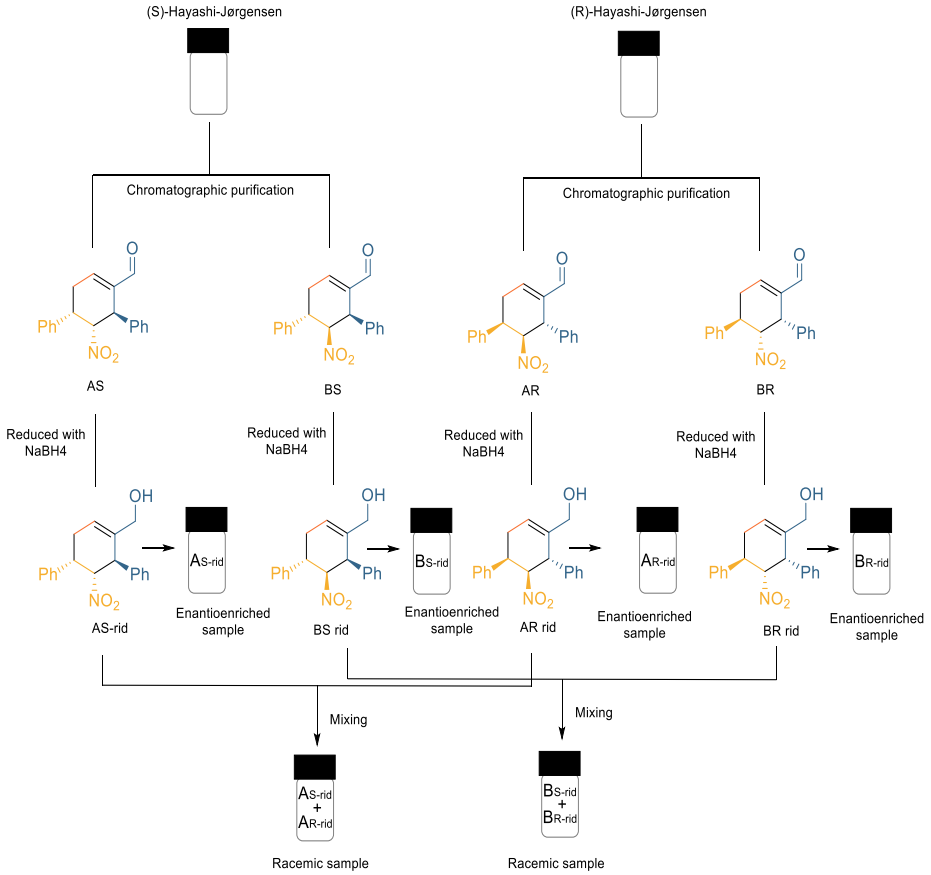

Scheme 1: Process to obtain the racemates avoiding the formation of undesired diastereomers.

This atypical preparation of the racemic samples was done to avoid the formation of undesired diastereomers using an equimolar mixture of both the enantiomers of the catalyst; being a multistep one-pot reaction it is not possible to guarantee that a chiral intermediate generated by one enantiomer of the catalyst will not do the second step using the other enantiomer of the catalyst.

(1'S,2'R,3'R)-2'-nitro-1',2',3',6'-tetrahydro-[1,1':3',1''-terphenyl]-4'-carbaldehyde **5a'**

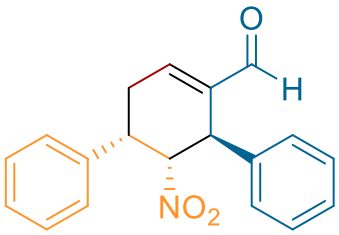

The desired product was obtained as an oil (24.3 mg, 0.0791 mmol, yield= 15.8%, ee >99%). 1H-NMR (400 MHz, CDCl3, 303 K) δ 9.53 (s, 1H), 7.35 – 7.11 (m, 10H), 5.33 – 5.26 (m, 1H), 4.73 (d, J = 4.8 Hz, 1H), 3.64 (m, 1H), 3.12 (m, 1H), 2.67 (m, 1H).. 13C NMR (101 MHz, CDCl3, 303 K) δ 190.7, 148.0, 140.1, 135.2, 129.0, 128.7, 128.6, 128.4, 127.7, 127.2, 89.2, 42.6, 37.8, 35.4, 29.7. HPLC (Lux 3µm i-Cellulose 5, 100 X 4.6 mm, Hexane/i-Propanol 80:20, flow: 0.5 mL/min, λ=210 nm), tminor: 17.8 min; tmajor: 24.2 min. [α]D25 = -111.6 (c = 1.9·10-3 g/mL, CHCl3). All analytical data were in agreement with reported data.[44]

(1'S,2'S,3'R)-2'-nitro-1',2',3',6'-tetrahydro-[1,1':3',1''-terphenyl]-4'-carbaldehyde **5a''**

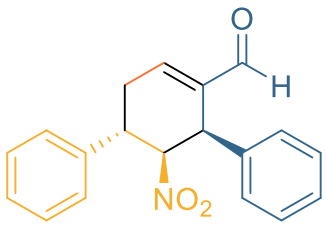

The desired product was obtained as an oil (42.1 mg, 0.137 mmol, yield = 27.4%, ee >99%). ^{1}H-NMR (400 MHz, $CDCl_3$, 303 K) δ 9.53 (s, 1H), 7.27 – 7.05 (m, 11H), 5.26 (dd, J = 12.5, 5.9 Hz, 1H), 4.71 (d, J = 5.6 Hz, 1H), 3.61 (td, J = 11.5, 6.8 Hz, 1H), 3.17 – 3.07 (m, 1H), 2.66 (dd, J = 20.7, 10.4 Hz, 1H). ^{13}C NMR (101 MHz, $CDCl_3$, 303 K) δ 190.8, 148.1, 140.2, 140.2, 135.3, 129.13, 128.8, 128.7, 128.6, 127.8, 127.3, 89.4, 42.8, 37.9, 35.5. HPLC (Lux 3µm i-Cellulose 5, 100 X 4.6 mm, Hexane/i-Propanol 80:20, flow: 0.5 mL/min, λ=210 nm), t_{minor}: 20.9 min; t_{major}: min. $[\alpha]_D^{25}$ = -124.0 (c = $3.4 \cdot 10^{-3}$ g/mL, $CHCl_3$).

(1'S,2'R,3'R)-4''-chloro-2'-nitro-1',2',3',6'-tetrahydro-[1,1':3',1''-terphenyl]-4'-carbaldehyde **5b'**

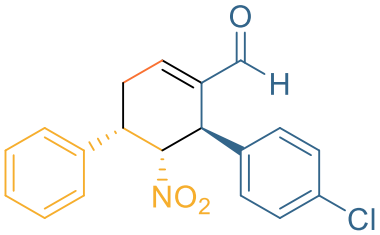

The desired product was obtained as an oil (43.2 mg, 0.126 mmol, yield = 25.3 %, ee >99%). ^{1}H NMR (400 MHz, $CDCl_3$, 303 K) δ 9.59 (s, 1H), 7.57 – 6.97 (m, 10H), 5.33 (m, 1H), 4.78 (m, 1H), 3.82 – 3.46 (m, 1H), 3.18 (m, 1H), 2.84 – 2.63 (m, 1H).. ^{13}C NMR (101 MHz, $CDCl_3$, 303 K) δ 190.7, 148.5, 147.6, 147.4, 140.2, 139.9, 139.8, 138.7, 135.1, 134.6, 133.9, 133.6, 129.9, 129.4, 129.3, 129.2, 129.1, 128.9, 128.8, 128.7, 128.7, 128.7, 128.6, 128.5, 127.9, 127.7, 127.3, 127.2, 89.2, 89.2, 77.2, 42.7, 42.3, 42.1, 37.9, 37.4, 35.4, 35.3, 35.1. HPLC (Lux 3µm i-Cellulose 5, 100 X 4.6 mm, Hexane/i-Propanol 80:20, flow: 0.5 mL/min, λ=210 nm), t_{minor}:

15.4 min; t_{major}: 22.2 min. $[\alpha]_D^{25}$ = -135.6 (c = $1.87 \cdot 10^{-3}$ g/mL, $CHCl_3$). ESI-MS: $C_{19}H_{16}ClNO_3Na$ [M+Na]+ calcd.: 364.0716, found: 364.0717.

(1'S,2'S,3'R)-4''-chloro-2'-nitro-1',2',3',6'-tetrahydro-[1,1':3',1''-terphenyl]-4'-carbaldehyde **5b''**

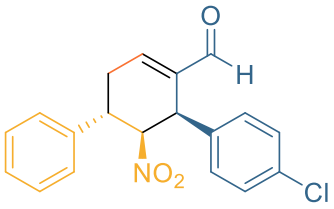

The desired product was obtained as an oil (66.7 mg, 0.195 mmol, yield = 39%, ee= 98%). ^{1}H-NMR (400 MHz, $CDCl_3$, 303 K) δ 9.52 (s, 1H), 7.24 (m, 8H), 7.05 – 6.97 (m, 1H), 6.94 (d, J = 8.6 Hz, 1H), 4.87 (m, 1H), 4.47 (d, J = 22.4 Hz, 1H), 3.37 – 3.09 (m, 2H), 2.92 – 2.77 (m, 1H).. ^{13}C NMR (101 MHz, $CDCl_3$, 303 K) δ 207.1, 191.6, 150.7, 150.3, 149.9, 138.8, 138.2, 138.0, 137.8, 137.5, 136.6, 134.1, 134.0, 129.5, 129.5, 129.4, 129.2, 129.2, 129.1, 128.9, 128.8, 128.2, 128.2, 128.1, 127.9, 127.4, 127.4, 91.1, 91.1, 43.2, 42.5, 40.0, 38.0, 37.5, 36.8, 28.0, 27.9. HPLC (Lux 3µm i-Cellulose 5, 100 X 4.6 mm, Hexane/i-Propanol 80:20, flow: 0.5 mL/min, λ=210 nm), t_{minor}: 56.8min; t_{major}: 26.8 min. $[\alpha]_D^{25}$ = -194.8 (c = $0.87 \cdot 10^{-3}$ g/mL, $CHCl_3$). ESI-MS: $C_{19}H_{16}ClNO_3Na$ [M+Na]+ calcd.: 364.0716, found: 364.0775.

(1'S,2'R,3'R)-4''-fluoro-2'-nitro-1',2',3',6'-tetrahydro-[1,1':3',1''-terphenyl]-4'-carbaldehyde **5c'**

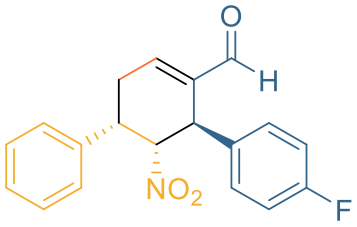

The desired product was obtained as an oil (31.4 mg, 0.0965 mmol, yield = 19.3%, ee >99%). ^{1}H NMR (400 MHz, $CDCl_3$, 303 K) δ 9.57 (s, 1H), 7.39 – 7.05 (m, 10H), 5.42 – 5.22 (m, 1H), 4.77 (m, 1H), 3.75 – 3.53 (m, 1H), 3.16 (dt, J = 10.8, 5.0 Hz, 1H), 2.81 – 2.54 (m, 1H).. ^{13}C NMR (101 MHz, $CDCl_3$, 303 K) δ 190.8, 164.1, 163.4, 161.6, 160.9, 148.3, 147.8, 140.1, 139.9, 135.8, 135.2, 131.2, 130.3, 130.2, 129.1, 129.0, 128.9, 128.8, 128.7, 128.6, 127.8, 127.3, 116.1, 115.9, 115.7, 89.5, 89.2, 42.7, 41.9, 37.8, 37.2, 35.4, 30.9, 29.8. HPLC (Lux 3µm i-Cellulose 5, 100 X 4.6 mm, Hexane/i-Propanol 80:20, flow: 0.5 mL/min, λ=210 nm), t_{minor}: 14.4 min; t_{major}: 19.3 min. $[\alpha]_D^{25}$ = -113.2 (c = $2.2 \cdot 10^{-3}$ g/mL, $CHCl_3$). ESI-MS: $C_{19}H_{16}FNO_3Na$ [M+Na]+ calcd.: 348.1012, found: 348.1056.

(1'S,2'S,3'R)-4''-fluoro-2'-nitro-1',2',3',6'-tetrahydro-[1,1':3',1''-terphenyl]-4'-carbaldehyde **5c''**

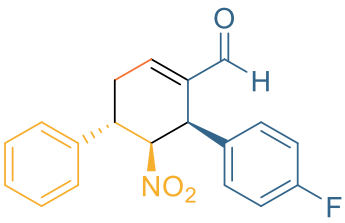

The desired product was obtained as an oil (34.8 mg, 0.107 mmol, yield = 21.4 %, ee= 96%). ^{1}H NMR (400 MHz, $CDCl_3$, 303 K) δ 9.59 (s, 1H), 7.49 – 6.77 (m, 10H), 4.92 (s, 1H), 4.53 (d, J = 11.6 Hz, 1H), 3.79 (m, 1H), 3.29 (m, 1H), 2.89 (m, 1H).. ^{13}C NMR (101 MHz, $CDCl_3$, 303 K) δ 191.7, 163.7, 163.7, 161.3, 161.2, 150.5, 149.9, 138.9, 138.34, 137.9, 134.8, 134.8, 133.9, 133.8, 129.8, 129.7, 129.4, 129.1, 129.1, 128.2, 128.2, 128.1, 127.4, 116.4, 116.2, 116.1, 115.9, 91.4, 91.3, 91.3, 43.2, 42.5, 38.3, 37.4, 36.8, 31.4, 29.8, 28.2, 28.1. HPLC (Lux 3µm i-Cellulose 5, 100 X 4.6 mm, Hexane/i-Propanol 80:20, flow: 0.5 mL/min, λ=210 nm), t_{minor}: 28,6 min; t_{major}: 46,6 min. $[\alpha]_D^{25}$ = -193.5 (c = $3.7 \cdot 10^{-3}$ g/mL, $CHCl_3$). ESI-MS: $C_{19}H_{16}FNO_3Na$ [M+Na]+ calcd.: 348.1012, found: 348.1012.

(1'S,2'R,3'R)-4''-methoxy-2'-nitro-1',2',3',6'-tetrahydro-[1,1':3',1''-terphenyl]-4'-carbaldehyde **5d'**

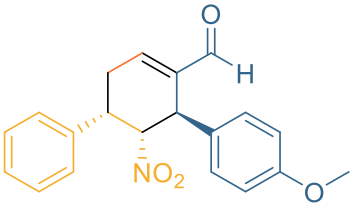

The desired product was obtained as an oil (58.5 mg, 0.173 mmol, yield = 34.7%, ee= 99%). ^{1}H NMR (400 MHz, $CDCl_3$, 303 K) δ 9.56 (s, 1H), 7.39 – 7.19 (m, 5H), 7.14 (d, J = 8.8 Hz, 1H), 7.07 – 7.02 (m, 1H), 6.95 (d, J = 8.8 Hz, 1H), 6.89 (d, J = 8.8 Hz, 1H), 6.80 (d, J = 8.8 Hz, 1H), 4.92 (m, 1H), 4.49 (d, J = 9.2 Hz, 1H), 3.77 (two s, rotamers, 3H), 3.42 – 3.31 (m, 1H), 3.30 – 3.14 (m, 1H), 2.94 – 2.81 (m, 1H).. ^{13}C NMR (101 MHz, $CDCl_3$, 303 K) δ 198.9, 191.8, 191.8, 191.7, 159.4, 159.3, 150.5, 150.2, 139.0, 138.4, 138.3, 138.2, 138.2, 130.9, 129.9, 129.3, 129.3, 129.2, 129.0, 128.5, 128.2, 128.1, 128.1, 127.5, 127.4, 114.7, 114.4, 91.6, 91.5, 79.5, 55.4, 55.4, 53.5, 46.5, 43.2, 42.5, 38.1, 37.3, 36.7, 29.8, 28.3, 27.9. HPLC (Lux 3µm i-Cellulose 5, 100 X 4.6 mm, Hexane/i-Propanol 80:20, flow: 0.5 mL/min, λ=210 nm), t_{minor}: 24.9 min; t_{major}: 31.4 min. $[\alpha]_D^{25}$ = -109.2 (c = $3.5 \cdot 10^{-3}$ g/mL, $CHCl_3$). ESI-MS: $C_{20}H_{19}NO_4Na$ [M+Na]+ calcd.: 360.1212, found: 360.1212.

(1'R,2'R,3'S)-4''-methoxy-2'-nitro-1',2',3',6'-tetrahydro-[1,1':3',1''-terphenyl]-4'-carbaldehyde **5d''**

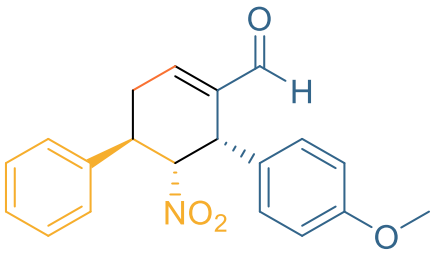

The desired product was obtained, using (R)-(**1**), as an oil (21 mg, 0.0622 mmol, yield = 12.4%, ee= >99% (R)-(**1**)). ^{1}H NMR (400 MHz, $CDCl_3$, 303 K) δ 9.50 (s, 1H), 7.29 (m, 3H), 7.25 – 7.16 (m, 2H), 7.13 – 6.99 (m, 4H), 6.82 (m, 1H), 5.27 – 5.16 (m, 1H), 4.67 (m, 1H), 3.76 (two s, rotamers, 3H), 3.57 (m, 1H), 3.08 (m, 1H), 2.63 (m, 1H).. ^{13}C NMR (101 MHz, $CDCl_3$, 303 K) δ 190.9, 190.9, 159.8, 159.1, 148.3, 147.8, 140.4, 140.3, 140.2, 135.4, 131.9, 129.8, 129.1, 128.8, 128.7, 128.5, 128.4, 127.7, 127.3, 127.2, 114.7, 114.5, 114.3, 89.7, 89.4, 55.5, 55.4, 55.3, 42.8, 42.1, 37.9, 37.1, 35.5, 35.5. HPLC (Lux 3μm i-Cellulose 5, 100 X 4.6 mm, Hexane/i-Propanol 80:20, flow: 0.5 mL/min, λ=210 nm), t_{minor}: 66.5 min; t_{major}: 65.1 min. $[\alpha]_D^{25}$ = +304.3 (c = $1.7 \cdot 10^{-3}$ g/mL, $CHCl_3$). ESI-MS: $C_{20}H_{19}NO_4Na$ [M+Na]+ calcd.: 360.1212, found: 360.1207.

(1'S,2'R,3'R)-4-methoxy-2'-nitro-1',2',3',6'-tetrahydro-[1,1':3',1''-terphenyl]-4'-carbaldehyde **5e'**

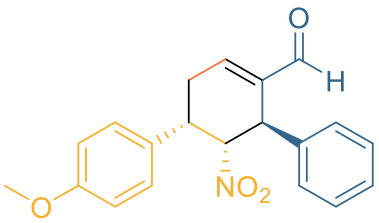

The desired product was obtained as an oil (24 mg, 0.0711 mmol, yield = 14.2%, ee >99%). ^{1}H NMR (400 MHz, $CDCl_3$, 303 K) δ 9.51 (s, 1H), 7.39 – 6.66 (m, 10H), 4.86 (m, 1H), 4.43 (d, J = 9.3 Hz, 1H), 3.72 (two s, rotamers, 3H), 3.36 – 3.07 (m, 2H), 2.82 (m, 1H).. ^{13}C NMR (101 MHz, $CDCl_3$, 303 K) δ 191.8, 191.8, 159.4, 159.4, 150.5, 150.2, 139.0, 138.5, 138.3, 138.2, 130.9, 129.9, 129.3, 129.2, 129.1, 128.5, 128.5, 128.1, 128.1, 127.4, 114.7, 114.4, 91.6, 91.5, 55.4, 55.4, 55.4, 43.2, 42.6, 37.3, 37.3, 36.7, 28.3, 27.9. HPLC (Lux 3μm i-Cellulose 5, 100 X 4.6 mm, Hexane/i-Propanol 80:20, flow: 0.5 mL/min, λ=210 nm), t_{minor}: 24.4 min; t_{major}: 30.9 min. $[\alpha]_D^{25}$ = -165.7 (c = $1.33 \cdot 10^{-3}$ g/mL, $CHCl_3$). ESI-MS: $C_{20}H_{19}NO_4Na$ [M+Na]+ calcd.: 360.1212, found: 360.1213.

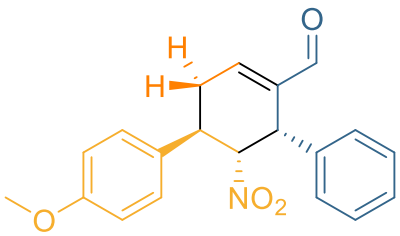

(1'R,2'R,3'S)-4-methoxy-2'-nitro-1',2',3',6'-tetrahydro-[1,1':3',1''-terphenyl]-4'-carbaldehyde ***5e''***The desired product was obtained, using (*R*)-(**1**), as an oil (17.5 mg, 0.0519 mmol, yield = 10.4%, ee >99%, (*R*)-(**1**)). ^{1}H NMR (400 MHz, $CDCl_3$, 303 K) δ 9.57 (s, 1H), 7.50 – 6.80 (m, 10H), 5.38 – 5.20 (m, 1H), 4.75 (d, J = 5.9 Hz, 1H), 3.83 (two s, rotamers, 3H), 3.68 – 3.51 (m, 1H), 3.15 (m, 1H), 2.78 – 2.60 (m, 1H).. ^{13}C NMR (101 MHz, $CDCl_3$, 303 K) δ 190.9, 190.9, 159.8, 159.1, 148.3, 148.3, 147.8, 140.2, 135.4, 131.9, 129.8, 129.1, 128.8, 128.7, 128.5, 128.4, 127.7, 127.3, 114.5, 114.3, 114.3, 89.7, 89.4, 55.4, 55.3, 42.8, 42.1,

37.9, 37.1, 35.5. HPLC (Lux 3µm i-Cellulose 5, 100 X 4.6 mm, Hexane/i-Propanol 80:20, flow: 0.5 mL/min, λ=210 nm), t_{minor}: 46.2 min; t_{major}: 36.5 min. $[\alpha]_D^{25}$ = +195.6 (c = $0.57 \cdot 10^{-3}$ g/mL, $CHCl_3$). ESI-MS: $C_{20}H_{19}NO_4Na$ [M+Na]+ calcd.: 360.1212, found: 360.1319.

(1'R,2'S,3'S)-2'-nitro-4-(trifluoromethyl)-1',2',3',6'-tetrahydro-[1,1':3',1''-terphenyl]-4'-carbaldehyde **5f'**

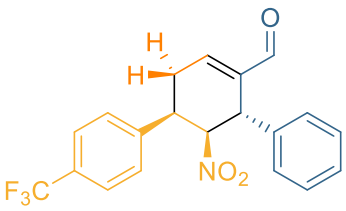

The desired product was obtained, using (R)-(**1**), as an oil (42.7 mg, 0.114 mmol, yield = 22.8%, ee >99%, (R)-(**1**)). ^{1}H NMR (400 MHz, $CDCl_3$, 303 K) δ 9.60 (s, 1H), 7.65 (d, J = 8.4 Hz, 1H), 7.55 (d, J = 8.4 Hz, 1H), 7.44 – 7.28 (m, 5H), 7.25 – 7.16 (m, 2H), 7.10 – 7.02 (m, 1H), 4.96 (m, 1H), 4.59 (m, 1H), 3.52 – 3.20 (m, 2H), 3.01 – 2.86 (m, 1H). . ^{13}C NMR (101 MHz, $CDCl_3$, 303 K) δ 191.6, 151.0, 149.5, 143.0, 138.7, 138.3, 137.9, 137.6, 129.5, 129.2, 128.6, 128.4, 128.3, 128.1, 127.9, 127.4, 126.5, 126.4, 126.4, 126.3, 126.1, 126.0, 90.9, 43.3, 42.9, 37.7, 37.2, 29.8, 28.1, 27.8. HPLC (Lux 3µm i-Cellulose 5, 100 X 4.6 mm, Hexane/i-Propanol 80:20, flow: 0.5 mL/min, λ=210 nm), t_{minor}: 21.7 min; t_{major}: 10.4 min. $[\alpha]_D^{25}$ = +92.4 (c = $2.95 \cdot 10^{-3}$ g/mL, $CHCl_3$). ESI-MS: $C_{20}H_{16}F_3NO_3Na$ [M+Na]+ calcd.: 398.0980, found: 398.1027.

(1'S,2'S,3'R)-2'-nitro-4-(trifluoromethyl)-1',2',3',6'-tetrahydro-[1,1':3',1''-terphenyl]-4'-carbaldehyde **5f''**

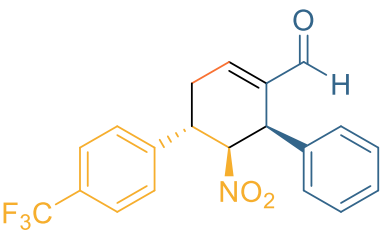

The desired product was obtained as an oil (34.1 mg, 0.0908 mmol, yield = 18.2%, ee= 97%; please note that at the λ= 254nm ratio signal/noise is too low and only λ= 210 nm has been used to calculate ee). ^{1}H NMR (400 MHz, $CDCl_3$, 303 K) δ 9.60 (s, 1H), 7.65 (d, J = 8.3 Hz, 2H), 7.55 (d, J = 8.6 Hz, 1H), 7.30 (m, 6H), 7.09 – 7.02 (m, 1H), 4.94 (m, 1H), 4.57 (m, 1H), 3.40 – 3.22 (m, 2H), 2.96 (m, 1H).. ^{13}C NMR (101 MHz, $CDCl_3$, 303 K) δ 191.5, 150.9, 143.0, 137.9, 137.6, 129.5, 129.2, 128.6, 128.4, 127.4, 126.4, 90.9, 42.9, 37.7, 29.9, 28.1. HPLC (Lux 3µm i-Cellulose 5, 100 X 4.6 mm, Hexane/i-Propanol 80:20, flow: 0.5 mL/min, λ=210 nm), t_{minor}: 18.2 min; t_{major}: 21.0 min. $[\alpha]_D^{25}$ = -160.4 (c = $5.95 \cdot 10^{-3}$ g/mL, $CHCl_3$). ESI-MS: $C_{20}H_{16}F_3NO_3Na$ [M+Na]+ calcd.: 398.0980, found: 398.0980.

(1'S,2'R,3'R)-4''-fluoro-4-methoxy-2'-nitro-1',2',3',6'-tetrahydro-[1,1':3',1''-terphenyl]-4'-carbaldehyde **5g'**

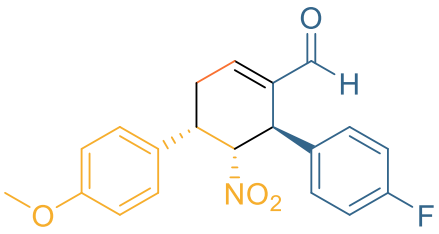

The desired product was obtained as an oil (18.9 mg, 0.0532 mmol, yield = 10.6%, ee >99%). ^{1}H NMR (400 MHz, $CDCl_3$, 303 K) δ 9.50 (s, 1H), 7.12 – 6.93 (m, 7H), 6.83 (m, 2H), 5.17 (m, 1H), 4.66 (d, J = 7.2 Hz, 1H), 3.76 (two s, rotamers, 3H), 3.63 – 3.44 (m, 1H), 3.14 – 2.99 (m, 1H), 2.70 – 2.57 (m, 1H).. ^{13}C NMR (101 MHz, $CDCl_3$, 303 K) δ 190.8, 190.8, 164.1, 163.4, 161.7, 159.8, 159.2, 148.4, 147.4, 140.4, 140.1, 131.7, 131.3, 131.3, 130.3, 130.3, 129.8, 129.0, 128.9, 128.4, 116.1, 115.9, 115.9, 115.7, 115.5, 114.6, 114.3, 114.3, 89.6, 89.5, 55.4, 55.3, 42.1, 42.0, 37.3, 37.1, 35.4. HPLC (Lux 3µm i-Cellulose 5, 100 X 4.6 mm, Hexane/i-Propanol 80:20, flow: 0.5 mL/min, λ=210 nm), t_{minor}: 19.8 min; t_{major}: 28.9 min. $[\alpha]_D^{25}$ = -99.5 (c = $2.95 \cdot 10^{-3}$ g/mL, $CHCl_3$). ESI-MS: $C_{20}H_{18}FNO_4Na$ [M+Na]+ calcd.: 378.1118, found: 378.1118.

(1'S,2'S,3'R)-4''-fluoro-4-methoxy-2'-nitro-1',2',3',6'-tetrahydro-[1,1':3',1''-terphenyl]-4'-carbaldehyde **5g''**

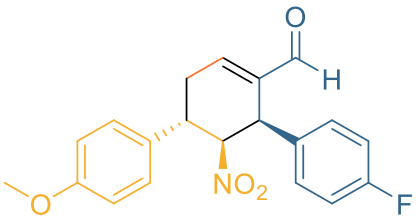

The desired product was obtained as an oil (27 mg, 0.076 mmol, yield = 15.2%, ee >99%). ^{1}H NMR (400 MHz, $CDCl_3$, 303 K) δ 9.57 (s, 1H), 7.42 – 6.73 (m, 9H), 4.97 – 4.78 (m, 1H), 4.48 (s, 1H), 3.79 (two s, rotamers, 3H), 3.37 – 3.28 (m, 1H), 3.27 – 3.15 (m, 1H), 2.88 (m, 1H).. ^{13}C NMR (101 MHz, $CDCl_3$, 303 K) δ 191.7, 163.7, 161.2, 159.5, 150.7, 149.7, 138.5, 138.3, 134.9, 134.8, 130.8, 129.8, 129.8, 129.2, 129.1, 128.5, 128.4, 116.4, 116.2, 116.1, 115.9, 114.8, 114.6, 114.5, 91.5, 91.5, 55.5, 55.4, 42.5, 42.4, 36.8, 36.7, 28.4, 28.2. HPLC (Lux 3µm i-Cellulose 5, 100 X 4.6 mm, Hexane/i-Propanol 80:20, flow: 0.5 mL/min, λ=210 nm), t_{minor}: 28.2 min; t_{major}: 29.4 min. $[\alpha]_D^{25}$ = -150.9 (c = $1.88 \cdot 10^{-3}$ g/mL, $CHCl_3$). ESI-MS: $C_{20}H_{18}FNO_4Na$ [M+Na]+ calcd.: 378.1118, found: 378.1131.

(1'R,2'S,3'S)-4,4''-dimethoxy-2'-nitro-1',2',3',6'-tetrahydro-[1,1':3',1''-terphenyl]-4'-carbaldehyde **5h'**

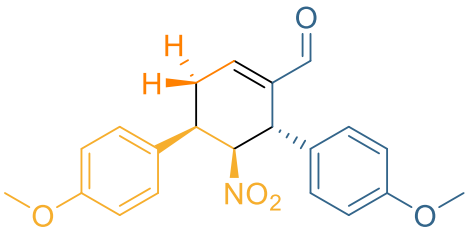

The desired product was obtained, using (R)-(**1**), as an oil (39.9 mg, 0.109 mmol, yield = 21.7%, ee >99%, (R)-(**1**)). ^{1}H NMR (400 MHz, $CDCl_3$, 303 K) δ 9.56 (s, 1H), 7.14 (d, J = 8.7 Hz, 3H), 6.98 (d, J = 8.8 Hz, 2H), 6.89 (d, J = 8.8 Hz, 2H), 6.82 (d, J = 12.0 Hz, 2H), 4.89 (s, 1H), 4.46 (s, 1H), 3.78 (d, J = 16.3 Hz, 7H), 3.41 – 3.29 (m, 1H), 3.19 (dd, J = 20.2, 11.1 Hz, 1H), 2.92 – 2.73 (m, 1H).. ^{13}C NMR (101 MHz, $CDCl_3$, 303 K) δ 199.1, 191.9, 159.4, 159.3, 159.3, 150.3, 138.4, 132.1, 130.9, 130.1, 130.1, 129.7, 129.2, 128.6, 128.5, 127.9, 114.7, 114.5, 114.4, 114.2, 91.7, 79.8, 60.5, 55.4, 55.4, 55.3, 55.3, 46.6, 42.5, 37.5, 36.6, 29.8, 28.3, 14.3. HPLC (Lux 3µm i-Cellulose 5, 100 X 4.6 mm, Hexane/i-Propanol 80:20, flow: 0.5 mL/min, λ=210 nm), t_{minor}: 58.0 min; t_{major}: 43.6 min. $[\alpha]_D^{25}$ = +188.8 (c = $2.31 \cdot 10^{-3}$ g/mL, $CHCl_3$). ESI-MS: $C_{21}H_{21}NO_5Na$ [M+Na]+ calcd.: 390.1317, found: 390.1334.

(1'R,2'R,3'S)-4,4''-dimethoxy-2'-nitro-1',2',3',6'-tetrahydro-[1,1':3',1''-terphenyl]-4'-carbaldehyde **5h''**

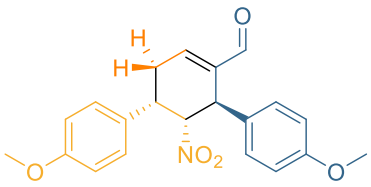

The desired product was obtained, using (R)-(**1**), as an oil (45.5 mg, 0.124 mmol, yield = 24.8%, ee >99%, (R)-(**1**)). ^{1}H NMR (400 MHz, $CDCl_3$, 303 K) δ 9.48 (s, 1H), 7.10 (d, J = 8.8 Hz, 2H), 7.01 (d, J = 8.8 Hz, 2H), 6.82 (m, 5H), 5.16 (dd, J = 12.3, 5.7 Hz, 1H), 4.63 (d, J = 4.9 Hz, 1H), 3.75 (two s, 6H), 3.58 – 3.44 (m, 1H), 3.10 – 2.98 (m, 1H), 2.59 (m, 1H).. ^{13}C NMR (101 MHz, $CDCl_3$, 303 K) δ 190.9, 190.6, 159.7, 159.1, 147.9, 140.3, 132.1, 129.7, 128.4, 127.3, 114.7, 114.5, 114.4, 114.2, 114.1, 89.7, 55.3, 55.3, 42.1, 37.1, 35.5, 29.8. HPLC (Lux 3µm i-Cellulose 5, 100 X 4.6 mm, Hexane/i-Propanol 80:20, flow: 0.5 mL/min, λ=210 nm), t_{minor}: 59.9 min; t_{major}: 47.4 min. $[\alpha]_D^{25}$ = +221.5 (c = $3.96 \cdot 10^{-3}$ g/mL, $CHCl_3$). ESI-MS: $C_{21}H_{21}NO_5Na$ [M+Na]+ calcd.: 390.1317, found: 390.1314.

(1'R,2'S,3'S)-4''-fluoro-2'-nitro-4-(trifluoromethyl)-1',2',3',6'-tetrahydro-[1,1':3',1''-terphenyl]-4'-carbaldehyde **5i'**

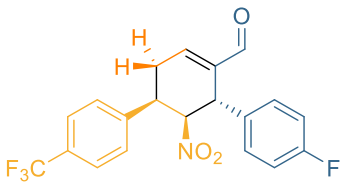

The desired product was obtained, using (R)-(**1**), as an oil (45.2 mg, 0.115 mmol, yield = 23%, ee= 99%, (R)-(**1**)). ^{1}H-NMR (400 MHz, $CDCl_3$, 303 K) δ 9.58 (s, 1H), 7.65 (d, J = 7.9 Hz, 1H), 7.57 (d, J = 8.0 Hz, 1H), 7.44 – 7.33 (m, 2H), 7.21 (m, 2H), 7.13 – 6.95 (m,

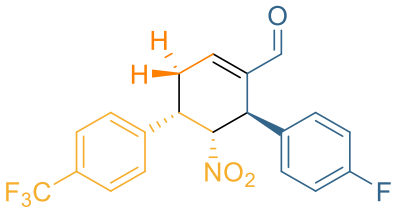

3H). 4.92 (d, J = 9.1 Hz, 1H), 4.57 (s, 1H), 3.47 – 3.33 (m, 1H), 3.32 – 3.19 (m, 1H), 2.95 (dt, J = 20.1, 5.2 Hz, 1H). ^{13}C NMR (101 MHz, $CDCl_3$, 303 K) δ 190.5, 148.3, 147.3, 140.3, 139.8, 139.4, 135.3, 130.8, 130.4, 130.3, 129.1, 129.0, 128.9, 128.1, 127.8, 126.2, 125.9, 125.9, 116.4, 116.2, 116.1, 115.9, 89.3, 88.9, 42.4, 41.9, 37.9, 37.4, 35.4, 35.1, 32.1, 29.9, 14.3. HPLC (Lux 3µm i-Cellulose 5, 100 X 4.6 mm, Hexane/i-Propanol 80:20, flow: 0.5 mL/min, λ=210 nm), t_{minor}: 14.4 min; t_{major}: 10.3 min. $[\alpha]_D^{25}$ = +67.2 (c = $4.1 \cdot 10^{-3}$ g/mL, $CHCl_3$. ESI-MS: $C_{20}H_{15}F_4NO_3Na$ [M+Na]+ calcd.: 416.0886, found: 416.0940.

(1'R,2'R,3'S)-4''-fluoro-2'-nitro-4-(trifluoromethyl)-1',2',3',6'-tetrahydro-[1,1':3',1''-terphenyl]-4'-carbaldehyde **5i''**

The desired product was obtained, using (*R*)-(**1**), as an oil (48.3 mg, 0.123 mmol, yield = 24.6%, ee> 99%, (*R*)-(**1**)). ^{1}H NMR (400 MHz, $CDCl_3$, 303 K) δ 9.59 (s, 1H), 7.65 (d, J = 8.3 Hz, 1H), 7.57 (d, J = 8.3 Hz, 1H), 7.43 – 7.33 (m, 2H), 7.25 – 7.17 (m, 2H), 7.12 – 6.97 (m, 3H), 4.91 (m, 1H), 4.56 (s, 1H), 3.52 – 3.17 (m, 2H), 2.94 (dt, J = 20.2, 5.5 Hz, 1H).. ^{13}C NMR (101 MHz, $CDCl_3$, 303 K) δ 191.4, 150.6, 149.6, 141.9, 138.3, 137.9, 134.5, 129.8, 129.7, 129.2, 129.1, 128.6, 127.9, 126.4, 126.1, 126.1, 116.6, 116.4, 116.3, 116.1, 90.9, 90.8, 42.9, 42.5, 37.2, 37.1, 29.9, 28.3, 27.8. HPLC (Lux 3µm i-Cellulose 5, 100 X 4.6 mm, Hexane/i-Propanol 80:20, flow: 0.5 mL/min, λ=210 nm), t_{minor}: 15.1 min; t_{major}: 7.9 min. $[\alpha]_D^{25}$ = -104.8 (c = $4.4 \cdot 10^{-3}$ g/mL, $CHCl_3$). ESI-MS: $C_{20}H_{15}F_4NO_3Na$ [M+Na]+ calcd.: 416.0886, found: 416.0886.

(1'R,2'S,3'S)-4''-methoxy-2'-nitro-4-(trifluoromethyl)-1',2',3',6'-tetrahydro-[1,1':3',1''-terphenyl]-4'-carbaldehyde **5j'**

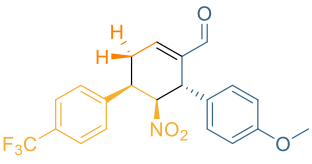

The desired product was obtained, using (R)-(**1**), as an oil (53.4 mg, 0.132 mmol, yield = 26.3%, ee= 99%, (R)-(**1**)). ^{1}H NMR (400 MHz, $CDCl_3$, 303 K) δ 9.59 (s, 1H), 7.64 (d, J = 8.3 Hz, 1H), 7.56 (d, J = 8.4 Hz, 1H), 7.46 – 7.30 (m, 3H), 7.18 (m, 1H), 6.97 (d, J = 8.8 Hz, 1H), 6.91 (d, J = 8.8 Hz, 1H), 6.82 (d, J = 8.8 Hz, 1H), 4.96 – 4.86 (m, 1H), 4.54 (s, 1H), 3.79 (two s, rotamers, 3H), 3.38 – 3.17 (m, 2H), 3.00 – 2.83 (m, 1H).. ^{13}C NMR (101 MHz, $CDCl_3$, 303 K) δ 191.6, 159.6, 151.1, 149.2, 143.11, 137.9, 129.4, 129.2, 128.6, 128.5, 127.9, 126.4, 126.3, 126.1, 114.9, 114.6, 91.1, 55.5, 55.4, 42.9, 42.6, 37.1, 29.9, 28.5, 27.8. HPLC (Lux 3µm i-Cellulose 5, 100 X 4.6 mm, Hexane/i-Propanol 80:20, flow: 0.5 mL/min, λ=210 nm),

t_{minor}: 25.4 min; t_{major}: min. $[\alpha]_D^{25}$ = +692.3 (c = $1.45 \cdot 10^{-3}$ g/mL, $CHCl_3$). ESI-MS: $C_{21}H_{18}F_3NO_4Na$ [M+Na]+ calcd.: 428.1086, found: 428.1086.

(1'R,2'R,3'S)-4''-methoxy-2'-nitro-4-(trifluoromethyl)-1',2',3',6'-tetrahydro-[1,1':3',1''-terphenyl]-4'-carbaldehyde **5j''**

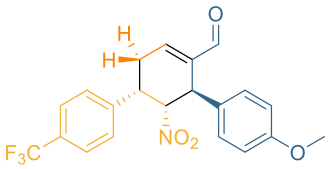

The desired product was obtained, using (R)-(**1**), as an oil (37.0 mg, 0.0913 mmol, yield = 18.3%, ee= 96%, (R)-(**1**)). ^{1}H NMR (400 MHz, $CDCl_3$, 303 K) δ 9.59 (s, 1H), 7.64 (d, J = 8.1 Hz, 1H), 7.56 (d, J = 8.2 Hz, 1H), 7.43 – 7.34 (m, 2H), 7.17 (m, 1H), 6.97 (d, J = 8.8 Hz, 1H), 6.91 (d, J = 8.8 Hz, 1H), 6.82 (d, J = 8.8 Hz, 2H), 4.95 – 4.86 (m, 1H), 4.54 (s, 1H), 3.79 (two s, rotamers, 3H), 3.37 – 3.17 (m, 2H), 2.92 (m, 1H).. ^{13}C NMR (101 MHz, $CDCl_3$, 303 K) δ 191.4, 163.8, 161.4, 150.5, 149.6, 141.9, 138.3, 137.9, 134.5, 130.8, 129.8, 129.7, 129.2, 129.1, 128.6, 127.9, 126.5, 126.4, 126.1, 126.1, 126.1, 116.6, 116.4, 116.3, 116.1, 90.9, 90.8, 42.9, 42.5, 37.3, 37.1, 29.9, 28.3, 27.8. HPLC (Lux 3µm i-Cellulose 5, 100 X 4.6 mm, Hexane/i-Propanol 80:20, flow: 0.5 mL/min, λ=210 nm), t_{minor}: 18.1 min; t_{major}: 14.5 min. $[\alpha]_D^{25}$ = +750.34 (c = $1.3 \cdot 10^{-3}$ g/mL, $CHCl_3$). ESI-MS: $C_{21}H_{18}F_3NO_4Na$ [M+Na]+ calcd.: 428.1086, found: 428.1075.

NMR spectra

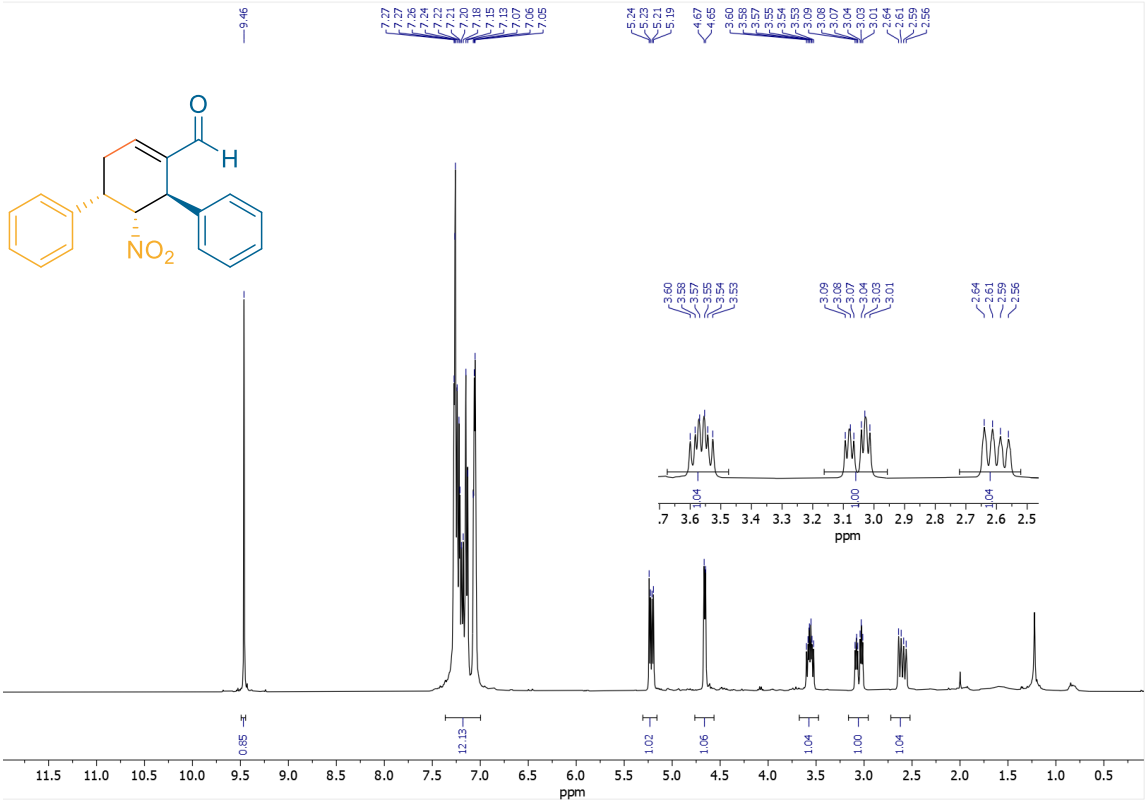

Figure S 1: ^{1}H-NMR (400 MHz) spectrum of 5a' in $CDCl_3$.

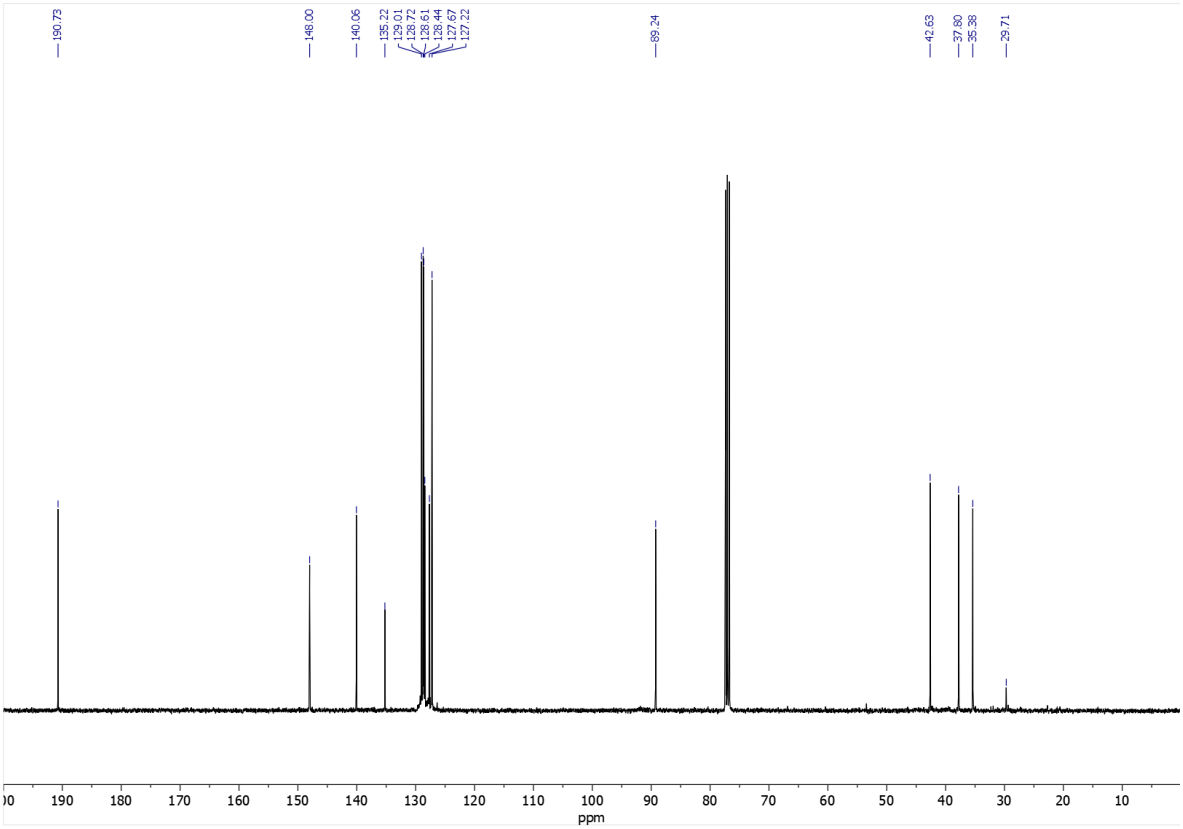

Figure S 2: ^{13}C-NMR (101 MHz) spectrum of 5a' in $CDCl_3$.

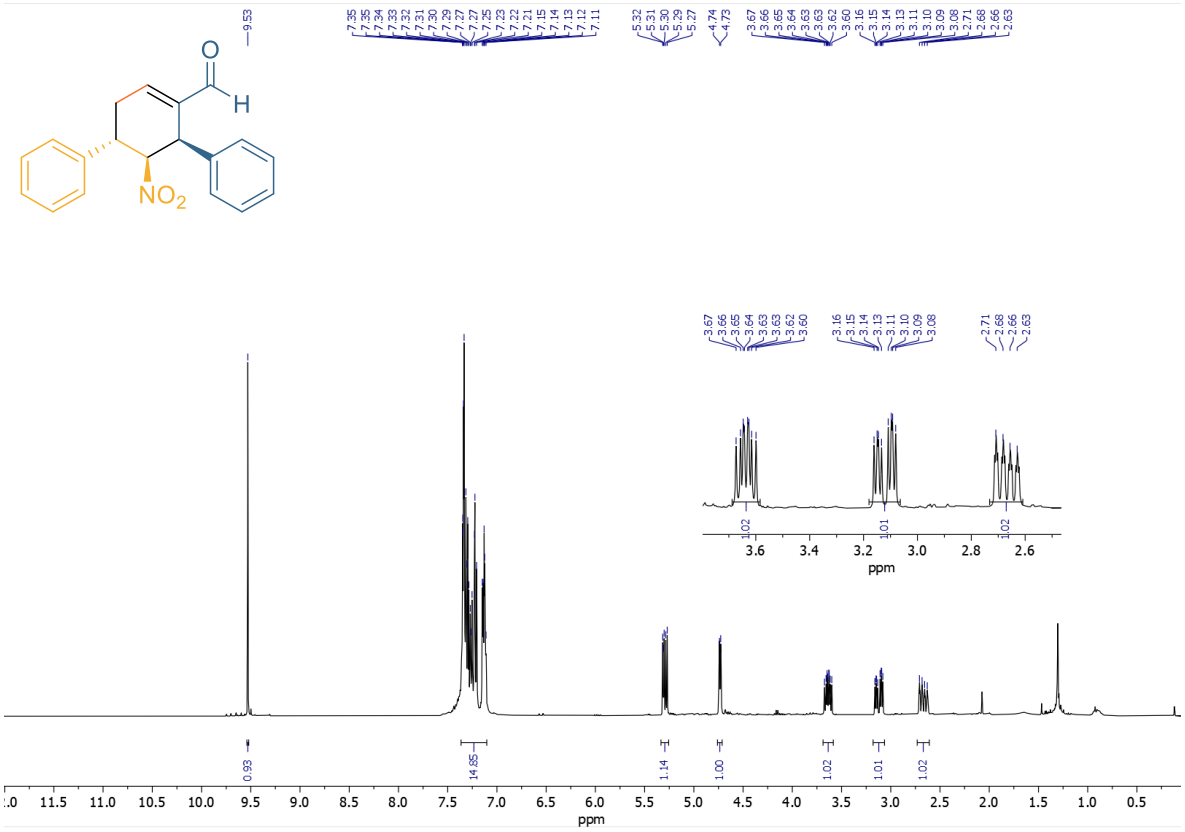

Figure S 3: ^{1}H-NMR (400 MHz) spectrum of 5a'' in $CDCl_3$.

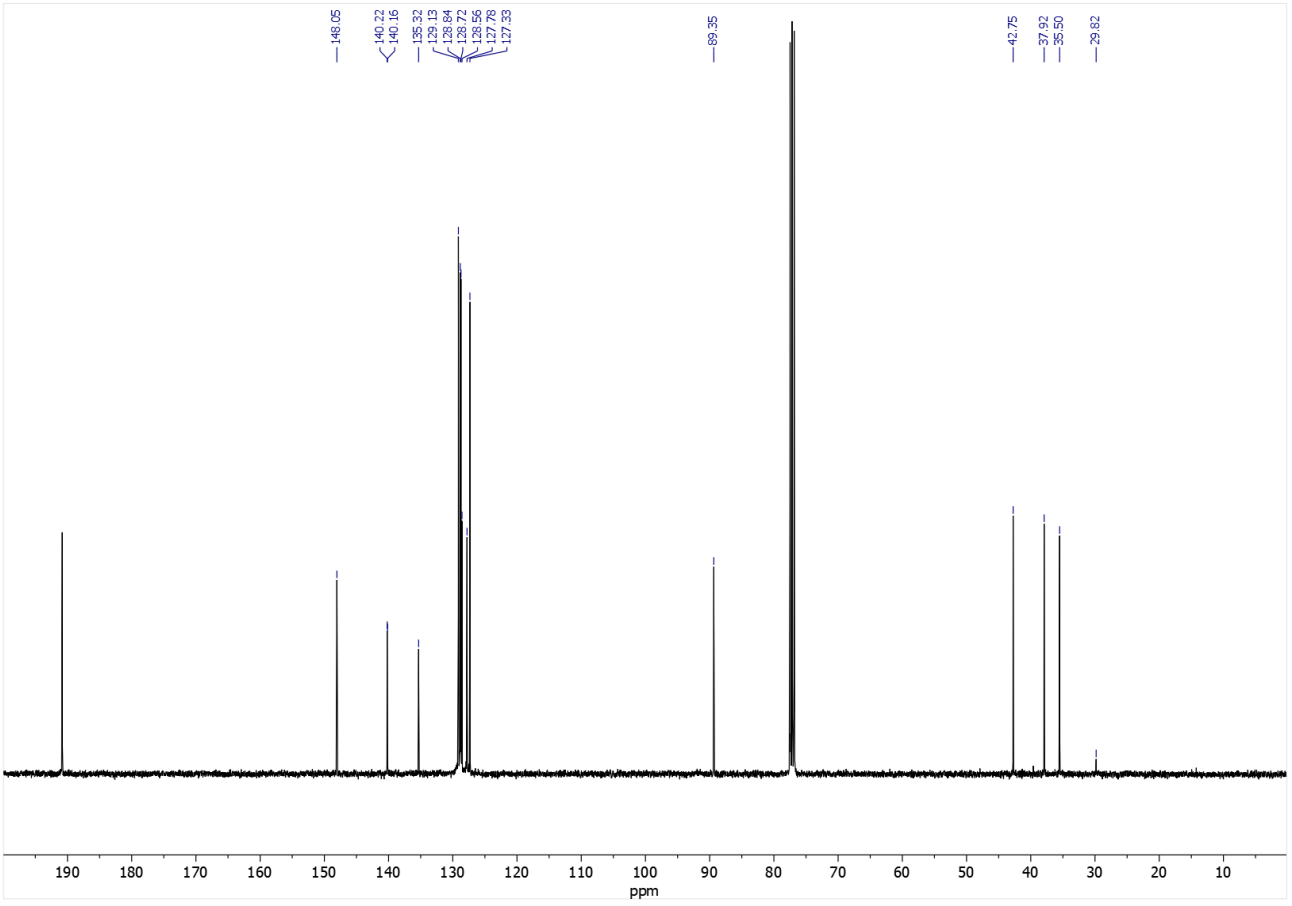

Figure S 4: ^{13}C-NMR (101 MHz) spectrum of 5a'' in $CDCl_3$.

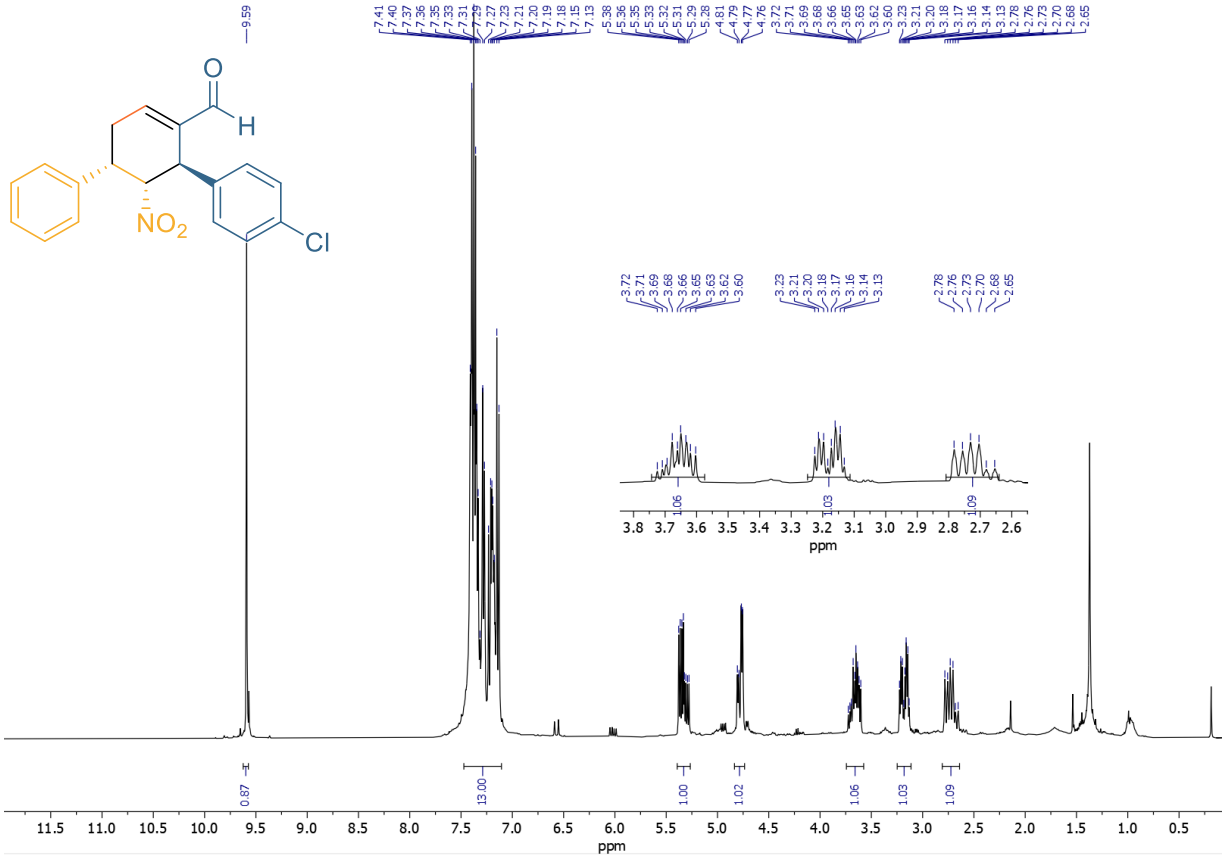

Figure S 5: ^{1}H-NMR (400 MHz) spectrum of 5b' in $CDCl_3$.

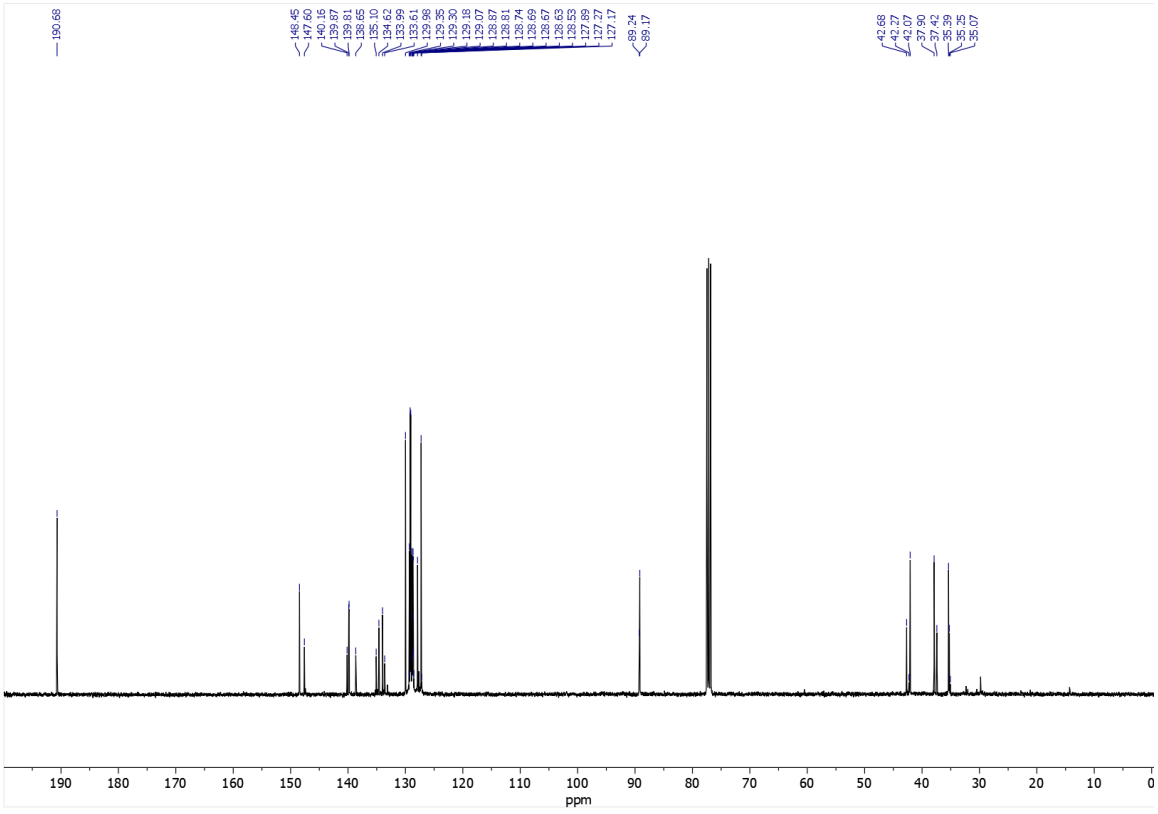

Figure S 6: ^{13}C-NMR (101 MHz) spectrum of 5b' in $CDCl_3$.

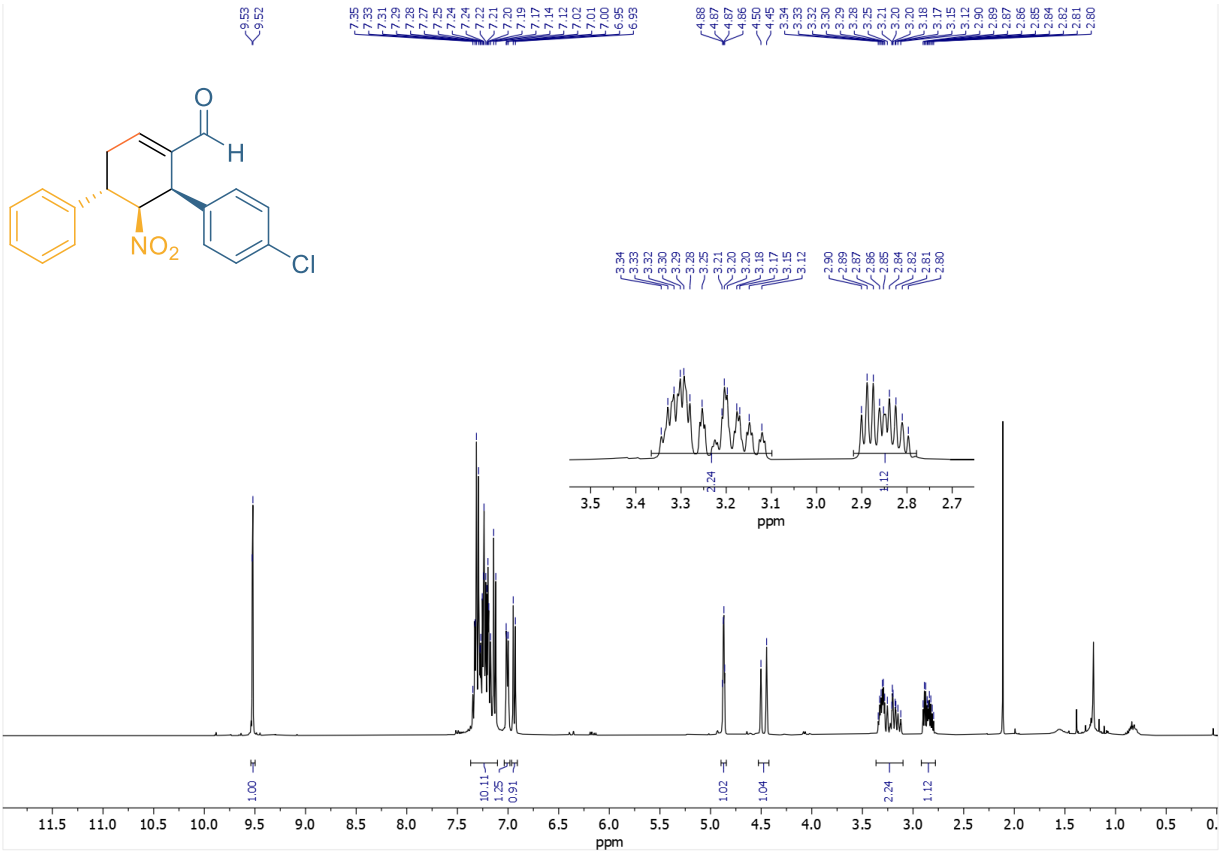

Figure S 7: ^{1}H-NMR (400 MHz) spectrum of 5b'' in $CDCl_3$.

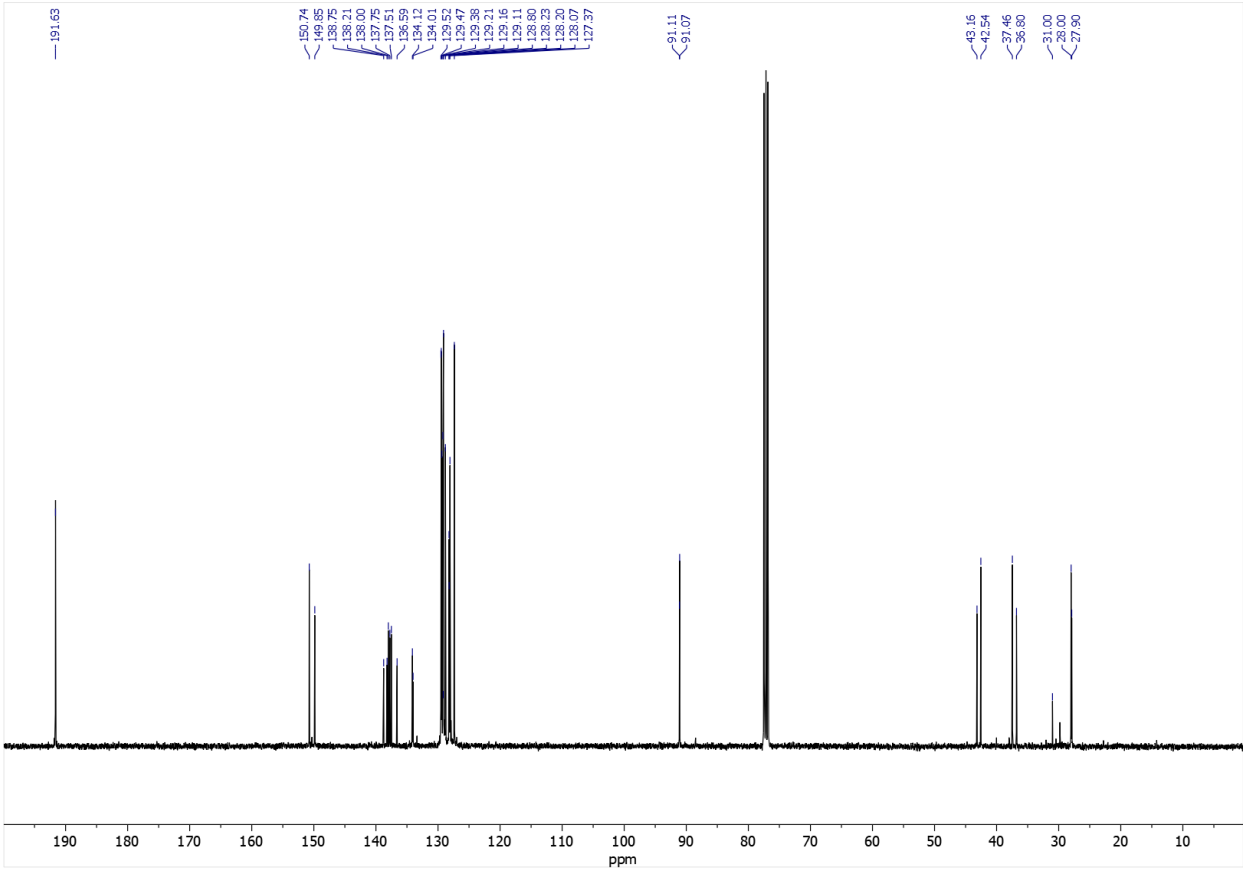

Figure S 8: ^{13}C-NMR (101 MHz) spectrum of 5b'' in $CDCl_3$.

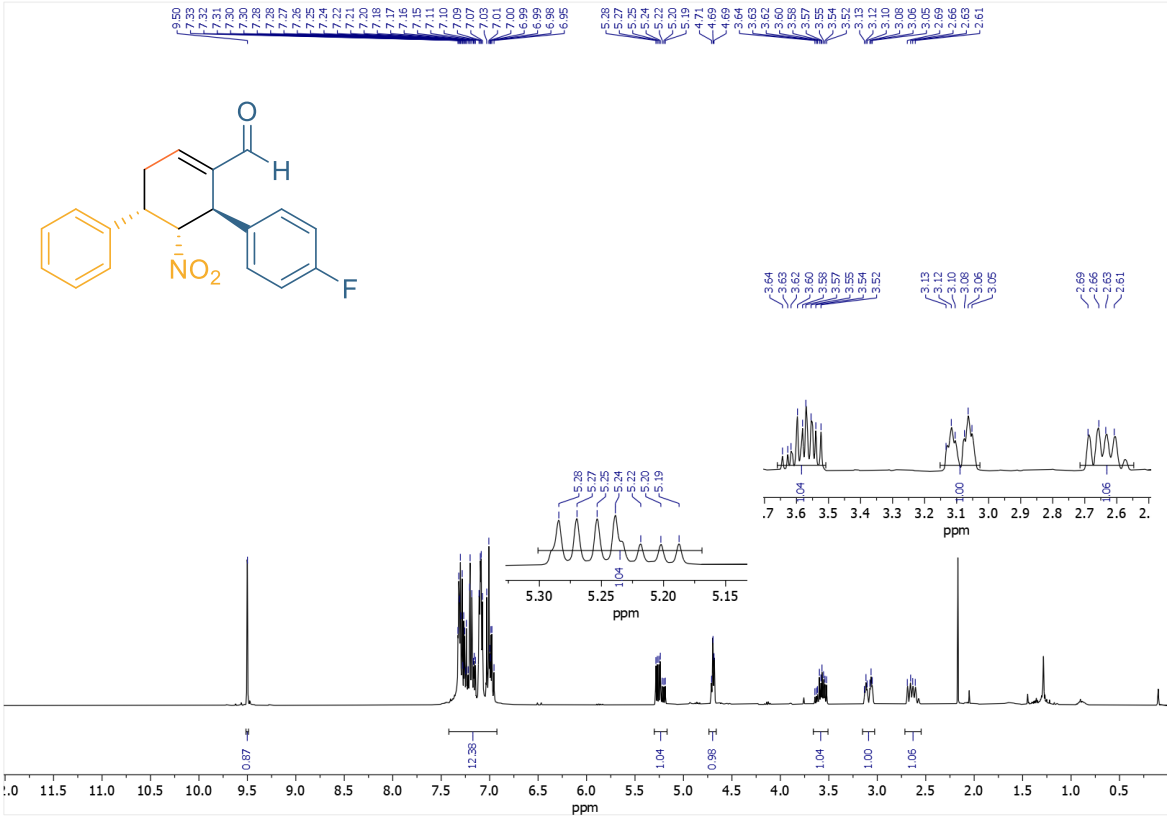

Figure S 9: ^{1}H-NMR (400 MHz) spectrum of 5c' in $CDCl_3$.

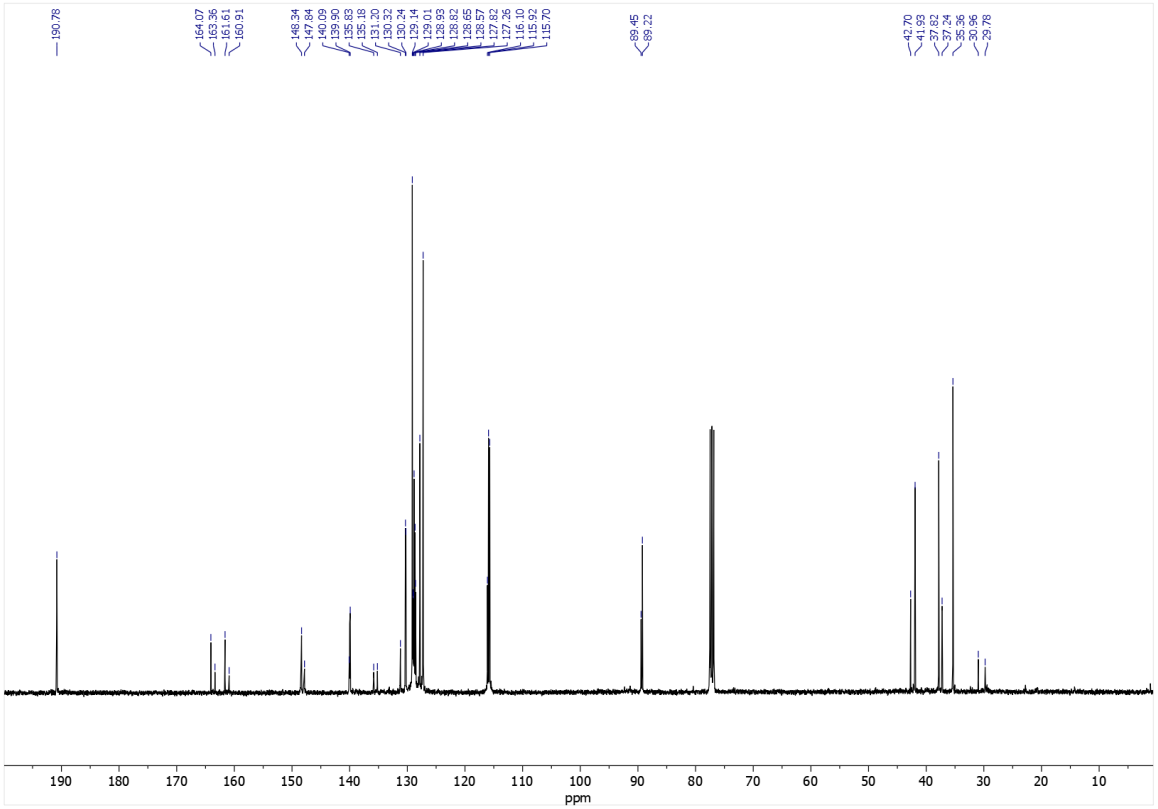

Figure S 10: ^{13}C-NMR (101 MHz) spectrum of 5c' in $CDCl_3$.

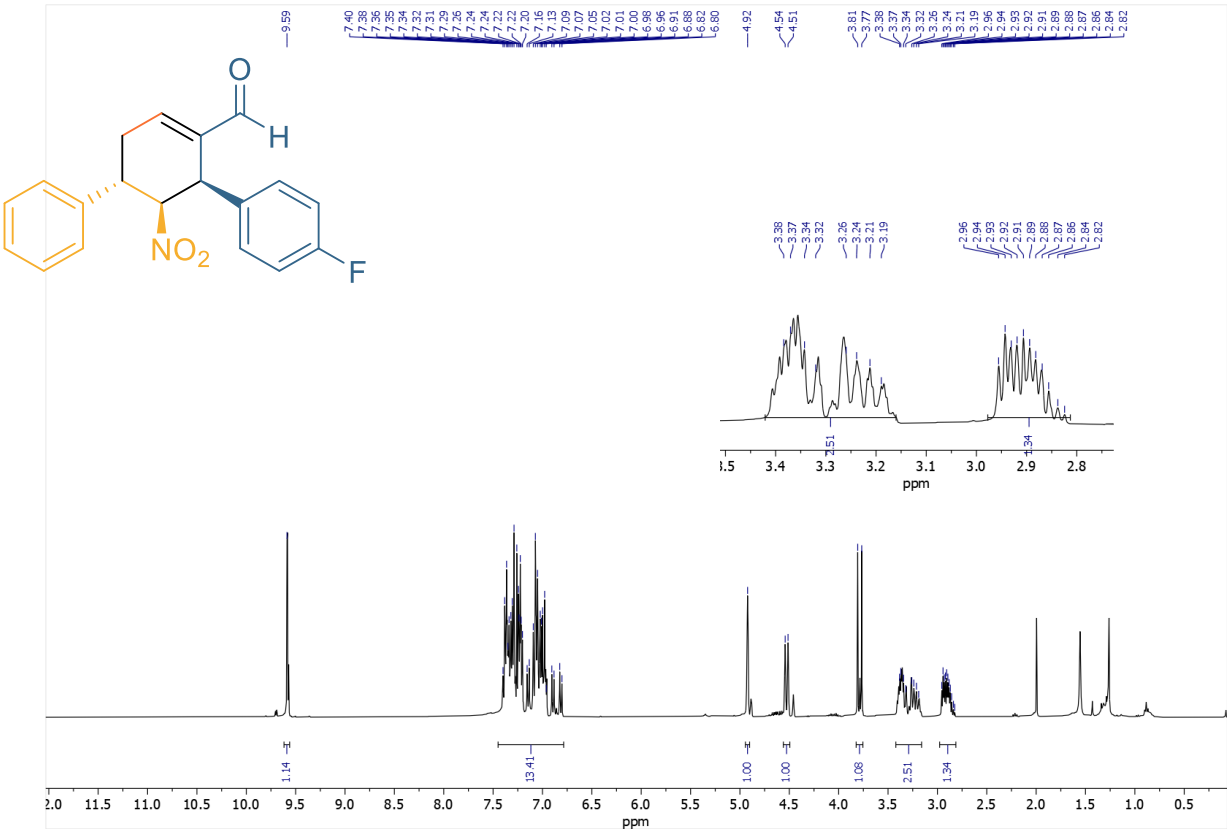

Figure S 11: ^{1}H-NMR (400 MHz) spectrum of 5c'' in $CDCl_3$.

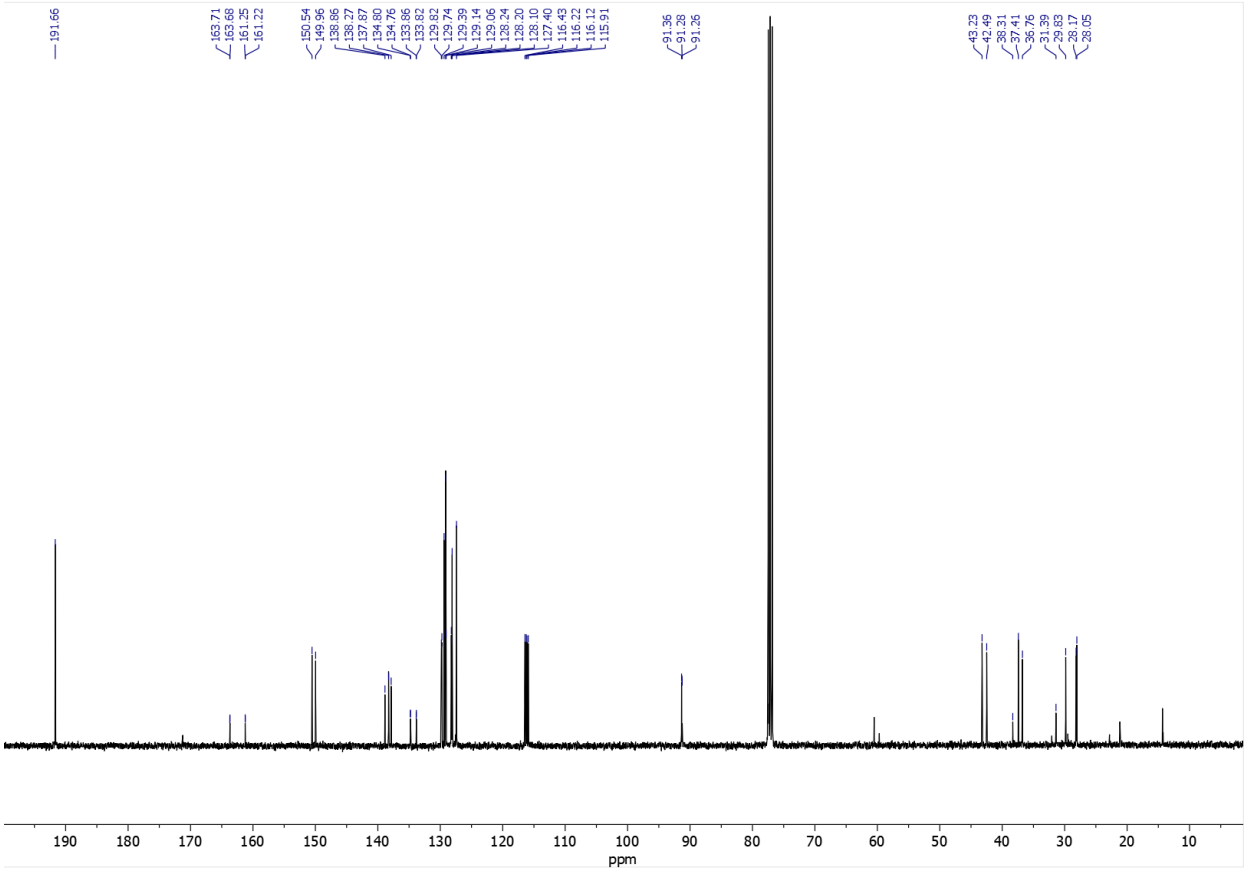

Figure S 12: ^{13}C-NMR (101 MHz) spectrum of 5c'' in $CDCl_3$.

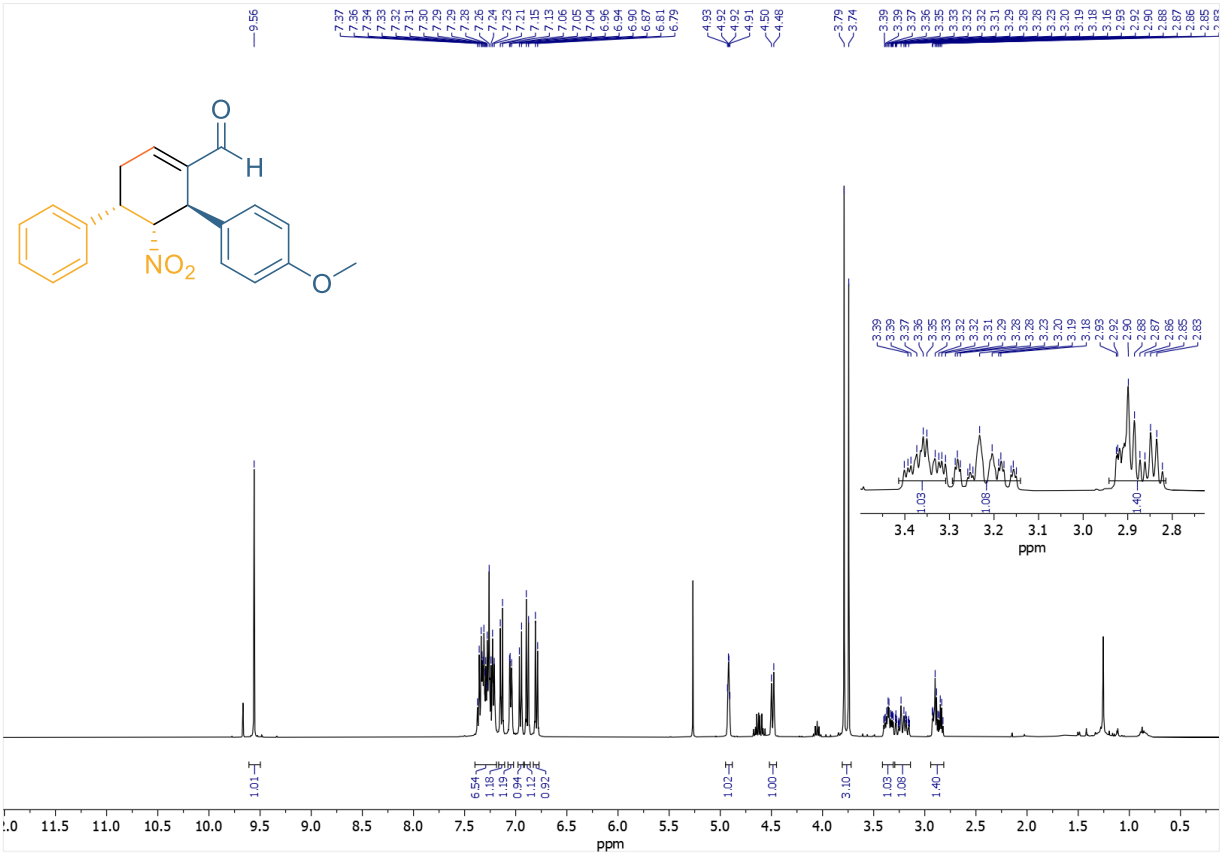

Figure S 13: ^{1}H-NMR (400 MHz) spectrum of 5d' in $CDCl_3$.

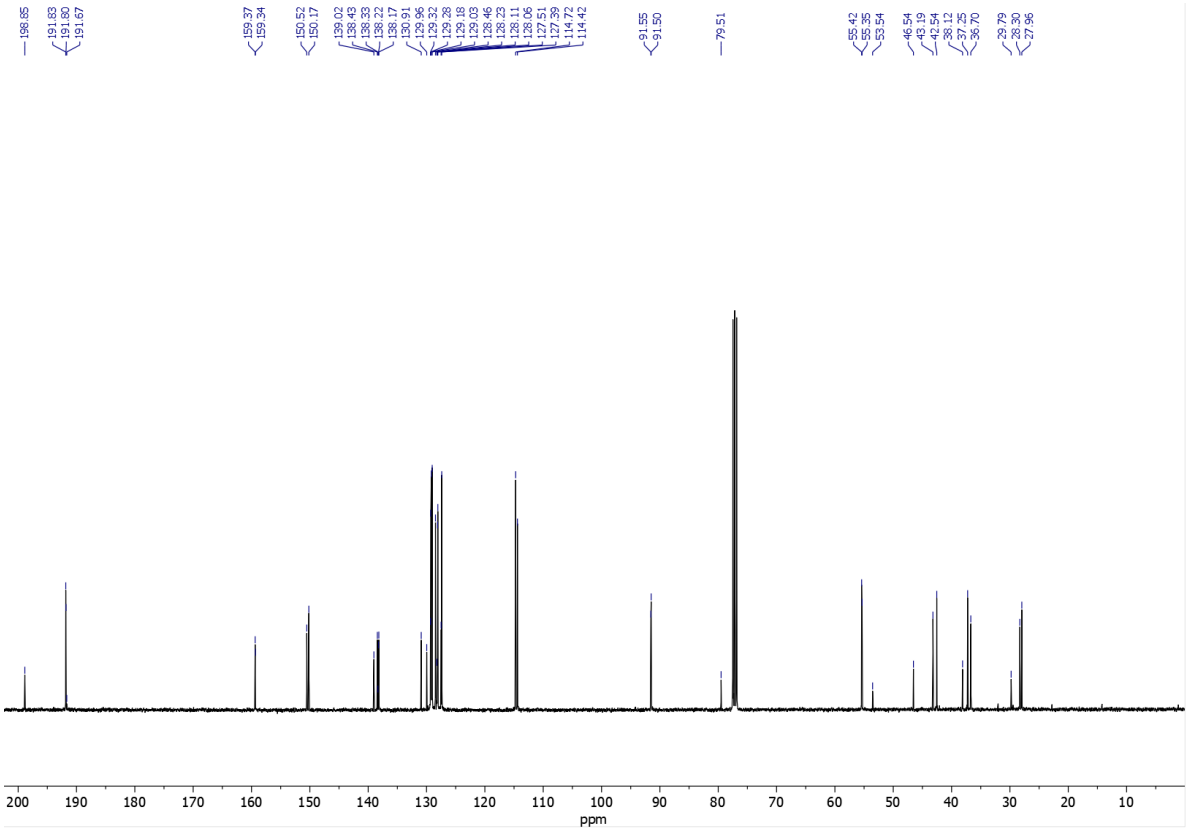

Figure S 14: ^{13}C-NMR (101 MHz) spectrum of 5d' in $CDCl_3$.

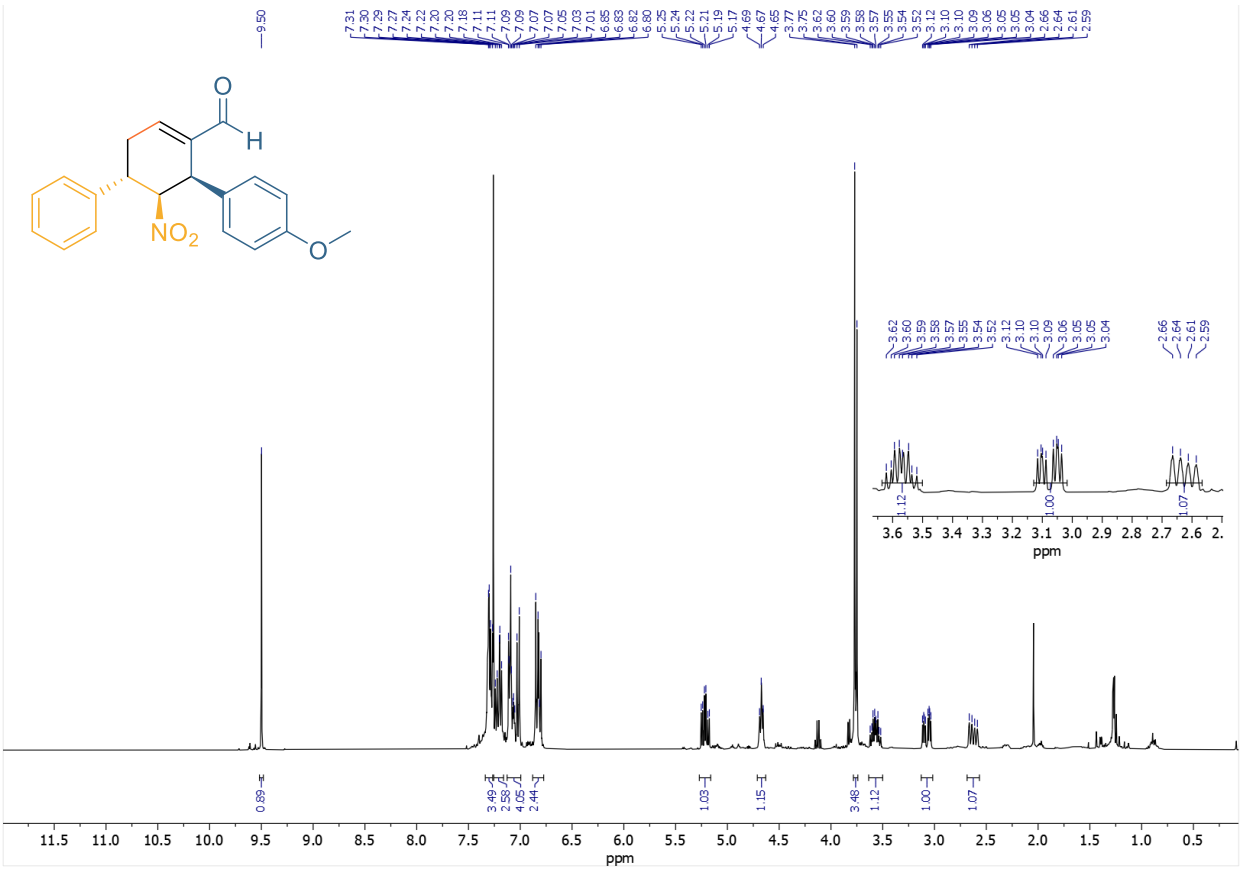

Figure S 15: ^{1}H-NMR (400 MHz) spectrum of 5d'' in $CDCl_3$.

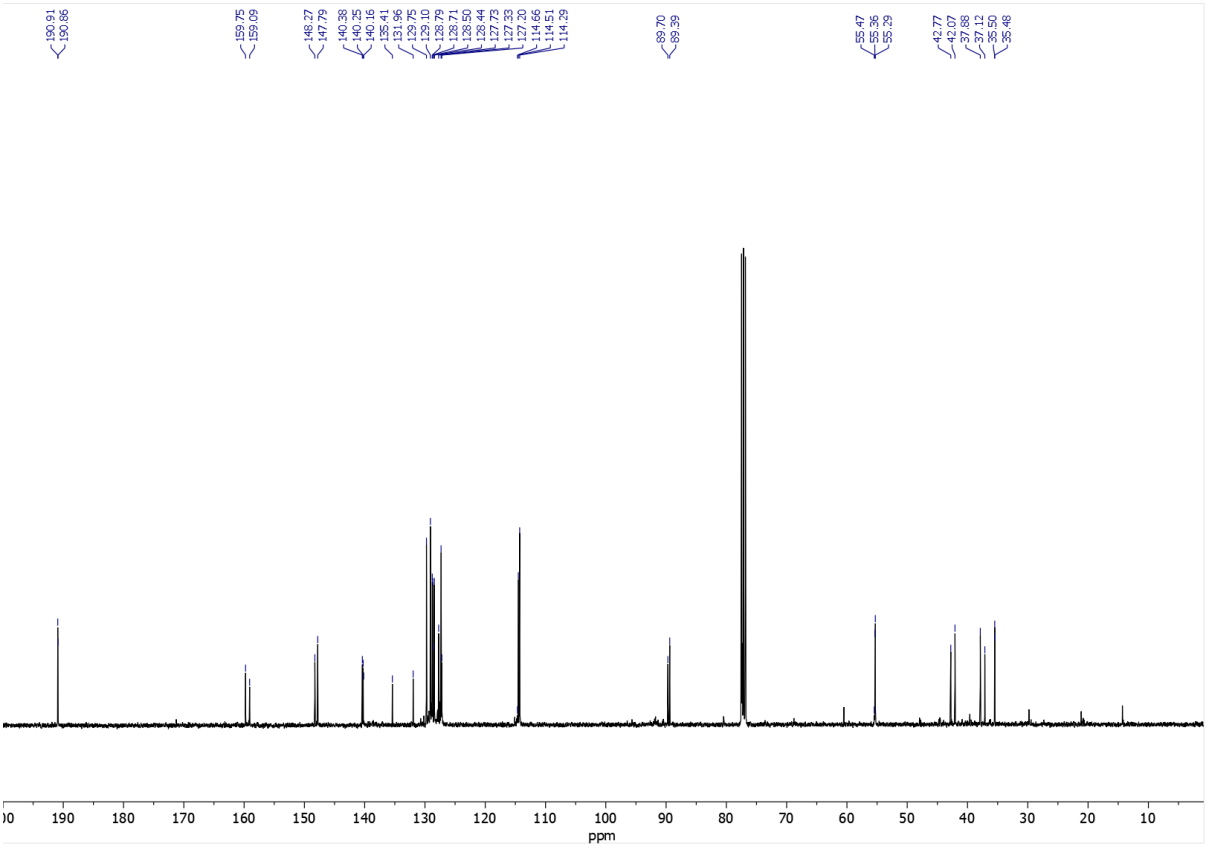

Figure S 16: ^{13}C-NMR (101 MHz) spectrum of 5d'' in $CDCl_3$.

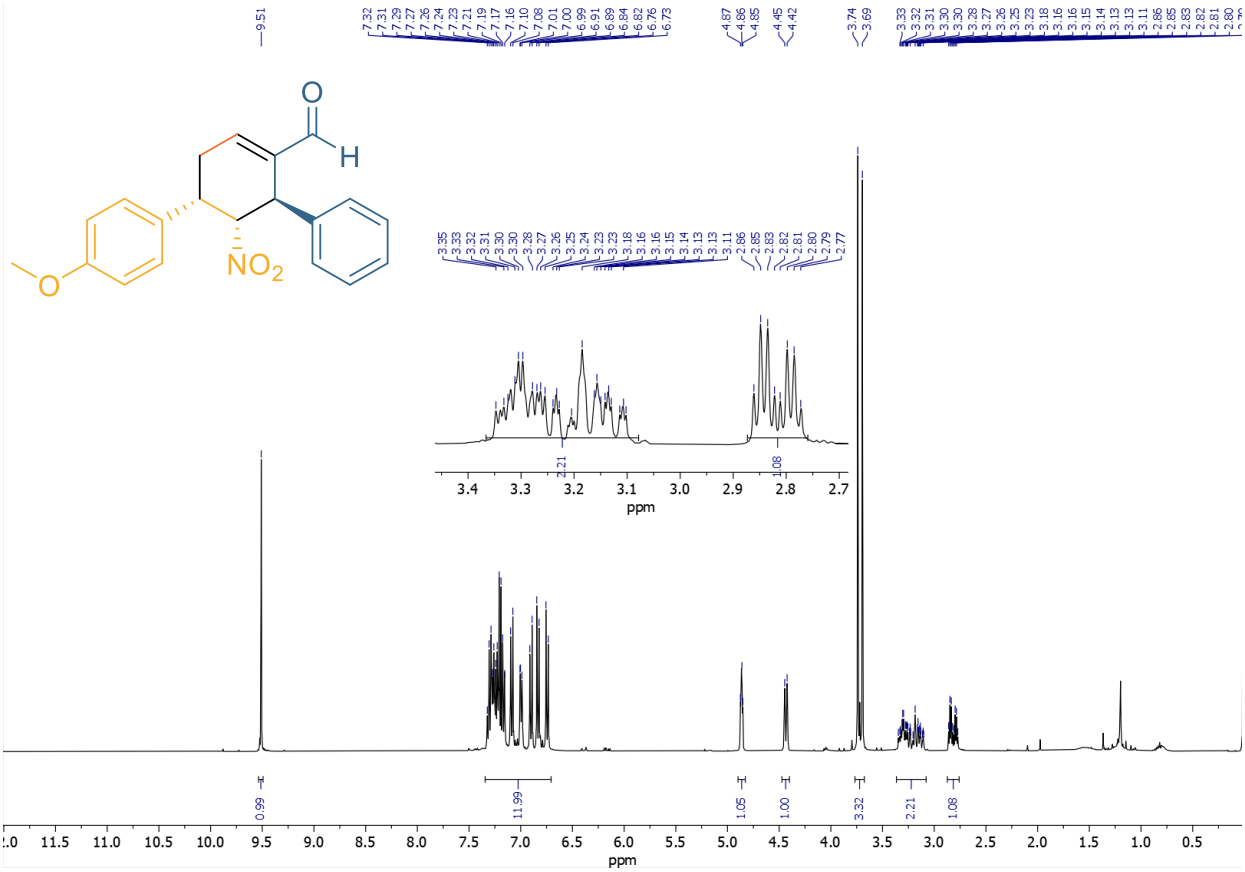

Figure S 17: ^{1}H-NMR (400 MHz) spectrum of 5e' in $CDCl_3$.

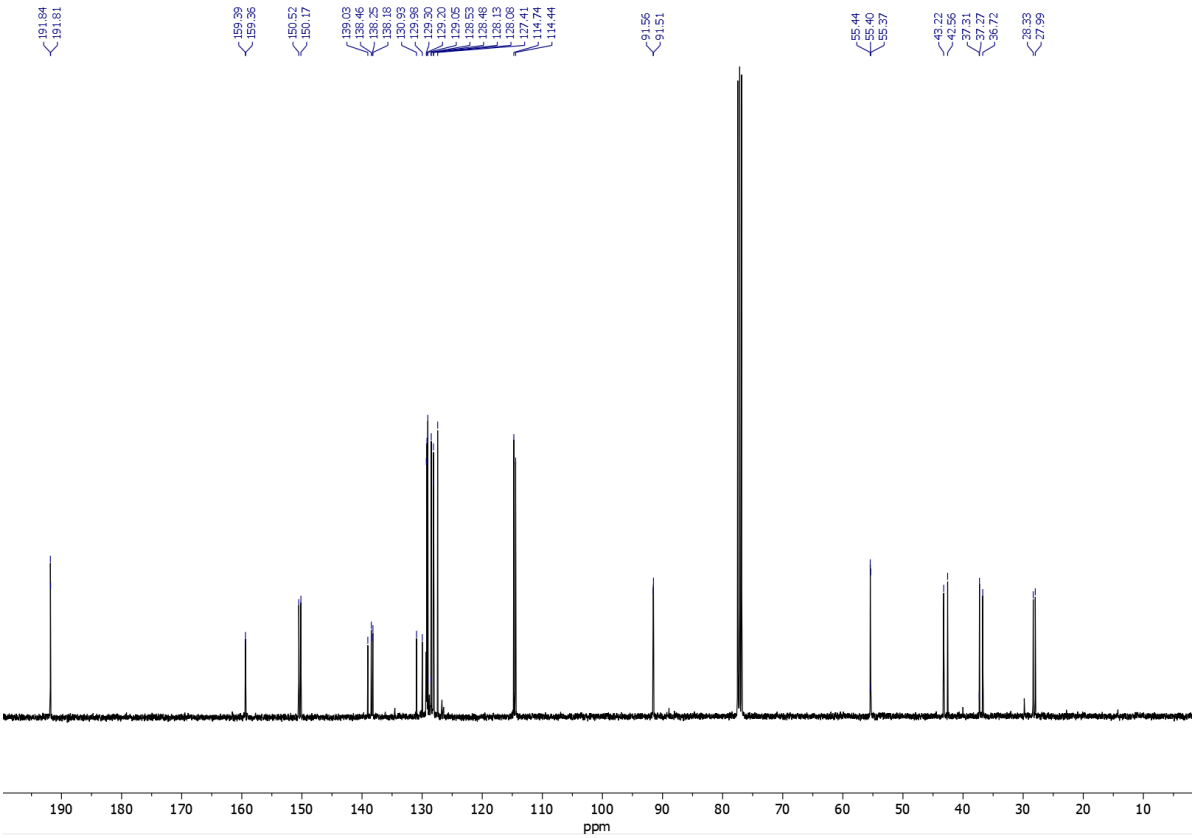

Figure S 18: ^{13}C-NMR (101 MHz) spectrum of 5e' in $CDCl_3$.

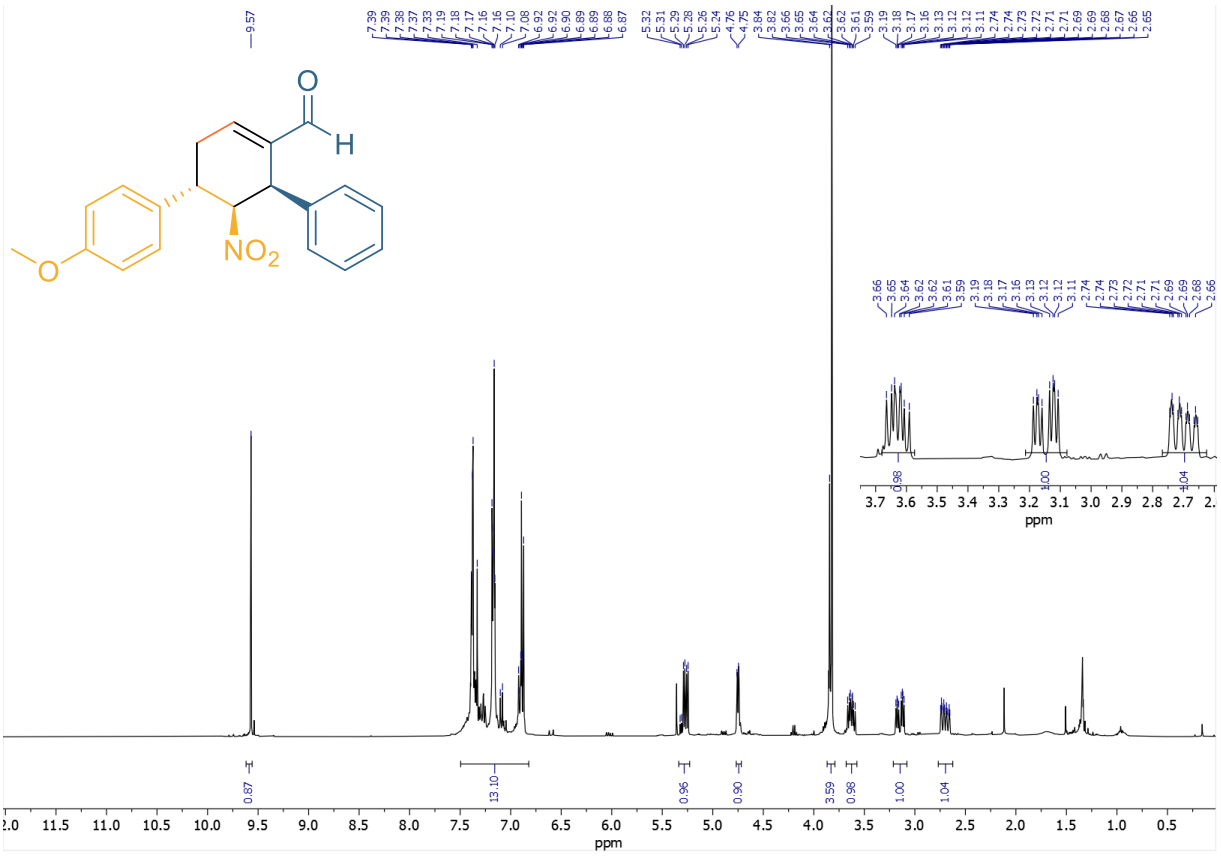

Figure S 19: ^{1}H-NMR (400 MHz) spectrum of 5e'' in $CDCl_3$.

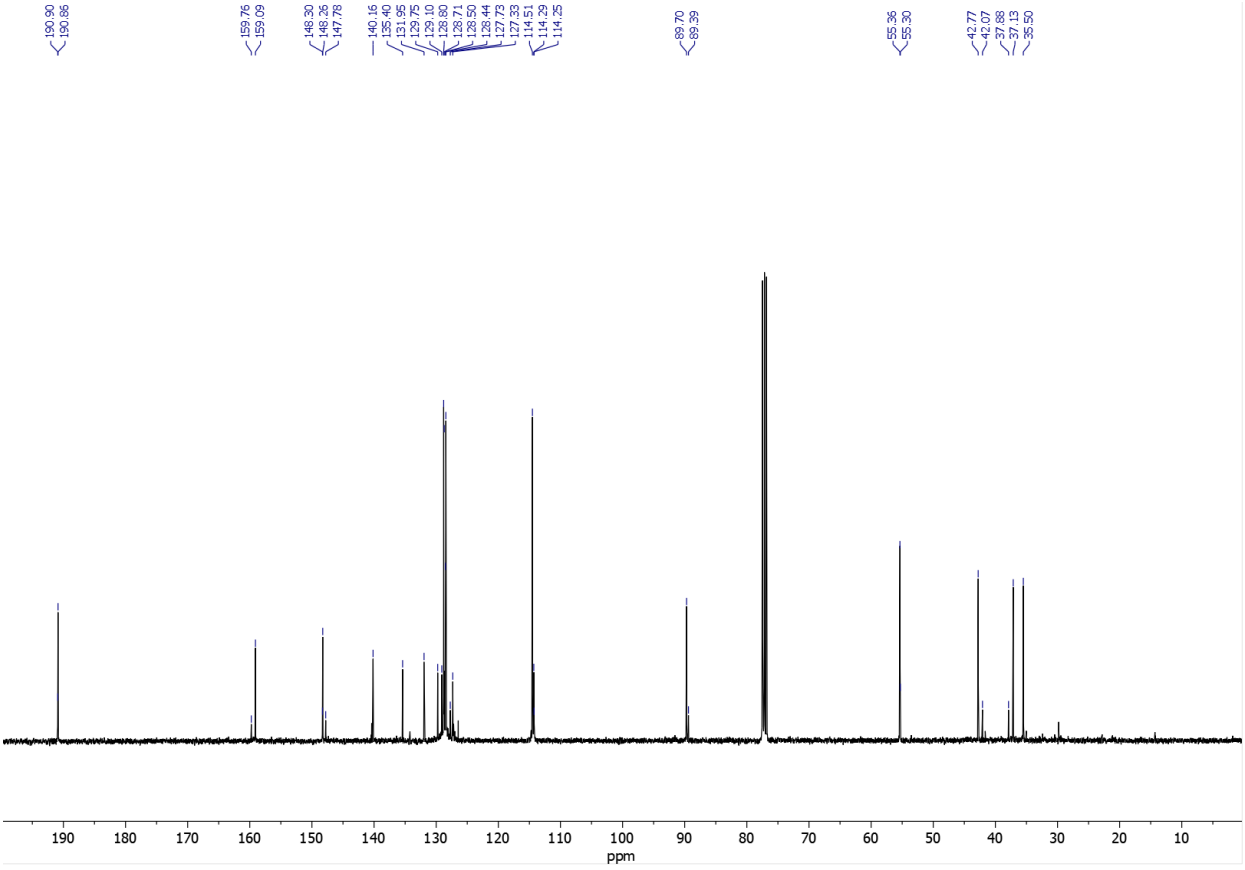

Figure S 20: ^{13}C-NMR (101 MHz) spectrum of 5e'' in $CDCl_3$.

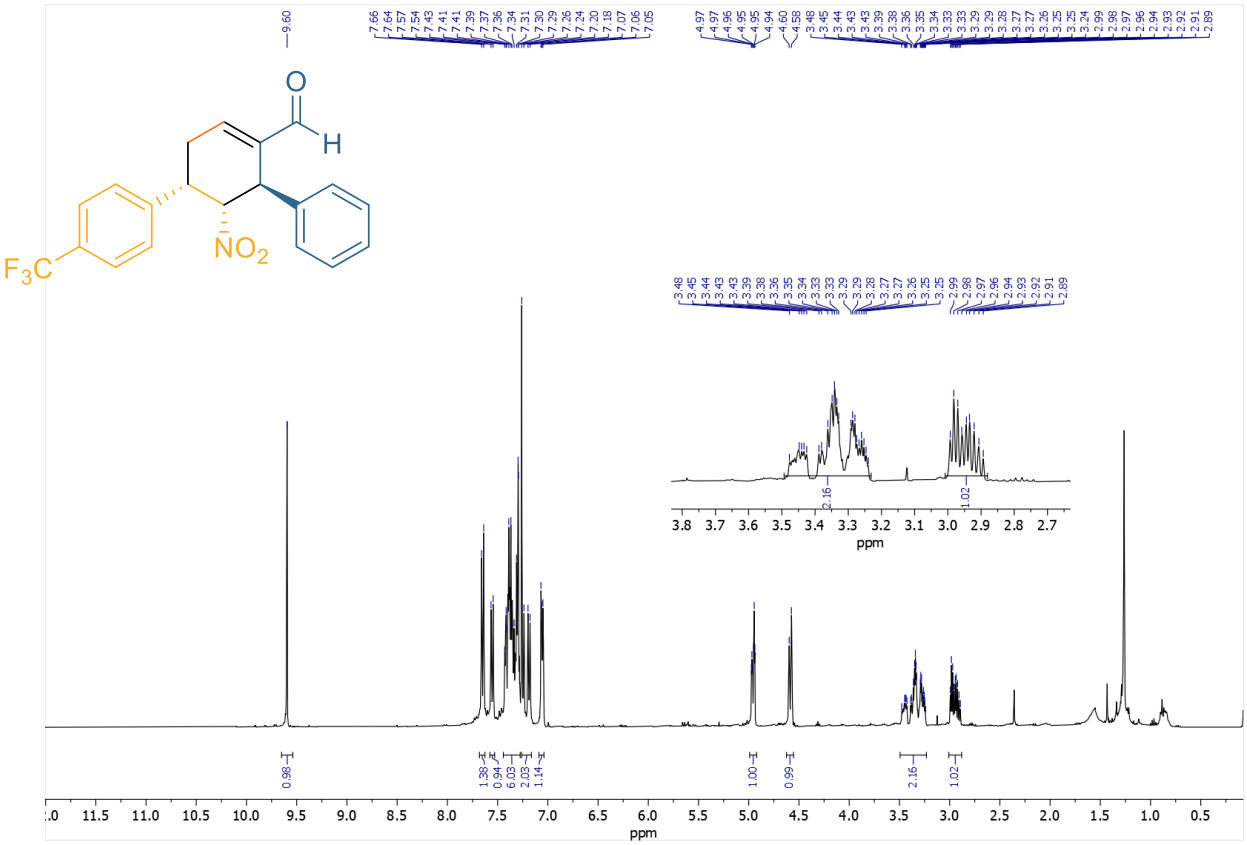

Figure S 21: ^{1}H-NMR (400 MHz) spectrum of 5f' in $CDCl_3$.

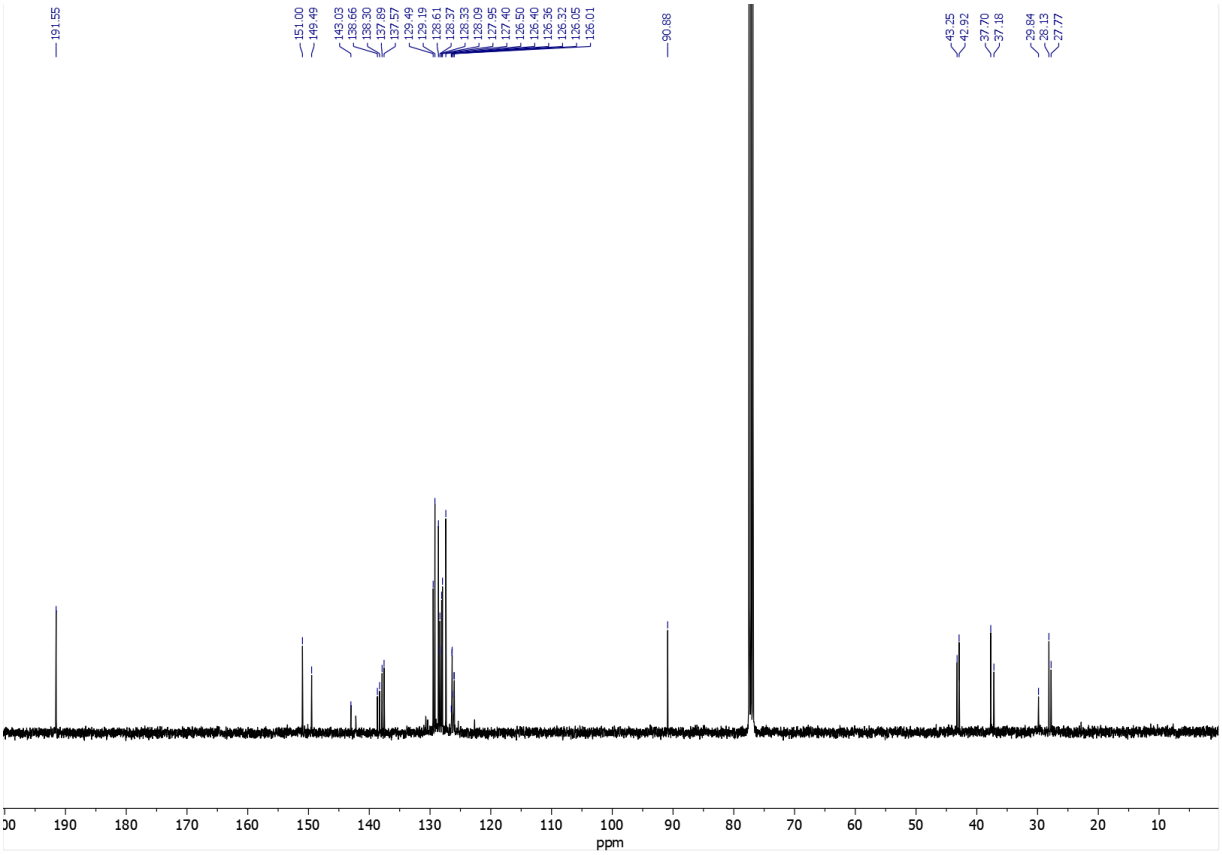

Figure S 22: ^{13}C-NMR (101 MHz) spectrum of 5f' in $CDCl_3$.

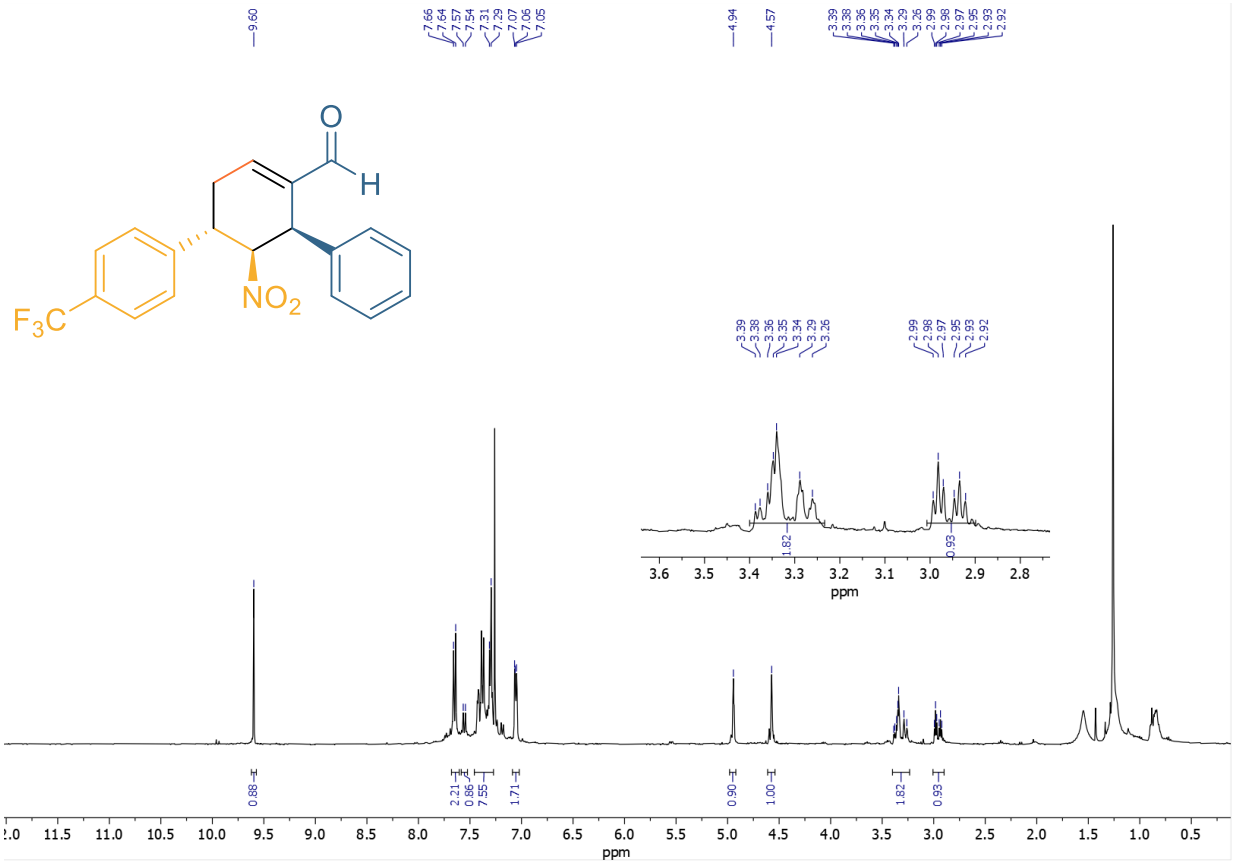

Figure S 23: ^{1}H-NMR (400 MHz) spectrum of 5f'' in $CDCl_3$.

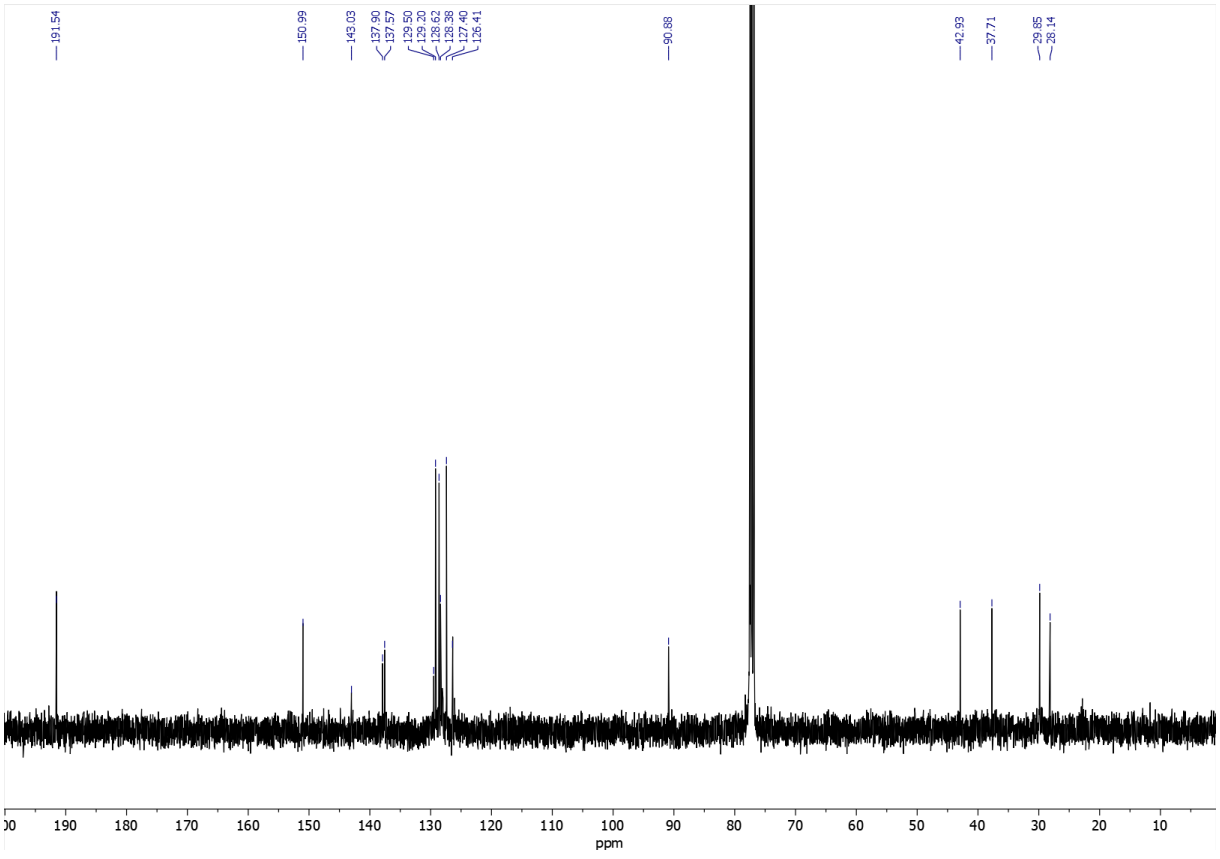

Figure S 24: ^{13}C-NMR (101 MHz) spectrum of 5f'' in $CDCl_3$.

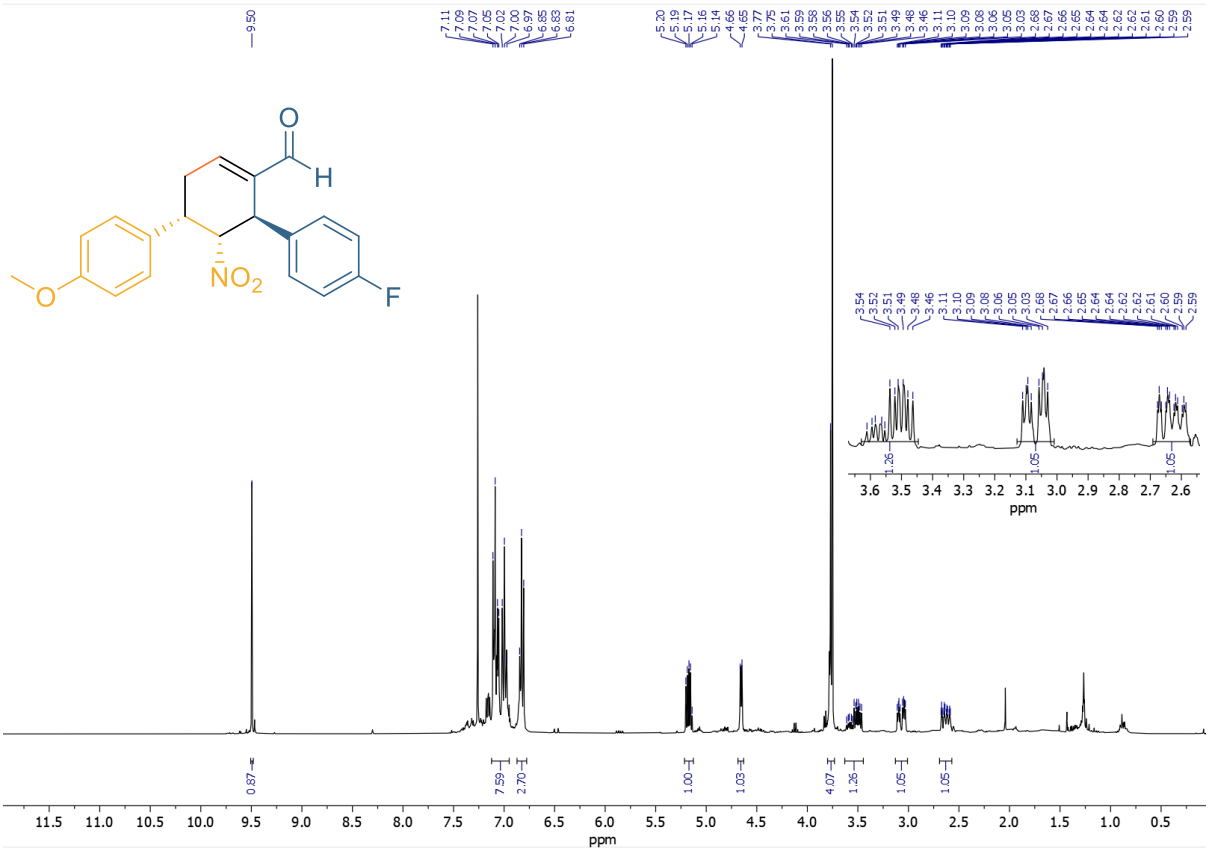

Figure S 25: ^{1}H-NMR (400 MHz) spectrum of 5g' in $CDCl_3$.

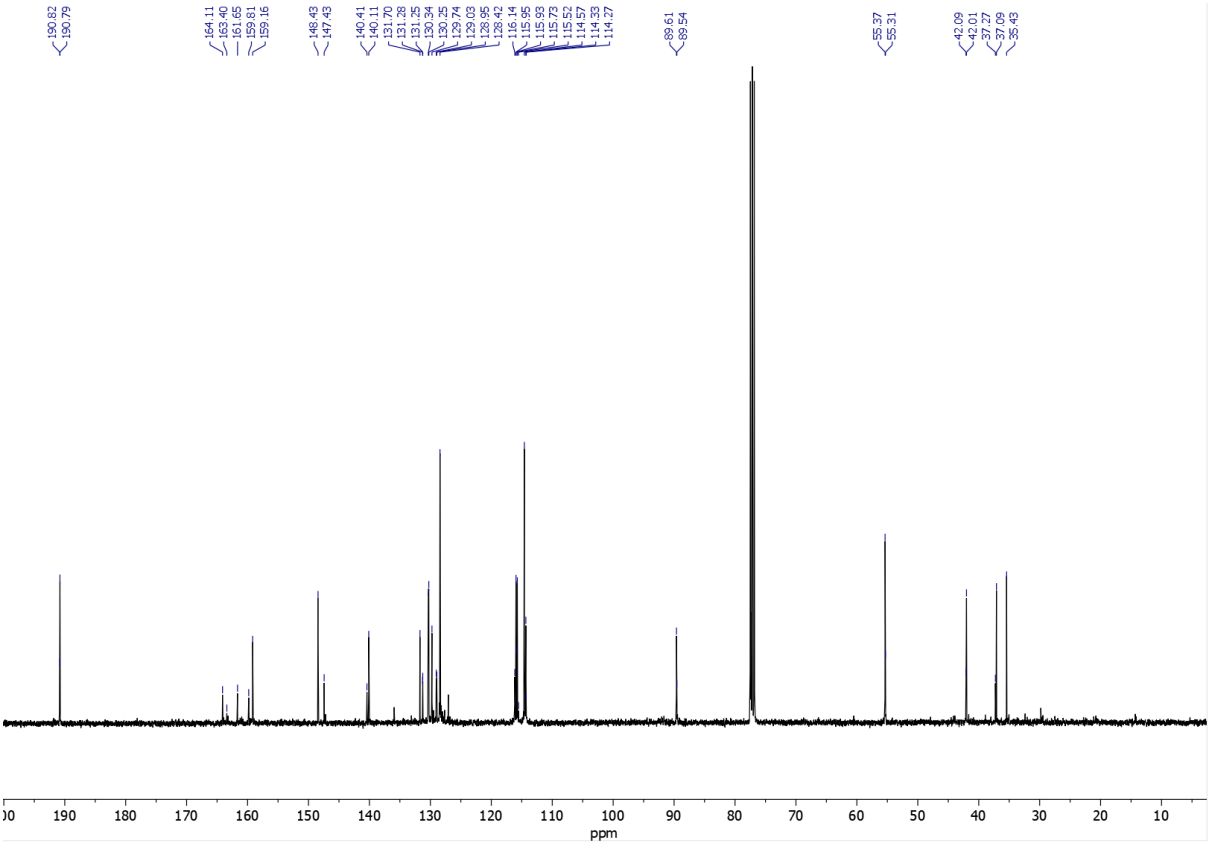

Figure S 26: ^{13}C-NMR (101 MHz) spectrum of 5g‘ in $CDCl_3$.

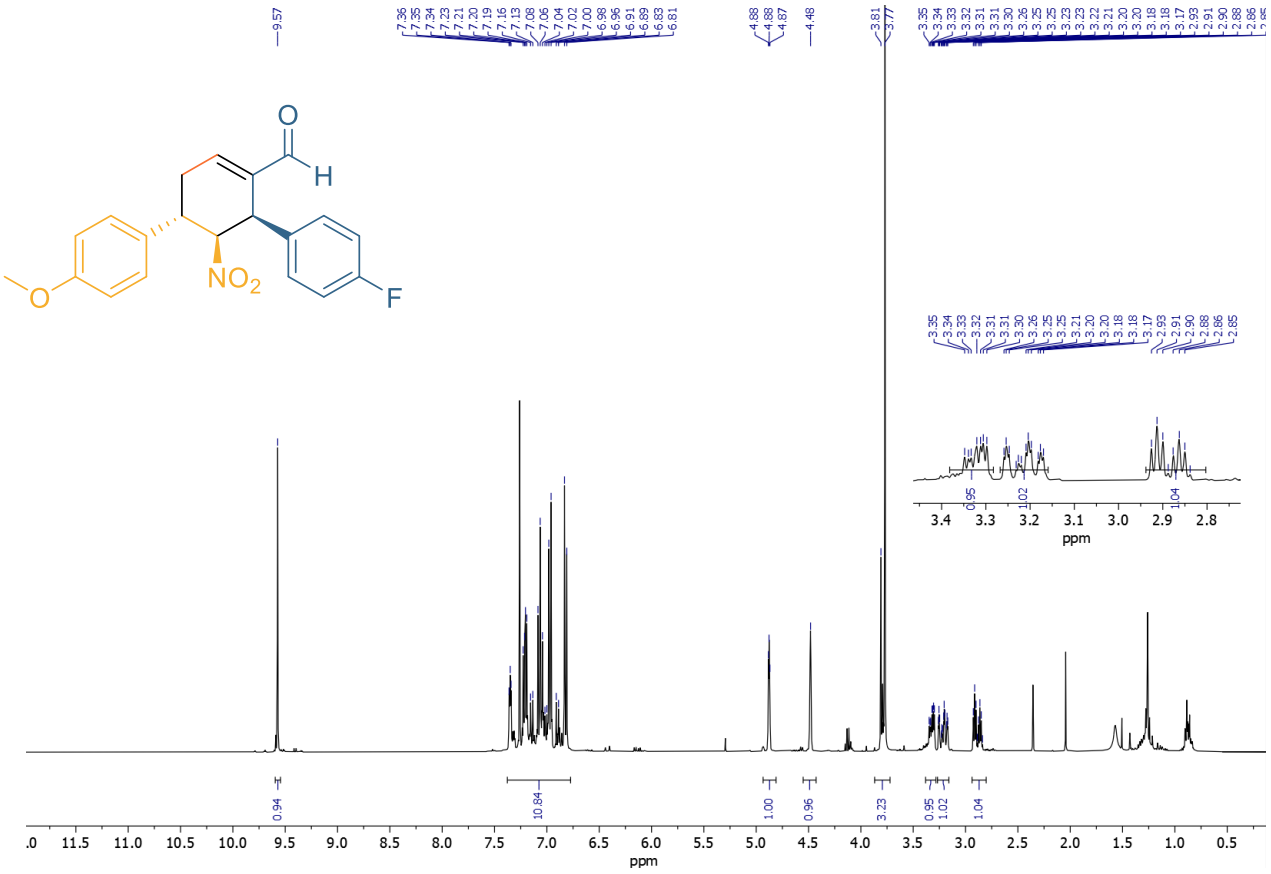

Figure S 27: ^{1}H-NMR (400 MHz) spectrum of 5g'' in $CDCl_3$.

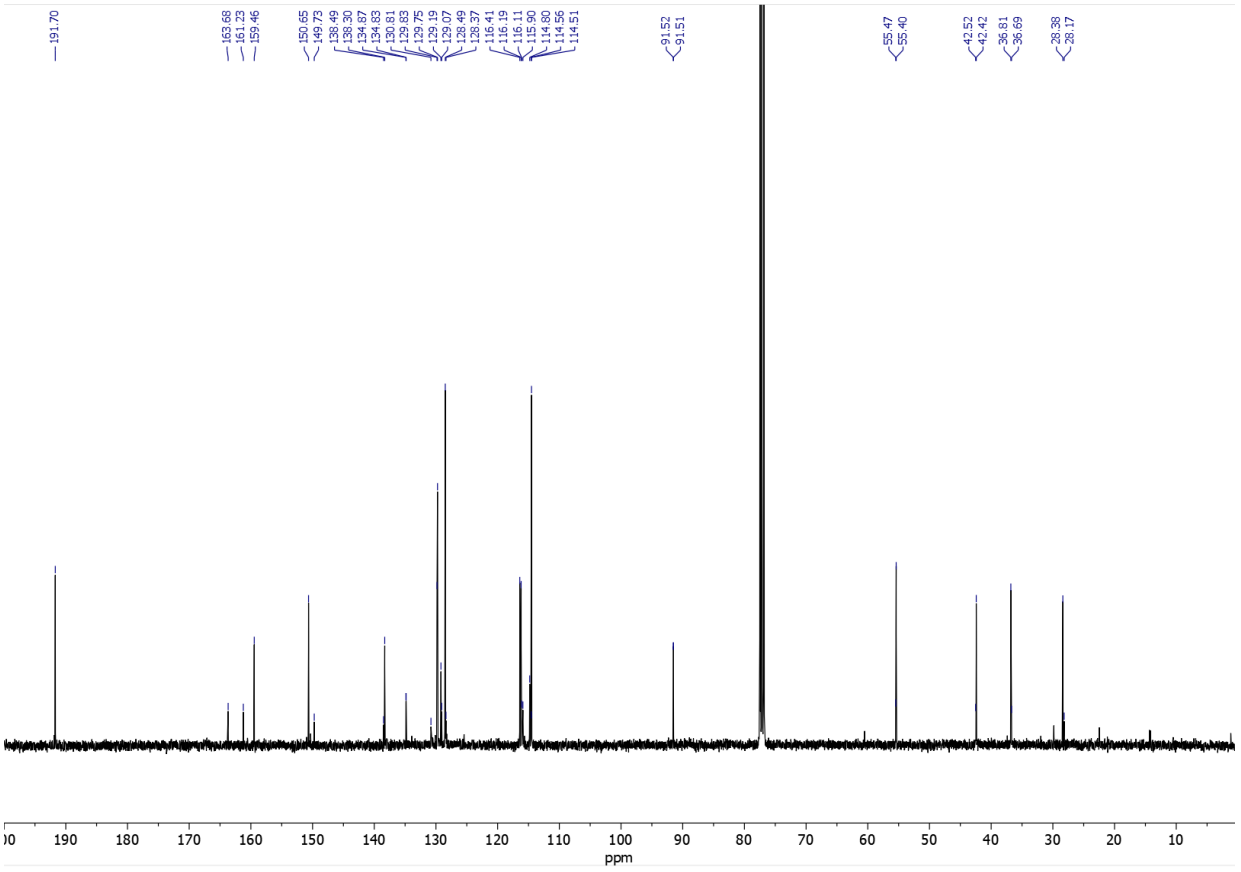

Figure S 28: ^{13}C-NMR (101 MHz) spectrum of 5g'' in $CDCl_3$.

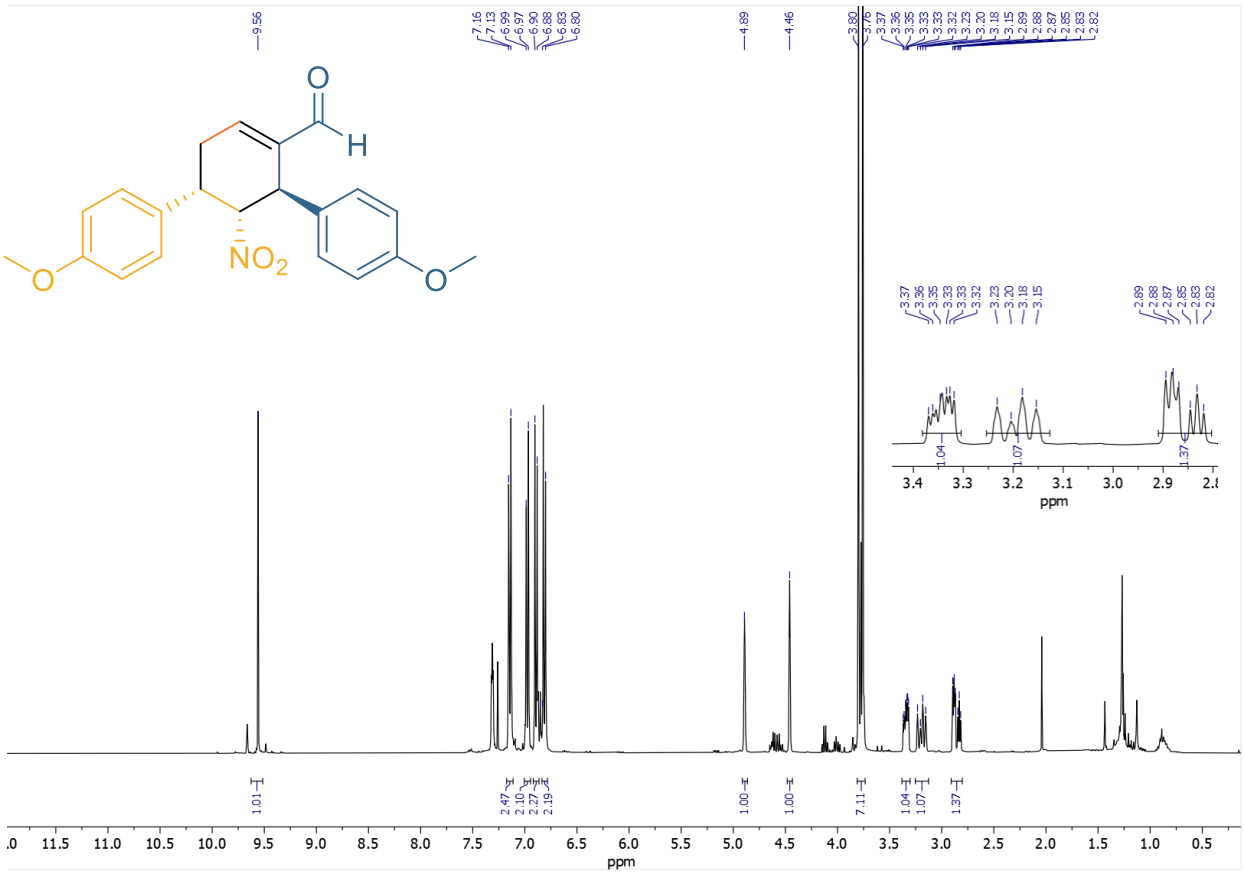

Figure S 29: ^{1}H-NMR (400 MHz) spectrum of 5h' in $CDCl_3$.

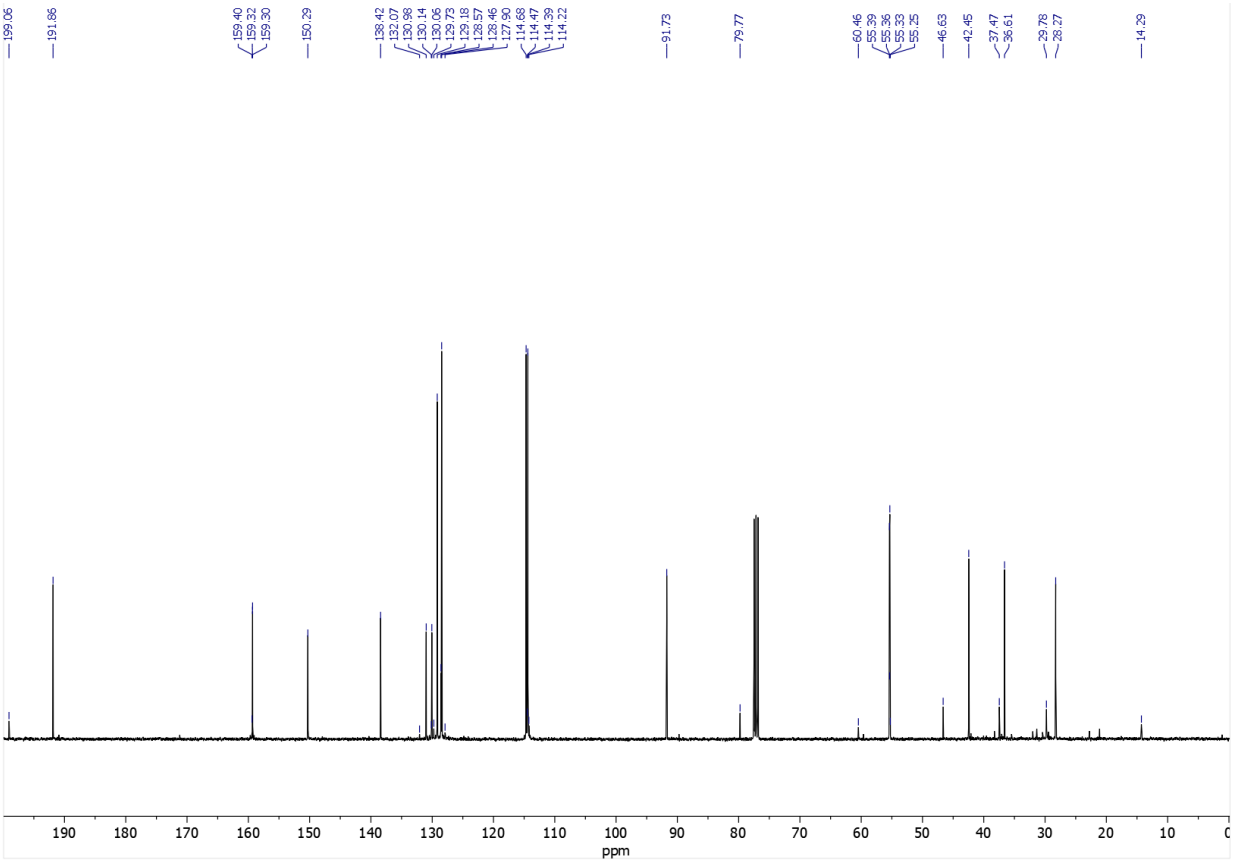

Figure S 30: ^{13}C-NMR (101 MHz) spectrum of 5h' in $CDCl_3$.

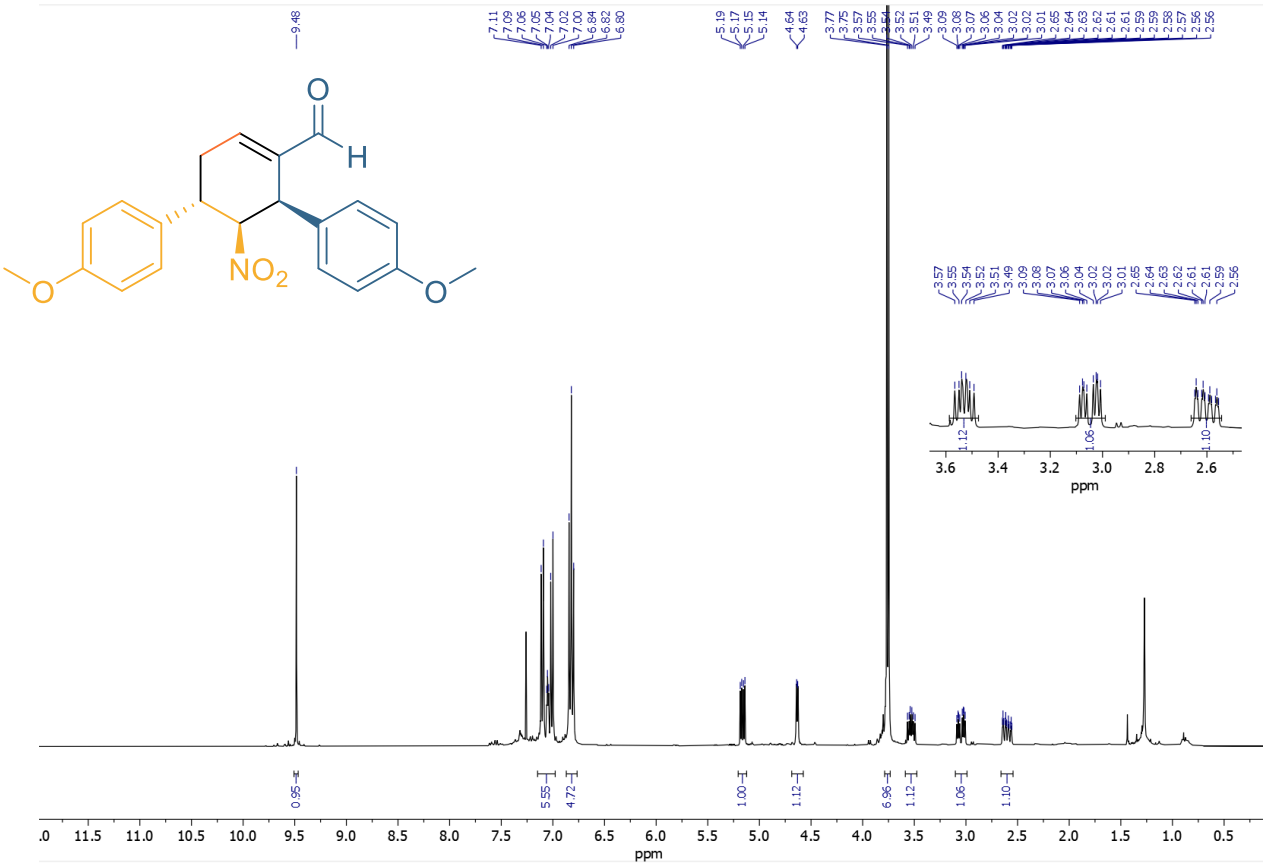

Figure S 31: ^{1}H-NMR (400 MHz) spectrum of 5h'' in $CDCl_3$.

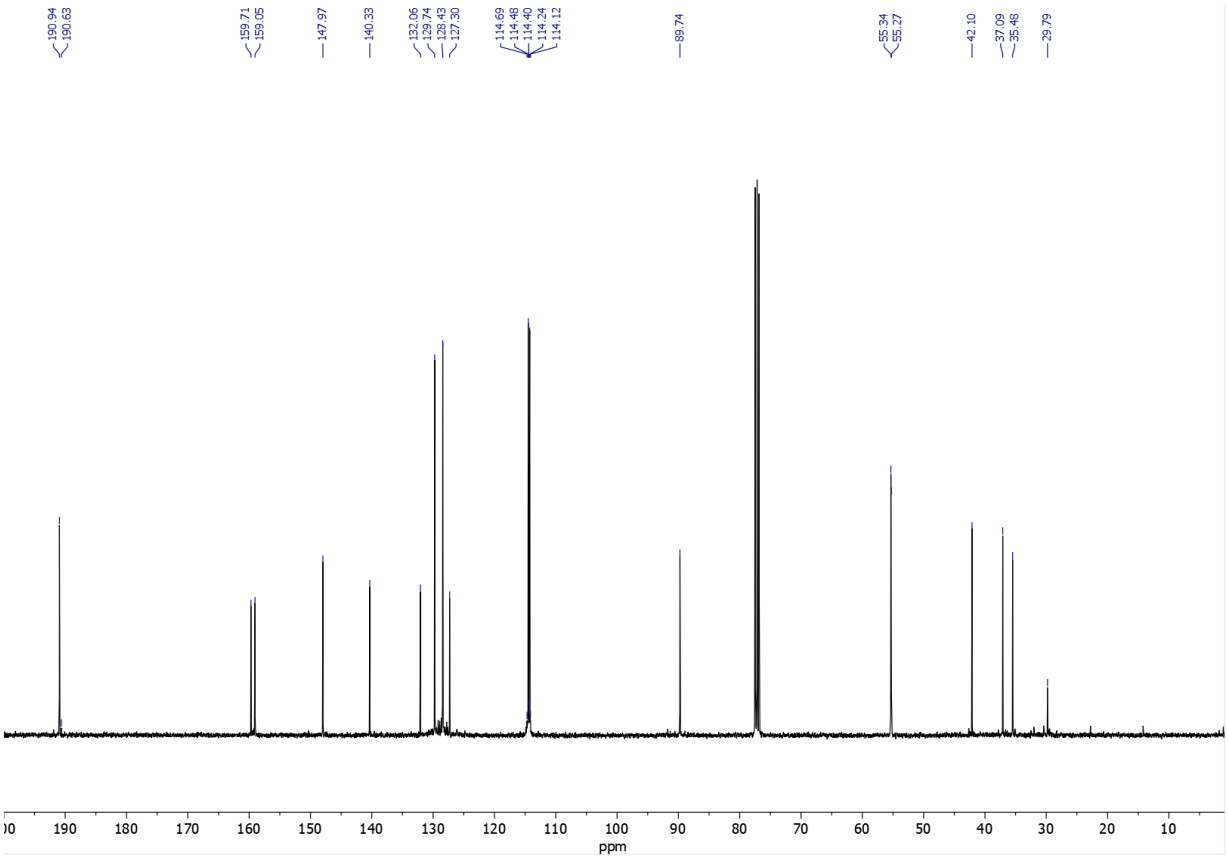

Figure S 32: ^{13}C-NMR (101 MHz) spectrum of 5h'' in $CDCl_3$.

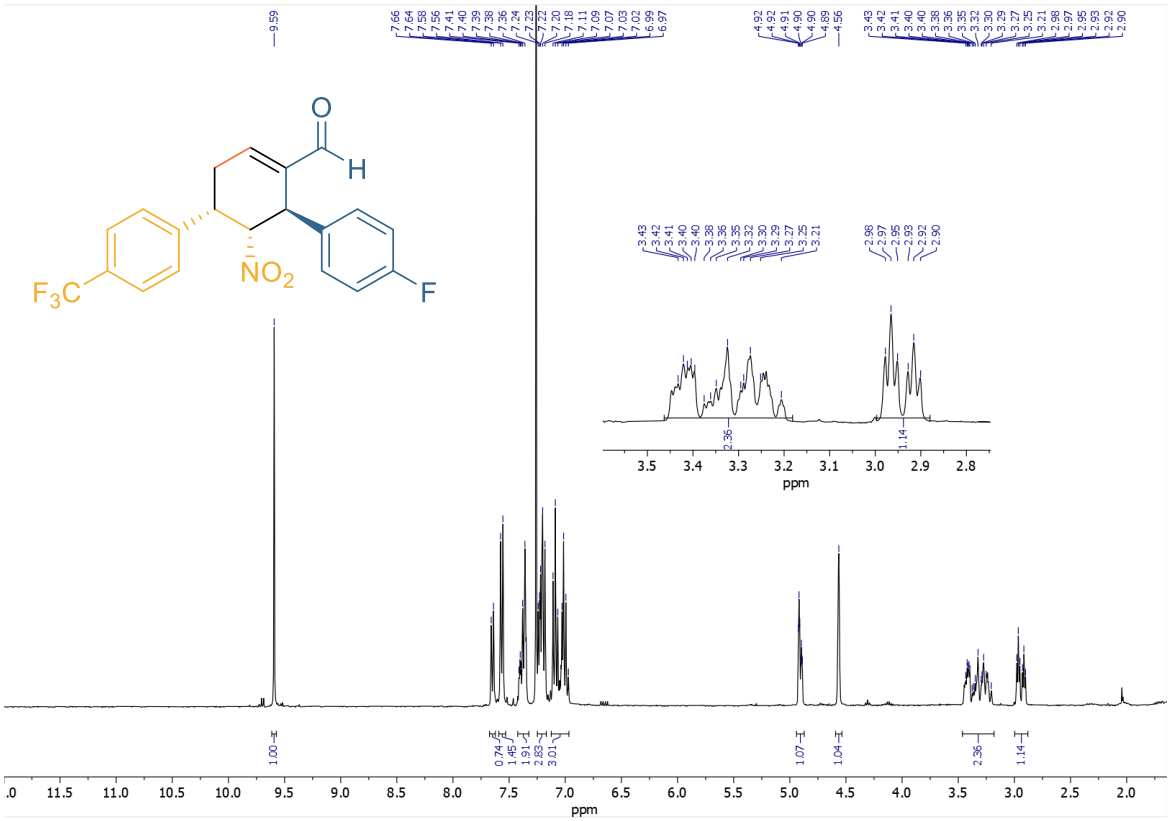

Figure S 33: ^{1}H-NMR (400 MHz) spectrum of 5i' in $CDCl_3$.

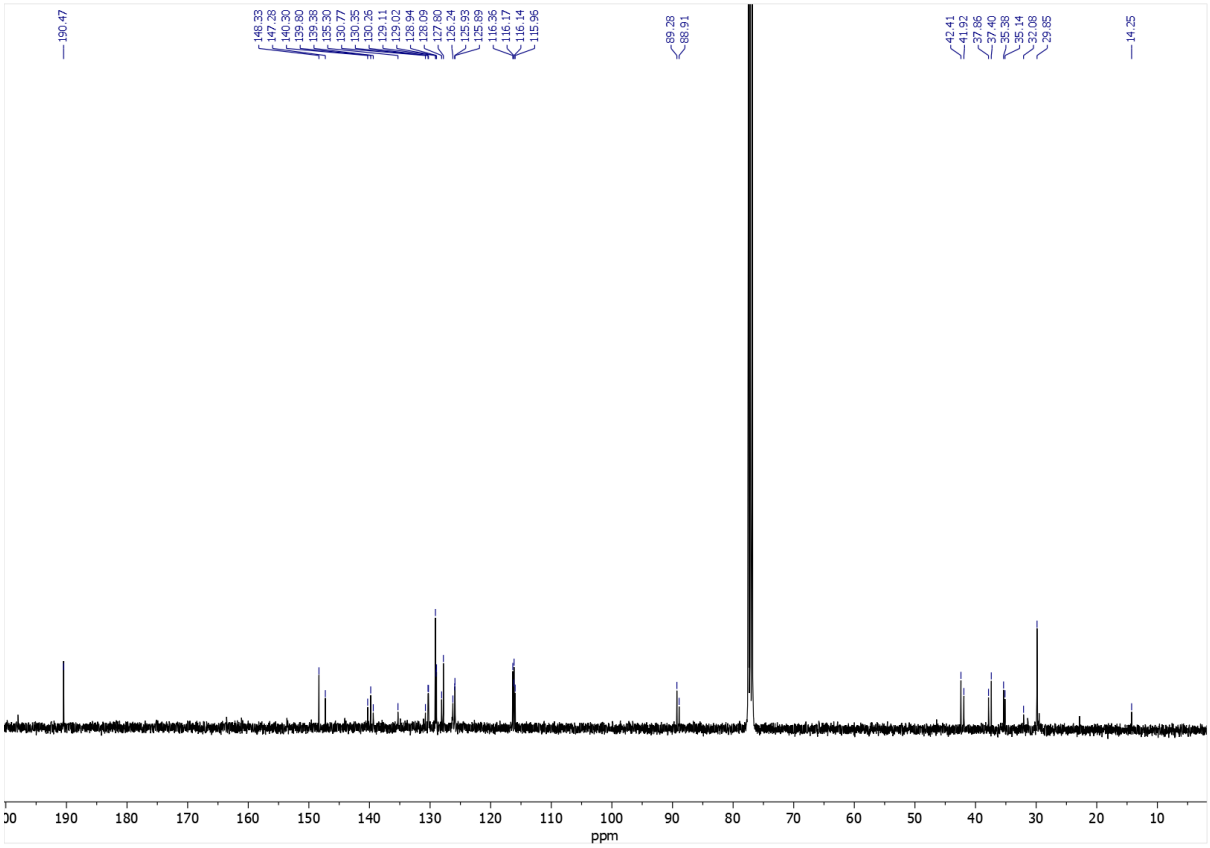

Figure S 34: : ^{13}C-NMR (101 MHz) spectrum of 5i' in $CDCl_3$.

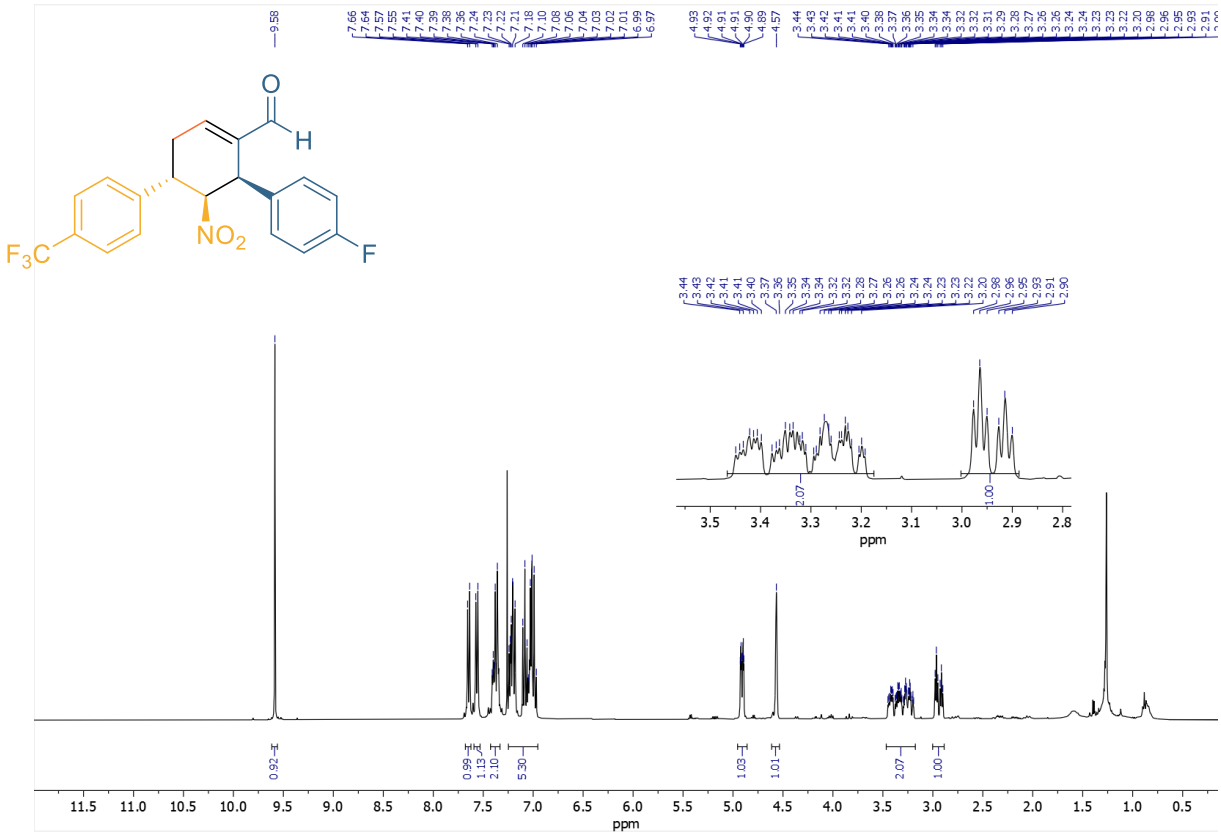

Figure S 35: ^{1}H-NMR (400 MHz) spectrum of 5i'' in $CDCl_3$.

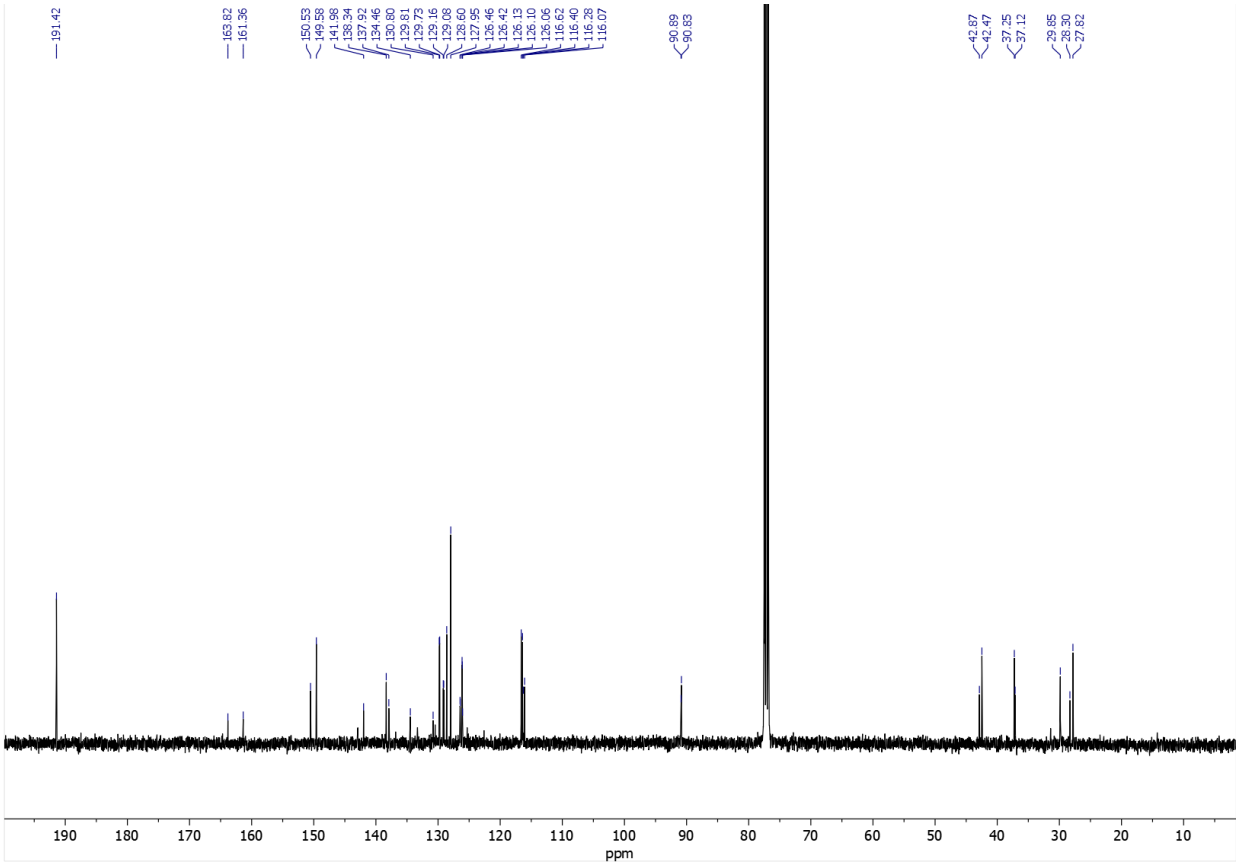

Figure S 36: : ^{13}C-NMR (101 MHz) spectrum of 5i'' in $CDCl_3$.

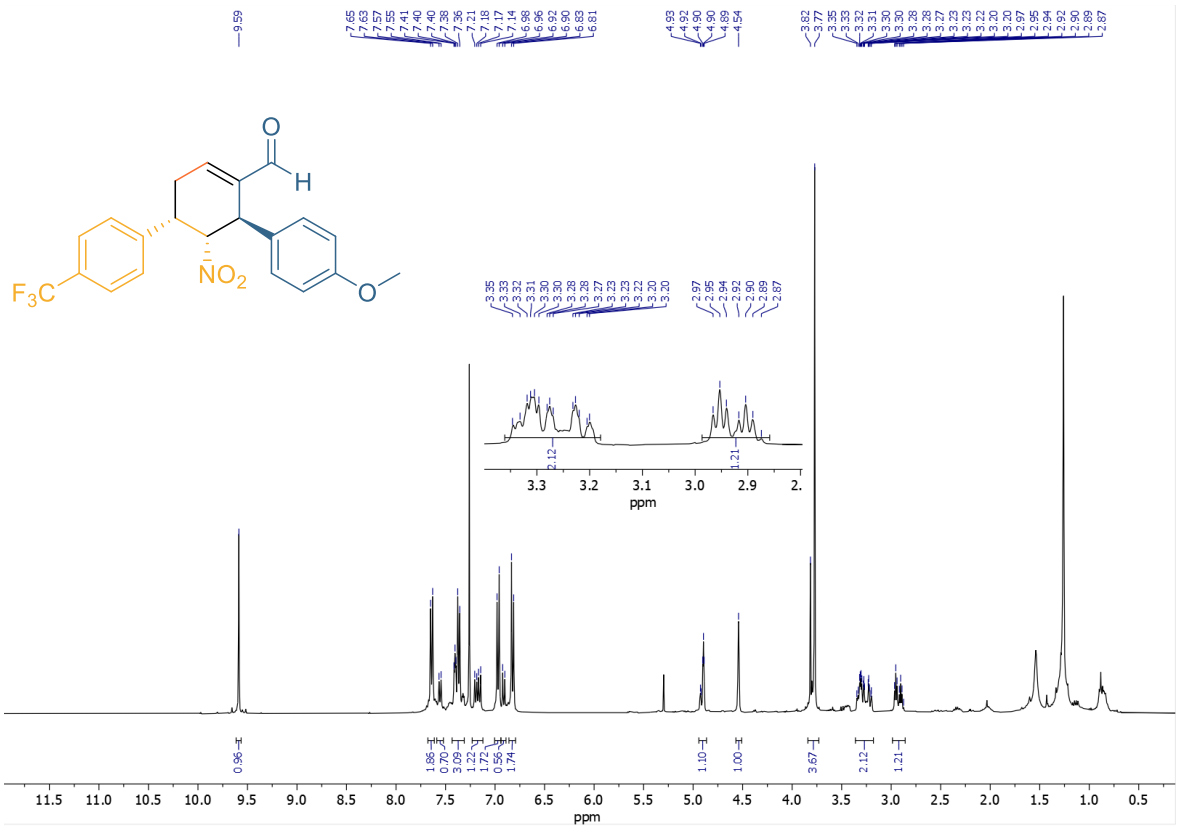

Figure S 37: ^{1}H-NMR (400 MHz) spectrum of 5j' in $CDCl_3$.

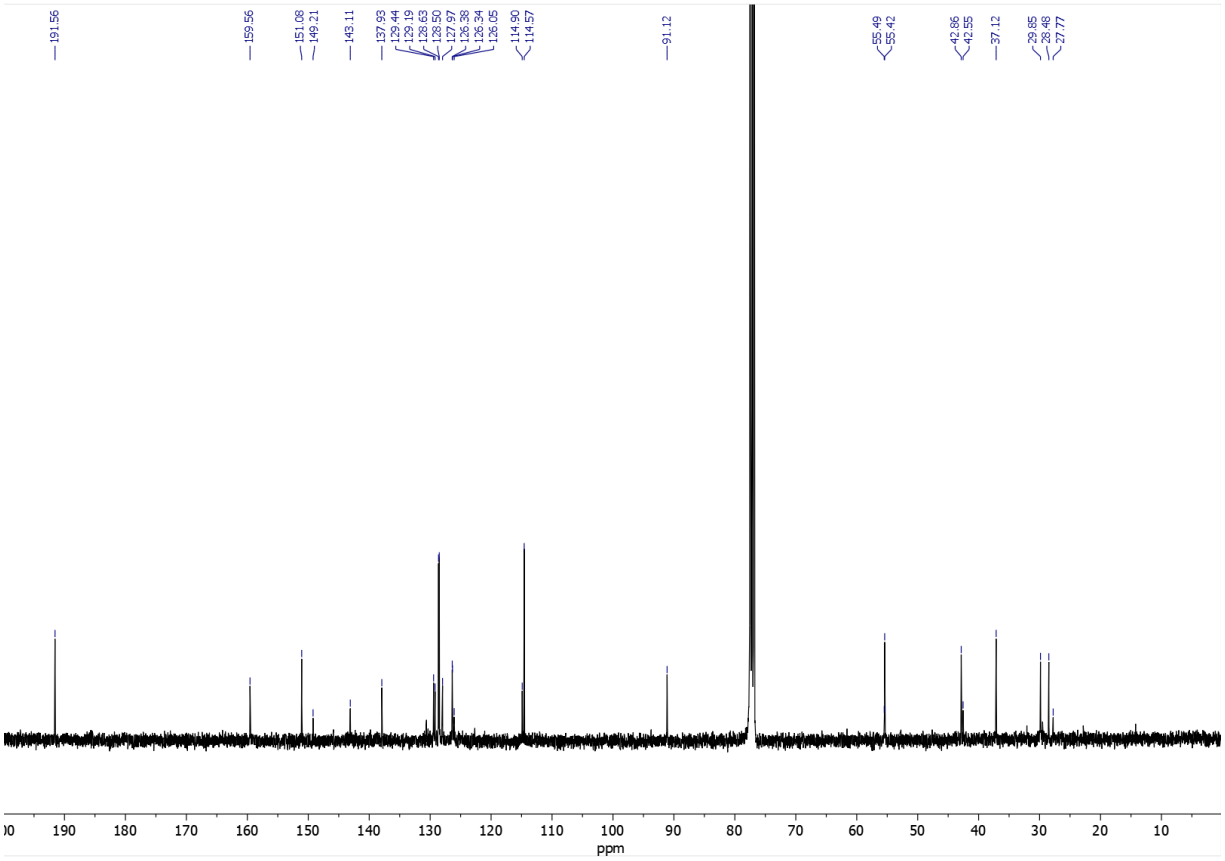

Figure S 38: ^{13}C-NMR (101 MHz) spectrum of 5j' in $CDCl_3$.

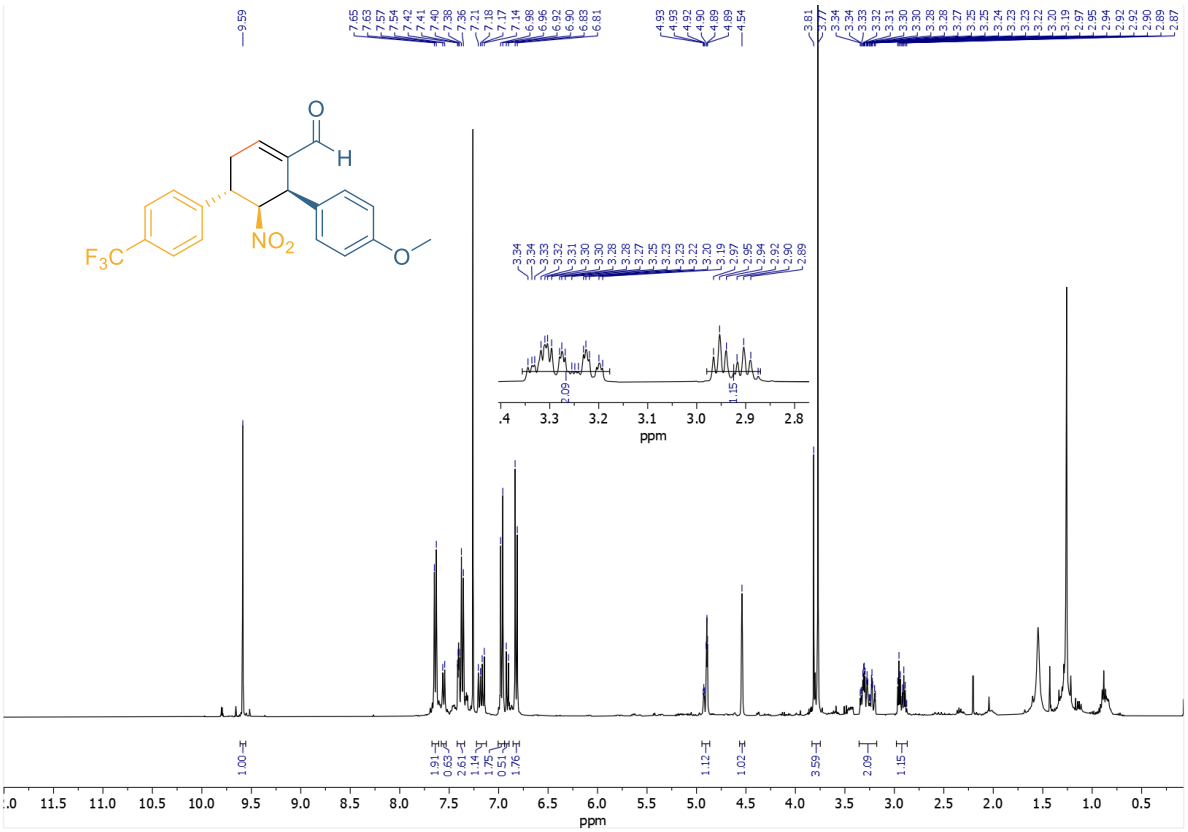

Figure S 39: ^{1}H-NMR (400 MHz) spectrum of 5j'' in $CDCl_3$.

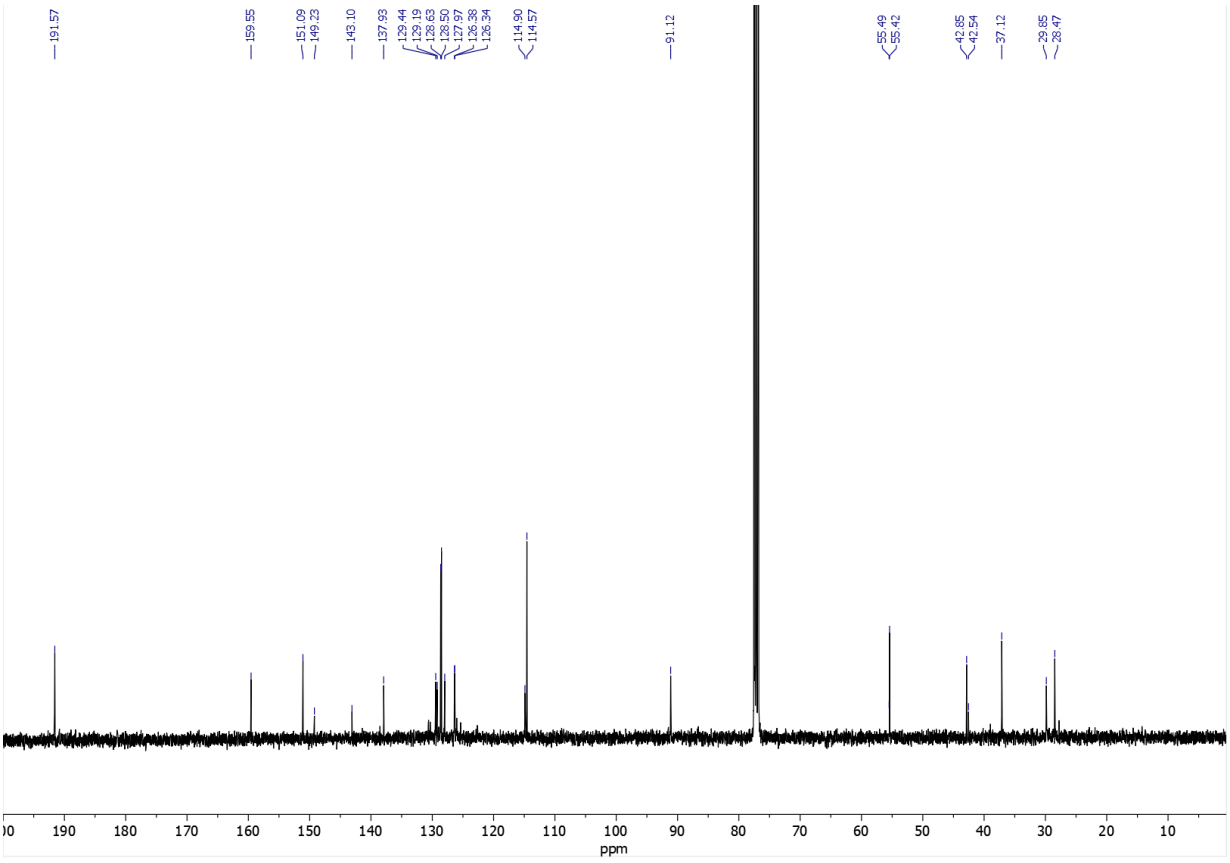

Figure S 40: ^{13}C-NMR (101 MHz) spectrum of 5j'' in $CDCl_3$.

HPLC spectra

5a’

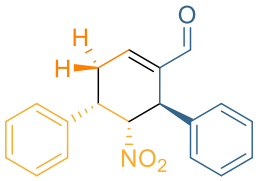

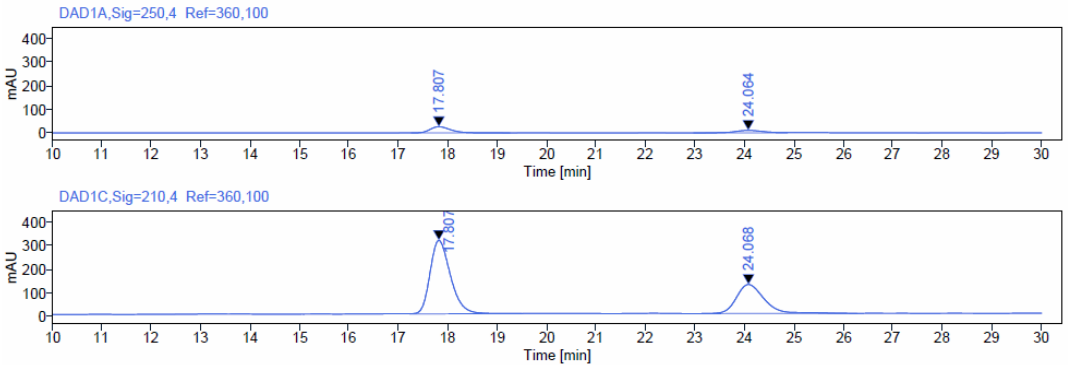

5a’ – Racemic sample

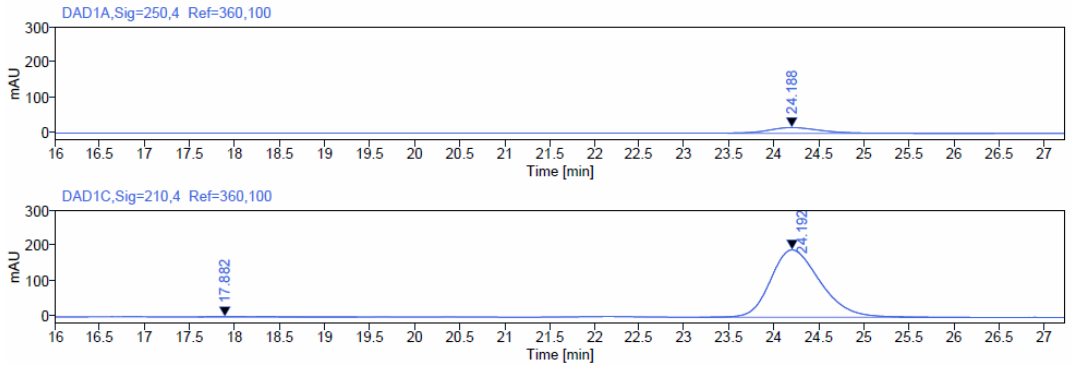

Signal: DAD1A,Sig=250,4 Ref=360,100

RT [min]	Type	Width [min]	Area	Height	Area%	Name
24.188	BB	3.35	660.58	16.22	100.00	
		Sum	660.58			

Signal: DAD1C,Sig=210,4 Ref=360,100

RT [min]	Type	Width [min]	Area	Height	Area%	Name
17.882	MM m	0.63	18.36	0.34	0.25	
24.192	BB	3.22	7378.80	191.59	99.75	
		Sum	7397.16			

5a’ - Enantioenriched sample

5a’’

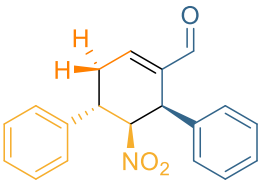

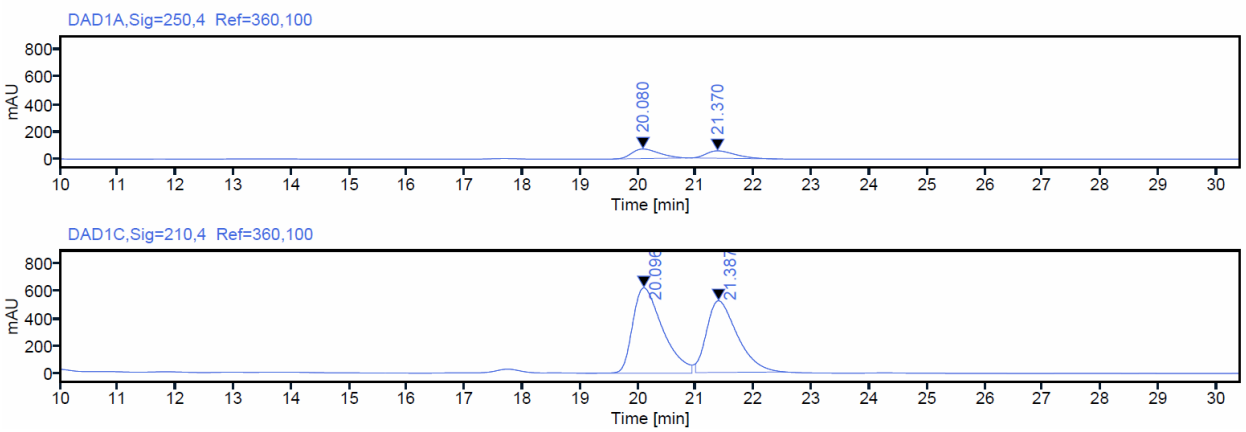

5a'' – Racemic sample

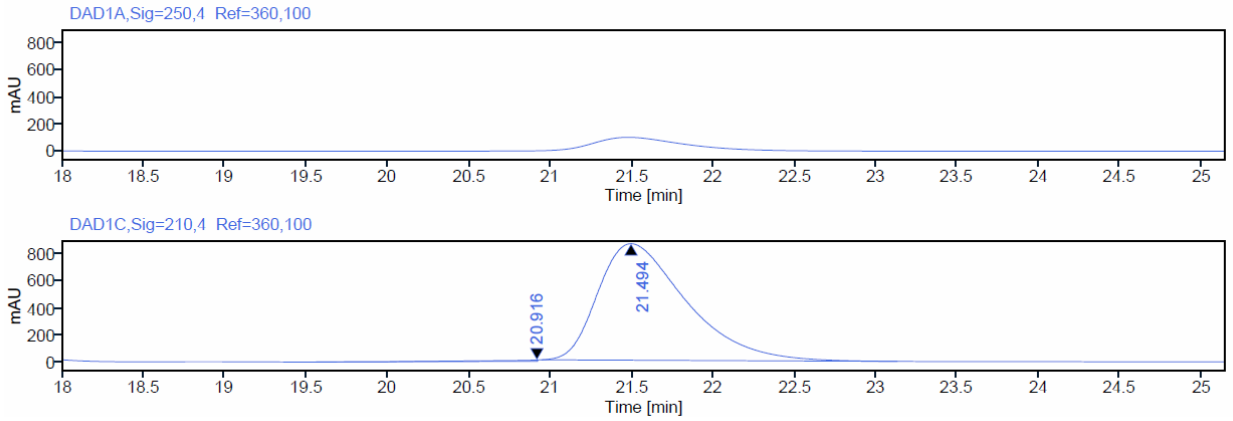

Signal: DAD1C,Sig=210,4 Ref=360,100

RT [min]	Type	Width [min]	Area	Height	Area%	Name
20.916	MM m	0.38	214.91	9.53	0.66	
21.494	MM m	0.57	32481.50	864.03	99.34	
		Sum	32696.41			

5a'' – Enantioenriched sample

5b'

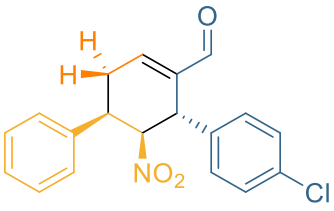

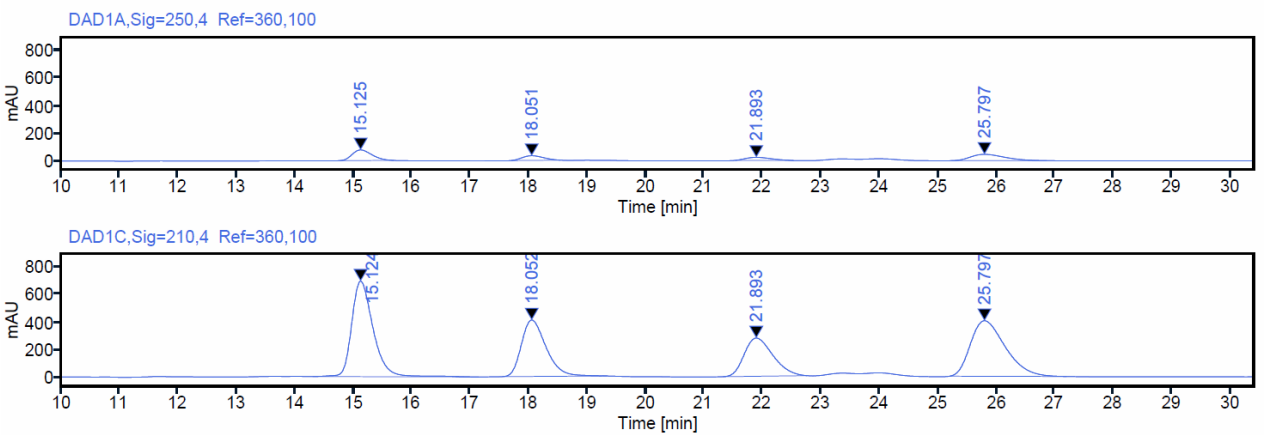

5b' – Racemic sample

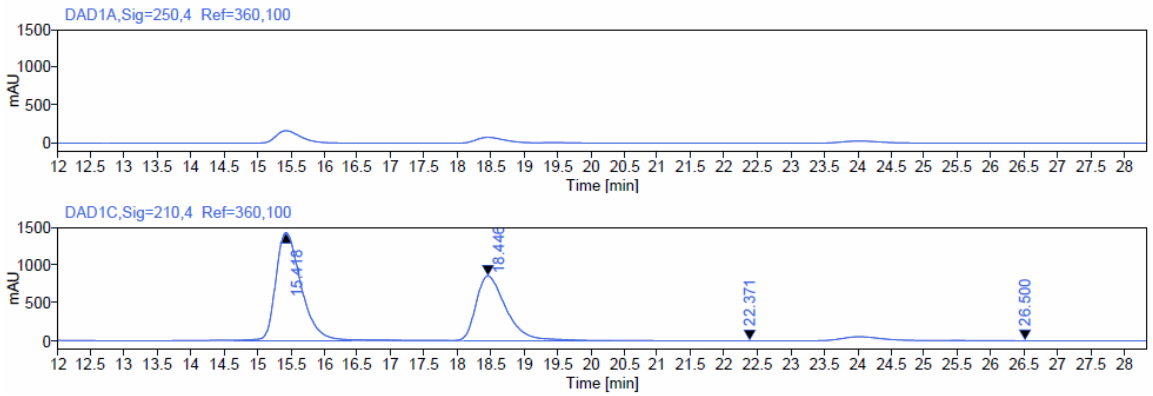

Signal: DAD1C,Sig=210,4 Ref=360,100

RT [min]	Type	Width [min]	Area	Height	Area%	Name
15.418	VB	2.90	38149.50	1426.22	58.63	
18.446	BV	2.78	26792.30	851.99	41.17	
22.371	MM n	0.22	8.25	0.45	0.01	
26.500	MM n	0.91	122.36	1.57	0.19	
		Sum	65072.41			

5b' – Enantioenriched sample

5b''

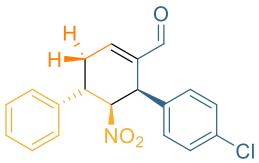

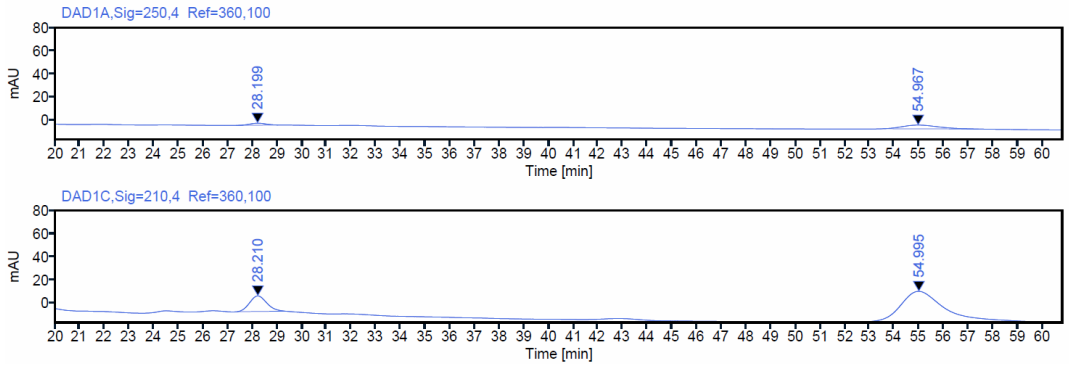

5b'' – Racemic sample

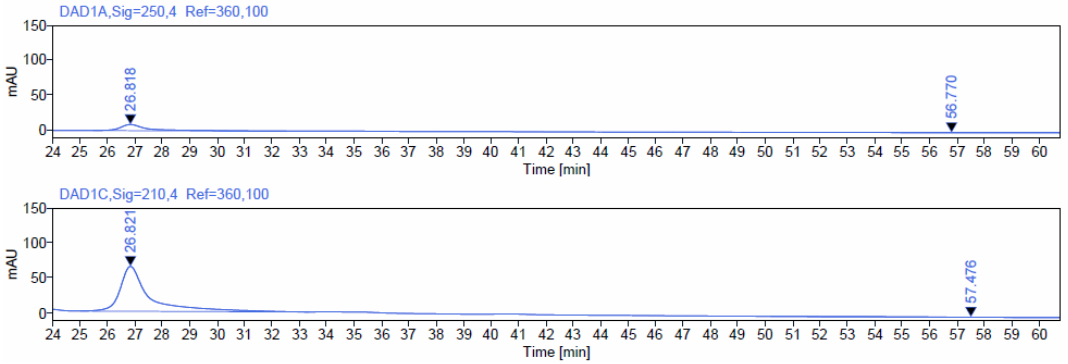

Signal: DAD1A,Sig=250,4 Ref=360,100

RT [min]	Type	Width [min]	Area	Height	Area%	Name
26.818	BB	7.05	606.35	8.72	99.01	
56.770	MM n	2.98	6.05	0.03	0.99	
		Sum	612.41			

Signal: DAD1C,Sig=210,4 Ref=360,100

RT [min]	Type	Width [min]	Area	Height	Area%	Name
26.821	BB	8.33	4757.97	64.08	99.43	
57.476	MM n	3.12	27.30	0.15	0.57	
		Sum	4785.27			

5b'' – Enantioenriched sample

5c'

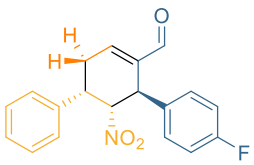

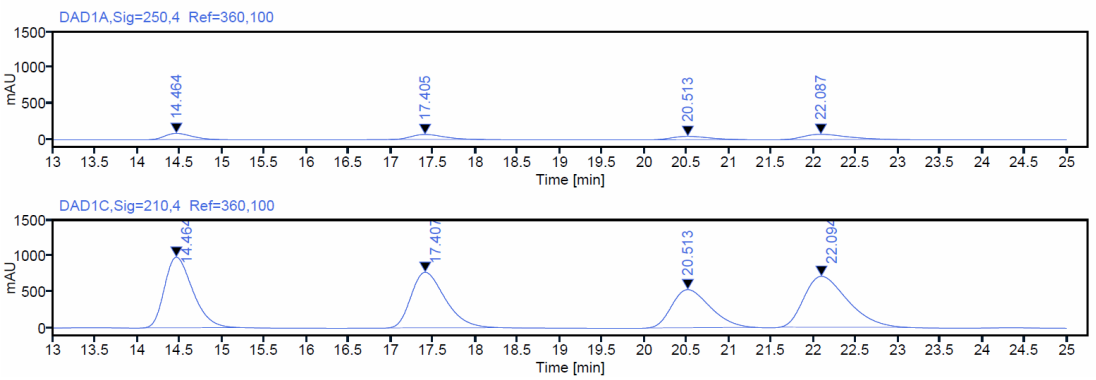

5c' – Racemic sample

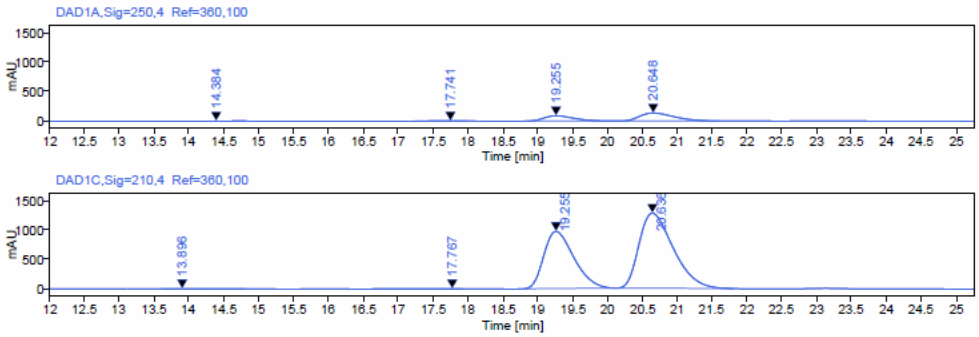

Signal: DAD1A,Sig=250,4 Ref=360,100

RT [min]	Type	Width [min]	Area	Height	Area%	Name
14.384	MM n	0.30	12.80	0.70	0.18	
17.741	MM m	0.13	9.14	1.58	0.13	
19.255	MM m	0.46	2605.63	88.39	35.75	
20.648	MM m	0.53	4661.82	136.36	63.95	
		Sum	7289.38			

Signal: DAD1C,Sig=210,4 Ref=360,100

RT [min]	Type	Width [min]	Area	Height	Area%	Name
13.896	MM m	0.28	68.29	3.53	0.09	
17.767	MM m	0.19	17.81	1.19	0.02	
19.255	MM m	0.46	29162.10	974.94	39.93	
20.636	MM m	0.53	43786.03	1281.22	59.95	
		Sum	73034.22			

5c' - Enantioenriched sample

5c''

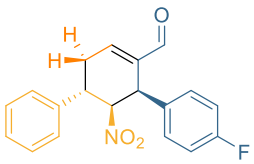

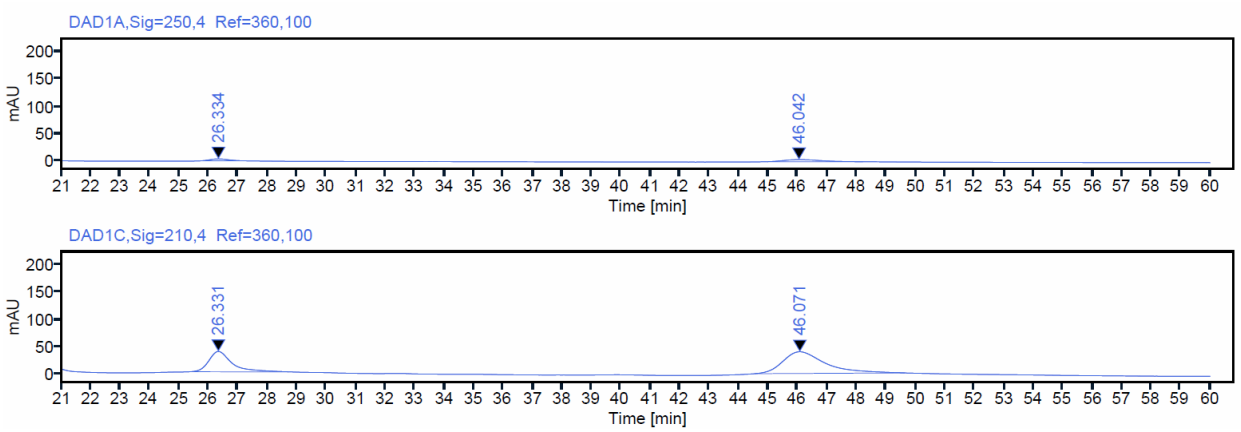

5c'' – Racemic sample

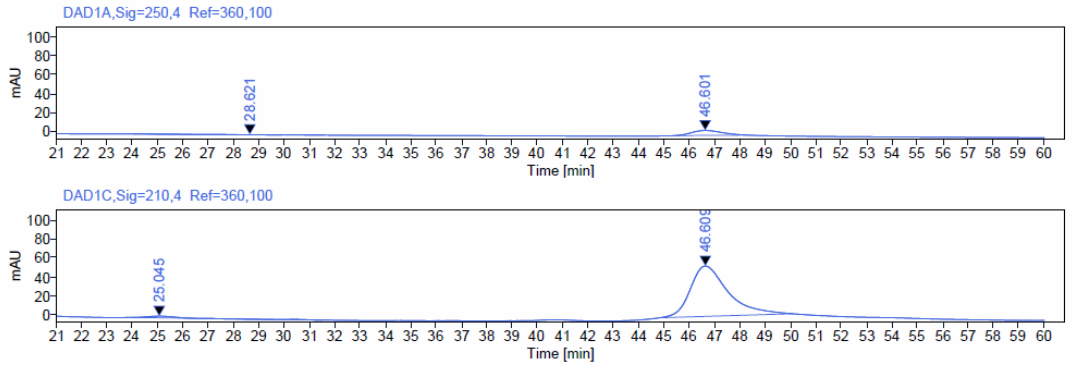

Signal: DAD1A,Sig=250,4 Ref=360,100

RT [min]	Type	Width [min]	Area	Height	Area%	Name
28.621	MM n	1.26	9.57	0.13	2.16	
46.601	MM m	0.98	434.16	5.23	97.84	
		Sum	443.73			

Signal: DAD1C,Sig=210,4 Ref=360,100

RT [min]	Type	Width [min]	Area	Height	Area%	Name
25.045	MM m	0.78	120.04	1.82	2.11	
46.609	MM m	1.39	5563.08	53.84	97.89	
		Sum	5683.12			

5c'' – Enantioenriched sample

5d'

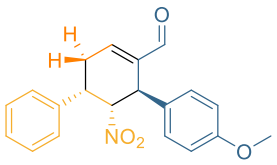

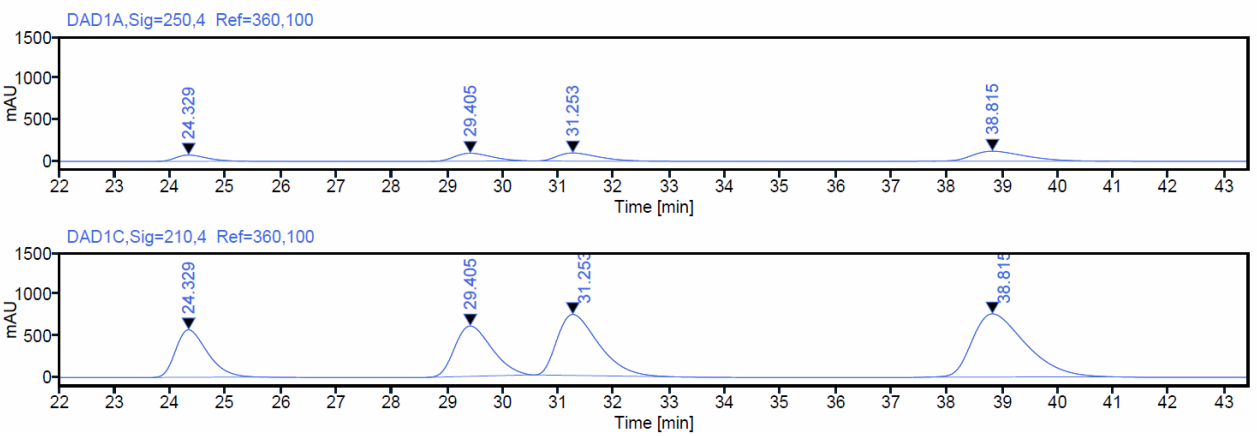

5d' – Racemic sample

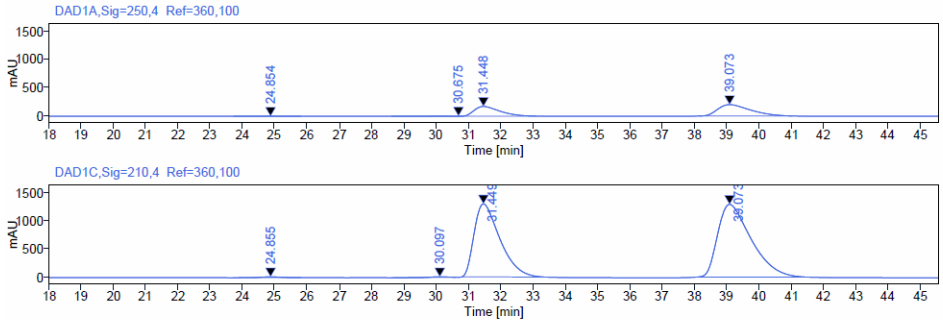

Signal: DAD1A,Sig=250,4 Ref=360,100

RT [min]	Type	Width [min]	Area	Height	Area%	Name
24.854	MM m	0.53	82.79	2.07	0.35	
30.675	MM n	0.67	82.84	2.07	0.35	
31.448	MM m	0.83	9352.40	171.93	39.37	
39.073	MM m	1.07	14234.94	203.13	59.93	
		Sum	23752.97			

Signal: DAD1C,Sig=210,4 Ref=360,100

RT [min]	Type	Width [min]	Area	Height	Area%	Name
24.855	MM m	0.58	615.48	15.40	0.37	
30.097	MM m	0.47	324.54	10.96	0.20	
31.449	MM m	0.84	71934.70	1296.17	43.52	
39.073	MM m	1.05	92400.15	1289.73	55.91	
		Sum	165274.87			

5d' – Enantioenriched sample

5d''

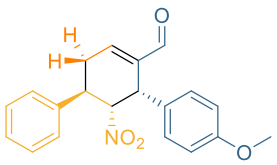

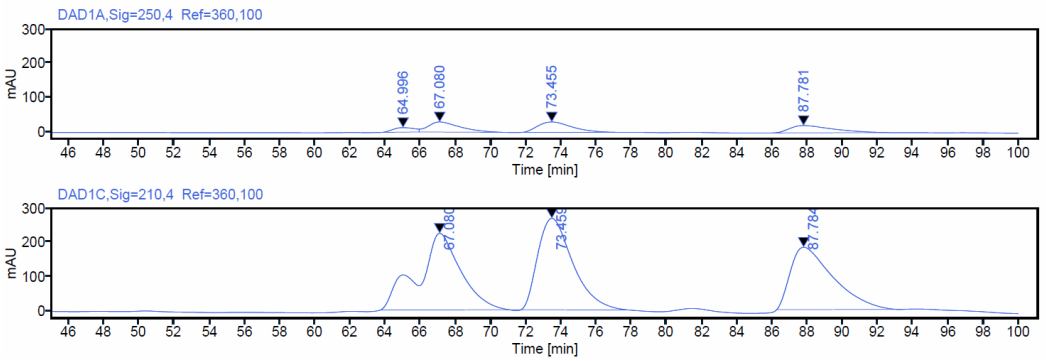

5d'' – Racemic sample

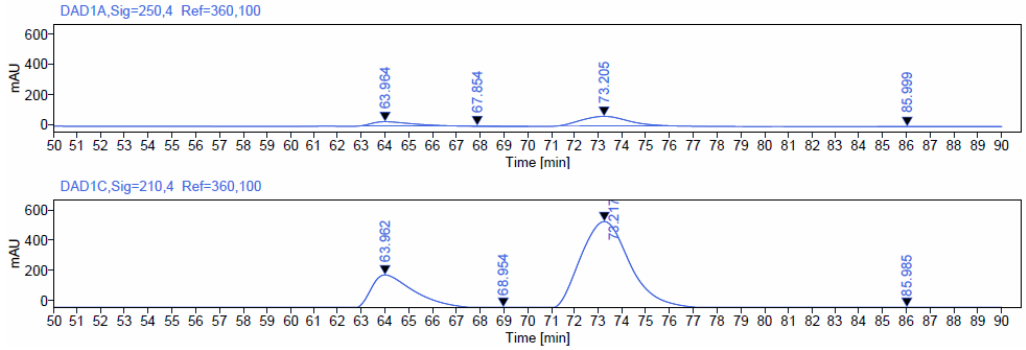

Signal: DAD1A,Sig=250,4 Ref=360,100

RT [min]	Type	Width [min]	Area	Height	Area%	Name
63.964	MM m	1.50	2989.23	27.27	26.02	
67.854	MM n	2.11	208.03	1.64	1.81	
73.205	MM m	1.88	8264.25	62.30	71.94	
85.999	MM m	1.21	26.73	0.26	0.23	
		Sum	11488.24			

Signal: DAD1C,Sig=210,4 Ref=360,100

RT [min]	Type	Width [min]	Area	Height	Area%	Name
63.962	MM m	1.82	28399.08	224.18	25.16	
68.954	MM n	1.28	141.37	1.84	0.13	
73.217	MM m	2.24	84143.74	581.97	74.54	
85.985	MM m	1.12	196.71	2.06	0.17	
		Sum	112880.90			

5d'' – Enantioenriched sample

5e'

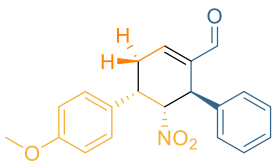

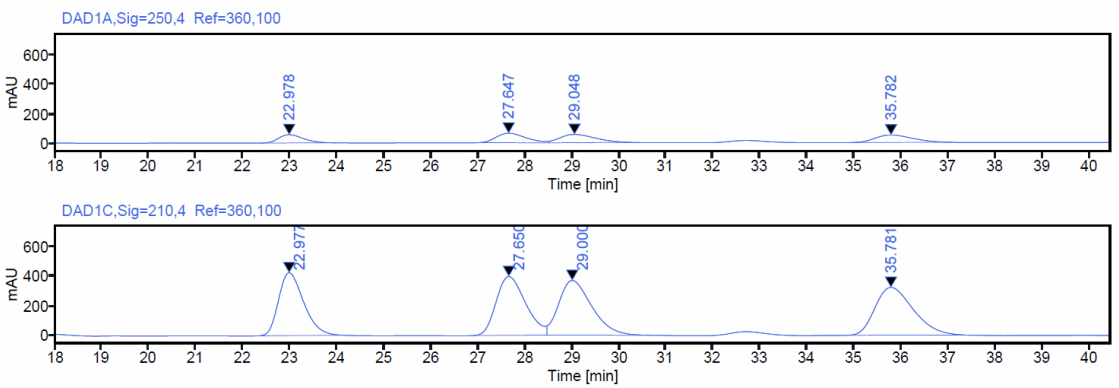

5e' – Racemic sample

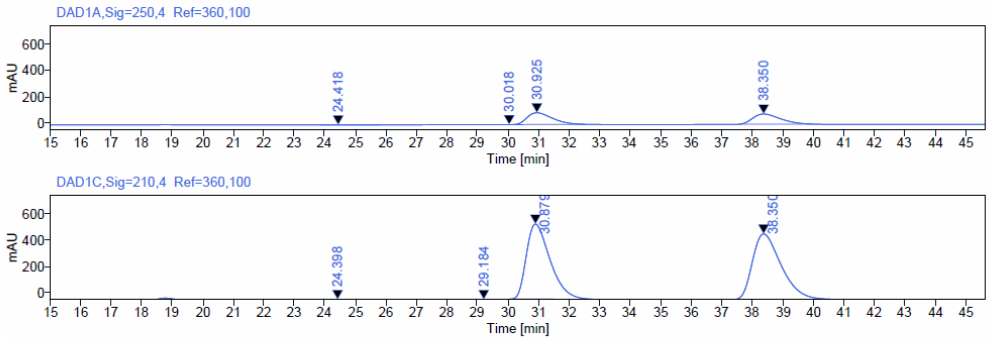

Signal: DAD1A,Sig=250,4 Ref=360,100

RT [min]	Type	Width [min]	Area	Height	Area%	Name
24.418	MM m	0.68	9.25	0.23	0.09	
30.018	MM n	0.30	3.16	0.18	0.03	
30.925	MM m	0.89	5150.29	90.07	51.30	
38.350	MM m	0.96	4877.54	78.51	48.58	
		Sum	10040.23			

Signal: DAD1C,Sig=210,4 Ref=360,100

RT [min]	Type	Width [min]	Area	Height	Area%	Name
24.398	MM m	0.54	69.44	1.53	0.11	
29.184	MM n	0.40	16.40	0.69	0.03	
30.879	MM m	0.83	31083.40	577.04	48.79	
38.350	MM m	0.99	32544.61	502.70	51.08	
		Sum	63713.84			

5e' – Enantioenriched sample

5e''

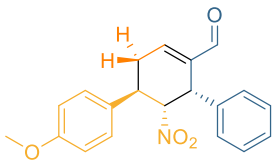

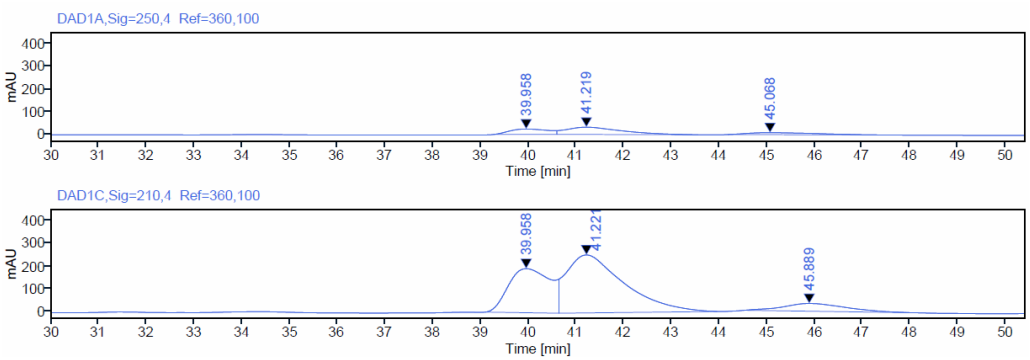

5e'' – Racemic sample

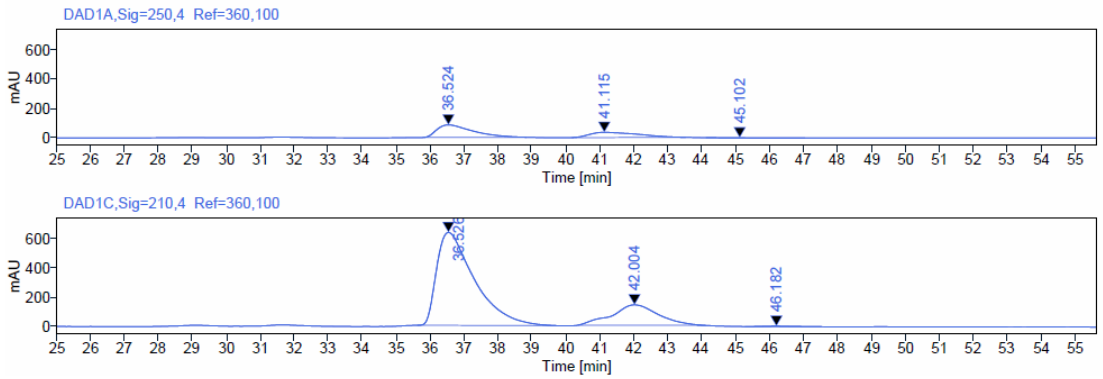

Signal: DAD1A,Sig=250,4 Ref=360,100

RT [min]	Type	Width [min]	Area	Height	Area%	Name
36.524	MM m	1.08	6373.19	86.51	63.62	
41.115	MM m	1.34	3589.18	36.15	35.83	
45.102	MM n	1.23	54.87	0.75	0.55	
		Sum	10017.25			

Signal: DAD1C,Sig=210,4 Ref=360,100

RT [min]	Type	Width [min]	Area	Height	Area%	Name
36.526	MM m	1.13	49559.88	641.56	78.49	
42.004	MM m	1.37	13392.49	140.92	21.21	
46.182	MM m	0.73	185.27	3.03	0.29	
		Sum	63137.63			

5e'' – Enantioenriched sample

5f’

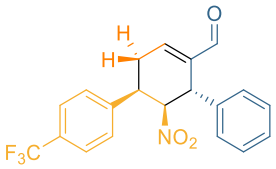

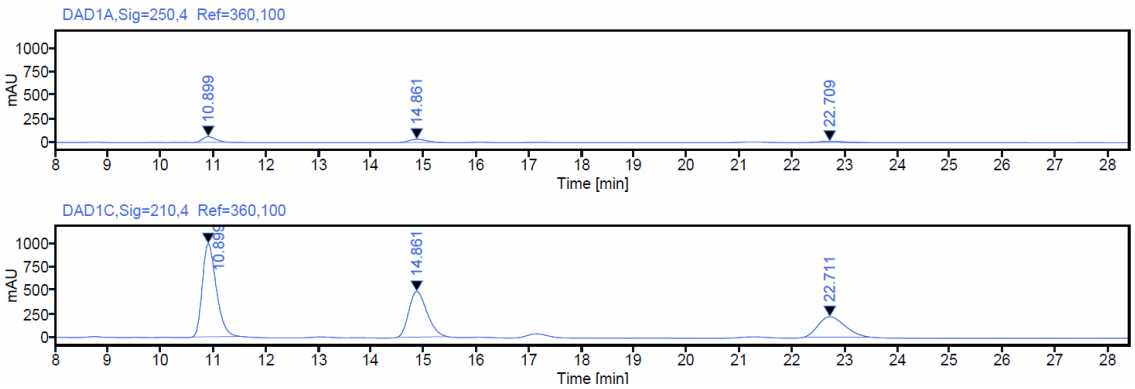

5f’ – Racemic sample

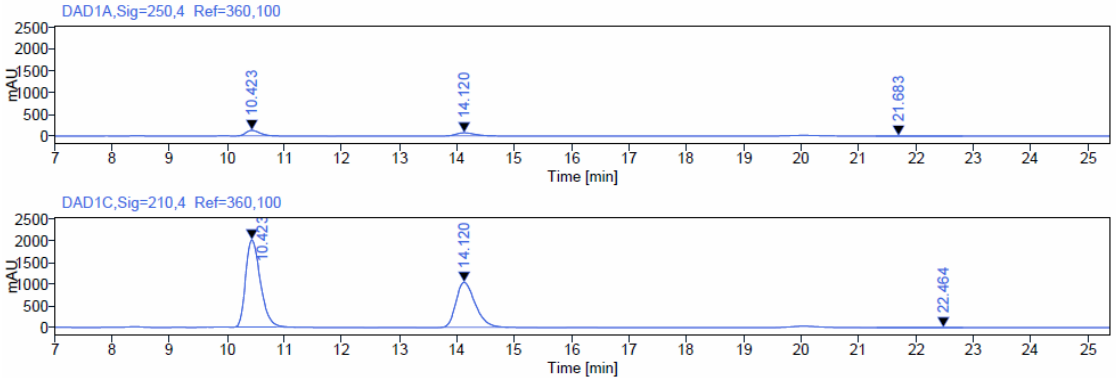

Signal: DAD1A,Sig=250,4 Ref=360,100

RT [min]	Type	Width [min]	Area	Height	Area%	Name
10.423	MM m	0.26	2173.03	129.24	57.24	
14.120	MM m	0.35	1619.06	73.25	42.64	
21.683	MM n	0.40	4.52	0.14	0.12	
		Sum	3796.60			

Signal: DAD1C,Sig=210,4 Ref=360,100

RT [min]	Type	Width [min]	Area	Height	Area%	Name
10.423	MM m	0.28	35949.17	2017.81	59.77	
14.120	MM m	0.36	24163.00	1043.40	40.17	
22.464	MM n	1.19	32.82	0.32	0.05	
		Sum	60144.99			

5f’ – Enantioenriched sample

5f’’

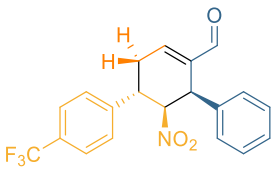

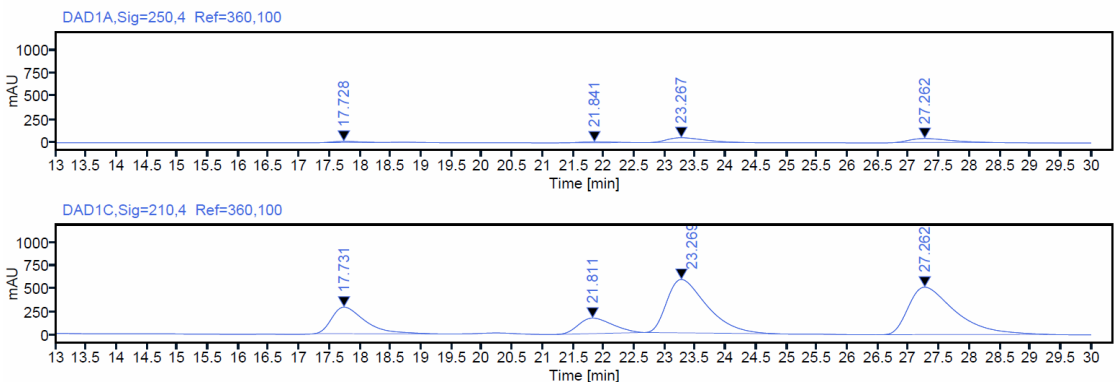

5f’’ – Racemic sample

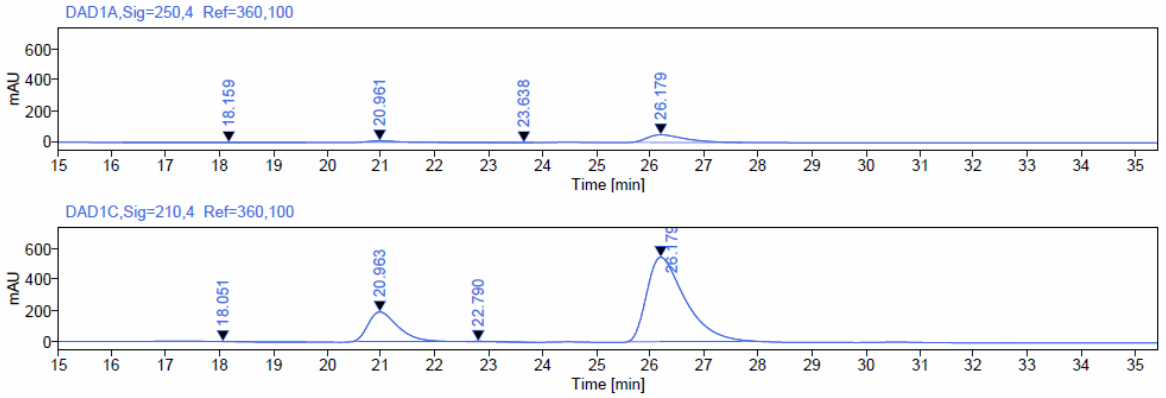

Signal: DAD1A,Sig=250,4 Ref=360,100

RT [min]	Type	Width [min]	Area	Height	Area%	Name
18.159	MM m	0.73	34.55	0.56	1.26	
20.961	MM m	0.51	310.76	9.40	11.35	
23.638	MM n	1.70	27.98	0.19	1.02	
26.179	MM m	0.71	2365.49	49.64	86.37	
		Sum	2738.78			

Signal: DAD1C,Sig=210,4 Ref=360,100

RT [min]	Type	Width [min]	Area	Height	Area%	Name
18.051	MM m	0.34	46.53	2.31	0.13	
20.963	MM m	0.58	7372.88	193.62	21.29	
22.790	MM m	0.40	92.00	2.85	0.27	
26.179	MM m	0.74	27120.62	551.02	78.31	
		Sum	34632.03			

5f'' – Enantioenriched sample

5g'

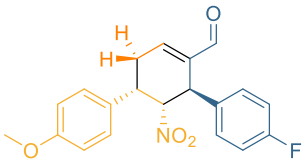

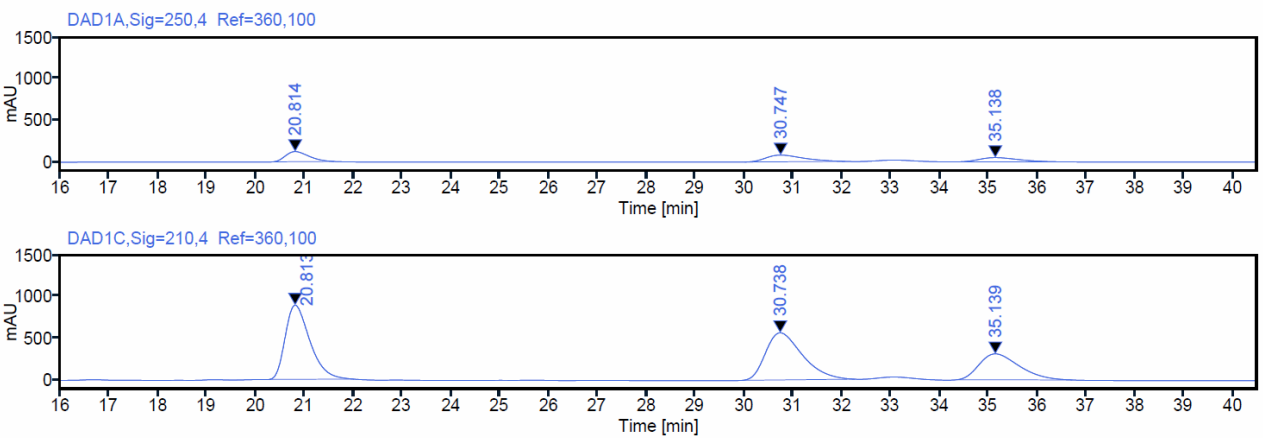

5g' – Racemic sample

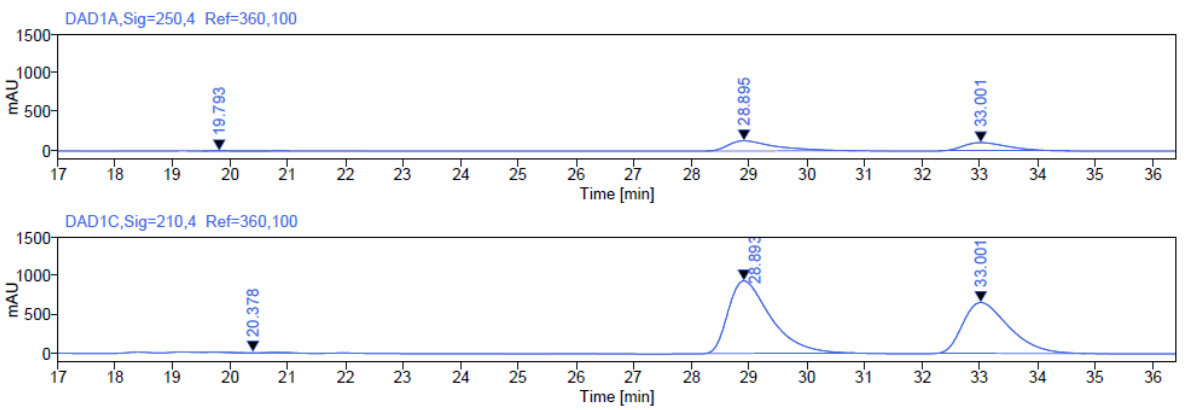

Signal: DAD1A,Sig=250,4 Ref=360,100

RT [min]	Type	Width [min]	Area	Height	Area%	Name
19.793	MM m	0.04	1.78	0.86	0.01	
28.895	MM m	0.83	7307.86	130.51	55.61	
33.001	MM m	0.84	5832.47	107.14	44.38	
		Sum	13142.10			

Signal: DAD1C,Sig=210,4 Ref=360,100

RT [min]	Type	Width [min]	Area	Height	Area%	Name
20.378	MM n	0.13	4.59	7.06	0.01	
28.893	MM m	0.77	47444.52	931.69	56.80	
33.001	MM m	0.85	36087.17	653.24	43.20	
		Sum	83536.29			

5g' – Enantioenriched sample

5g''

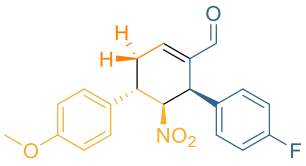

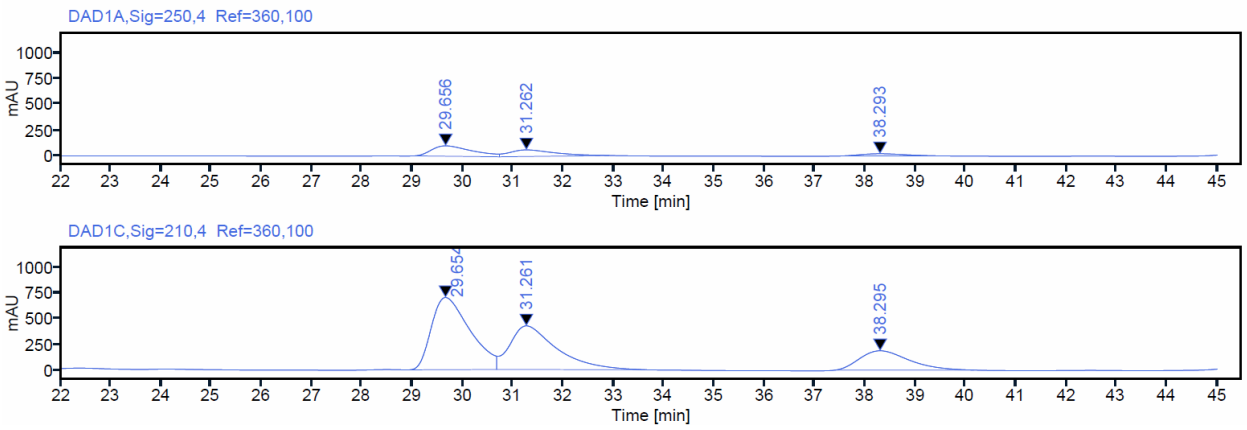

5g'' – Racemic sample

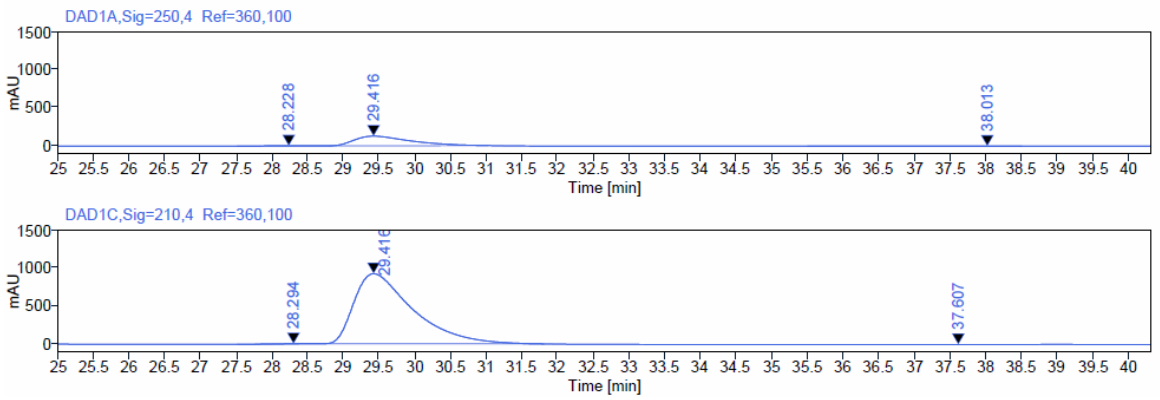

Signal: DAD1A,Sig=250,4 Ref=360,100

RT [min]	Type	Width [min]	Area	Height	Area%	Name
28.228	MM m	0.20	13.12	1.08	0.19	
29.416	MM m	0.82	6828.19	126.14	99.54	
38.013	MM n	1.03	18.19	0.21	0.27	
		Sum	6859.50			

Signal: DAD1C,Sig=210,4 Ref=360,100

RT [min]	Type	Width [min]	Area	Height	Area%	Name
28.294	MM m	0.24	22.46	1.56	0.04	
29.416	MM m	0.85	52631.49	921.00	99.69	
37.607	MM n	1.35	142.18	1.24	0.27	
		Sum	52796.13			

5g'' – Enantioenriched sample

5h'

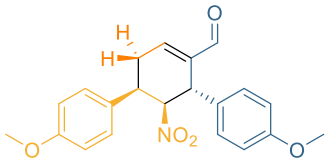

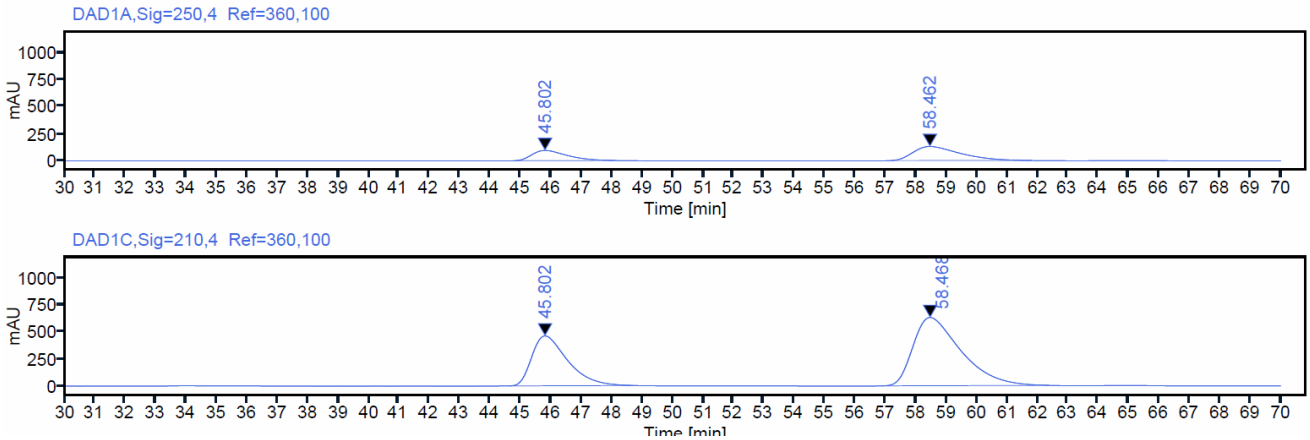

5h' – Racemic sample

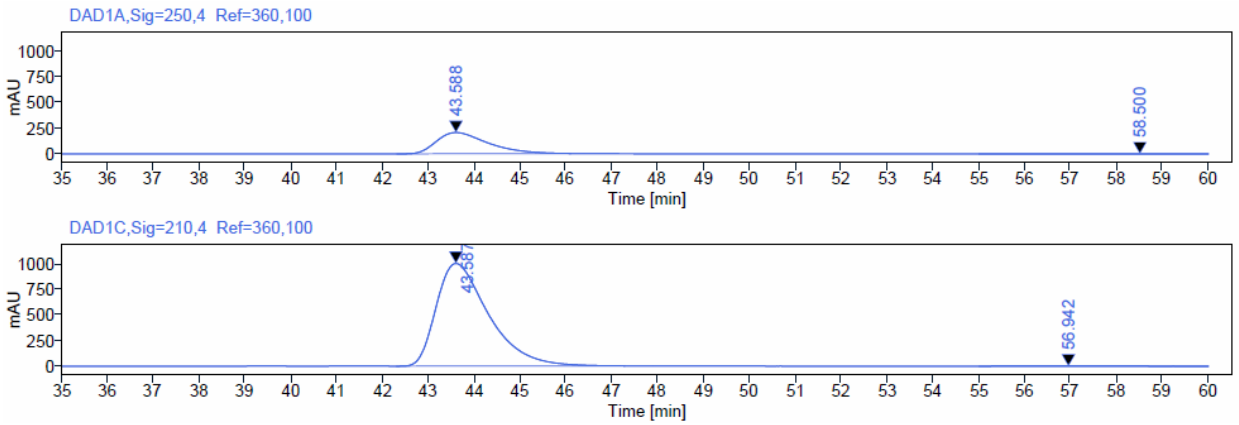

Signal: DAD1A,Sig=250,4 Ref=360,100

RT [min]	Type	Width [min]	Area	Height	Area%	Name
43.588	BM m	1.18	16173.44	208.34	99.85	
58.500	MM m	1.87	24.02	0.15	0.15	
		Sum	16197.45			

Signal: DAD1C,Sig=210,4 Ref=360,100

RT [min]	Type	Width [min]	Area	Height	Area%	Name
43.587	BM m	1.20	79886.47	1007.89	99.90	
56.942	MM m	1.69	81.35	0.56	0.10	
		Sum	79967.82			

5h' – Enantioenriched sample

5h''

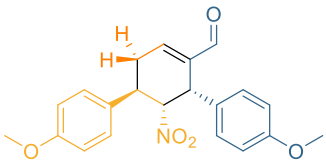

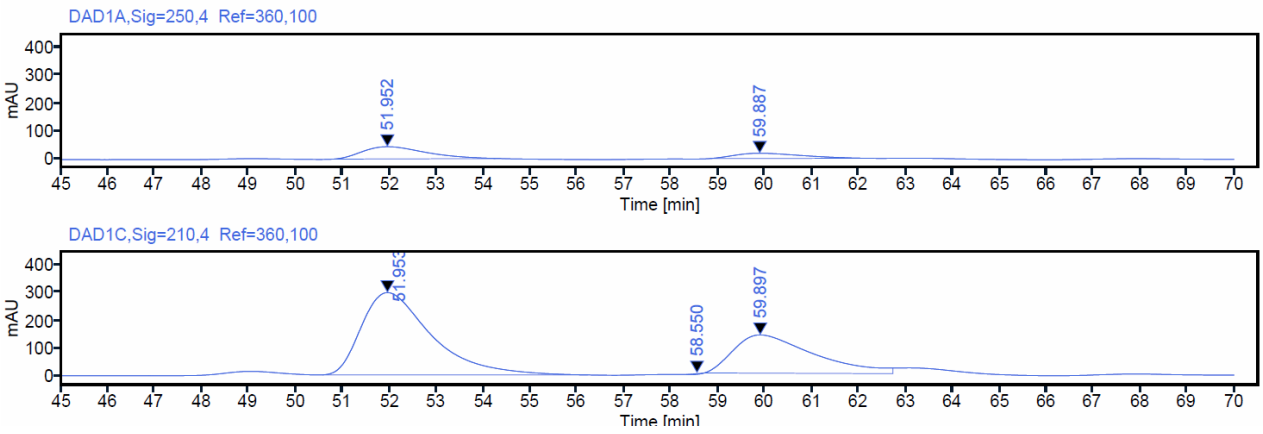

5h'' – Racemic sample

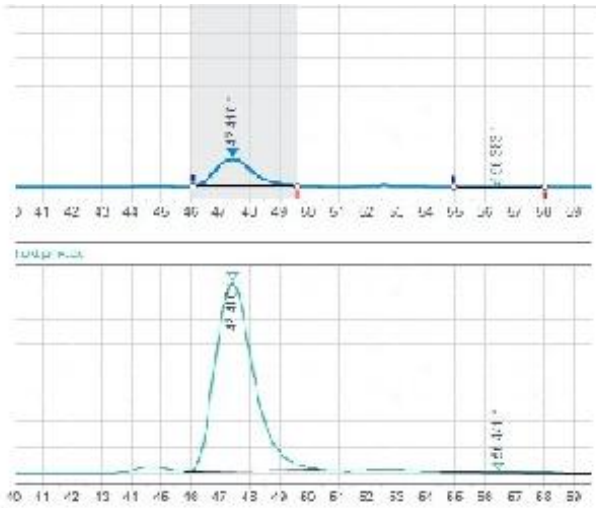

Signal: DAD1A,Sig=250,4 Ref=360,100

RT [min]	Type	Width [min]	Area	Height	Area%	Name
47.410	MM m	1.37	9719.53	110.51	99.95	
59.850	MM n	1.16	5.29	0.05	0.05	
		Sum	9724.82			

Signal: DAD1C,Sig=210,4 Ref=360,100

RT [min]	Type	Width [min]	Area	Height	Area%	Name
47.410	MM m	1.41	66247.48	727.78	99.54	
56.441	MM m	1.06	306.58	3.40	0.46	
		Sum	66554.06			

5h'' – Enantioenriched sample

5i'

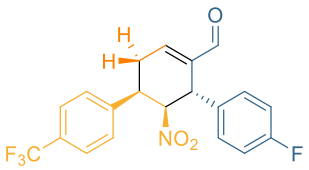

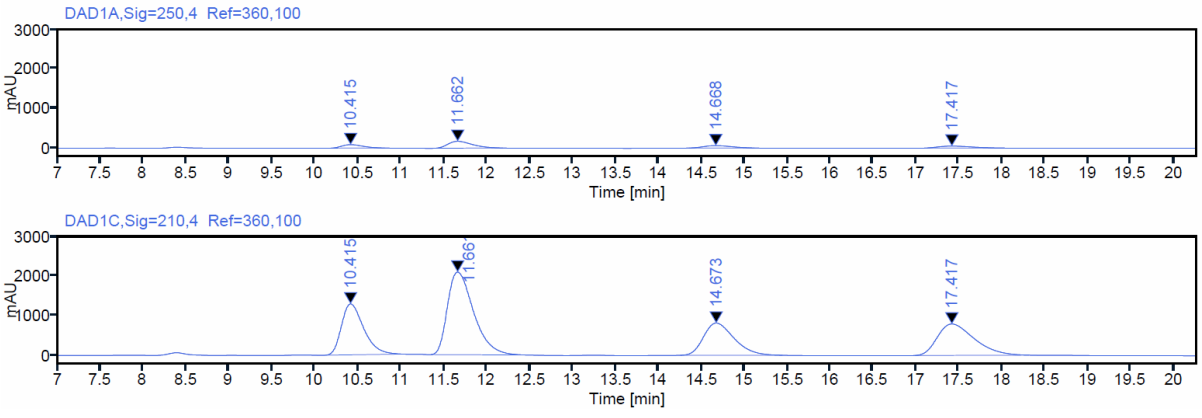

5i' – Racemic sample

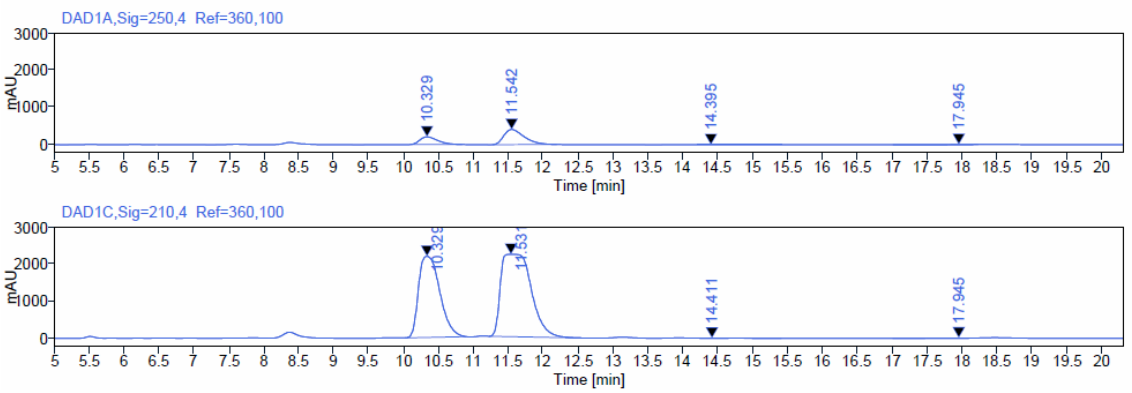

Signal: DAD1A,Sig=250,4 Ref=360,100

RT [min]	Type	Width [min]	Area	Height	Area%	Name
10.329	MM m	0.27	3630.48	205.74	30.27	
11.542	MM m	0.31	8229.88	405.87	68.61	
14.395	MM n	0.16	2.30	0.18	0.02	
17.945	MM n	0.67	132.23	3.30	1.10	
		Sum	11994.89			

Signal: DAD1C,Sig=210,4 Ref=360,100

RT [min]	Type	Width [min]	Area	Height	Area%	Name
10.329	MM m	0.33	46062.44	2180.57	40.63	
11.531	MM m	0.37	67041.17	2213.72	59.14	
14.411	MM n	0.23	35.99	2.66	0.03	
17.945	MM n	0.55	223.37	6.77	0.20	
		Sum	113362.97			

5i' – Enantioenriched sample

5i''

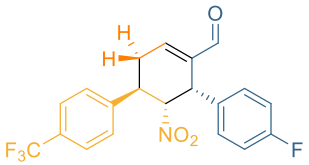

5i

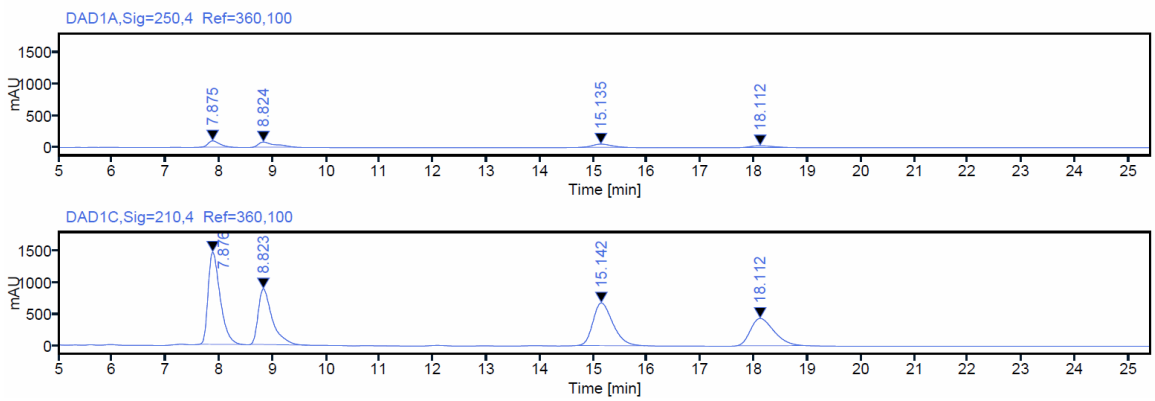

5i'' – Racemic sample

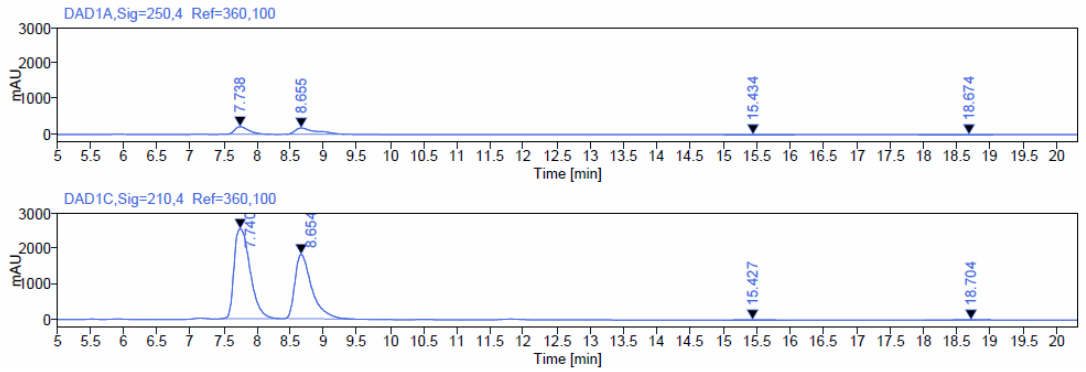

Signal: DAD1A,Sig=250,4 Ref=360,100

RT [min]	Type	Width [min]	Area	Height	Area%	Name
7.738	MM m	0.22	3108.90	212.79	44.40	
8.655	MM m	0.31	3880.17	177.77	55.41	
15.434	MM m	0.28	7.13	0.30	0.10	
18.674	MM m	0.31	6.26	0.25	0.09	
		Sum	7002.45			

Signal: DAD1C,Sig=210,4 Ref=360,100

RT [min]	Type	Width [min]	Area	Height	Area%	Name
7.740	MM m	0.26	42136.29	2521.36	56.94	
8.654	MM m	0.27	31735.90	1808.05	42.89	
15.427	MM m	0.36	78.44	3.22	0.11	
18.704	MM m	0.31	47.46	2.11	0.06	
		Sum	73998.09			

5i'' – Enantioenriched sample

5j'

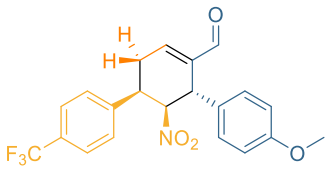

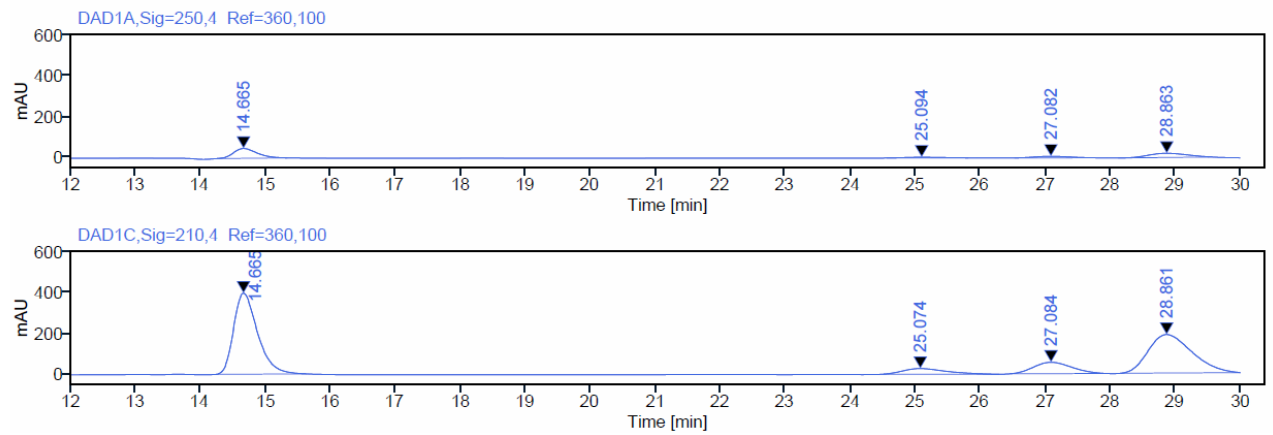

5j' - Racemic sample

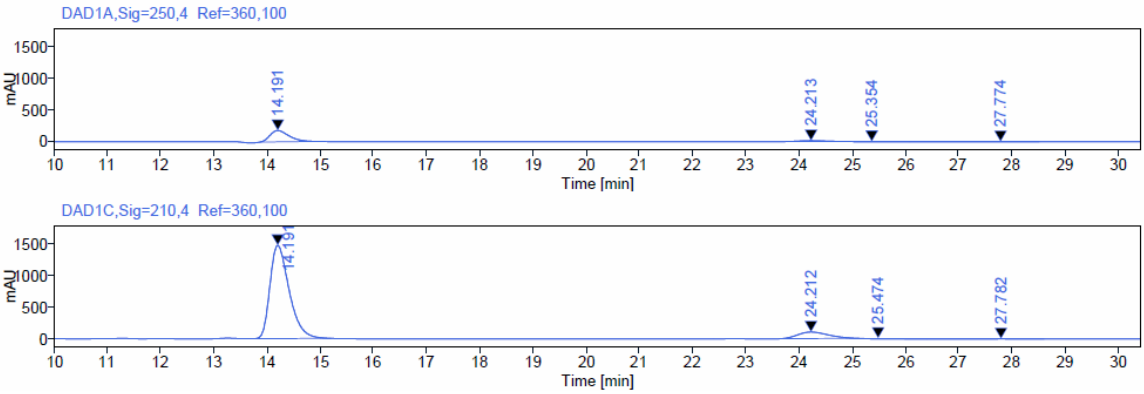

Signal: DAD1A,Sig=250,4 Ref=360,100

RT [min]	Type	Width [min]	Area	Height	Area%	Name
14.191	MM m	0.38	4414.69	179.51	91.98	
24.213	MM m	0.50	342.19	11.39	7.13	
25.354	MM n	0.65	28.39	0.73	0.59	
27.774	MM m	0.56	14.29	0.30	0.30	
		Sum	4799.56			

Signal: DAD1C,Sig=210,4 Ref=360,100

RT [min]	Type	Width [min]	Area	Height	Area%	Name
14.191	MM m	0.39	37107.66	1477.53	89.28	
24.212	MM m	0.63	4087.80	102.87	9.84	
25.474	MM n	0.81	222.17	4.55	0.53	
27.782	MM m	0.60	146.16	2.90	0.35	
		Sum	41563.79			

5j' – Enantioenriched sample

5j''

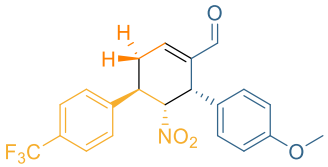

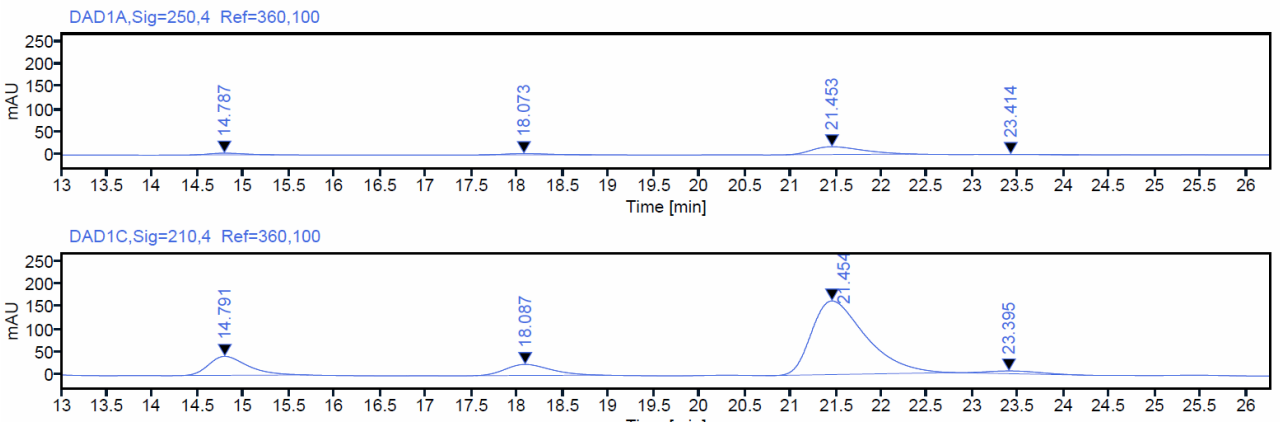

5j'' – Racemic sample

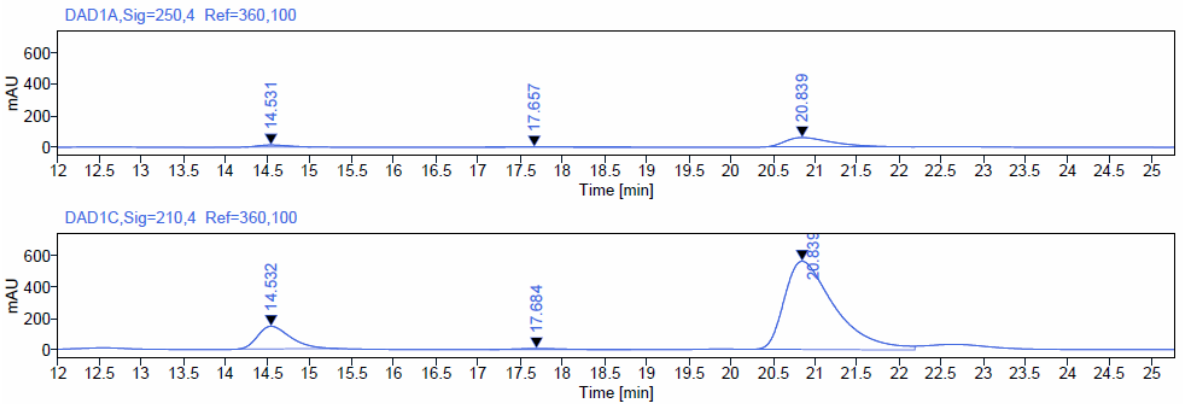

Signal: DAD1A,Sig=250,4 Ref=360,100

RT [min]	Type	Width [min]	Area	Height	Area%	Name
14.531	MM m	0.37	305.36	12.95	11.81	
17.657	MM m	0.50	82.12	2.01	3.18	
20.839	MM m	0.57	2198.33	58.39	85.01	
		Sum	2585.82			

Signal: DAD1C,Sig=210,4 Ref=360,100

RT [min]	Type	Width [min]	Area	Height	Area%	Name
14.532	MM m	0.41	3919.63	145.64	14.19	
17.684	MM m	0.50	256.33	6.48	0.93	
20.839	MM m	0.62	23447.62	567.40	84.88	
		Sum	27623.58			

5j'' – Enantioenriched sample

Bibliography

(1) List, B. Introduction: Organocatalysis. *Chemical Reviews*. December 2007, pp 5413–5415. https://doi.org/10.1021/cr078412e.

(2) von Liebig, J. Ueber Die Bildung Des Oxamids Aus Cyan. *Justus Liebigs Ann Chem* 1860, *113* (2), 246–247. https://doi.org/10.1002/jlac.18601130213.

(3) Neises Bernhard; Steglich Wolfgang. *Simple Method for the Esterification of Carboxylic Acids*; Bonn, 1978. https://doi.org/10.1002/anie.197805221.

(4) László Kürti; Barbara Czakó. *Strategic Applications of Named Reactions in Organic Synthesis*; 2005.

(5) Shoppee, C. W.; Johnson, F. P.; Lack, E.; Hajos, Z. G.; Parrish, D. R. *Synthesis of Bicyclic Intermediates Asymmetric Synthesis of Bicyclic Intermediates of Natural Product Chemistry*; UTC, 1974; Vol. 39. https://pubs.acs.org/sharingguidelines.

(6) Hoang, L.; Bahmanyar, S.; Houk, K. N.; List, B. Kinetic and Stereochemical Evidence for the Involvement of Only One Proline Molecule in the Transition States of Proline-Catalyzed Intra- and Intermolecular Aldol Reactions. *J Am Chem Soc* 2003, *125* (1), 16–17. https://doi.org/10.1021/ja028634o.

(7) Bahmanyar, S.; Houk, K. N. Transition States of Amine-Catalyzed Aldol Reactions Involving Enamine Intermediates- Theoretical Studies of Mechanism, Reactivity, and Stereoselectivity. *J Am Chem Soc* 2001, *123* (45), 11273–11283. https://doi.org/10.1021/ja011403h.

(8) Frohn, M.; Shi, Y. Chiral Ketone-Catalyzed Asymmetric Epoxidation of Olefins. *Synthesis (Stuttg)* 2000, *2000* (14), 1979–2000. https://doi.org/10.1055/s-2000-8715.

(9) Curci, R.; Fiorentino, M.; Serio, M. R. Asymmetric Epoxidation of Unfunctionalized Alkenes by Dioxirane Intermediates Generated from Potassium Peroxomonosulphate and Chiral Ketones. *J Chem Soc Chem Commun* 1984, No. 3, 155. https://doi.org/10.1039/c39840000155.

(10) Tu, Y.; Wang, Z.-X.; Shi, Y. An Efficient Asymmetric Epoxidation Method for *Trans* -Olefins Mediated by a Fructose-Derived Ketone. *J Am Chem Soc* 1996, *118* (40), 9806–9807. https://doi.org/10.1021/ja962345g.

(11) List, B.; Lerner, R. A.; Barbas, C. F. Proline-Catalyzed Direct Asymmetric Aldol Reactions [13]. *Journal of the American Chemical Society*. March 15, 2000, pp 2395–2396. https://doi.org/10.1021/ja994280y.

(12) Ahrendt, K. A.; Borths, C. J.; MacMillan, D. W. C. New Strategies for Organic Catalysis: The First Highly Enantioselective Organocatalytic Diels - Alder Reaction [16]. *Journal of the American Chemical Society*. May 3, 2000, pp 4243–4244. https://doi.org/10.1021/ja000092s.

(13) *The 2021 Nobel prize in chemistry*. https://www.nobelprize.org/prizes/chemistry/2021/summary/.

(14) *IUPAC, Compendium of Chemical Terminology*, 2nd ed.; 1997.

(15) Mayr, H.; Patz, M. Scales of Nucleophilicity and Electrophilicity: A System for Ordering Polar Organic and Organometallic Reactions. *Angewandte Chemie International Edition in English* 1994, *33* (9), 938–957. https://doi.org/10.1002/anie.199409381.

(16) Appel, R.; Mayr, H. Quantification of the Electrophilic Reactivities of Aldehydes, Imines, and Enones. *J Am Chem Soc* 2011, *133* (21), 8240–8251. https://doi.org/10.1021/ja200820m.

(17) Lakhdar, S.; Tokuyasu, T.; Mayr, H. Electrophilic Reactivities of α,β-Unsaturated Iminium Ions. *Angewandte Chemie International Edition* 2008, *47* (45), 8723–8726. https://doi.org/10.1002/anie.200802889.

(18) Lakhdar, S.; Ammer, J.; Mayr, H. Generation of α,β-Unsaturated Iminium Ions by Laser Flash Photolysis. *Angewandte Chemie International Edition* 2011, *50* (42), 9953–9956. https://doi.org/10.1002/anie.201103683.

(19) *'Glossary of Class Names of Organic Compounds and Reactivity Intermediates Based on Structure*; 1995.

(20) Kempf, B.; Hampel, N.; Ofial, A. R.; Mayr, H. Structure–Nucleophilicity Relationships for Enamines. *Chemistry – A European Journal* 2003, *9* (10), 2209–2218. https://doi.org/10.1002/chem.200204666.

(21) Lakhdar, S.; Maji, B.; Mayr, H. Imidazolidinone-Derived Enamines: Nucleophiles with Low Reactivity. *Angewandte Chemie International Edition* 2012, *51* (23), 5739–5742. https://doi.org/10.1002/anie.201201240.

(22) Mayr, H.; Kempf, B.; Ofial, A. R. π-Nucleophilicity in Carbon–Carbon Bond-Forming Reactions. *Acc Chem Res* 2003, *36* (1), 66–77. https://doi.org/10.1021/ar020094c.

(23) Leonov, A. I.; Timofeeva, D. S.; Ofial, A. R.; Mayr, H. Metal Enolates - Enamines - Enol Ethers: How Do Enolate Equivalents Differ in Nucleophilic Reactivity? *Synthesis (Germany)* 2019, *51* (5), 1157–1170. https://doi.org/10.1055/s-0037-1611634.

(24) List, B. The Ying and Yang of Asymmetric Aminocatalysis. *Chemical Communications* 2006, No. 8, 819. https://doi.org/10.1039/b514296m.

(25) Doyle, A. G.; Jacobsen, E. N. Small-Molecule H-Bond Donors in Asymmetric Catalysis. *Chemical Reviews*. December 2007, pp 5713–5743. https://doi.org/10.1021/cr068373r.

(26) Mahlau, M.; List, B. Asymmetric Counteranion-Directed Catalysis: Concept, Definition, and Applications. *Angewandte Chemie International Edition* 2013, *52* (2), 518–533. https://doi.org/10.1002/anie.201205343.

(27) Mayer, S.; List, B. Asymmetric Counteranion-Directed Catalysis. *Angewandte Chemie International Edition* 2006, *45* (25), 4193–4195. https://doi.org/10.1002/anie.200600512.

(28) Xu, Z.; Zheng, C.; Lin, J.; Huang, W.; Song, D.; Zhong, W.; Ling, F. Asymmetric Counteranion-Directed Electrocatalysis for Enantioselective Control of Radical Cation. *Angewandte Chemie International Edition* 2025, *64* (1). https://doi.org/10.1002/anie.202413601.

(29) Mayer, S.; List, B. Asymmetric Counteranion-Directed Catalysis. *Angewandte Chemie International Edition* 2006, *45* (25), 4193–4195. https://doi.org/10.1002/anie.200600512.

(30) Yang, J. W.; Hechavarria Fonseca, M. T.; List, B. A Metal-Free Transfer Hydrogenation: Organocatalytic Conjugate Reduction of α,β-Unsaturated Aldehydes. *Angewandte Chemie International Edition* 2004, *43* (48), 6660–6662. https://doi.org/10.1002/anie.200461816.

(31) Enders, D.; Hüttl, M. R. M.; Grondal, C.; Raabe, G. Control of Four Stereocentres in a Triple Cascade Organocatalytic Reaction. *Nature* 2006, *441* (7095), 861–863. https://doi.org/10.1038/nature04820.

(32) Kumar, M.; Kumar, A.; Rizvi, M. A.; Shah, B. A. Acetaldehyde in Asymmetric Organocatalytic Transformations. *RSC Adv* 2015, *5* (69), 55926–55937. https://doi.org/10.1039/c5ra05695k.

(33) García-García, P.; Ladépêche, A.; Halder, R.; List, B. Catalytic Asymmetric Michael Reactions of Acetaldehyde. *Angewandte Chemie International Edition* 2008, *47* (25), 4719–4721. https://doi.org/10.1002/anie.200800847.

(34) Hayashi, Y.; Itoh, T.; Ohkubo, M.; Ishikawa, H. Asymmetric Michael Reaction of Acetaldehyde Catalyzed by Diphenylprolinol Silyl Ether. *Angewandte Chemie International Edition* 2008, *47* (25), 4722–4724. https://doi.org/10.1002/anie.200801130.

(35) Hayashi, Y.; Itoh, T.; Aratake, S.; Ishikawa, H. A Diarylprolinol in an Asymmetric, Catalytic, and Direct Crossed-Aldol Reaction of Acetaldehyde. *Angewandte Chemie International Edition* 2008, *47* (11), 2082–2084. https://doi.org/10.1002/anie.200704870.

(36) Zhang, W.; Wang, N.; Yang, Z.; Li, Y.; Yu, Y.; Pu, X.; Yu, X. Lipase-Initiated Tandem Biginelli Reactions *via in Situ* -Formed Acetaldehydes in One Pot: Discovery of Single-Ring Deep Blue Luminogens. *Adv Synth Catal* 2017, *359* (19), 3397–3406. https://doi.org/10.1002/adsc.201700599.

(37) Boxer, M. B.; Yamamoto, H. Tris(Trimethylsilyl)Silyl-Governed Aldehyde Cross-Aldol Cascade Reaction. *J Am Chem Soc* 2006, *128* (1), 48–49. https://doi.org/10.1021/ja054725k.

(38) Biewenga, L.; Kunzendorf, A.; Poelarends, G. J. In Situ Acetaldehyde Synthesis for Carboligation Reactions. *ChemBioChem* 2020, *21* (10), 1505–1509. https://doi.org/10.1002/cbic.201900666.

(39) Fan, X.; Rodríguez-Escrich, C.; Sayalero, S.; Pericàs, M. A. Paraldehyde as an Acetaldehyde Precursor in Asymmetric Michael Reactions Promoted by Site-Isolated Incompatible Catalysts. *Chemistry – A European Journal* 2013, *19* (33), 10814–10817. https://doi.org/10.1002/chem.201302087.

(40) Casacchia, M. E.; Giorgianni, G.; Allegritti, E.; Giansanti, L.; Carlone, A.; Pesciaioli, F. Organocatalytic Synthesis of γ-Amino Acid Precursors via Masked Acetaldehyde under Micellar Catalysis. *SynOpen* 2023, *07* (01), 29–32. https://doi.org/10.1055/a-1996-8940.

(41) Giorgianni, G.; Bernardi, L.; Fini, F.; Pesciaioli, F.; Secci, F.; Carlone, A. Asymmetric Organocatalysis—A Powerful Technology Platform for Academia and Industry: Pregabalin as a Case Study. *Catalysts* 2022, *12* (8), 912. https://doi.org/10.3390/catal12080912.

(42) Giorgianni, G.; Nori, V.; Baschieri, A.; Palombi, L.; Carlone, A. Organocatalyzed Michael Addition to Nitroalkenes via Masked Acetaldehyde. *Catalysts* 2020, *10* (11), 1296. https://doi.org/10.3390/catal10111296.

(43) Enders, D.; Krüll, R.; Bettray, W. Microwave-Assisted Organocatalytic Quadruple Domino Reactions of Acetaldehyde and Nitroalkenes. *Synthesis (Stuttg)* 2010, *2010* (04), 567–572. https://doi.org/10.1055/s-0029-1217146.

(44) Enders, D.; Jeanty, M.; Bats, J. Organocatalytic Asymmetric Triple Domino Reactions of Nitromethane with α,β-Unsaturated Aldehydes. *Synlett* 2009, *2009* (19), 3175–3178. https://doi.org/10.1055/s-0029-1218282.

(45) Vigneron, J. P.; Dhaenens, M.; Horeau, A. Nouvelle Methode Pour Porter Au Maximum La Purete Optique d'un Produit Partiellement Dedouble sans l'aide d'aucune Substance Chirale. *Tetrahedron* 1973, *29* (7), 1055–1059. https://doi.org/10.1016/0040-4020(73)80060-2.

(46) Świderek, K.; Nödling, A. R.; Tsai, Y. H.; Luk, L. Y. P.; Moliner, V. Reaction Mechanism of Organocatalytic Michael Addition of Nitromethane to Cinnamaldehyde: A Case Study on Catalyst Regeneration and Solvent Effects. *Journal of Physical Chemistry A* 2018, *122* (1), 451–459. https://doi.org/10.1021/acs.jpca.7b11803.

(47) Wheeler, S. E.; Seguin, T. J.; Guan, Y.; Doney, A. C. Noncovalent Interactions in Organocatalysis and the Prospect of Computational Catalyst Design. *Acc Chem Res* 2016, *49* (5), 1061–1069. https://doi.org/10.1021/acs.accounts.6b00096.

(48) Wagner, J. P.; Schreiner, P. R. London Dispersion in Molecular Chemistry—Reconsidering Steric Effects. *Angewandte Chemie International Edition* 2015, *54* (42), 12274–12296. https://doi.org/10.1002/anie.201503476.

(49) Krenske, E. H.; Houk, K. N. Aromatic Interactions as Control Elements in Stereoselective Organic Reactions. *Acc Chem Res* 2013, *46* (4), 979–989. https://doi.org/10.1021/ar3000794.

(50) Brusa, A.; Iapadre, D.; Casacchia, M. E.; Carioscia, A.; Giorgianni, G.; Magagnano, G.; Pesciaioli, F.; Carlone, A. Acetaldehyde in the Enders Triple Cascade Reaction via Acetaldehyde Dimethyl Acetal. *Beilstein Journal of Organic Chemistry* 2023, *19*, 1243–1250. https://doi.org/10.3762/bjoc.19.92.

Chapter 2 - Organo-photocatalyzed α-functionalization of carbonyl compounds with aryl-diazo compounds

This project is about the asymmetric α-functionalization of carbonyl compounds using aryldiazosulphones as aryl-donating agents under photochemical conditions. In our intentions, the asymmetric induction is done by an asymmetric secondary amine through an enamine intermediate. It follows a brief introduction on the basic principles of photocatalysis in general, as these are used both here and in the next chapters.

Introduction- photochemistry and photocatalysis

Photochemistry is a branch of chemistry which studies the interaction of matter with light, in particular the reactivity induced to matter thanks to photo absorption.[1] One important pioneering contribution was by Giacomo Ciamician in 1912, using sunlight to carry out chemical reactions on the roof of the chemistry department in Bologna (Figure 37).

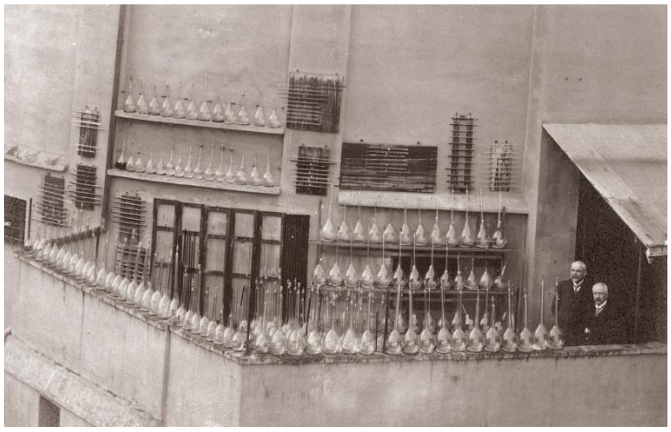

Figure 37 - First examples of photocatalysis in 1912

Aside the chemistry discovered with sunlight, the important contribution of Ciamician is also *conceptual*: the use of light to induce chemical reactivity, and the fact that this would have been something of ground importance in the future. He dreamt about laboratories with glass walls, in which chemical reactions were induced simply exposing solutions to natural irradiance. Aside from the braveness of imaging all this with air conditioning still to be invented at the time, this actually became somehow true: currently, many research groups focus on photochemistry, as there has been a burst in this research field in the last two decades.

“Simple”, uncatalyzed photochemistry in the field of organic chemistry normally works by two activation modes: the first is by simple excitation of organic molecules. Excited state of these molecules than presents some peculiar reactivity, for example pericyclic chemistry or biradical behavior. The second activation mode consists in the direct homolysis of bonds between atoms by light excitation, usually the weakest ones such as carbon-halogen sp^3 bond or oxygen-oxygen bond in the peroxide compounds. Some notable examples of photochemistry applied in organic synthesis are [2+2] cycloaddition to make cyclobutanones from olefins (Figure 38) and Norrish[2] type-II rearrangement, to make cyclobutanols (Figure 39). An interesting example coming from natural substances is the photo-induced rearrangement of α-santonin (Figure 40).

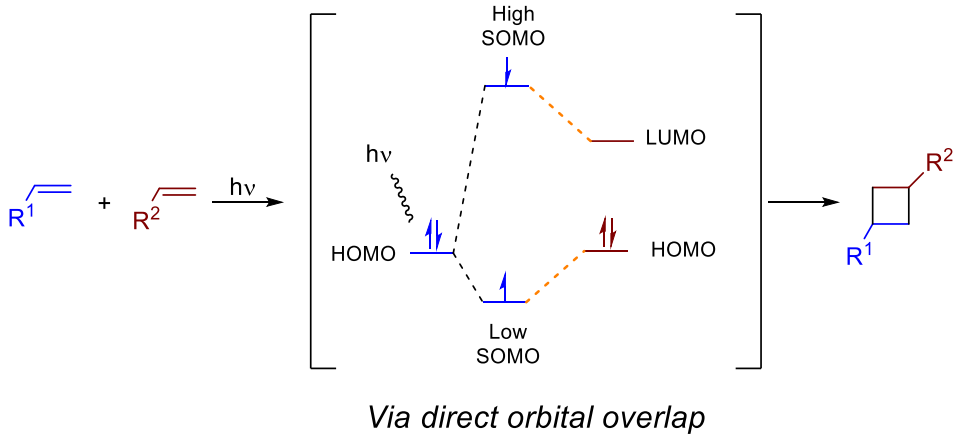

Figure 38 - [2+2] cycloaddition of olefins

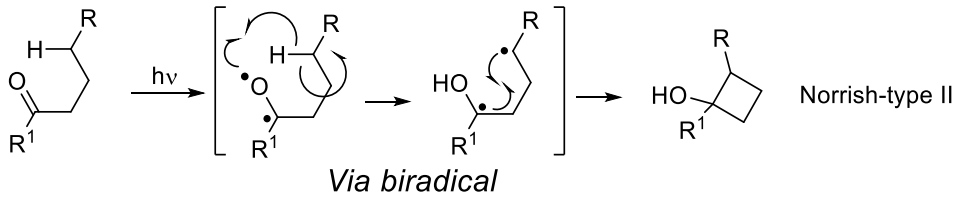

Figure 39 - Norrish-type II rearrangement

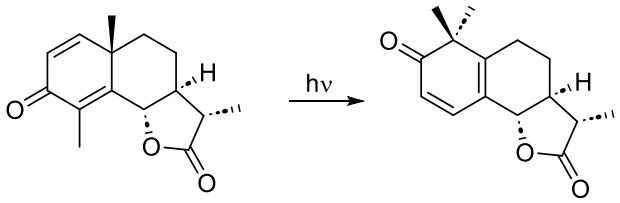

Figure 40 - Photo-induced rearrangment of α-santonin

Photocatalysis is the change in the rate of a chemical reaction or its initiation under the action of light in the presence of a substance, the photocatalyst, that absorbs

light and is involved in the chemical transformation of the reaction partners.[3] Photocatalysis is thus a sub-field of photochemistry, and its applications in organic synthesis has been extensively studied in the last years, especially after the pioneering work by Mac Millan and Nicewicz in 2008, showing that photo-redox merged with organocatalysis opens new possibilities.[4]

Photocatalysis and photochemistry in general represent a powerful tool for the synthesis of complex organic molecules. Indeed, photocatalysis not only speeds up chemical reactivity in general but also unlocks peculiar reactivity patterns thanks to radical chemistry (Figure 41).

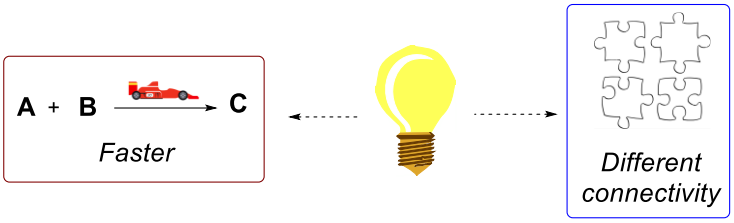

Figure 41 - Main advantages of photocatalysis in organic synthesis

An example of unusual pattern is represented by the anti-Markovnikov addition of mineral acids to styrene-derivatives (Figure 42).[5]

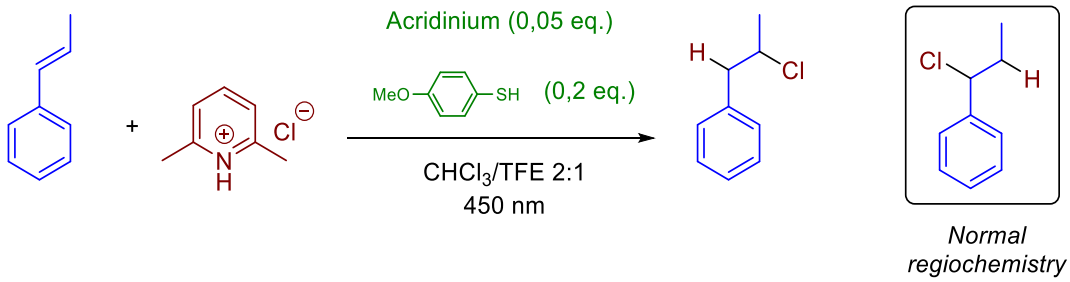

Figure 42 - Photocatalyzed anti-Markovnikov addition of mineral acids

The radical reaction induced by the photocatalytic pathway induces first the attack of the chloride anion to the mono-oxidized olefin, then hydrogen atom transfer (HAT) closes the catalytic cycle. In this way, anti-Markovnokov selectivity was induced on the substrate. With classical polar reactivity, the benzyl chloride would have been obtained.

If compared to photochemistry, photocatalysis has another advantage: the use of less energetic wavelengths. Indeed, photochemistry usually needs high-energetic radiation to induce reactivity, such as UV light. This has implicit disadvantages such as the difficulty in scaling-up for the radiation diffusion, the danger associated with UV radiation, which damages seriously vision and skin of operators, and the low functional group tolerance. Thanks to photocatalysis, energy from photons can be *efficiently and selectively* transmitted to the reactive system.

Basic principles of photocatalysis

The presence of the photocatalyst (PC) is a key point of the whole process, as it absorbs light generating an exited state (PC*). It is the reactivity of PC* in the systems that transfers the energy of the photons through different pathways triggering the substrates. To make this possible, the PC usually needs to be phosphorescent, as phosphorescent pathways involve a long-living triplet PC*. This elongates the excited state half-life time enough to be quenched by bimolecular mechanisms and efficiently transfer the energy accumulated with absorption.[6] Other relaxation pathways of PC* do not lead usually to any chemical change in the system of interest. The most common relaxation paths are resumed in a simplified Jablonski diagram[7] below (Figure 43).

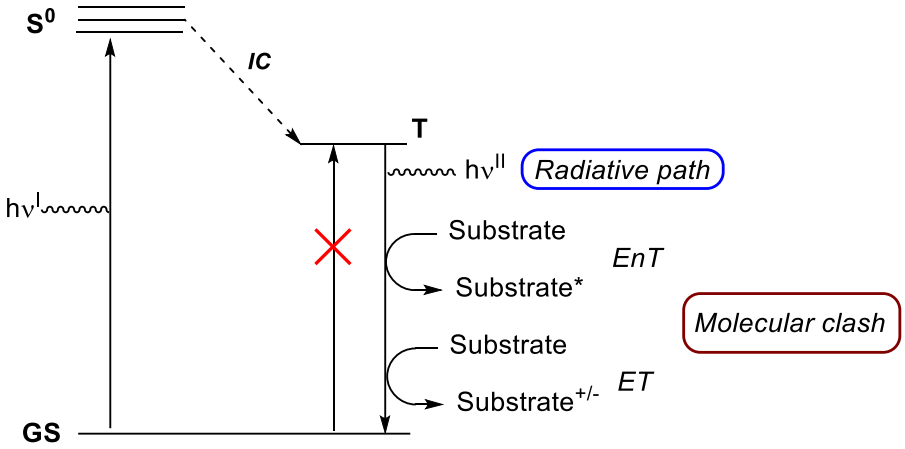

Figure 43 - Jablonski diagram

The radiation ν^{I} excites PC in the ground state (GS), generating a singlet state (S^0), which then converts to a triplet state (T) via inter-system crossing (IC). The triplet state is a relatively long living state, as the normal decay to GS is spin-forbidden. This gives T enough time to undergo a quench by molecular clash. Of course, radiative re-emission of ν^{II} is possible, causing the fluorescent phenomenon. The energy transfer from PC* to the substrate is the key event in photocatalysis, and it can happen both via simple energy transfer (EnT), or via electron transfer (ET). EnT is very important in photocatalysis. For example, all the reactions involving triplet transfer, such as singlet dioxygen chemistry, require this activation mode. However, this activation mode is not discussed here, as it was not exploited once in the preparation of a starting material in the total synthesis of norcembranoid diterpenes (chapter 5), but not in photocatalysis projects. ET is the other photo-activation mode. As the name says, what happens is that PC* exchanges an electron with the substrate. If the electron is *given* to the substrate it's called

"oxidative quenching", if the electron is *taken* from the substrate it's called "reductive quenching".[6, IV] ET events in photocatalysis are shown in Figure 44.

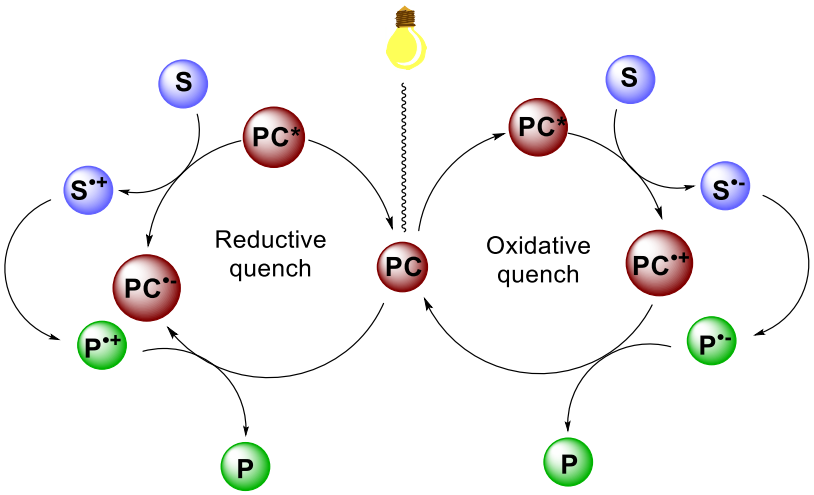

Figure 44 - ET activation mode in photocatalysis

These are fundamental steps and the key idea of photo-redox catalysis: being able to *transfer* an electron from one molecule to another one in a controlled manner creates powerful reactive intermediates which can be exploited to do non-trivial chemistry. The redox quenching events need fundamentally two conditions to happen: first, an electronic matching between PC* and substrate (S), in order to induce the triplet decay. This property is not straightforward to predict, and usually there is not a real rational design for this step. Literature data can be of support, but the photoinduced ET event for new substrate-PC couples is somehow empirical. However, the quenching properties of the couple *can* be tested by Stern-Volmer experiments, a typical control experiment to study photocatalytic systems. The fluorescence spectrum of PC is first recorded as isolated, then recorded with increasing concentrations of the investigated quencher. The attenuation of the emission spectrum observed for increasing concentration of quencher is the positive signal that the quenching happens for real, otherwise there are no significant quenching events. Second, the electron transfer event must be *thermodynamically allowed*, i.e. electrons must go to lower electronic potential. Thus, redox potentials of both PC and the substrate must be known for a correct design. Electrostatic potentials of isolable species can be estimated via cyclovoltammetry (CV). CV is an experiment in which two electrodes are soaked into a solution containing the substrate of interest. The electrostatic potential generated by the electrode is then scanned over a certain range using a proper electronic setup, usually using a potentiostat. The induced electric current intensity is recorded at the same time, all in a regime of static fluid. The redox potentials

[IV] The adjective refers to PC*

values of the analyte are then extrapolated from the curves obtained plotting electronic potential and current intensity. Moreover, the stability of the radical species can be deduced from the *shape* of the curve. Potentially, also the kinetics of radical decomposition can be deduced. An example of CV diagram is shown in Figure 45.[V]

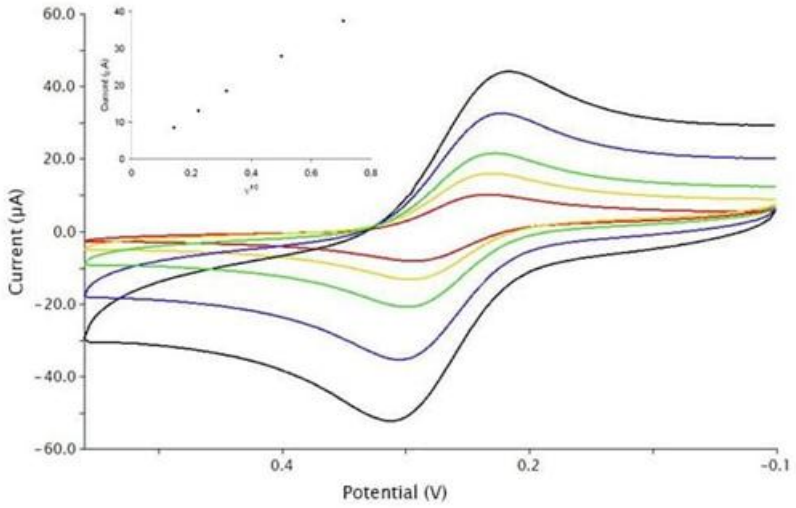

Figure 45 - Example of CV

Of course, CV can measure *only* ground state species, which is ok for the substrate. For PC, the redox potential of the excited state is actually needed and can be estimated using the *Rehm-Weller* equation. The simplest version of Rehm-Weller equation corrects the redox potential with the electronic energy gained with absorption, named E_{00}, and measured as the interception curve between absorption and emission spectra of PC, to exclude the vibrational contribution of different energetic levels. Looking at the molecular orbital of the triplet state, it is evident that both oxidizing and reducing the excited species takes less energy compared to the ground state (Figure 46).

[V] Different scan rates are shown in the picture.

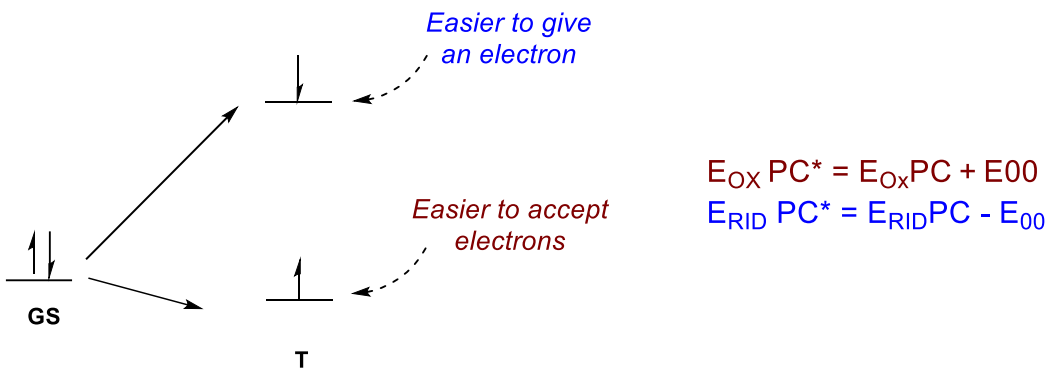

Figure 46 - Orbital diagram for excited redox potential

The electron transfer event not only needs to be thermodynamically favored, but some *overpotential* is needed to make the electron transfer fast, as stated by the Marcus theory. Indeed, there is usually a potential barrier to overcome for the electron to migrate from one species to another of greater electronic potential. As for the quenching events, the design of SET step is not an easy task, as Marcus' equation parameters are very complex. However, for catalytic applications in organic chemistry, usually an overpotential of 200-300 mV is considered good enough as a rule of thumb, and this make the SET design easy to do. Finally, for the design of the photo-redox mechanism, back-electron transfer events also needs to be considered: taking as example reductive quench in Figure 44, the back electron transfer from $PC^{\bullet-}$ to $S^{\bullet+}$ is a possible (and favored event), which liberates the accumulated energy as heat, without any chemical change induced. Sometimes to suppress back-electron transfer events $S^{\bullet+}$ or $S^{\bullet-}$ are designed to undergo fast cleavage, making this process irreversible. Last but not least, the electron transfer should also be allowed in the final electron transfer event to close the catalytic cycle – a usually overlooked design parameter in literature reports. The other events in the middle of the catalytic cycle are radical, radical cation or radical anion chemical events, which follow the rules of radical chemistry.[8] The basic "chess moves" possible in radical chemistry are radical addition to multiple bond, β-scission of σ-bonds and atom- transfer reactions, in particular hydrogen atom transfer (HAT) and halogen bond transfer (XAT) (Figure 47).

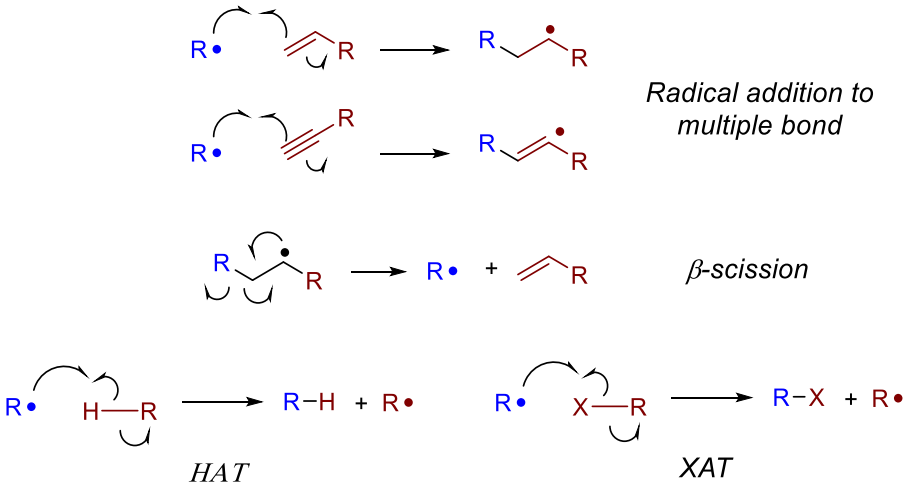

Figure 47 - Basic steps in radical reactivity

Radical cations and radical anions usually tend to react to split charge and spin into different species (or different parts of the molecules), following then radical and/or polar chemistry. The reactivity of radical type containing species of any type is not introduced here.

The combination of photochemically induced events (excitation, quench and SET) and radical type reactivity overall contribute to the design and development of photocatalytic process. In this thesis, it is shown how catalytic design and experimental approach are iteratively compared and shape each other in the overall development of photocatalyzed process. I anticipate that both failures and success have been obtained with this approach.

Photochemistry aryldiazosulphones: introduction

Aryldiazosulphones are compounds with the following general chemical structure (Figure 48):

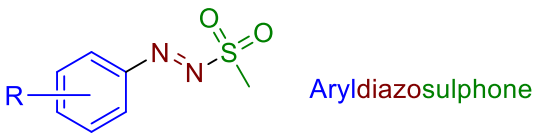

Figure 48 - Aryldiazosulphone structure

Their structure embeds a reactive diazo group connected to an aryl group and a sulphone group, usually a methyl-sulphone. These compounds are intensely yellow-colored solids, unstable to light because of their photochemical properties. They are cheap and easy to synthesize from the corresponding anilines through diazotization and nucleophilic attack by a sulphinate sodium salt. Another

convenient synthesis method is the copper-catalyzed oxidation of the corresponding hydrazine in the presence of a sulphonyl chloride (Figure 49).

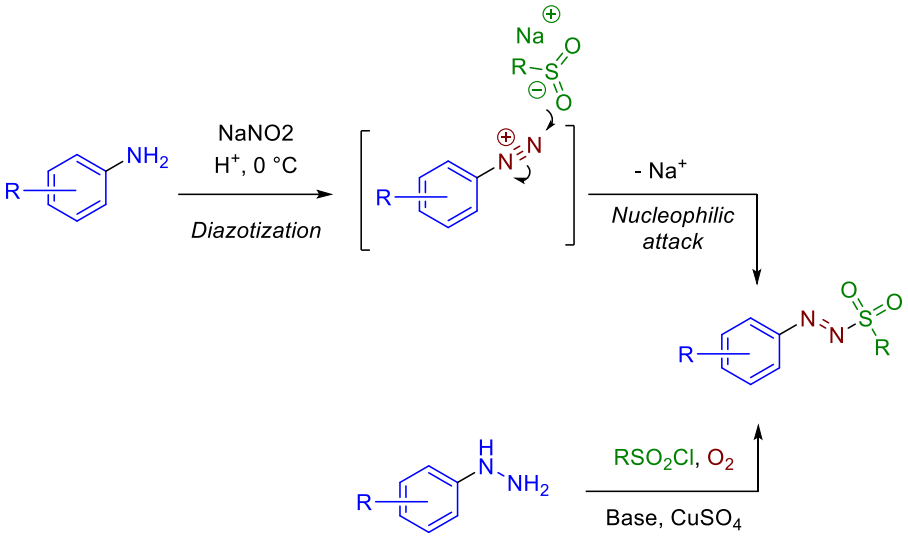

Figure 49 - General synthesis of aryldiazosulphones

Aryldiazosulphones can be seen as bench stable synthetic equivalents of diazo compounds, as after light activation they are able to generate similar intermediates, such as aryl-diazonium radicals and aryl-diazonium cations, and all the corresponding reactive intermediates obtainable by deazotation.[9]

Despite have being reported in the 70's,[10] their photochemistry was not deeply investigated until 2016,[9] with the seminal work of S. Protti, M. Fagnoni and co-workers from the University of Pavia.[9] In general, aryldiazosulphones have absorption peaks between 300 and 360 nm and between 400 and 450 nm. These correspond to a π–π* and a n-π* transition, respectively (Figure 50).

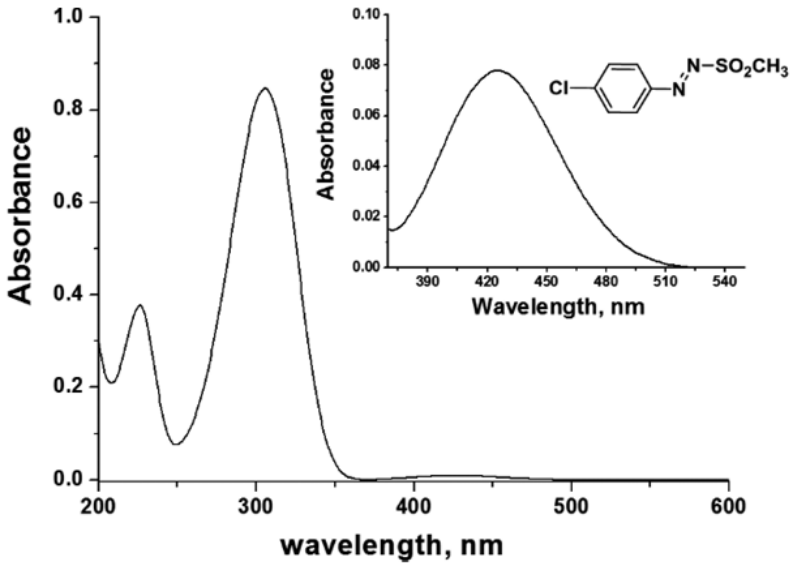

Figure 50 - A representative absorption spectrum of aryldiazosulphones[11]

In particular, the n-π* transition, probably together with the contribution of diazo-isomerization,[12] is associated with the homolysis of N-S bond, generating an aryl-diazo radical (Ar-N_2•) and a sulfonyl radical (RSO_2•). Thus, aryldiazosulphones under visible light irradiation are a mild source of radicals, without the need for a photocatalyst – it's pure photochemistry. In the last years aryldiazosulphones have been exploited for many different photocatalyzed aryl functionalization and arylation reactions.[11] Some notable examples are represented in Figure 51.

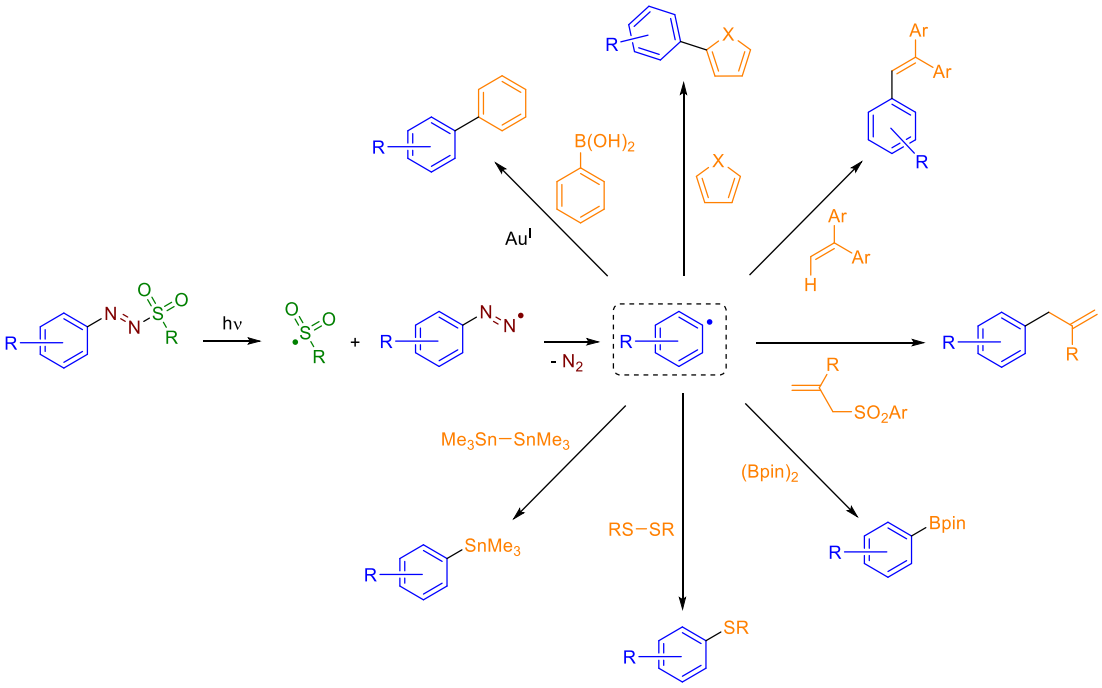

Figure 51 - Examples of aryldiazosulphones light-induced reactivity

Aryldiazosulphones have been used for gold-catalyzed Suzuki-type aryl-aryl cross-coupling,[13] heteroarene C-H activation,[9] metal free Heck reaction of 1,1-disubstituted alkenes,[14] allylation of aromatic scaffolds,[15] borylation,[16,17] sulphuration[17] and stannylation.[18] In general, all this type of chemistry (and other examples not cited here), is supposed to pass through the aryl radical intermediate generated via photolysis of the aryldiazosulphones, generating another radical. Then, the sulphonyl radical plays the role of HAT agent, stopping the radical chain and generating the corresponding *sulfinic* acid. Alternatively, if functionalization reagents of RX-XR type are used, where X is a heteroatom, there are probably chain propagation phenomena induced by RX•, which probably recombines at the end with RSO_2•. Thus, in general it seems that the sulfonyl radical is not very reactive in these systems and has more the role of "radical quencher".

Asymmetric organocatalyzed α – arylation with aryldiazosulphones

Despite the numerous examples of aryldiazosulphones used in organic synthesis, to the best of our knowledge there is still no use of these versatile compounds in *asymmetric* reactions. The same is true for enamine-organocatalysis: there are still no examples of organocatalytic-induced reactivity with aryldiazosulphones. Thus, it was decided to cooperate with Professor Protti from the university of Pavia to merge asymmetric enamine catalysis and the photochemistry of aryldiazosulphones.

The core ideas of our catalytic design rely on basic principles of organocatalysis, aryldiazosulphones photochemistry and radical chemistry. First, alkyl aldehydes in the presence of a secondary amine catalyst reversibly form a small amount of reactive enamine, which is nucleophilic at C2. Second, aryldiazosulphones under irradiation at around 450 nm undergo homolytic cleavage of N-S bond as discussed above, generating an aryldiazoradical and a sulphonyl radical. The former decomposes freeing dinitrogen and an electrophilic aryl radical; the latter usually behaves as final quencher of the radical cascade. It is straightforward to think that the aryl radical can attack the enamine as the most nucleophilic species in the system, enantioselectively arylating C2. The following mechanism was designed (Figure 52).

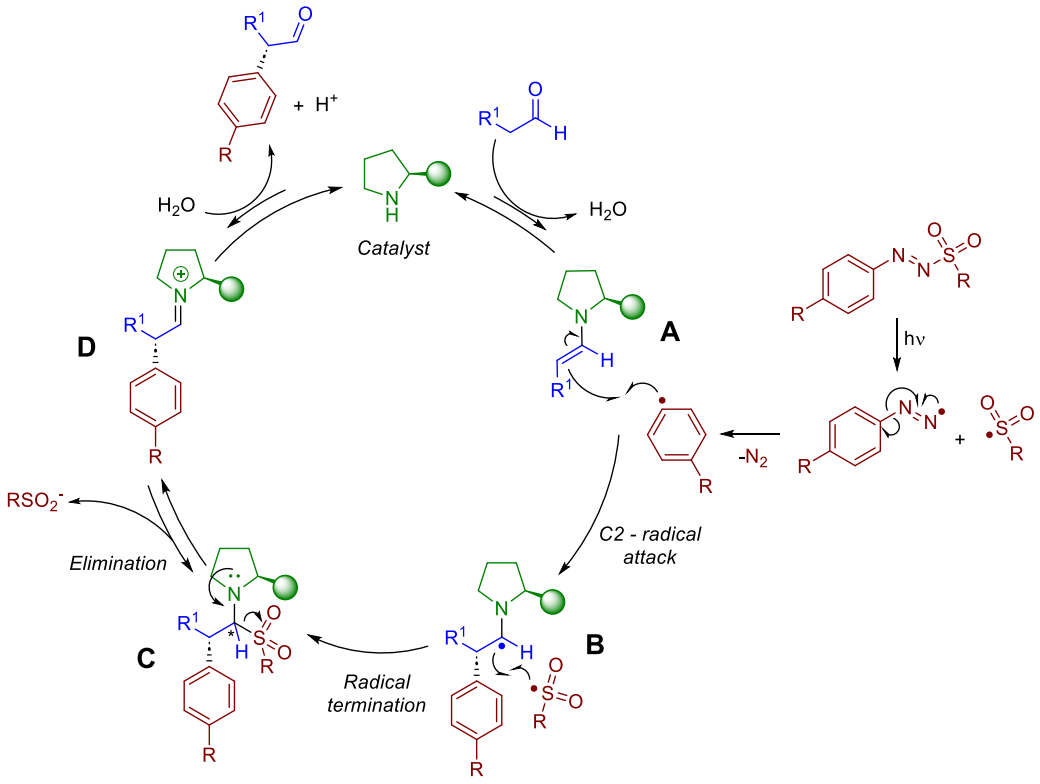

Figure 52 - Design of asymmetric organocatalyzed C2-arylation with aryldiazosulphones

On the photochemistry side the irradiation of aryldiazosulphone induces the homolysis of N-S bond and subsequent dinitrogen loss to form an electrophilic aryl radical species. In our plans, aryl radical attacks **A-type** enamine at C2 position, forming **B-type** intermediate. The attack of electrophilic radicals to enamines is not something novel – for example, it was the key bond-forming event in the first report of asymmetric-organocatalyzed photoredox catalysis.[19]

Then, radical re-binding between **B-type** and sulphonyl radical should generate **C**. The diastereoselectivity of this bond forming event is not much important, as **C** should eliminate sulfinate anion at the equilibrium to yield iminium ion **D**, and the α - arylated enantioenriched product after hydrolysis. The overall reaction balance gives a sulfinic acid as coproduct. Its accumulation in the reaction environment would shift the iminium-enamine equilibrium toward iminium. So, the presence of a base to neutralize the acid produced could be essential.

If this design is effective, the resulting methodology would be of interest in our opinion, as to the best of our knowledge there is *only one* example asymmetric α-arylation of aldehydes reported by MacMillan and co-workers.[19] The arylation was realized through cooperative enamine-copper catalysis, using diphenyl iodonium triflates as arylation agent. The key activation steps are reported in Figure 53.

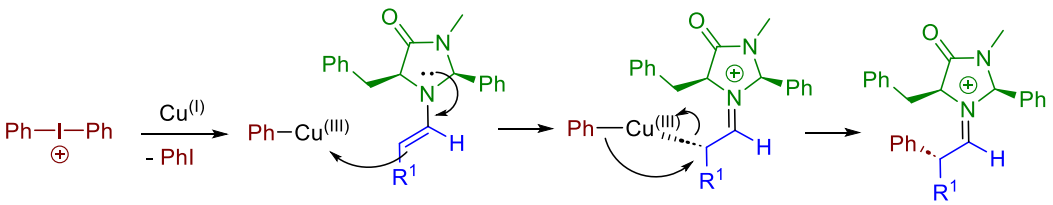

Figure 53 - Activation mode reported in the α - arylation of aldehydes

Potentially, our designed methodology would avoid the use of a transition metal catalyst and iodonium reagents, which are made starting from the corresponding aryl iodides in a one-pot procedure. Aryldiazosulphones represent a valid synthetic alternative from our point of view, as they are synthetized in a one-pot procedure starting from the corresponding anilines. Moreover, to the best of our knowledge, there is no reported asymmetric methodology involving the use of aryldiazosulphones. This would introduce a further degree of innovation, paving the way for further asymmetric photochemistry discovery for these peculiar compounds.

Other possible α - functionalization paths

In the previous paragraph, the design of α - arylation of aldehydes with aryldiazosulphones process was designed, assuming that the aryl radical produced

after photolysis of the starting material would have been the effective electrophile in the system. However, other two other possible electrophilic radical were taken into account (Figure 54).

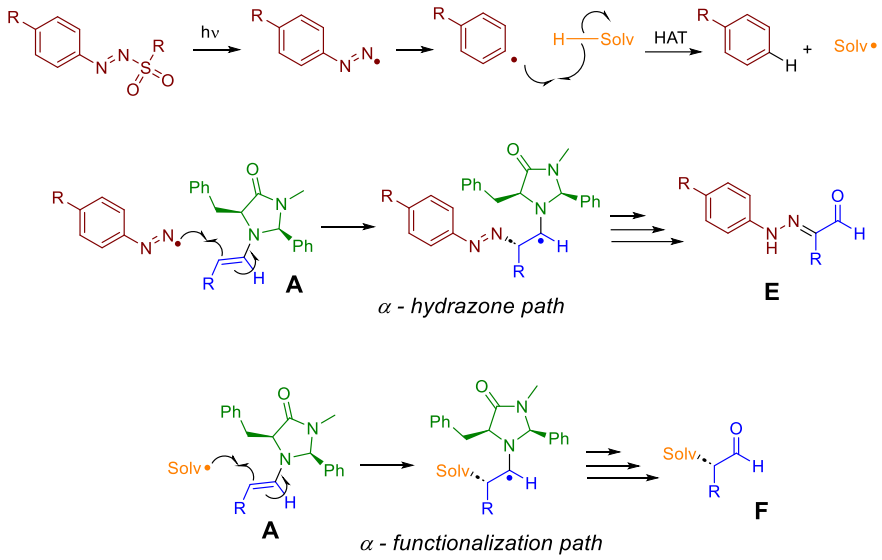

Figure 54 - Other possible a - functionalization paths

First, aryldiazoradical itself can potentially react with **A**, being a strongly electrophilic radical. An analogous reactivity was also reported by Protti, Fagnoni and co-workers with silyl-enol ethers.[20] After catalytic cycle closure, thermodynamics would probably induce the tautomerization of N=N bond with the carbonyl α - position, yielding an α - hydrazone of **type E**. On the other hand, if the enamine is not reactive enough, phenyl radical goes for HAT on the solvent, to form a more stable alkyl radical. This radical, if electrophilic, can potentially attack the enamine, leading to an F-**type product**. Depending on the solvent used, different α - functionalization can be performed. While we are not interested in **E-type** products, **F-type** structure is appealing for us: asymmetric transformations such these are not trivial to develop. Just to make an example, if the solvent is acetonitrile, the α - cyanomethylation is the reaction. There are only three examples of enantioselective α - cyanomethylation of aldehydes, a reaction pioneered by MacMillan and co-workers.[21] Other variants developed by Melchiorre's[22] and Vetica's[23] groups use the same chemistry, just changing the photocatalyst. All these methodologies use a photocatalyst and bromoacetonitrile , an expensive and toxic reagent, or chloroacetonitrile, a nasty reagent. The use of cheap aryldiazosulphone derived for example from the inexpensive p-toluidine and acetonitrile has its advantages.

Experimental

Catalyst-aryldiazosulphone compatibility

To verify our reactivity hypothesis, we started to check the compatibility of aryldiazosulphones with secondary amine catalysts, as amines usually react with these compounds. Hayashi catalyst (**1**), Mac Millan (II) imidazolidinone (**2**) and Melchiorre's catalyst (**3**) were mixed with p-tolylarildiazosolfone **4** in dark conditions for 24 hours (Figure 55). The results are reported in Table 7.

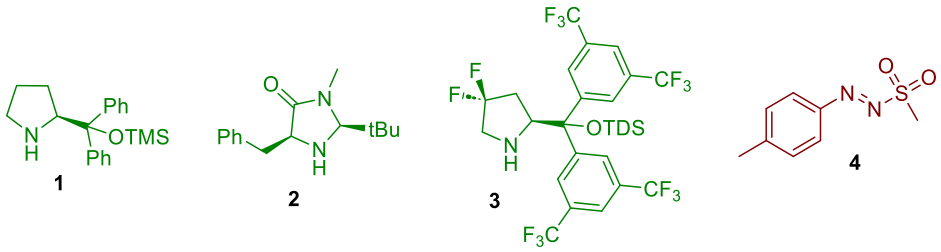

Figure 55 - Substrates used in compatibility tests

Entry	Reagents	Solvent	Result
1	1 + 4	Toluene	Degradation of 1
2	2 + 4	Toluene	Degradation of 2
3	3 + 4	Toluene	3 is stable
4	1 + 4	$CHCl_3$	Degradation of 1
5	2 + 4	$CHCl_3$	Partial degradation of 2
6	3 + 4	$CHCl_3$	3 is stable

Table 7 - Secondary amine catalyst - aryldiazosolfone compatibility test

Toluene and chloroform were used as model solvents, being common reaction media in organocatalytic processes. **1** always undergoes fast degradation in both solvents (entry 1 and 4), so it was ruled out immediately, as it reasonably cannot be competitive in any other media. **2** was degraded in toluene (entry 2), while it was only partially degraded in chloroform (entry 5). This is good news for oxazolidinones – there is some chance of being used as catalyst, at least in chloroform. Finally, **3** was a rock: there was absolutely no trace of degradation, not even by TLC. Thus, it was decided to start the experimentation using both **2** and **3** as organocatalyst. It is worth noting that the stability of the organocatalyst increases as the amine group becomes more electron-poor. This result is in good agreement with the fact that aryldiazosulphones (or their derived radicals) are electrophiles: stronger nucleophiles react faster, whatever the degradation mechanism is.

Reactivity test – static conditions

The reactivity of our system was then tested using different organocatalysts common in solvents, catalyst **2** and **3**, and **4** as aryldiazosulphone and 3-phenylpropionaldehyde (**5**) as model substrates. The results are shown in Table 8.

Entry	Catalyst	Solvent	Results
1	3	ACN	Unidentified products from degradation of 4. 3 and 5 unaffected.
2	3	Toluene	Unidentified products from degradation of 4. 3 and 5 unaffected.
3	3	$CHCl_3$	Unidentified products from degradation of 4. 3 and 5 unaffected.
4	2	Toluene	Unidentified products from degradation of 4 and 2. 5 unaffected.
5	2	ACN	Unidentified products from degradation of 4 and 2. 5 unaffected.
6	2	$CHCl_3$	Slight difference in degradation products compared to entry 4 and entry 5

Table 8 - Reaction screening

Reactions run with 4 (1 eq.), 5 (1 eq.), organocatalyst (0,2 eq.), $NaHCO_3$ (2 eq.), solvent (0,14 M) into a UFO[24] vial. Irradiation with a Kessil lamp at 440 nm, max power. UFO reactor used as light-delivering system. Suspensions undergo 10 minutes of sparging with N_2 before irradiation. Sodium bicarbonate is introduced as a base to quench the metansulfinic acid formed.

From the first screening tests, some critical points emerged. First of all, it seems that in the presence of **3** there is no reactivity at all, despite the catalyst is completely unaffected in these reaction conditions. There are two possible reasons for this: first, the designed reactivity simply does not happen – enamine is not reactive enough and other paths are followed by the radical intermediates after photolysis. In this case, not much can be done if not re-design the reaction, as fundamental chemistry is as it is. Second, there is an extremely low concentration of enamine, or no enamine at all in the system. Assuming to keep the same organocatalyst loading and that at least some enamine is actually there, a possible solution is "diluting" the aryldiazosulphone in the system, to have a comparable enamine concentration. In other words, the organocatalyst must have enough time to produce some new enamine and close the catalytic cycle. Otherwise, the photochemistry of aryldiazosulphone is just too fast and decomposition paths overcome the desired reactivity. To do this, slow addition of **4** with a syringe pump can be adopted, while continuously irradiating the system.

Another critical point is that **2** is degraded under irradiation in the presence of **4**, while it is partially stable in the dark. However, degradation products were not

identified, as not much can be done to avoid this reactivity. In our opinion, the only possible solution again is the slow injection of **4**, assuming that **type-A** enamine is more reactive than the organocatalyst itself. With enough enamine around, there is the possibility that a very small amount of photo-generated radical attacks preferentially the enamine, giving time to the system to re-generate some fresh enamine.

To rule out the possibility of having some reacted aldehyde at C-H bond, which is a weak bond, and/or other possible reaction paths, some blank tests were done. First, compound **4** undergoes the same reaction conditions of Table 8 and the decomposition products are compared to entry 1, 2 and 3, and are identical. This confirms that the aldehyde was not involved at all in the photochemical process. Second, entry 4 was repeated, without the aldehyde. As expected, **2** was decomposed and the same products were observed. Part of these products are the same found in the **4**-decomposition blank test, and other are new, presumably coming from **2** somehow. To summarize the first round of experiments, catalyst **2** gets decomposed during the photochemical process and **4** itself disappears, as expected. However, catalyst **3** and **5** are inert under these conditions, underling the fact that a completely different reaction pathway, whatever it is, is favored. No products compatible with the designed organocatalytic path were detected, so the enamine is not reactive enough, or not enough enamine is present. Further investigation was carried out, trying to answer these questions and make things work.

Enamine synthesis

Given the difficult scenario, it was decided to *directly* sample the reactivity of enamines with aryldiazosulphones under photocatalytic conditions. Indeed, trying to find photochemical-flow injection conditions to give the desired product at this stage would have probably been fruitless, since there is no experimental evidence or previous knowledge about this system.

To make enamines quantitatively, water has to be removed from the system to shift the carbonyl-enamine equilibrium. Both molecular sieves and azeotropic distillation were tested as water removing methods. Both 3-phenylproprionaldehyde (**5**) and phenylacetaldehyde (**6**) and amine organocatalysts combinations were tested as well. The results are resumed in Table 9.

Entry	Substrates	Conditions	Results
1	3 + 5	Benzene, 4 Å MS, r.t., 3 days, inert atmosphere	No enamine observed
2	3 + 5	ACN, 4 Å MS, r.t., 3 days, inert atmosphere	No enamine observed
3	2 + 5	Benzene, 4 Å MS, r.t., 3 days, inert atmosphere	No enamine observed
4	2 + 5	ACN, 4 Å MS, r.t., 3 days, inert atmosphere	No enamine observed
5	2 + 5	1 % p-TSA, toluene, reflux 22 h, inert atmosphere	Partial enamine formation (7)
6	2^{I} + 6	1 % p-TSA, toluene, reflux 2 h, inert atmosphere	Enamine isolated (7^{I})

Table 9 - Enamine preparation

Using the conditions reported by Melchiorre and co-workers for the enamine quantitative formation,[25] both substrates **3** and **5** (entry 1 and 2) and substrates **2** and **5** (entry 3 and 4) were combined, but without success. There was no enamine formation at, at least at the sensitivity level of a 60 MHz NMR. For some reason I'm not able to understand, these conditions, which worked well for amines like **1** or similar, are not able to induce enamine formation. Thus, it was decided to change strategy, using the conditions reported by Mayr and co-workers:[26] instead of using molecular sieves to remove water, azeotropic distillation in toluene was tested to remove water. Instead of using **2**, (S)-5-benzyl-2,2,3-trimethylimidazolidin-4-one (Mac Millan catalyst, 1st generation - $\mathbf{2^{I}}$) was used for the enamine formation in entry 6. Moreover, the addition of 1% p-toluensulfonic acid (p-TSA) should help with the enamine formation as well, offering the catalytic acidity necessary for reaction to go faster. Indeed, the enamine of **2** and **5** after 22 hours of reflux was finally observed, despite being in low amount. Since this type of enamine has never been isolated,[VI] it was decided to use this crude *directly* for photochemistry tests. Replacing substrate **5** to for **6** and 2 for $\mathbf{2^{I}}$, which is reported, in only 2 hours gave full conversion. Evidently, the enamine stabilization due to the phenyl group presence pays back. It was also possible to isolate the resulting enamine $\mathbf{7^{I}}$ by column chromatography, as reported. $\mathbf{7^{I}}$ was then used as model substrate for photochemical tests.

The enamine synthesis test made us question if the formation of enamines from catalyst **3** is *possible* in principle under these conditions, as an enamine such this

[VI] Given the low resolution it was also very difficult to state if the reaction was actually successful or not, as can be seen by the data in the supporting information.

is not reported at all in scientific literature, with the exception of an intramolecular aldol reaction[27](Figure 56).

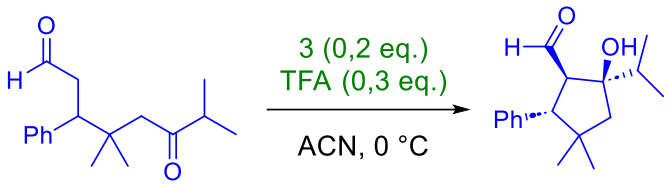

Figure 56 - Example of enamine catalysis by 3

The massive presence of a *strong* acid compared to the amount of catalyst **3** is somehow unusual to induce the enamine formation, and probably this is needed for the nature of catalyst **3** itself. Apparently, the formation of the enamine in the neutral environment is too slow, and this *could* explain why no reactivity at all was observed in the initial photochemical conditions.

To support the strong acid hypothesis, a control test was done: the enamine-catalyzed aldol reaction of propionaldehyde with β-nitrostyrene was run both with **1** and **3** as catalyst (Figure 57).

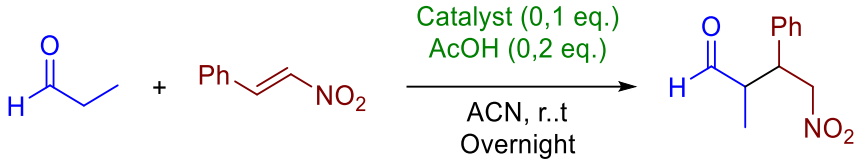

Figure 57 - Enamine reactivity blank test

As reported, **1** gave full conversion to give a diastereomeric mixture of products, while **3** did not induce product. From this test, it is evident that to unlock enamine formation of **3** a stronger acid than acetic acid, such as trifluoroacetic acid, is needed. However, this investigation was done just before the end of the working period, and results are updated to 31st July 2025. Further investigation will be undertaken for sure on this line, as it is certain that **3**-derived enamines can be formed. The use of **3** would be certainly an advantage over **2**, as it is insensitive to aryldiazosulphone, even under photolytic conditions.

It follows the investigation done with enamine **7** and other activation modes.

Direct reaction of enamine with aryldiazosulphones

Enamine **7** was reacted with p-Cl-aryldiazosulphone **8** in different common organic solvents suitable for organocatalytic processes, hoping to observe product **9** (Figure 58).

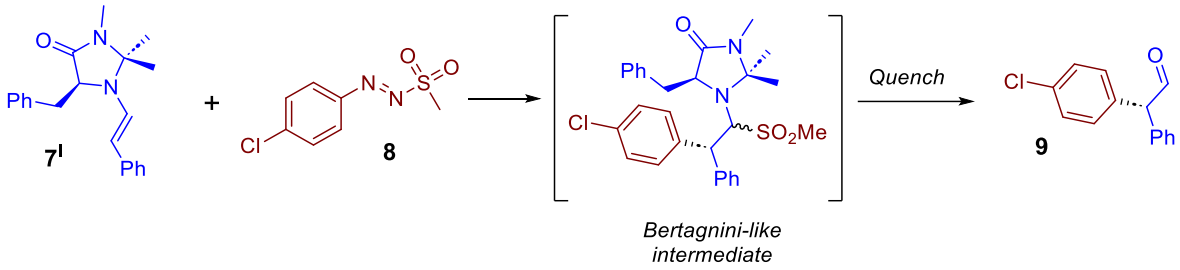

Figure 58 - Direct reaction of 7 with 8

If the mechanistic hypothesis is true, the photochemically induced reaction of **7** with **8** should generate a "Bertagnini-like" intermediate, which should eliminate methylsulfinate after aqueous quench. If a consistent amount of product **9** is thus detected, the slow addition of **8** in the reaction environment should give a catalytic version of the reaction. The solvent screening tests are resumed in Figure 59.

Entry	Solvent	Light	Results
1	Toluene	Yes	Complex crude. Pre- and post-quench look different
2	THF	Yes	Complex crude. Pre- and post-quench look different
3	DCM	Yes	Complex crude. Pre- and post-quench look different
4	ACN	Yes	Complex crude. Pre- and post-quench look the same
5	ACN	No	Dark test, different reactivity

Figure 59 - Direct combination of 7ᴵ and 8 - solvent screening

Reactions run with 7ᴵ (1 eq.) and 8 (1 eq.), UFO vial. Irradiation with a Kessil lamp at 427 nm, 50% power. 4h of irradiation. UFO reactor[24] used as light-delivering system. Solution undergoes 10 minutes of sparging with N_2 before irradiation.

The solvent screening revealed immediately a somehow unexpected very complex behave of these systems. First, all the reaction crude analyzed by HNMR show a multitude of compounds, making the interpretation practically impossible, especially with a 60 MHz NMR available at the time. Moreover, after aqueous quench all crude showed a completely different signal pattern, so we're probably hydrolyzing something. The only invariant system is entry 4 with ACN. The products obtained were separated by column chromatography, attempting to at least identify some products. However, the high resolution HNMR spectrum of these products is very complex, demonstrating an inherent fragility of the products, whatever they are. Moreover, just slight traces of aldehyde peaks are detected, not present in the final products. One example of HNMR spectrum of an isolated product is shown in Figure 60.

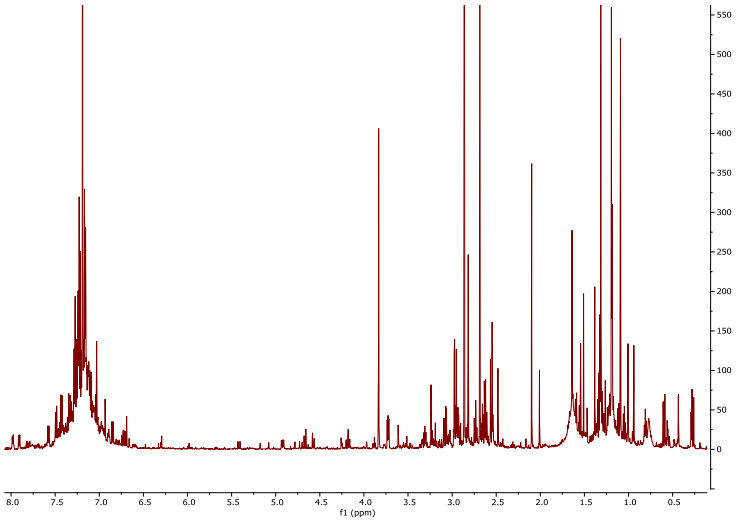

Figure 60 - HNMR of a single-spot isolated sample from reaction of 7 and 8 in acetonitrile

The presence of a molecular structure derived from **2** seems evident for the presence of methyl groups, presumably coming from both the N-methyl and tertbutyl present in the structure.

GC/MS analysis gives some clues about the products structure; the chloride pattern is not visible in the mass spectrum in any product. Moreover, then aryl moiety is not present for sure in the final isolated products. One of the mother peaks can be attributed to an addition product of **7'** and methyl sulfinate somehow, but the fine structure is difficult to deduce. Furthermore, entry 5 shows that the observed reactivity in entry 4 is really photochemically induced: entry 5 was run in the same conditions, but without light. There *is* a partial conversion, but to different, unknown products.

These first experiments using pure enamine do not give any appreciable amount of the expected product **9**. The data show a very complex mixture of products, and little was really understood about that. In our opinion, maybe the reason for this messy behavior is some sort of oligomerization process by the enamine itself (Figure 61): this would explain the almost total absence of aldehydes after hydrolysis and the complex NMR spectra recorded.

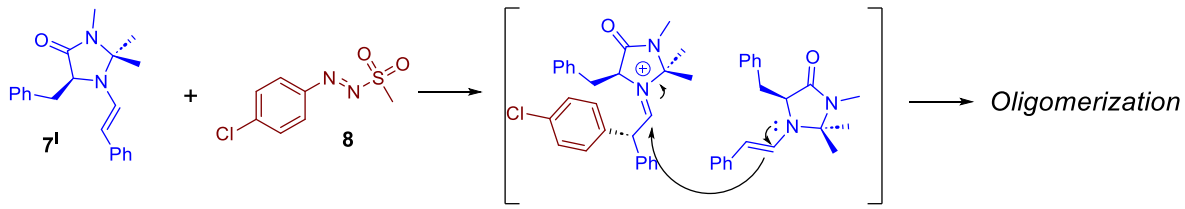

Figure 61 - An example of oligomerization process

Aside from the reason why other reactive paths are followed, it is clear that these series of experiments did not demonstrate our initial mechanistic hypothesis. The only possible way to keep hoping that this reaction can work is to assume that the high enamine concentration induces the complex product formation. Maybe the low concentration of enamine, typical of classical organocatalytic conditions, is essential for this process to work. However, as already learnt from previous experimentation, the catalytic formation of enamine is incompatible with the presence of catalyst **1** and **2**, if not by slow injection via syringe pump, whom ideal conditions are difficult to find. These findings narrow the possible development possibilities to very careful optimization of injection photocatalytic set-up and the use of **3** as organocatalyst with trifluoracetic acid as cocatalyst.

For these reasons, another activation mode was tested to conjugate organocatalysis with aryldiazosulphones photochemistry.

Re-design of reaction: enol chemistry

From early experimentation, it turns out that the activation of the α-position of aldehydes via enamine presents intrinsic problems associated with it: the secondary amine tends to be decomposed in the presence of aryldiazosulphones, both via direct reaction and via photo-induced pathways. More resistant amines on the other side tend to form enamines less readily, offering secondary reaction paths to the photogenerated radicals. In this situation, it was decided to try the asymmetric enol-chemistry, using BINOL-derived phosphoric acid. Enol-chemistry was introduced by List and co-workers,[28] and it basically consists in the acid-base catalyzed formation of ketone-derived enols thanks to the bifunctional phosphate nature. The enol is bound via hydrogen-bond to the phosphate group of the catalyst, which transmits stereochemical information directing the attack of electrophile E to one face of the enol (Figure 62).

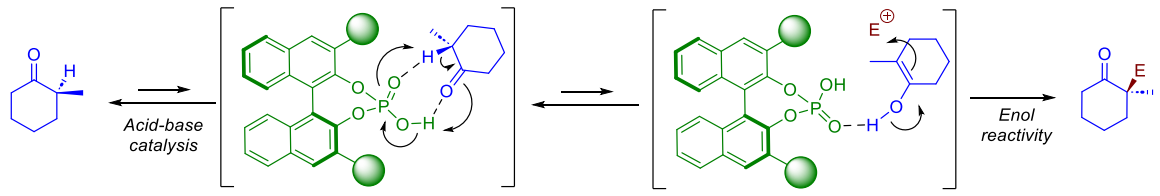

Figure 62 - Enol chemistry activation mode scheme

The regioselectivity of the attack is on the more sterically hindered atom in the α-position, so reasonably the preferred enol is the most hindered. Different electrophiles can be reacted such as Michael acceptors,[28] palladium-allyl complexes[29], diazo-dicarboxylates[30] and nitroso-compounds[31].

Thus, this is a mild organocatalytic method to generate asymmetric enol, a synthetic equivalent of an enamine. The chiral phosphoric acid should be much less sensitive to the electrophilic aryldiazosulphones, even under photocatalytic conditions, as the enol is more nucleophilic than the aromatic ring. It was then decided to test this catalytic system for α-arylation.

Experimental

The investigation started using racemic 2-methyl-phenylacetaldehyde (**10**) and 2-methylcyclohexanone (**11**), as we wanted to test both aldehydes and ketones. The conditions to induce enolization were taken from literature,[29] using toluene as solvent. Aware that enolization is slow under these conditions (days of reaction time), it was decided to slowly inject a solution of aryldiazosulphone, keeping the receiving flask under constant irradiation and heating (Figure 63).

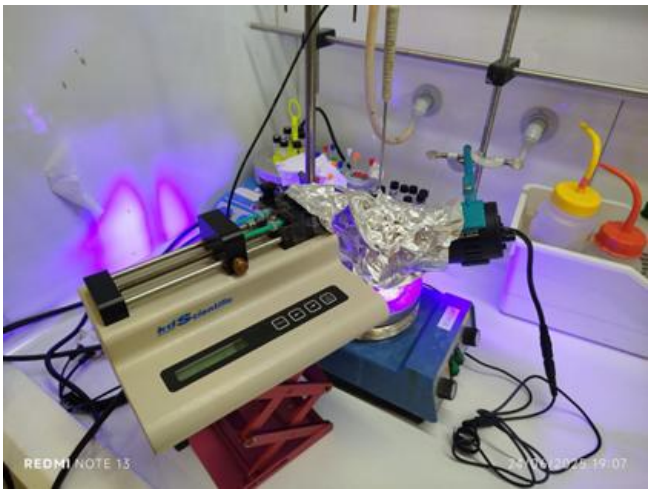

Figure 63 - Slow injection of compounds under heating and irradiation

Indeed, at least in toluene, the system must be kept at around 50 °C to obtain appreciable amounts of products – reasonably to accelerate the enolization processes. It is known that aryldiazosulphones are also thermally liable, but being slowly added under intense irradiation it was assumed that the radical fragmentation would have been much faster. The seminal tests performed with this activation mode are resumed in Table 10.

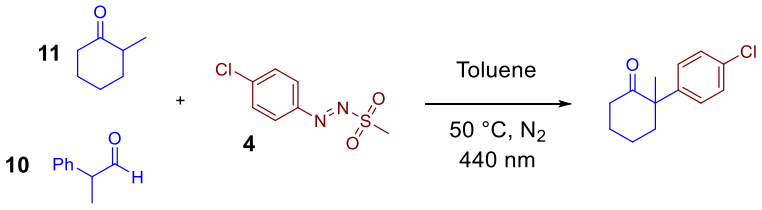

Entry	Substrate	Acid catalyst	Results
1	10	TRIP (0,1 eq.)	Complex mixture
2	10	Benzoic acid (0,1 eq.)	Complex mixture
3	11	TRIP (0,1 eq.)	SM unreacted, chloride-containing products.
4	11	HCl (0,2 eq.)[a]	SM unreacted, chloride-containing products.
5	\	\	Blank test. Chloride-containing products.

Table 10 - Photocatalyzed alpha-arylation of carbonyl compounds with aryldiazosulfones - seminal tests
Reactions run with 8 (1,2 eq.) and carbonyl (1 eq.), in toluene into a vial at 50 °C. Irradiation with a Kessil lamp at 440 nm, 100% power. Slow injection of 4 over 16 h. Solution undergoes 10 minutes of sparging with N_2 before irradiating.
[a] Hydrogen chloride introduced as dioxane solution to avoid water addition.

It was clear immediately from entry 1 and entry 2 that substrate 9 was not suitable for this reaction, as complex mixtures were isolated from these reactions. The HNMR spectra again seemed to be of great complexity even after chromatographic purification. Benzoic acid (entry 2) was tested as alternative acid to induce the enolization of aldehyde **9**. Entry 3 and entry 4 showed no reactivity of the substrate, both with TRIP and HCl as acid catalysts. However, three isomass products containing the chloride atom were detected by GC/MS. Entry 5 is a blank test, performed to confirm that there is no role by **10** or acid catalyst. The same products were found. It turns out that toluene was arylated, as reported by Protti and Fagnoni with aryldiazosulphones.[9] The mechanism is shown in Figure 64.

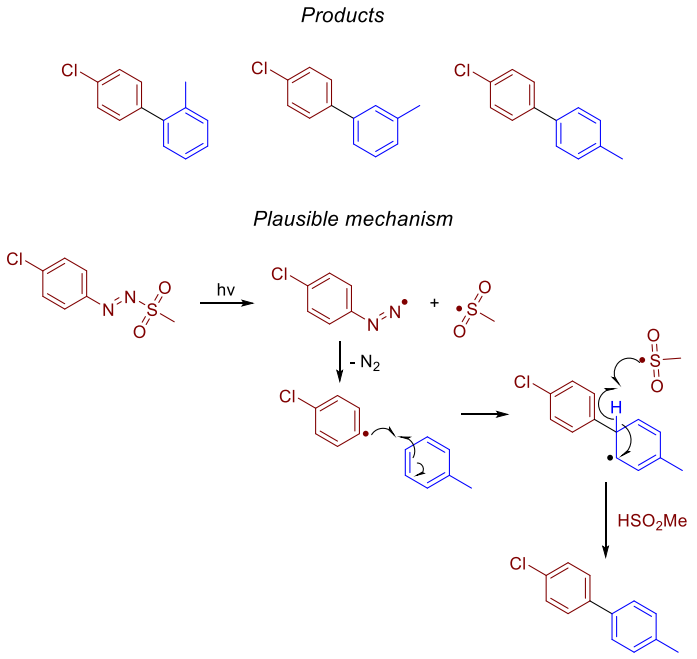

Figure 64 - Radical arylation of toluene

Despite being an interesting result, metal-free arylation of aromatic compounds is a difficult reaction, it is already reported and there is no possibility of having regioselectivity here with simple methods. Toluene is then ruled out as possible reaction solvent. The experimentation was stopped at this point for time reasons. Other less electrophilic solvents compatible with aryldiazosulphones will be tested in the future. ACN and DCM indeed already reported to work for enolization with phosphoric acids as well.[31]

Conclusions

Enantioselective α-arylation of carbonyl compounds, in particular aldehydes, is an important reaction to forge asymmetric benzyl-substituted compounds. The same is true for other α-functionalization of aldehydes. While α-coupling with sp^3 electrophiles is well known to proceed via enamine catalysis, the reaction with sp^2 electrophiles, for example aryl groups, is less straightforward, as it requires the intermediation by copper (I) and the use of iodonium salts as reagents.[32] The development of transition metal-free methods and/or different arylation agents are thus highly desirable. In particular, different arylation agents allow to start from functional groups different from iodine.

Aryldiazosulphones are interesting compounds made of an aryl moiety, a diazo group, and sulphone. They are prone to photolysis, both heterolytic and homolytic. The latter activation mode has been exploited by the group of Professor Protti and Fagnoni for many synthetic applications, as it is a source of both aryl-diazo radicals and aryl radicals.

The core idea for this project is to merge the reactivity of aryl-diazo compounds with organocatalysis via enamine or enol: the C2 position of these compounds is indeed nucleophilic and could theoretically capture the aryl radical generated photochemically. Here the seminal experimentation of this asymmetric organocatalyzed asymmetric arylation is reported. It was found that the 3,3-difluorinated prolinol-derived structures are suitable catalysts, but they struggle to form enamines in the conditions tested. MacMillan (II)-type catalysts are photodegraded, and their enamines too under different conditions. In the future, 3,3-difluorinated prolinols will be tested in the presence of a *strong acid* as catalyst, with slow addition of aryldiazosulphones under constant irradiation. At the same time, seminal tests were performed for the enol activation of both aldehydes and ketones, using chiral phosphoric acids and achiral acids. Up to now, arylation of toluene was obtained. In the future other less reactive solvents such

as ACN and DCM, already reported to work for enol chemistry, will be tested, hoping to capture the elusive aryl radicals with the catalytically formed enols.

Supporting information

It follows the experimental details on the most significant tests that were done. Most of the unsuccessful results are not shown.

Catalyst stability test

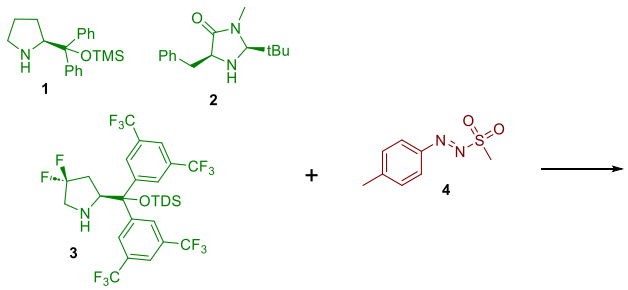

The catalyst (0.2 equiv.) was weighed into a vial and dissolved into 250 ul of toluene or chloroform. Then, 10 mg (1 equiv.) of aryldiazosulphone 4 was added as solid. The samples were stored in the dark for 24 hours, then analyzed by TLC. It was observed the complete degradation of **1**, partial degradation of **2** and no new spots for **3**.

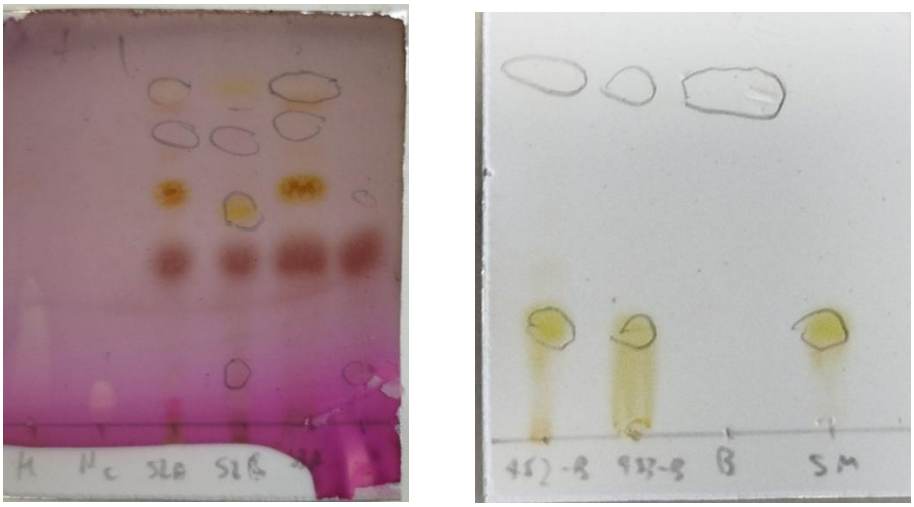

On the left TLC degradation of **1** and **2**. On the right catalyst **3** showed no degradation at all.

Photochemical α–arylation of aldehydes *via* enamine catalysis

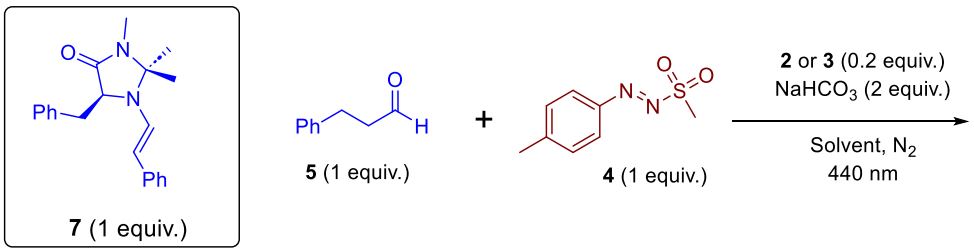

0.2 equiv. of catalyst **2** or **3** were weighed into a vial and then dissolved into 0,5 ml of ACN, toluene or chloroform. Then, 10.1 ul (0.076 mmol, 1 equiv.) of 3-Ph-propenal (**5**) are then added and the solution allowed to stir for 10 minutes (give time to the enamine to be formed). Then, 12,7 mg (0.15 mmol, 2 equiv.) of $NaHCO_3$ were added, followed by 15 mg (0.076 mmol, 1 equiv.) of aryldiazosulphone **4**. The reaction is in the dark stirring for 40 minutes and monitored by TLC. Ok, no degradation. The solution is degassed (10 minutes using N_2), then put into the UFO reactor overnight 440 nm, max power.

Quench: filter the crude over celite, washing with DCM. Then, solvents were evaporated. All HNMR and GC/MS analysis were performed and all chromatographic separation attempts produced unreadable data.

A similar procedure was used also for enamine arylation. The 1 equivalent of enamine **7** instead of aldehyde and organocatalyst can be used pre-dissolved in acetonitrile.

7 - (2S,5S)-5-benzyl-2-(tert-butyl)-3-methyl-1-((E)-3-phenylprop-1-en-1-yl)imidazolidin-4-one

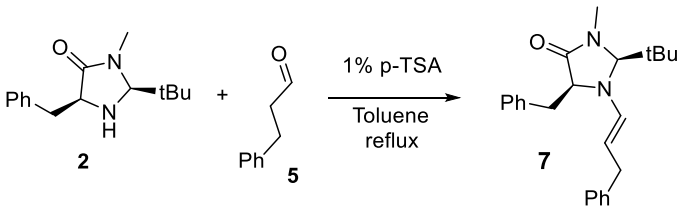

100 mg (0.406 mmol) of **2** were loaded into a 1 neck 5 ml round bottom flask. It followed the addition of 1 ml of toluene, 53,9 ul (0.406 mmol) of aldehyde **5** and 0,7 mg (4.6 μmol) of p-TSA. A small Dean-Stark apparatus was installed and the reaction put under inert atmosphere though N_2/vacuum cycles. Then, the system was set-up to reflux for 22 h.

After 22 h the system was allowed to go to room temperature. Then, 500 ul of the solution was transferred into a well-flamed NMR tube under inert atmosphere and analyzed by HNMR. There is partial enamine formation. The solution containing **7** was used as it is for further photochemical tests.

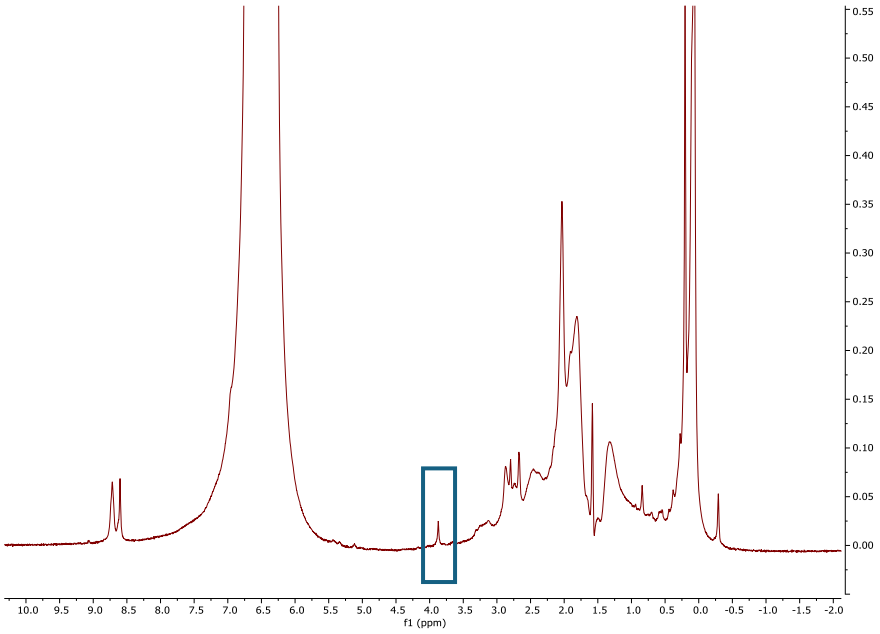

1HNMR - 60 MHz – toluene with solvent suppression. Peak of the enamine detected. It was not possible to characterize it better.

7^{I} - (2S,5S)-5-benzyl-2-(tert-butyl)-3-methyl-1-((E)-styryl)imidazolidin-4-one

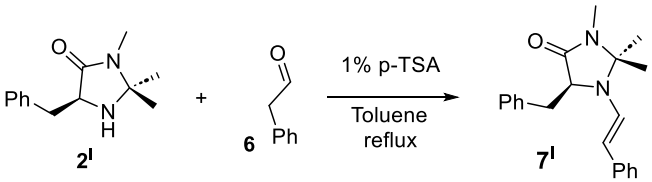

400 mg (1.57 mmol) of **2**^{I} as hydrochloride salt were weighed and dissolved in 0,1 M NaOH (3 ml, pH check), extracting with 3 ml of DCM. The organic phase was washed twice with water to remove any residual NaOH. Once evaporated the amine was stripped with toluene a couple of times to remove water. Then, it was dissolved in 2,5 ml of toluene. Into a 5 ml round bottom flask, 2,7 mg (0.0157 mmol) of p-TSA were weighted, followed by the addition of the toluene solution of amine. Finally, 175 ul (1.57 mmol) of aldehyde **6** were added and the reaction put under nitrogen in a Dean-stark system. The trap was filled with 4 Å MS (activated and kept in the dryer) and rinsed with toluene, in order to don't lose it. The system was refluxed for 2 h. After this time, we have a yellow solution. A TLC anaylis was done (PE:AcOEt 7:3 + 1% TEA) showed no aldehyde left-

The toluene was then removed under reduced pressure and in the meantime a column was set up. Short column using oven dry silica (200 °C, 2 days) in order to do not hydrolyze it. Then the crude is diluted in DCM and loaded into the column.

Eluent: 1 Volume 9:1 PE:AcOEt + 1% TEA to elute the aldehyde, then 7:3 PE:AcOEt + 1% TEA. 472,6 mg of **7** were obtained (95% yield).

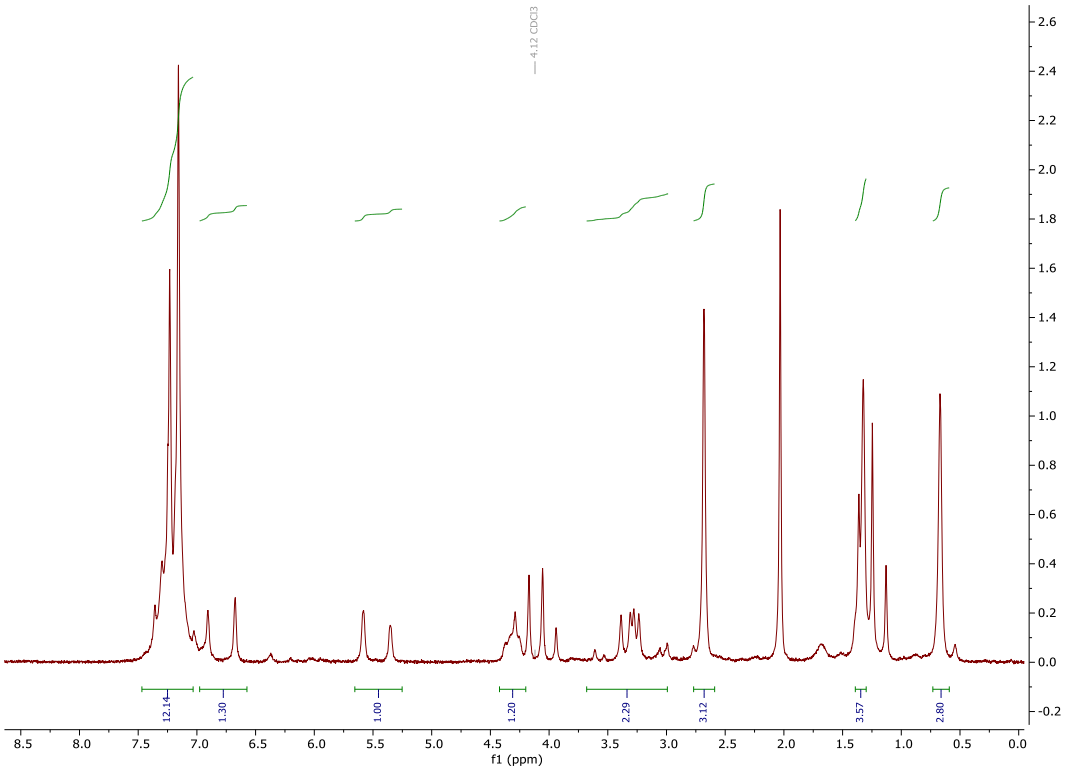

7[I] - ^{1}H NMR (61 MHz) δ 7.38 – 7.09 (m, 5H), 6.79 (d, *J* = 14.2 Hz, 1H), 5.47 (d, *J* = 14.3 Hz, 1H), 4.29 (m, 1H), 3.49 – 2.99 (m, 2H), 2.67 (s, 3H), 1.34 (s, 3H), 0.67 (s, 3H)

Photochemical α–arylation of carbonyl compounds *via* enol catalysis

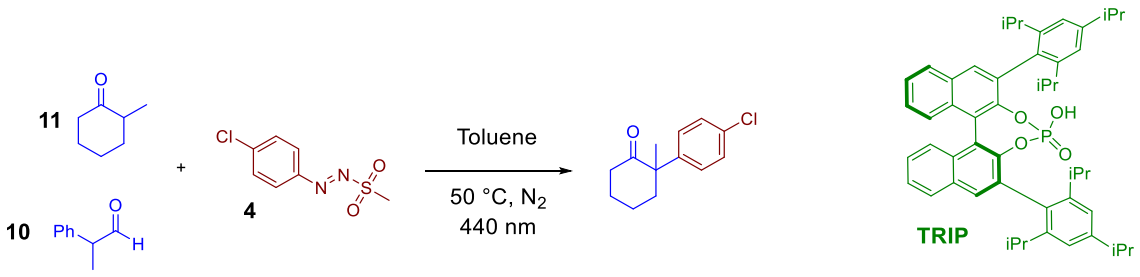

9.15 µmol of acid catalyst was weighted[VII] and added to a vial, which was then set under inert atmosphere. Then, dry toluene (250 ul) was added, dissolving it. Then, 0.09 mmol of carbonyl compound **10** or **11** were injected.

Into another vial 20 mg (0.11 mmol) of aryldiazo compound **4** were weighted and put under inert atmosphere, then dissolved into 250 ul of dry toluene and withdrawn with a syringe under inert atmosphere. Then, the syringe containing **4** was covered with aluminum foil to avoid light decomposition and injected into the main vial in around 16 h (flow = 0,3 ul/min). The main vial in the meantime is irradiated with a Kessil lamp, max power, 440 nm. Reaction is conducted at 50°C. Reaction is then quenched with water and toluene phase is separated, removing the solvent under reduced pressure. The set up is shown below.

The only defined and characterized products are the arylated toluene isomers. The GC/MS spectrum is shown below.

[VII] In case HCl is used some HCl 37% n water is taken and put into a vial

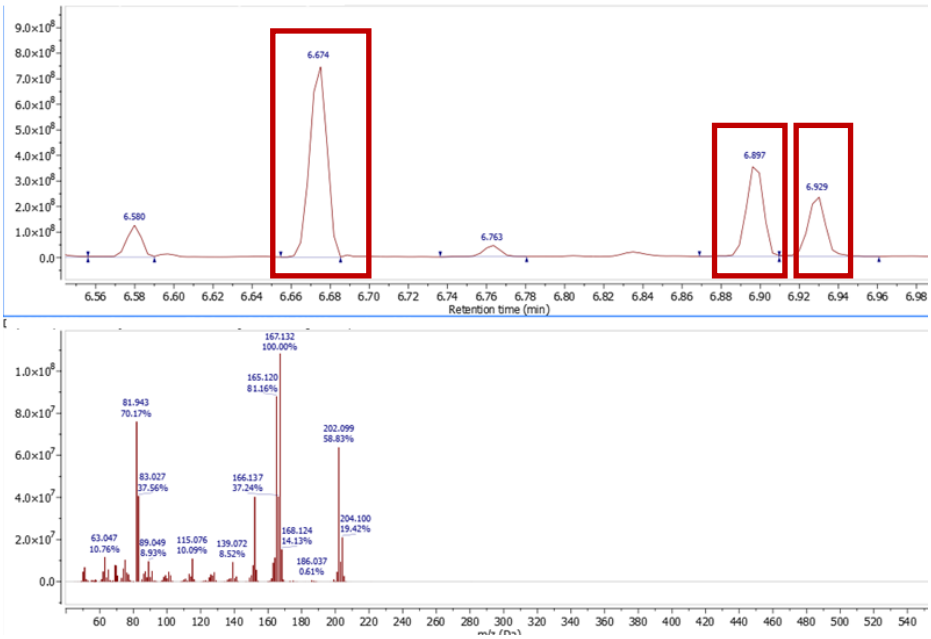

m/z = 204.100, 202.099, 3:1 ratio as $^{35}Cl/^{37}Cl$

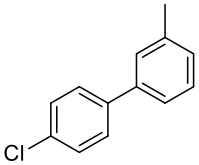

m/z: 202.05 (100.0%), 204.05 (32.0%), 203.06 (14.2%), 205.06 (4.6%)

Only the first peak on the left is shown. The other two have the same molecular ion peak, but with a different fragmentation pattern.

Bibliography

(1) Photochemistry. In *The IUPAC Compendium of Chemical Terminology*; International Union of Pure and Applied Chemistry (IUPAC): Research Triangle Park, NC, 2014. https://doi.org/10.1351/goldbook.P04588.

(2) Norrish, R. G. W.; Bamford, C. H. Photo-Decomposition of Aldehydes and Ketones. *Nature* 1937, *140* (3535), 195–196. https://doi.org/10.1038/140195b0.

(3) Photocatalysis. In *The IUPAC Compendium of Chemical Terminology*; International Union of Pure and Applied Chemistry (IUPAC): Research Triangle Park, NC, 2014. https://doi.org/10.1351/goldbook.P04580.

(4) Nicewicz, D. A.; MacMillan, D. W. C. Merging Photoredox Catalysis with Organocatalysis: The Direct Asymmetric Alkylation of Aldehydes. *Science (1979)* 2008, *322* (5898), 77–80. https://doi.org/10.1126/science.1161976.

(5) Wilger, D. J.; Grandjean, J.-M. M.; Lammert, T. R.; Nicewicz, D. A. The Direct Anti-Markovnikov Addition of Mineral Acids to Styrenes. *Nat Chem* 2014, *6* (8), 720–726. https://doi.org/10.1038/nchem.2000.

(6) Tucker, J. W.; Stephenson, C. R. J. Shining Light on Photoredox Catalysis: Theory and Synthetic Applications. *J Org Chem* 2012, *77* (4), 1617–1622. https://doi.org/10.1021/jo202538x.

(7) Jablonski Diagram. In *The IUPAC Compendium of Chemical Terminology*; International Union of Pure and Applied Chemistry (IUPAC): Research Triangle Park, NC, 2014. https://doi.org/10.1351/goldbook.J03360.

(8) Parsaee, F.; Senarathna, M. C.; Kannangara, P. B.; Alexander, S. N.; Arche, P. D. E.; Welin, E. R. Radical Philicity and Its Role in Selective Organic Transformations. *Nature Reviews Chemistry*. Nature Research July 1, 2021, pp 486–499. https://doi.org/10.1038/s41570-021-00284-3.

(9) Crespi, S.; Protti, S.; Fagnoni, M. Wavelength Selective Generation of Aryl Radicals and Aryl Cations for Metal-Free Photoarylations. *Journal of Organic Chemistry* 2016, *81* (20), 9612–9619. https://doi.org/10.1021/acs.joc.6b01619.

(10) Kobayashi, M.; Fujii, S.; Minato, H. Photolysis of Phenylazo *p* -Tolyl Sulfones. *Bull Chem Soc Jpn* 1972, *45* (7), 2039–2042. https://doi.org/10.1246/bcsj.45.2039.

(11) Qiu, D.; Lian, C.; Mao, J.; Fagnoni, M.; Protti, S. Dyedauxiliary Groups, an Emerging Approach in Organic Chemistry. The Case of Arylazo Sulfones. *Journal of Organic Chemistry* 2020, *85* (20), 12813–12822. https://doi.org/10.1021/acs.joc.0c01895.

(12) Kamigata, N.; Kobayashi, M. Azosulfones: Versatile Precursors for Aryl Radicals, Aryl Cations, Aryl Anions, Carbenes, and Benzynes. *Sulfur reports* 1982, *2* (3), 87–128. https://doi.org/10.1080/01961778208082429.

(13) Sauer, C.; Liu, Y.; De Nisi, A.; Protti, S.; Fagnoni, M.; Bandini, M. Photocatalyst-free, Visible Light Driven, Gold Promoted Suzuki Synthesis of (Hetero)Biaryls. *ChemCatChem* 2017, *9* (24), 4456–4459. https://doi.org/10.1002/cctc.201701436.

(14) Onuigbo, L.; Raviola, C.; Di Fonzo, A.; Protti, S.; Fagnoni, M. Sunlight-Driven Synthesis of Triarylethylenes (TAEs) via Metal-Free Mizoroki–Heck-Type Coupling. *European J Org Chem* 2018, *2018* (38), 5297–5303. https://doi.org/10.1002/ejoc.201800883.

(15) Dossena, A.; Sampaolesi, S.; Palmieri, A.; Protti, S.; Fagnoni, M. Visible Light Promoted Metal- and Photocatalyst-Free Synthesis of Allylarenes. *J Org Chem* 2017, *82* (19), 10687–10692. https://doi.org/10.1021/acs.joc.7b01532.

(16) Xu, Y.; Yang, X.; Fang, H. Additive- and Photocatalyst-Free Borylation of Arylazo Sulfones under Visible Light. *J Org Chem* 2018, *83* (20), 12831–12837. https://doi.org/10.1021/acs.joc.8b01662.

(17) Blank, L.; Fagnoni, M.; Protti, S.; Rueping, M. Visible Light-Promoted Formation of C–B and C–S Bonds under Metal- and Photocatalyst-Free Conditions. *Synthesis (Stuttg)* 2019, *51* (05), 1243–1252. https://doi.org/10.1055/s-0037-1611648.

(18) Lian, C.; Yue, G.; Mao, J.; Liu, D.; Ding, Y.; Liu, Z.; Qiu, D.; Zhao, X.; Lu, K.; Fagnoni, M.; Protti, S. Visible-Light-Driven Synthesis of Arylstannanes from Arylazo Sulfones. *Org Lett* 2019, *21* (13), 5187–5191. https://doi.org/10.1021/acs.orglett.9b01788.

(19) Nicewicz, D. A.; MacMillan, D. W. C. Merging Photoredox Catalysis with Organocatalysis: The Direct Asymmetric Alkylation of Aldehydes. *Science (1979)* 2008, *322* (5898), 77–80. https://doi.org/10.1126/science.1161976.

(20) Othman Abdulla, H.; Scaringi, S.; Amin, A. A.; Mella, M.; Protti, S.; Fagnoni, M. Aryldiazenyl Radicals from Arylazo Sulfones: Visible Light-Driven Diazenylation of Enol Silyl Ethers. *Adv Synth Catal* 2020, *362* (11), 2150–2154. https://doi.org/10.1002/adsc.201901424.

(21) Welin, E. R.; Warkentin, A. A.; Conrad, J. C.; MacMillan, D. W. C. Enantioselective α-Alkylation of Aldehydes by Photoredox Organocatalysis: Rapid Access to Pharmacophore Fragments from β-Cyanoaldehydes. *Angewandte Chemie International Edition* 2015, *54* (33), 9668–9672. https://doi.org/10.1002/anie.201503789.

(22) Schweitzer-Chaput, B.; Horwitz, M. A.; de Pedro Beato, E.; Melchiorre, P. Photochemical Generation of Radicals from Alkyl Electrophiles Using a Nucleophilic Organic Catalyst. *Nat Chem* 2019, *11* (2), 129–135. https://doi.org/10.1038/s41557-018-0173-x.

(23) Di Sabato, A.; Santoni, M.; Moldoveanu, V. G.; Camilli, A.; Feroci, M.; Olivo, G.; Simonis, B.; Sturabotti, E.; Leonelli, F.; Vetica, F. Synergistic Visible Light Nanophotocatalysis and Asymmetric Organocatalysis for the Stereoselective α-Alkylation of Aldehydes. *Adv Synth Catal* 2025, *367* (13). https://doi.org/10.1002/adsc.202500354.

(24) Masson, T. M.; Zondag, S. D. A.; Schuurmans, J. H. A.; Noël, T. Open-Source 3D Printed Reactors for Reproducible Batch and Continuous-Flow Photon-Induced Chemistry: Design and Characterization. *React Chem Eng* 2024, *9* (8), 2218–2225. https://doi.org/10.1039/D4RE00081A.

(25) Silvi, M.; Arceo, E.; Jurberg, I. D.; Cassani, C.; Melchiorre, P. Enantioselective Organocatalytic Alkylation of Aldehydes and Enals Driven by the Direct

Photoexcitation of Enamines. *J Am Chem Soc* 2015, *137* (19), 6120–6123. https://doi.org/10.1021/jacs.5b01662.

(26) Lakhdar, S.; Maji, B.; Mayr, H. Imidazolidinone-Derived Enamines: Nucleophiles with Low Reactivity. *Angewandte Chemie International Edition* 2012, *51* (23), 5739–5742. https://doi.org/10.1002/anie.201201240.

(27) Woźniak, Ł.; Magagnano, G.; Melchiorre, P. Enantioselective Photochemical Organocascade Catalysis. *Angewandte Chemie International Edition* 2018, *57* (4), 1068–1072. https://doi.org/10.1002/anie.201711397.

(28) Felker, I.; Pupo, G.; Kraft, P.; List, B. Design and Enantioselective Synthesis of Cashmeran Odorants by Using "enol Catalysis. *Angewandte Chemie - International Edition* 2015, *54* (6), 1960–1964. https://doi.org/10.1002/anie.201409591.

(29) Pupo, G.; Properzi, R.; List, B. Asymmetrische Katalyse Mit CO 2 : Die Direkte A-Allylierung von Ketonen . *Angewandte Chemie* 2016, *128* (20), 6204–6207. https://doi.org/10.1002/ange.201601545.

(30) Shevchenko, G. A.; Pupo, G.; List, B. Catalytic Asymmetric α-Amination of α-Branched Ketones via Enol Catalysis. *Synlett* 2015, *26* (10), 1413–1416. https://doi.org/10.1055/s-0034-1380680.

(31) Shevchenko, G. A.; Pupo, G.; List, B. Direct Asymmetric α-Hydroxylation of Cyclic α-Branched Ketones through Enol Catalysis. *Synlett* 2019, *30* (1), 49–53. https://doi.org/10.1055/s-0037-1611084.

(32) Allen, A. E.; MacMillan, D. W. C. Enantioselective α-Arylation of Aldehydes via the Productive Merger of Iodonium Salts and Organocatalysis. *J Am Chem Soc* 2011, *133* (12), 4260–4263. https://doi.org/10.1021/ja2008906.

Chapter 3 – Organosilicon chemistry

Introduction

Organosilicon chemistry, an important branch of organic chemistry, is the study of compounds containing carbon-silicon bonds. Silicon is a precious alley in organic chemistry, as the presence of carbon-silicon compounds is essential for many technological areas. For example, polysiloxanes are important materials which have widespread application in everyday life. Another emerging application of organosilicon compounds is bioactive molecules: silicon-containing bioactive molecules have shown interesting chemical-physical properties, especially diffusion in biological tissues, and it's currently a hot research topic.[1,2]

The area of synthetic chemistry also benefits the presence of silicon. Indeed, there are several name reactions involving organosilicon chemistry[3] and silyl-ethers are a fundamental class of protecting groups.

Properties of silicon

It follows a brief description of silicon fundamental properties in the context of organic chemistry to introduce the main concepts used in this chapter. First, carbon–silicon bond is strong enough for the trialkyl silyl group to survive synthetic transformations on the rest of the molecule but weak enough for it to be cleaved by specifical methodologies employing different nucleophiles, especially fluoride anion. Another important factor is the length of the C–Si bond (1.89 Å) - it is significantly longer than a typical C–C bond (1.54 Å). Silicon has a lower electronegativity (1.8) than carbon (2.5) and therefore C–Si bonds are polarized towards carbon. This makes silicon susceptible to attack by nucleophiles, despite the strength of the C–Si bond means that alkyl silanes are stable under common operative conditions.

Silicon makes strong bonds with electronegative elements, especially oxygen, fluoride (one of the strongest bonds in nature) and the other halides. Indeed, the Si-X (X = heteroatom) bond formation is thermodynamic pushing to break a C-Si bond in organosilicon chemistry. Moreover, silicon can be easily extruded from positively charged organic molecules via pure cationization as R_3Si^+, to be then captured by a nucleophile in the reaction environment (Figure 65).[4,5]

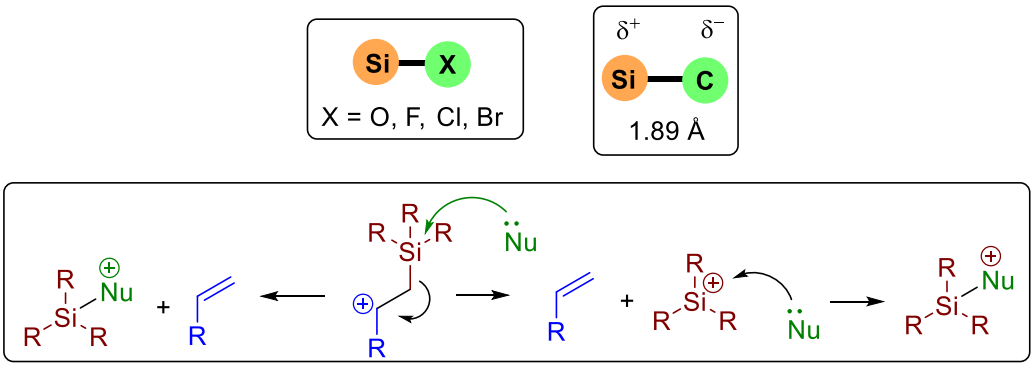

Figure 65 - Fundamental chemical properties of silicon in organic molecules

Silicon moieties interact with π-systems and p-orbitals by coplanar σ–C-Si bonds, which have a higher energy compared to C-C bonds and a more favorable geometry, and can thus donate more electron density. This interaction has deep consequences on the chemistry of organosilicon compounds, modulating the energy of both ground states and reaction intermediates. The interaction between a π-system of a C=C bond and the σ–C-Si *increases* the HOMO energy of the olefin (ground state destabilization). This makes that olefin much more nucleophilic, as shown by the molecular orbital sketch in Figure 66.[4]

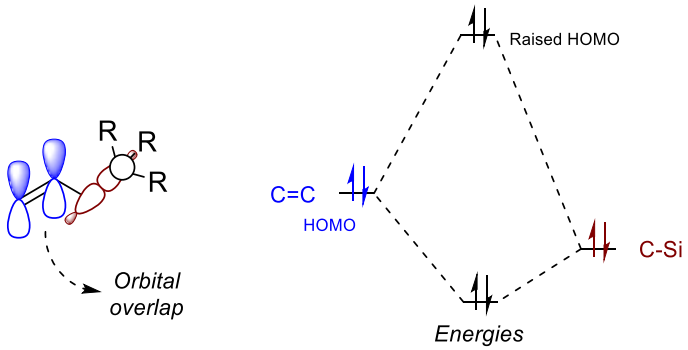

Figure 66 - Orbital interaction with π - system

Moreover, the σ–C-Si can overlap with the empty p-orbital of carbocations, significantly stabilizing it. This makes the reaction with electrophiles even faster, as the energy to access the high energy-intermediate is lower compared to a classical olefin, alkyne or allene (Figure 67).[4]

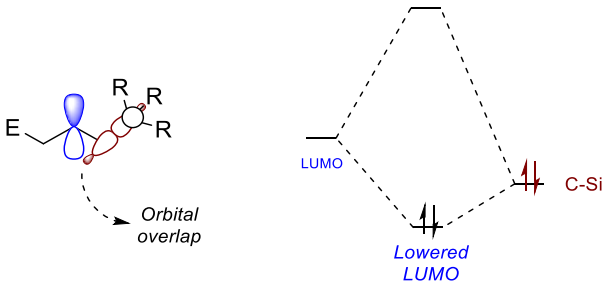

Figure 67 - Orbital interaction with empty p-orbital

Both these effects contribute to the general enhanced reactivity of silicon-containing olefins, alkynes, allenes and arene compound compared to their purely alkyl counterpart. This phenomenon is called "β-silicon effect", as the silicon is always in the β-position respect to the carbon carrying the positive charge to be effective. This kinetic effect is considered among the strongest in organic chemistry, and it can be well exemplified comparing the N values of the Mayr scale for two similar alkenes (Figure 68).[4]

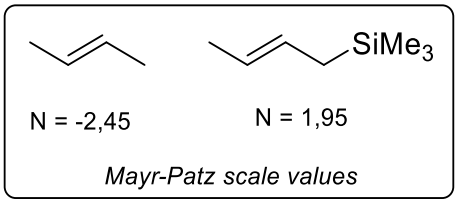

Figure 68 - Mayr scale N-values for normal olefin and allyl silane with a similar structure

The difference of N is 3,5, which means that the reaction of an electrophile with the allyl silane is expected to be around 3100 times faster than the corresponding olefin.

The termination of these polar reactions can be both desilylation or nucleophilic addition to saturate the electronic vacancy. Given the conjugation of σ–C-Si bond with an empty orbital, this bond is very weak and has a great tendency to break, so in the majority of cases silicon elimination is the dominant process. Moreover, [1,2]- silicon-migration events are sometimes observed as well, helped by the liability of the conjugated σ–C-Si bond.

Different unsaturated groups can be activated by the β-silicon effect, yielding products with various substitution patterns. A summary of the main reactive groups is shown in Figure 69, taking the elimination reaction es example.

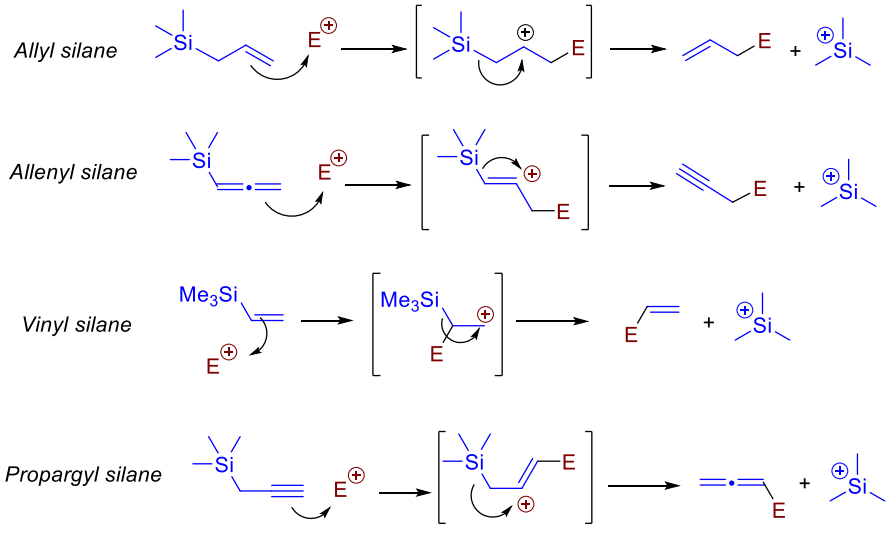

Figure 69 - Different silanes regiochemistry

Danheiser cyclopentane annulation

The Danheiser cyclopentane annulation is a reaction developed by Professor Rick L. Danheiser and co-workers in 1981.[6] It is a formal [3+2] cycloaddition between an allenylsilane and a Michael acceptor, typically a ketone or ester.[6,7] The reaction is thought to proceed via a β-silyl vinyl cation which then undergoes [1,2]-silicon shift and intramolecular nucleophilic attack by the enolate generated (Figure 70).

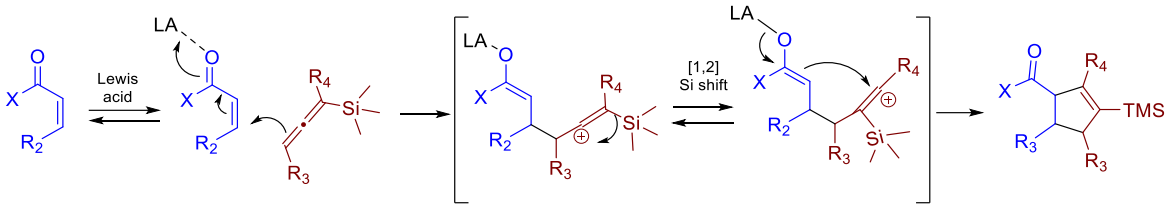

Figure 70 - Danheiser annulation – mechanism

An alternative fate is possible for the stabilized silyl cation before the [1,2]-shift: enolate C-attack to obtain a 4-membered ring, enolate O-attack to obtain a dihydropyran or nucleophilic attack at silicon that triggers elimination to obtain a propargylation product (Figure 71).

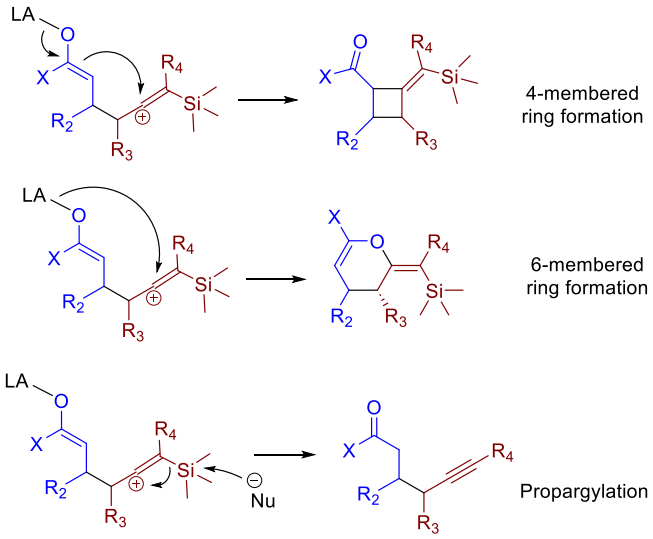

Figure 71 - Possible side reactions of Danheiser cyclopentane annulation

Danheiser annulation can also be done with simple carbonyl compounds as electrophiles, and in that case, heterocycles are generated. However, these reaction variants are not introduced here as they are not considered in our work. The most common Lewis acid used is over stoichiometric $TiCl_4$, with some rare examples of Sc^{3+} complexes in heteroatomic variants, i.e. *very strong Lewis acids* are needed to make this reaction work.

The 5-membered carbocyclic products are very common structures in natural products and pharmaceuticals compounds. Thus, the [3+2] all-carbon addition is a very interesting reaction in our opinion, as it is difficult to realize by other means

Indeed, Danheiser pentane annulation found application in natural products synthesis.[3] One example is the racemic synthesis of **GB18** by Shenvi and co-workers,[8] in which the [3+2] annulation is the on the key skeleton-forging steps (Figure 72).

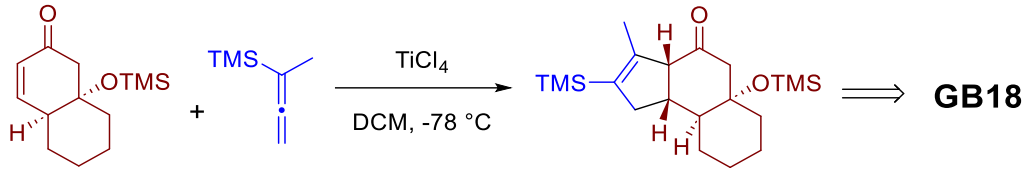

Figure 72 - Application of Danheiser cyclopentane annulation to the synthesis of natural products

Despite the high synthetic value of Danheiser cyclopentane annulation, there are no *asymmetric* examples of this *specific* all-carbon reaction. One notable example of asymmetric hetero-Danheiser cycloaddition was reported by Evans and co-workers in the synthesis of chiral dihydrofurans: the researchers used a Sc^{3+} complex with an asymmetric oxazolidine as chiral ligand (Figure 73).

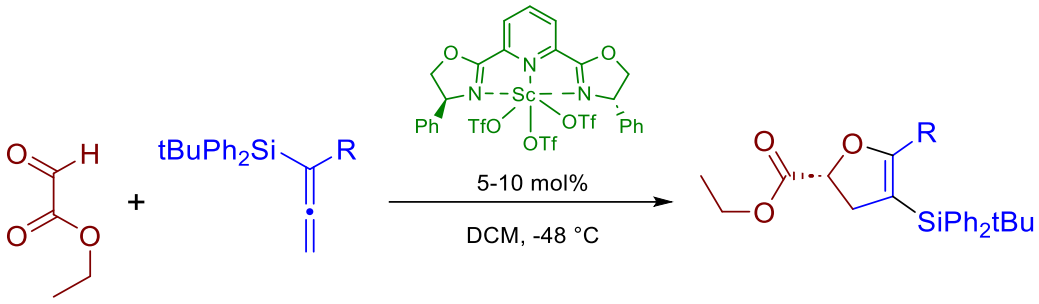

Figure 73 - Evans' asymmetric hetero-Danheiser cycloaddition

Given the high synthetic value of Danheiser cyclopentane annulation, the development of an *asymmetric* and *mild* version of the reaction is highly desirable.

Design of an organocatalyzed asymmetric Danheiser cyclopentane annulation

Given our interest in the field of organocatalysis, we thought that the key bond-forming event between the Michael acceptor and silyl allene can be triggered by an α,β-unsaturated iminium ion as electrophile. The use of an asymmetric organocatalyst as amine, for example a prolinol-derived or a MacMillan-type catalyst, would drive the attack by nucleophilic silyl allene preferentially on one face of the aldehyde-derived iminium ion, forging a stereocenter and generating an

intermediate enamine-vinylsilyl cation (Figure 74). The electrophilic activation in this way would be possible thanks to the LUMO lowering induced by the iminium ion formation.

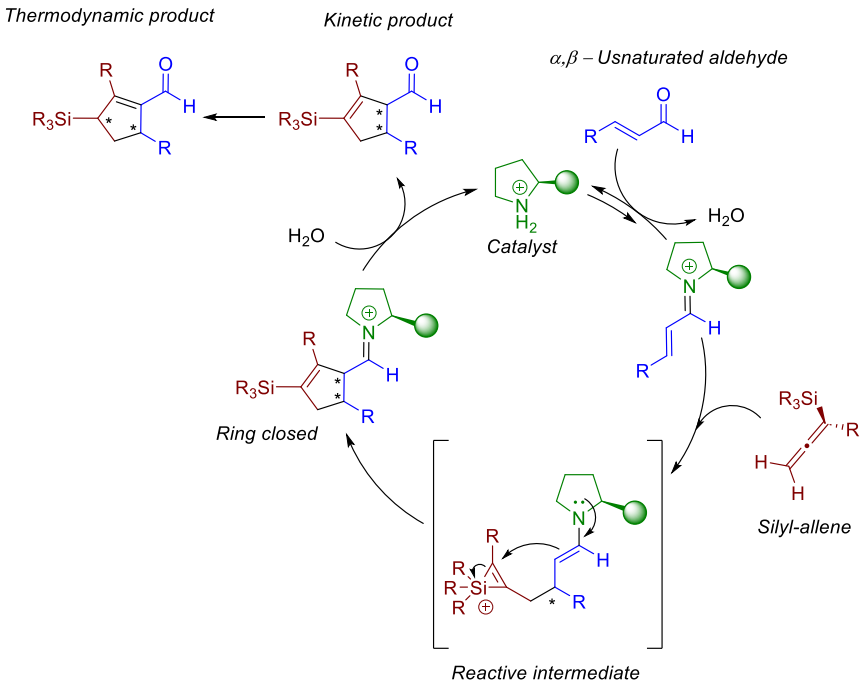

Figure 74 - Catalytic cycle design

This reactive intermediate in our plans undergoes [1,2]-silicon shift, the silicon migrating on the internal carbon. At this point, the C2 of the enamine should attack the terminal vinyl cation closing the 5-membered carbon ring. This reactivity hypothesis is inspired by the example of Danheiser annulation, mimicking the titanium enolate attack. The saturated iminium ion obtained after this attack can then undergo hydrolysis restoring the catalyst and yielding a kinetic product, with a de-conjugated alkene. The action of the acidic environment or the presence of the organocatalyst in theory could induce the isomerization to the conjugated, thermodynamic product.

Taking into account the possibility of side-reactivity events, such as enamine hydrolysis, vinyl cation solvation, or 4-membered ring closure, it is evident that the major difficulty for the realization of an organocatalyzed Danheiser pentane annulation is the attack of silyl allene to the α,β - unsaturated iminium ion. Moreover, even if side reactions can attack the intermediate enamine-vinyl cation, the bond-forming event itself could be of interest, whatever the fate of the silyl-cation (Figure 75).

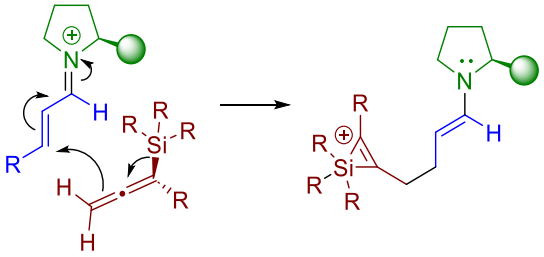

Figure 75 - Bond forming-event between allyl-silane and iminium ion - reactive enough?

To the best of our knowledge, the N-parameter on the Mayr-Patz scale for allenylsilanes has *not* been measured, so a direct estimation on the reactivity of this electrophile/nucleophile couple cannot be done. However, both vinyl-silanes and allyl silanes N-parameter values have been measured, so at least a gross prediction can be made (Figure 76).

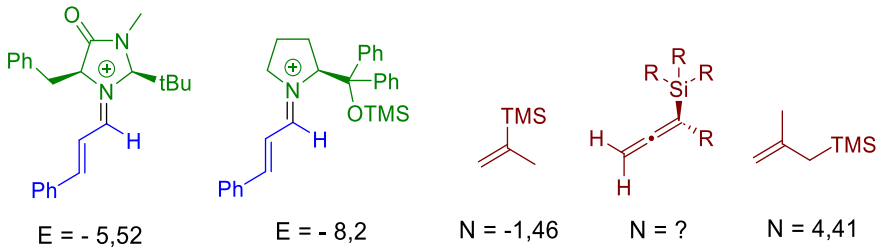

Figure 76 - Known N-values for reaction design

The reactivity of an allyl silane must rely between allyl and vinyl silanes. Assuming to use MacMillan (II) as catalyst, log(k) ranges between -6,96 and -1,11 – which means something that *not feasible* and something *feasible*, respectively. To verify our hypothesis, we started to screen different organocatalytic conditions, searching for some kind of reactivity.

Experimental

Materials synthesis

Cinnamaldehyde (**1**) was chosen as model Michael acceptor, as aldehydes readily form iminium ions with secondary amines catalysts. The choice of silyl allene is less straightforward: 1,1 or 1 – substituted silyl allenes are achiral, so there are no match-mismatch effects with the chiral iminium ion, a good simplification of the reactive system for initial studies. However, tertiary or quaternary silyl allene are more electron-rich, so they are more nucleophilic and can react faster.

As we did not find any commercially available material at a reasonable price in the providers catalogue, we decided to synthesize the allenes by different simple methodologies: conjugate addition of organocuprates to propargylic substrates[9,10],

conjugated reduction of propargylic substrates[11] (Figure 77) and direct allenylation of silyl chlorides[12] (*Figure 77*).

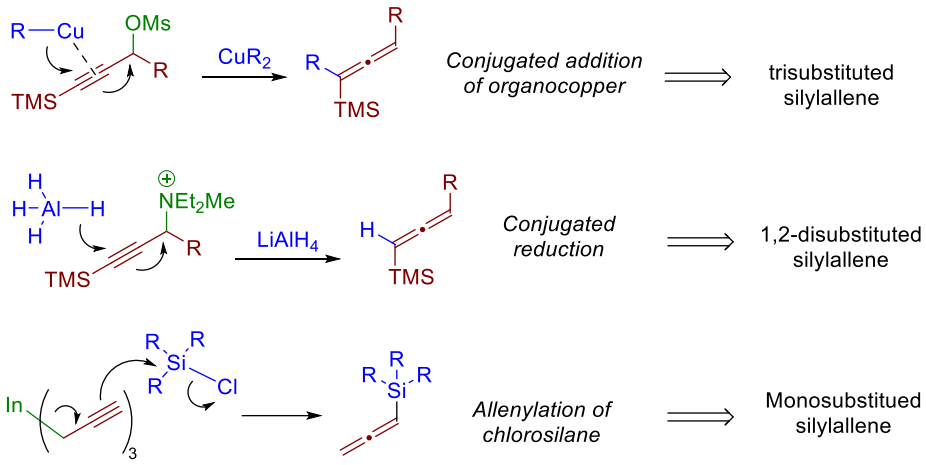

Figure 77 - Synthetic approaches to different substituted silyl allenes

The propargylic substrates were obtained simply by addition of a lithium acetylide to an aldehyde, reacting the alcoholate with methanesulfonyl chloride[9,10] (Figure 78).

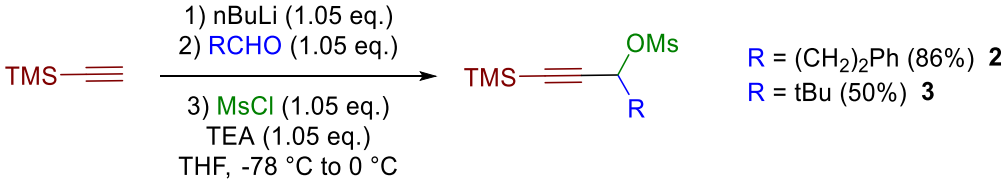

Figure 78 - Preparation of propargyl mesylates

The conjugated addition of alkyl moieties generated with copper (I) iodide gave poor results in our hands, as well as the conjugated reduction with lithium aluminum hydride. Instead, the use of CuBr•LiBr complex to generate the reactive organocopper using methyl lithium provided the desired silyl allene in high yield and total conversion (Figure 79).[VIII]

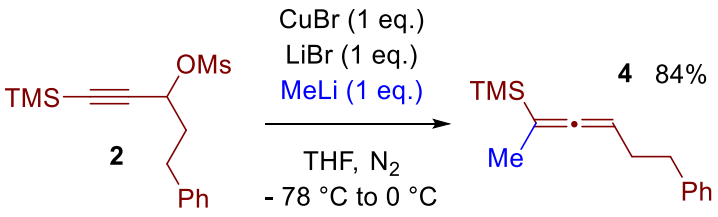

Figure 79 - Synthesis of 4

[VIII] The use of a robust methodology based on CuCN as copper precursor was not attempted for the prohibitive cost associated with the transport, as it is considered hydrogen cyanide by one of the main commercial suppliers.

The synthesis of monosubstituted dienes via organoindium proved more challenging. The reported procedure[12] generates the silyl allenes in high yield, but the aqueous quenching procedure described destroys them, probably because In^{3+} promotes oligomerization. To remove most of the metal complex from the DMF environment we directly extracted the products in pentane. Moreover, monosubstituted silyl allenes have more issues: TMS-allene gave very low yield as it evaporates too fast, and $tBuPh_2Si$-allene could not be synthesized as probably the organoindium is not reactive enough. The only allene synthesized in this manner is the MePh2Si-derivative **5**, Figure 80.

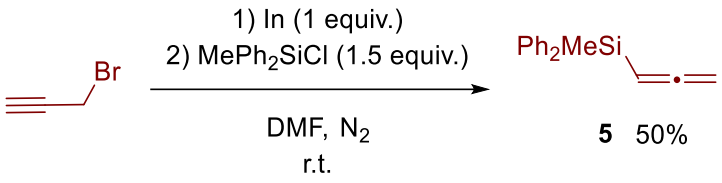

Figure 80 - Synthesis of 5

Screening campaign

The screening campaign was conducted using Hayashi (**6**), Hayashi-Jørgensen (**7**), MacMillan (I) (**8**) and MacMillan (II) (**9**) catalysts under different common reaction conditions (Figure 81): 1.2 equivalents of allene **5**, 1 equivalent of cinnamaldehyde, 20% of organocatalyst loading, 20% of acid co-catalyst in different solvents at room temperature.

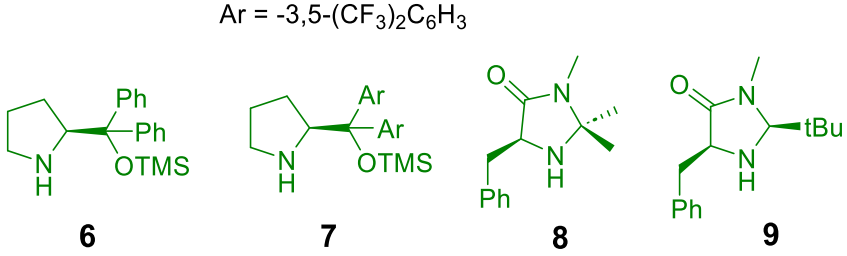

Figure 81 - Asymmetric secondary amines used in the screening campaign

The first screening was attempted using prolinol derived catalysts (*Table 11*).

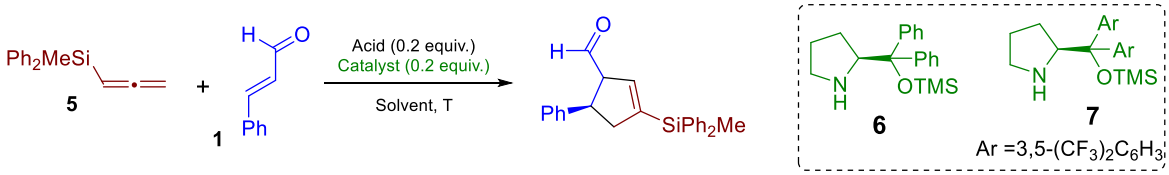

Entry	Catalyst	Acid	Solvent	Temp.	Time	Conversion	Yield
1	6	2-F-benzoic acid	Toluene	r.t. to 50 °C	65 h	0%	0%

2	7	2-F-benzoic acid	Toluene	r.t. to 50 °C	65 h	0%	0%
3	6	2-F-benzoic acid	$CHCl_3$	r.t.	65 h	0%	0%
4	6	Amberlyst-15	$CHCl_3$	r.t.	65 h	0%	0%
5	6	Amberlyst-15	Toluene	r.t. to 65 °C	65 h	0%	0%
6	6	p-NO_2-benzoic acid	$CHCl_3$	r.t. to 65 °C	65 h	0%	0%
7	6	p-NO_2-benzoic acid	Toluene	r.t. to 65 °C	65 h	0%	0%
8	6	F_3CCOOH	$CHCl_3$	r.t. to 65 °C	65 h	0%	0%
9	6	F_3CCOOH	Toluene	r.t. to 65 °C	65 h	0%	0%

Table 11 - Screening with prolinol-derived catalysts

All the tests were run in toluene or chloroform, both at room temperature and up to 65 °C for around 65 h – a long reaction time. Different acids were used to modulate the reactivity of the iminium ion: 2-F-benzoic acid (entry 1 to 33), Amberlyst-15 (entry 4 and 5),[IX] p-NO_2-benzoic acid (entry 6 and 7) and trifluoroacetic acid (entry 8 and 9). No reactivity at all was observed in these systems. The more electrophilic MacMillan oxazolidinones were then tested. The results are resumed in Table 12.

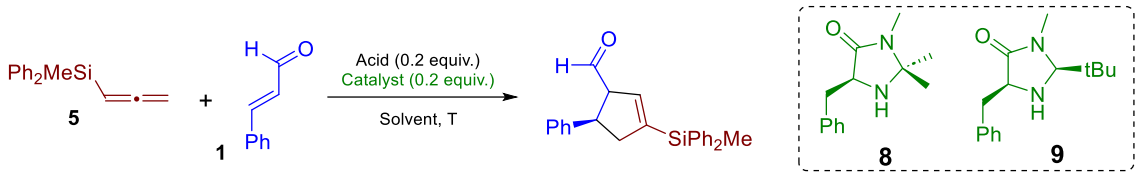

Entry	Catalyst	Acid	Solvent	Temp.	Time	Conversion	Yield
1	8 (0,2 eq.)	HCl[a]	MeOH/H_2O 95:5	r.t.	48 h	Reactivity	0%
2	8 (0,2 eq.)	HCl	THF/H2O 9:1	r.t.	48 h	0%	0%
3	8 (0,2 eq.)	HCl	EtOH	r.t.	48 h	Reactivity	0%
4	8 (0,2 eq.)	HCl	THF/MeOH 9:1	r.t.	48 h	0%	0%
5	8 (0,2 eq.)	HCl	THF/MeOH 1:1	r.t.	48 h	Reactivity	0%
6	9 (0,2 eq.)	*p*-TSA	MeOH/H_2O 9:1	r.t.	72 h	Reactivity	0%

[IX] A sulphonic acid resin easily removable by filtration.

7	9 (0,4 eq.)	HCl	MeOH/H_2O 95:5	r.t.	100 h	Reactivity	0%
8	9 (0,2 eq.)	p-TSA	Acetone	r.t.	24	Reactivity	0%
9	9 (0,2 eq.)	p-TSA	CHCl3	r.t.	100 h	0%	0%
10	9 (0,2 eq.)	p-TSA	Toluene	r.t.	100 h	0%	0%
11	9 (0,2 eq.)	p-TSA	DCM	r.t.	24 h	0%	0%

Table 12 - Screening with oxazolidinone-derived catalyst
[a] = 8 directly introduced in the environment as hydrochloride salt.

First, the cheaper **8** was tested as hydrochloride salt in MeOH/H_2O 95:5 (entry 1), THF/H_2O (entry 2), ethanol (entry 3), THF/MeOH 9:1 (entry 4) and THF/MeOH 1:1 (entry 5). Some reactivity was observed only for entry 1 and entry 3, giving different products. Excited for the results, we explored the reactivity of **8** in different solvents using p-toluenesulfonic acid, except for entry 7 in which we used hydrogen chloride. Again, a water/methanol system (entry 6) showed a good conversion of cinnamaldehyde to yield the same products of entry 1. The conditions were slightly changed, and the reaction time was extended to 100 h aiming to obtain higher conversions (entry 7). The product was then isolated and characterized (see below). Then, acetone (entry 8), chloroform (entry 9), toluene (entry 10) and dichloromethane (entry 11) were tested as well and only acetone gave a new product. Finally, a shy tentative of ACDC activation was conducted as well using TRIP and morpholine in dioxane at 50 °C for 100 h, but only a slight amount of Michael-addition of morpholine to cinnamaldehyde was observed by GC/MS.

The product observed in the presence of methanol (**10**) was isolated and characterized: it's the Michael addition of methanol and tandem acetal formation. A plausible rection mechanism is the following (Figure 82):

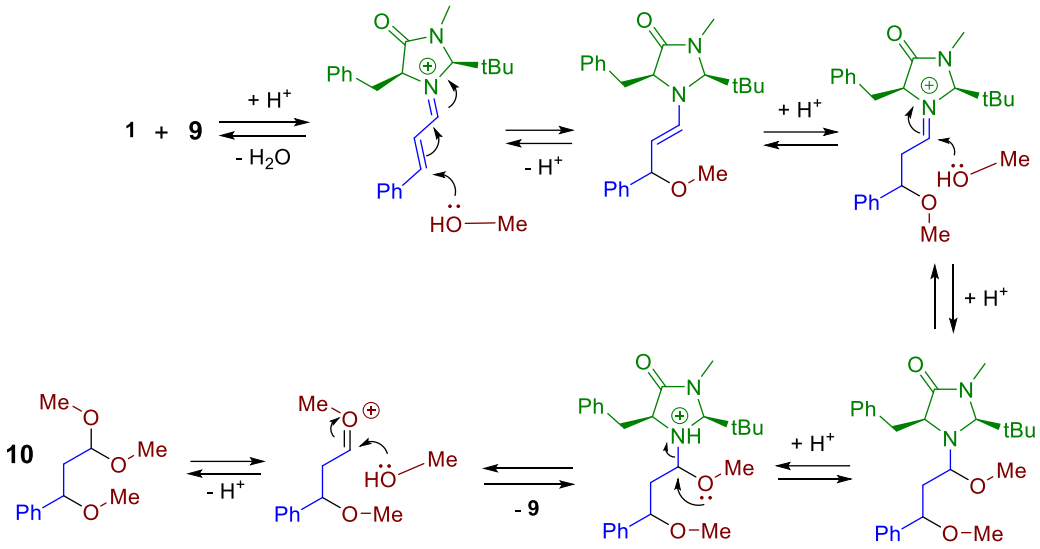

Figure 82 - Mechanism of formation of 10

There is probably an oxa-Michael reaction with methanol triggered by the reactive α,β-unsaturated iminium ion. The formation of the saturated iminium ion then probably catalyzes the formation of the acetal in the carbonyl attack phase, which then proceeds to yield **10** and re-generating **9**. Both the oxa-Michael addition and the acetal formation are reversible reactions and the equilibrium is shifted as methanol is the solvent. The organocatalyzed asymmetric *direct* oxa-Michael reaction is potentially interesting: to the best of our knowledge, there are only two examples reported in literature: two reports by Marouka and co-workers using a bis-amino-BINOL-derived catalyst, with modest enantiomeric excess.[13,14] The other example is just a simple observation of the same type of reactivity by Pihko and co-workers[15] working with **9**, although with a discouraging 6 % yield.

Unluckily, product **10** was racemic, maybe for the low asymmetric induction induced by the catalyst with such a small nucleophile, or maybe for the reaction being an equilibrium that slowly induced the overall product racemization. Considering also that the reaction is already sluggish (50 % conversion in 4 days), we decided to not catch the opportunity to prosecute the work in this unexpected direction, continuing to explore the Danheiser-type reactivity.

After the first catalyst screening, silyl allene in these conditions seem to be reluctant to react. Indeed, **5** has always been recovered untouched as a spectator component. Before continuing the experimental investigation, it was decided to computationally estimate if the overall process is at least *feasible*.

Computational investigation

Aware of the complexity and computation time required for simulating a potential energy surface (PES) of an organic reaction, in particular for transition states, it was decided to focus *only* on the energy difference between the iminium ion ground state (**A**) and the vinylsilylcation (**B**) before the postulated [1,2]-silicon shift event (Figure 83).

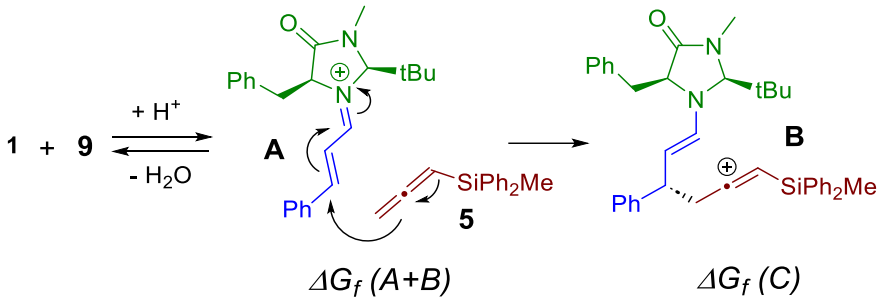

Figure 83 - Computational task - ground state energies

The result of the simple equation $\Delta G_f°(C) - \Delta G_f°(A+B)$ will clarify if the process is physically feasible or not. Of course, the level of the method used (base of function, DFT functional, implicit or explicit solvation, calculation of dispersion forces and so on...) can significantly change the final energy output. However, the target of this calculation is not a super-fine predicted structure, it's just the energy difference between two *significantly different* stabilized cations. So, despite running a gross calculation, it should not be difficult to spot large energy differences. In other words, we just wanted to make sure we were not trying to jump the empire state building, to make the experimental effort is worth it.

Cheap calculation

Another aspect considered before the calculation is the computational power required: with the target of doing more of these calculations in the future for novel reactivity processes developed in the laboratory of Professor Carlone, we aimed to use only a standard workstation. This will allow us to work *immediately* on the calculations without any waiting time.

Thus, a "cheap" approach to the problem was chosen to exploit our computational power. The calculation parameters chosen are M062X-6-311G(d,P)- CPCM (Chloroform). 6-311G(d,P) was selected to accommodate the larger orbitals of silicon, while implicit solvation was selected to shorten the calculation time, assuming as negligible the additional energy stabilization. ORCA[16,17] is the software used for the whole calculation process. Avogadro[18,19] was used for molecule visualization and for format conversion.

The ground state structure optimization of **A** (Figure 83) was relatively easy, as previous studies on the ground state energy of iminium ions as tetrafluoroborate were realized by Costa and co-workers:[20] the reported ground state for **A** was used without any further geometrical optimization[X] for energy calculation. Determination of ground state for **5** followed a classical approach: use of a semi-empiric method to get close to the minimum as fast as possible, followed by coordinates refining using the more accurate method. Luckily, **5** is a monosubstituted allene, so only a few bonds are able to rotate, shrinking the accessible conformational space and leading to painless energy minimization. Finally, (Figure 83) undergoes the same treatment as **5**: optimization with semi-empirical methods and final refinement with the more accurate method. Importantly, it was noticed that the angle between C-Si and C=C is 97,8 °. This is far from the cyclopropenyl cation representation usually adopted in Danheiser's reports.

The final structures are shown in Figure 84.

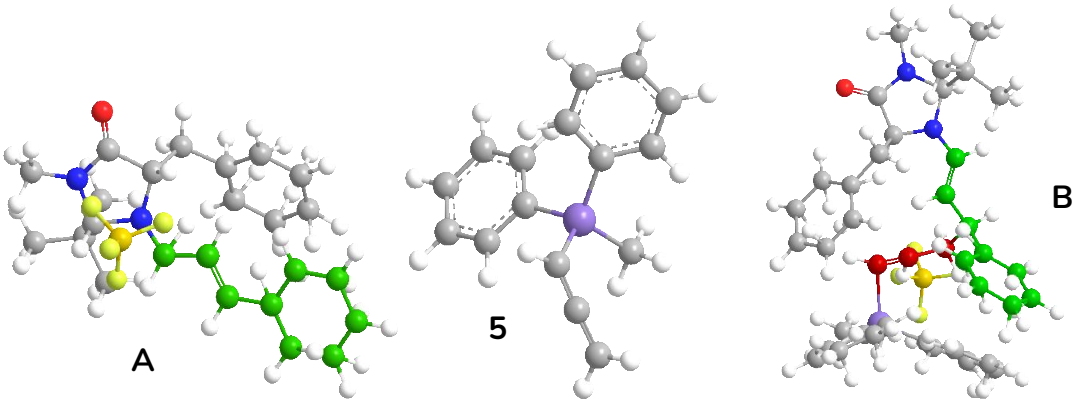

Figure 84 - Optimized ground state structures

The calculated difference of $\Delta G_f°$ is astonishing: around 55 kcal/more are found, a tremendous amount of energy. It is virtually *impossible* that such a high energy intermediate is generated at accessible temperatures. Moreover, it is required to come from an unstable intermediate, iminium ion, which is already around 12 kcal/mol over the reagents[20] (Figure 85).

[X] Actually, a negative frequence in the vibrational spectrum, corresponding to the rotation of tert-butyl group, was found. The group was rapidly rotated of a degrees and the real minimum found with very little computational effort.

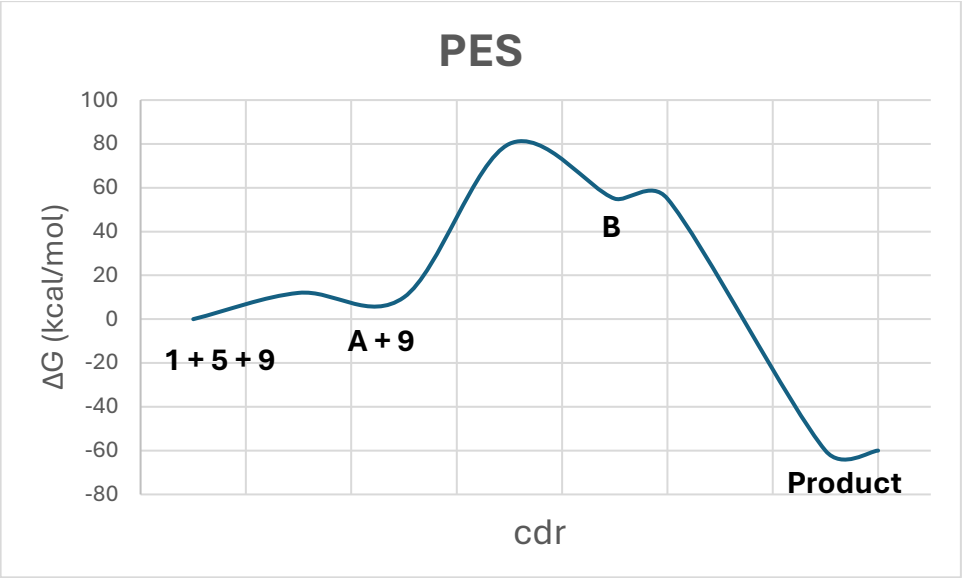

Figure 85 - Sketched PES

In our opinion such a difference in energy rules-out every possible design improving for organocatalyzed Danheiser reaction: a more substituted silyl allene, a less coordinating counter-ion, a different solvent or higher temperature will not significantly influence the PES.

Unfortunately, it was demonstrated that the reaction design was flawed, so the organocatalytic approach was ruled out. To compensate for that energy difference in the bond event formation, we tried to give energy with light. A photocatalytic approach was attempted.

Re-design of Danheiser cyclopentane annulation: photocatalysis

In the previous paragraph it was shown that the nucleophilic attack of allenyl silanes to catalytically-generated iminium ions was not feasible, we though to re-design the reacting system introducing light activation. Indeed, one of the positive aspects of photocatalysis is the possibility of overcoming high activation barriers, as light gives energy to the system. *Back-of-the-envelope calculation* can give a gross idea about this: the energy for the formation of **B** from **A** is 2,38 eV (calculated as single event), while the energy carried by a blue photon at 420 nm is around 2,95 eV. Clearly, harnessing of the light inputs in the system can *potentially* solve the reactivity problem met in the first catalytic cycle design. Thus, it was decided to test a photocatalytic approach.

Starting from the originally designed catalytic cycle (Figure 74) it is straightforward thinking to photoexcite the iminium ion **A**, which would act as photocatlyst.[21] In this scenario, this intermediate would induce the monoelectronic oxidation of **5** and

subsequent radical recoupling (Figure 86). The rest of the designed catalytic cycle is the same as before, as the focus is on the first binding event, of which the feasibility must be proven as first step in the realization of this methodology.

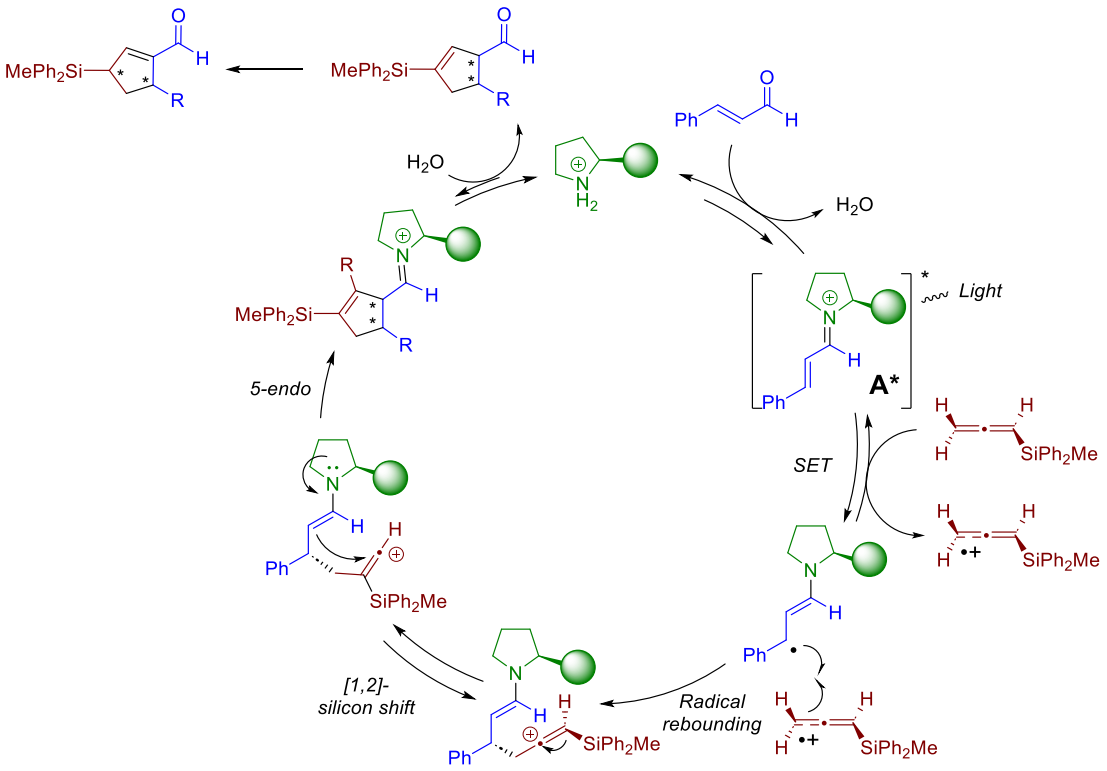

Figure 86 - Designed photocatalytic cycle

This hypothesis is not exotic, as the activation of allenes via mono-oxidation using photoexcited iminium ions have already been reported by Melchiorre and co-workers.[22] In that work the allene is oxidized, but the radical cation is immediately trapped by the carboxylic acid moiety present by intramolecular nucleophilic attack on the central carbon atom, leading to an allyl radical. This probably shuts down the back electron-transfer process and other possible side reactions, forcing the reaction to product formation. Aware of the difficulty of this reaction, it was decided anyway to give this process a chance using normal silyl allenes without any trapping groups.

Experimental – first attempt

Using **1** and **5** as model substrates, the first experimentation was conducted using Melchiorre's reported conditions. Both **9** and the difluoroprolinol-derived catalyst **10** (Figure 87) were used as organocatalyst.[21]

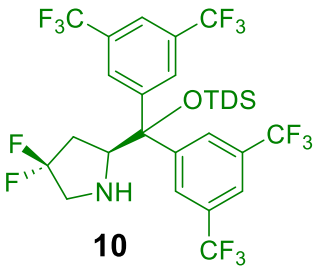

10

Figure 87 - Structure of 10

The results are resumed in Table 13.

Entry	Catalyst	Solvent	Time	Results
1	10 (0,2 eq.)	ACN	72 h	No reaction
2	10 (0,2 eq.)	ACN:DCE 1:1	72 h	No reaction
3	10 (0,2 eq.)	DCE	72 h	<5% traces of some product by HNMR
4	9 (0,2 eq.)	ACN	18 h	No reaction

Table 13 – Asymmetric organo-photocatalyzed Danheiser pentane annulation of cinnamaldeyde
All the reactions were performed using 0,2 eq. of trifluoroacetic acid in a sealed vial, using a 427 nm Kessil lamp set at maximum power, using a UFO reactor[23]. The system undergoes freeze-pump-thaw procedure before starting to irradiate.

Acetonitrile and DCE are the solvents tested for this reaction, as they are reported to work with photoexcited iminium ion. DCE was explored as non-nucleophilic solvent, as oxidized silicon-containing substrates typically undergo Si-C bond cleavage through nucleophilic attack.[24,25] For our designed reaction system, the silicon needs to be bound on the structure to forge the 5-membered ring.

The first tests did not lead to any sort of reactivity. Before screening the reaction conditions deeper (solvent, allene and acid) it was thought to be more reasonable to change the photochemical activation mode. Indeed, it is strange that nothing at all happened: once the allenylsilane is oxidized it should be very reactive. Even a decomposition of the reagents would make sense. The fact that nothing is observed probably means that there has been no SET event at all. Changing the photoexcited reactive species could then be fruitful, so another photo-activation mode was tested. It follows a brief introduction about this.

Alternative photo-activation mode design

A hybrid acridinium-iminium ion photocatalytic system, again reported by Melchiorre and co-workers,[26] was tested. The principle is represented in Figure 88.

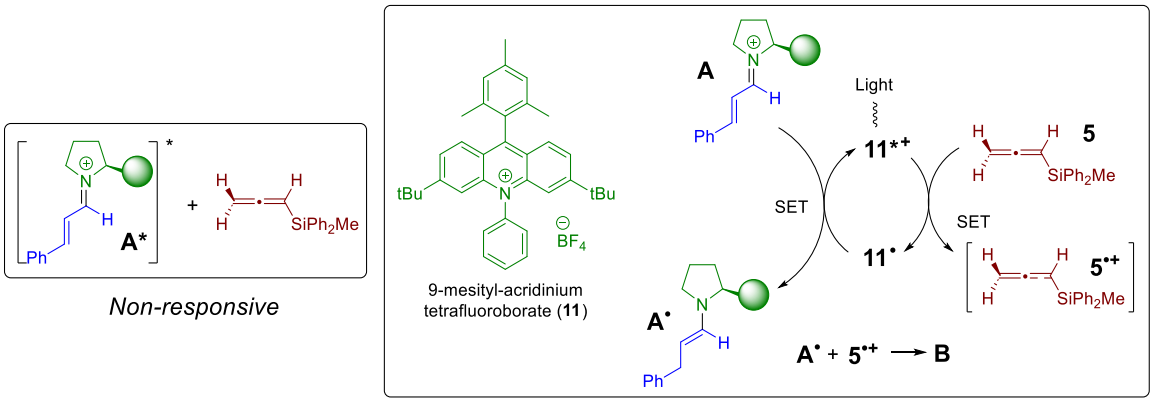

Figure 88 - Acridinium mediated iminium ion oxidation

Photoexcited acridinium catalyst **11*** acts as oxidant on **5**, producing **5**$^{\bullet+}$ and **11**$^{\bullet}$, which is now a reducing agent. **A**, is the most reducible species in the system and acts as electron sink, restoring **11** and producing **A**$^{\bullet}$. **A**$^{\bullet}$ and **5**$^{\bullet+}$ can then react to make **B** and closing the Danheiser reaction enamine cascade.

The electron transfer between **11**$^{\bullet}$ and **A** is another parameter to be careful about: E_{RED} **A**$_{(10)}$ ≈ -647 mV, E_{RED} **A**$_{(9)}$ ≈ -539 mV[24] and E_{RED} **11**$^{\bullet}$ ≈ -570 mV vs SCE. Thus, the reduction of iminium ion derived from **10** is counter-thermodynamic, while the reduction of iminium ion derived from **9** is thermodynamically favored for miserable 31 mV – not enough to be a *fast* process, considering that typically an overpotential of 200 – 300 mV is recommended in organic photo-redox catalysis. Luckily, the system is under irradiation, so both **11**$^{\bullet}$ and **A** can be excited, generating **11**$^{\bullet *}$ and **A***. Acridinium photocatalysts are typically irradiate around 450 nm and 420 nm, so 427 nm available in our laboratory should do the job. **A**$_{(10)}$ and **A**$_{(9)}$ are both excited at the same wavelength: E_{OX} **A**$_{(10)}$* ≈ +2773 mV, E_{OX} **A**$_{(9)}$* ≈ +2411 mV[24] vs SCE. Under these conditions the electron transfer is thermodynamically favored, despite probably being slow, as we're in the Marcus inversion region. The same principle can be exploited exciting **11**$^{\bullet}$: Nicewicz and co-workers reported that at 390 nm not only **11*** acts as oxidant, but also **11**$^{\bullet}$ gets photo-excited and acts as a strong reducing agent: E_{RED} **11**$^{\bullet *}$ = -3360 mV vs SCE – more than enough to reduce every **A**-type species.[27]

Experimental – second attempt

The hybrid photocatalytic approach was then experimentally tested. The tests are resumed in Table 14.

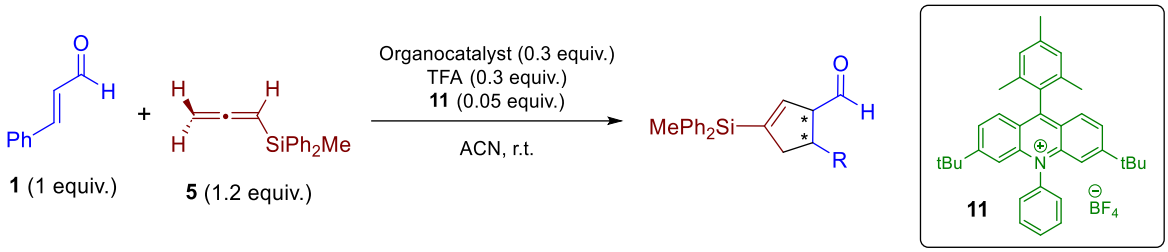

Entry	Organocatalyst	Wavelength	Result
1	10 (0,3 eq.)	427 nm (100% power)	Low 1 conversion – products observed
2	10 (0,3 eq.)	390 nm (50% power)[a]	Low conversion of 1 – products observed
3	9 (0,3 eq.)	390 nm (50% power)	Low 1 conversion of 1 – same products as entry 1 and 2 and 1 more product

Table 14 - Hybrid photocatalytic system tests

All the tests were conducted reacting 1 and 5 in acetonitrile, using 0,3 eq. of TFA as acid catalyst and 0,05 eq. of 11. The reactions were conducted in a sealed vial, using a Kessil lamp and a UFO reactor. The system undergoes freeze-pump-thaw procedure before starting to irradiate. [a] Low power otherwise to keep the temperature low.

Both 427 nm and 390 nm (entry 1 and entry 2, respectively), showed a low conversion of the aldehyde, yielding some products, which are not the desired product. Using **9** as photocatalyst (entry 3) the systems behaved similarly, but two additional byproducts were obtained.

The common byproducts obtained from entry 1, 2 and 3 were then characterized, deducing also a possible mechanism of formation. It turns out that two diastereomeric aldehydes **12**^{I} and **12**^{II} are formed in 1:1 ratio (Figure 89).

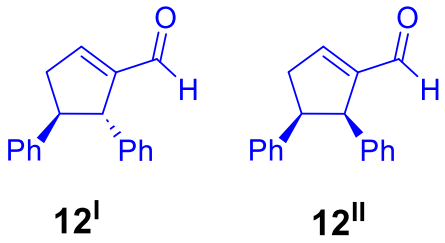

12^{I} **12**^{II}

Figure 89 – 12^{I} and 12^{II} structures

It was decided to investigate deeper the formation of these new products, both because understanding what processes are really taking place is important to suppress them, and because the products themselves are interesting and have potential in the synthesis of natural products. The studies about this homocoupling process are fully exposed in chapter 6. Moreover, from these first tests also other fluorinated compounds were observed in traces. Probably, the fluorinated compounds come from the decomposition of trifluoroacetate ion under oxidizing

conditions. The other products in entry 3 probably come from catalyst decomposition, so nothing interesting happened.

In general, **5** seems to play a spectator role even under photocatalytic conditions, as confirmed later by fluorescence-quenching experiments with **9** (see supporting information). The oxidation potential of **5** was measured by cyclovoltammetry, revealing that E_{OX} **5** ≈ 1800 – 1900 mV – compatible with the oxidation potential of all the photocatalysts used. Moreover, blank test with O_2 as oxidant showed that the allene can be fully converted using **11** as photocatalyst, but no reactivity is observed during the reaction. Probably, **5** is not a good quencher for **9***, while with **11** the back-electron transfer is probably too fast. To summarize, for now **5** showed no reactivity in the tested conditions, demonstrating different issues in physicochemical characterization tests.

It was then decided to investigate similar reaction conditions using **4**, a more substituted allenyl-silane. The tertiary substitution of **4** makes the whole system more electron rich compared to **5**. This should lower the oxidation potential, making the SET easier for the photocatalyst. Moreover, the radical cation **4**$^{\bullet+}$ should be more stabilized for the electro-dotation effect, so its lifetime should be higher than **5**$^{\bullet+}$. Due to time limit, only one test has been performed right now (Figure 90).

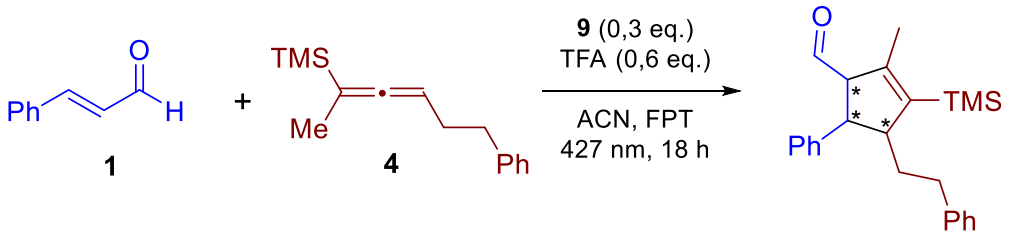

Figure 90 - Reaction of 1 with 4

Under these conditions **1** is fully converted, yielding multiple products: **12**^{I} and **12**^{II} were detected, together with two diastereomeric aldehydes in 1.2:1 ratio. The determination of the exact structure needs further investigation with mass spectrometry and CNMR spectroscopy, which are not currently not available in our laboratory. However, some basic structural features can be deduced: first, the products have probably an open chain structure, as the aldehyde are triplets. Second, the silicon atom is probably gone, as there are no methyl groups with a coherent chemical shift or area. Third, these isolated products are probably derived from the attack of the silyl allene to the aldehyde, as the number of peaks detected in the HNMR and the complexity of the spectrum must come from a molecule with more carbon than simple cinnamaldehyde. The presence of two close methyl groups supports this hypothesis, as these must come from **4**. A blank test with only

0,6 eq. of TFA was also conducted to verify that the process is not induced by the acidic environment was also conducted, and indeed no reactivity was observed.

Moreover, from this preliminary test reactivity, it can be deduced that this allene, and probably more substituted ones, *could be* the key to unlock the SET event and the consequential reactivity. The full conversion of cinnamaldehyde and the reductive coupling products obtained are a positive signal of a fully working catalytic cycle.

There will be further experimentation using less nucleophilic solvents to keep the silicon atom in the structure. Of course, full characterization of the products will be conducted to fully understand the process.

Low-order Danheiser cyclopentane annulation

The classical Danheiser cyclopentanone annulation is used to make *unsaturated* cyclopentanes, and this requires the use of allenyl silanes. However, the first experimental evidence reveals how difficult the photoactivation of these substrates is, especially without any stabilization path available to the radical cation formed. Thus, we started to investigate also the possibility of a "lower order" cycloaddition reaction with *allyl silanes*, as reported by Danheiser[28], Knölker[29,30] and Ohe[31] (Figure 91).

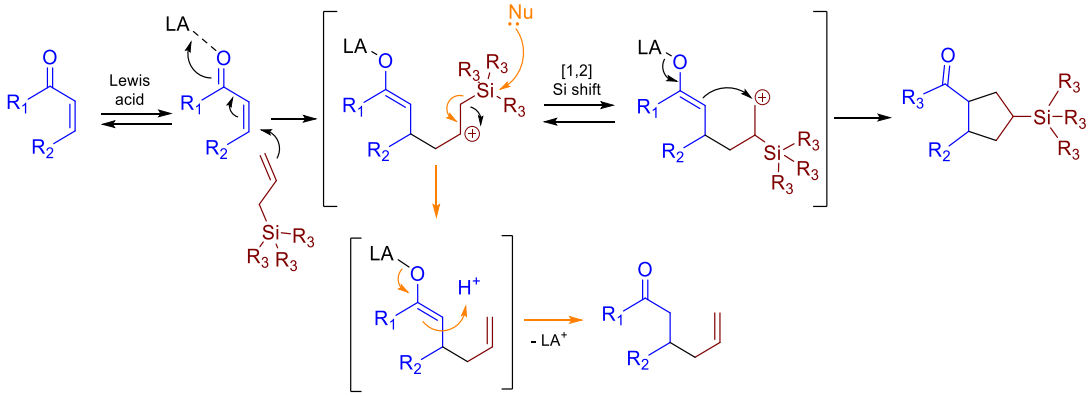

Figure 91 - Low order Danheiser cycloaddition mechanism

The conjugated attack of allyl silane produces a β-stabilized sp^2-cation, which can then undergo [1,2]-silicon shift and subsequent 5-exo ring closure with the enolate. In the same conditions, it is reported that silicon undergoes SN_2 by a nucleophile, freeing the allyl moiety (orange path) and generating the conjugated allylation product. This reaction path is known in literature as "conjugated Hosomi-Sakurai reaction". The chemoselectivity of the process depends on dimension of the R_3 group. If R_3 is small the nucleophilic attach to silicon is favored. If R_3 is bulky, the [1,2]-shift is favored for the stronger electron donation effect, and at the same time

the SN_2 is slowed down. These two factors favor in general the ring-closing cycle process.

As for the "classical" Danheiser cyclopentanone addition reaction, there are nor asymmetric versions of this reaction, nor metal-free catalytic systems. Thus, we are interested also in lower-order annulation reactions. It follows the report of the first, seminal experiments.

Experimental – third attempt

The low-order annulation reaction photocatalyzed reaction was tested both in acetonitrile and 1,2-dichloroethane.

The results are reported in Table 15.

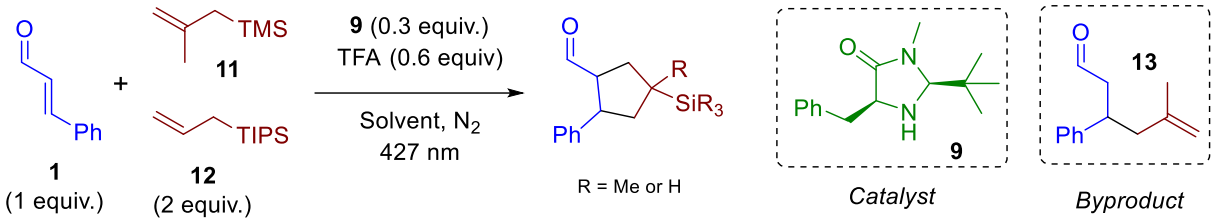

Entry	Allyl silane	Solvent	Conversion[a]	Yield[b]
1	11	ACN	35 %	20% of 13, 10% of unknown (I)
2	11	1,2-DCE	>20 %[c]	20% of 13 + unknown (II)
3	12	ACN	100 %	30 % of 14 + other products

Table 15 - Low-order asymmetric organo-photocatalyzed Danheiser annulation - seminal tests
All reactions were performed in a Schlenk tube using 1 equivalent of cinnamaldehyde, 2 equivalents of allyl silane, 0.3 equivalents of catalyst 9, 0.6 equivalents of trifluoroacetic acid in the indicated solvent. UFO reactor was used as photosystem, irradiating with a 427 nm Kessil lamp set at 100 % power for 18 hours. The system undergoes freeze-pump-thaw procedure before starting to irradiate.
[a] Conversion evaluated by HNMR based on cinnamaldehyde aldehydic peak
[b] Conversion evaluated by HNMR based on cinnamaldehyde aldehydic peak
[b] One of the detected products hidden under starting material, so integration not possible

The screening conditions are inspired by the report of Melchiorre and co-workers,[25] as in those conditions the iminium ion under photocatalytic conditions showed to oxidize allyl silanes for sure. However, we decided to use Mac Millan catalyst **9** to start instead of **11**, being a cheaper and simpler catalyst. As explained above, we were initially interested in testing if different allyl silanes in different solvents are able to do the Danheiser reaction instead of Hosomi-Sakurai. First, allyl silane **11** was used both in acetonitrile (entry 1) and 1,2-DCE (entry 2). Despite the low conversion, the formation of different products in the two batches was observed.

Using acetonitrile, some Hosomi-Sakurai product **13**[XI] was observed, together with another not identified aldehyde peak in around 10% yield. Running the reaction in 1,2-DCE the formation of the other product was somehow hampered, and a new triplet is formed under the signal of cinnamaldehyde.[XII]

The use of the more hindered and electron-rich **12** (entry 3) showed full conversion, yielding different, unidentified products. We're dealing with 7 different aldehydic peaks, so a messy reactive system. However, one peak is prevalent over the others, showing around 60% abundance (Figure 94). This product (**14**) was already isolated during the optimization of the homocoupling of cinnamaldehyde to yield **12**[I] and **12**[II] (see next chapter). The structure is shown in Figure 92, together with the possible formation mechanisms.

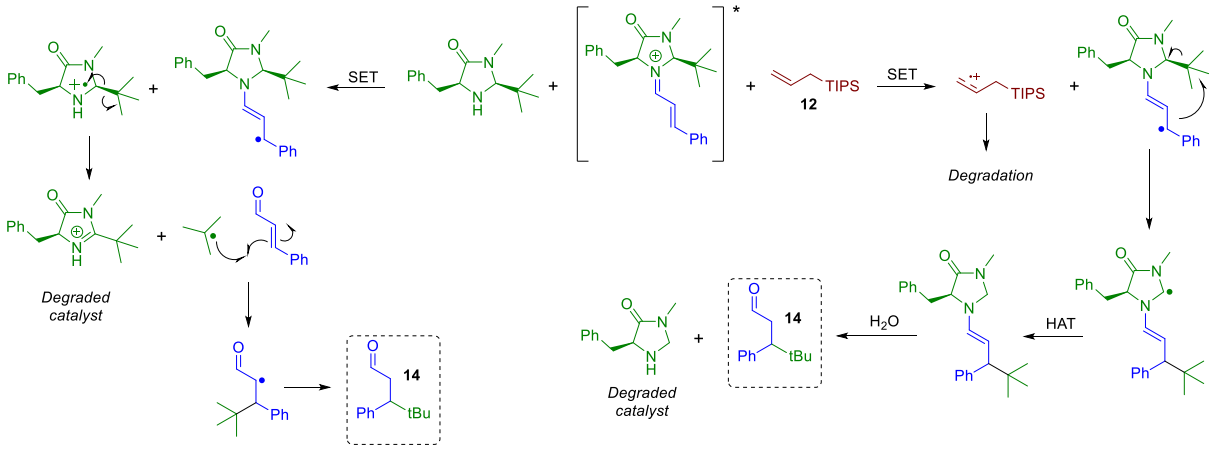

Figure 92 - Product 14 formation

The formation of **14** was somehow surprising for us, as the transfer of a tertbutyl group from the catalyst is difficult to imagine. The fragmentation of the radical enamine to free a tert-butyl group would be difficult, as the span between the initial and final radical cannot account for a β-fragmentation process (Figure 93).

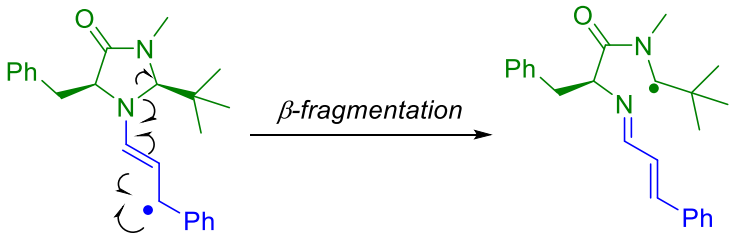

Figure 93 - β–fragmentation of radical enamine

[XI] The aldehyde peak looks very similar to Melchiorre's report, both as chemical shift and coupling constant. GC/MS showed the presence of that product, so probably that triplet at HNMR corresponds really to **13**.

[XII] Identification by mass spectrum is difficult in this case, as with electronic impact the molecular ion is difficult to identify. So no prediction are done in this case.

Thus, it was sketched an intramolecular nucleophilic radical substitution to justify the product, although all of this would need more theoretical support. Another possible, and more mechanistically familiar path,[24] would be the direct mono-oxidation of the catalyst free amine, followed by radical fragmentation. However, the problem with this path is that theoretically there are more oxidizable species than **9** in the reaction environment, such as DIPEA (see next chapter). To account for this, the selectivity in the quenching of excited species should be better investigated – maybe **9** is somehow a better quencher than other species. Further investigation is needed to clarify this point.

The crude spectrum of entry 3 contains also **12**^{I} and **12**^{II} as products, together with probably the Hosomi-Sakurai allylation product. Other unidentified aldehydes are present, so further analysis of this reaction is needed (Figure 94).

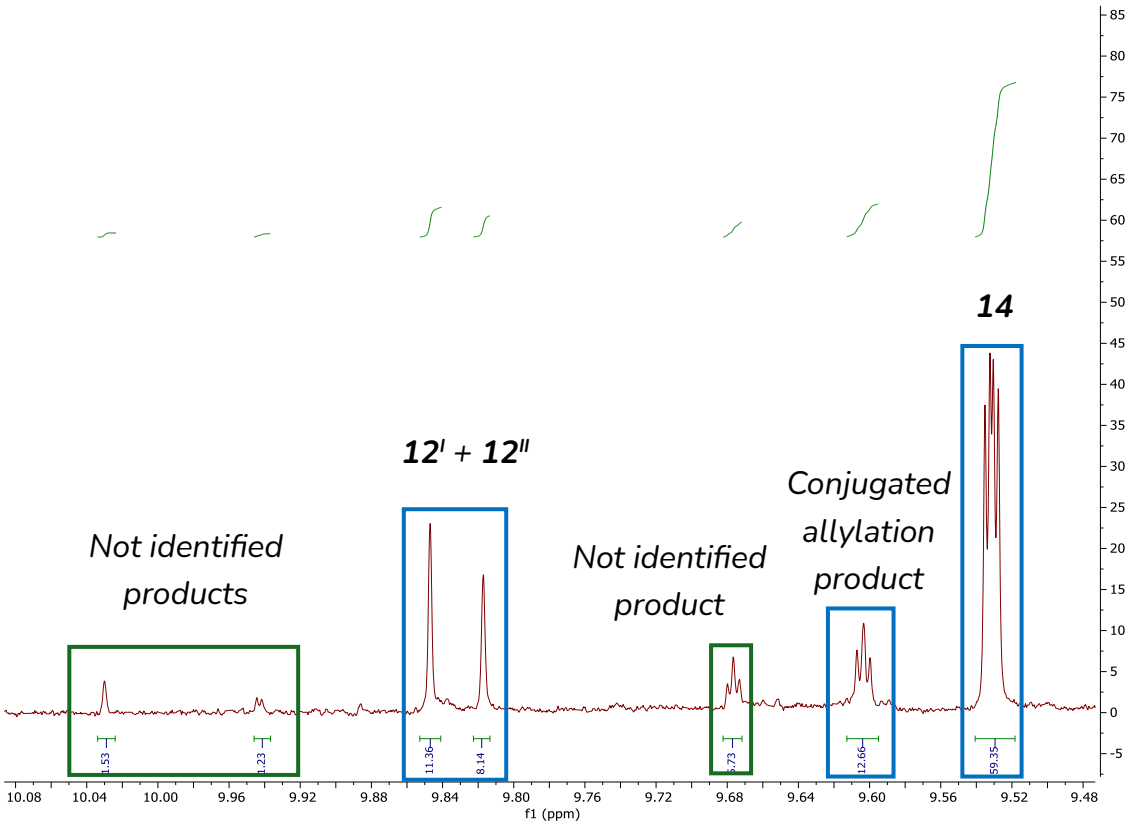

Figure 94 - Aldehyde region on the crude spectrum of entry 3

A deeper analysis of the crude was not possible for time reasons, so these are results based on aldehyde peaks and some other characteristic peak in the spectrum.

Considering the discovery of the tert-butyl transfer process and that most of the identified products are known reaction paths (see also the next chapter), two information can be deduced. First, somehow the photoexcited iminium ion or the radical enamine tend to eliminate tert-butyl group degrading the catalyst if not

captured fast enough. However, the ally-TIPS moiety is not present, at least in the majority of the products. The only possible allyl moiety seems to be the conjugated allylation product. Probably, the radical cation derived from substrate **12** is degraded fast, which is reasonable considering that acetonitrile is nucleophilic.

In the future, all products will need to be characterized properly to at least finish to trace all the reaction paths. Moreover, 1,2-DCE as solvent can be tested again, trying to make **12**$^{\bullet+}$ survive long enough to be attacked. Also, Melchiorre's catalyst **10** can be taken into consideration again, as now the degradation problem of **9** have been observed.

Conclusions

Danheiser cyclopentane annulation is a [3+2] all-carbon annulation involving a silyl allene and an enone. It is an important chemical reaction for the straightforward synthesis of cyclopentanes, used also in natural product synthesis. To realize this transformation in the all-carbon version, stoichiometric titanium tetrachloride is necessary. This methodology is thus not very tolerant of other functional groups, dangerous and inconvenient on a large scale. Importantly, to the best of our knowledge no asymmetric versions of this reaction are reported. The development of an asymmetric version is highly desirable, as would allow the straightforward synthesis of chiral cyclopentanes. In this project, we attempted a novel approach for the Danheiser reaction, trying to activate an α,β–unsaturated aldehyde via iminium ion. The use of organocatalysis for this type of substrate would introduce both chirality and a much milder activation method. Moreover, to the best of our knowledge it would be the first example of silyl allenes used in organocatalysis, and the first example of Danheiser annulation on aldehydes.

First, classical iminium activation was attempted, supported by Mayr-Patz scale-based predictions. However, after different tests we doubt if doing this reaction was possible at all. So, a ground state energy estimation by DFT of the different intermediates involved in the key step was done. It was discovered that the key step was *strongly counter thermodynamic* - ΔG = 55 kcal/mol. Thus, the iminium ion activation was abandoned.

It was decided to completely change approach, trying to overcome the energy barrier with light. Thus, direct photocatalytic activation of the iminium ion was attempted, hoping to at least induce some bond-forming process. After some experimentation it was observed that the silyl allene seems reluctant to react with both simple iminium photocatalytic systems and photocatalyst-iminium systems,

at least in the case of monosubstituted silyl allenes. The only reactivity observed was the reductive homocoupling of cinnamaldehyde, studied deeper in the next chapter. In this case, the key to obtain reactivity with silyl allenes was to have substituted silyl allenes, which gave full conversion and a complex product in probably two diastereoisomers, still to be fully characterized. However, at a first sight it seems that we have developed some sort of new reactivity, despite the desired Danheiser annulation product was not observed, because the alkyl silicon peaks are missing from the HNMR spectrum.

Moreover, following a literature report by Danheiser, a pentane annulation reaction with allyl silanes was also attempted. Allyl silanes are easier to oxidize, as the silyl cations formed are much more stabilized. Indeed, an iminium-based photocatalyzed process involving allyl silane was reported by Melchiorre and co-workers. During our seminal experimentation, we tried to force the cycloaddition of substrates starting from Melchiorre's conditions. Using 2-methyl substituted allyl trimethylsilanes the formation of both the Hosomi-Sakurai product and a new, not identified product were observed. For sure, a divergent reaction path was activated.[XIII] Using the bulkier-at-silicon allyl-TIPS the formation of new products was observed, but most of them are undesired products, derived both from catalyt degradation and probably allyl silane radical cation degradation. Again, the identification of products was not possible for time reasons.

In the future, the products of these seminal tests on Danheiser reaction will be properly characterized and other reaction conditions explored, trying to understand the mechanistic pathways involved in their formation. We hope that the isolated products can have a real synthetic application.

Supporting information

It follows the main experimental detail of this work. Starting materials preparation, isolated products (both identified and unidentified) and typical catalysis experimental setup are exposed. Computed structures are reported as well. Products **12** and **13** are characterized in the next chapter as these information come from that project.

2 - 5-phenyl-1-(trimethylsilyl)pent-1-yn-3-yl methanesulfonate

[XIII] I thank Davide Carboni, one of the original Melchiorre's paper author, to have confirmed me that no byproducts were identified during their experimentation.

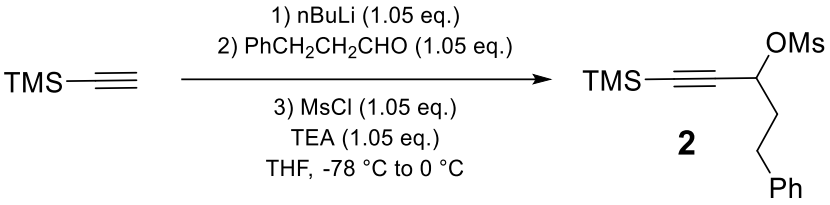

Trimethylsilylacetylene (3.3 ml, 23.2 mmol) was dissolved in 20 ml of dry THF and the temperature lowered to 0 °C. It follows the addition of 2.5 M n-BuLi (8,94 ml, 22.1 mmol) at the same temperature, waiting 40 minutes for the metalation process. Then, 3-phenyl proprionaldehyde (2.97 ml, 22.1 mmol) was added, waiting 30 minutes. Then, MsCl (1,82 ml, 23.2 mmol) was added, followed by dry TEA (3,26 ml, 23.2 mmol) always at 0 °C. After 30 minutes the reaction was allowed to go to room temperature. After 6 hours stirring the reaction was quenched with saturated aqueous NH_4Cl and extracted with DCM. Then, the organic phase was dried over Na_2SO_4, filtered and the solvent removed under reduced pressure. The crude was purified by column chromatography (Hex:AcOEt 99:1 2 CV, then 95:5). 5.96 g of **2** were recovered (87% yield).

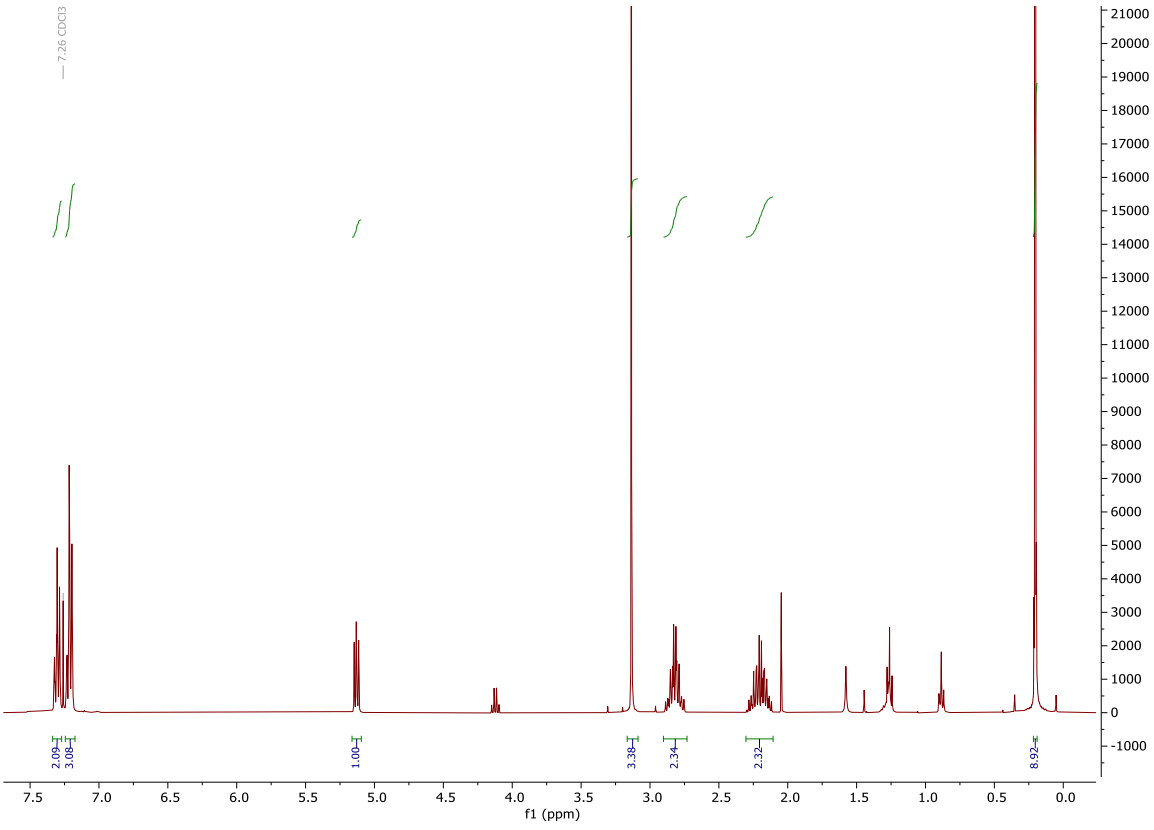

2 - 1H NMR (400 MHz, CDCl3) δ 7.33 – 7.28 (m, 2H), 7.21 (m, 3H), 5.13 (dd, J = 7.1, 5.9 Hz, 1H), 3.14 (s, 3H), 2.90 – 2.74 (m, 2H), 2.30 – 2.12 (m, 2H), 0.20 (s, 9H). Small traces of AcOEt and petroleum ether present.

3 – 4,4-dimethyl-1-(trimethylsilyl)pent-1-yn-3-yl methanesulfonate

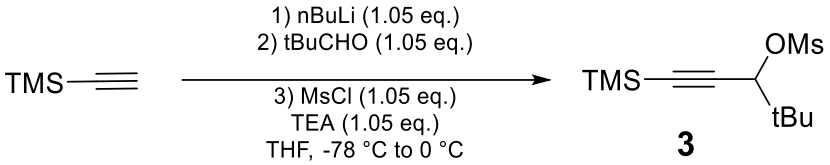

3

TMS acetylene (2.4 ml, 28 mmol) was dissolved in 15 ml of dry THF and the temperature lowered down to 0 °C. It follows the addition of 2,5 M n-BuLi (7 ml, 29.4 mmol) at the same temperature, waiting 40 minutes for the metalation process. Then, pivalaldehyde (1,8 ml, 28 mmol) was added, waiting 30 minutes. Then, MsCl (1,37 ml, 29.4 mmol) was added, followed by dry TEA (2.5 ml,) always at 0 °C. Wait for 30 minutes, then go to room temperature. After 1 hours the reaction was quenched with saturated aqueous NH_4Cl and extracted with DCM. The organic phase dried over Na_2SO_4, filtered and the solvent removed under reduced pressure. The product looks pure by HNMR analysis, so it was stored as it is. 4.42 g isolated (60 % yield).

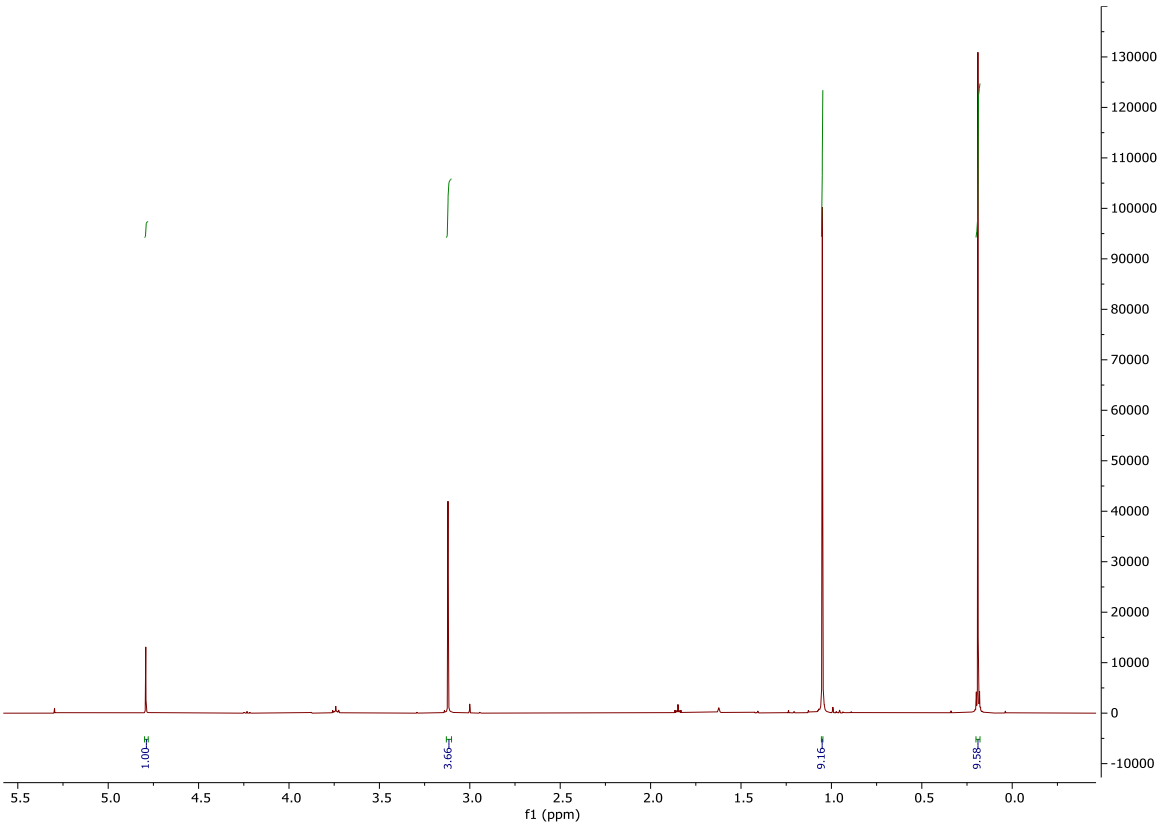

3 - 1H NMR (400 MHz, CDCl3) δ 4.79 (s, 1H), 3.12 (s, 3H), 1.05 (s, 9H), 0.19 (s, 9H). Small traces of solvent present.

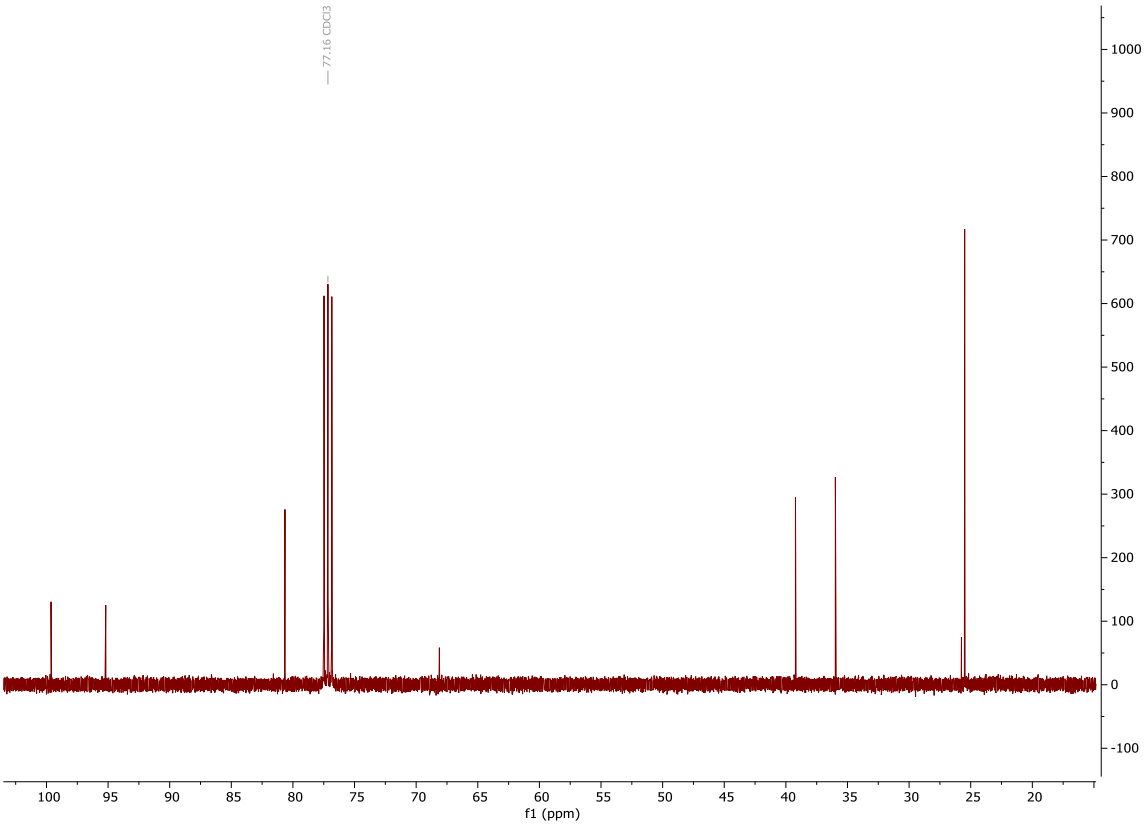

3 - 13C NMR (101 MHz, CDCl3) δ 99.63, 95.19, 80.65, 77.48, 77.16, 76.84, 68.12, 39.22, 35.98, 35.98, 25.49, -0.27, -0.28.

4 - trimethyl(6-phenylhexa-2,3-dien-2-yl)silane

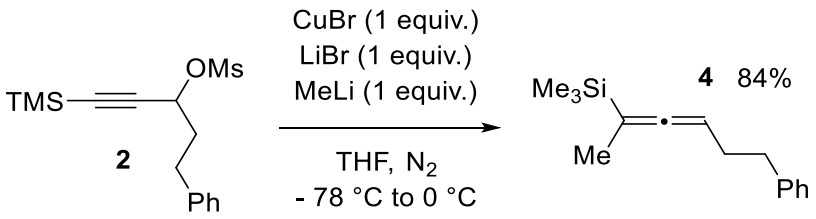

400 mg (2.79 mmol) of CuBr were added to a flamed vial, followed by 242 mg (2.79 mmol) of LiBr. Then, the round bottom flask was filled with 5,2 ml of dry THF and the reaction was put at 0 °C. Then, 1.6 M MeLi (1.74 ml, 2.79 mmol) was added dropwise and the reaction stirred for 30 minutes. In the meantime, 866 mg (2.79 mmol) of **2** were added to a vial, then dissolved into 2,2 ml of dry THF under inert atmosphere. The vial with the organometal was put at -80 °C, then the solution of **2** was added dropwise and the reaction left to go to room temperature and stirred until the next day. The reaction was then quenched with saturated aqueous NH_4Cl and extracted with hexane. The organic phase was then washed with concentrated aqueous NH_4OH to remove copper traces, washed with water and brine and dried over Na_2SO_4. The organic phase was then filtered and the solvent removed under

reduced pressure. 541 mg of **4** were recovered (84% yield). The product was used as it is without any further purification.

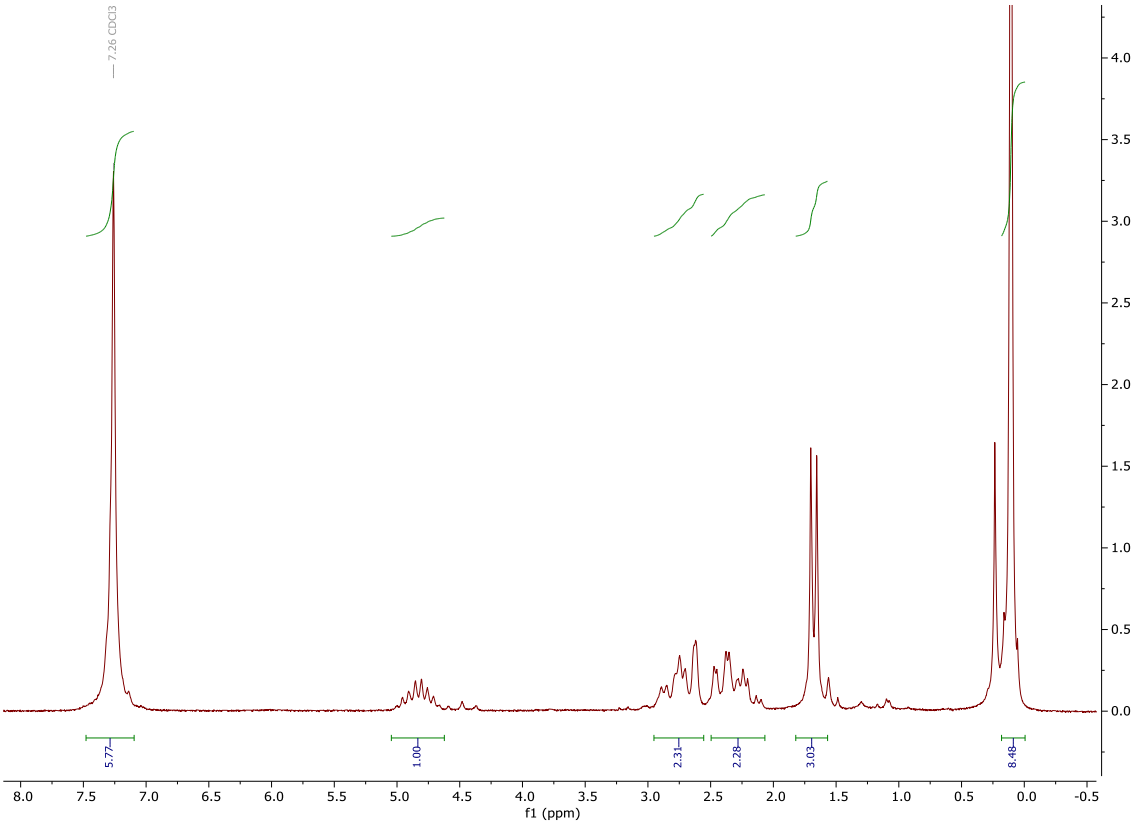

5 - 1H NMR (61 MHz) δ 7.26 (bs, 5H), 4.83 (dq, J = 6.0, 3.0 Hz, 1H), 2.94 – 2.58 (m, 2H), 2.50 – 2.06 (m, 2H), 1.68 (d, J = 2.9 Hz, 3H), 0.11 (s, 9H).

5 – methyldiphenyl(propa-1,2-dien-1-yl)silane

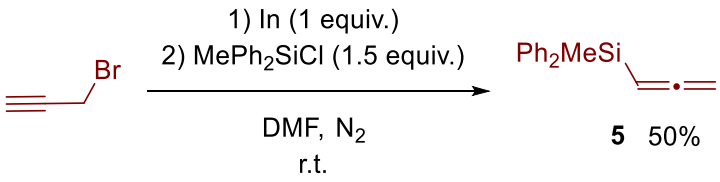

800 mg (6.67 mmol) of indium metal powder were weighted into a round bottom flask and set under inter atmosphere using vacuum/N2 cycles. Then, 14 ml of dry DMF were added, followed by 1 ml (10.5 mmol) of 80% w/w proprargyl bromide in toluene and the reaction is left to stir at r.t. for 1 h, to allow oxidative insertion taking place. Then, the $MePh_2SiCl$ (1,48 ml, 6.97 mmol) was added dropwise and the reaction is left to stir overnight. After, the DMF solution was extracted with pentane (25 ml x 6). The pentane solution was washed water (50 ml x 4) and with brine (x2). The solution was then dried over Na_2SO4, filtered and evaporated under reduced pressure (40 °C, 650 mbar, to avoid allene evaporation). The crude was

then purified by plug over silica using pure pentane as eluent. Finally, pentane was removed under reduced pressure in the same conditions. 831 mg of **5** were recovered (50% yield).

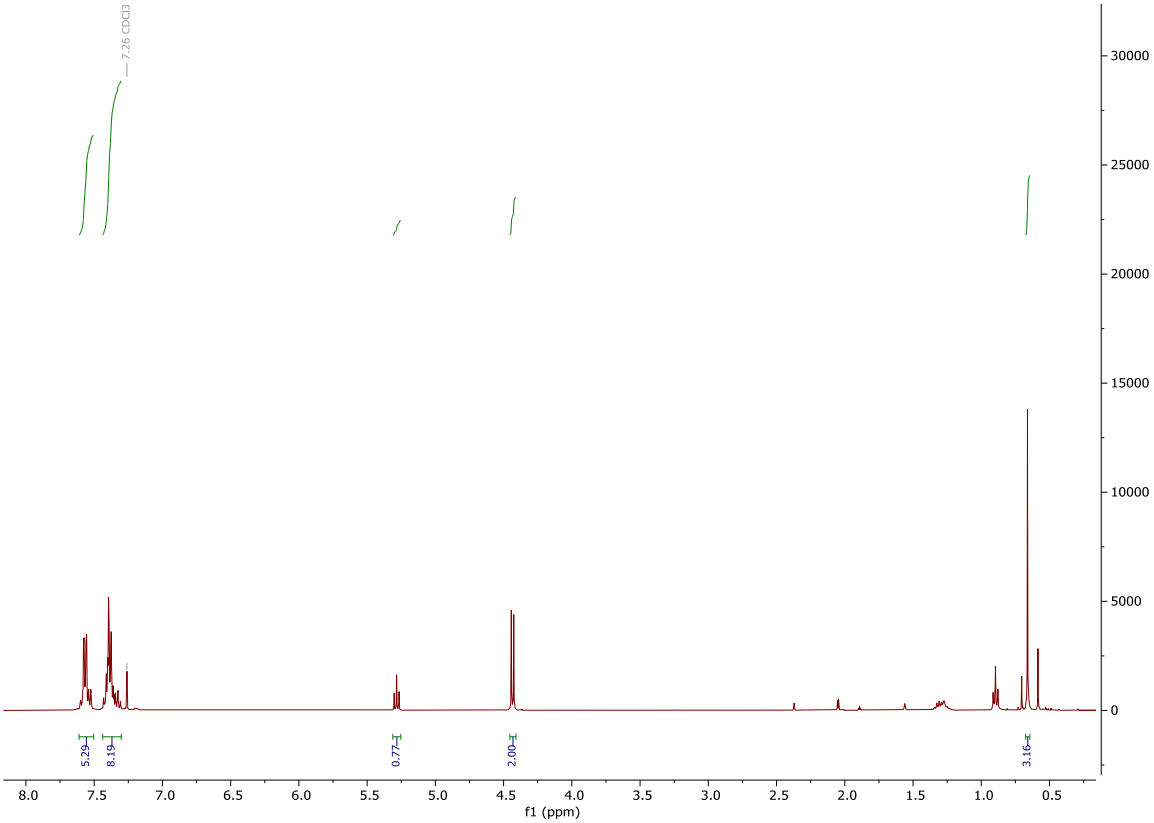

5 - 1H NMR (400 MHz, CDCl3) δ 7.59 – 7.55 (m, 5H), 7.41 - 7.37 (m, 5H), 5.28 (t, J = 7.1 Hz, 1H), 4.43 (d, J = 7.1 Hz, 2H), 0.66 (s, 3H).

10 - (1,3,3-trimethoxypropyl)benzene

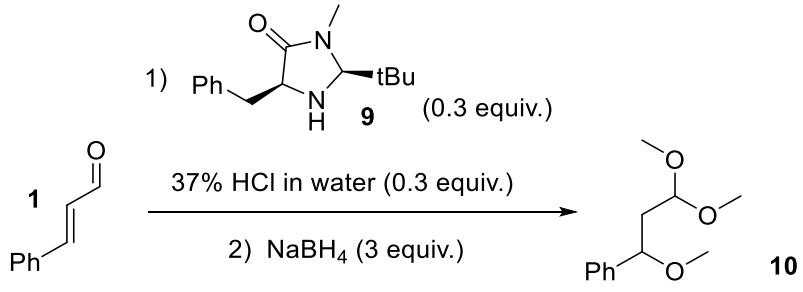

36 mg (0.146 mmol) of catalyst **9** were weighted into a vial and dissolved in MeOH (1530 ul), followed by the addition of 137 ul of 3,7 % HCl (0.146 mmol) in water (water is already there, so no more water was added later). Finally, cinnamaldehyde (61,2 ul, 0.487 mmol) was added. The reaction was left to stir for 4 days at room temperature. After this time, the reaction was quenched with water and extracted with Et2O. The solvent was then removed under reduced pressure.

To remove the cinnamaldehyde, the crude was dissolved in 1 ml of MeOH, and 55 mg (1.46 mmol) $NaBH_4$ were added. The reaction was then quenched with saturated aqueous NH_4Cl, extracted with Et_2O. The solvent was then removed under reduced pressure and the curde plugged over silica to remove the traces of borates and cinnamic alcohol (plug 9:1 PE:AcOEt). The spectrum looks the same, and clean enough. The structure of compound **10** was then confirmed by NMR and GC/MS analysis.

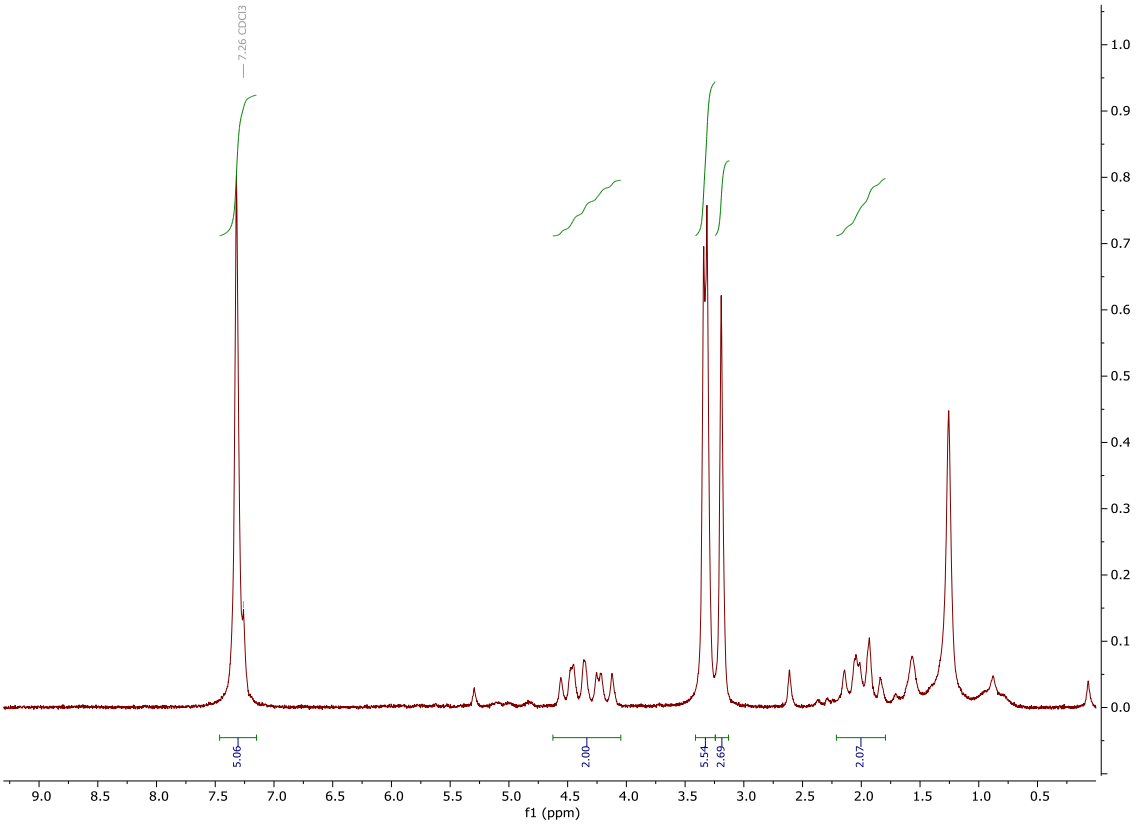

10 - 1H NMR (61 MHz) δ 7.32 (bs, 5H), 4.66 – 4.00 (m, 2H), 3.34 (s, 3H), 3.31 (s, 3H), 3.19 (s, 3H), 1.83-2.13 (m, 2H). Some residual solvents present.

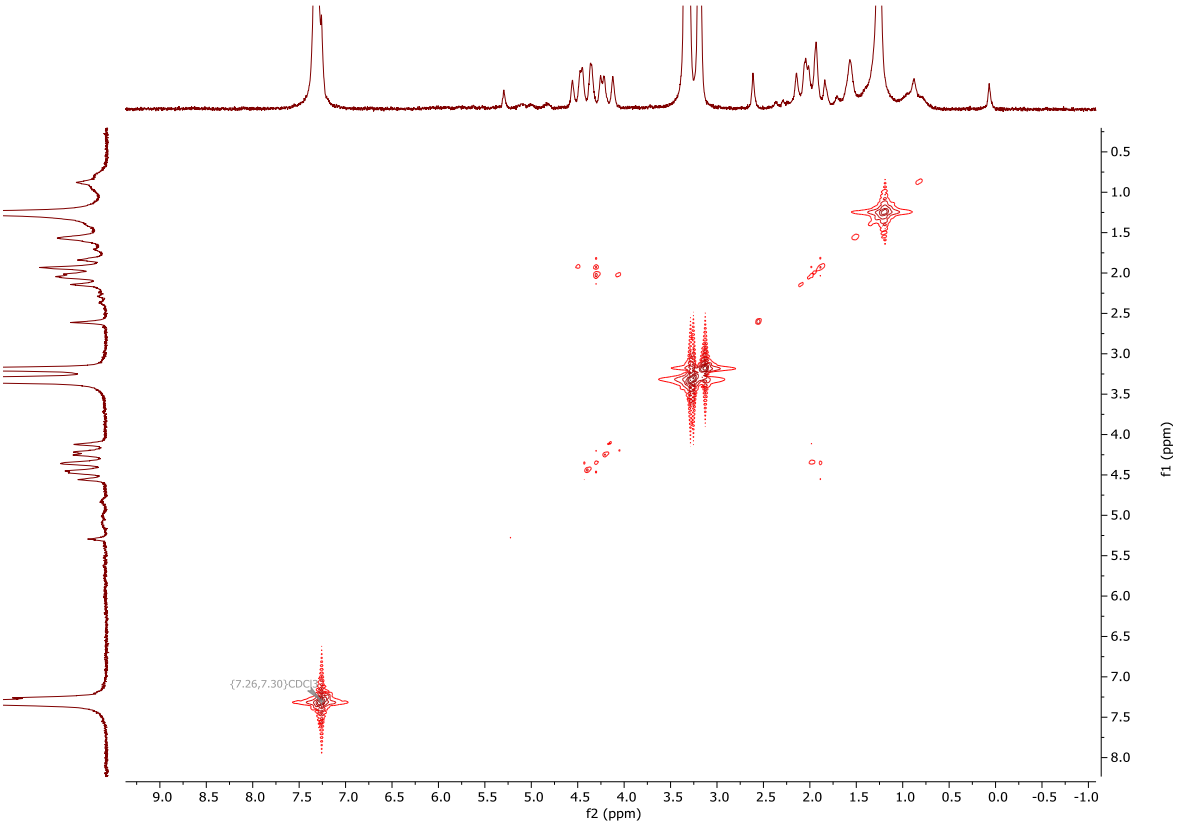

COSY

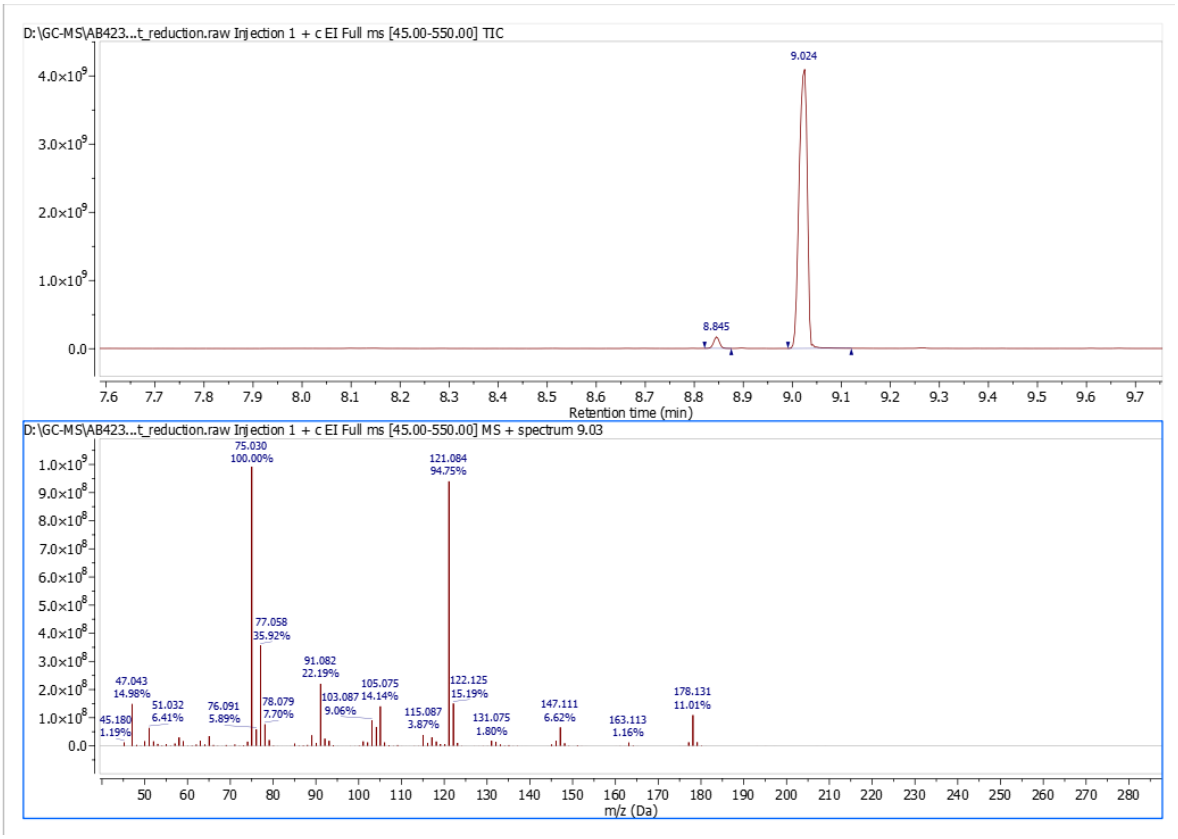

m/z = 210.13 – 178.131 = 32 (corresponding to methanol loss)

12 – allyltriisopropylsilane

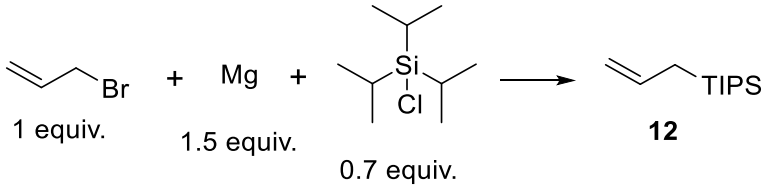

Procedure:

171 mg (7 mmol) of metallic magnesium turnings were weighted into a 2 neck round bottom flask, flaming the system under vacuum. It followed the addition of 5 ml of dry THF, 1 small piece of elemental iodine and then 400 ul (4.68 mmol) of allyl bromide were added. The solution was heated up to trigger the formation of the Grignard reagent. Once formed, it was kept for 2 h at 45 °C. Then, TIPSCl (700 ul, 3.27 mmol) was added and the reaction set-up to reflux overnight.

In the morning the reaction was allowed to cool down (it forms a gel, probably some THF is gone). 3 ml of dry THF were added to improve rheology, then the reaction was put at 0 °C using an ice bath. Then, 10 ml of cold saturated aqueous NH_4Cl were added portion wise (everything turns yellow). Then, the emulsion was put into a separatory funnel, diluted with more water and extracted with Et_2O. Then, the organic phases were merged and washed with brine to remove water. The solvent was then removed under reduced pressure and the crude was loaded directly over silica for a plug using pure hexane. 99 mg of product were recovered (11 % yield).

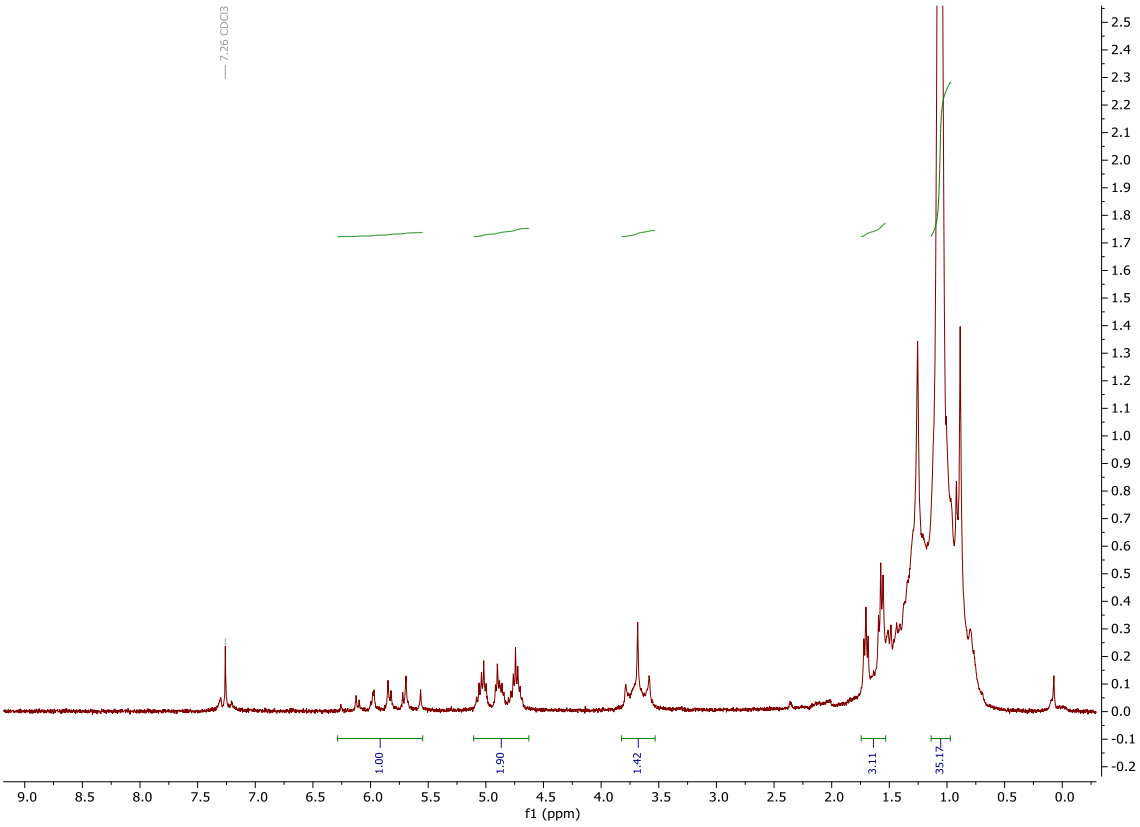

General photocatalysis experimental procedure

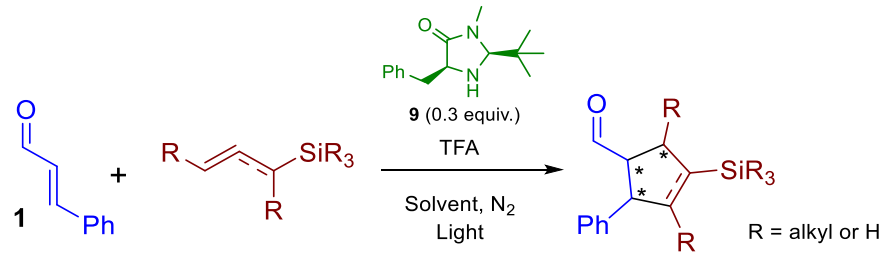

8 mg (0.0325 mmol, 0.3 equivalents) of **9** were weighted into a UFO vial or a Schlenk tube. If indicated, a photocatalyst such as acridinium was added

Then, the system was put under inter atmosphere with N_2/vacuum cycles. It follows the addition of 0,3 ml of dry ACN. Then, 13,6 ul (0.1 mmol, 1 equivalent) of cinnamaldehyde were added, followed by the silane compound (in liquid form). Finally, the indicated amount of trifluoroacetic acid was inject in solution. The system undergoes freeze-pump-thaw to remove oxygen. The solution was then irradiated overnight at 427nm (100% power) or 390 nm (50% power) using a Kessil lamp. UFO reactors were always used as photosystem. After the appropriate reaction time, the reaction was always quenched with water to remove the catalyst and TFA, extracting the organic products with Et_2O.

New products detection (only synthetically interesting results shown)

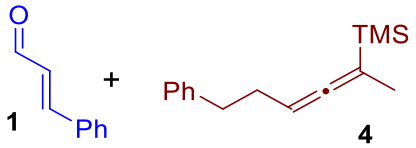

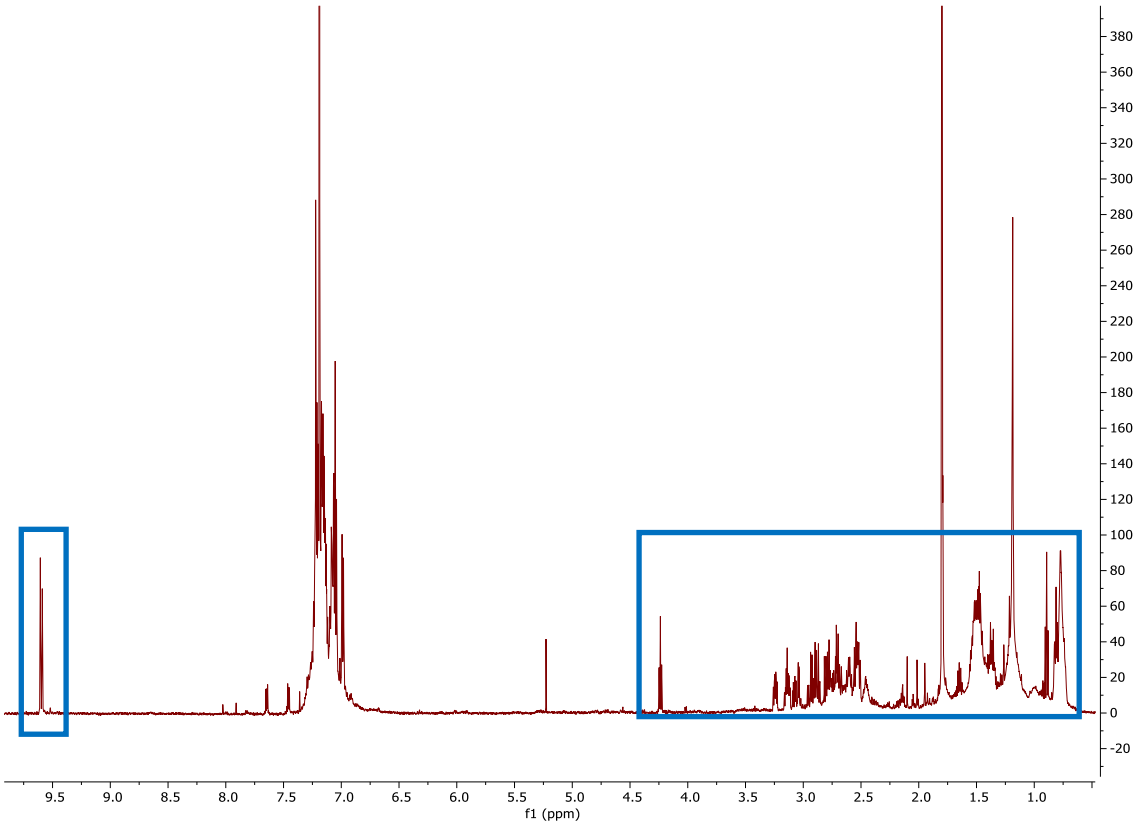

It seems a mixture of 2 diastereoisomers in roughly equal amount (see aldehyde peaks). The alkyl region has interesting complexity, probably presence of chiral centers.

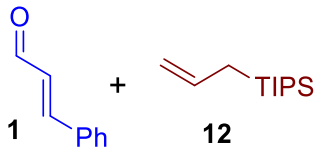

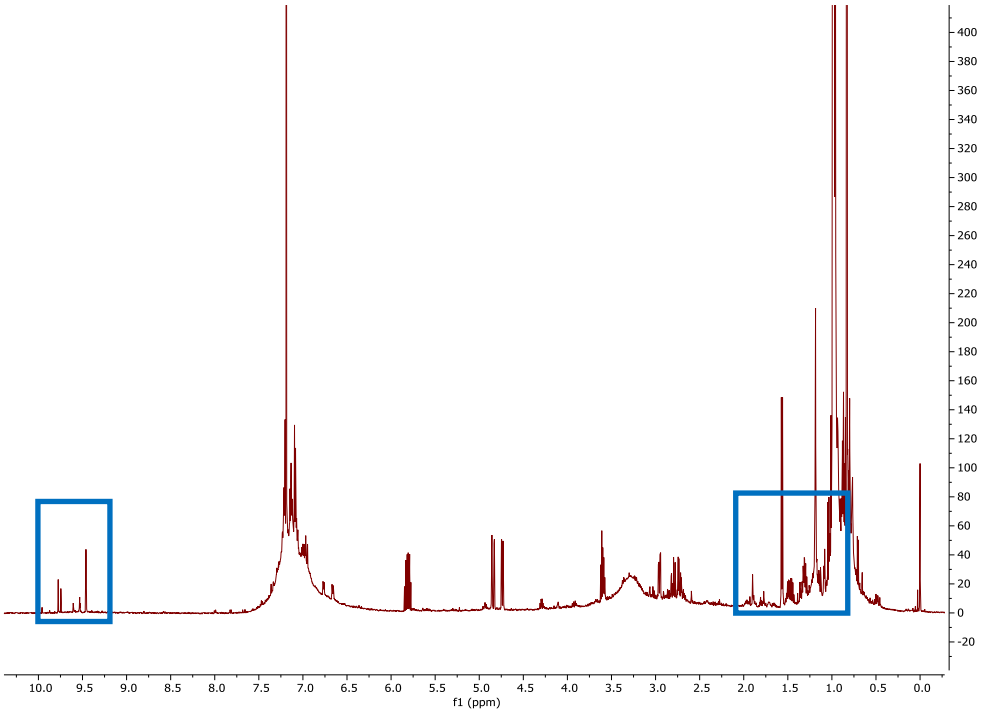

Interesting patterns observed in the crude.

Cyclovoltammetry

The cyclovoltammetry measurement was run on an Electrasyn 2.0. Reference electrode Ag/Ag⁺ (Ag⁺ solution contains 0.01 M AgNO3 and 0.1 M KPF_6 in acetonitrile). Working electrode in graphite (3 mm), counter-electrode in platinum metal. 70 ul of **5** are used to detect the signal. The resulting CVs are shown below.

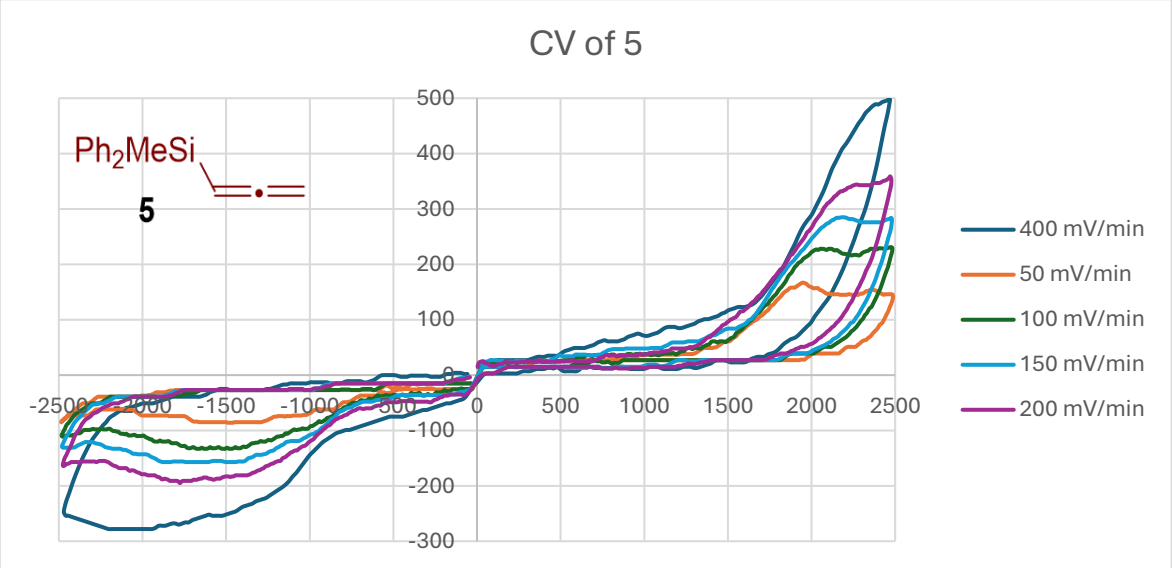

$E°(5)_{OX}$ = 1860 mV, calculated by linear regression of the oxidation peaks at different scan rate for scan rate approaching zero. From the curve shapes it can be deduced that **5** undergoes irreversible mono-oxidation.

Quenching experiment of 5

A degassed solution of trifluoroacetic acid in acetonitrile was prepared and the fluorescence spectrum recorded as background reference. A degassed solution of containing catalyst **9** (0.2 equivalents), trifluoroacetic acid (0.2 equivalents) and cinnamaldehyde (1 equivalent) in acetonitrile was prepared and the fluorescence spectrum recorded. In the same solution 1 equivalent of **5** was added under inert atmosphere, recording the fluorescence spectrum. No significant change in the emission intensity was observed, so it can be concluded that 5 is not a good quencher for iminium ion derived from **9**, cinnamaldehyde (1) and trifluoroacetic acid.

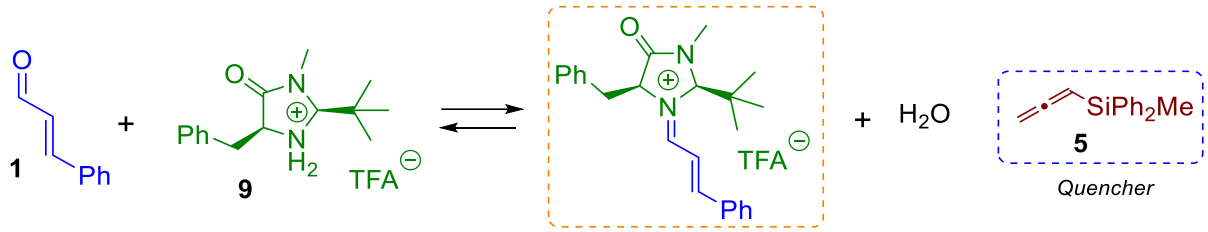

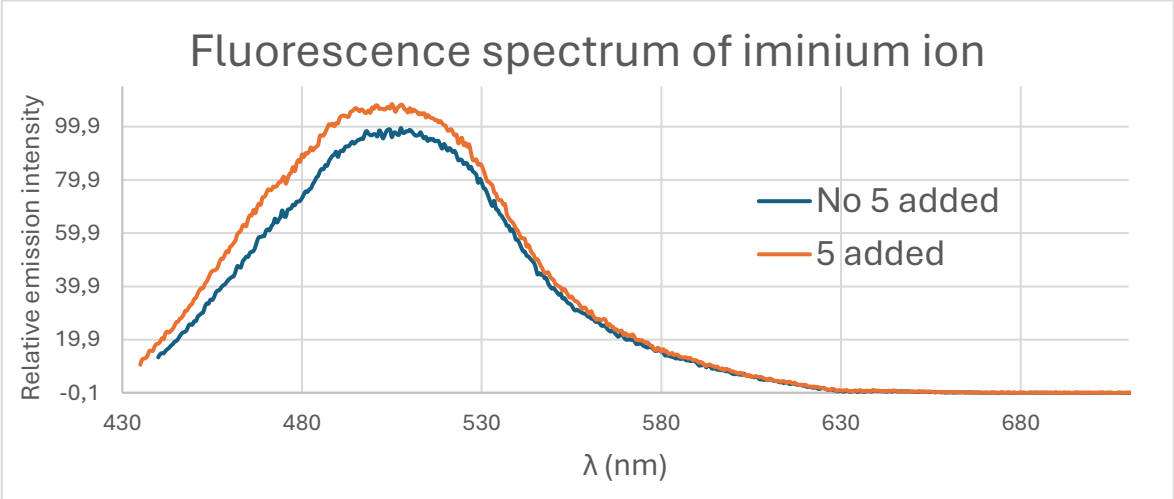

Computational data

Minium energy calculation was run using density functional theory (DFT), using M062X as functional, CPCM in chloroform (implicit solvation) and 6-311G(d,P) as base. ORCA was used as calculation software. It follows the coordinates of the minimized energy structures and the table with the final energy calculation.

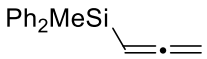

5

CARTESIAN COORDINATES (ANGSTROEM)

C	-0.631979	4.530801	-0.299593
C	-0.453718	3.296257	-0.683393
H	-1.629462	4.929273	-0.149038
H	0.213896	5.189054	-0.133525
C	-0.270442	2.048058	-1.012976
H	-0.222762	1.783704	-2.069191
Si	-0.080191	0.718221	0.298903
C	-0.182622	1.508489	1.990245
H	0.576001	2.285355	2.115436
C	-1.462355	-0.535817	0.052077
H	-1.164717	1.968654	2.125211
H	-0.045346	0.757008	2.772027
C	1.572408	-0.151061	0.072084
H	-2.843551	0.883159	-0.801012
H	-4.692760	-0.728770	-1.027272
C	-2.697621	-0.144447	-0.480300
C	1.779548	-1.032969	-0.998433
H	-0.359869	-2.209282	0.855981
H	-4.384874	-3.084542	-0.315226
C	-3.745149	-1.052261	-0.611753
C	-1.308593	-1.871521	0.448541
H	-2.213760	-3.812374	0.631261
C	-3.572773	-2.374070	-0.211000
C	-2.352554	-2.783116	0.320340
H	2.512693	0.764866	1.784088
C	2.641141	0.088263	0.944669
H	4.689216	-0.334317	1.446036
C	4.060463	-1.401217	-0.311438

H	5.019763	-1.884140	-0.458441
C	3.875057	-0.530468	0.757598
C	3.009969	-1.652546	-1.191398
H	0.966912	-1.246085	-1.688006
H	3.150031	-2.333161	-2.023502

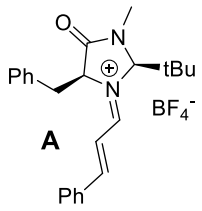

CARTESIAN COORDINATES (ANGSTROEM)

C	1.287327	-0.225602	-0.400328
C	-0.080159	-0.512074	-0.683233
N	-1.057845	-0.553802	0.170516
C	-0.922589	-0.483311	1.634840
C	-2.400454	-1.069465	-0.237536
H	1.606594	-0.092164	0.623099
C	2.145210	-0.141690	-1.438605
H	1.751116	-0.262601	-2.445697
H	-0.026364	-1.038532	1.920547
H	-0.341188	-0.739740	-1.710055
C	3.574714	0.127400	-1.341200
C	6.305275	0.703879	-1.236948
C	4.261218	0.087517	-0.117951
C	4.280812	0.440514	-2.509798
C	5.637863	0.734043	-2.457339
C	5.616050	0.373839	-0.069022
H	3.736973	-0.179263	0.792113
H	3.754272	0.457934	-3.458169
H	6.174172	0.981634	-3.365260
H	6.141531	0.335918	0.877748

H	7.364567	0.928611	-1.193620
C	-3.287545	-0.037933	-0.983700
C	-0.927454	0.924097	2.260066
H	-0.917873	0.749273	3.339035
H	-1.862874	1.431217	2.018877
C	0.259588	1.753560	1.850981
C	2.543678	3.104787	0.961854
C	1.466693	1.639799	2.546071
C	0.202614	2.577819	0.727522
C	1.338844	3.247777	0.281508
C	2.602586	2.308576	2.103803
H	1.515271	1.008842	3.428454
H	-0.731329	2.683135	0.185170
H	1.284792	3.875313	-0.600628
H	3.536352	2.204609	2.644555
H	3.432368	3.615917	0.609846
C	-2.136666	-1.270986	2.095942
N	-2.939765	-1.515294	1.033597
C	-3.938256	-2.573264	1.124188
H	-3.651296	-3.233738	1.941577
H	-3.946023	-3.137700	0.191519
H	-4.934127	-2.173124	1.318057
O	-2.337757	-1.602818	3.243333
B	0.166791	-3.574160	0.198647
F	0.642333	-4.877327	0.170086
F	-0.035451	-3.102996	-1.119725
F	-1.059614	-3.506944	0.885904
F	1.088021	-2.729707	0.850486
H	-2.214737	-1.933611	-0.885350
C	-3.637860	1.158340	-0.099328
H	-2.761141	1.779490	0.091952

H	-4.065769	0.841777	0.854953
H	-4.374099	1.781613	-0.612388
C	-4.577977	-0.756922	-1.404403
H	-4.360668	-1.675114	-1.957423
H	-5.154963	-0.096710	-2.055341
H	-5.202971	-1.003493	-0.545619
C	-2.580216	0.458704	-2.249638
H	-1.700424	1.064111	-2.016087
H	-3.269804	1.091164	-2.812735
H	-2.282365	-0.371122	-2.898110

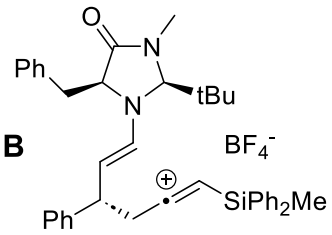

CARTESIAN COORDINATES (ANGSTROEM)

C	4.345521	1.444061	0.924469
C	2.886854	1.042547	0.827397
N	2.766427	0.008323	1.836335
C	4.025833	-0.235937	2.545310
N	4.945422	0.640789	1.826250
C	3.919006	0.065408	4.065806
C	1.897575	2.222749	0.973444
C	6.383216	0.674798	2.022132
O	4.883555	2.318585	0.267322
C	5.198032	-0.373199	4.791671
C	2.750268	-0.745417	4.640028
C	3.668204	1.557557	4.289499
C	1.260492	2.651841	-0.330323
C	2.029409	2.776788	-1.492168
C	1.450296	3.197977	-2.685896

C	0.093379	3.515096	-2.735237
C	-0.681339	3.395898	-1.583847
C	-0.101745	2.958081	-0.394395
C	1.867356	-1.016279	1.611214
C	0.816769	-0.915785	0.786822
C	-0.142731	-2.030674	0.478059
C	-0.197119	-2.259348	-1.063022
C	-1.541107	-1.813702	1.034383
C	-2.078315	-0.538186	1.211648
C	-3.372582	-0.376537	1.703587
C	-4.143425	-1.487743	2.028879
C	-3.610907	-2.763950	1.863705
C	-2.321987	-2.922311	1.367875
C	-0.366369	-1.014516	-1.777281
C	-0.506300	0.055660	-2.358665
Si	-2.294647	-0.388408	-3.342817
C	-1.693696	-0.371570	-5.093781
C	-3.197031	1.159628	-2.830325
C	-3.592783	1.397042	-1.506964
C	-4.266103	2.563445	-1.163383
C	-4.540109	3.520680	-2.137989
C	-4.135993	3.309654	-3.452724
C	-3.470110	2.135686	-3.797396
C	-3.056657	-1.994136	-2.822293
C	-2.744072	-3.130725	-3.582364
C	-3.268938	-4.373920	-3.249622
C	-4.132596	-4.493734	-2.165637
C	-4.464093	-3.371149	-1.410343
C	-3.925126	-2.129704	-1.729146
H	2.751869	0.588791	-0.166290
H	4.339113	-1.281320	2.416027

H	1.119189	1.930548	1.682686
H	2.423342	3.077847	1.411053
H	6.671665	1.397515	2.788991
H	6.733143	-0.316764	2.308644
H	6.842810	0.966330	1.078161
H	5.039961	-0.307523	5.870996
H	6.053324	0.256864	4.548814
H	5.450769	-1.411008	4.552785
H	2.710250	-0.603657	5.722526
H	1.793963	-0.426567	4.220562
H	2.877332	-1.815670	4.447040
H	4.518295	2.160583	3.958706
H	2.775992	1.887051	3.749191
H	3.508933	1.751673	5.353105
H	3.092390	2.559544	-1.450841
H	2.061536	3.287012	-3.576549
H	-0.356344	3.853747	-3.661975
H	-1.738398	3.635749	-1.615057
H	-0.712684	2.861132	0.498235
H	2.062929	-1.933518	2.159694
H	0.624778	0.029640	0.286388
H	0.241405	-2.965991	0.893701
H	-0.997655	-2.947533	-1.362475
H	0.732285	-2.702270	-1.431648
H	-1.483432	0.338795	0.975972
H	-3.775975	0.621741	1.837179
H	-5.146479	-1.360904	2.419228
H	-4.200008	-3.636519	2.122143
H	-1.912529	-3.919414	1.234818
H	-0.196869	1.046950	-2.656462
H	-2.539371	-0.513446	-5.772777

H	-0.979384	-1.184695	-5.237655
H	-1.204295	0.575601	-5.330481
H	-3.362083	0.676582	-0.730876
H	-4.569892	2.729001	-0.136007
H	-5.063095	4.431759	-1.871372
H	-4.339859	4.055949	-4.211665
H	-3.166073	1.984901	-4.828359
H	-2.068552	-3.062792	-4.424586
H	-2.990229	-5.240736	-3.836541
H	-4.546555	-5.461311	-1.905721
H	-5.135085	-3.461755	-0.564454
H	-4.190260	-1.275454	-1.115370
B	0.373920	-4.091613	-4.041756
F	-0.480244	-4.546956	-5.058270
F	0.029603	-4.698159	-2.824751
F	1.700879	-4.375094	-4.360805
F	0.216939	-2.684996	-3.911119

Bibliography

(1) Showell, G. A.; Mills, J. S. Chemistry Challenges in Lead Optimization: Silicon Isosteres in Drug Discovery. *Drug Discov Today* 2003, *8* (12), 551–556. https://doi.org/10.1016/S1359-6446(03)02726-0.

(2) Panayides, J.-L.; Riley, D. L.; Hasenmaile, F.; van Otterlo, W. A. L. The Role of Silicon in Drug Discovery: A Review. *RSC Med Chem* 2024, *15* (10), 3286–3344. https://doi.org/10.1039/D4MD00169A.

(3) Kürti László; Czakó Barbara. Strategic Applications of Named Reactions in Organic Synthesis. In *Strategic Applications of Named Reactions in Organic Synthesis*; 2005.

(4) Curtis-Long, M. J.; Aye, Y. Vinyl-, Propargyl-, and Allenylsilicon Reagents in Asymmetric Synthesis: A Relatively Untapped Resource of Environmentally Benign Reagents. *Chemistry - A European Journal*. May 25, 2009, pp 5402–5416. https://doi.org/10.1002/chem.200900337.

(5) Clyaden Jonathan; Greeves Nick; Warren Stuart. *Organic Chemistry*, Second.; Oxford, 2012.

(6) Danheiser, R. L.; Carini, D. J.; Basak, A. (Trimethylsilyl)Cyclopentene Annulation: A Regiocontrolled Approach to the Synthesis of Five-Membered Rings. *J Am Chem Soc* 1981, *103* (6), 1604–1606. https://doi.org/10.1021/ja00396a071.

(7) Danheiser, R. L.; Carini, D. J.; Fink, D. M.; Basak, A. Scope and Stereochemical Course of the (Trimethylsilyl)Cyclopentene Annulation. *Tetrahedron* 1983, *39* (6), 935–947. https://doi.org/10.1016/S0040-4020(01)88592-6.

(8) Woo, S.; Shenvi, R. A. Synthesis and Target Annotation of the Alkaloid GB18. *Nature* 2022, *606* (7916), 917–921. https://doi.org/10.1038/s41586-022-04840-9.

(9) Westmuze H.; Vermeer P. A New and General Route to 1-Trimethylsilyl-1,2-Alkadienes. *Synth Commun* 1979.

(10) Sharma, R.; Manpadi, M.; Zhang, Y.; Kim, H.; Ahkmedov, N. G.; Williams, L. J. Spirodiepoxide-Based Cascades: Direct Access to Diverse Motifs. *Org Lett* 2011, *13* (13), 3352–3355. https://doi.org/10.1021/ol201101e.

(11) Alf, C.; Lars-Inge, O. Allenes and Acetylenes. 22. Mechanistic Aspects of the Allene-Forming Reductions (SN2' Reaction) of Chiral Propargylic Derivatives with Hydride Reagents. *J Am Chem Soc* 1979, *101* (24), 7302–7311. https://doi.org/10.1021/ja00518a028.

(12) Li, Z.; Yang, C.; Zheng, H.; Qiu, H.; Lai, G. Selective Mono- and Di-Allylation and Allenylation of Chlorosilanes Using Indium. *J Organomet Chem* 2008, *693* (25), 3771–3779. https://doi.org/10.1016/j.jorganchem.2008.08.028.

(13) Kano, T.; Tanaka, Y.; Maruoka, K. Organocatalytic Oxy-Michael Addition of Alcohols to α,β-Unsaturated Aldehydes. *Tetrahedron Lett* 2006, *47* (18), 3039–3041. https://doi.org/10.1016/j.tetlet.2006.03.001.

(14) Kano, T.; Tanaka, Y.; Maruoka, K. Asymmetric Organocatalytic Oxy-Michael Addition of Alcohols to α,β-Unsaturated Aldehydes. *Tetrahedron* 2007, *63* (35), 8658–8664. https://doi.org/10.1016/j.tet.2007.03.179.

(15) Pohjakallio, A.; Pihko, P. M.; Laitinen, U. M. Synthesis of 2-Isoxazolines: Enantioselective and Racemic Methods Based on Conjugate Additions of Oximes. *Chemistry – A European Journal* 2010, *16* (37), 11325–11339. https://doi.org/10.1002/chem.201000861.

(16) Neese, F. Software Update: The <scp>ORCA</Scp> Program System—Version 5.0. *WIREs Computational Molecular Science* 2022, *12* (5). https://doi.org/10.1002/wcms.1606.

(17) Neese, F. The ORCA Program System. *WIREs Computational Molecular Science* 2012, *2* (1), 73–78. https://doi.org/10.1002/wcms.81.

(18) Hanwell, M. D.; Curtis, D. E.; Lonie, D. C.; Vandermeersch, T.; Zurek, E.; Hutchison, G. R. Avogadro: An Advanced Semantic Chemical Editor, Visualization, and Analysis Platform. *J Cheminform* 2012, *4* (1), 17. https://doi.org/10.1186/1758-2946-4-17.

(19) *http://avogadro.cc/*.

(20) Costa, A. M.; Castro-Alvarez, A.; Fillot, D.; Vilarrasa, J. Computational Comparison of the Stability of Iminium Ions and Salts from Enals and Pyrrolidine Derivatives (Aminocatalysts). *European J Org Chem* 2022, *2022* (35). https://doi.org/10.1002/ejoc.202200627.

(21) Silvi, M.; Verrier, C.; Rey, Y. P.; Buzzetti, L.; Melchiorre, P. Visible-Light Excitation of Iminium Ions Enables the Enantioselective Catalytic β-Alkylation of Enals. *Nat Chem* 2017, *9* (9), 868–873. https://doi.org/10.1038/nchem.2748.

(22) Perego, L. A.; Bonilla, P.; Melchiorre, P. Photo-Organocatalytic Enantioselective Radical Cascade Enabled by Single-Electron Transfer Activation of Allenes. *Adv Synth Catal* 2020, *362* (2), 302–307. https://doi.org/10.1002/adsc.201900973.

(23) Masson, T. M.; Zondag, S. D. A.; Schuurmans, J. H. A.; Noël, T. Open-Source 3D Printed Reactors for Reproducible Batch and Continuous-Flow Photon-Induced Chemistry: Design and Characterization. *React Chem Eng* 2024, *9* (8), 2218–2225. https://doi.org/10.1039/D4RE00081A.

(24) Silvi, M.; Verrier, C.; Rey, Y. P.; Buzzetti, L.; Melchiorre, P. Visible-Light Excitation of Iminium Ions Enables the Enantioselective Catalytic β-Alkylation of Enals. *Nat Chem* 2017, *9* (9), 868–873. https://doi.org/10.1038/nchem.2748.

(25) Berger, M.; Carboni, D.; Melchiorre, P. Photochemical Organocatalytic Regio- and Enantioselective Conjugate Addition of Allyl Groups to Enals. *Angewandte Chemie - International Edition* 2021, *60* (50), 26373–26377. https://doi.org/10.1002/anie.202111648.

(26) Le Saux, E.; Ma, D.; Bonilla, P.; Holden, C. M.; Lustosa, D.; Melchiorre, P. A General Organocatalytic System for Enantioselective Radical Conjugate Additions to Enals. *Angewandte Chemie - International Edition* 2021, *60* (10), 5357–5362. https://doi.org/10.1002/anie.202014876.

(27) Venditto, N. J.; Liang, Y. S.; El Mokadem, R. K.; Nicewicz, D. A. Ketone–Olefin Coupling of Aliphatic and Aromatic Carbonyls Catalyzed by Excited-State Acridine Radicals. *J Am Chem Soc* 2022, *144* (26), 11888–11896. https://doi.org/10.1021/jacs.2c04822.

(28) Danheiser Rick L.; Dixon Brian R.; Gleason Robert W. Dixon-et-al-2002-Five-Membered-Ring-Annulation-via-Propargyl-and-Allylsilanes. *Journal of Organic Chemistry* 1992, *57*.

(29) Knölker, H. J.; Foitzik, N.; Goesmann, H.; Graf, R.; Jones, P. G.; Wanzl, G. Highly Stereoselective Synthesis of Bicyclo[n.3.0]Alkanes by Titanium Tetrachloride Promoted [3 + 2] Cycloaddition of Allylsilanes and 1-Acetylcycloalkenes. *Chemistry - A European Journal* 1997, *3* (4), 538–551. https://doi.org/10.1002/chem.19970030409.

(30) Knölker, H.; Foitzik, N.; Goesmann, H.; Graf, R. Eine Vielseitige Und Effiziente Synthese Anellierter Cyclopentane Durch Stereoselektive Cycloaddition von Allylsilanen Und Cycloalkenylmethylketonen. *Angewandte Chemie* 1993, *105* (7), 1104–1106. https://doi.org/10.1002/ange.19931050725.

(31) Okamoto, K.; Tamura, E.; Ohe, K. Stereoselective Construction of 1,3-Disilylcyclopentane Derivatives by Scandium-Catalyzed [3+2] Cycloaddition of Allylsilanes to B-Silylenones. *Angewandte Chemie International Edition* 2014, *53* (38), 10195–10199. https://doi.org/10.1002/anie.201404218.

Chapter 4 – Asymmetric photo-organocatalyzed reductive coupling

This chapter is connected with chapter 5, so the numeration continues.

Mechanistic investigation

As anticipated in chapter 5, compounds **12**^{I} and **12**^{II} (Figure 95) were obtained as byproducts of the attempted Danheiser reaction. After chromatographic separation, only one of the diastereoisomers was characterized by HNMR, COSY and mass spectrometry (m/z = 248,174). The correct assignation of each diastereoisomer to the recorded spectrum was attempted. Despite the use of a simulation software[1], it was not possible to reach any conclusion. Luckily, there is a literature report in which the stereochemistry is assigned thanks to a separate synthesis of the compounds.[2]

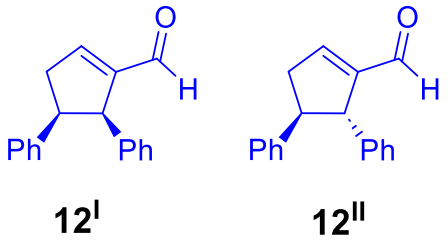

Figure 95 - 12^{I} and 12^{II} structures

To understand how these byproducts get generated, some blank tests were done, working on the conditions that yielded the byproduct (Table 16).

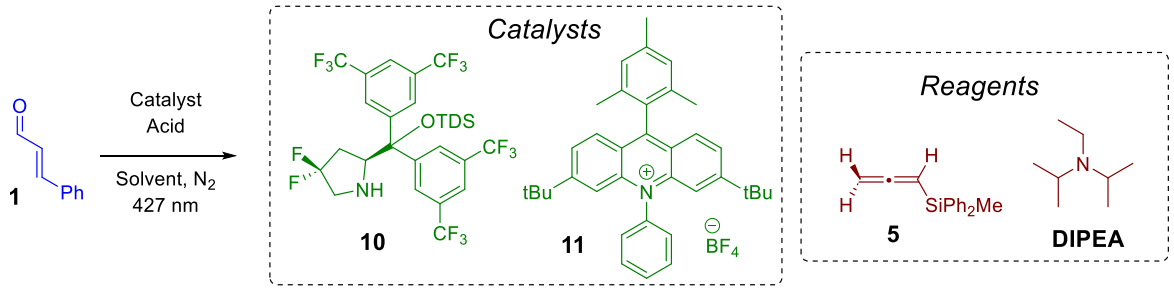

Entry	Reagents	Catalyst	λ	Solvent	Time	Results
1	1	10 (0,3 eq.) + TFA (0,3 eq.)	427 nm	ACN	18 h	12^{I} and 12^{II} detected
2	1	10 (0,3 eq.) + TFA (0,3 eq.)	390 nm	ACN	18 h	12^{I} and 12^{II} detected
3	1	11 (0,05 eq.) + TFA (0,3 eq.)	390 nm	ACN	18 h	No reaction
4	1 + 5	11 (0,05 eq.) + TFA (0,3 eq.)	390 nm	ACN	18 h	No reaction

5	1 + DIPEA	11 (0,05 eq.)	390 nm	ACN	18 h	12^{I} and 12^{II} detected

Table 16 - Blank tests

All reactions were performed in a Schlenk tube or a vial in the indicated conditions. UFO reactor was used as photosystem, irradiating with a 427 nm Kessil lamp set at 100 % power for 18 hours. The system undergoes freeze-pump-thaw procedure before starting to irradiate.

The reaction conducted in the presence of catalyst **10** at 427 nm without allene **5** led to the formation of 12^{I} and 12^{II} (entry 1). This confirms that allenyl silane has no active role in the formation of the homocoupling products. The same test was conducted at 390 nm (entry 2), to check if a lower wavelength somehow gives different results, but essentially the same events were observed. The use of *only* acridinium as photocatalyst with TFA (entry 3) in the same conditions of entry 2 gave no reaction. Another test conducted in the same conditions with both **4** and TFA again showed no reactivity, ruling out any role of **4** also in a photosystem with only acridinium. Finally, **1** and diisopropylethylamine (DIPEA) in the presence of **11** at 390 nm yielded $\mathbf{12^{I}}$ and $\mathbf{12^{II}}$.

These results, taken together with the previous experimental observations, gave the following information:

- **9**, **10** and **11** are all able to act as photocatalysts, both at 390 nm and 427 nm irradiation.
- **5** is not involved at all in the photocatalysis process: nor as reagent, or co-catalyst.
- The reaction works only in the presence of something *oxidizable*, such as DIPEA of TFA *anion*. This is in good agreement both with the overall process stoichiometry, which is a reductive coupling, and with some fluorinated byproducts detected in the first tests, together with $\mathbf{12^{I}}$ and $\mathbf{12^{II}}$. Probably the $\bullet CF_3$ acts as chain terminator. The reaction of entry 5 is indeed much cleaner, as only starting material, catalyst and products were detected by mass spectroscopy.

Two simple mechanistic hypotheses for the different photocatalytic systems were then formulated.

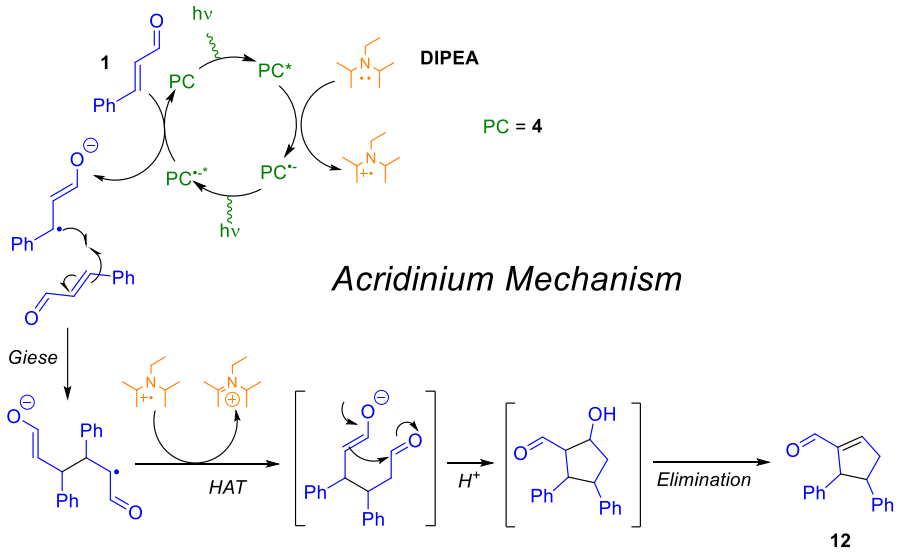

Figure 96 – Acridinium-based mechanism

In the acridinium-based photocatalytic system (Figure 96) the photoexcited catalyst oxidizes DIPEA, generating the corresponding radical cation. Thanks to the excitation of the reduced photocatalyst, the latter reduces **1**, generating a strongly nucleophilic radical-enolate species. This radical then operated Giese addition on another molecule of **1**, generating an intermediate species, which undergoes HAT from the DIPEA-radical cation, generating the enolate ion and the iminium ion co-product. It follows intramolecular aldol reaction and elimination, yielding **12**-type products. It is reasonable to think enolate ion to be responsible for aldol reaction, but nothing excludes the possibility of hydrolyzing the oxidized DIPEA, generating a secondary amine that acts as organocatalyst.

The iminium-based mechanism (Figure 97) should follow a different path.

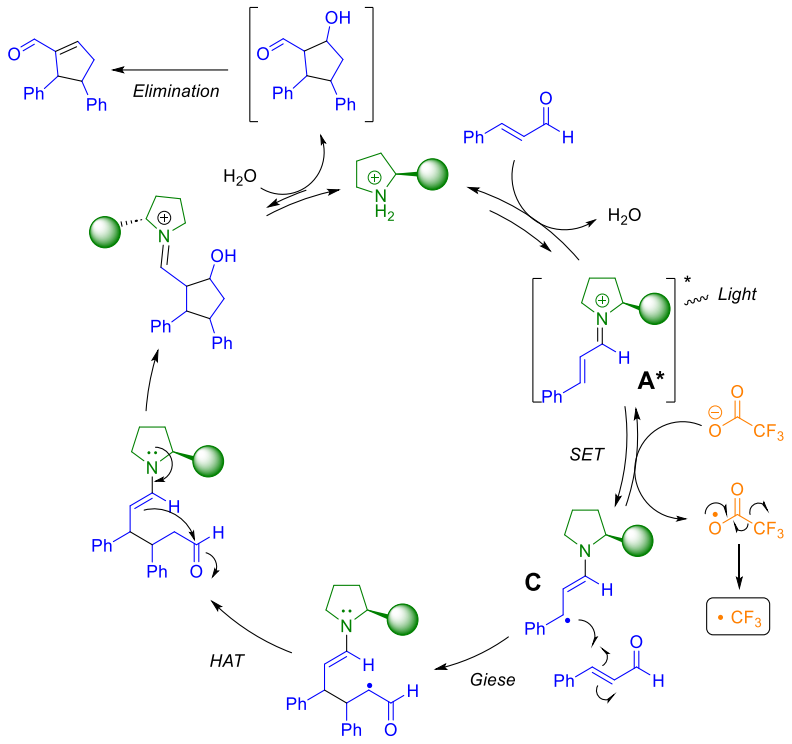

Figure 97 – Iminium-based reaction

For sure, it must start from the photoexcited iminium ion, which is a strong oxidizing agent: mono-oxidation of trifluoroacetate, despite difficult, is thermodynamically allowed, and the following decarboxylation is fast, generating •CF_3 species. The Giese addition of the so generated enamine radical **C** is reasonably followed by a HAT event, and then by intramolecular aldol reaction. The hydrolysis of organocatalyst and the elimination of the aldol yield **12**-type products. The exact sequence of events is probably more complex, as the organocatalyst can be hydrolyzed in different steps, and organocatalyzed events contribute to the elimination step too. Some radical termination or addition events of •CF_3 explain the presence of complex fluorinated products.

12-type products are densely functionalized and are general structures which could be useful for synthetic application. It follows a brief overview of reductive coupling methodologies on similar substrates, and asymmetric synthesis to have similar products.

Literature background

To the best of our knowledge, the intermolecular reductive coupling of α,β-unsaturated aldehyde followed by intramolecular aldol reaction has no examples in literature – doing this in an *asymmetric* fashion would be of great interest. The reductive coupling of ketones is a much more common reaction, as hundreds of

examples are available in literature. Reduction usually occurs via radical methodologies, such as electrochemistry, SmI_2 reduction and Cr^{II} reduction. Notably, there is only one example of asymmetric reductive coupling reported by Sundén and co-workers:[3] using a asymmetric triazolium-based ionic liquid as solvent, in the presence of DBU as base and methanol, the *in situ* formed NHC carbene is able to operate an enantioselective reductive coupling (Figure 98).

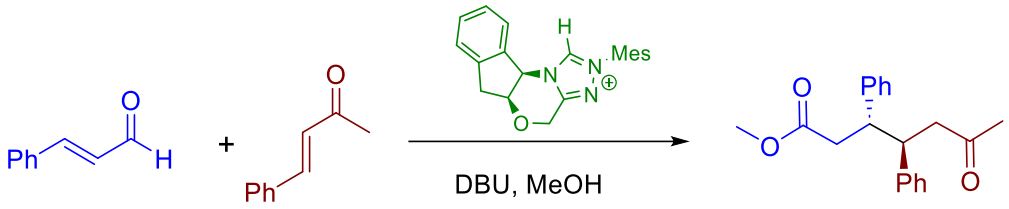

Figure 98 - The only example of enantioselective reductive coupling

Moreover, asymmetric structures close to **12** can be obtained by other photocatalytic methodologies coupling a α-cyclopropyl-ketone with an olefin with asymmetric gadolinium catalyst,[4] and by coupling an α,β-unsaturated aldehyde with a cyclopropanol via iminium-ion photocatalysis[5] (Figure 99).

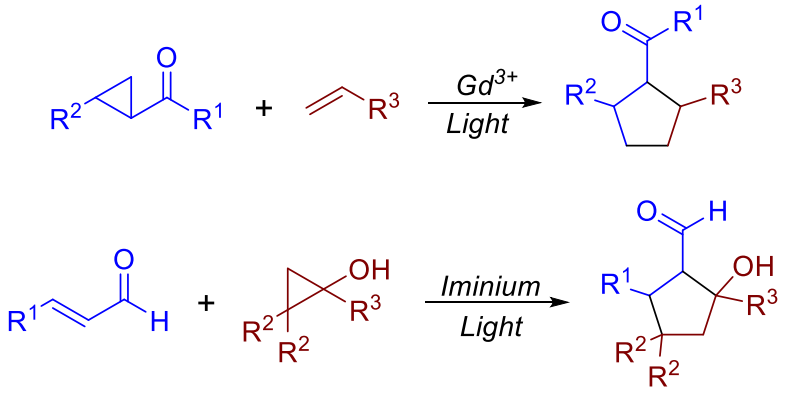

Figure 99 - Examples of similar 5-membered structure synthesized via other photocatalyzed asymmetric methodologies

Despite these are valid asymmetric methodologies, they are substrate-limited and use cyclopropane substrates, which need to be synthesized. Our access to substrates of **12**-type is more straightforward, as only widely available α,β-unsaturated carbonyl compounds would be used instead.

Experimental - homocoupling

The experimentation started testing different reducing agents, using the homocoupling of **1** as reaction model. The results are shown in Table 17:

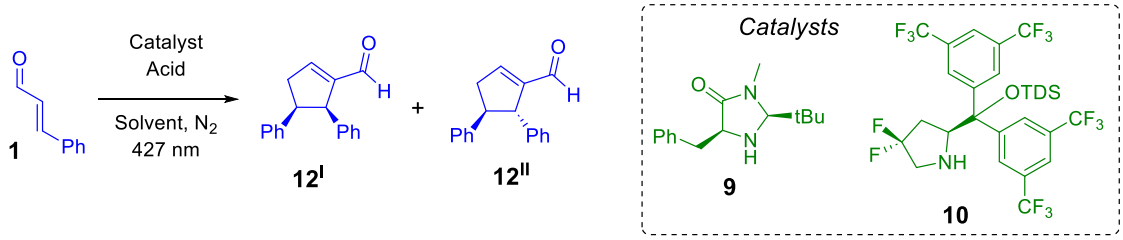

Entry	Reducing agent	Catalyst	Time	Conversion of 1[a]	Products
1	DIPEA (2 eq.)	9 (0,3 eq.) TFA (0,6 eq.)	48 h	Low	12 + 13[b]
2	Oxalic acid[c] (0,6 eq.)	9 (0,3 eq.)	48 h	-	12 and 13
3	Oxalic acid (3 eq.)	9 (0,3 eq.)	18 h	100 %	12[d] and 13
4	Oxalic acid (3 eq.)	9 (0,1 eq.)	18 h	-	Only 13
5	Oxalic acid (1.1 eq.)	9 (0,3 eq.)	22 h	100 %	12 and 13
6	Oxalic acid (3 eq.)	10 (0,2 eq.)	18 h	Low	12, 13 and other aldehydes
7[e]	Oxalic acid (3 eq.)	9 (0,3 eq.)	18 h	100 %	12 and 13 and other compounds

Table 17 - Homocoupling reactivity optimization

All the reaction were run in ACN, using a Schlenk tube or a UFO vial, irradiating at 427 nm with a Kessil lamp set at maximum power. The system undergoes freeze-pump-thaw before irradiation. UFO reactor[6] was used as photocatalytic set-up.

[a] = Conversion evaluated by HNMR, [b] = 13 is the product of direct tert-butyl addition to cinnamaldehyde shown in the previous chapter [c] = oxalic acid dihydrate used, [d] = enantiomeric excess of 12^{I} = 5,5%, ee of 12^{II} = 45,5%, [e] = solution purged with dinitrogen for 5 minutes.

DIPEA was tested as reducing agent, using 0,3 eq. of **9** as organocatalyst and 0,6 eq. of TFA as acid co-catalyst. Despite the real proton source is DIPEA completely deprotonating TFA, the formation of the iminium ion is still visible by the yellow color. After 48 h of irradiation the conversion **12-type** products were obtained with a low conversion of cinnamaldehyde. Moreover, **13** was obtained (Figure 100).

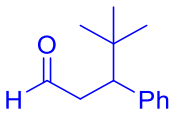

13

Figure 100 - 13-type products structure

Entry 2 introduces the use of oxalic acid both as reducing agent and acid co-catalyst to help the formation of iminium ion. We reasoned that oxalic acid has no

R-residues that can free R• after the decarboxylation process, as the species •COOH is known to act as simple HAT agent with the emission of a second equivalent of carbon dioxide. This is important, as previously •CF_3 was observed to attack the reaction intermediate, giving an insanely complex reaction mixture (Figure 101).

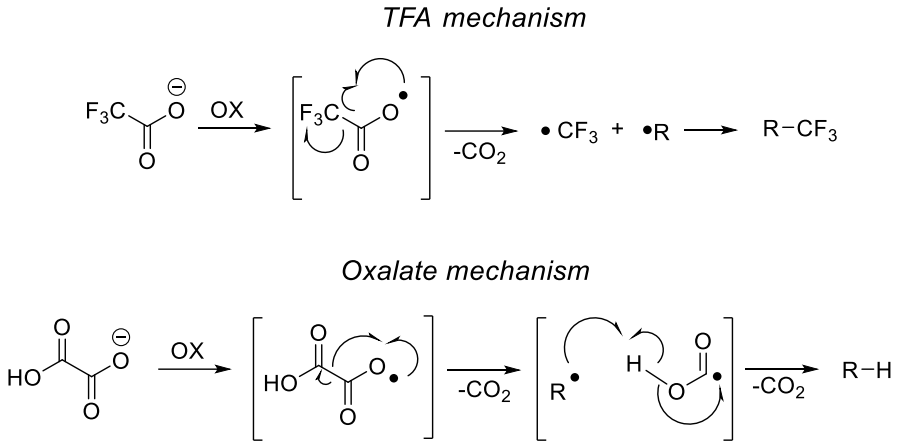

Figure 101 - Difference between oxalic acid and TFA mechanism

Moreover, oxalic acids have been successfully used as reducing agent in electrochemistry, so there are precedents for its use in radical-mediated processes. Indeed, with 0.6 equivalents of oxalic acid a partial conversion after 48 h of irradiation was observed. This first result was encouraging, especially taking into account that the reducing agent was used in sub-stoichiometric amount. 3 equivalents of oxalic acid (entry 3) showed full conversion. 0.1 equivalents of catalyst **9** and 3 equivalents of oxalic acid gave a partial conversion with the same reaction time – more catalyst is needed for full conversion in 18 hours (entry 4). Then, 1.1 equivalents of oxalic acid and 0.3 equivalents of **9** gave full conversion – a slight excess of reagent is enough to complete the reaction (entry 5). 0.2 equivalents of catalyst **10** (entry 5) revealed a much milder reactivity in the same conditions, excluding for the moment the use of **10**, also much more expensive than **9**. Finally, entry 7 has the same exact conditions as entry 3, but the solution is purged for 5 minutes with N_2 instead of undergoing freeze-pump-thaw. The results are somehow different, as very colored impurities are formed together with the usual products. This was not investigated further, as the information of being O_2 sensible is now acquired.

The enantiomeric excess of **12**^{I} and **12**^{II} were then measured, being 45,5 % and 5,5 %. However, as stated above we are still not sure about which diastereoisomer is which. The enantiomeric excess values are drastically different, considering that the values come from the same reaction. This gives further insights into the mechanism of **12-type** products formation (Figure 102).

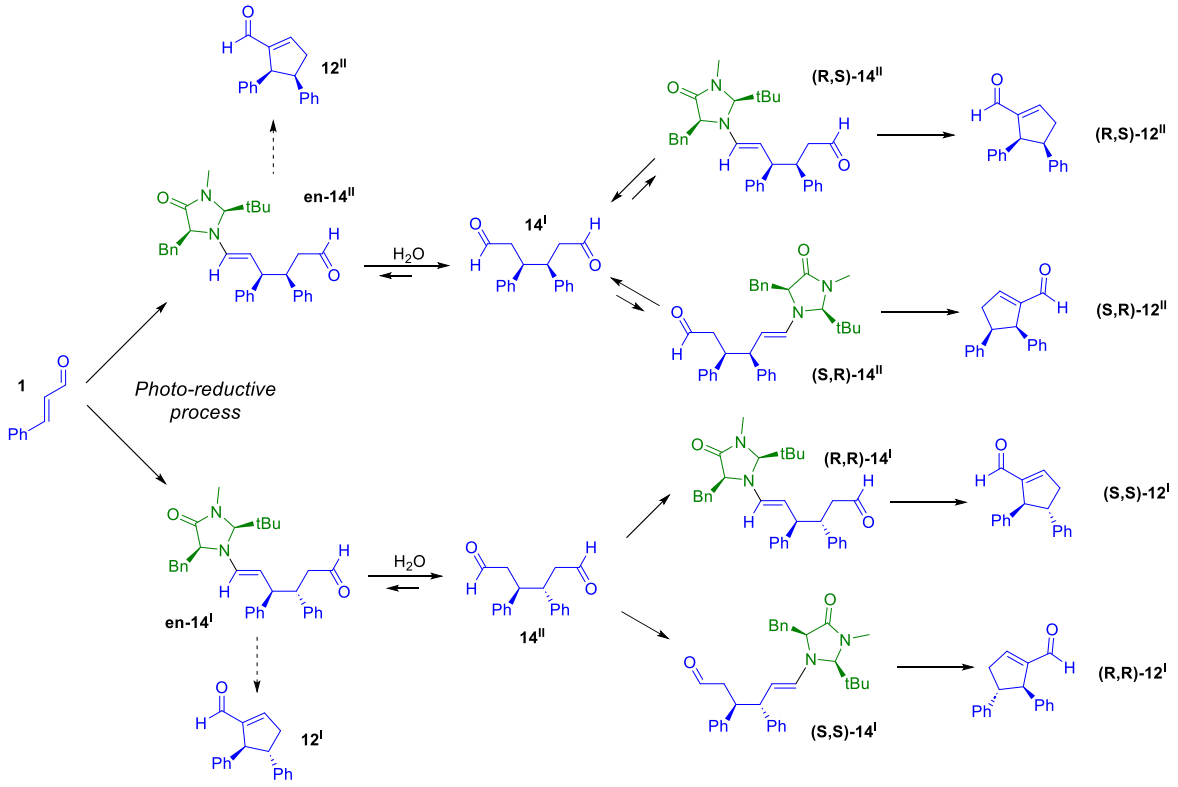

Figure 102 - Intramolecular aldol reaction to forge 12-type products

Once **1** reacts via iminium ion through photoactivation, the species **en-14^{I}** and **en-14^{II}** are then produced. If the intramolecular aldol happens (dashed arrow), the enantiomeric excess of **12^{I}** and **12^{II}** is the direct expression of the enantioselectivity in the radical-olefin bond forming event. However, if **en-14-type** intermediates are hydrolyzed to give **14^{I}** and **14^{II}**, the chirality transfer mechanism is different, with a desymmetrization process going on. Indeed, having two similar aldehydes, two different enamines can be generated (**14^{I} → (S,S)–12^{I}**, **(R,R)-12^{I}** and **14^{II} → (R,S)–12^{II}**, **(S,R)-12^{II}**). The different enamines generated from the same compound are converted into the two enantiomeric products. In other words, which enantiomer is generated depends on which side of the chain the enamine functionality is formed. Of course, this peculiar enantioenriching process is valid only for homocoupling – other products do not show this, as they would just generate different regio-isomers. Nothing excludes that both paths represented in Figure 102 operate at the same time, and the observed enantiomeric excess is the net result of both. Further efforts will be necessary to upgrade the model reaction. The future working ideas are briefly exposed in the next paragraph.

Future work

First, the oxalic acid used during the experimentation is dihydrate, as the dry form was not available in our laboratory, and water itself is the co-product of aldol

condensation. Thus, there is plus-stoichiometric water in the system, which shifts even more the equilibrium of iminium ion formation, lowering the reaction rate in general – iminium ion is essential for the photocatalytic activation.

Dry oxalic acid will thus be tested, as potentially this could raise the enantiomeric excess of the overall process, giving all information about the chirality induction mechanism itself. Moreover, having higher concentrations of iminium ions would speed up the overall reaction rate, so a lower irradiation time would be possible.

Second, the fragmentation of catalyst **9**, whatever the exact mechanism is, destroys the catalyst and lowers the yield of desired products. This could be due to the structure of **9** itself, maybe for ring constrain associated with the *syn* substituents. The relative rate of homocoupling/catalyst degradation curiously seems to be similar, at least using 0.3 equivalent of catalyst. It has to be investigated if lowering the amount of catalyst has some effect, as in that case losing a small amount of catalyst for a difficult reaction is tolerable. Moreover, the redox potential of oxalic acid, which is lower than the nitrogen mono-oxidation of proline-derived catalysts, can be exploited: using Hayashi-Jorgensen type catalysts could lead to the same results, opening new possibilities, as in that case there is no need of fluorinated catalysts anymore. In that case the catalyst decomposition rate could be low.

Third, it is important to determine which diastereoisomer corresponds to the recorded spectra. A more accurate simulation using quantum chemical calculations and/or hydrogens distance measurements will be done in order to clarify the structures.

Hetero coupling

In the meantime, the hetero coupling of different Michael acceptors with cinnamaldehyde was studied. Enones, nitroalkenes and substituted cinnamaldehyde were tested, analyzing the results simply via GC/MS, just to sample if heterocoupling is possible in these conditions. The substrates structure is represented in Figure 103, and the reaction tests are reported in Table 18.

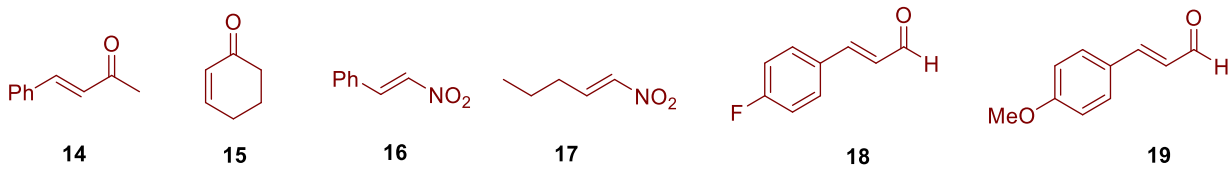

Figure 103 - Michael acceptors tested

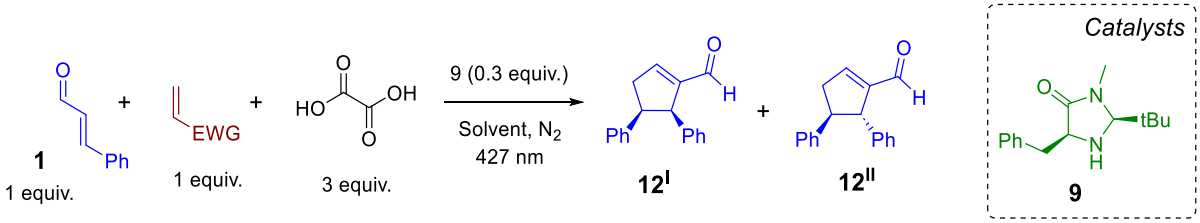

Entry	Substrates	Result[a]
1	1 + 14	12 + 13
2	1 + 15	12 + 13
3	1 + 16	No reaction
4	1 + 17	13 + other products
5	1 + 18	12 + 13 + homocoupling of 18 + heterocoupling products
6	18 + 19	No reaction

Table 18 - Heterocoupling tests

All the reaction were run in ACN with 1 equivalent of cinnamaldehyde, 1 equivalent of coupling partner and 3 equivalents of oxalic acid. Reactions were run in a Schlenk tube or a UFO vial, irradiating at 427 nm with a Kessil lamp set at maximum power. The system undergoes freeze-pump-thaw before irradiation. UFO reactor was used as photocatalytic set-up.

[a] = Results analyzed with 60 MHz NMR and GC/MS with electronic impact

Substrate **14** and substrate **15** (entry 1 and entry 2) did not react at all, and only the usual homocoupling reaction of **1** was observed. Thus, it can be concluded that in these conditions enones are not good Michael acceptors for intermolecular coupling. This is not surprising, as unsaturated aldehydes are usually more electrophilic substrates compared to enones. Substrate **16** (entry 3) shuts down completely all the reactivity, probably because of its yellow color, which inhibits the light absorption by iminium ion. Substrate **17** (entry 4) yielded not identified products by EI-MS spectrum, together with **13**. Curiously, the intramolecular aldol addition was inhibited. Further work and ESI-MS analysis are necessary to detect heterocoupling products. Reaction with **18** (entry 5) showed both homocoupling and heterocoupling products of **1** and **18**. Finally, reaction between **18** and **19** did not yield any product (entry 6).

Despite these seminal results don't seem very encouraging, they actually unveil important information. First, the fact that the incorporation of nitroalkenes as electrophilic Michael acceptors in the final products is less straightforward than expected: most of the detected product is indeed **13**.

The heterocoupling of substituted aldehydes at first sight could seem not feasible, as the presence of all the possible coupling products would be expected (homocoupling of both partners and heterocoupling in both addition and ring closure orders). However, considering the reaction mechanism theorized above, theoretically the products formation selectivity could be as follows in Figure 104:

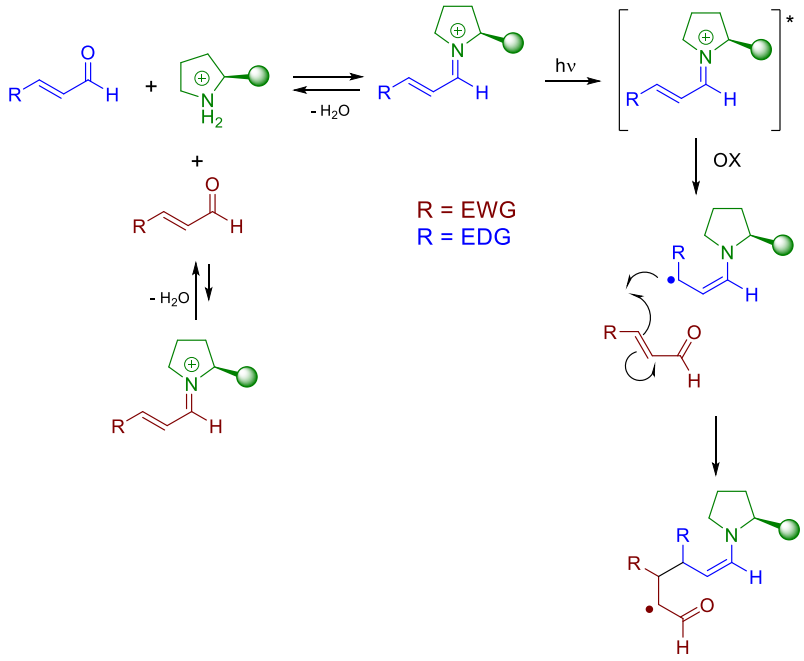

Figure 104 - Selectivity design in the heterocoupling of unsaturated aldehydes

Assuming to have different aldehydes, one with EDG group and one with EWG group, these will compete for the iminium ion formation with the organocatalyst. The EWG group stabilizes the iminium ion more, so most of the iminium ion species at the equilibrium will be derived from the electron-rich aldehyde. In this way, the photoexcitation of iminium ion will activate only the electron-rich aldehyde and the corresponding enamine radical is thus generated. The enamine radical will then react with the *second* most electrophilic species in the system, the electron-poor aldehyde. The most electrophilic species is of course iminium ion, but being very diluted, as the radical enamine, it is assumed that the meeting probability is very low, shutting down the homocoupling process. To have the best selectivity possible, it is necessary to have a great difference in both iminium ion formation equilibrium constants and electrophilicity. Also, the difference in absorption spectrum of the desired and undesired iminium ion to excite could be of great help, hampering the photoactivation of the undesired iminium ion.

The first results of heterocoupling (entry 5 and entry 6) demonstrates that at least the process is possible. Indeed, in entry 5 *both* heterocoupling products are obtained. Presumably, the difference in energy between **1** and **18** is not enough to have a preferential product, or **18** can be photoactivated too. In entry 6, **18** is not activated at all, and this means the iminium ion was formed only with **19**, which is probably not photoactive, as not being reported in literature.[7,8] Of course, this is only a proof of concept, and different aldehyde system need to be tested to further confirms these seminal results and obtain synthetically useful yields.

Future work

Some future work will be done to optimize heterocoupling reaction. First, the actual products need to be isolated and fully characterized, and the enantiomeric excess should have acceptable values. Second, different Michael acceptors must be tested in couples, to understand which substitution patterns are comparable with the reaction design shown in Figure 104. Second, the use of alkyl aldehydes will be tested: these are more electrophilic than aromatic aldehyde and their iminium ion is not photoactive – an ideal substrate for our purposes. Third, an intramolecular version of this reaction would be highly desirable, as it would forge asymmetric 5- or 6-member rings in a novel manner. Fourth, other Michael acceptors will be tested as well, such as Knoevenagel adducts derived from different malonates. These are good electrophiles, and their acidic protons ensure a regiochemically defined intramolecular nucleophilic attack (Figure 105).

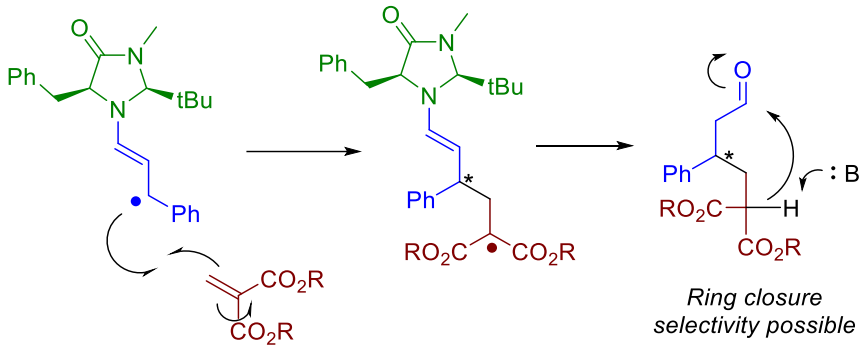

Figure 105 - Coupling of cinnamaldehyde with a Knoevenagel adduct as electrophilic olefin

Conclusions

An asymmetric organo-photocatalyzed reductive homocoupling of cinnamaldehyde was developed, starting from byproducts detected in the Danheiser annulation project. Different catalysts were tested (acridinium, Melchiorre's catalyst and MacMillan (II) catalyst), together with both DIPEA and oxalic acid as reducing agents. MacMillan (II) catalyst and oxalic acid proved to be an efficient couple, as total conversion can be achieved with a slight excess of oxalic acid. However, the seminal results show that there is competitive catalyst fragmentation mechanism. Moreover, probably the asymmetric induction event is the intramolecular aldol reaction, de-symmetrizing the open chain intermediate. Seminal tests of heterocoupling reaction were performed, achieving the heterocoupling of cinnamaldehyde and p-F-cinnamaldehyde. This is considered a good starting point, despite the reaction mixture contains all the possible combinations of coupling products between different aldehydes. Further work will be done to increase the rate of intramolecular aldol reaction, the enantiomeric

excess and to achieve clean heterocoupling reactions. This will be done both combining different unsaturated aldehydes, exploiting the iminium ion thermodynamic distribution, and both using different Michael acceptors, such as Knoevenagel adducts. These should be reactive enough to capture the elusive radical-enamine intermediate. Moreover, thanks to the acidity of malonic protons, the regiochemistry of the intramolecular Michael addition should not be an issue anymore.

Finally, the redox reaction between the oxalate anion and the iminium ion deserves some brief comment. To the best of our knowledge, the monoelectronic reduction of iminium ion to induce umpolung reactivity change in γ-position has not been reported yet. The use of oxalic acid as reducing agent is advantageous, as oxalic acid is cheap, the reaction with photoexcited iminium ion showed to be fast and the only coproduct is carbon dioxide. Moreover, the oxidation potential of oxalate is lower than proline or prolinol-derived catalysts, potentially unlocking their use in exited-iminium ion-type processes. The substitution of Melchiorre's catalyst would be highly desirable, as it requires a long and expensive synthesis.[8] Moreover, the easiness of radical enamine formation can potentially be exploited in many reactions, such as enantioselective conjugated reduction, addition to Michael acceptors in general and cross-coupling reaction via radical cross-over. We speculate that this photoredox system will be used in the future for the development of novel methodologies.

Supporting information

It follows experimental data related to the compounds characterization and the photocatalytic reductive cinnamaldehyde homocoupling with oxalic acid in the best version developed until now.

General photocatalytic conditions

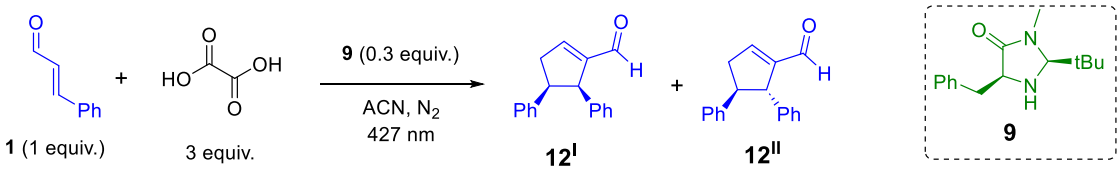

8,6 mg (0.035 mmol) of organocatalyst **9** were weighted into a Schlenk tube, followed by 44,1 mg (0.35 mmol) of oxalic acid dihydrate. Then, the Schlenk tube was put under inter atmosphere with N_2/vacuum cycles. It follows the addition of 0,5 ml of dry ACN. Then, 17 ul of cinnamaldehyde (0.12 mmol) were finally added.

The system undergoes freeze-pump thaw, then it was irradiated overnight at 427 nm using a Kessil lamp 100% power. UFO reactor used. Overnight irradiation. The reaction was then quenched with water, extracting with Et_2O to remove the catalyst. The solvent was removed under reduced pressure and the crude analyzed by HNMR and GC/MS. Assuming that all cinnamaldehyde was converted into **12** and **13**, around 65% of **12** and 35% of **13** are present by HNMR integration. The pure compounds were isolated in previous experiments. GC/MS showed a very clean reaction: only slight traces of cinnamaldehyde left, and the presence of only **12** and **13**.

The crude was separated by column chromatography over silica gel, isolating $\mathbf{12}^{I}$ and $\mathbf{12}^{II}$. Eluent 95:5 Hexane:Et_2O.

This fraction was analyzed by chiral HPLC, showing 5,5% enantiomeric excess for one compound, and 45,5% enantiomeric excess for the other.

Racemic samples preparation

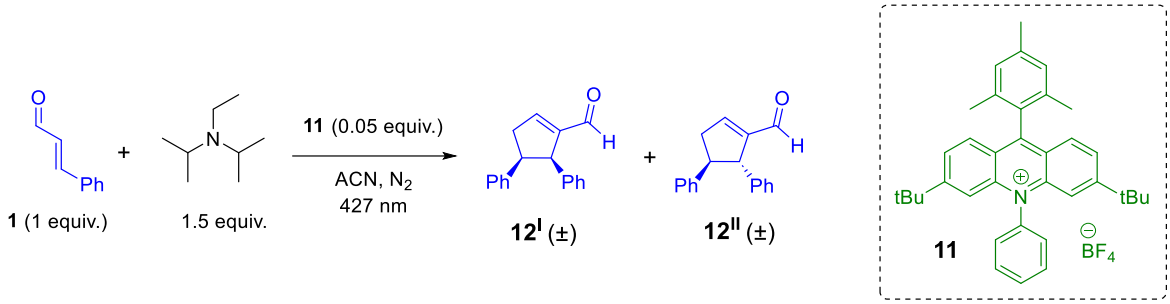

3,4 mg of photocatalyst **11** (6 µmol) were weighted into a UFO vial, then put under inter atmosphere with N_2/vacuum cycles. It follows the addition of 0,5 ml of dry ACN. Then, 15 ul (0.12 mmol) of cinnamaldehyde were added, followed by 31 ul (0.18 mmol) of DIPEA. The system undergoes FPT, then it is irradiated overnight at 390 nm using a Kessil lamp 50% power. UFO reactor used.

The reaction was then quenched with water, extracting with Et_2O to remove the catalyst and the solvent removed under reduced pressure. The crude was separated by column chromatography over silica gel, isolating $\mathbf{12}^{I}$ and $\mathbf{12}^{II}$. Eluent 95:5 Hexane:Et_2O. Both samples were checked by GC/MS to ensure their purity, and both samples were slightly polluted with the other diastereoisomer. The enantiomers were separated via chiral HPLC. Eluent 90:10 Hex:IPA, 0,5 ml/min, 30 minutes of elution. All 4 compound elute at different retention times, and cinnamaldehyde and 13 have much lower retention times. Thus, this method can be used directly to check the enantiomeric excess of a crude mixture.

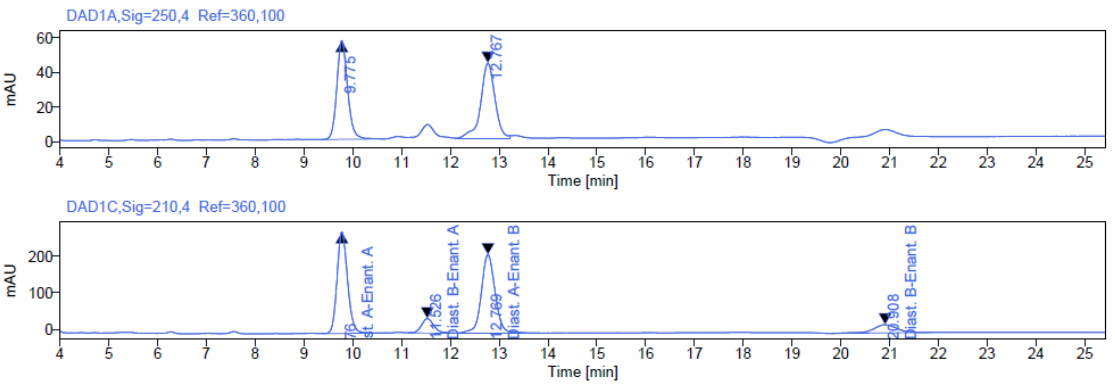

Diastereoisomer A			
Enantiomer	**Retention time**	**Area**	**Area %**
A	9.775 min	873.57	49.97
B	12.767 min	874.69	50.03

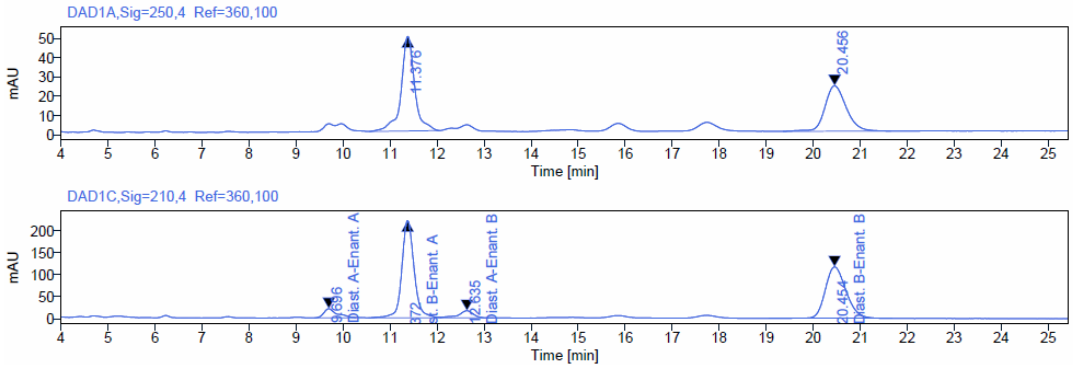

Diastereoisomer B			
Enantiomer	**Retention time**	**Area**	**Area %**
A	11.376	3988.48	52.5
B	20.456	3596.26	47.5

12^{II} - (4S,5S)-4,5-diphenylcyclopent-1-ene-1-carbaldehyde[XIV]

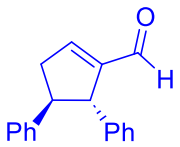

12^{II}

12^{II} – 1H NMR (600 MHz, CDCl3) δ 9.82 (s, 1H), 7.31 – 7.27 (m, 3H), 7.25 – 7.18 (m, 3H), 7.15 – 7.12 (m, 3H), 7.08 – 7.05 (m, 2H), 4.18 (dd, J = 5.6, 2.2 Hz, 1H),

[XIV] It was not possible to assign the absolute chemistry yet.

3.44 (dt, J = 8.9, 5.6 Hz, 1H), 3.26 (ddt, J = 19.7, 8.8, 2.5 Hz, 1H), 2.81 (dddd, J = 19.7, 5.7, 2.7, 1.8 Hz, 1H). The spectrum has traces of the other diastereoisomer.

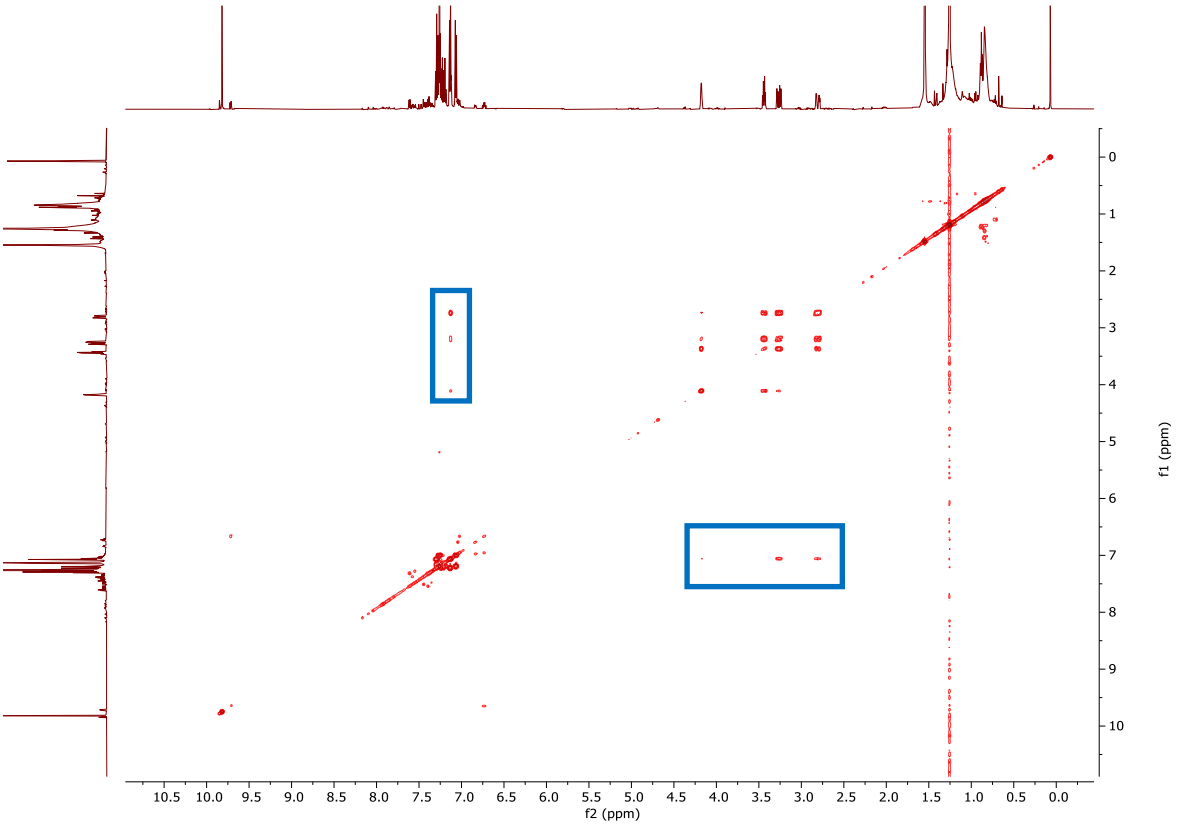

12^{II} – COSY

(4S,5R)-4,5-diphenylcyclopent-1-ene-1-carbaldehyde[XV]

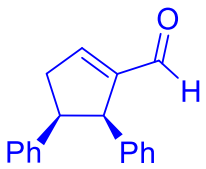

12^{I}

[XV] It was not possible to assign the absolute chemistry yet.

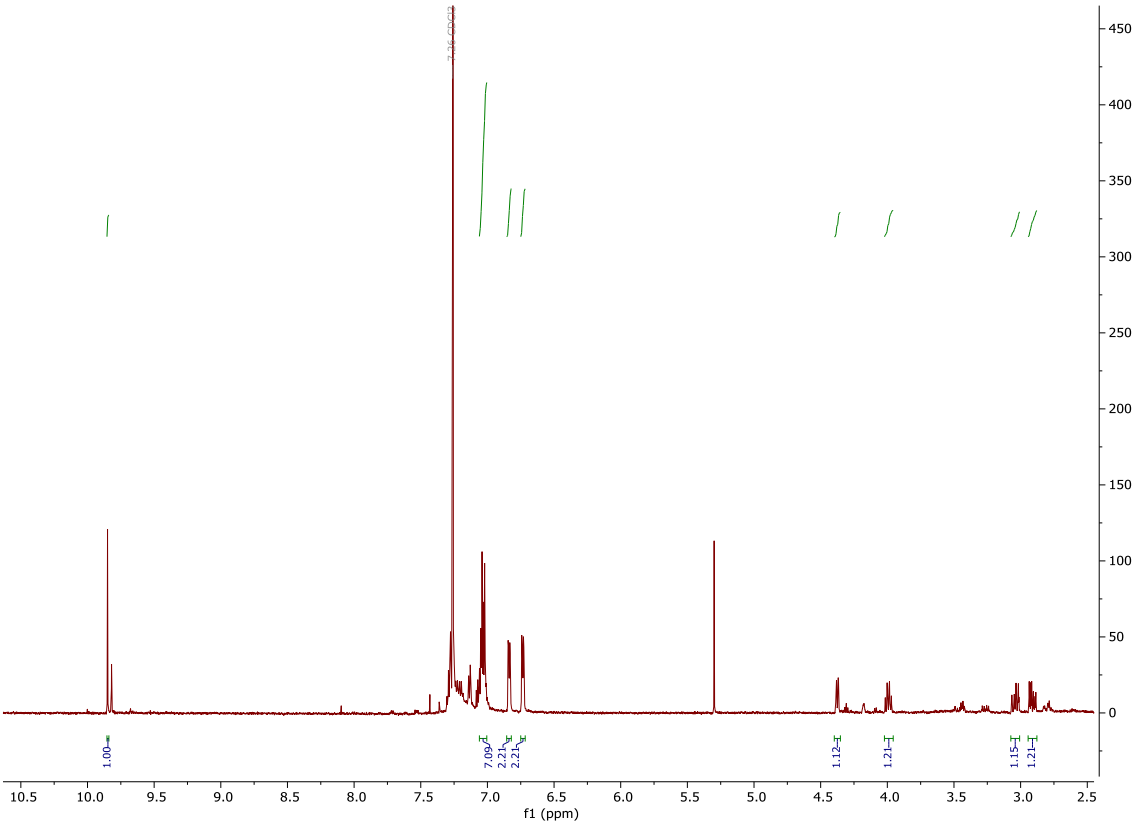

12[I] – 1H NMR (600 MHz, CDCl3) δ 9.85 (s, 1H), 7.07 – 6.99 (m, 7H), 6.84 (dd, J = 7.4, 2.2 Hz, 2H), 6.73 (dd, J = 7.3, 2.2 Hz, 2H), 4.37 (d, J = 9.3 Hz, 1H), 4.02 – 3.96 (m, 1H), 3.04 (ddt, J = 18.7, 10.7, 2.2 Hz, 1H), 2.91 (ddd, J = 18.7, 7.9, 3.1 Hz, 1H). The spectrum has traces of the other diastereoisomer.

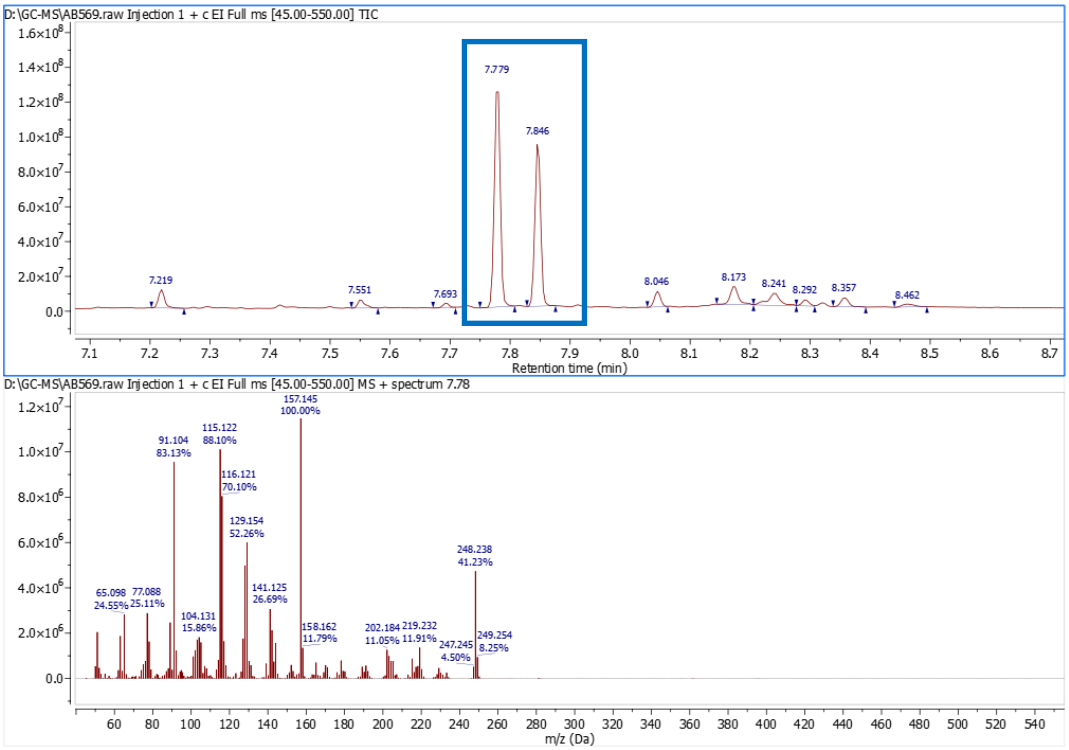

The two diastereoisomers elute at slightly different retention time (7.779 min and 7.846 min). Both have mother peak at 248.238 u, which corresponds to the exact mass of **12**^{I} and **12**^{II}.

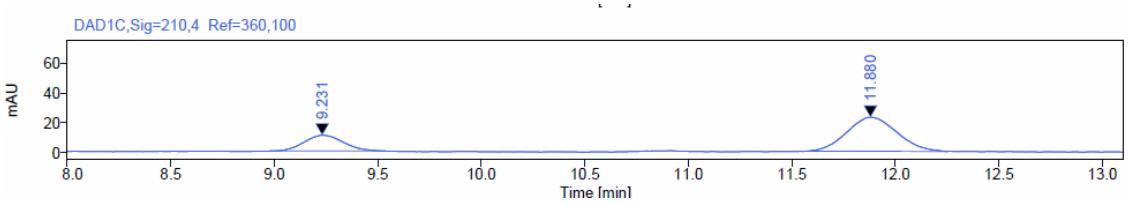

Signal: DAD1C,Sig=210,4 Ref=360,100

RT [min]	Type	Width [min]	Area	Height	Area%
9.231	MM m	0.56	139.66	10.60	26.64
11.880	MM m	0.68	384.60	22.86	73.36
		Sum	524.26		

ee = 47%

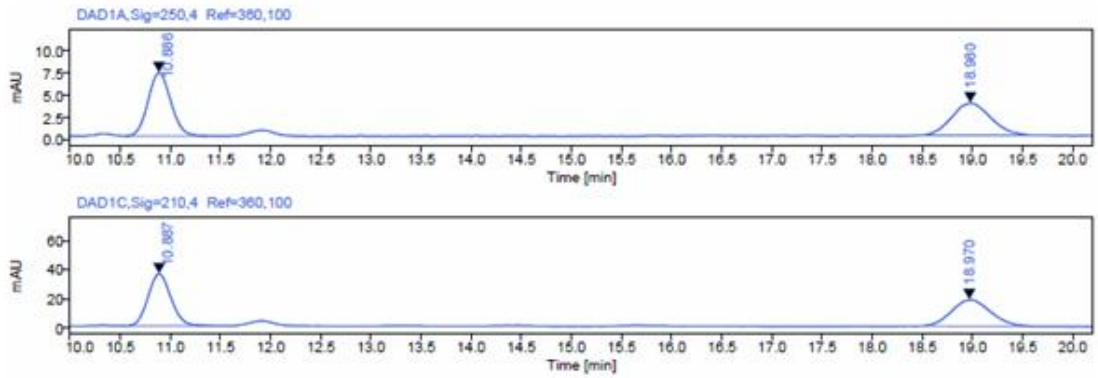

Signal: DAD1C,Sig=210,4 Ref=360,100

RT [min]	Type	Width [min]	Area	Height	Area%	Name
10.887	MM m	0.94	568.74	35.71	53.50	
18.970	MM m	1.30	494.38	18.13	46.50	
		Sum	1063.12			

ee = 6%

13 – 4,4-dimethyl-3-phenylpentanal

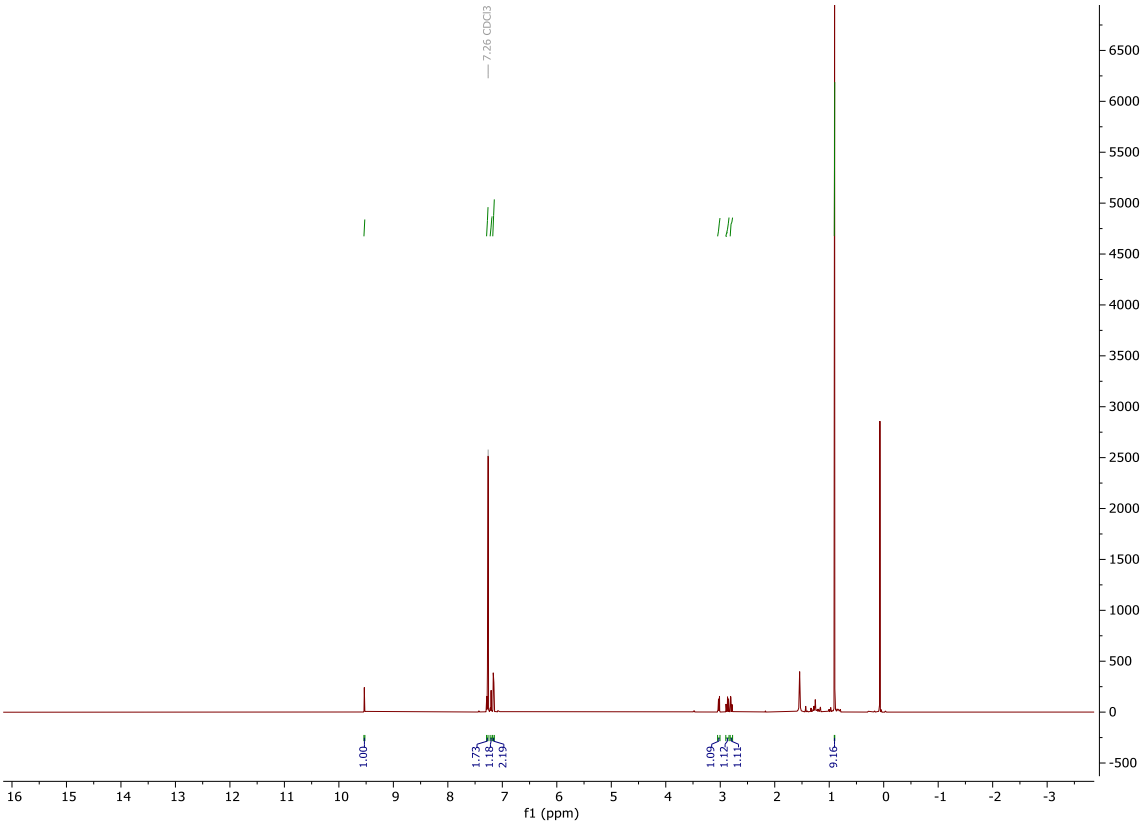

13 - 1H NMR (600 MHz, CDCl3) δ 9.53 (dd, J = 2.8, 1.7 Hz, 1H), 7.29 – 7.27 (m, 2H), 7.23 – 7.18 (m, 1H), 7.18 – 7.14 (m, 2H), 3.03 (dd, J = 10.8, 4.5 Hz, 1H), 2.87 (ddd, J = 16.5, 10.8, 2.9 Hz, 1H), 2.80 (ddd, J = 16.4, 4.6, 1.7 Hz, 1H), 0.90 (s, 9H).

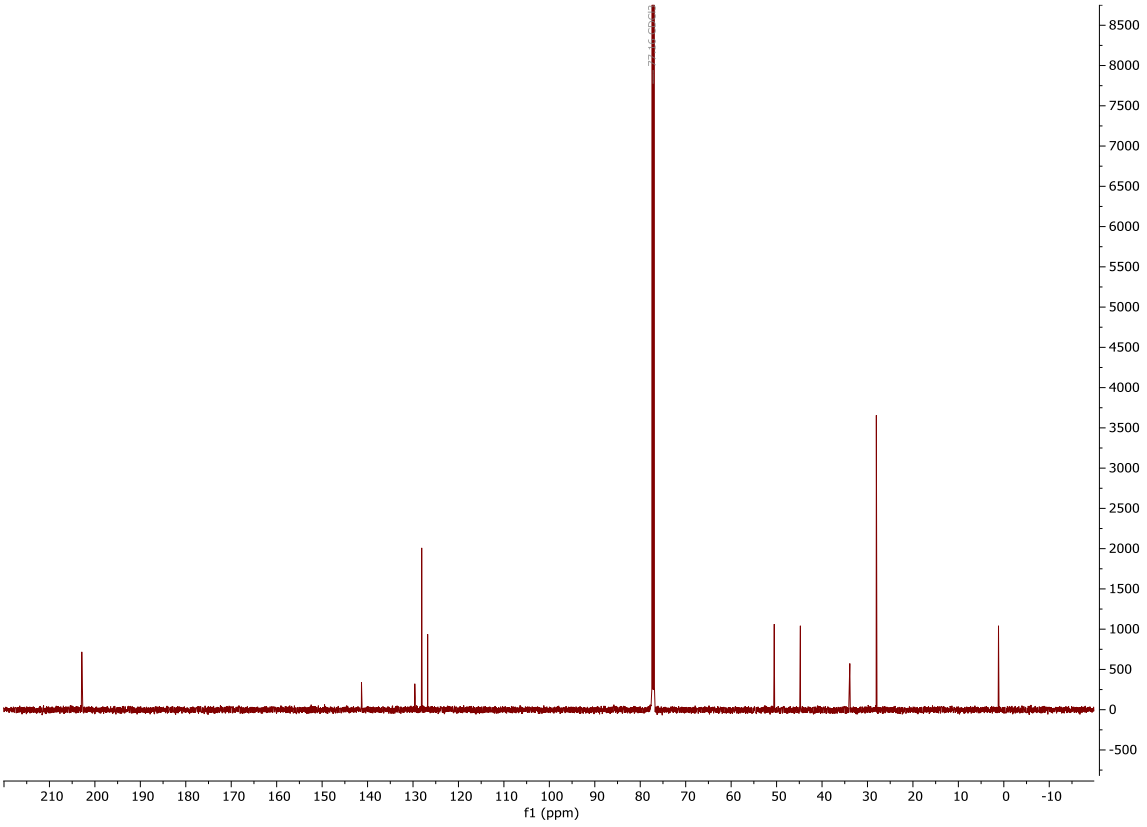

13 - 13C NMR (151 MHz, CDCl3) δ 202.88, 141.34, 129.60, 128.09, 126.78, 77.37, 77.16, 76.95, 50.51, 44.77, 33.89, 28.05.

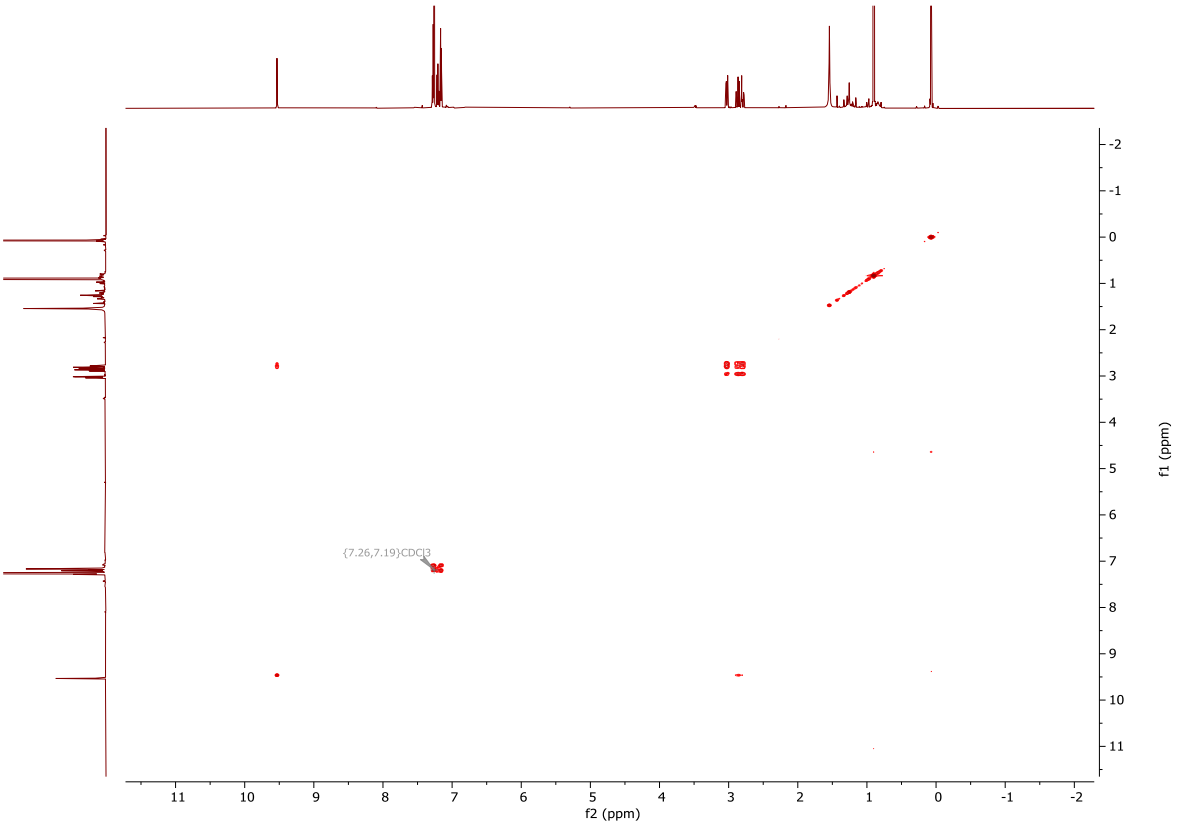

COSY

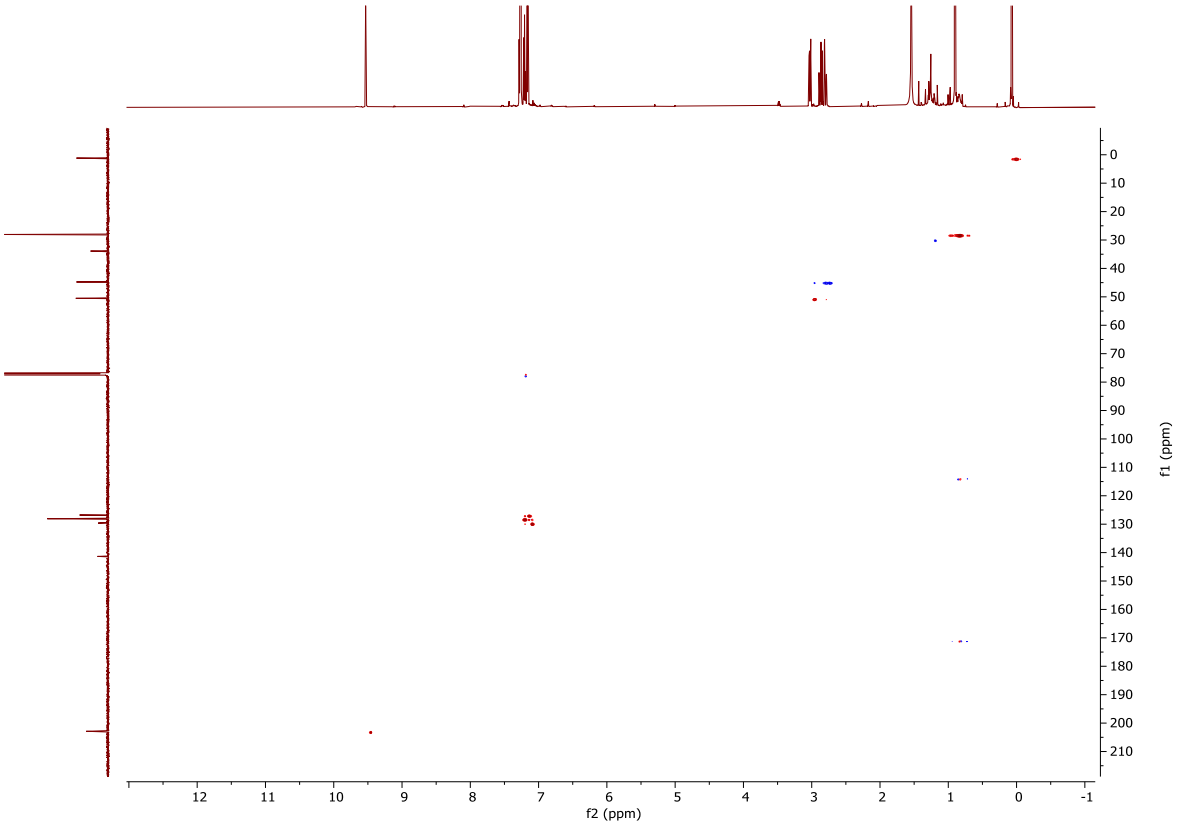

Bibliography

(1) *https://www.nmrdb.org/about/*.

(2) Ta, L.; Axelsson, A.; Bijl, J.; Haukka, M.; Sundén, H. Ionic Liquids as Precatalysts in the Highly Stereoselective Conjugate Addition of α,β-Unsaturated Aldehydes to Chalcones. *Chemistry – A European Journal* 2014, *20* (43), 13889–13893. https://doi.org/10.1002/chem.201404288.

(3) Amador, A. G.; Sherbrook, E. M.; Yoon, T. P. Enantioselective Photocatalytic [3 + 2] Cycloadditions of Aryl Cyclopropyl Ketones. *J Am Chem Soc* 2016, *138* (14), 4722–4725. https://doi.org/10.1021/jacs.6b01728.

(4) Woźniak, Ł.; Magagnano, G.; Melchiorre, P. Enantioselective Photochemical Organocascade Catalysis. *Angewandte Chemie* 2018, *130* (4), 1080–1084. https://doi.org/10.1002/ange.201711397.

(5) Masson, T. M.; Zondag, S. D. A.; Schuurmans, J. H. A.; Noël, T. Open-Source 3D Printed Reactors for Reproducible Batch and Continuous-Flow Photon-Induced Chemistry: Design and Characterization. *React Chem Eng* 2024, *9* (8), 2218–2225. https://doi.org/10.1039/D4RE00081A.

(6) Silvi, M.; Verrier, C.; Rey, Y. P.; Buzzetti, L.; Melchiorre, P. Visible-Light Excitation of Iminium Ions Enables the Enantioselective Catalytic β-Alkylation of Enals. *Nat Chem* 2017, *9* (9), 868–873. https://doi.org/10.1038/nchem.2748.

Chapter 5 – Divergent total synthesis of polycyclic norcembranoid diterpenes

Introduction

The C_{19} norcembranoid and C_{20} cembranoid diterpenoids represent a rare and intriguing class of natural products found in both terrestrial and marine environments, particularly in the soft corals of *Sinularia* genus (Figure 106). The complex, highly oxygenated and caged polycyclic structures of norcembranoid diterpenes have captured the interest of the synthesis community., What makes these compounds even more interesting is their wide array of promising bioactivities and the fact their mechanism of action is or unknown to date.[1,2] Some examples include Bielschowskysin, a cytotoxic cyclobutanoid highly active against EKVX non-small cell lung cancer,[3] the mildly cytotoxic Intricarene[4] and Rameswaralide.[5] Moreover, many furano-butenolides found in the same soft corals show interesting biological activity. These furano-butenolides are probably the biological precursors of C_{19} norcembranoid and C_{20} cembranoid diterpenoids.[1]

Figure 106 - Sinularia Flexibilis - one example of Sinularia coral

The discovery of this natural product family dates back to 1995, with the isolation of Dissectolide from *S. Maxima*, from the coast of India (Figure 107).[6] The molecule contains a peculiar structure of 5-, 6-, and 7-membered carbocyclic rings linked to a 5-ring lactone.

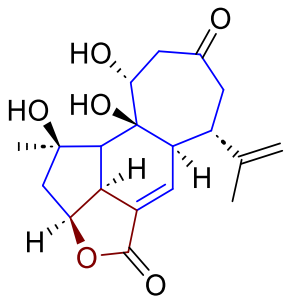

Figure 107 - Dissectolide structure

Yonarolide was isolated also from *Sinularia* species in Okinawa in the same year.[7] Ineleganolide was isolated in 1999 from corals of *S. Inelegans* sited in Taiwain.[8] The structure of this diterpene was determined by X-ray crystallography. The poly-oxygenated condensed tetra-cycle is also present here, but with the 6- and 7-memebered ring swapped, with the addition of one more 5-membered oxygenated bridge-ring. Scabrolide-A and Scabrolide-B were then isolated from the Taiwanese coral *S. Scabria* in 2002.[9] Also Dissectolide and Ineleganolide were detected in the same species. Lastly, Sinulochmodin C was isolated from the soft coral *S. Lochmodes* in 2005.[10] Sinulochmodin C shows a similar tetracyclic framework with an oxygenated 5-memebered bridge-ring as Ineleganolide.

During my visiting period at the University of Texas at Dallas I worked in the laboratory of Professor F. Romiti. The main research interest of Romiti's group is the total synthesis of naturally occurring and bioactive compounds, using innovative strategies and methodologies. I was involved in the total synthesis of norcembranoid diterpenes family, leveraging a common mid-stage intermediate.

It follows an overview of the different strategies developed in the synthetic community until august 2025. Only the fundamental skeletal-forging reactions are illustrated.

Reported synthetic approaches

Despite the first member of the polycyclic norcembranoid diterpenes was isolated in 1995, it was not until 2006 that a member of the family, Intricarene (Figure 108), succumbed to total synthesis, using a [5+2] cycloaddition strategy.[11,12]

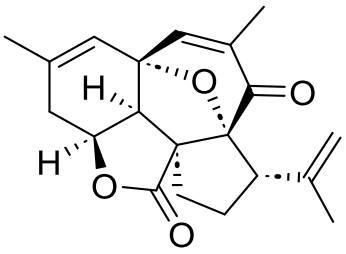

Figure 108 - Intricarene

However, the condensed polycyclic system is different from the rest of the family members we're interested in (Figure 125).

Over the years, there have been extensive efforts to synthesize other members of the family with the Dissectolide core structure[1]. The first total synthesis of Scabrolide A was finally achieved in 2020 by the group of Stoltz.[13] In the space of a few years, many other strategies were outlined: Wood in 2022[14] (synthesis of

Ineleganolide and Sinulochmodin C), Fürstner 2022[15] (Scabrolide A and nominal Scabrolide B), Stoltz in 2023[16] (Ineleganolide), Sarlah in 2023 (Scabrolide A and Yonarolide)[17] and 2024[18] (Scabrolide B, Ineleganolide, and other norcembranoids), Fürstner in 2024[19] (Scabrolide B correct structure, Sinulochmodin C, Ineleganolide and Horiolide), Hu and Hong in 2024[20] (Scabrolide A and Havellockate) and Zhang[21] in 2024 (Sinulochmodin C). Moreover, in 2022, Romo reported the first total synthesis of Rameswaralide,[22] another related member of the polycyclic norcembranoid diterpenes.

Stoltz's strategy for Scabrolide A

The synthesis strategy adopted by Stolz for Scabrolide A[13] starts from the chiral pool and the preparation of intermediates **6** and **7**, obtained in a few steps from (*R*)-linalool and (*R*)-carvone, respectively (Figure 109).

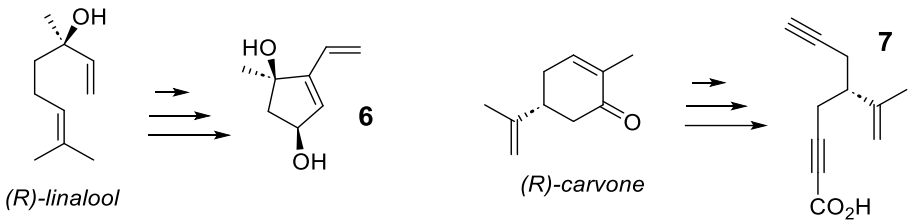

Figure 109 - Synthesis of 6 and 7

The 5-membered carbocycle is synthesized following a streamlined procedure reported by Maimone,[23] which involves RCM of (*R*)-linalool followed by allylic oxidation as fundamental ring-forming steps. **7** is obtained from (R)-carvone via oxidation, ring opening and alkynylation sequence. Then, **6** and **7** are condensed together yielding the reactive ester **16**. The 5-membered lactone ring and the 6-membered carbocyclic ring are then forged simultaneously by an intramolecular thermal Diels-Alder reaction, yielding **17** (Figure 110).

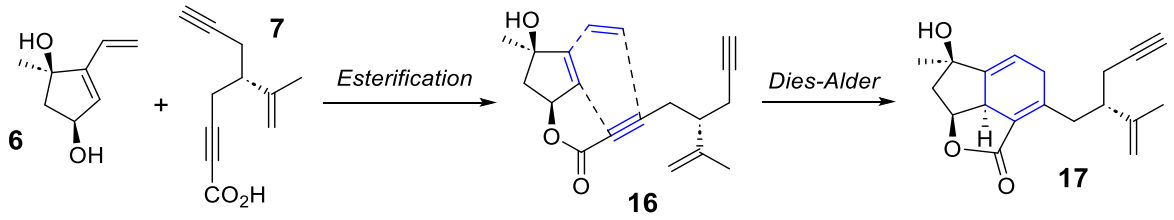

Figure 110 - Esterification and Diels-Alder reaction

Intermediate **17** undergoes further synthetic elaboration until a [2+2] reaction forges the strained cyclobutene structure **24** from diene **21**. The silicon atom is important as the Tamao-Fleming oxidation installs the required oxygen atom in the appropriate position. Intermediate **4a** undergoes an oxidative rearrangement-

elimination sequence. The ring-expansion forges the desired cycloheptanone ring, yielding the final product (Figure 111).

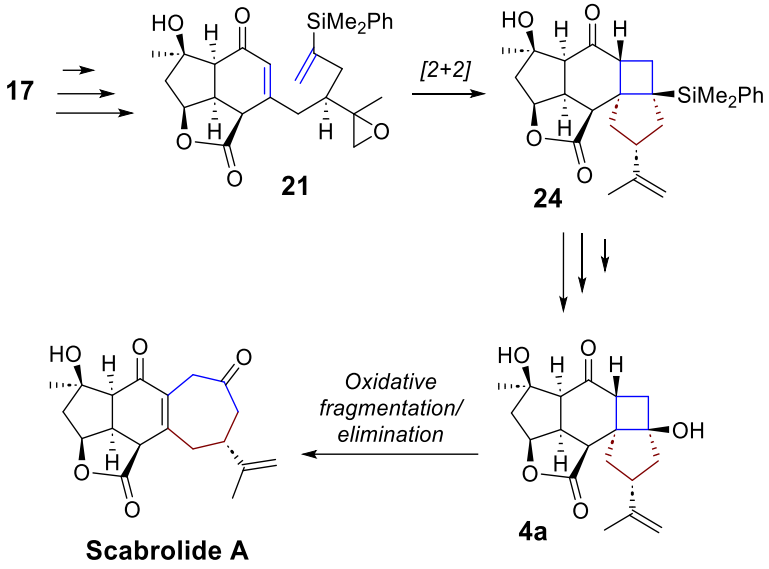

Figure 111 - Cycloheptanone ring formation main steps

Sarlah's strategy for Scabrolide A and Yanorolide

The Sarlah's approach for the synthesis of Scabrolide A and Yanorolide[17] is a convergent synthesis. As Stoltz, two different building blocks from the chiral pool are used for the synthesis and merged together in the late stages. The cycloheptanone ring structure (**7**) is forged enantioselectively from (S)-perillyl alcohol in 2 steps. The 5-memebered carbocycle **6**, also known as "Maimone's ketone" is synthesized from (S)-linalool in two steps[23] (Figure 112).

Figure 112 - Synthesis of 6 and 7

Then, the lactone ring contained in **12**[l] was synthesized by direct annulation of **6** with vinylcyclopropane, oxidative opening, reduction and intramolecular esterification (Figure 113).

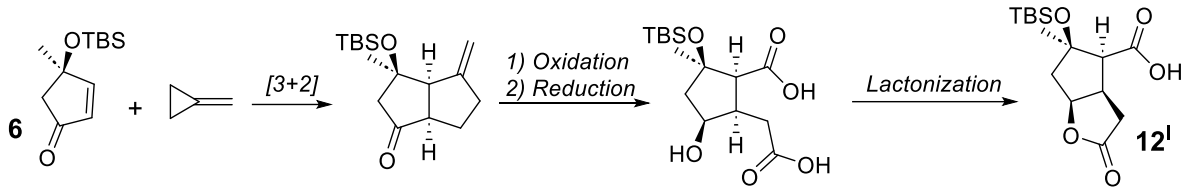

Figure 113 - Synthesis of intermediate 12^{I}

The 6-membered ring was made in 2 additional steps: **15**, prepared from **7**, was coupled with **13**, synthesiszed from **12^{I}**, through a Liebeskind–Srogl cross-coupling reaction yielding **16**. The ring was then closed via an intramolecular Michael addition of enolate-elimination sequence, yielding **3** (*Figure 114*).

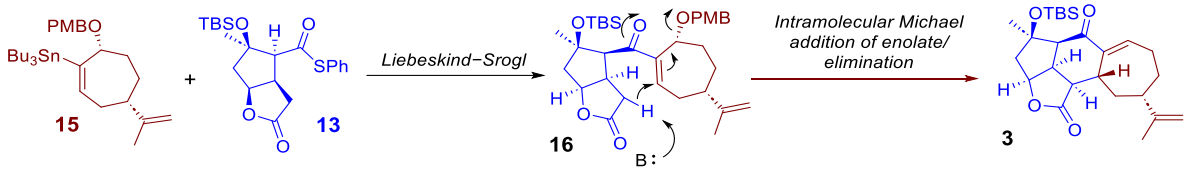

Figure 114 - Synthesis of 3

The final products were obtained after a few more steps mainly entailing oxidation state adjustments.

Fürstner's strategy for Scabrolide A

Fürstner's strategy for the synthesis of Scabrolide A[15] is somewhat similar to Sarlah's approach in the initial stages, but requires a higher number of chemical transformations to conclude the synthesis. First, the 5-membered carbocyclic ring **15** is Maimone's ketone made from *(R)-linalool* (**15**). The 7-membered ring **9** is made by Tiffeneau-Demjanov cyclo-expansion of (*R*)-carvone (Figure 115).

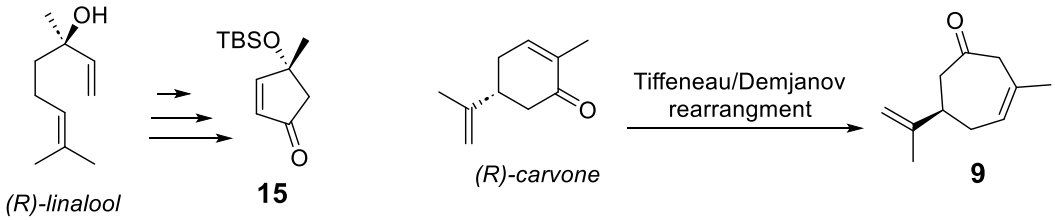

Figure 115 - Synthesis of 15 and 9

The lactone ring, contained in intermediate **17** was built from **15** by a sequence concerning cycloaddition, oxidative cleavage and intramolecular oxidative lactonization (Figure 116).

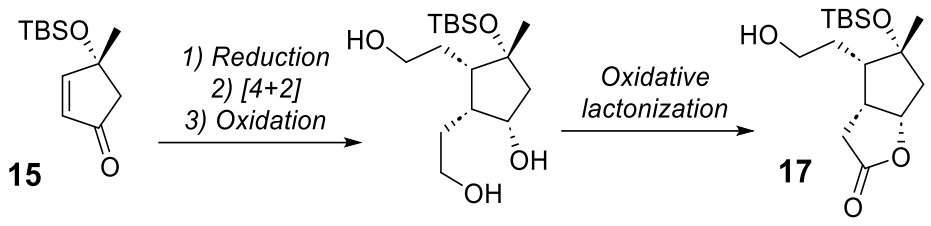

Figure 116 - Synthesis of 17

9 and **17** are further elaborated and merged together to form intermediate ylide **24**, which undergoes a [3+2] sigmatropic rearrangement, forging the first bond to make the 6-membered cycle. Base-promoted equilibration and de-sulphuration yield **28**. Finally, the 6-membered ring was formed by RCM generating **29** (Figure 117).

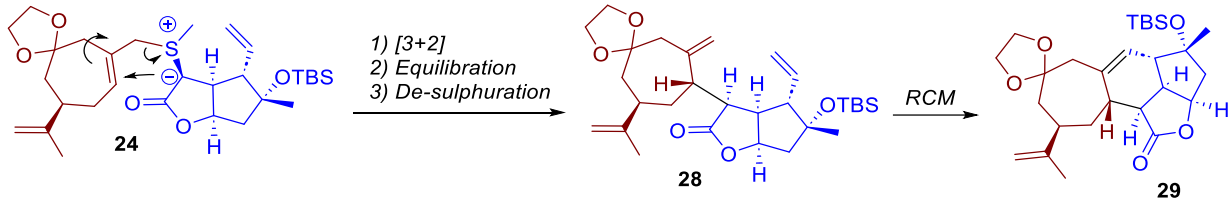

Figure 117 - Synthesis of 28 and 29

Further oxidation of **29** and global deprotection afforded Scabrolide A.

Wood's strategy for Ineleganolide and Sinlochmodin C

Wood's strategy for the synthesis of Ineleganolide[14] starts from Maimone's ketone too, which is decorated with the furane ring, a key player in the endgame (**17**). The lactone ring is forged by Ueno-Stork/lactol oxidation sequence delivering **12** (Figure 118).

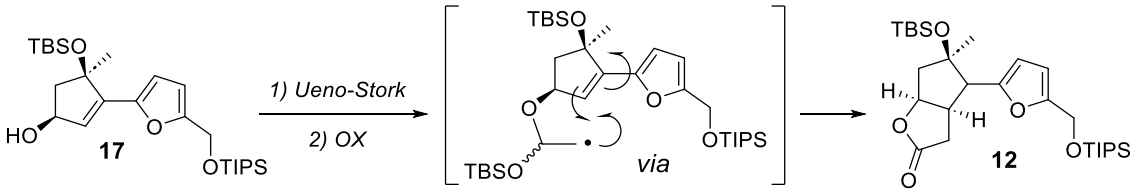

Figure 118 - Synthesis of 12

The intricate 6,7-condensed ring system featuring the oxo-bridge is forged in a biomimetic way: first, a 12-membered ring featuring the furane unit is generated by Nozaki-Hiyama-Kishi macrocyclization reaction (**28a** to **29** - Figure 119).

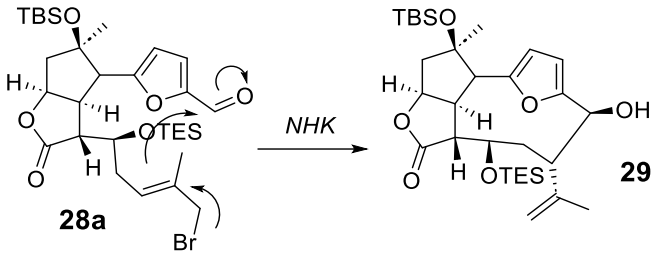

Figure 119 - Intermediate 29 synthesis

Then, **42** undergoes a [4+2] cycloaddition between the furane ring and singlet O_2 followed by ring opening and intramolecular oxa-Michael reaction to yield **9**. Finally, treatment with LiHMDS triggers an intramolecular Michael addition that installs the 6 and 7-membered ring simultaneously and delivering Sinulochmodin C and Ineleganolide (Figure 120).

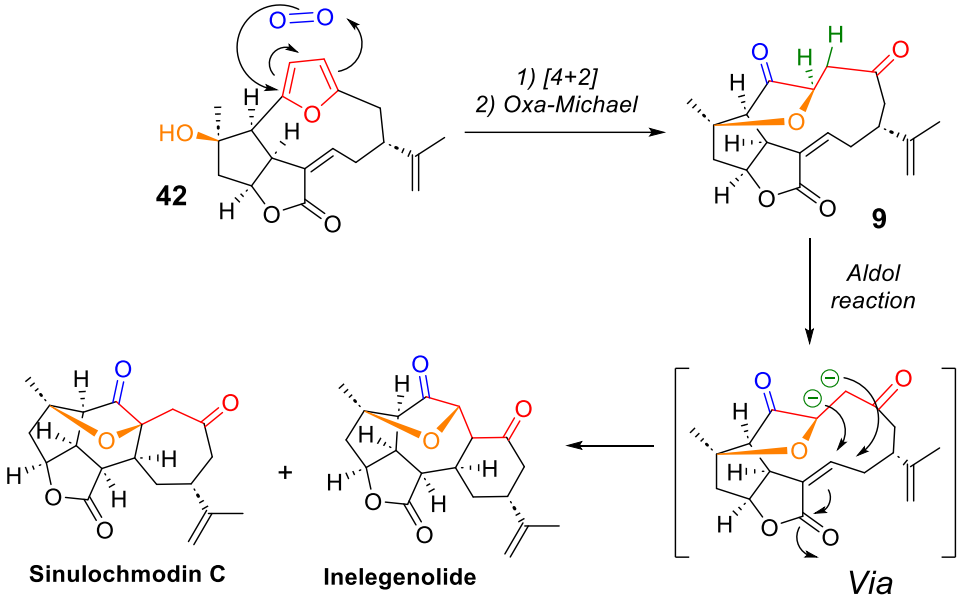

Figure 120 - Sinuochmodin C and Ineleganolide synthesis

Fürstner's strategy for Scabrolide B, Sinuscalide C, Ineleganolide and Horiolide

With the aid of DFT calculations, Fürstner's and co-workers re-assigned the structure of Scabrolide B [19], which was also confirm by X-ray crystallography.[24] Scabrolide B has the 6 and 7-membered ring "exchanged" compared to Scabrolide A, so a different strategy was devised. First, the 6-membered ring is synthesized starting from cyclohexenone in 3 steps by Rh-catalyzed enantioselective prenylation and Segusa-Ito oxidation, while the 5,5-membered ring condensed system (**22**) is prepared from Maimone's ketone as previously reported by the same group[15] (Figure 121).

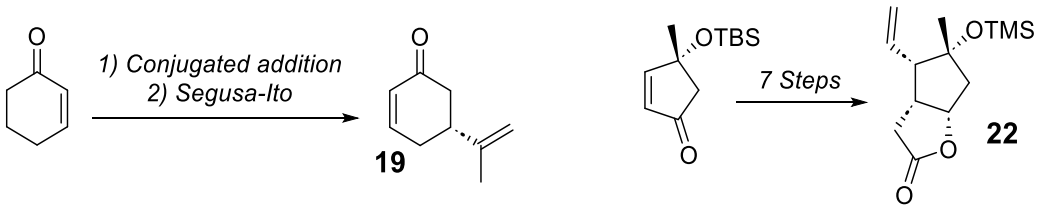

Figure 121 - 19 and 22 synthesis

The 7-membered ring was then forged in two steps by lanthanum(III) triflate catalyzed Mukayama-Michael reaction (**25**) followed by intramolecular enolate cross coupling reaction promoted by a Pd-based complex (**28** - Figure 122).

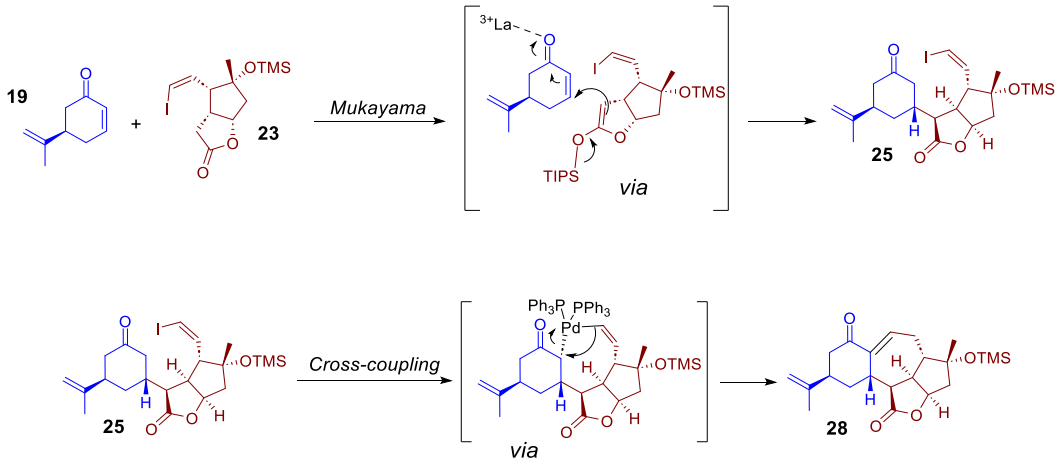

Figure 122 - Intermediate 28 synthesis

Scabrolide B was obtained after further synthetic elaboration. Finally, similarly to Wood's strategy, Ineleganolide was obtained by intramolecular oxa-Michael addition and isomerization. They showed that Horiolide could be obtained from Ineleganolide by a sequence entailing retro-Michael, retro-aldol and Micheal addition reaction (Figure 123).

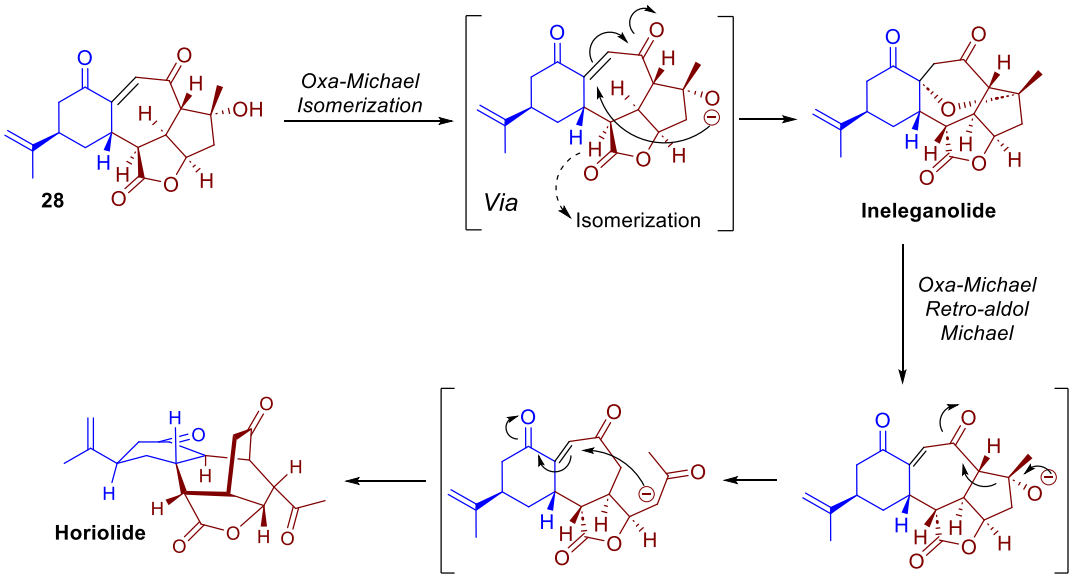

Figure 123 - Ineleganolide and Horiolide synthesis

Zhang strategy for Sinulochmodin C

Zhang's strategy[21] exploits a commercially available enantiopure compound as 5-membered carbocycle moiety. The 7-membered ring derives from commercially available cycloheptenone. **10** (derived from the cyclopentane), and **17**, prepared from cycloheptenone, are linked by the addition of the organolithium species derived from **10** to the aldehyde functionality and oxidation, to obtain intermediate **18c**, which undergoes esterification with malonate to obtain **19**. Finally, double Michael addition of the malonate unit onto the dienone system simultaneously builds the 5-membered lactone and 6-membered ring (Figure 124).

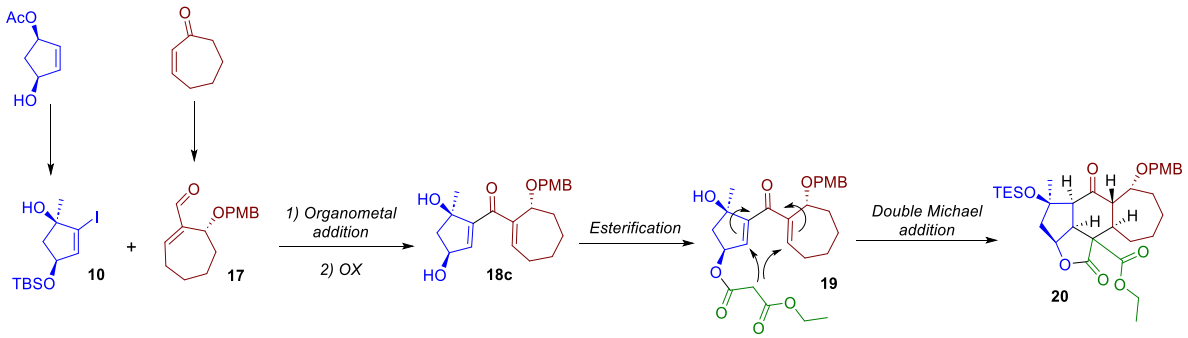

Figure 124 - Synthesis of intermediate 20

Further synthetic elaboration yields Sinulochmodin C.

Our synthetic plan

The idea at the core of our strategy is that most of the norcembranoid diterpenes family members share a common skeletal motif, as shown in Figure 125.

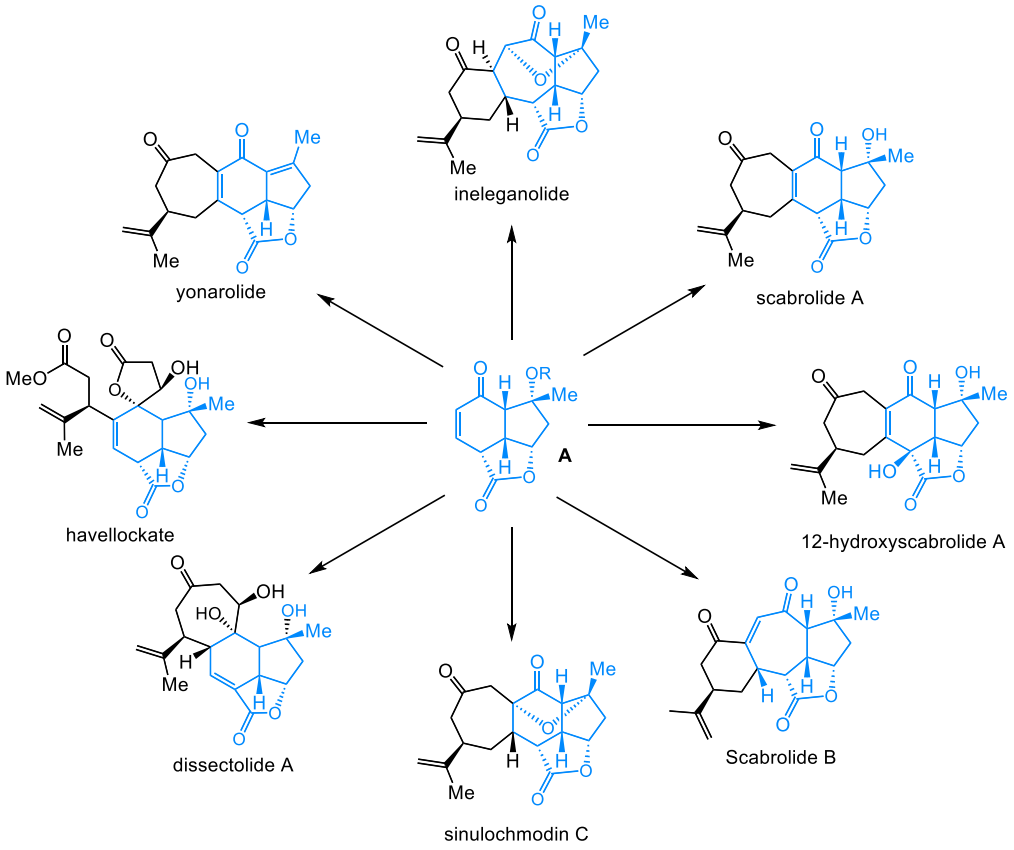

Figure 125 - Norcembranoid diterpenes common skeletal motif

Our initial goal was the efficient and scalable synthesis of structure of type **A,** we identified as the common mid-stage intermediatefeaturing the 5- and 6-membered carbon rings as well as the 5-membered lactone. Once **A** is made, the synthesis paths *diverge*. In particular, the 7-membered ring of Sinulochmodin C, Scabrolide A and Scabrolide B, Yanarolide, 12-hydroxyscabrolide and Dissectolide A can be synthesized with the same strategy yielding 6 natural products. Ineleganolide and Scabrolide B have a similar ring system, but the 6- and 7- membered rings are swapped – in this case a ring expansion followed by the last 6-membered ring is needed. Lastly, Havellockate needs a separate late-stage synthesis strategy.

This approach, if realized in a concise and efficient manner, can guarantee fast access to all norcembranoid diterpenes family in meaningful quantities for detailed biological investigations.

The efficient and succinct synthesis of intermediate **A** is the first step towards the realization of an ambitious natural products cascade synthesis plan.All the

experimental work described in this chapter focused on the synthesis of **A**, so only a brief overview of the general synthesis strategies followed by the group is provided.

Radical cascade

Our first approach involved the preparation of the 5-membered carbocyclic ring using established protocols, then forging the lactone and the 6-membered ring through a radical cascade. The envision radical cascades can involve a wide array of functional groups, both as radical initiators and reactive groups, chosen according to the radical-philicity rules. A general representation of the approach is shown in Figure 126.

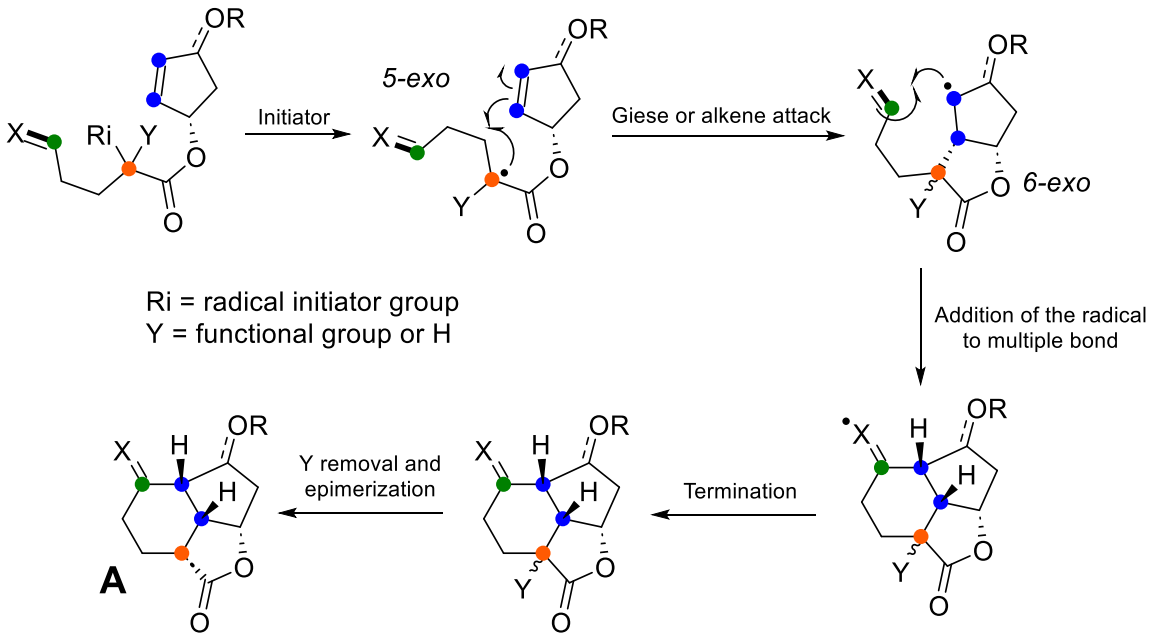

Figure 126 - Radical cascade approach to A

The stereoselectivity of the attack would be induced by the O-bound chiral center, which in our plans forces a *syn* attack on the 5-membered ring. Importantly, "Y" can correspond to different structures, able to trigger radical formation and tune the radical reactivity. "Y" is a hydrogen atom in the final product, so it must be removed as an additional step. Importantly, while the formation of the chiral centers on the 5-membered carbocycle (blue carbons) is locked by conformation, the other stereogenic center originating from the attack (orange) is not so well defined, as it depends on the approach of the radical. However, it is reported that the epimerization of this center favors the desired product, so we did not pay attention to the stereochemistry of that stereogenic carbon center in our design.

Diels-Alder

Our second approach relied on a Diels-Alder reaction on the same cyclopenten(on)e moiety. Different dienes and dienophiles, as well as catalysts were explored. Moreover, both intermolecular and intramolecular reaction, as well as substrate- or catalyst-controlled stereoselectivity were tested (Figure 127).

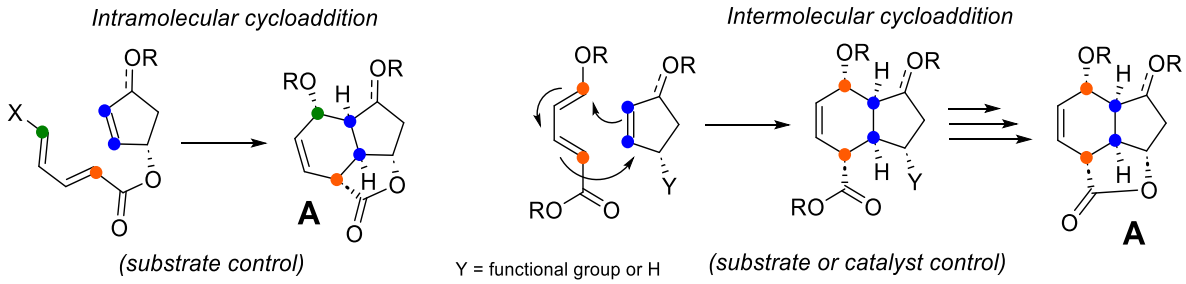

Figure 127 - Diels-Alder approach to A

As for radicals, in the case of intramolecular Diels-Alder reaction, the stereochemical outcome is controlled by the already existing stereocenters. In the case of intermolecular reaction, both catalyst control and substrate control are viable options. The former can be induced using an enantioenriched catalyst, while the latter is induced by the presence of a substituent “Y” in the structure. In case intermolecular cycloaddition is used, the closure of the lactone ring in a separate step should be considered. Depending on the nature of group “Y”, it can be realized with different chemistry: C-H activation, esterification, or oxa-Michael addition.

Michael addition-aldol condensation

An alternative strategy, albeit less direct, entails the intermolecular Michael addition reaction between a cyclopentenone and a malonate unit followed by intramolecular aldol condensation and intermolecular oxa-Michael addition on cyclopentenone or an oxygenated derivative (Figure 128).

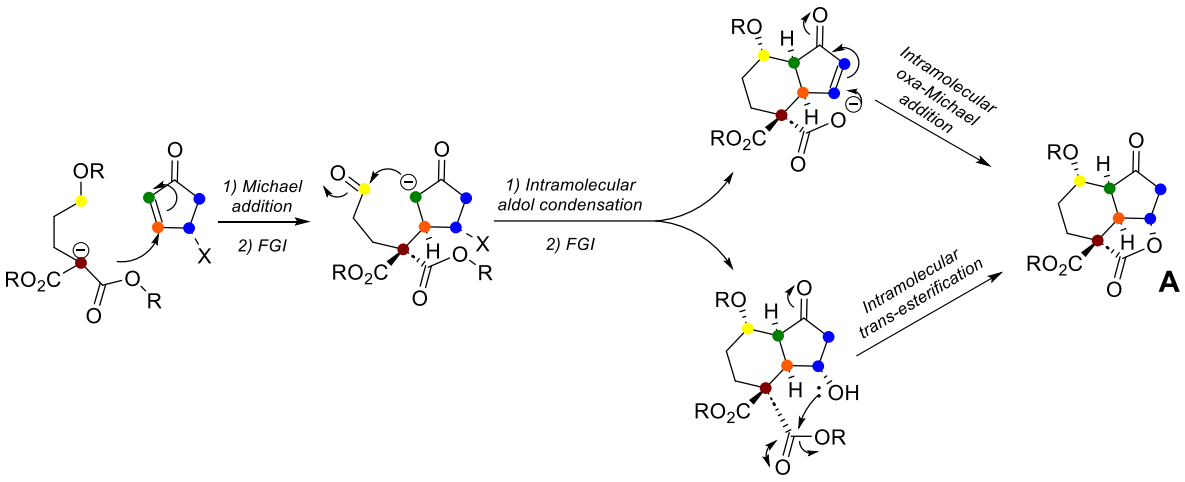

Figure 128 – Michal addition-aldol condensation approach to A

The chiral center is installed by enantioselective catalysis using cyclopentenone as Michael acceptor. An intramolecular aldol condensation was envisioned to close the 6-membered ring. Finally, the lactone can be forged either by intramolecular oxa-Michael addition exploiting the carboxylate moiety, or by intramolecular trans-esterification. Luckily, Reisman and co-workers outlined the enantioselective Michal addition – aldol reaction sequence [25,26]. Thus, we were able to synthesize the required intermediate in an enantioselctive fashion and test some synthetic elaboration.

Experimental

The next section described the main experimental results I have obtained. For every strategy, different structures, functional groups and methodologies have also been investigated by A. Lanzirotta (PhD Student) and N. Chandra (Postdocs). Their experimental activity is not reported in the experimental results.

Radical cyclization

The first strategy I explored relied on an intramolecular radical cyclization. The 5-membered carbocyclic ring was synthesized following the 2-steps protocol from linalool as outlined by Maimone[23] (Figure 129).

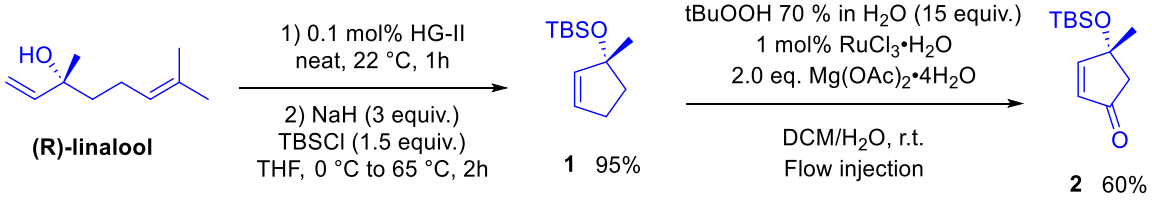

Figure 129 – Synthesis of 2

Starting from (*R*)-linalool, a feedstock chemical extracted from plants, the 5-membered ring was generated by alkene metathesis using Hoveyda-Grubbs second generation complex (HG-II) as the catalyst. The tertiary alcohol is protected as tert-butyl-dimethylsilyl ether to give **1** in 95% yield. Then, **1** undergoes ruthenium tetroxide catalyzed allylic oxidation in the presence of *tert*-butyl hydroperoxide as the oxidant to deliver **2** in 60 % yield. The allylic oxidation step is very sensitive to reaction conditions. Curiously, we observed that along with the quality of the tBuOOH, vigorous stirring was crucial to break the emulsion and ensure a successful outcome. A small deviation from these optimal conditions caused a dramatic decrease in the yield (*i.e.*, down to 25 % in certain cases). Enone **2** was then converted to alcohol **3** by reduction of the ketone unit with lithium aluminum hydride in the presence of LiI as the additive (Figure 130).

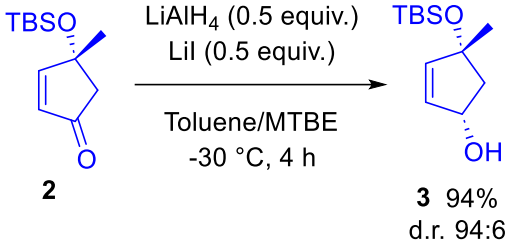

Figure 130 – Synthesis of 3

These peculiar conditions were adopted as more efficient alternative to the classical Luche reduction of enones,[27] which led to a d.r. 10:1 and a lower yield compared to literature report in our hands, despite performing the reaction at – 80 °C.[20] The low yield is probably due to substrate polymerization, as cyclopentenones are known to easily polymerize in the presence of Lewis acids. The use of lithium iodide in 1:1 ratio with lithium aluminum hydride probably forms another aluminum-based species – structure not investigated to date – which favors *syn* reduction of β-hydroxy-ketones silyl ethers.[28,29]

The sidechain of the molecule was synthesized starting from the commercially availableethyl 4-bromobutanoate by displacement of the bromide with cyanide (**4**) and subsequent saponification with sodium hydroxide, to yield carboxylic acid **5** in 99% yield over 2 steps.

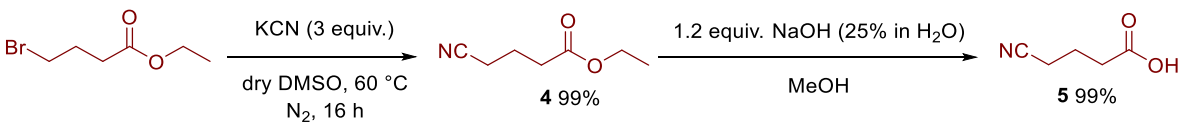

Figure 131 - Synthesis of fragment 5

Then, the carboxylic acid **5** undergoes esterification with **3** to yield fragment **6** in 69% yield. HATU was used as the coupling agent (Figure 132) as the use of DIC

delivered the product in low yield, while reacting the corresponding acyl chloride of **5** with the alcohol resulting in no reaction at all.

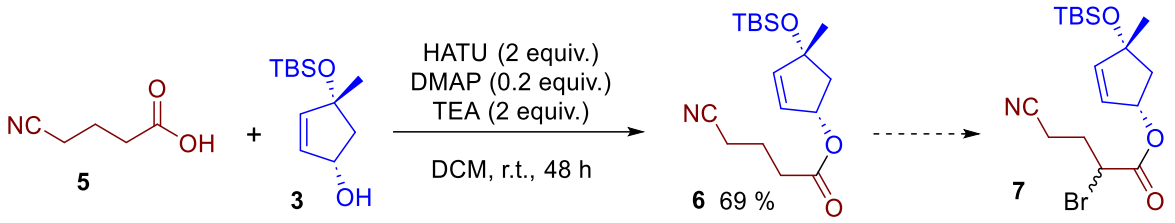

Figure 132 - Synthesis of fragments 6 and 7

However, despite our efforts, we could not install the required bromide α to the ester unit of **6** to obtain **7**. Bromination via enolate formation and via silyl enol ether were attempted, using both NBS and Br_2 as brominating agents.

The idea behind this synthetic sequence was to trigger the radical formation from the alkyl bromide using tributyltin hydride. Despite not being very common, the use of nitril group is strategical, as it would yield immediately ketone **8** (Figure 133).[30]

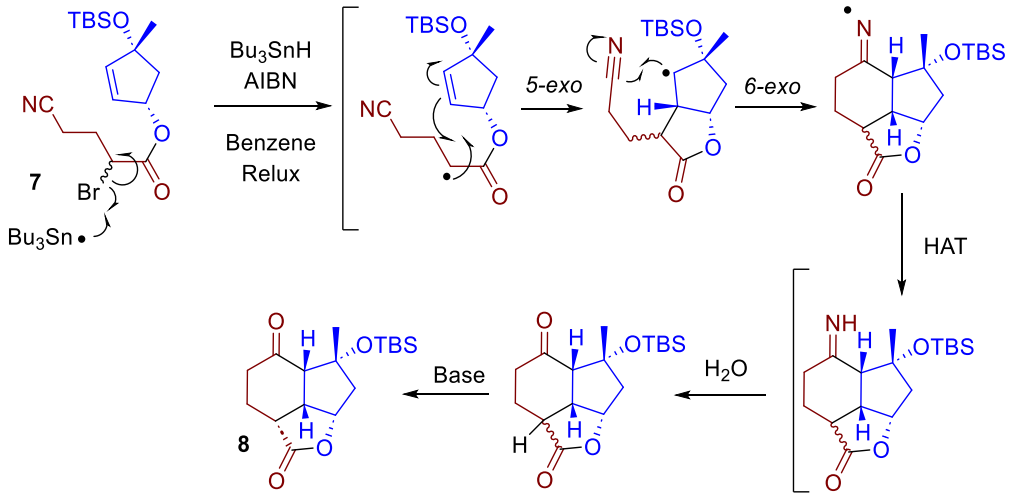

Figure 133 - Radical cascade designed with nitrile group

After this failed attempt, we tried to pursue the radical cyclization approach using an allene as radical acceptor. This in our plan should give two advantages: first, the bromination of an allene substrate via enolate should not be as problematic due to the absence of additional acidic protons. Second, allenes are known to be very reactive substrates, so there is a higher chance to form the second ring, this time via a *6-endo* addition mode, as shown in Figure 134.

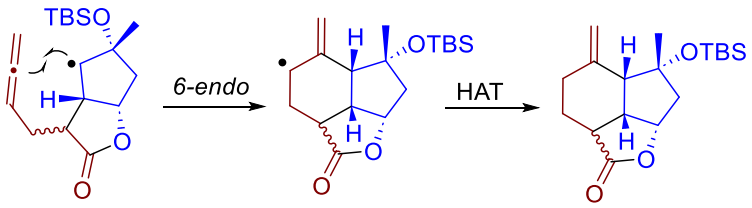

Figure 134 - Radical cascade with allene

Since the direct bromination of the latter chain was not working, we decided to attempt the bromination first and make the ester later. We started condensing the commercially available pent-4-ynoic acid with tert-butanol using DCC, obtaining **9** in 77 % yield. Then, **9** undergoes Crabbè homologation reaction[31], giving allene **10** in 61% yield. Regrettably, even allene **10** could not undergo α-bromination in our hands.

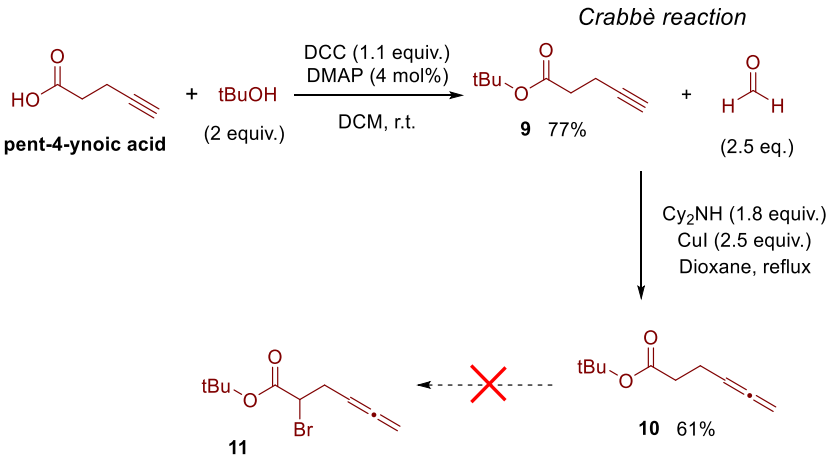

Figure 135 - Intermediate 11 synthesis

Then, we decided to explore the formation of malonate radicals, as we were able to make α-functionalized malonic esters of **3**. Different substrates were synthesized this time, and two different methodologies were studied, to explore the influence of structural features.

The malonate moiety was prepared in 2 steps starting from dimethyl malonate via alkylation to obtain Dielsters of type-**12** (Figure 136).

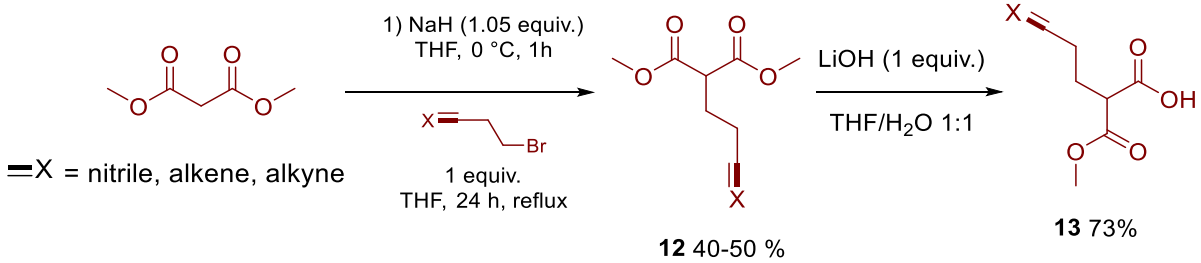

Figure 136 - Intermediates 13 synthesis

Different side chains were used to install nitrile, alkene and alkyne as terminal groups. The malonate alkylation gave between 40 % and 50 % yield of intermediates of type-**12**. Diester **12** then undergoes saponification of only one ester moiety yielding carboxylic acids of type-**13.**

Acid **13** was then condensed to allylic alcohols of type-**3** using HATU as the coupling agent, with a yield of esters of type 14 ranging between 40% and 60% (Figure 137).

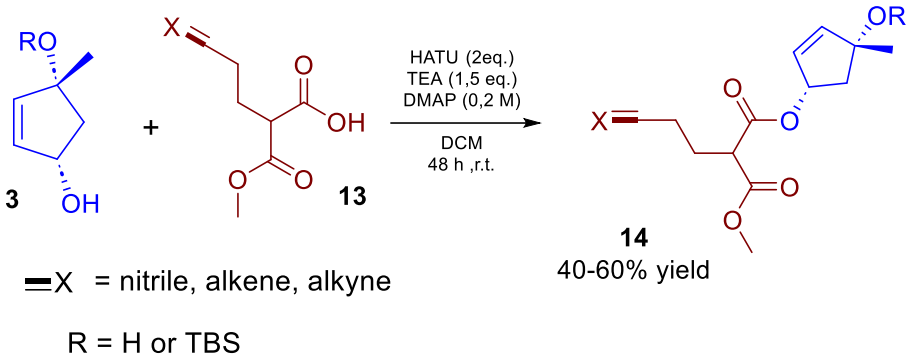

Figure 137 - Intermediates 14 synthesis

Intermediates of type **14** were then tested for Mn^{3+}-induced radical cyclization, as reported by Snider and co-workers[32]. The methodologies are shown in Figure 138, together with the proposed mechanism.

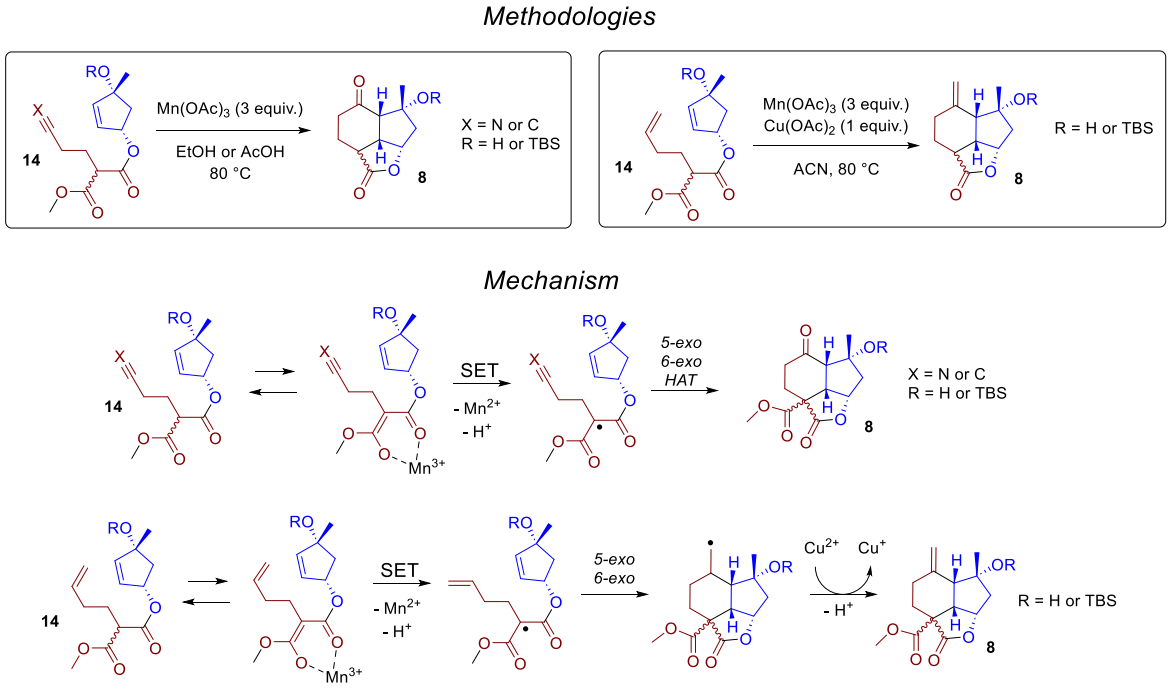

Figure 138 - Manganese-induced cyclization

Mn^{3+} is able to oxidize the malonate by SET generatingthe corresponding radical. It is reasonable to think that this oxidation goes via enolization of the malonate,

coordination to Mn^{3+} and intramolecular SET process. Snider and co-workers reported this methodology to trigger radical cyclization on simpler substrates, which is the evidence of the formation of a radical intermediate under those conditions. After the designed 5-exo-trig/6-exo-trig or -dig sequence, HAT yields the final product in case triple-bond are used as acceptors. In the case of alkenes, acetonitrile is used as solvent and Cu^{2+} as co-oxidant to convert the terminal alkyl radical to the required alkene.

Despite our efforts, even in this case radical cyclization did not delivered any product, but only unreacted starting material, decomposition or byproducts were observed.

Why radical cyclization does not work

Many radical cyclizations were investigated in the attempt of making the **A** ring system. However, no complete reaction was ever observed. Only R_i removal or a 4-exo attack on X group were detected, as shown in Figure 139.

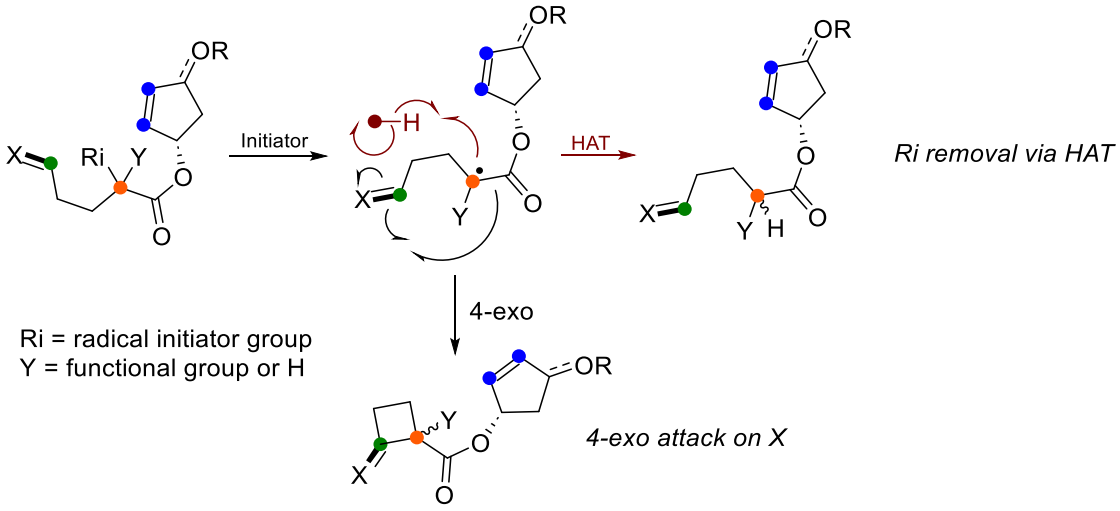

Figure 139 - Main side reactions observed during radical cyclization experiments

There was only one case in which the first of the *desired* bond-forming events (i..e., the initial 5-exo-trig process) was observed: the Ueno-Stork-type radical cyclization of intermediate **15**,[33] shown in Figure 140.

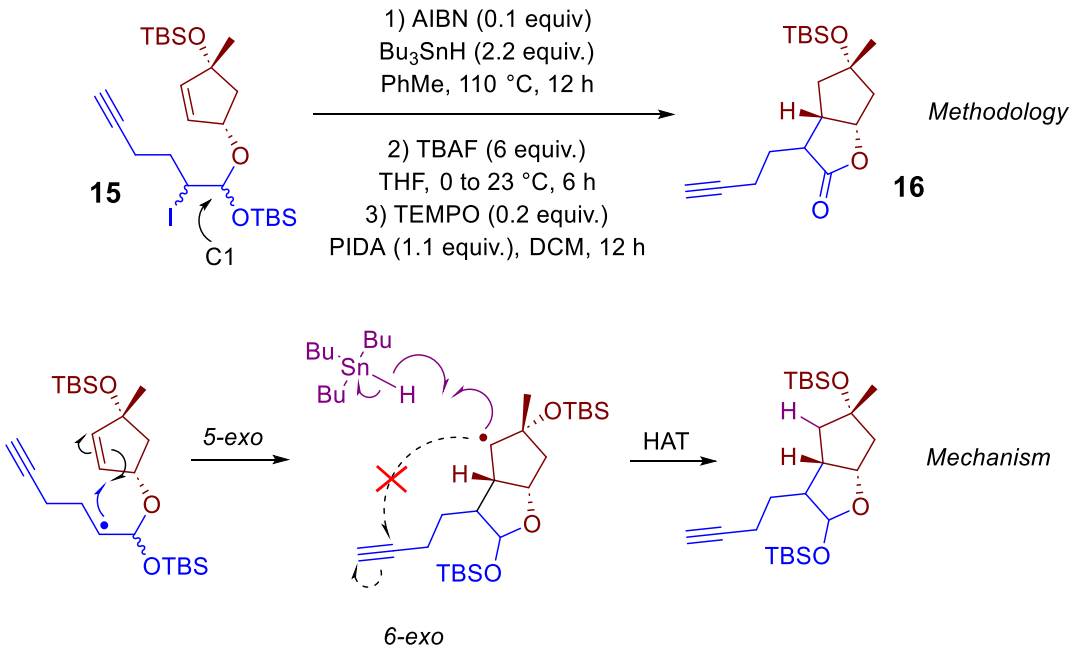

Figure 140 - Ueno-Stork radical cyclization

Product **16** was observed, and this means the radical intermediate generated after the halogen atom abstraction (XAT) undergoes 5-exo-trig cyclization, but the cascade is interrupted by the HAT process operated by tributyltin hydride, which is presumably faster than the 6-exo-dig cyclization. The only significant structural difference between **15** and **14-type** intermediates is the hybridization of C1: sp^3 for **15**, sp^2 for **14**. Thus, it is reasonable to think that the structural constrain imposed by sp^2 C1 brings the radical center in a non-reactive position (too far or with an unfavorable orbital overlap), and the ΔG^{++} is too high. In this situation, the side reactions shown in Figure 139 become competitive. On the other hand, the sp^3 C1 forces a tighter geometry on the corresponding radical, somehow lowering the ΔG^{++} - a nice example of Ingold-Thorpe effect.[XVI] Unfortunately, the next step probably has another conformational issue, so the reaction stops there.

To summarize, we are facing an intricated geometrical issue in the key cyclization step, which we could not solve. Some additional conditions and substrates could have been tested, such as different X groups to facilitate the 6-exo step in the Ueno-Stork reaction, or milder radical reducing agents, such as Et_3SiH, or Tris(trimethylsilyl)silane to slow down the competitive HAT process.[34] However, just a few weeks after we started the radical cyclization investigation, Hong, Hu and co-workers[20] reported the radical cyclization approach for the synthesis of the same ring system in the total synthesis of Scabrolide A and Havellockate, forcing us to change strategy.

[XVI] There are actually 2 isomers of 15 synthesized. I do not speculate on which one reacted faster.

The radical cascade outlined by Hong and Hu has a completely different geometry, featuring two reactive vinyl radicals, the same C1-sp^3 carbon and the radical cascade performed from the other side of the molecule (5-exo/5-exo/5-endo) - Figure 141 .

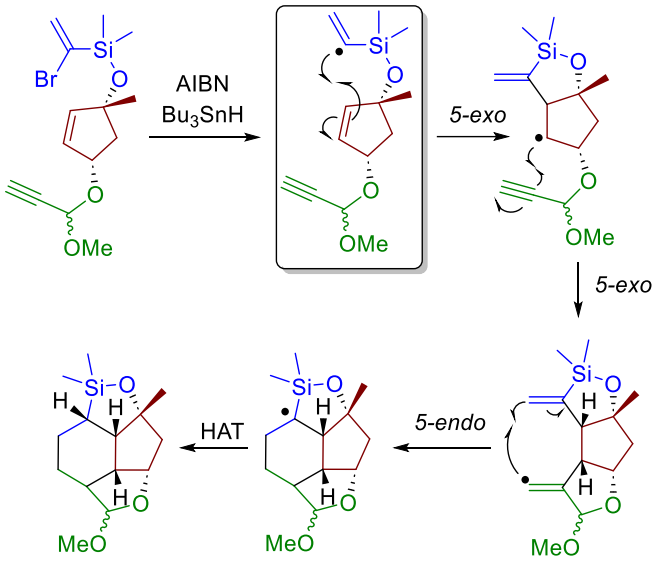

Figure 141 - 5-exo/5-exo/5-endo cascade by Hong and Hu

Diels-Alder strategy

The Diels-Alder (DA) strategy, as explained in the strategy introduction, is based on the construction of the 5-membered carbocyclic ring, followed by 6-membered ring formation by [4+2] cycloaddition reaction. The lactone ring can be forged contemporary or at a later stage using different methodologies.

Diels-Alder reaction (DAR) was attempted using different activation modes and substrates, trying to overcome the issue of the lack of reactivity generally observed. We attempted the cycloaddition via thermal activation, classic Lewis Acid activation, Corey-Bakshi-Shibata (CBS) catalyst – Lewis Acid complex activation, radical cation activation and organocatalysis activation, especially via iminium ion. The different experimental results are organized and discussed by activation mode.

Thermal activation

First, simple *intermolecular* normal-demand DA cycloaddition was tested. The electron-rich dienes tested are furane **17**, Danishefsky's diene (**18**)[35] and Rawal's diene[36] (**18**). These substrates were chosen as model substrates both for their reactivity and for the presence of a heteroatom, which allows for further functionalization to obtain the desired 6-membered enone. The electron-poor

dienophiles tested are the 2-carboxycyclopentenone **20** and cyclopentenone (**21**). **20** and **21** were chosen as model substrates as they feature a 5-membered carbocycle (Figure 142), so only a few steps are needed after cycloaddition to obtain **A**.

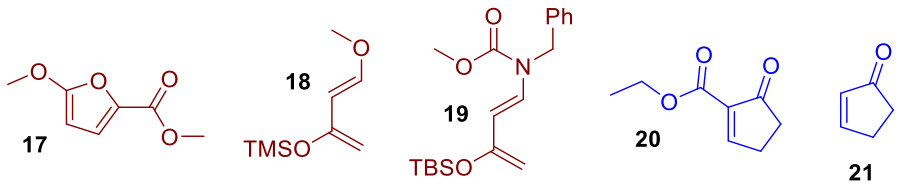

Figure 142 - Substrates used for thermal activation

All the reactions were carried out in toluene under heating, without any means of chiral induction, as we wanted to initially test the reactivity of cyclopentenone scaffold as dienophile. The reactions are shown in Table 19.

Entry	Reaction	Outcome
1[a]	17 + 20	Enone decomposition
2	18 + 20	No reaction
3	18 + 21	Decomposition
4	19 + 21	Decomposition
5	19 + 20	Decomposition

Table 19 - Thermal DAR screening

All the reactions were performed in toluene at 110 °C. [a] 140 °C

Unfortunately, only decomposition of one of the two components or no reaction was observed. From this early experimentation it can already be observed that cyclopentenones are substrates reluctanct to react in DAR. Indeed, there are only a few reports concerning this substrate, despite this should be a common reaction in the synthesis of natural products.

Given the scarce results obtained with intermolecular DAR, *intramolecular* DAR was investigated, starting from the use of furan derivatives as the diene and using an optically pure cyclopentenone-derived substrate (**29**). The synthetic sequence was already available in literature, and it's shown in Figure 143.

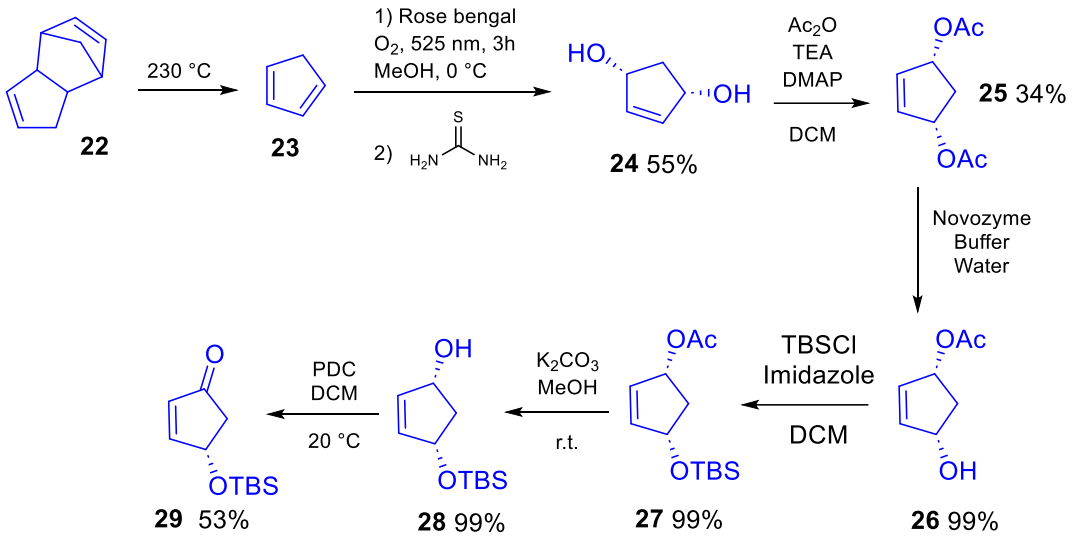

Figure 143 - Intermediate 29 synthesis

The sequence starts with dicyclopentadiene **22**, which undergoes retro-DAR upon heating yielding **23**. Then, **23** undergoes [4+2] cycloaddition with singlet O_2 under photocatalytic conditions, using rose Bengal as photosensitizer.[37] The peroxide is reduced *in situ* by treatment with thiourea, yielding **24**. Diol **24** is then quantitatively acetylated using acetic anhydride to give **25**. Dielster **25** undergoes desymmetrization by enantioselective biocatalytic hydrolysis using novoenzyme which delivered enantioenriched alcohol **26** in 99% yield and >99.5:0.5 e.r.[38] Then, the free alcohol group of **26** is protected with TBS, again with full conversion, yielding **27**. Cleavage of the acetate group with methanol in the presence of K_2CO_3 gives alcohol **28**. Finally, the desired ketone **29** is obtained by oxidation with pyridinium dichromate[39] (PDC). If desired, the other enantiomer of **29** can be obtained by using a slightly modified procedure that utilizes a different enzyme: pancreatic lipase. Moreover, the racemic version of **29,** useful as model substrate, can be obtained by Piancatelli rearrangement[40] of furfuryl alcohol (to obtain ketone **30**) followed by silylation (Figure 144). We found the Piancatelli rearrangement-based methodology straightforward, as simple and cheap reagents were used to synthesize in one step fundamental building block. However, after chromatographic isolation, a lower yield than reported was recovered.

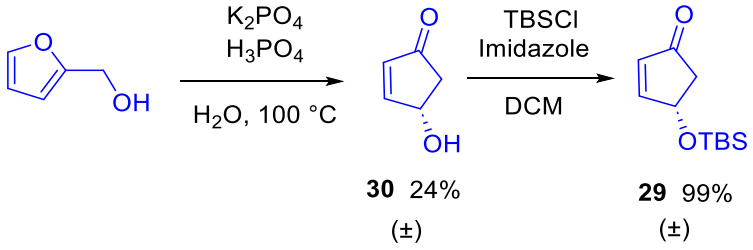

Figure 144 - Racemic 29 synthesis via Piancatelli rearrangment

The desired substrate was then obtained by merging fragment **29** and furfuryl alcohol (Figure 145).

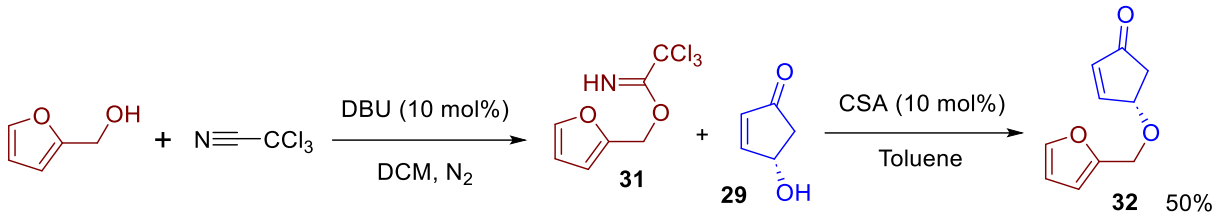

Figure 145 - Synthesis of fragment 32

The hydroxide group of furfuryl alcoho was activated using trichloroacetonitrile to afford **31**. Trichloroacetimidate **31** undergoes substitution by **29** under acidic conditions yielding **32** in 50 % yield. Ether **32** was then subjected to thermal cycloaddition by heating the reaction up to 140 °C in xylenes. Regrettably, no reaction was observed (Figure 146).

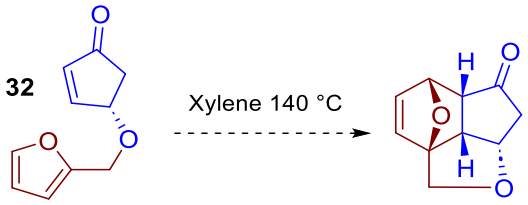

Figure 146 - Thermal DA of 32

The fact that no reaction at all was observed, despite the electronic match between the enone and the furane units, led us to think that maybe the intramolecular reaction was somehow hampered by conformational issues. The transition state requires alignment of the orbitals of the two π systems, and maybe the -OCH_2- bridge cannot accommodate this with an acceptable energy cost. However, it is not possible to insert or delete atoms in the linker, as we would make another molecule.

Thus, inspired by Nicolau's approach for the synthesis of the C-ring of Taxol,[41] we decided to follow the "template" strategy which takes advantage of a transient link between the two π systems to favor the required geometry (Figure 147).

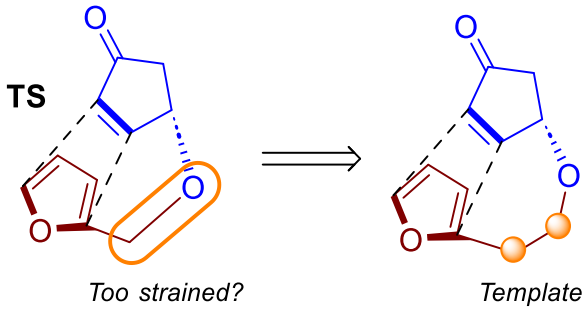

Figure 147 - Template strategy

Moreover, different dienes were synthesized as side chains, inspired by literature reports and by the necessity of having a heteroatom in the newly formed 6-membered ring to install the required ketone functionality. A boron-containing diene (**39,** Figure 148) and silicon-containing dienes (**43**, **44** and **45**) were thus synthesized.

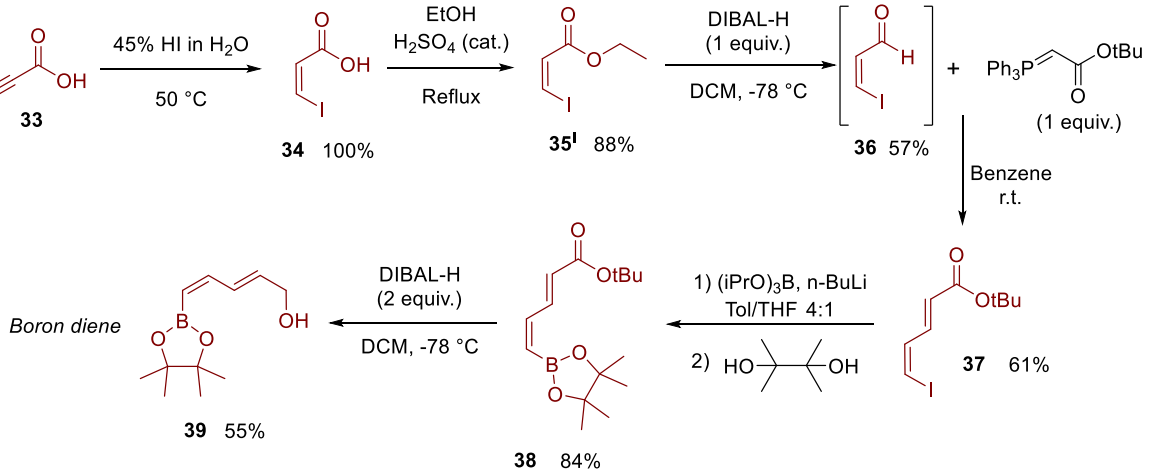

Figure 148 - Synthesis of fragment 39

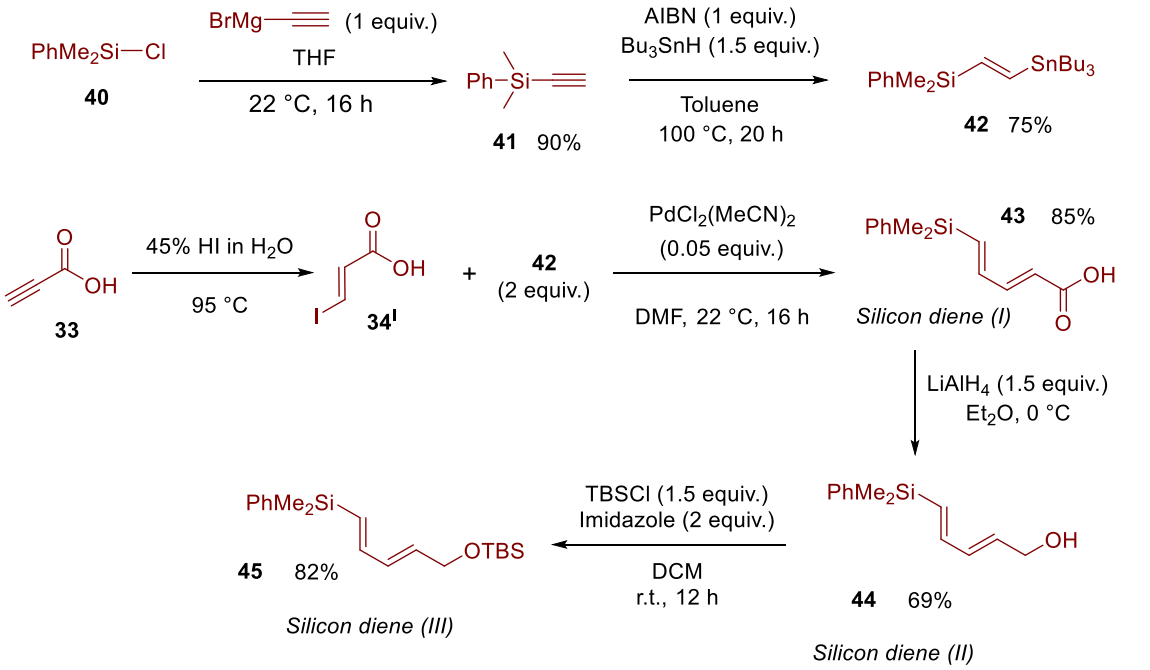

Figure 149 - Fragment 43, 44 and 45 syntheses

Alkenyl boronate **39** was synthesized starting from the commercially available propiolic acid **33** by iodic acid addition (**34**^{I}),[42] esterification (**35**)[43], reduction to aldehyde with DIBAL-H (**36**), Wittig olefination (**37**), metalation-borylation-pinacol ester formation (**38**)[44] and final reduction to alcohol.

The silicon dienes we employed were synthesized following the same synthesis sequence starting from silyl chloride **40** by addition of a Grignard reagent to yield

41, followed by hydrostannylation with Bu_3SnH to yield **42**.[45] Alkenyl iodide **34**[I] was prepared by iodic acid addition to **33** at a higher temperature. Next, Stille cross-coupling[46] between **34**[I] and **42** afforded diene **43**. Reduction of the carboxylic acid unit with $LiAlH_4$ yields directly alcohol **44**, which is then TBS-protected to yield **45**.

Dienyl boronate **39** was then reacted with alcohol **29** in the presence of phenylboronic acid in toluene under azeotropic conditions. At the equilibrium **39** and **29** should generate a mixed ester with boronic acid, creating a template. In our design, this intermediate is activated for DA reaction. The mixed ester would then be easily hydrolyzed upon work-up at the end of the reaction (Figure 150). However, once again no cycloaddition reaction was observed.

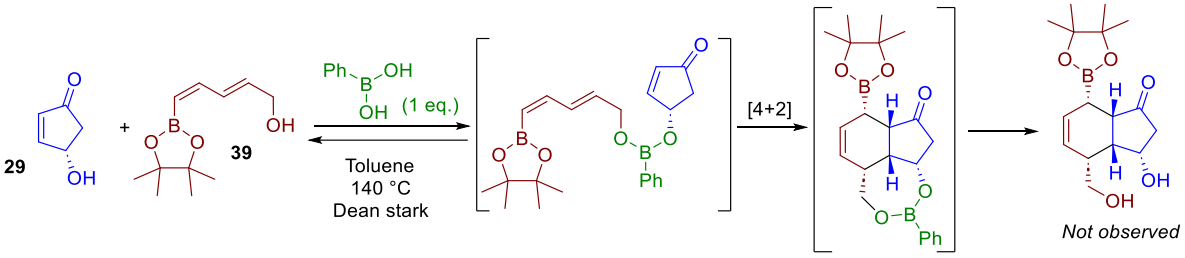

Figure 150 - Boronic acid template reactivity

The silicon tether[47] was installed by sequential chloride substitutions, obtaining **45**. However, thermal Diels-Alder reaction failed to deliver any product. Mild H-bond activation with BHT and HFIP did not improve matters (Figure 151).

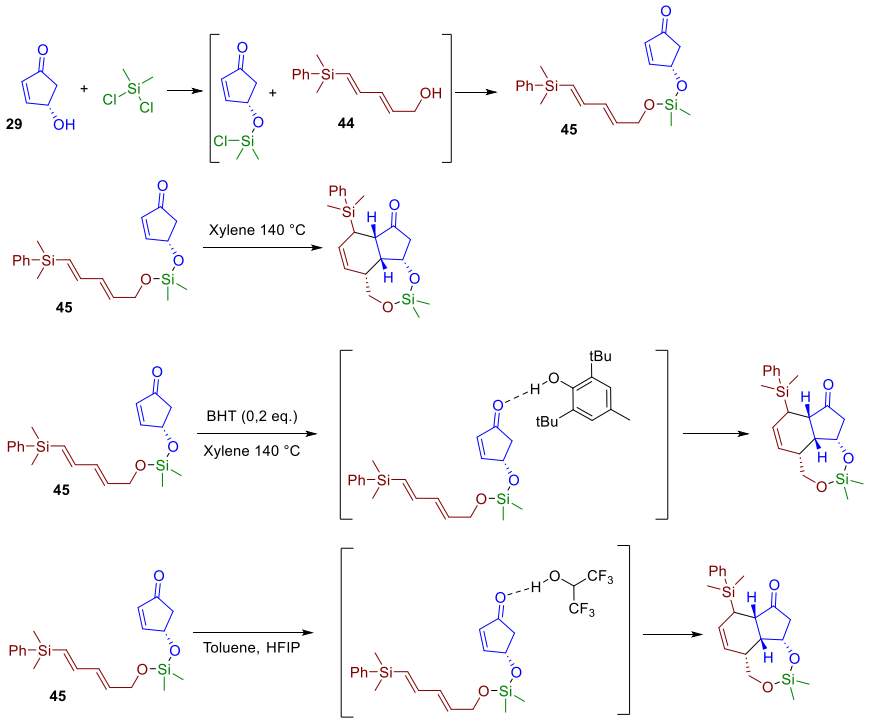

Figure 151 - Silicon template synthesis and reactivity

Given that thermal activation did not trigger any cycloaddition, despite the different geometries and electronic system tested, we decided to test different ways to activate the dienophile.

Hole-catalyzed Diels-Alder reaction

"Hole catalysis" is the activation of substrates using only single electrons as catalyst. In these chemical events the electron has a TON >1 by definition.[48] This type of catalysis has been successfully used to promote Diels-Alder reaction: the cycloaddition between a conjugated radical cation and an alkene is usually orders of magnitude faster than the classic [4+2] reactions. This is especially useful in cases in which two *neutral* reaction partners are coupled, as the electrophilic or nucleophilic activation cannot be used to speed up the process.

The activation mode of hole-catalysis applied to cycloadditions is shown in Figure 152, taking the classical butadiene-ethylene reaction as example.

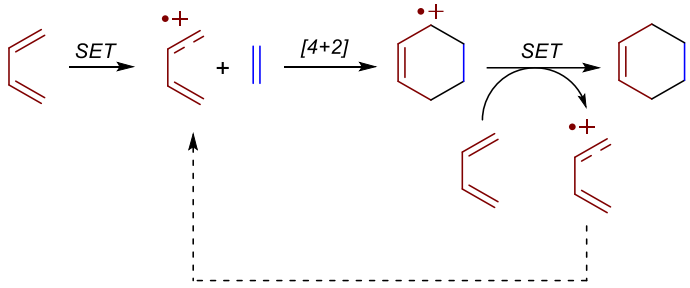

Figure 152 - Hole-catalyzed [4+2] cycloaddition

To activate the cycle an initial SET on the most oxidation-prone substrate, in this case the diene, is needed. The oxidation can be performed using strong chemical oxidants, photocatalysis or electrocatalysis. The generated radical cation very quickly undergoes cycloaddition with the dienophile, generating an alkyl radical cation, which has a higher oxidation potential then conjugated radical cation. The alkyl radical cation then oxidizes the diene, yielding the product and initiating another catalytic cycle.

To overcome our troubles with Diels-Alder reaction, we tested this activation mode on different substrates and different radical cation-generation methods. Our design was based on oxidizing the *dienophile* first, to avoid dealing with diene-radical cations. Indeed, these could react *directly* with other dienes playing the role of dienophiles,[49] generating undesired byproducts (Figure 153).

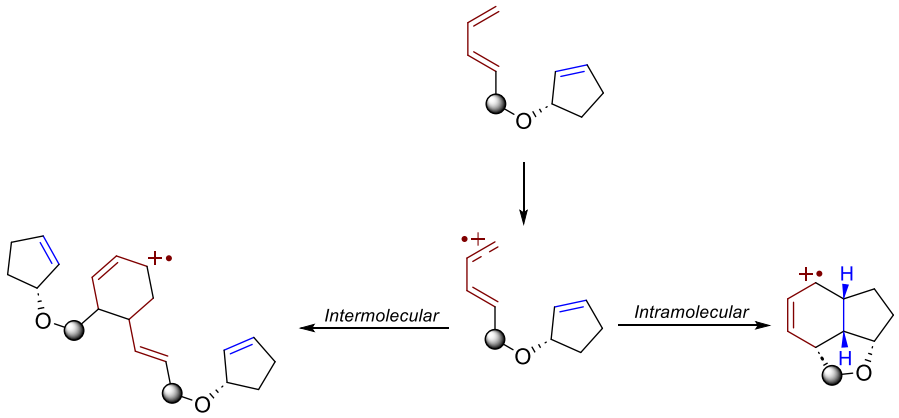

Figure 153 - Intermolecular side-reaction

To realize this plan, the dienophile must have an oxidation potential *lower* than the diene. Thus, diene was always decorated with an EWG group (*i.e.*, a carboxylate) to have the lactone structure embedded in the cycloaddition product. The heteroatom of choice was silicon, as it was available at that moment.

The desired precursor **46** was then obtained by ester coupling with **3** using HATU (Figure 154).

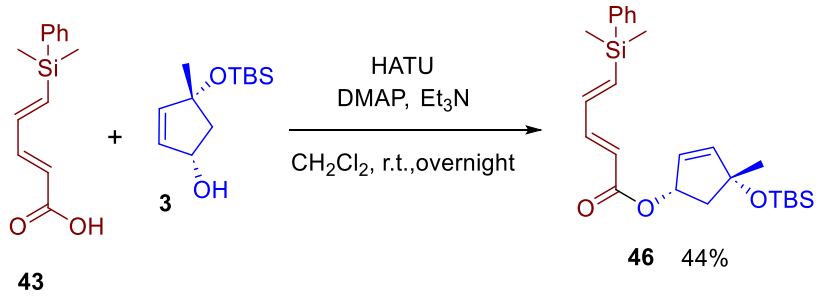

Figure 154 - Fragment 46 synthesis

Our radical-cation cycloaddition attempts are shown in Figure 155.

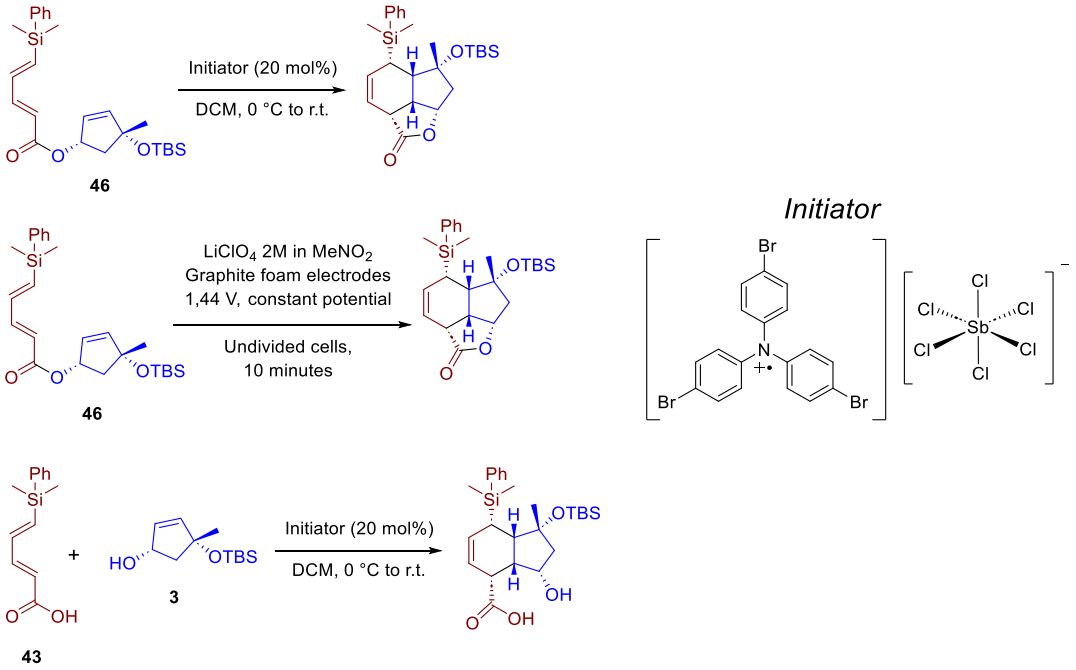

Figure 155 - Radical cation DAR

The intramolecular cycloaddition of **46** was attempted using both a commercially available amino-radical cation as initiator,[49] and an electrochemical method.[50] Both reactions showed complete conversion in a few minutes, but no desired cycloaddition product was detected, as only unidentified byproducts were obtained. The same can be said for the intermolecular reaction between diene **43** and alkene **3**: only byproducts and some unreacted starting materials were observed. At this point it was clear for us that other reaction paths were promoted under the reaction conditions instead of DA, so this activation mode was considered not worth investigating.

Classical Lewis acid activation

Given the scarce results obtained using thermal activation and hole catalysis, we decided to explore the classical Lewis acid activation. The idea behind this activation mode is simple: if thermal activation is not sufficient and radical-cation activation is slower than other side reactions, maybe activation of the dienophile by Lewis acids is the key to trigger the desired reactivity. As for the other activation modes, both intermolecular and intramolecular reactions were tested, as well as the use of templates and racemic reactions for reactivity studies.

For intermolecular cycloadditions, **19**, **44**, **45**, **21** and **29** were investigated as substrates. $AlCl_3$, $CrCl_2$, Et_2AlCl, BF_3, $ZnCl_2$ and $TiCl_4$ were screened as the Lewis acid. The experimental results are summarized in Figure 156.

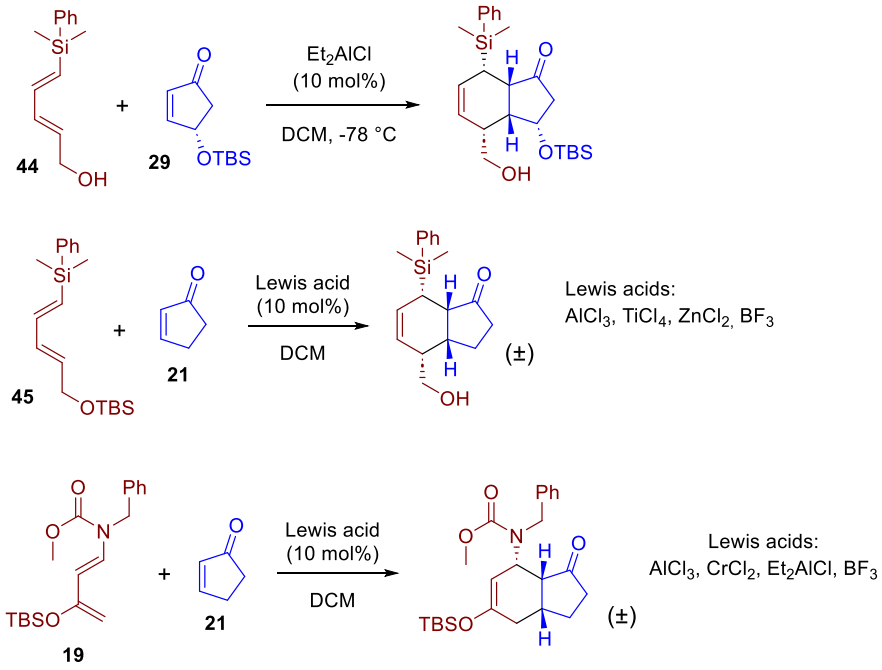

Figure 156 - Intermolecular classic Lewis acids-catalyzed DAR

In all cases, decomposition products or no reaction was observed. The reaction between **44** and **29** deserves some comments; the free hydroxyl group of **44** was intentionally left unprotected, as it is reported that Et_2AlCl can coordinate it and, in some cases, enhance the reactivity. In our case, only a by-product derived from **44** was observed, probably the substitution of the OH with a chlorine . Moreover, the diastereoselectivity design is peculiar, as we predicted that **44** would have attacked **29** *on the same side* of the bulky -OTBS group. It is reported that the reaction between **29** and butadiene in the presence of $AlCl_3$ as the catalyst shows a *syn* stereochemical outcome[51]. This is due to transition state-stabilizing orbital effects in the presence of strong Lewis acids.[51] This orbital effect was considered also for the design of other cycloadditions.

The reactions between **21** and **19** and **45** were tested at different temperatures up to reflux of the solvent. **45** again showed to give a byproduct, probably the same chlorination underwent by **44**, while Rawal diene **19** decomposes generating unidentified byproducts.

Thus we turned our attention to the reaction between furan-derived substrates and cyclopentenone-derived substrates under Lewis acids catalysis and triflic acid catalysis, both via *in situ* template formation (Figure 157 and Figure 158) and directly on **32** (Figure 159).

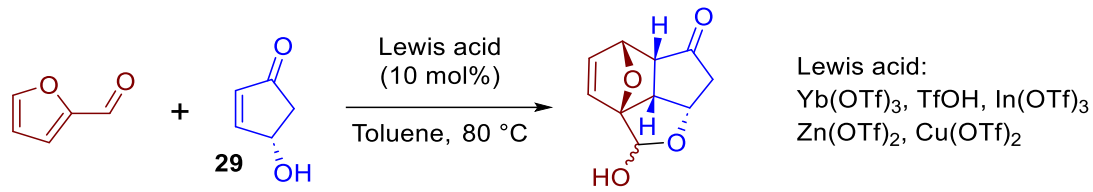

Figure 157 - Lewis acid catalyzed reaction DAR between furfural and 29

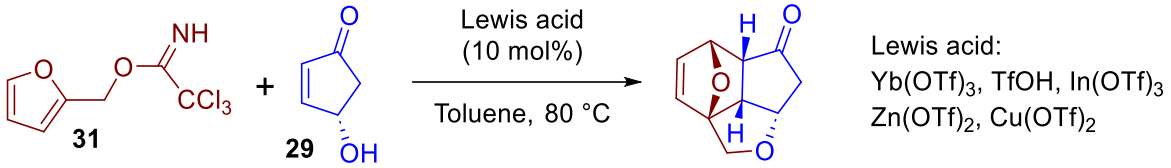

Figure 158 - Lewis acid catalyzed cycloaddition reaction between 31 and 29

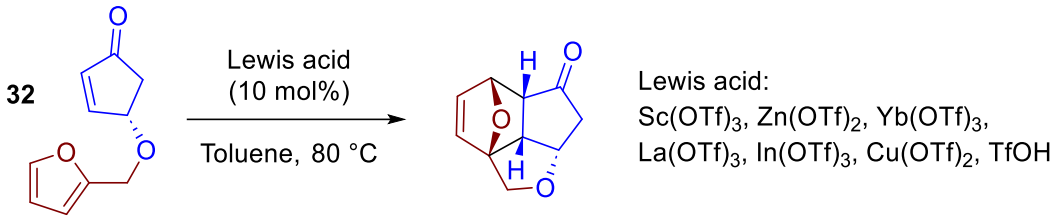

Figure 159 - Intramolecular Lewis acid catalyzed DAR of 32

Inspired by the report of Baskaran and co-workers[52], the reaction between furfural and **29** was designed to go through the reversible formation of the corresponding two hemiacetal diastereoisomers. We postulated that one of the two diastereoisomers, presumably the (*S*,*S*) one, should force the furane ring to lay under the cyclopentenone plane accelerating the reaction by proximity effect. The lactol obtained could then be oxidized to the corresponding lactone and reduced by SmI_2, forming an intermediate metalated species which should cleave the oxa-bridge to form a strong Sm-O bond releasing the strain of the system, yielding the desired product (Figure 160).

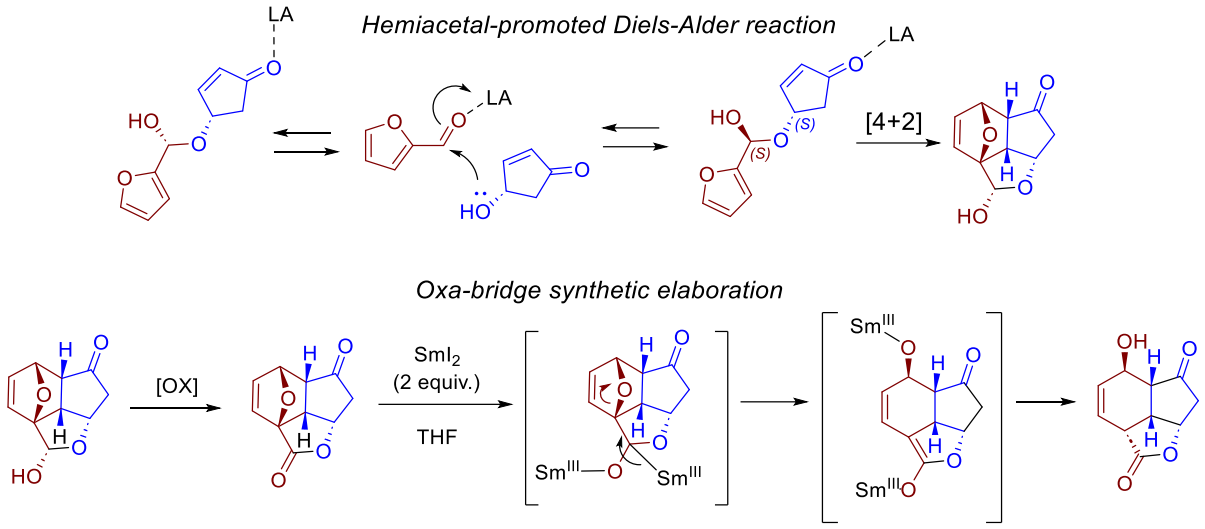

Figure 160 - Hemiacetal-promoted DAR and ox-bridge synthetic elaboration plan

Despite our efforts, no cycloaddition product was ever observed: only decomposition or formation of unidentified byproducts was detected.

The reaction between **29** and **31** follows an analogous logic: *in situ* formation of the adduct **32** and Lewis acid-promoted cycloaddition, followed by the same oxa-bridge synthetic elaboration. Again, only decomposition or unidentified products were detected even in this instace. Not even **32** was observed, so we decided to test **32** directly under similar reaction conditions. Even this time, only decomposition or the formation of unidentified byproducts was observed.

Finally, intermolecular cycloaddition with oxygenated diene **47** and **21** was attempted (Figure 161). **47** can be obtained in 5 steps from **48** and was available in our laboratory.

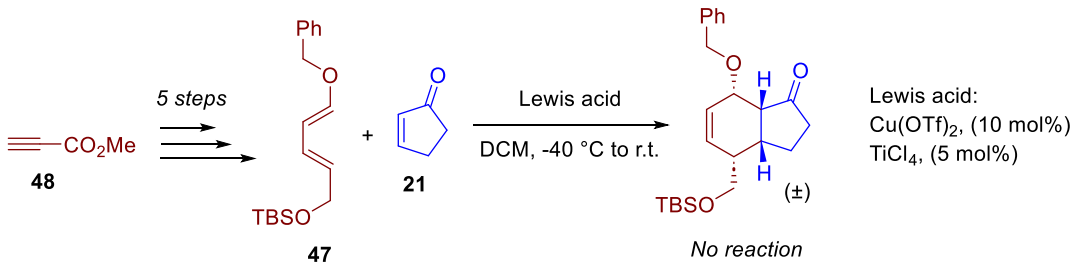

Figure 161 - Intermolecular classical Lewis-acid catalyzed DAR

Despite the use of an electron-rich diene such as **47** and the presence of strong Lewis acids, such as $Cu(OTf)_2$ and $TiCl_4$, the system proved to be reluctanct to react.

In summary, we observed that the use of a Lewis acid as the catalyst gave much more decomposition compared to thermal activation. Probably, Lewis acids tend to bind also the heteroatoms present in the diene, promoting decomposition pathways and/or self-cycloaddition. Moreover, the Diels-Alder reaction on

cyclopentenones or related substrates is much less commonly reported compared to other substrates, so there is probably an intrinsic difficulty in DAR. Thus, we decided to test different catalytic systems: organocatalysis and CBS – Lewis acid complex catalyst. The former is much milder, as the activation via iminium ion involves only the ketone itself, so diene decomposition should be circumvented. Importantly, iminium organocatalysis and CBS-Lewis acid complex have been reported to work on **21** and analogous substrates.

Organocatalysis

DA cycloaddition can be catalyzed both via H-bonding or iminium ion, as shown in Figure 162. Both activation modes act on the enone, rendering it more electrophilic and therefore more prone to undergo cycloaddition.

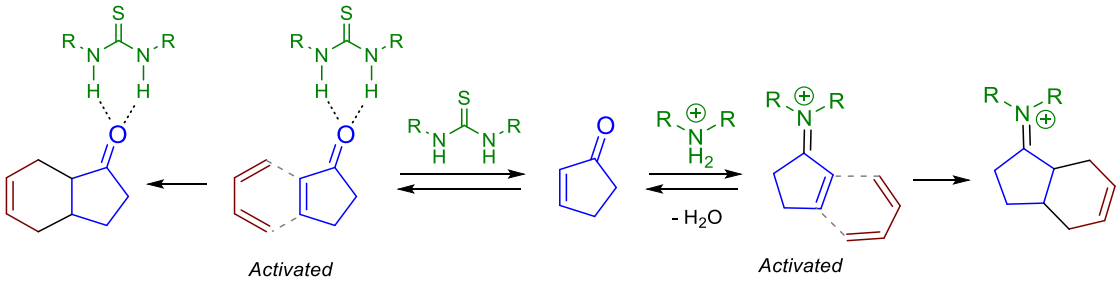

Figure 162 - Activation of cyclopentenone via organocatalysis

Initial screening of activation modes was done with Schreiner thiourea,[53] TRIP,[54] hydrogen chloride and pyrrolidine using **32** as model substrate (Figure 163).

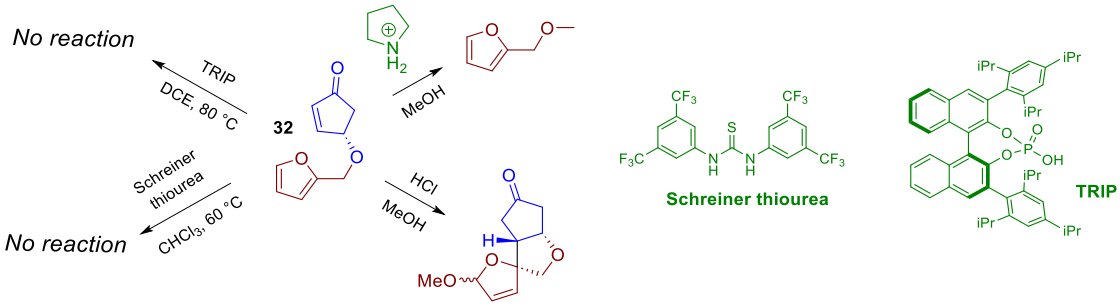

Figure 163 - Activation mode tested

Only hydrogen chloride and pyrrolidine showed some reactivity, while thiourea and TRIP did not promote any reaction. However, hydrogen chloride promoted Michael addition generating a byproduct that was tentatively assigned to be **49^{I}**, and pyrrolidine-derived iminium ion induced Grob fragmentation or SN_2 reaction with methanol, generating **49^{II}** and unidentified oligomers (Figure 164).

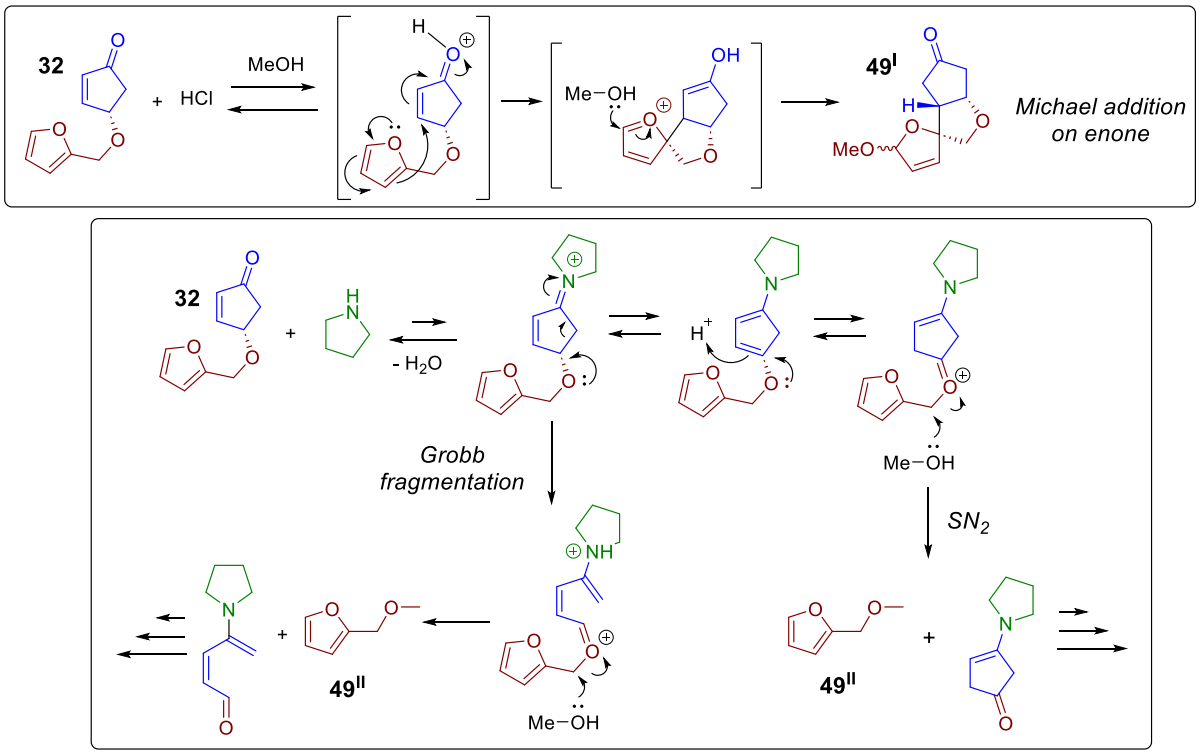

Figure 164 - Parasite reactions of 32 with hydrogen chloride and pyrrolidine

Despite promoting undesired side reactions instead of the DA, we decided to further test iminium ion catalysis for intermolecular cycloadditions, as it is a well-established chemistry. Inspired by the seminal work of Mac Millan and co-workers,[55] we decided to test the reactivity between dienophile **21** and the electron-rich dienes **47** and **48**, which was obtained in two steps from **35**^{I} and an oxa-alkyne[56–58] by Suzuki cross-coupling reaction in the presence of RuPhos G3 palladium complex[59] (Figure 165).[XVII]

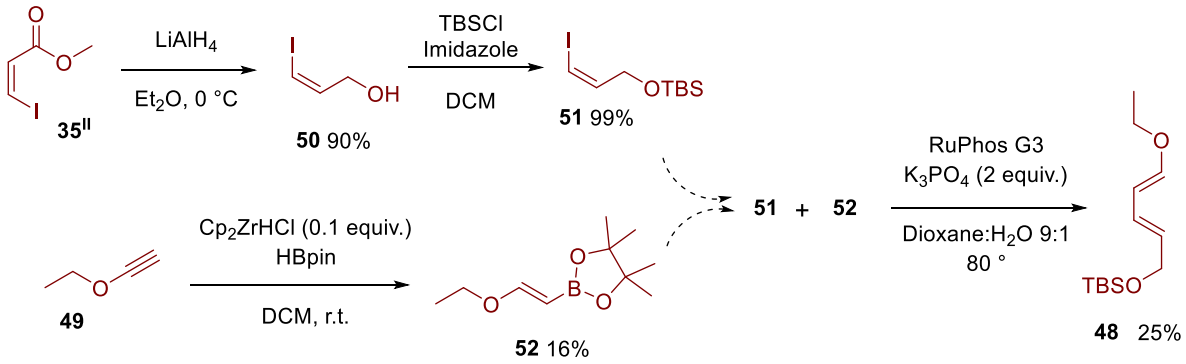

Figure 165 - Synthesis of fragment 48

[XVII] Product **52** was obtained in low yield for accidental spilling. The reaction was not repeated as **48** did not react in the key cycloaddition step.

The synthesis of **48** is justified by the possible steric clash between the oxygen substituent and the catalyst, as shown in Figure 166. Moreover, the absence of a benzylic position lowers the possibility of enol-ether deprotection.

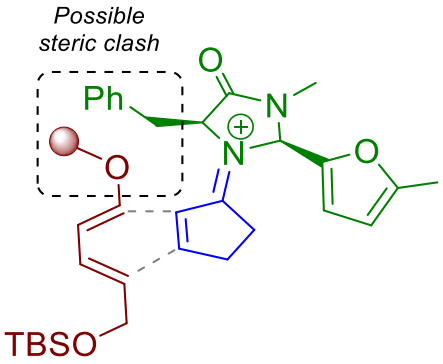

Figure 166 - Possible steric clash in the transition state of asymmetric organocatalyzed DAR

The attempted DA asymmetric cycloadditions via iminium ion are resumed in Table 20:

Entry	Reaction	Catalyst	Conditions	Result
1	21 + 47	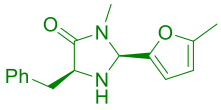	Cat•$HClO_4$ (20 mol%) Water or EtOH for catalyst loading -30 °C to r.t.	No reaction
2	21 + 48	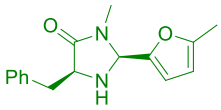	Cat•$HClO_4$ (20 mol%) Water or EtOH for catalyst loading -30 °C to r.t.	Diene decomposition
3	21 + 47	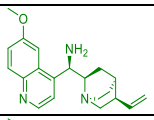	Cat (5 mol%) TFA (20 mol%) DCM, r.t.	Diene decomposition
4	21 + 48	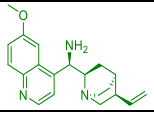	Cat (5 mol%) TFA (20 mol%) DCM, r.t.	Diene decomposition

Table 20 - Asymmetric organocatalyzed DAR

Both MacMillan (II) catalyst[60] (entry 1 and 2) and 9-amino-epiquinidine[61] (entry 3 and 4) were tested in the reported conditions for DA reaction, to explore both primary and secondary amine – derived iminium ions as active species. However, only ino reaction or direct diene decomposition were observed after several days. The diene decomposition is probably due to the acidic environment, as enol ethers are in general sensitive to these conditions.

Moreover, the reaction between **21** and **18** was tested under pyrrolidine catalysis without any acid additive. This reaction led to the formation of an unidentified byproduct in minutes with full conversion (Figure 167), but the desired cycloadduct was not observed.

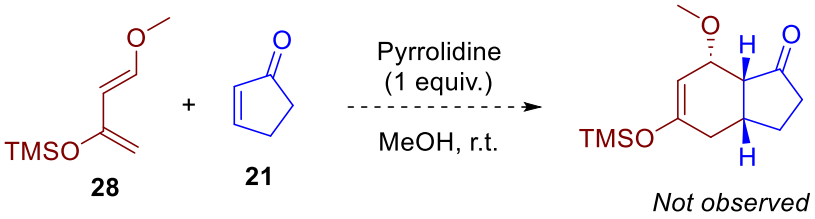

Figure 167 - Pyrrolidine catalyzed DAR between 21 and 28

We then decided to explore CBS catalysis.

CBS

CBS catalysts are a class of oxazaboroles, obtained from diphenyl-prolinol in one step by condensation with a boronic anhydride or a boronic acid. It is usually employed for the enantioselective reduction of ketones, but many other catalytic applications are known, especially cycloadditions.[62] Indeed, it has been reported by Corey and co-workers that oxazaboroles if activated with a Lewis acid[63,64] or a Brønsted acid[64,65] can become a catalyst for enantioselective Diels-Alder reactions. The additive binds the nitrogen lone pair, breaking the conjugation with the neighboring boron atom. The boron atom in this way has a low energy LUMO, able to bind the carbonyl group of enones, while the oxygen atom binds the γ-H via H-bonding. The enone-CBS complex activates the enone toward the cycloaddition reaction and shields one face, inducing enantioselectivity (Figure 168).[66–68]

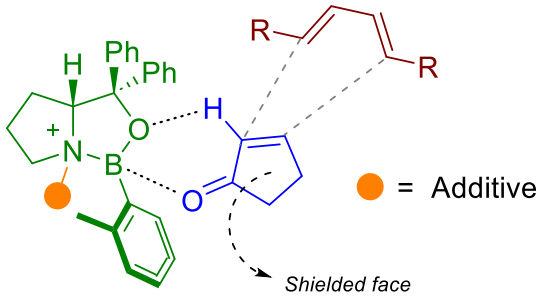

Figure 168 - CBS activation of enones

Moreover, CBS catalysts are reported to be effective on **21** and are very easy to synthesize from common precursors. Thus, we decided to explore the combination of CBS catalysts with $AlBr_3$ and Tf_2NH as additives, using the conditions reported by Corey and co-workers. The electron-donating dienes tested are **41**, **45** and TBS-protected furfuryl alcohol (**53**). The screening is shown in Table 21.

Entry	Reaction	Catalyst	Conditions	Result
1	41 + 21	CBS-Tf_2NH (0.2 equiv.)	DCM, -78 °C to r.t.	Enone polymerization

2	45 + 21	CBS-Tf_2NH (0.2 equiv.)	DCM, -78 °C to r.t.	Enone polymerization
3	53 + 21	CBS-Tf_2NH (0.2 equiv.)	DCM, -78 °C to r.t.	Enone polymerization
4	41 + 21	CBS-$AlBr_3$ (0.05 equiv.)	DCM, -78 °C to r.t.	Diene decomposition
5	45 + 21	CBS-$AlBr_3$ (0.05 equiv.)	DCM, -78 °C to r.t.	Diene decomposition
6	53 + 21	CBS-$AlBr_3$ (0.05 equiv.)	DCM, -78 °C to r.t.	Diene decomposition

Table 21 - CBS-catalyzed asymmetric DAR

The presence of Bronsted acid induced enone polymerization, while the presence of the Lewis acid induced diene decomposition, which was also observed in previous experiments (see above).

As also this catalytic system failed, together with other experiments carried out by our team, we decided to stop the investigations on the Diels-Alder cycloaddition, focusing on the intermolecular Micheal addition strategy.

Why Diels-Alder cycloaddition does not work

As many different DA catalytic systems proved ineffective, the possible problems affecting this reaction are worth discussing.

First, to the best of our knowledge DAR on **21** or δ-oxygenated **21** derivatives and a C4-substituted diene of type **C** have been reported only *once* under harsh conditions,[69] with an opposite regiochemistry compared to the desired one (Figure 169).

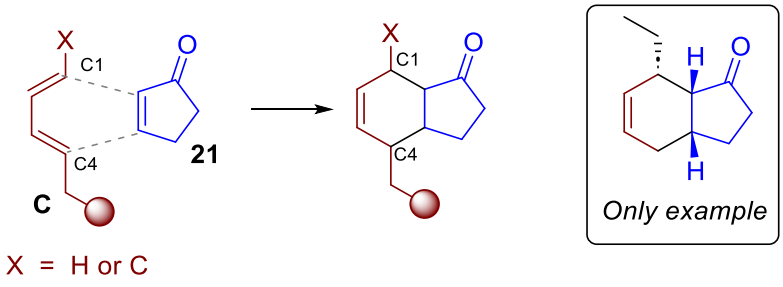

Figure 169 - Issues with cycloadditions of A to 21

This means that probably there are some issues with *that particular DAR*. However, without further studies it is difficult to give a reasonable explanation. The additionally functionalized carbon bound to C4 is vital for our strategy, so no other different dienes can be used. The C1 side of the diene should give less interference

in this reaction, as C1-unfuctionalized dienes with CBS catalytic system were tested as well in Romiti's lab, without any lack. The only exception to this behavior is the reactivity of cyclopentadiene, but in that case probably the contribution of ring strain plays a key role as well.

A factor penalizing the *intramolecular* DAR is the unfavorable conformation of the ester group. Indeed, esters can exist in *syn* or *anti* conformation, depending on where the substituent connected to the sp^3 O is oriented compared to the carbonyl group.[XVIII] With some exceptions, *syn* is generally the more stable one.[70] Despite possessing a low rotational barrier which give access to both conformation, the energy difference between *syn* and *anti*-conformations is significant: it was experimentally determined that for methyl formate the barrier is 4.75 ± 0.2 kcal/mol, while for methyl acetate is 8.5 ± 1 kcal/mol.[70]

In the case of an intramolecular DAR with an ester, the *anti* conformation is the reactive one. Considering that for a substrate as simple as methyl acetate the difference in energy is 8.5 kcal/mol, for a substrate as complex as **B** that difference should be significantly higher (Figure 170). This would theoretically render the reactive conformer not accessible.[XIX] A sketched PES representation is shown in Figure 171.

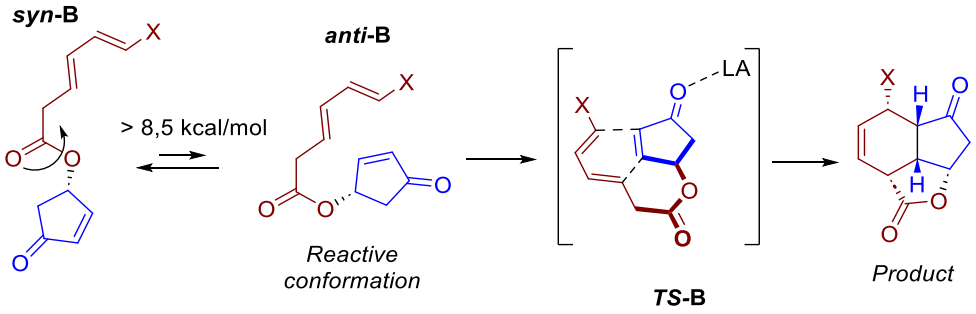

Figure 170 - Conformations of B and DAR

[XVIII] I would like to thank Dr. N. Tampellini for the fruitful discussion.

[XIX] Using Botlzmann distribution equation at 140 °C at only 0,000058% of molecules the equilibrium is in the desired conformation. This is synonym of a sluggish reactivity.

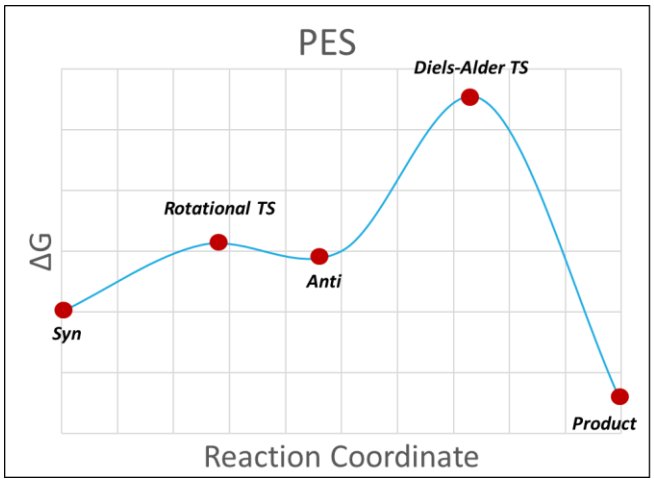

Figure 171 - PES representation of B reaction

Finally, our efforts were focused on intermediate **32**. A negative result was particularly surprising for us, as a similar *intramolecular* cycloaddition is reported as part of an aza-Piancatelli/[4+2][71] sequence (Figure 172).

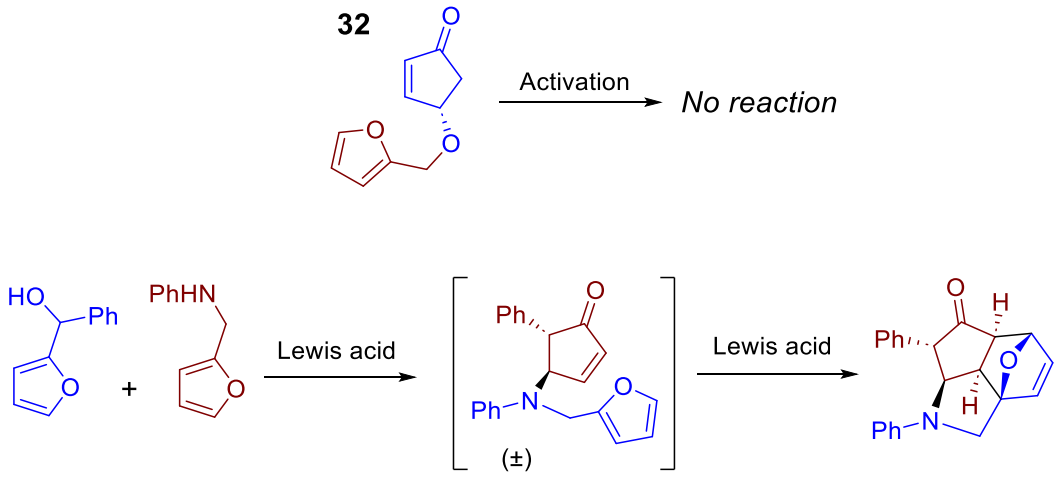

Figure 172 - Comparison between 32 and intermolecular DAR

Probably the substitution on the lateral chain and the presence of the phenyl group on the 5-membered ring helps somehow the reaction to proceed.

DAR of substituted furane and γ-oxygenated cyclopentenones is also reported (Figure 173).[72]

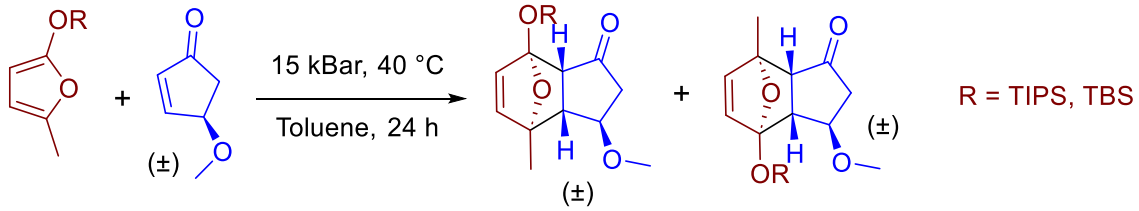

Figure 173 - DA cycloaddition on γ-oxygenated cyclopentenones

However, the presence of Lewis acids induced Michael addition of the furane ring on the enone system, as we observed with hydrogen chloride treatment. Only strong pressure can induce the formation of the cycloadduct, with a ca. 1:1 regioselectivity as the *syn* DA to the oxygenated group is induced only in the presence of Lewis acids.[72] The reason why high pressure is needed is the reversibility of the reaction: normally, DA cycloaddition is thermodynamically favored as in the overall energetic balance 2 π bonds are broken to form 2 σ bonds. However, in the case of furan cycloaddition to enones one π bond broken is conjugated and the two other π bonds broken are part of an aromatic system. In the product the new π bond is isolated, with an additional strain due to the oxa-bridge and the strained condensed 5-membered ring. The overall energy balance *could be*[XX] in favor of the reagents.[73] This is a known problem of [4+2] cycloaddition of furan, i.e. it's the reason why cantaridine – an antifungal compound – is synthesized in similar conditions in industry.[74]

The use of high pressure represents an efficient mean to force the equilibrium toward the product: indeed, $\Delta V_{Reaction} < 0$, and the equilibrium is shifted right for Le Châtelier principle. Moreover, $\Delta V^{(\ddagger)} < 0$, so high pressure shows also a catalytic effect (Figure 174).

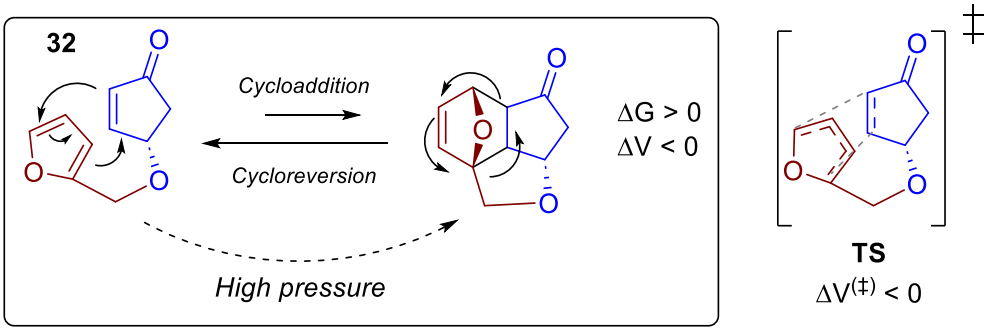

Figure 174 - Thermodynamic of DA reaction of 32

Thus, one possible method to obtain the product from **32** is to conduct the reaction at high pressure in hydrocarbons. However, high-pressure equipment is not available in the laboratories of UTD.

Another interesting methodology, currently not explored for our goals, is the use of 3-borylated furans. These promote both the reaction kinetics and the thermodynamics of the process, shutting down the retro-DA process.[75] Theoretically, this would allow to obtain the desired product with a pre-

[XX] A similar behavior is observed for furane/maleic anhydride reaction. So, it was deduced that probably cyclopentenone could undergo a similar phenomenon.

functionalization, useful to access the norcembranoid diterpenes family (Figure 175).

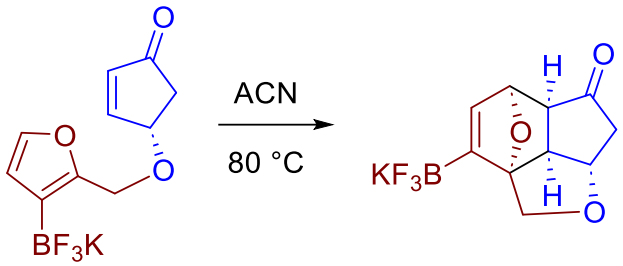

Figure 175 - 3-borylated furane option

Michael addition-intramolecular aldol reaction

The investigations of the Michal addition-intramolecular aldol reaction started with the synthesis of intermediate **54**, reproducing the sequence reported by Reisman and co-workers (Figure 176).[26]

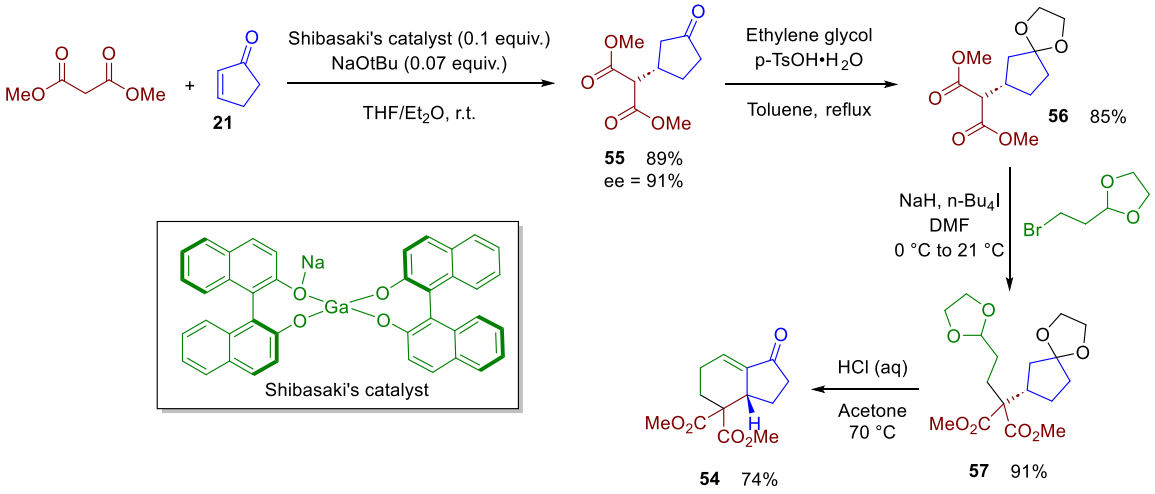

Figure 176 - Intermediate 54 synthesis

The sequence starts with the enantioselective Michael addition of dimethyl malonate to cyclopentenone **21** under the conditions developed by Shibasaki and co-workers,[76] using a gallium-based complex. Adduct **55** was isolated in 89% yield and 95.5:4.5 e.r. It follows ketone protection as acetal to give in 85% yield. Then Dielster **56** undergoes alkylation with the acetal of 3-bromo acrolein to yield **57** in 91% yield. Finally, treatment of intermediate **57** with hydrochloric acid triggers double acetal hydrolysis and intramolecular aldol reaction with concomitant elimination to give **54** in 74% yield.

To introduce the oxygen atom in the 6-membered ring, we decided to perform a boryl- or silyl- conjugated addition to the enone unit. Then, Tamao-Fleming oxidation or oxidative de-borylation can be used to install the desired oxygen atom.

The silyl conjugated addition was attempted via the formation of a silicon-zincate[77] or a silicon-cuprate[78] species. Both methodologies caused the decomposition of **54**.

The borylation was attempted both using copper catalysis and the metal free-carbene catalytic system developed by Hoveyda and co-workers,[79] using bis(pinacolato)diboron as the source of the boron-containing group. Only the copper mediated reaction worked, yielding intermediate **58** in up to 55% yield after purification optimization[XXI] (Figure 177).

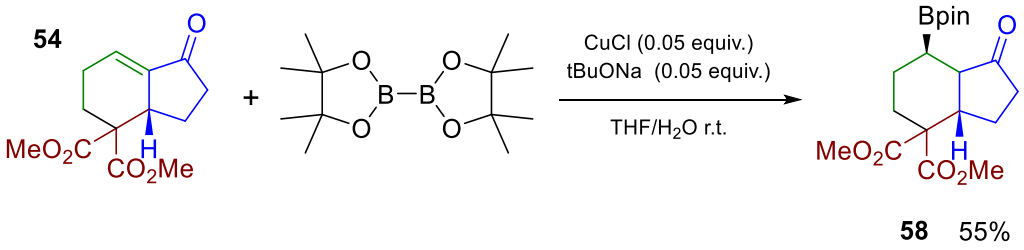

Figure 177 - Copper-catalyzed conjugated borylation

However, after the first batches of **58** were produced, it was not possible to make more material, as the results proved to be not reproducible. The synthesis path towards **58** is shown in any case.

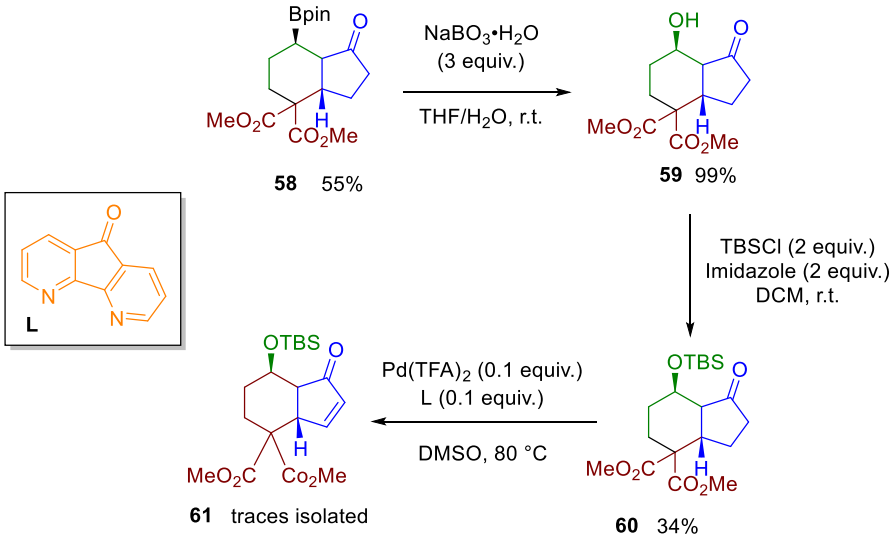

Figure 178 - Intermediates 59, 60 and 61 syntheses

The hydroxyl group on **58** was introduced by oxidation of the B(pin) unit with sodium perborate, generating **59** in quantitative yield. Then, **59** was TBS-protected giving **60** in 34% yield. The first desaturation test on **60** was done using the method developed by Sthal and co-workers.[80] Indeed, thanks to palladium catalysis and the presence of a fluorenone ligand, the alkene functionality can be

[XXI] The silica used during chromatographic purification induced partial hydrolysis of the pinacol borane.

introduced using simple oxygen as the stoichiometric oxidant. The enone functionality of **61** was detected by ^{1}HNMR, but chromatographic isolation yielded only traces of product. Probably **60** undergoes decomposition upon chromatographic purification. The synthetic sequence could not be improved as the synthesis of **58** was not reproducible. For the same reason, the configuration on the α-carbon was not determined, as **58** was not used anymore.

As the boryl- and silyl-conjugated addition proved difficult, we tested the introduction of the oxygen atom via an epoxide-containing intermediate. In our plans, epoxide can be opened by radical reductive processes, yielding an alcohol and the *cis* bicyclic system once the lactone is forged with the correct stereochemistry (Figure 179).

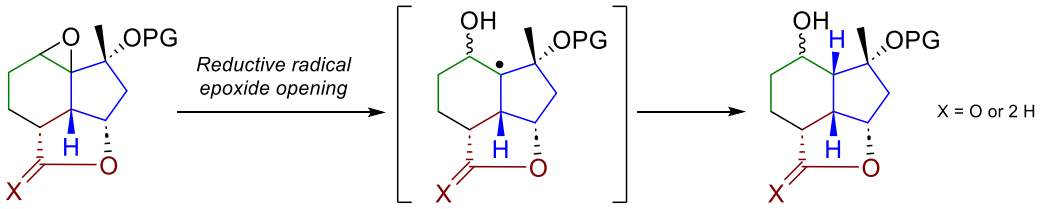

Figure 179 – Planned reductive ring-opening of the epoxide

Given the configuration of **54**, we attempted the addition of methyl-lithium to the ketone, as it would attack the convex face of the molecule. Indeed, **62** was obtained as single diastereoisomer with full conversion by 1H NMR. However, **62** and its derivatives proved very difficult to handle because prone to decomposition (Figure 180).

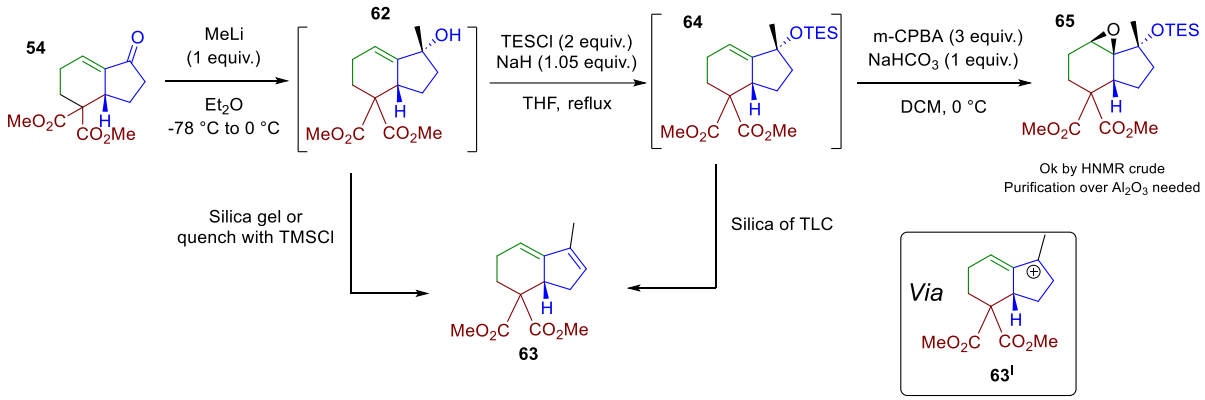

Figure 180 - Synthesis of intermediates 62, 64 and 65

The contact of **62** with silica gel for purification induced the elimination of the tertiary alcohol to give byproduct **63**. An attempt of silylation with TMSCl on the alcoholate was done, but that triggered elimination too. Probably, the tertiary alcohol spontaneously forms the highly stabilized carbocation **63^{I}**, which then eliminates.

62 was then deprotonated with sodium hydride and silylated with TESCl. **64** was cleanly observed by 1H NMR, but even silica TLC triggered elimination to give **63**. Thus, the crude was directly treated with *m*-CPBA in a basic environment, yielding epoxide **65**. This was kept in the freezer, as we wanted to purify it using alumina. **65** was not isolated and fully characterized because of time constraints.

As the epoxidation of **65** seemed to stabilize the system, **62** was subjected to epoxidation with m-CPBA and fully converted to **66** (detected by 1H NMR). However, chromatographic purification on silica gel triggered a fragmentation, surprisingly yielding **54**[XXII] (Figure 181).

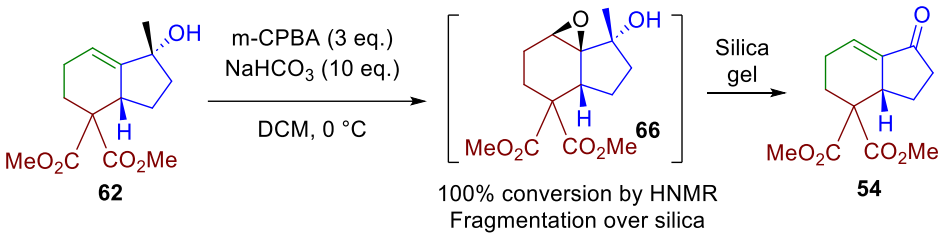

Figure 181 - Synthesis of intermediate 66 and demethylation event

I cannot give any reasonable explanation for the demethylation reaction, but it would be interesting to investigate it further as it is a peculiar event. Moreover, from this functionalization campaign we observed a general tendency to elimination by the tertiary alcohol. The same elimination reaction was also observed while working on "Romo's intermediate" (not shown). The protection of the alcohol unit with a silicon-based protecting group and careful purification avoiding silica seems vital for those intermediates.

Finally, we wanted to test if the *endo* epoxide was better suited for our purposes as the alcohol unit would be ultimately oxidized to the corresponding ketone rendering its stereochemical configuration inconsequential. The *endo* oxidation was performed in two steps, following Reisman's report (Figure 182).[26]

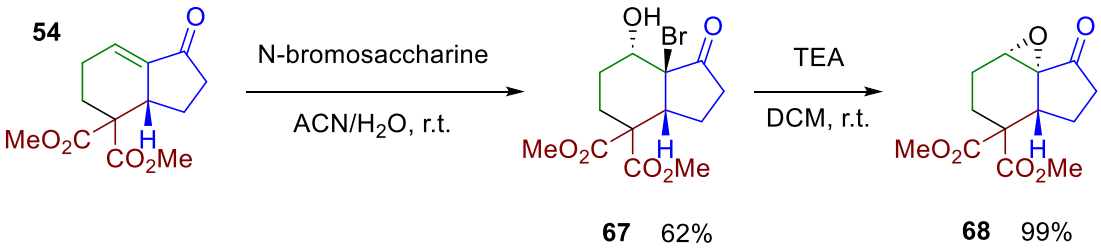

Figure 182 - Synthetis of intermediate 68

[XXII] The experiment was repeated, the product isolated and HNMR and CNMR match perfectly our spectra of **54** and the spectra reported by Reisman and co-workers.

54 was efficiently transformed into the corresponding halohydrin using N-bromosaccharine as brominating agent in the presence of water. The reaction follows the *exo* selectivity, and **67** could be isolated in 62% yield. Treatment of **67** with triethylamine in DCM triggered the formation of the epoxide **68** in quantitative yield.

68 was then treated with methyl lithium, yielding **69** in 50% yield as a 1:1 mixture of diastereoisomers. Interestingly, **69** was stable over silica gel but not to other acidic environments, as we detected the presence of two isomass compounds on a purified sample. The silylation of **69** with TSMOTf and 2,6-lutidine afforded **70** in 25% yield as inseparable 1:1 diastereoisomeric mixture (Figure 183).

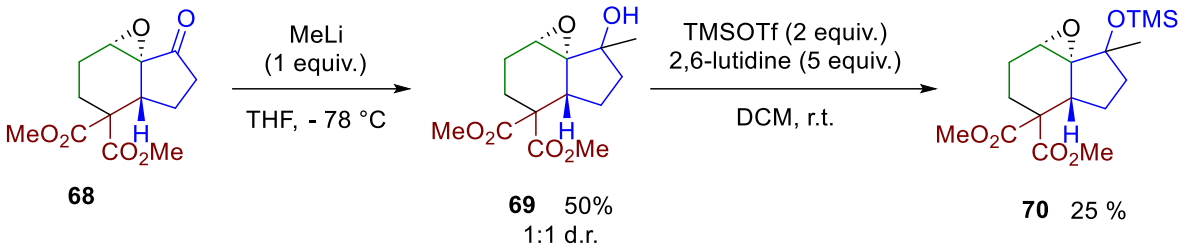

Figure 183 - Synthesis of intermediate 70

Interestingly, the attack of the nucleophile occurred both from the convex and the concave face. Probably the epoxide functionality of **68** somehow chelates the organolithium species directing the attack on the concave face. There was an attempt to break such chelation and force the attack on the convex face using a stoichiometric additive. BBu_2OTf, $MgBr_2 \bullet Et_2O$ and $Zn(OTf)_2$ were tested, but no significant improvement was obtained.

Given the poor diastereomeric ratio obtained, the difficulties encountered in the chromatographic purification of several intermediates and the fact this is an early-stage intermediate in the synthesis sequence, we decided to abandon this strategy

Best results with Diels-Alder and cut-and-sew strategy

The best results obtained with Diels-Alder reaction and the ongoing synthesis strategy are briefly resumed, to give a complete picture of the project.

Inspired by the report of Sarpong co-workers,[81] an enantioselective Diels-Alder reaction between methyl 5-oxocyclopent-1-ene-1-carboxylate (**71**) and **47** has been developed: Yb(III) triflate in combination with an enatioenriched phosphine-oxazolidine ligand works as catalyst, yielding the desired product **72** in 46% yield and 70:30 e.r. (Figure 184).

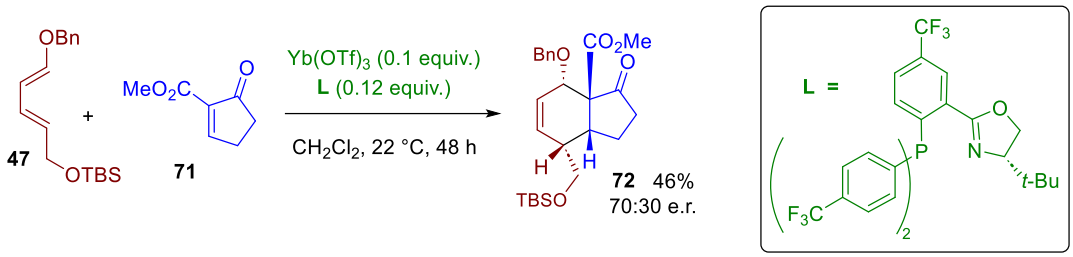

Figure 184 - Advancements in Diels-Alder reaction

72 was then converted into the corresponding triethylsilyl-enolether (**73**) and undergoes Segusa-Ito oxidation under Larock conditions[82] to give **74**.[XXIII] Then, **74** is elegantly converted to **75** by treatment with the Jones reagent. The TBS protecting group is removed under acidic conditions, the resulting primary alcohol is then oxidized to the corresponding carboxylic acid which undergoes oxa-Michael reaction to forge the lactone ring in one-pot fashion.

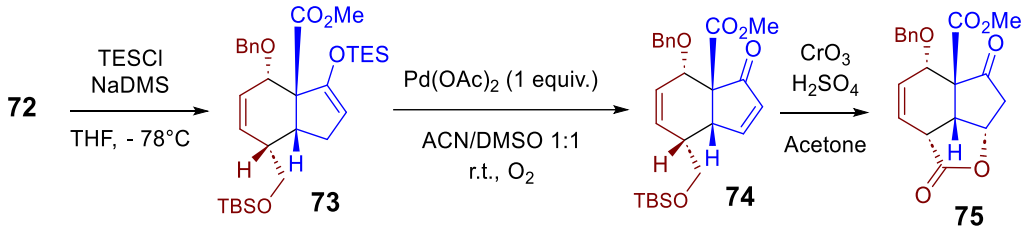

Figure 185 - Intermediate 75 synthesis

However, the synthetic elaboration of **75** to give an **A**-type product proved too hard, and the DA route was definitely abandoned.

Currently, the Romiti lab is investigating the "cut-and-sew" route. The latter describes a type of reactivity in which a Rh-based catalyst undergoes insertion into an activated C-C single bond followed by reaction with a π-system, for example of an olefin. Typically, mildly activated C-C bond activation is possible thanks to Rh^{I}-Rh^{III} catalysis. Indeed, Rh^{I}–based complexes are able to undergo oxidative insertion into C-C bonds (cut), followed by migratory insertion of the Rh-C bond to a X=X double bond and final reductive elimination (sew) to yield the desired product (Figure 186).[83]

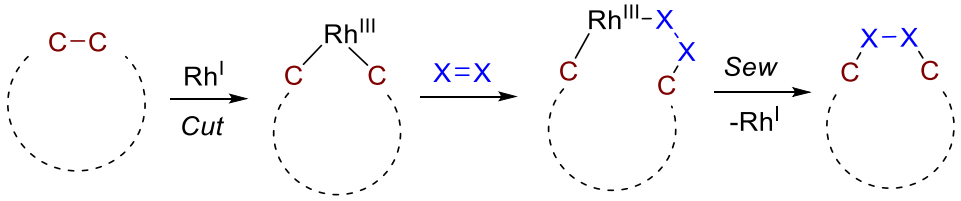

Figure 186 - Cut and sew strategy

[XXIII] Despite the use of O_2 as terminal oxidant one equivalent of palladium is needed.

Specifically, in 2014 Guangbin Dong and co-workers introduced a novel a formal [4+2] reaction between cyclobutanones and alkenes that they named “cut-and-sew".[84] This strategy can be adopted for the synthesis of the 6-membered ring such as of intermediate of type-**A** : the 5 membered ring can be derived from the usual Maimone’s ketone, and then a cyclobutanone ring can be bound (type-**B**), setting the stage for Rh-catalyzed [4+2] cycloaddition (Figure 187).

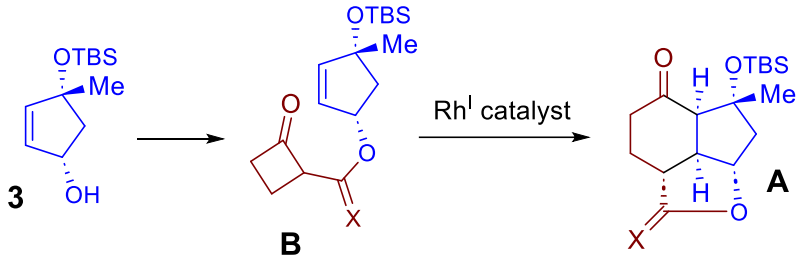

Figure 187 - Cut and sew approach to A

If this strategy works, it would be an out-of-the-box and elegant strategy to rapidly access **A**, which involve a novel cut-and-sew process.

Conclusions

The norcembranoid diterpenes are a family of natural products found in the *Sinularia* corals, showcasing interesting biological activity and unique structural features. These characteristics render norcembranoid diterpenes interesting targets for complex molecule synthesis, as evidenced by the several recent total syntheses of most family members. All the key approaches to forge the highly functionalized core have been briefly resumed in the introduction. The target of this project is to develop a general streamlined approach to the whole familythrough a mid-stage common intermediate of type **A**. This would allow quick access to these natural products for detailed biological studies and possibly pave the way for medicinal chemistry, in particular decorating the rings forges starting from **A**.

Different strategies have been tested to synthesize **A:**

- Radical cascade: starting from optically pure 5-membered carbocycles obtained through reported methodologies that is connected to a sidechain featuring a functional group capable of forming a radical and a π-system as terminal bond \. After this, radical cascade was triggered by different means, trying to induce a 5-exo/6-exo radical cascade. Different reactive groups for radicals were tested, as well as different radical initiators. However, side reactions were always observed, especially de-halogenation, which seems faster than any cyclization event. There is probably some geometrical

constraint that slows down the rate or hampers the cyclization, but we could not overcome this issue. Moreover, during the work on radical cyclization, a radical cascade approach for the synthesis of Scabrolide A and havellockate[20] was reported.

- Diels-Alder: the 6-membered ring can be constructed by a Diels-Alder reaction with a cyclopentene or cyclopentenone derivative. Optically pure 5-membered carbocyclic rings were thus synthesized using reported methodologies. These can be linked to a proper sidechain containing the diene necessary for the [4+2] intramolecular process or can be reacted *directly* with a diene intermolecularly. Different dienes, dienophiles and tethered substrates were synthesized and tested under different activation modes reported for Diels-Alder reactions: thermal, "hole" catalysis, rare earth or transition metal cations as Lewis acids, activated CBS as Lewis acid and organocatalysis via iminium ion. However, no cycloaddition product has ever been observed. we postulated that the lack of reactivity is, once again, due to geometrical constrains, but we are currently unable to provide an exhaustive rationale for *ll* the failed results. However, it was discussed that probably the ester configuration and the furane tendency to undergo retro-cycloaddition somehow contributed to the failure of this strategy. After extensive efforts by the group, the only successful Diels-Alder reaction uses a 2-carboxycyclopentenone as dienophile, with modest yield and enantiomeric excess.

Michael addition-intramolecular aldol reaction: another possible method to synthesize the 6-membered ring enatils the Michael addition of an appropriate nucleophile to a cyclopentenone derivative, followed by intramolecular aldol reaction and lactone ring closure. Reisman and co-workers[26] reported the synthesis of a very similar bicyclic system using Shibasaki catalyst[76] for the enantioselective Michael addition step. We then tested the functionalization of **54**, and we found it difficult to handle the products, as they tend to decompose. Also the methyl addition to **68** is not diastereoselective. The only positive result is the preparation of epoxde **65**. However, this synthetic route is not very appealing, as it requires several steps. To summarize, despite our efforts we could not gain any significant advance in the synthesis of norcenmbranoid diterpenes family. Currently, the "cut-and-sew" methodology is under investigation in the laboratories of UTD.

Supporting information

It follows the experimental data collected for the total synthesis of nocernmbranoid diterpenes. NMR spectra were recorded using a Bruker Ascend ™ 500 Avance NEO

with Prodigy cryoprobe. Only the most meaningful experiments and the isolated products cited in the thesis are reported, together with their experimental preparation.

3 - (1S,4R)-4-((tert-butyldimethylsilyl)oxy)-4-methylcyclopent-2-en-1-ol

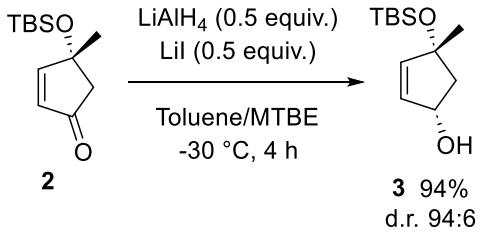

LiI (960 mg, 7,18 mmol) was punt under nitrogen and at -30 °C and then 41 ml of dry toluene were added, followed by 9,3 ml of 1M LiAlH4 (9,33 mmol). Then, the solution was treated dropwise with a solution of the ketone **2** (3,25 g) in MTBE (16,25 ml). The solution was stirred at the same temperature until the disappearance of the SM monitored by TLC. Quench: NH4Cl, then extraction with AcOEt. Dry over $MgSO_4$, filter, remove solvent. 3,02 g of **3** were recovered (92 % yield). The product was used as it is for the next steps. If desired, the product can be purified by column chromatography to remove the undesired diastereoisomer. d.r. 94:6 (C-H under the alcohol monitored). d.r. can drop down to 90:10 scaling-up the reaction, probably for temperature control due to high scale.

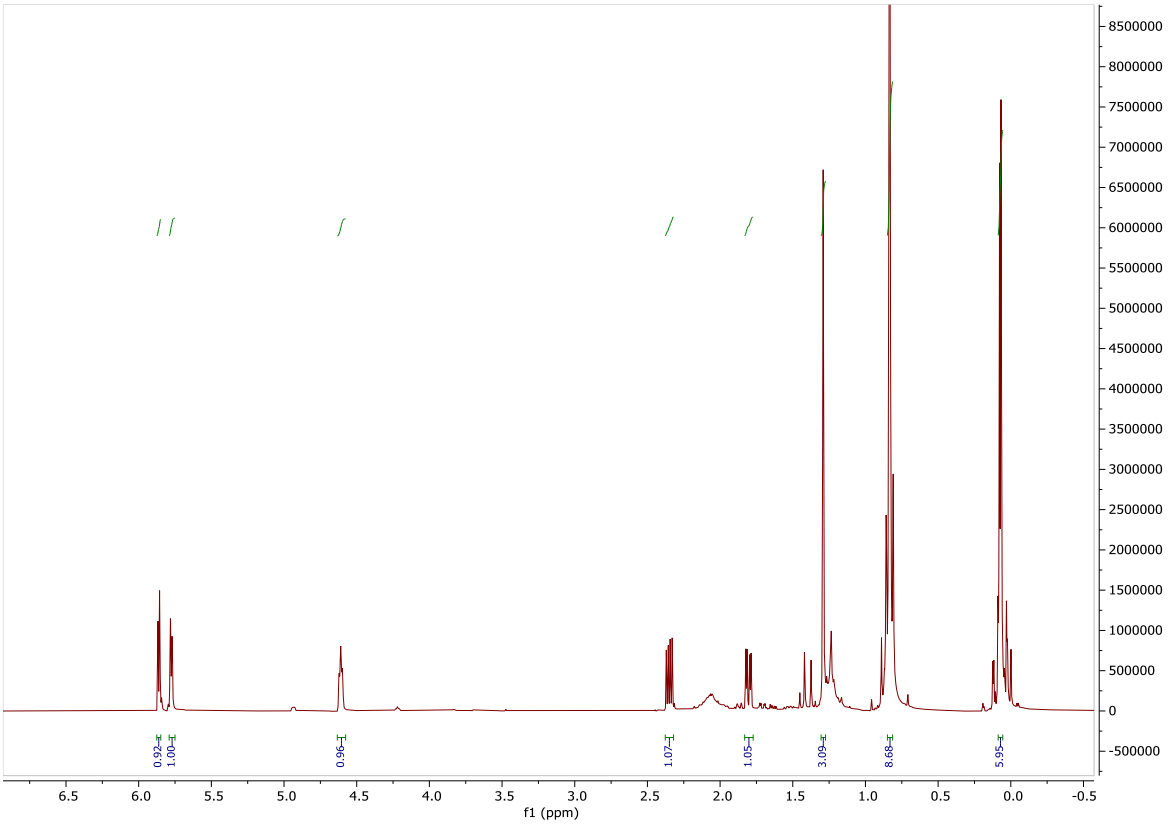

3 - 1H NMR (500 MHz, CDCl3) δ 5.86 (d, J = 5.7 Hz, 1H), 5.78 (dd, J = 5.6, 1.9 Hz, 1H), 4.61 (m, 1H), 2.35 (dd, J = 13.3, 6.9 Hz, 1H), 1.81 (dd, J = 13.3, 4.7 Hz, 1H), 1.29 (s, 3H), 0.077 (s, 3H), 0.067 (s, 3H).

4 - ethyl 4-cyanobutanoate

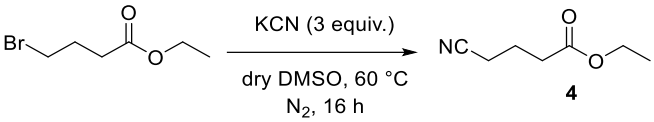

3 g of the bromo ester (15,28 mmol) are put into a 100 ml 1neck RBF. Then, 35 ml of dry DMSO are added, followed by 3 g (46,14 mmol) of KCN. The system is brought to 60 °C for 18 h. Then, the solution is quenched with 123 ml of water and the system is extracted with ethyl acetate (80 ml x 3). Then, the organic phase is washed with brine (80 ml) and the dried over MgSO4. The solvent is then removed under reduced pressure. More washing with water could be necessary to remove completely the residual DMSO. After solvent removal, 2,165 g are obtained for a 99% yield. The products was used as it is for the next step.

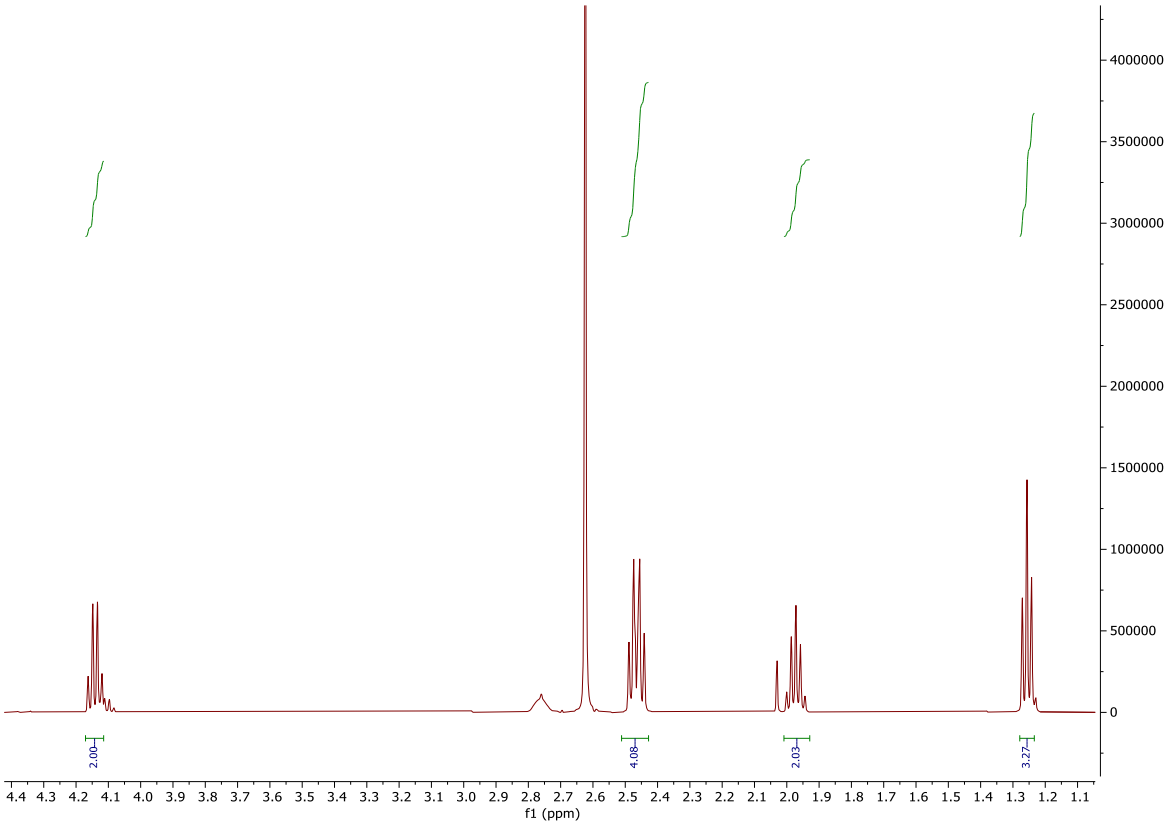

4 - 1H NMR (500 MHz, CDCl3) δ 4.12 (t, J = 7.2 Hz, 2H), 2.47 (ddd, J = 10.1, 8.0, 6.6 Hz, 4H), 2.05 – 1.92 (m, 2H), 1.29 – 1.21 (t, J = 6.9 Hz 3H). (Residual DMSO in the spectrum, later removed).

5 – 4-cyanobutanoic acid

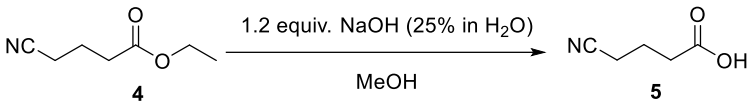

2,17 g (15,3 mmol) of the target compound 4 were transferred into a RBF using 10 ml of MeOH. Then, 1 ml of NaOH 50% in water was added. After 4 h the reaction was quenched with 12 ml of 4 M HCl. Then, 125 ml of water were added and the solution is extracted with EtOAc several times. Then, the organic phase is dried over MgSO4, filtered and the solvent removed under reduced pressure. To yield 1,73 g of 5 (99 % yield).

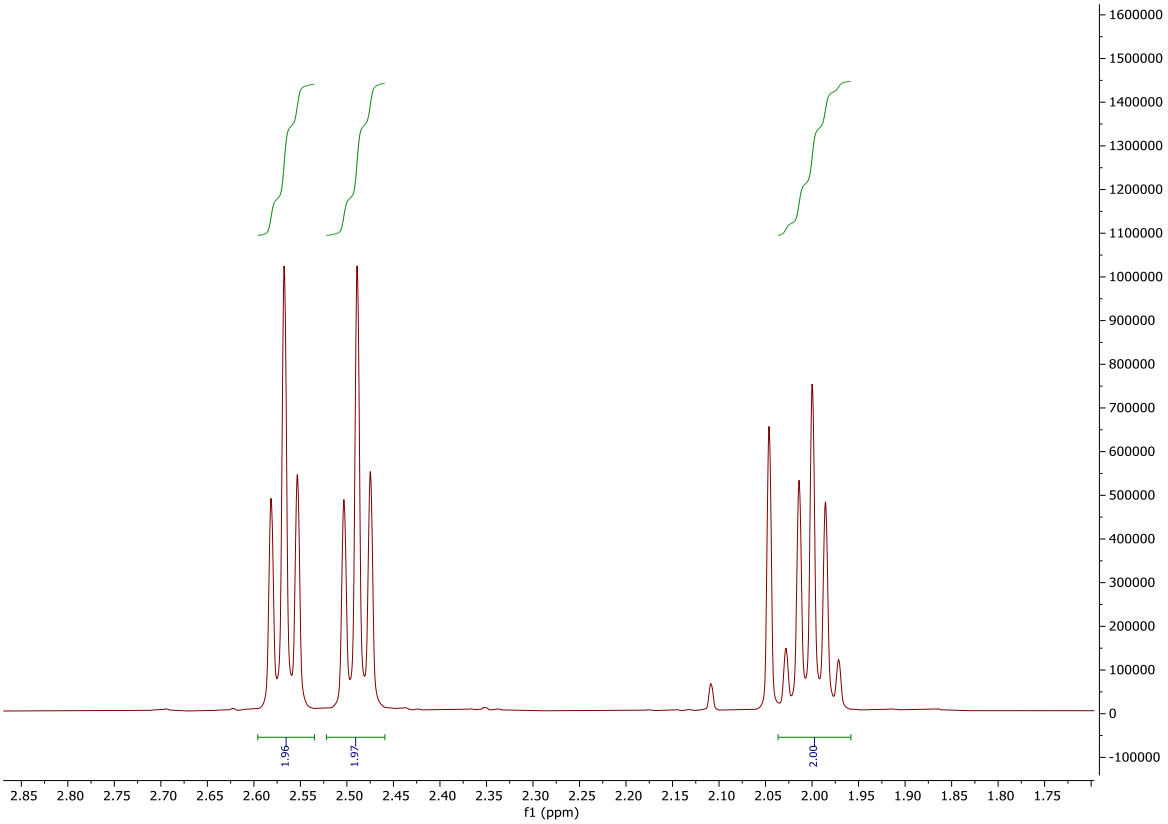

5 - 1HNMR (500 MHz, CDCl3) δ 2.57 (t, J = 7.0 Hz, 1H), 2.49 (t, J = 7.1 Hz, 1H), 2.00 (t, J = 7.1 Hz, 1H). Spectrum has small traces of ethyl acetate.

6 – (1S,4R)-4-((tert-butyldimethylsilyl)oxy)-4-methylcyclopent-2-en-1-yl 4-cyanobutanoate

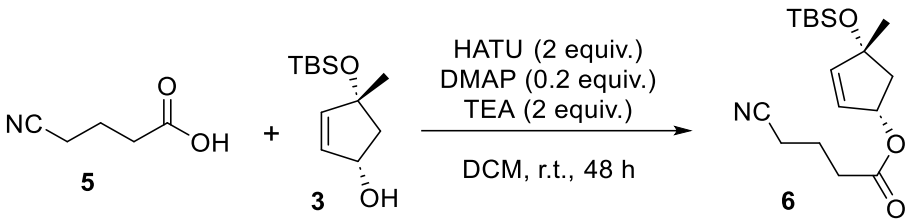

59 mg of the acid (0,5 mmol) were weighted into a 50 ml 2 neck RBF and put under N2. Into a separated vial, 100 mg of the alcohol (0,86 mmol) were weighted and put under inert atmosphere. Then, 3,9 ml of dry DCM were used to dissolve the alcohol and are transferred to the acid. Then, TEA (119 ul, 0,88 mmol) is injected, followed by DMAP (10,7 mg, 0,09 mmol). Finally, 333 mg (0,88 mmol) of HATU were added. The reaction is left to stirr at r.t. for 48 h.

Quench: the reaction is quenched with water and extracted with DCM. Then, the organic phase is dried over MgSO4, filtered and the solvent is removed under reduced pressure.

TLC (4:1 Hex-AcOEt) shows the formation of one product (but when isolated it's a by-product). SM and product not separated by TLC. HNMR monitoring is needed.

Column using Combiflash (method saved - 95:5 to 90:10, direct gradient)

94,8 mg of **6** recovered (70 % yield). By 1HNMR the two diastereoisomers formation is clearly visible. It comes in the same ratio of the starting material 3 (9:1).

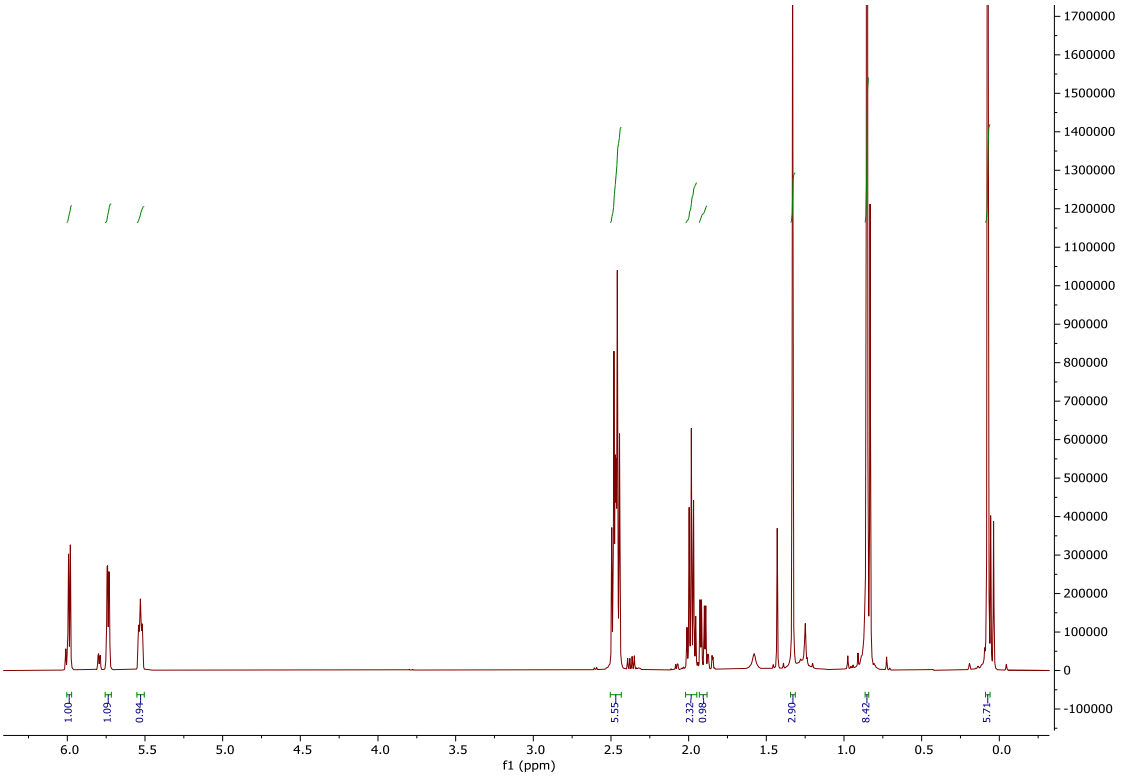

6 - 1H NMR (500 MHz, CDCl3) δ 5.99 (dd, J = 5.6, 1.2 Hz, 1H), 5.74 (dd, J = 5.5, 2.0 Hz, 1H), 5.55 – 5.51 (m, 1H), 2.47 (dt, J = 10.9, 7.2 Hz, 6H), 1.98 (p, J = 7.0 Hz, 2H), 1.91 (dd, J = 13.8, 4.8 Hz, 1H), 1.33 (s, 3H), 0.85 (s, 8H), 0.07 (d, J = 1.6 Hz, 6H).

9 - tert-butyl pent-4-ynoate

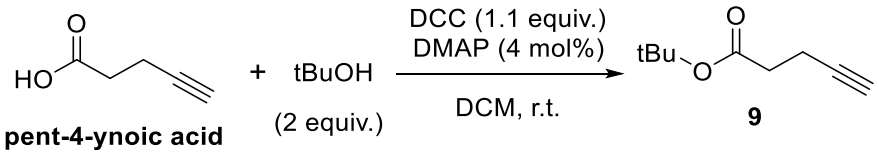

2 g (20,4 mmol) of acid were dissolved in dry DCM (8 ml). It follows the addition of tBuOH (3,9 ml, 40,8 mmol), DMAP (100 mg, 0,8 mmol). Then, 4,63 g (22,4 mmol) of DCC dissolved in 8 ml of dry DCM are added over the other DCM solution. The reaction was left to stir overnight. In the morning, the reaction was quenched with water and the organic phase separated. The aqueous phase was then extracted with DCM. The organic phases were then merged and the solvent is removed under reduced pressure. Then, ester **9** is purified by column chromatography, recovering 2,43 g (77 % yield). 1H NMR spectrum was not very clear, but the next step after purification confirmed product formation.

10 – tert-butyl hexa-4,5-dienoate

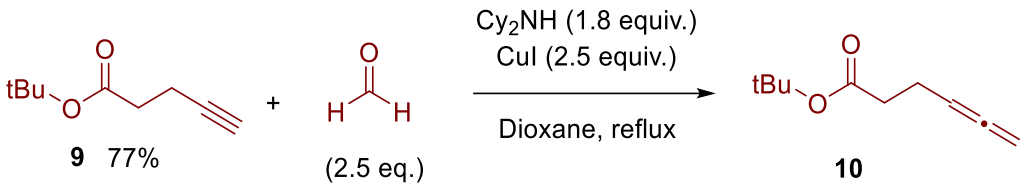

2,43 g (15,8 mmol) of alkyne **9** are weighted into a round bottom flask. Then, paraformaldehyde (900 mg, 39,4 mmol), and CuI (1,50 g, 7,9 mmol) were added and put under inert atmosphere. Then, dry dioxane (22,5 ml) was added to dissolve everything, followed by the addition of Cy_2NH (5,64 ml, 28,4 mmol). The reaction is refluxed overnight. Then, after cooling to room temperature the solution was filtered through a pad of celite, washing with Et2O. Then, the solution was diluted with 70 ml of Et2O and washed with 70 ml of HCl 1M. The aqueous phase is then extracted further with Et2O. The organic phase was washed with NaHCO3, then washed with brine, dried over MgSO4, filtered and the solvent was removed under reduced pressure.

The crude is purified directly by column chromatography (Hex:Et2O 9:1, TLC check 1:1). 1,68 g of material were recovered. However, by HNMR the presence of dioxane was still detected (it was not possible to remove it completely during the work-up). By peak integration the mass of compound was calculated to be around 1,61 g, (61 % yield).

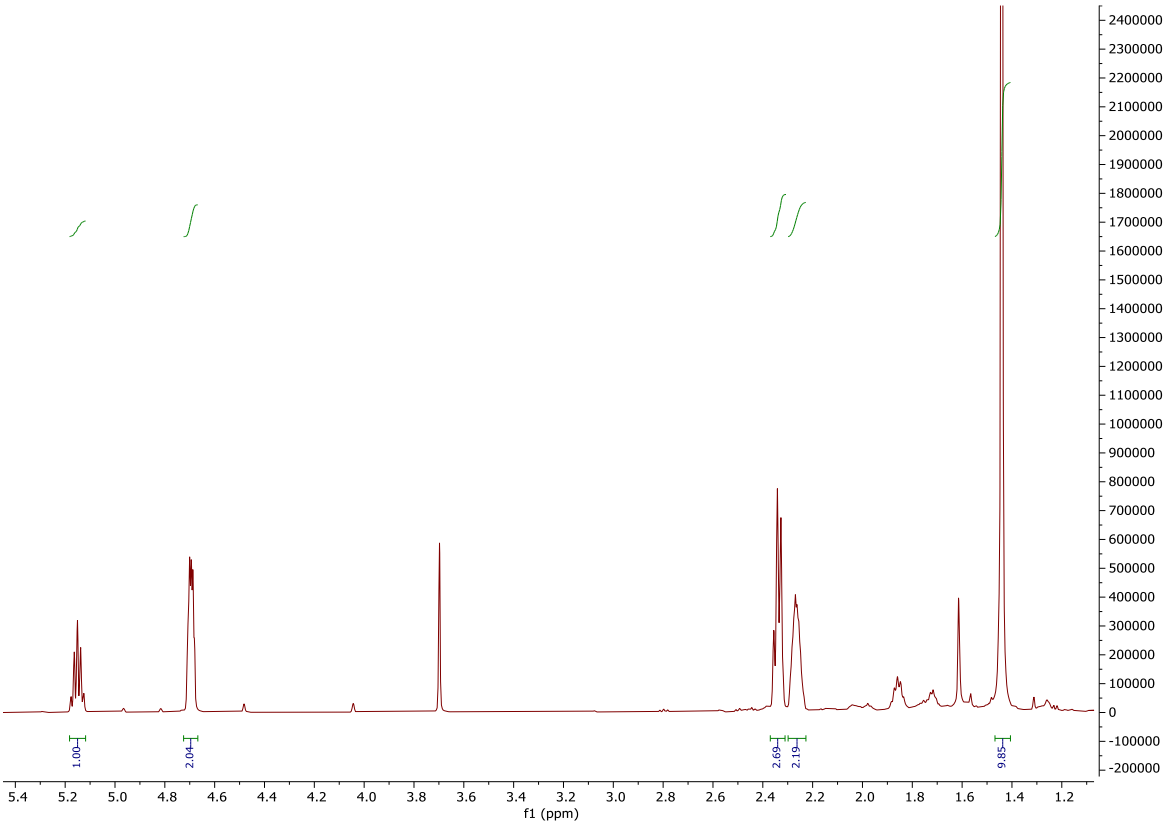

10 - 1H NMR (500 MHz, CDCl3) δ 5.15 (p, J = 6.4 Hz, 1H), 4.70 (dq, J = 6.6, 2.7 Hz, 2H), 2.34 (t, J = 7.3 Hz, 3H), 2.27 (dq, J = 7.3, 3.6 Hz, 2H), 1.44 (d, J = 1.9 Hz, 9H).

12^{I} – dimethyl 2-(but-3-en-1-yl)malonate

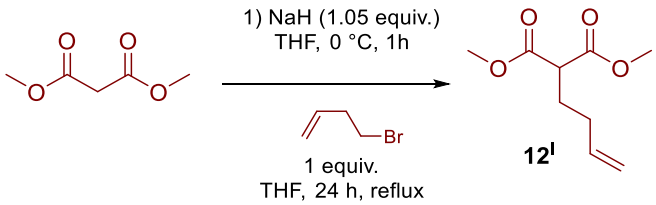

3 g (22,7 mmol) of dimethyl malonate were put into a round bottom flask and dissolved in 75 ml of dry THF. It follows the addition of sodium hydride (953 mg, 23,8 mmol) and the reaction is left to stir for 10 minutes. Then, 4-bromobutane (3,07 g, 23,8 mmol) was added and the reaction is set/up to reflux for 24 h. The reaction is quenched with saturated NaHCO3 (10 ml) and extracted with AcOEt. The organic phase is dried over MgSO4, filtered and the solid is removed under reduced pressure. Then, the product is purified by column chromatography. 1,67 g of **12**^{I} were recovered (40 % yield).

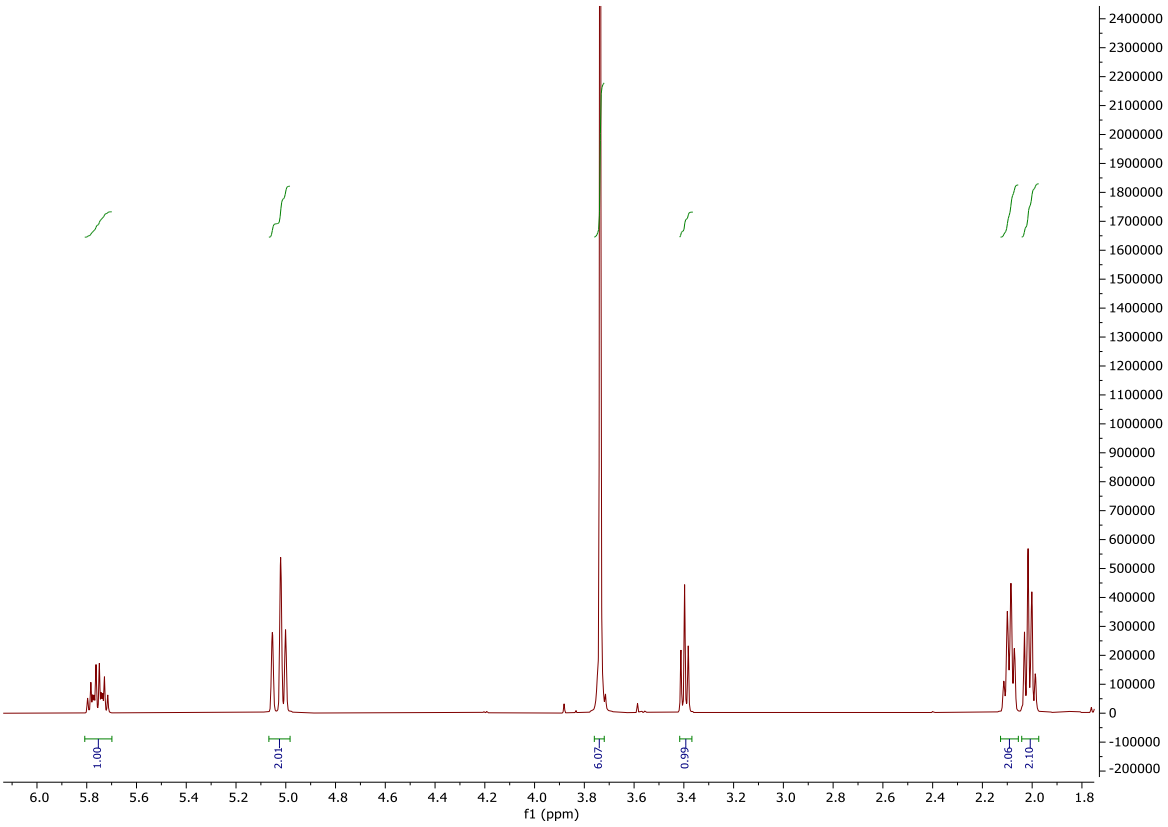

12^{I} - 1H NMR (500 MHz, CDCl3) δ 5.76 (ddt, J = 16.9, 10.2, 6.6 Hz, 1H), 5.11 – 4.88 (m, 2H), 3.74 (s, 6 H), 3.40 (t, J = 7.3 Hz, 1H), 2.09 (m, 2H), 2.04 – 1.97 (m, 2H).

13^{I} - 2-(ethoxycarbonyl)hex-5-enoic acid

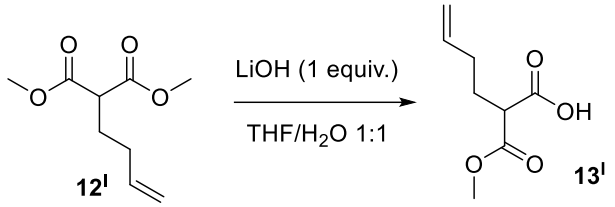

To a solution of 1,67 g (9 mmol) of substrate **12**^{I} in THF (89 ml) and water (8,9 ml), a solution of KOH (603 mg) in water (28 ml) was added. The reaction is left to stir overnight at room temperature. The reaction is quenched with 50 ml of 0,5 M HCl. Then, the reaction is partitioned between brine and AcOEt, extracting with AcOEt. The organic phase is dried over MgSO4, filtered and the solvent is removed under reduced pressure. HNMR confirms complete conversion and a practical quantitative recovery of **13**^{I}. The product was used as it is for other transformations.

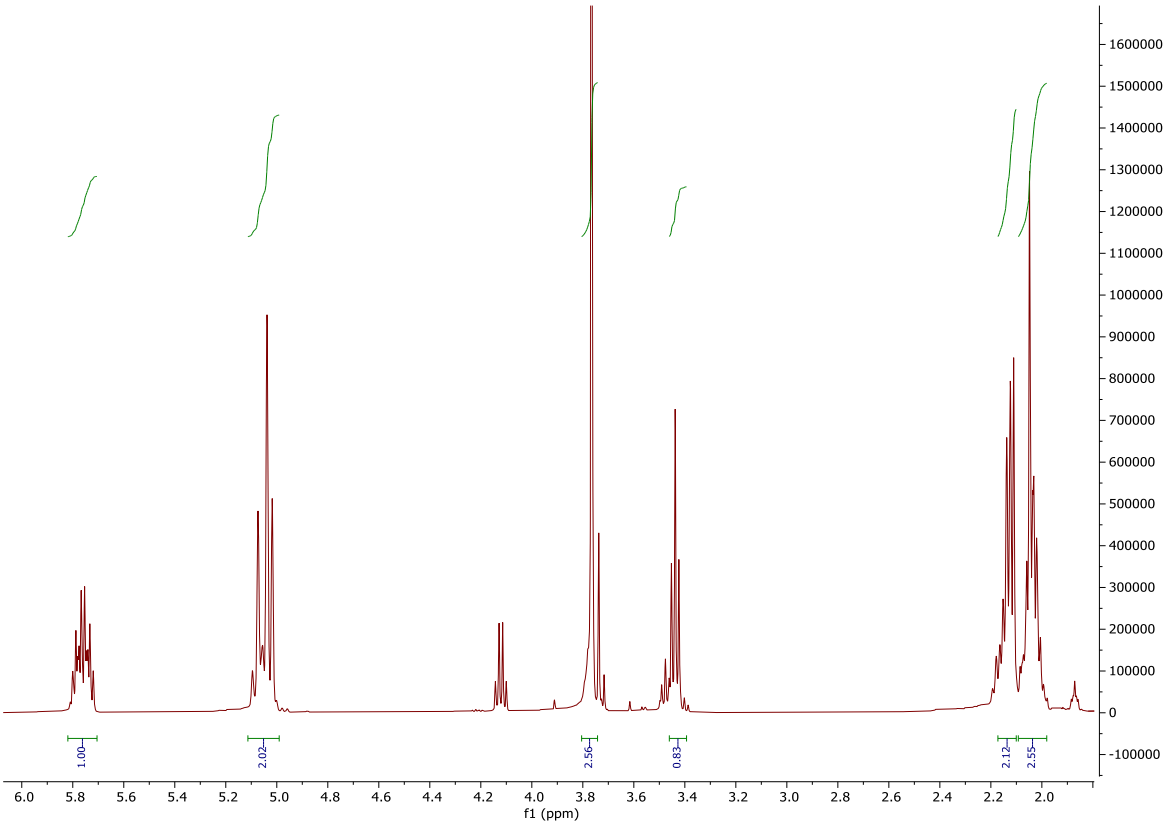

13^{I} - 1H NMR (500 MHz, CDCl3) δ 5.76 (m, 1H), 5.12 – 4.96 (m, 2H), 3.77 (s, 2H), 3.44 (t, J = 7.3 Hz, 1H), 2.13 (dd, J = 14.0, 6.8 Hz, 2H), 2.09 – 1.99 (m, 2H). (traces of ethyl acetate in the spectrum).

13^{II} - 4-cyano-2-(ethoxycarbonyl)butanoic acid

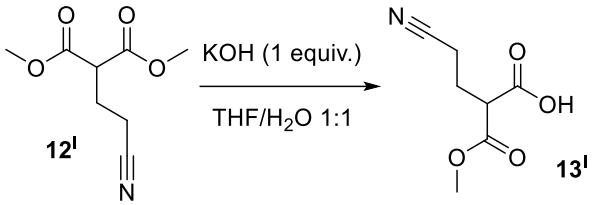

To a solution of 1,33 g (7,18 mmol) of diethyl 2-(2-cyanoethyl)malonate in THF (104 ml) and water (10,4 ml), a solution of KOH (489 mg, 8,62 mmol) in water (33 ml) was added. The reaction is left to stirred overnight at room temperature. The reaction was quenched with 50 ml of 0,5 M HCl. Then, the reaction was partitioned between brine and AcOEt, extracting with AcOEt. The organic phase is dried over MgSO4, filtered and the solvent is removed under reduced pressure.

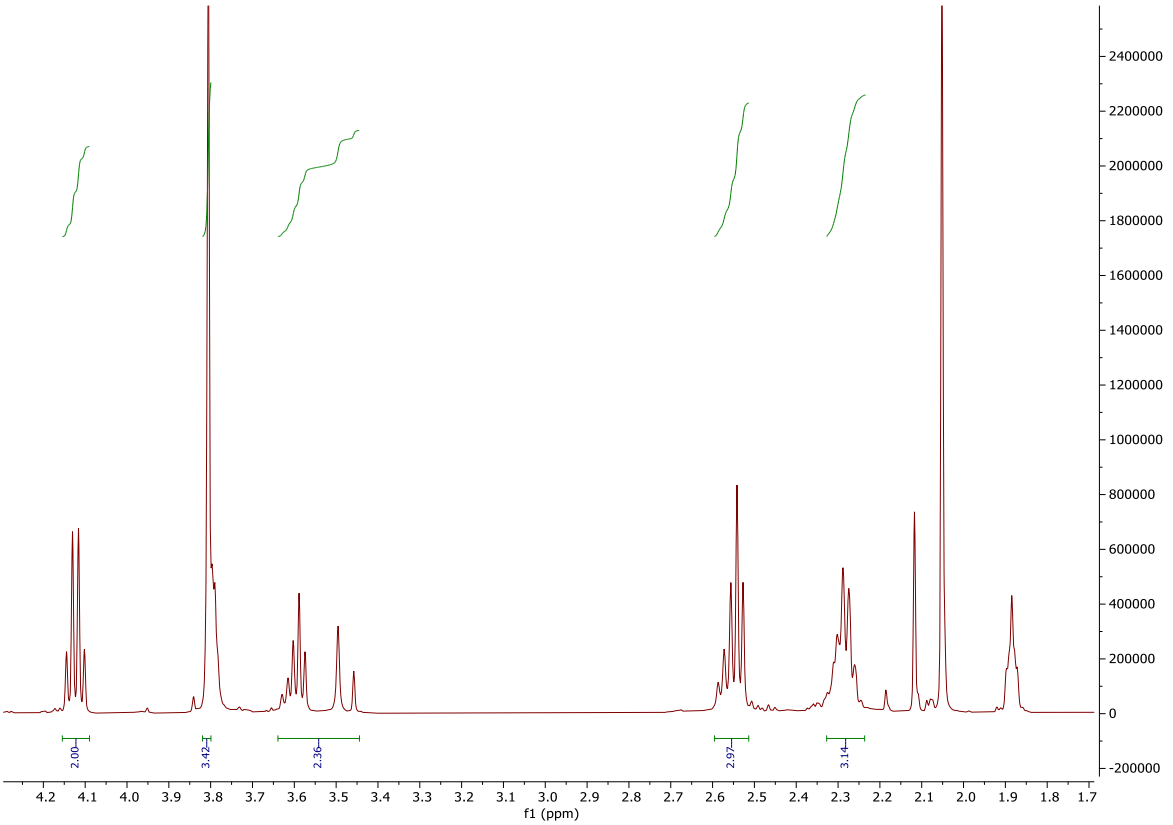

13^{II} - 1H NMR (500 MHz, CDCl3) δ 4.12 (q, J = 7.1 Hz, 1H), 3.81 (s, 2H), 3.64 – 3.44 (m, 1H), 2.56 (m, 3H), 2.33 – 2.23 (m, 3H). Spectrum contains traces of THF and ethyl acetate.

14[I] - 1-((1S,4R)-4-hydroxy-4-methylcyclopent-2-en-1-yl) 3-methyl 2-allylmalonate

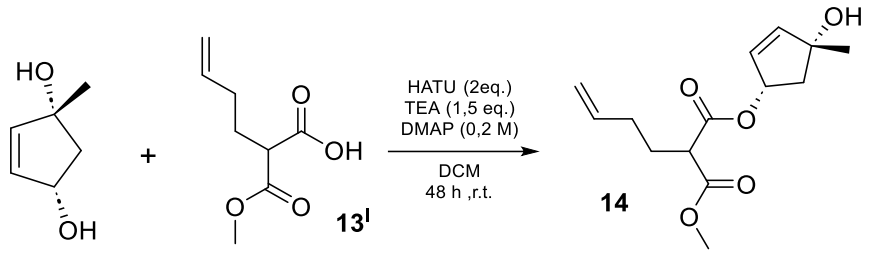

181 mg of diol (1.6 mmol) were weighted into a vial and put under inert atmosphere. Then, 5 ml of dry DCM were used to dissolve the substrate. Then TEA (332 ul, 2.4 mmol) was added, followed by DMAP (58 mg, 0.46 mmol) and finally by DIC (372 ul, 2.4 mmol). The reaction was left to stir 24 h. After this time, reaction quenched with aqueous NH4Cl, separating the organic layer. The organic layer was then dried over MgSO4, filtered and the solvent removed under reduced pressure. Crude was purified by column chromatography in pure ethyl acetate, recovering 174 mg of product (43% yield). HNMR is very complicated, as two diastereoisomers are formed (carboxylic acid is racemic). It is not possible to characterize the two isomers peak by peak. Moreover, looking at the spectrum there is maybe a third diastereoisomer, maybe coming from the isomerization of allylic position happened somehow. Another hypothesis is that there are rotamers around. In any case the isolated product mixture was used for the next steps, without showing any relevant reactivity.

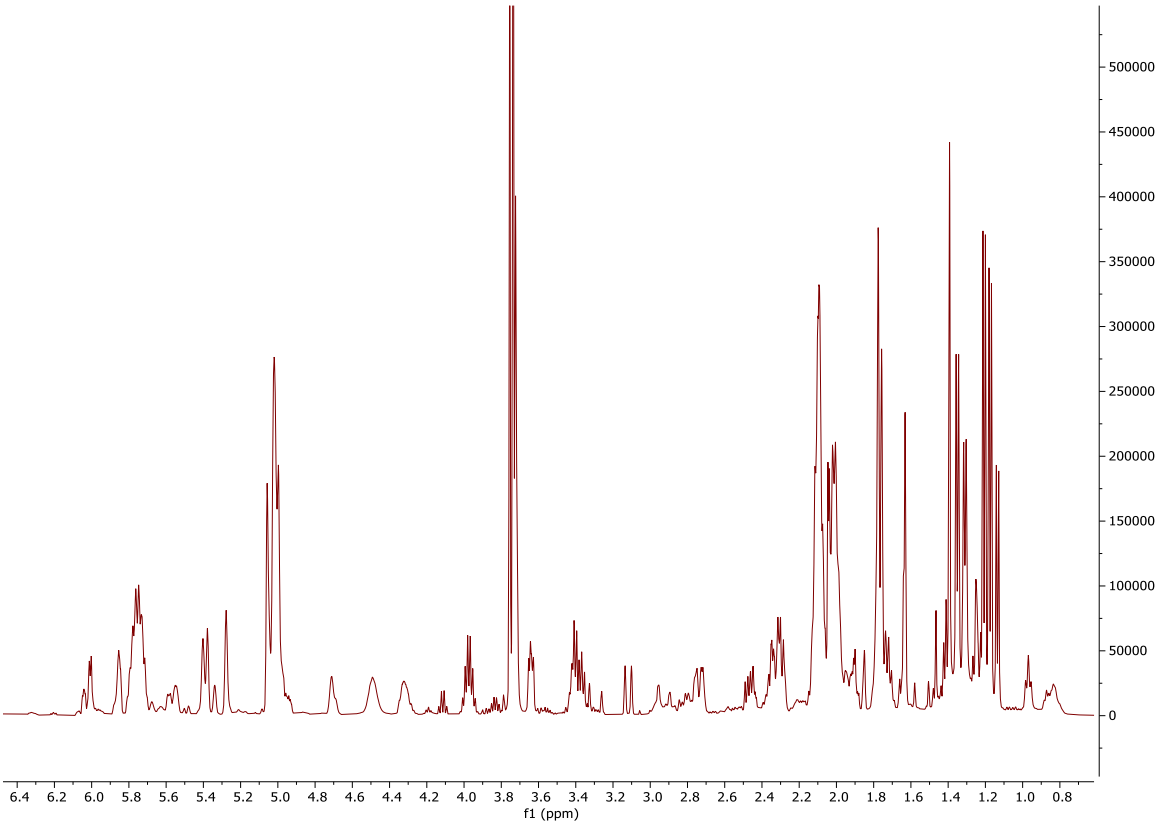

14^{II} - 1-((1S,4R)-4-((tert-butyldimethylsilyl)oxy)-4-methylcyclopent-2-en-1-yl) 3-methyl 2-allylmalonate

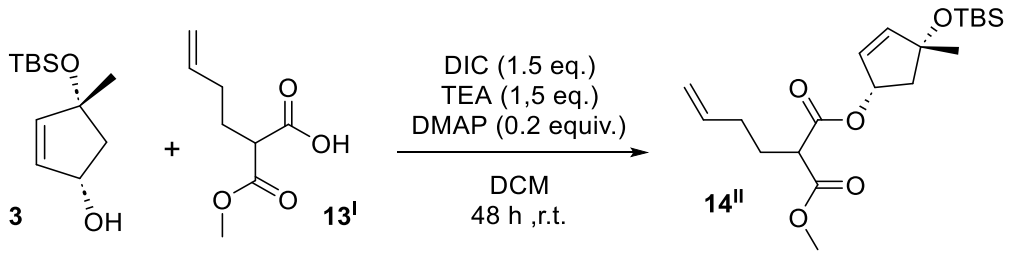

200 mg of alcohol **3** (0.87 mmol) were weighted into a vial and put under inert atmosphere. Then, 5 ml of dry DCM were used to dissolve substrate 13^{I}. The DCM solution was injecting the vial containing **3**, making an homogeneous solution. Then TEA (147 ul, 1.05 mmol) was added, followed by DMAP (21.4 mg, 0.175 mmol) and finally by DIC (206 ul, 1.05 mmol). The reaction was left to stir 24 h. After this time, reaction quenched with aqueous NH4Cl, separating the organic layer. The organic layer was then dried over MgSO4, filtered and the solvent removed under reduced pressure. Crude was purified by column chromatography in pure ethyl acetate, recovering 32 mg of product (9% yield). Other byproducts were recovered. HNMR is very complicated, as two diastereoisomers are formed (carboxylic acid is racemic). It is not possible to characterize the two isomers peak by peak. Another hypothesis is that there are rotamers around. In any case the

isolated product mixture was used for the next steps, without showing any relevant reactivity.

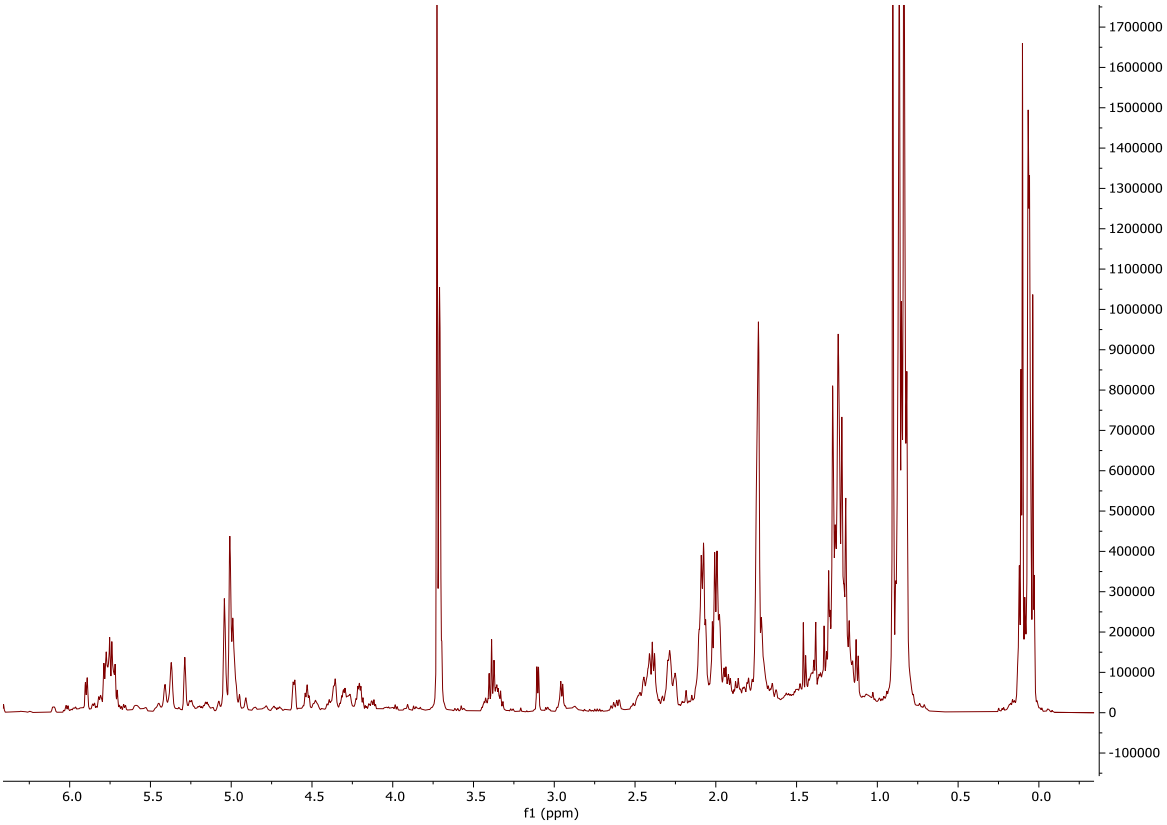

14^{III} - 1-((1S,4R)-4-((tert-butyldimethylsilyl)oxy)-4-methylcyclopent-2-en-1-yl) 3-methyl 2-(2-cyanoethyl)malonate

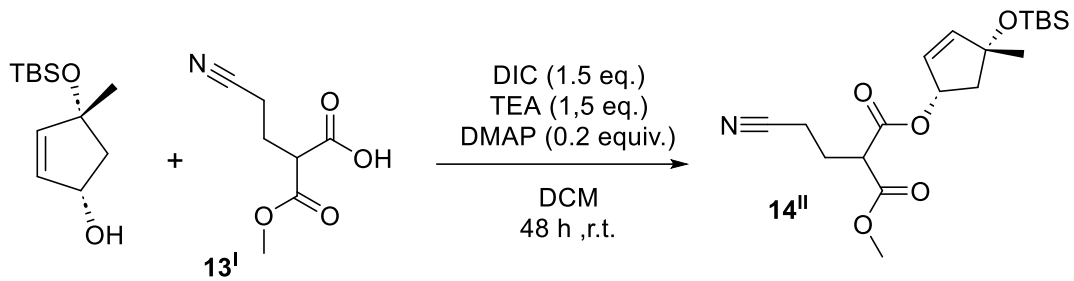

450 mg (2.63 mmol) of the acid were weighted into a round bottom flask and put under N2. Into a separated vial, 400 mg (1.75 mmol) of the alcohol 3 were weighted and put under inert atmosphere. Then, 32 ml of dry DCM were used to dissolve the alcohol and are transferred to the acid. Then, TEA (477 ul, 3.50 mmol) is injected, followed by DMAP (43 mg, 0.35 mmol). Finally 1,33 g (3.5 mmol) of HATU were added. The reaction is left to stirr at r.t. for 48 h.

Quench: the reaction is quenched with water and extracted with DCM. Then, the organic phase is dried over MgSO4, filtered and the solvent is removed under

reduced pressure. Separation by column chromatography yields product **14**^{III}. Curiously, this seems to be mostly on diastereoisomer.

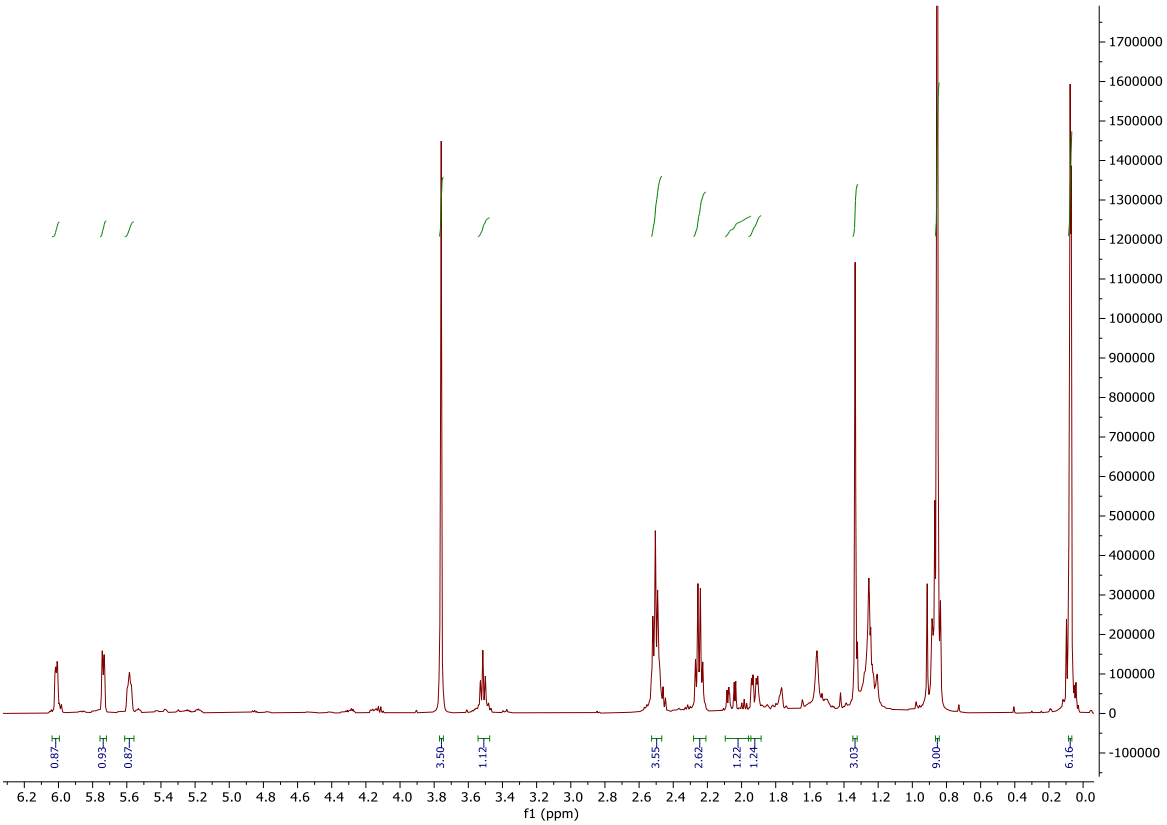

14^{III} - 1H NMR (500 MHz, CDCl3) δ 6.04 – 5.99 (m, 1H), 5.74 (d, J = 5.6 Hz, 1H), 5.58 (t, J = 6.4 Hz, 1H), 3.76 (s, 3H), 3.51 (t, J = 7.2 Hz, 1H), 2.50 (q, J = 6.5 Hz, 4H), 2.25 (q, J = 7.2 Hz, 2H), 2.10 – 2.03 (m, 1H), 1.92 (dd, J = 13.9, 4.9 Hz, 1H), 1.33 (s, 3H), 0.85 (s, 9H), 0.07 (d, J = 3.3 Hz, 6H).

20 - ethyl 5-oxocyclopent-1-ene-1-carboxylate

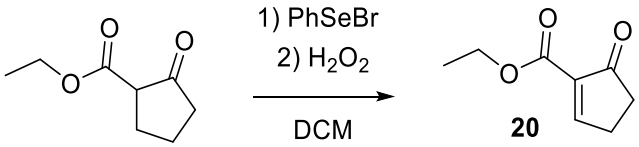

PhSeBr (5 g, 21.1 mmol) was weighted into a round bottom flask and set-under inert atmosphere. It follows the addition of 130 ml of dry DCM and 2,32 ml of dry pyridine. Then, the acylcyclopentanone (3 g, 19.2 mmol) was added dropwise and the reaction left to stir overnight.

Then, HCl 1 M (135 ml) is added to quench the reaction and the organic phase is washed with NaHCO3 and dried over MgSO4, before undergoing the addition of

35% H2O2 (5 ml, 58 mmol) and left to stir at room temperature for 2 hours. Then, the reaction is quenched with water and NaHCO3, directly separating the organic phase, which is then dried over MgSO4, filtered and the DCM is removed under reduced pressure. Product 20 was then purified by column chromatogtaphy (1:1 AcOEt:Hex). 2.2 g of 21 were recovered (74% yield).

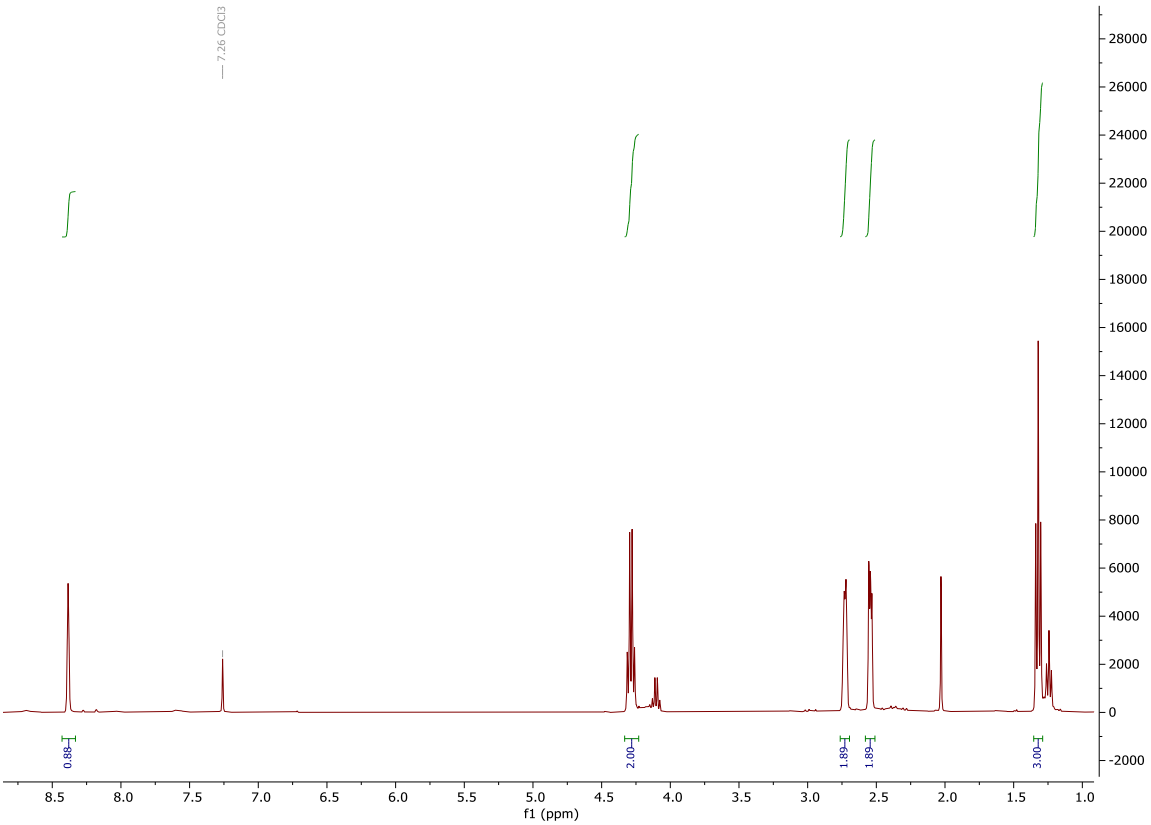

1H NMR (400 MHz, CDCl3) δ 8.42 – 8.34 (m, 1H), 4.29 (qd, J = 7.1, 1.1 Hz, 2H), 2.76 – 2.69 (m, 2H), 2.57 – 2.52 (m, 2H), 1.32 (td, J = 7.2, 1.1 Hz, 3H). Small traces of ethyl acetate are left.

23 – cyclopenta-1,3-diene

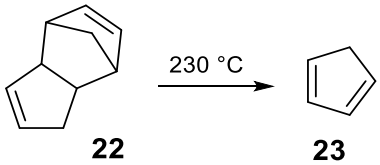

23 was obtained by destructive retro Diels-Alder of bis-cyclopentadiene. It is sufficient to heat the material to at least 170 °C and condense the vapors with a short-distillation path condenser in which ice-bath water circulates. To minimize losses, the trap was soaked in a bath of acetone and dry ice. In this way, up to 20

g of **23** could be made. An image of the distillation system is shown below. The product was used immediately as it is to avoid degradation. However, I tested that the product lasts for at least a few days in the dry ice box without visible degradation.

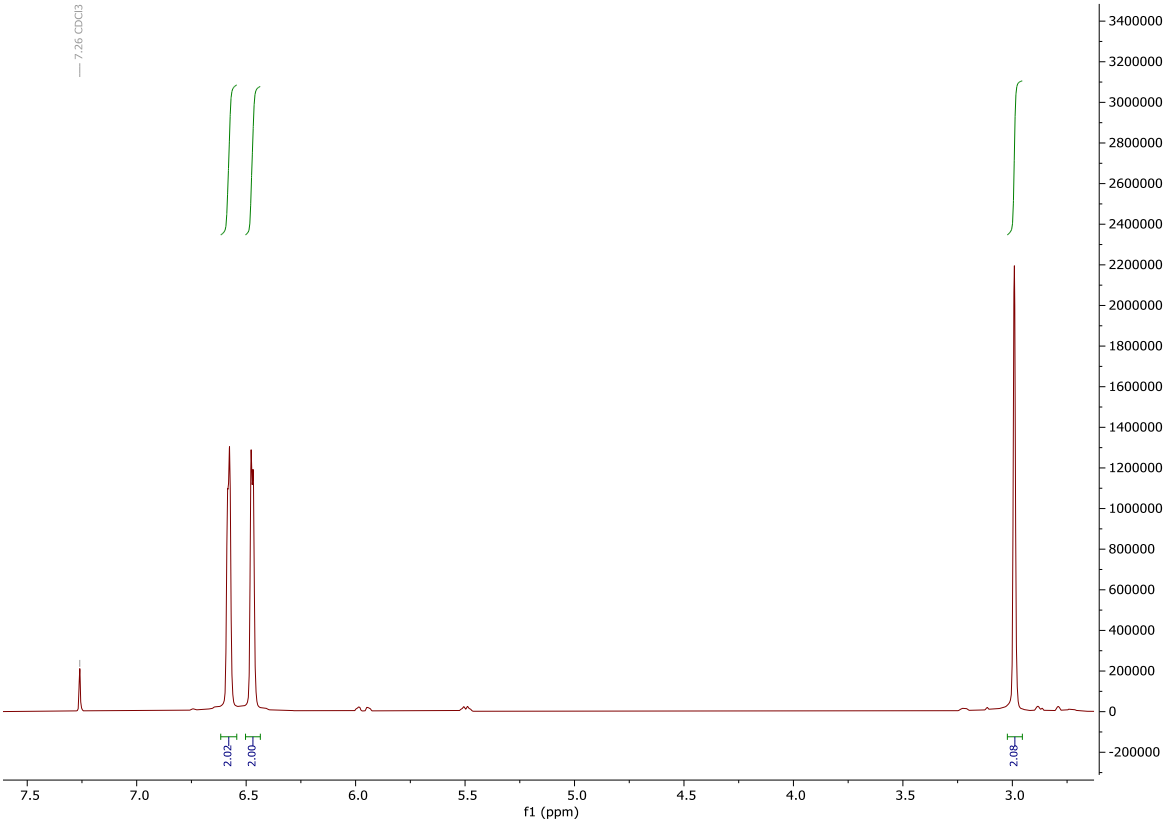

23 - 1H NMR (500 MHz, CDCl3) δ 6.58 (q, J = 2.1 Hz, 2H), 6.47 (t, J = 5.0 Hz, 2H), 2.99 (s, 2H).

24 – (1R,3S)-cyclopent-4-ene-1,3-diol

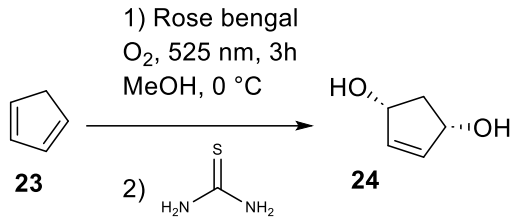

23,5 g of freshly prepared **23** were dissolved in 1 liter of methanol. It followed the addition of 723 mg of rose Bengal. Then, the environment was saturated with O_2. A balloon filled with O_2 feeds the system. The solution was irradiated for 3 hours with a 525 nm Kessil lamp at full power, keeping the solution at 0 °C with an ice bath. Conversion can be checked easily by HNMR. After this time 27,1 g of thiourea were added and the solution allowed to stir for 16 hours. After this time, methanol was removed under reduced pressure and **24** purified by column chromatography (19,5 g, 55% yield).

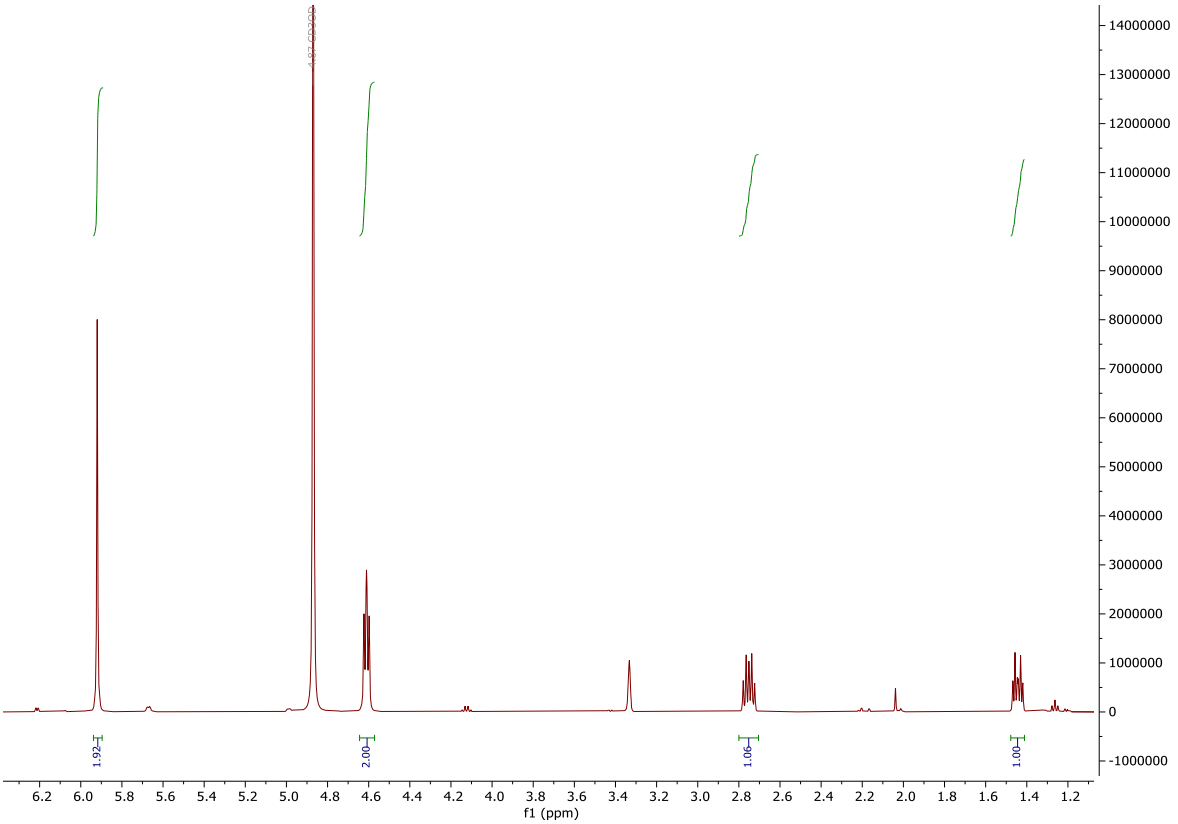

24 - 1H NMR (500 MHz, MeOD) δ 5.92 (s, 2H), 4.61 (dd, J = 7.2, 5.4 Hz, 2H), 2.75 (dt, J = 14.1, 7.3 Hz, 1H), 1.44 (dt, J = 13.4, 5.4 Hz, 1H).

25 - (1R,3S)-cyclopent-4-ene-1,3-diyl diacetate

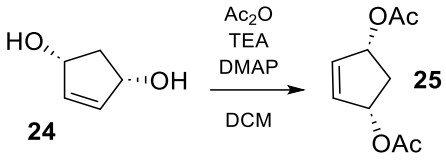

1,04 g (10,4 mmol) of 24 were dissolved into 20 ml of dry DCM under inert atmosphere. Then, 4,34 ml of triethylamine (31,2 mmol) were added, followed by 2,95 ml of acetic anhydride (31,2 mmol). The reaction was left to stir at room temperature for xxx hours. After this time the reaction was quenched with water and extracted with DCM. The organic solvent was then removed under reduced pressure and the compound purified by column chromatography (9:1 Hex:AcOEt). 750 mg were recovered (39 % yield).

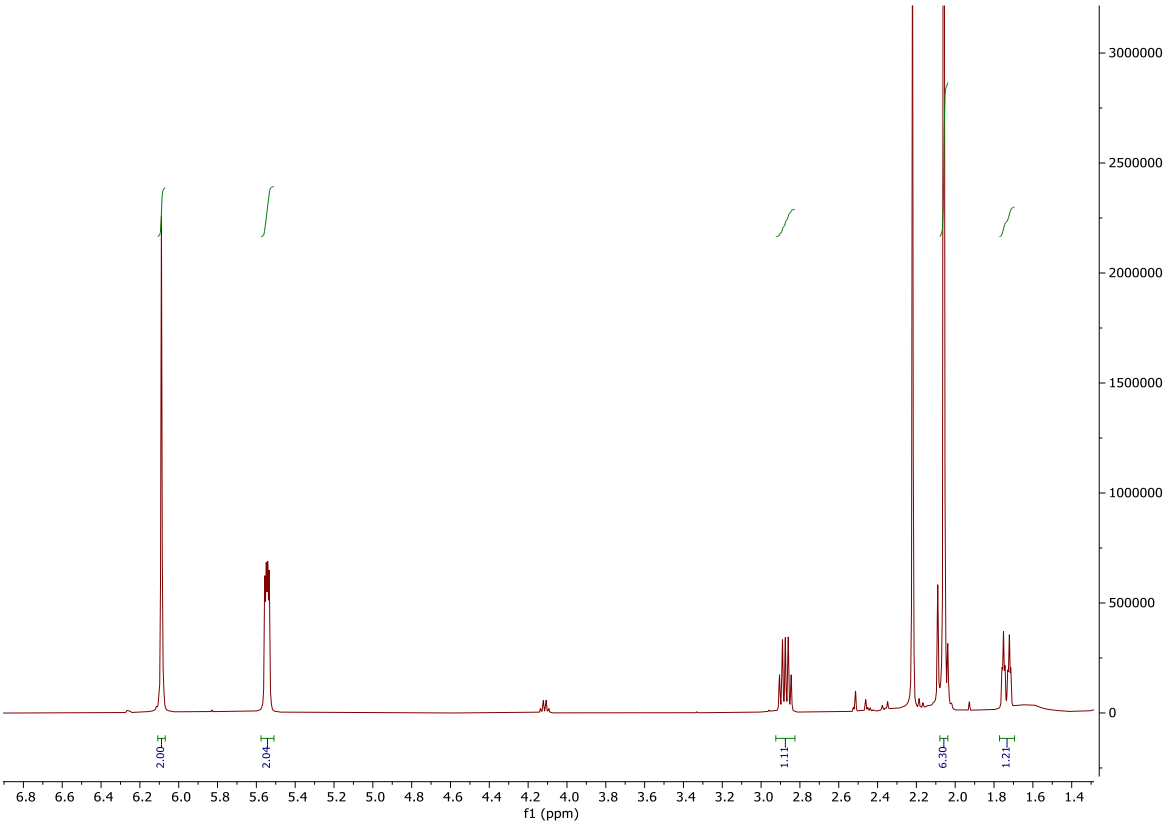

25 - 1H NMR (500 MHz, CDCl3) δ 6.09 (s, 2H), 5.55 (dd, J = 7.8, 3.8 Hz, 2H), 2.88 (dt, J = 15.0, 7.5 Hz, 1H), 2.06 (s, 3H), 1.74 (dt, J = 15.0, 3.9 Hz, 1H). Spectrum contains traces of ethyl acetate.

26 - (1R,4S)-4-hydroxycyclopent-2-en-1-yl acetate

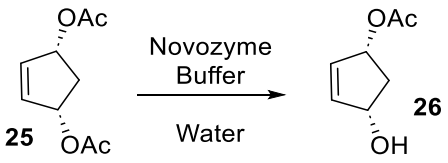

To 3 g (16,3 mmol) of diacetate **25** 25, 91 ml of a buffer solution of NaH2PO4/K2PO4 0,05 M were added. Then, 360 mg of Novoenzyme on spheres was added, stirring slowly at 25 °C. After 16 hours TLC check shows complete consumption. The aqueos phase was extracted with ethyl acetate and the solvent removed under reduced pressur, recoring around 2,29 g of product (99% yield). HNMR check shows a clean product **26**. The product is used as it is for the next step.

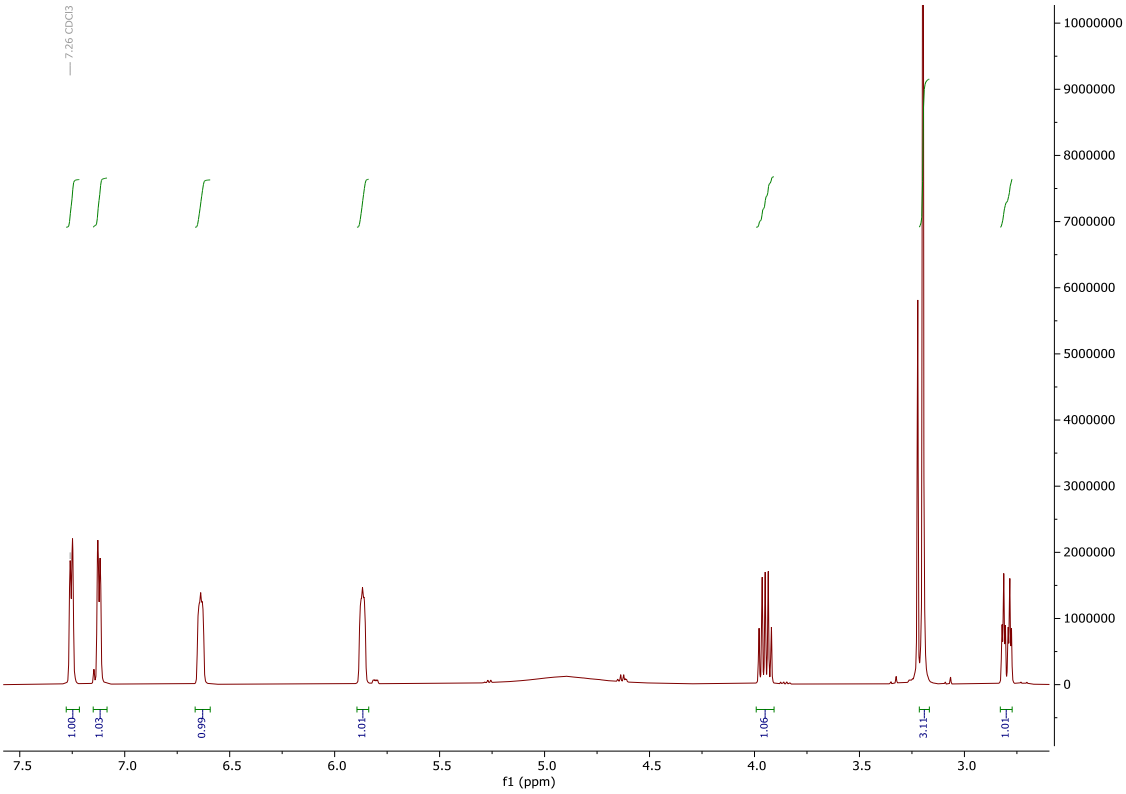

26 - 1H NMR (500 MHz, CDCl3) δ 7.26 (dd, J = 5.6, 1.9 Hz, 1H), 7.15 – 7.08 (m, 1H), 6.66 – 6.60 (m, 1H), 5.87 (dt, J = 8.1, 3.1 Hz, 1H), 3.95 (dt, J = 14.5, 7.4 Hz, 1H), 3.20 (s, 3H), 2.80 (dt, J = 14.7, 3.9 Hz, 1H). Small traces of bis-hydrolyzed products are visible (not influence the next step).

27 - (1R,4S)-4-((tert-butyldimethylsilyl)oxy)cyclopent-2-en-1-yl acetate

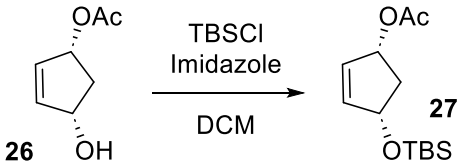

5 g (35,2 mmol) of **26** were dissolved into 47 ml of dry DCM under inert atmosphere. Then, 2,63 g (38,7 mmol) of imidazole were added, followed by 5,30 g (35,2 mmol) of tert-butyl dimethylsilyl chloride, under continuous stirring. After 30 minutes TLC check shows complete conversion. The reaction is quenched with water, separating the organic phase. The aqueous phase is then extracted with AcOEt. The organic phases are merged and the organic solvents removed under reduced pressure. 8,72 g of **27** were isolated (97% yield). HNMR confirms the purity of the compound, which is then used as it is for the next step.

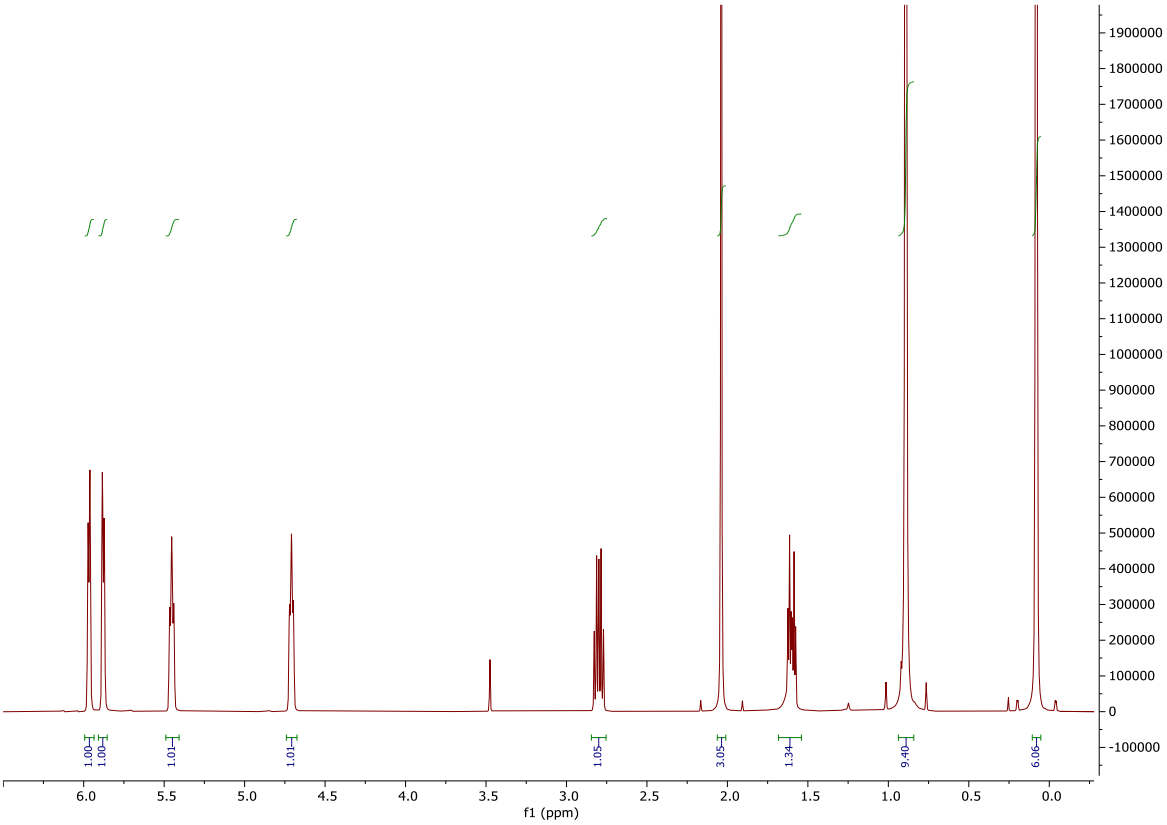

27 - 1H NMR (500 MHz, CDCl3) δ 6.00 – 5.92 (m, 1H), 5.92 – 5.83 (m, 1H), 5.45 (t, J = 6.4 Hz, 1H), 4.71 (t, J = 6.2 Hz, 1H), 2.80 (dt, J = 14.3, 7.3 Hz, 1H), 2.04 (d, J = 1.2 Hz, 3H), 1.60 (dt, J = 13.8, 5.1 Hz, 1H), 0.89 (d, J = 1.5 Hz, 9H), 0.08 (d, J = 3.2 Hz, 6H).

28 - (1S,4R)-4-((tert-butyldimethylsilyl)oxy)cyclopent-2-en-1-ol

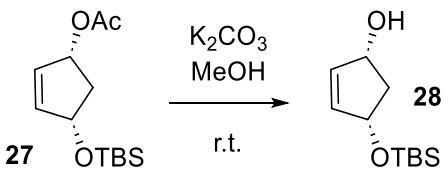

4,33 g (16,9 mmol) of **27** were dissolved into 77 mol of methanol. Then, 17,3 ml of saturated aqueous potassium carbonate solution are added, stirring

continuously. After 30 minutes TLC check shows complete conversion, so the reaction is quenched.

Quench: dilution with DCM, addition of brine and partition into separatory funnel. Aqueous phase extracted with DCM. The organic phase was then dried over MgSO4, filtered, and the solvent removed under reduced pressure. 3,58 g of **29** recovered (99% yield). HNMR analysis confirms the purity of the product, which was used as it is for the next step.

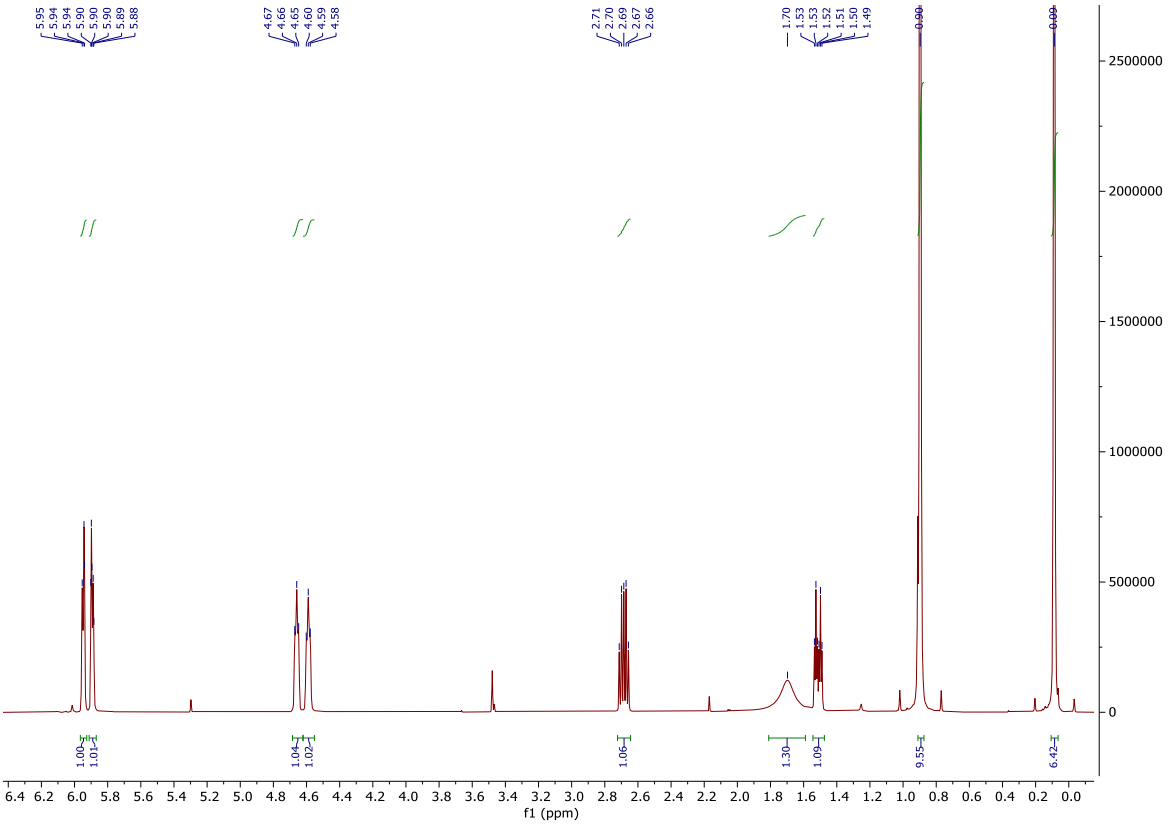

28 - 1H NMR (500 MHz, $CDCl_3$) δ 5.95 (q, *J* = 3.5 Hz, 1H), 5.89 (d, *J* = 5.5 Hz, 1H), 4.66 (q, *J* = 5.9 Hz, 1H), 4.59 (dq, *J* = 24.6, 6.0 Hz, 1H), 2.69 (dt, *J* = 13.9, 7.1 Hz, 1H), 1.70 (s, 1H), 1.51 (dt, *J* = 13.7, 4.5 Hz, 1H), 0.90 (s, 9H), 0.09 (s, 6H).

29 - (R)-4-((tert-butyldimethylsilyl)oxy)cyclopent-2-en-1-one

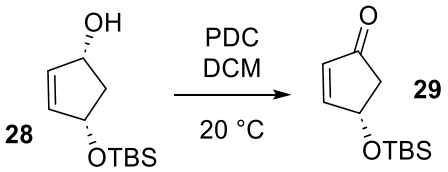

9,16 g of PDC (24,35 mmol) and 13,56 g of celite were stirred in DCM (170 ml) at room temperature. Substrate **28** (3,48 g) was then added as solution in DCM (13,4 ml). The reaction is left to stir until complete conversion of the SM (should be

around 2 h). Actually, after 3 h the reaction was not complete. So, 1 more equivalent (4,5 g) of PDC was added. After 18 h the reaction was complete by TLC (4:1 Hex:AcOEt). Work-up: the solution was filtered through a pad of celite (4 cm) and silica gel (4 cm) using Et2O/Hex 1:1 as eluent. The solvent was removed under reduced pressure and the crude purified by column chromatography. 1,81 g of **29** were recovered (53% yield).

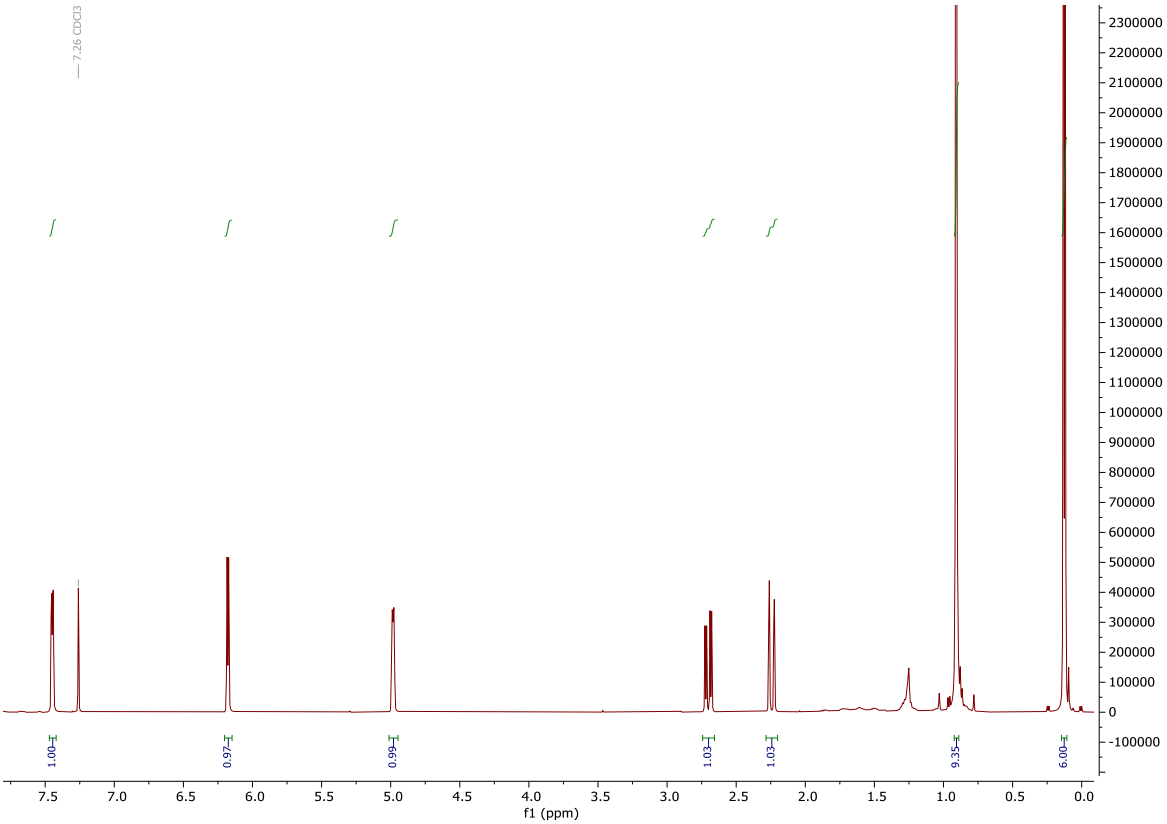

29 - 1H NMR (500 MHz, CDCl3) δ 7.45 (dd, J = 5.7, 2.1 Hz, 1H), 6.18 (d, J = 5.6 Hz, 1H), 4.98 (dt, J = 6.1, 2.1 Hz, 1H), 2.70 (dd, J = 18.2, 6.0 Hz, 1H), 2.24 (dd, J = 18.4, 2.1 Hz, 1H), 0.91 (s, 9H), 0.13 (s, 3H), 0.12 (s, 3H).

30 - (S)-4-hydroxycyclopent-2-en-1-one *(racemic)*

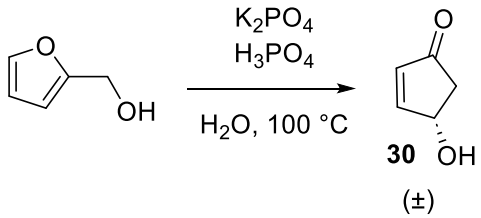

Furan-2-ylmethanol (1 g, 10.2 mmol) was dispersed in 31 ml of water, together with 49 mg (0.36 mmol) of KH_2PO_4. pH is corrected with HCl to 4,1. Then, the suspension was heated to 100 °C for 24 hours into a pressurized vial

The aqueous phase was then diluted with brine and extracted with AcOEt (x 5). The organic phase is then dried over MgSO4, filter and the solvent is removed under reduced pressure. The product is isolated via column chromatography (90:10 to 50:50 Hex:AcOEt). 240 mg of product **30** were recovered (24% yield).

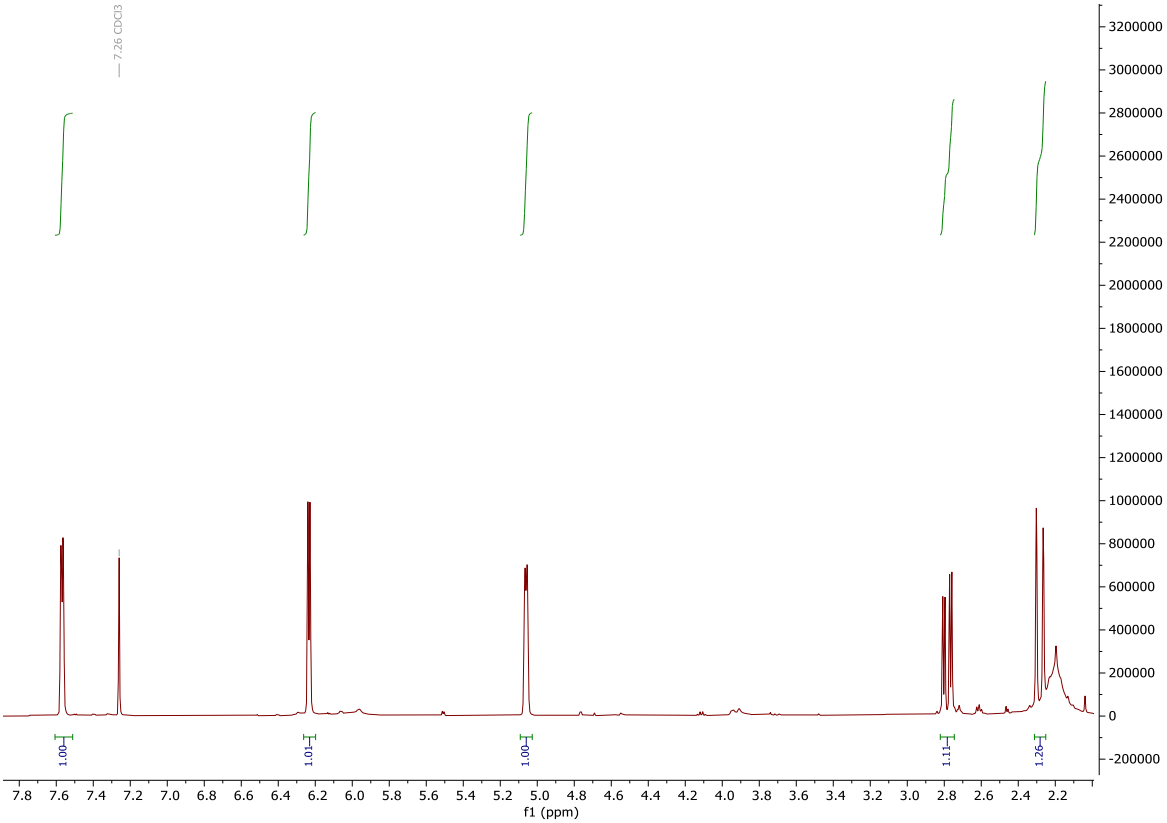

30 - 1H NMR (500 MHz, CDCl3) δ 7.57 (dd, J = 5.8, 2.1 Hz, 1H), 6.23 (d, J = 5.6 Hz, 1H), 5.08 – 5.03 (m, 1H), 2.78 (ddd, J = 18.5, 6.2, 1.6 Hz, 1H), 2.28 (dd, J = 18.6, 2.2 Hz, 1H).

31 - furan-2-ylmethyl 2,2,2-trichloroacetimidate

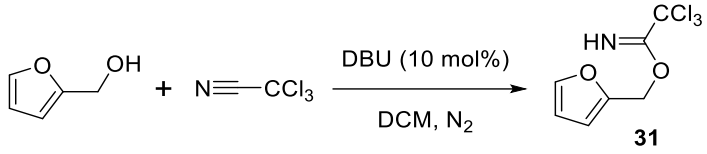

1 g (10.2 mmol) of furfuryl alcohol were put under inert atmosphere and dissolved into 20 ml of dry DCM. Then, 1,53 ml (15.3 mmol) of trichloroacetonitrile (1,53 ml) and DBU (152 ul, 1.02 mmol). The reaction was left to stir at room temperature for 24 hours. The solvent was then removed under reduced pressure and the product

was purified by column chromatography (Hex:AcOEt 3:1 + 5 % TEA as eluent). 1.71 g of **31** were recovered (69 % yield).

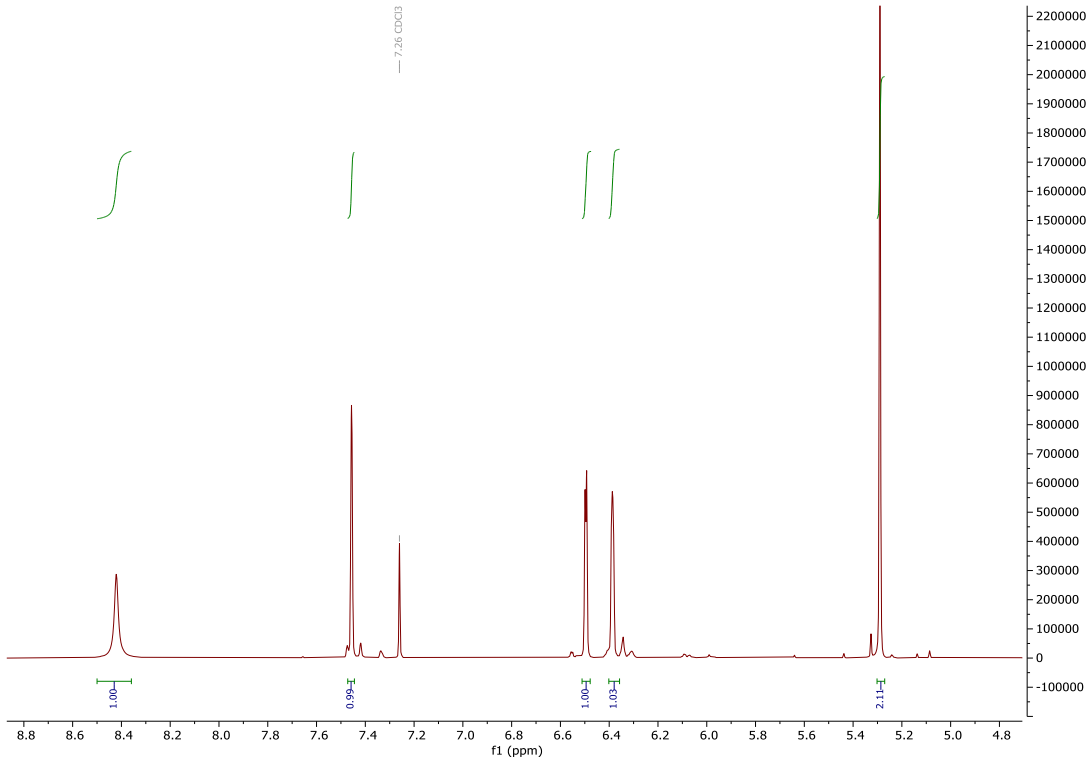

31 - 1H NMR (500 MHz, CDCl3) δ 8.42 (s, 1H), 7.46 (d, J = 1.9 Hz, 1H), 6.50 (d, J = 3.2 Hz, 1H), 6.39 (dd, J = 3.1, 1.8 Hz, 1H), 5.29 (s, 2H).

32 – (S)-4-(furan-2-ylmethoxy)cyclopent-2-en-1-one

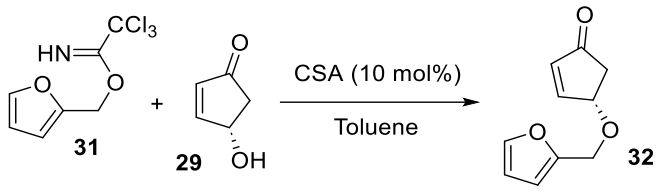

Alcohol **29** (585 mg, 6 mmol) and trichloroacetimidate 31 (1.45 g, 6 mmol) were weighted into a round bottom flask and put under inert atmosphere. Then, 60 ml of dry toluene were added, followed by 205 mg (1.2 mmol) p-toluensulphonic acid. The reaction was left to stir ar room temperature overnight. The solution turns black. The reaction was quenched with acqueous NaHCO3, and the organic layer separated. The solvent was then removed under reduced pressure, and the product was purified by column chromatography. 550 mg of 32 were recovedered (52 % yield).

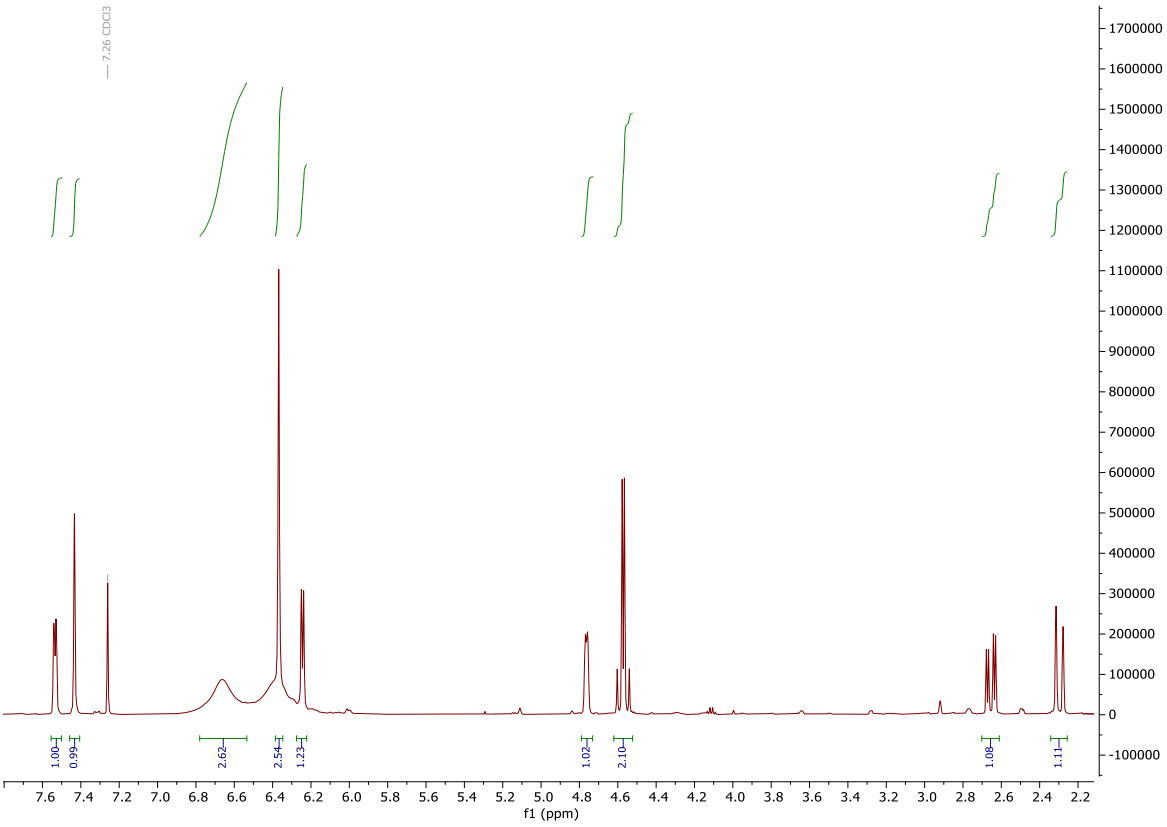

1H NMR (500 MHz, CDCl3) δ 7.53 (dd, J = 5.7, 2.2 Hz, 1H), 7.43 (s, 1H), 6.66 (s, 3H), 6.37 (bs, 1H), 6.24 (dd, J = 5.7, 1.3 Hz, 1H), 4.76 (d, J = 5.8 Hz, 1H), 4.57 (t, J = 11.9 Hz, 2H), 2.65 (dd, J = 18.3, 5.9 Hz, 1H), 2.30 (dt, J = 18.4, 1.5 Hz, 1H). It can be noted that in the furane peak area the is a broadening effect, probably due to rotamers and aggregates. Indeed, the same sample in different concentrations shows different peak broadening. Spectra on similar systems also showed the same phenomena.

34 - (Z)-3-iodoacrylic acid

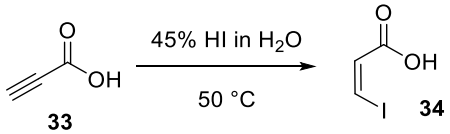

33 **34**

Propiolic acid (4,4 g, 71,4 mmol) was dissolved in HI 55% in water (17,8 ml). It follows the addition of the same volume of water. The reaction is set up at 50 °C overnight (17 h is recommended). The reaction is then left to go to room temperature. Some more water is then added, and the solution is extracted with Et_2O several times. The organic phase was then dried over $MgSO_4$, filtered and the solvent was removed under reduced pressure. 13,48 g of product **34** were isolated (95 % yield). The crude undergoes direct HNMR analysis, showing an essentially clean product, which is used as it is in the next step.

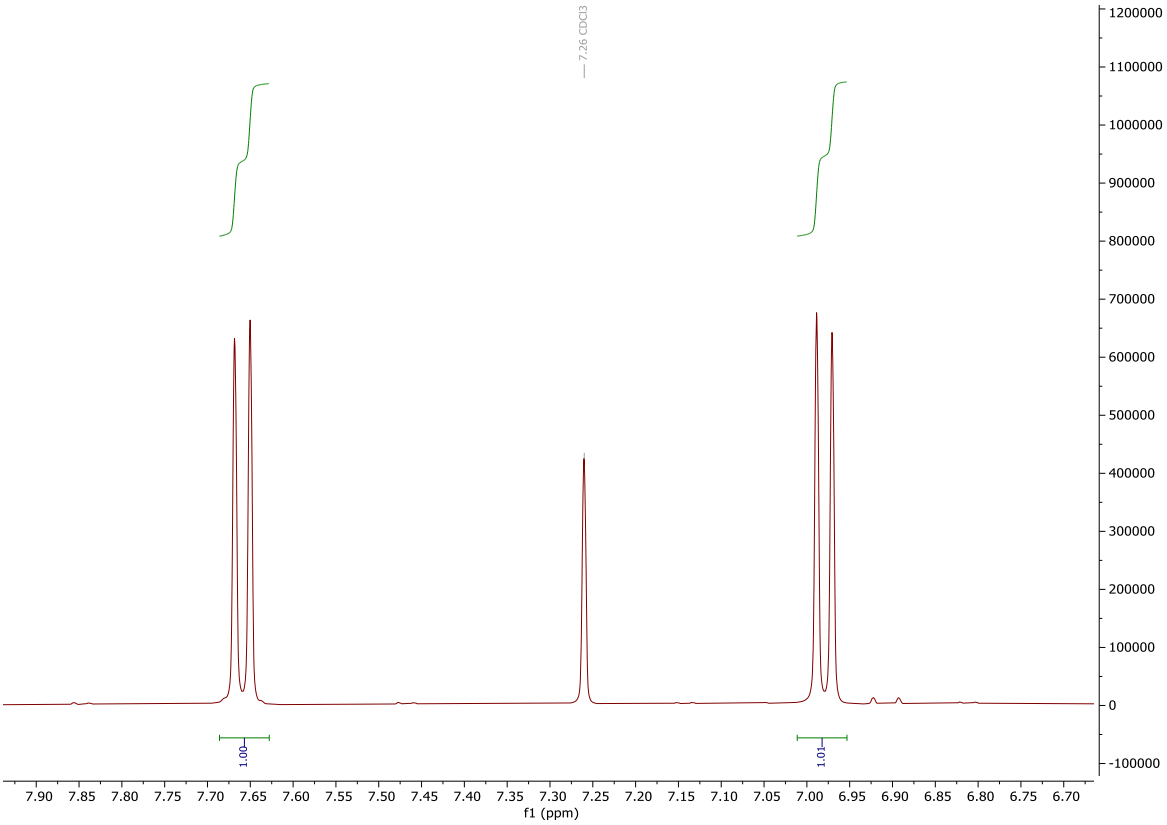

1H NMR (500 MHz, CDCl3) δ 7.66 (dd, J = 9.1, 1.2 Hz, 1H), 6.98 (d, J = 9.2 Hz, 1H). The spectrum shows a small trace of isomerized product and some residual diethyl ether.

35 - ethyl (Z)-3-iodoacrylate

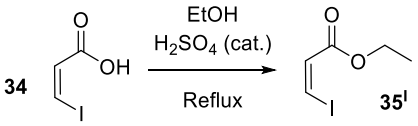

14,13 g (71,4 mmol) of **34** were dissolved in 43 ml of ethanol. Then, 1,42 ml of H2SO4 were added. The system is set-up to reflux overnight. The solution was quenched adding water and extracted with Et2O several times. The organic phase was dried over MgSO4, filtered and then the solvent is removed under reduced pressure. 14,2 g of **35** were recovered (88% yield).

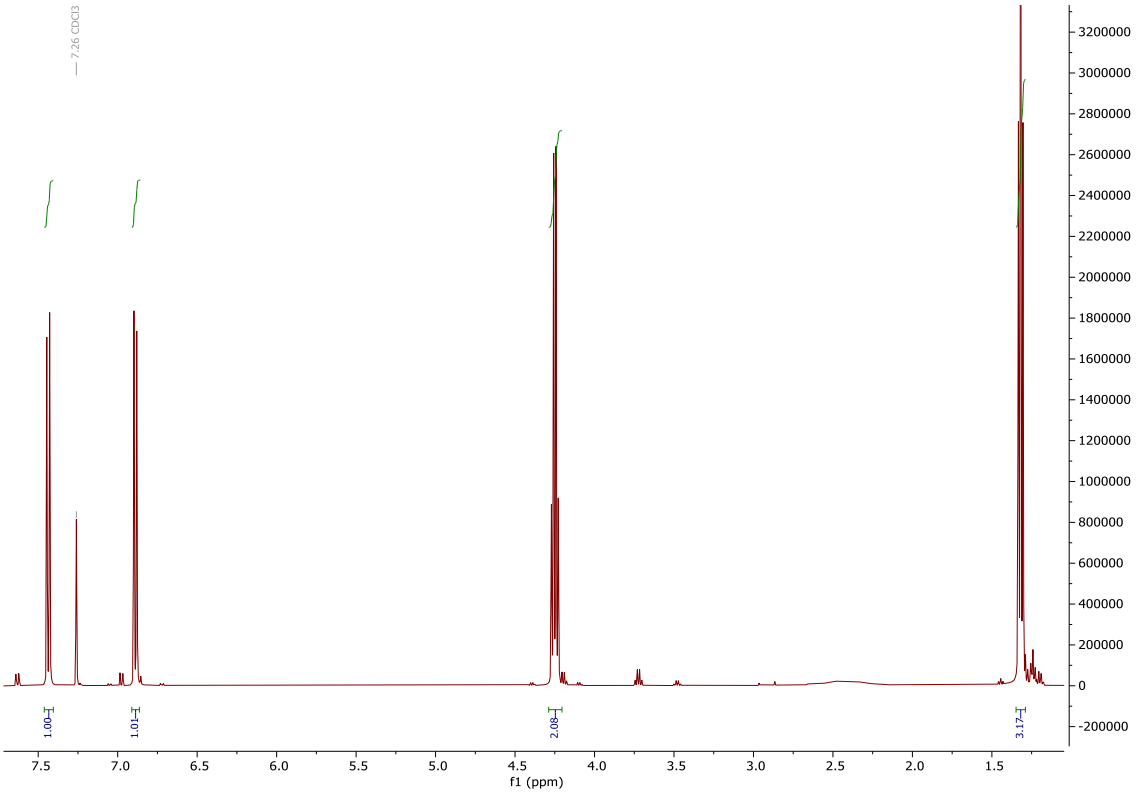

35 - 1H NMR (500 MHz, CDCl3) δ 7.44 (d, J = 8.9 Hz, 1H), 6.89 (d, J = 8.9 Hz, 1H), 4.25 (q, J = 7.1 Hz, 2H), 1.32 (t, J = 7.2 Hz, 3H).

36 - (Z)-3-iodoacrylaldehyde

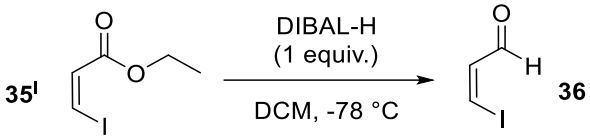

35 (2,64 g, 11,7 mmol) was dissolved in dry DCM (27 ml) under inert atmosphere and the solution was put at -78 °C. Then, 12,85 ml of DIBAL-H 1 M in eptane (12,9 mmol) were added dropwise. And the system was covered with aluminum foil. After 2 hours TLC check showed complete conversion. The reaction was quenched at the same temperature with 2 ml of MeOH, then allowed to go to room temperature. Then, 27 ml of Et2O were added, followed by 50 ml of a 15% weight solution of sodium-potassium tartrate. The suspension was stirred for 1 h at 1000 rpm. The phases were then allowed to separate and the aqueous layer discarded. The organic phase was dried over $MgSO_4$, filtered and the solvent removed under reduced pressure. 1,21 g of aldehyde 36 were recovered (57% yield).

NB: yield is low because the aldehyde is volatile. DIBAL-H in heptane was used because we found that DIBAL-H in DCM was giving other products, but this could be due to a defective batch. The peculiar event was not investigated further.

37 - tert-butyl (2E,4Z)-5-iodopenta-2,4-dienoate

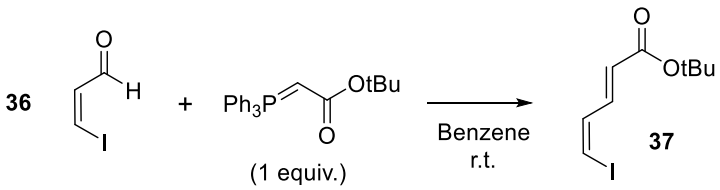

586 mg (3,22 mmol) of aldehyde **36** were dissolved in 10 ml of dry benzene under inert atmosphere. It follows the addition of 1,33 g (3,54 mmol) of the phosphonium ylide. The reaction is left to stir at room temperature overnight. After this time, the solvent is directly removed and the crude was dissolved in Et2O, precipitating Ph3P=O. The precipitate is removed through filtration over celite. The product was isolated by column chromatography (gradient from 1% to 10% Hex:Et_2O). 478 mg of **37** were recorded (53% yield).

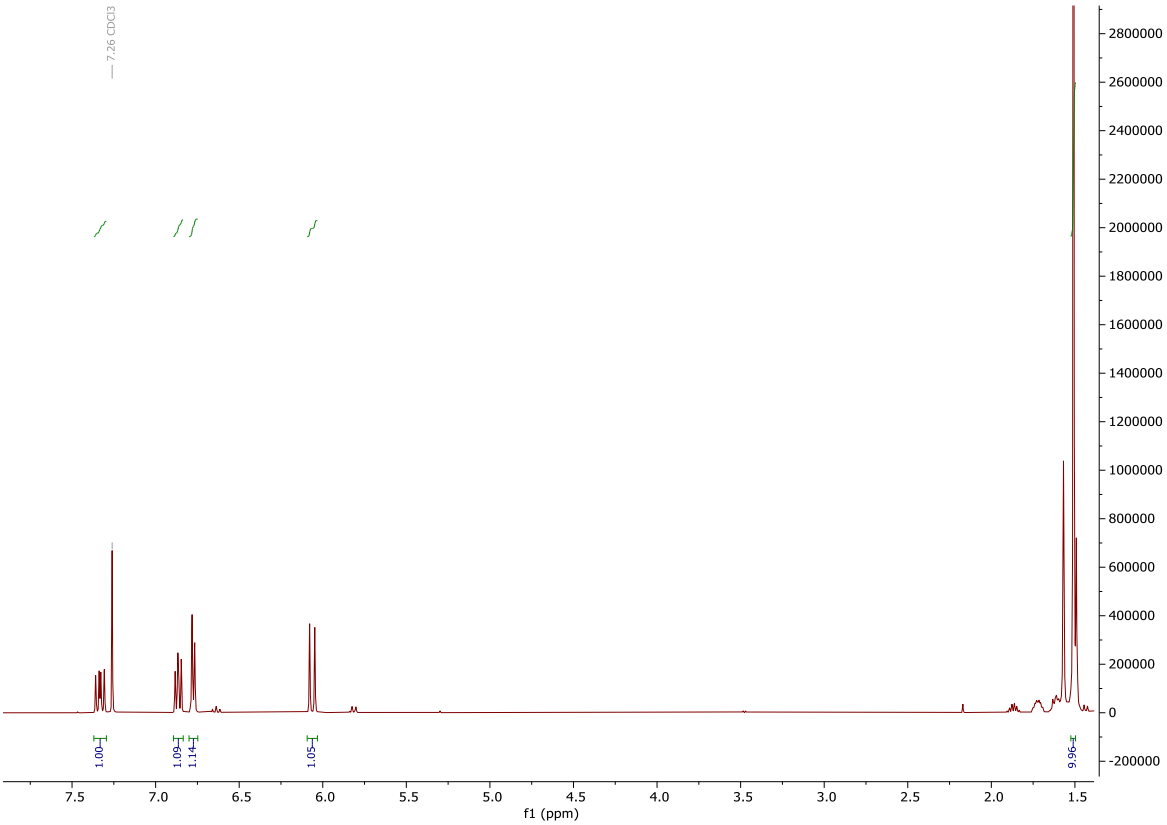

37 - 1H NMR (500 MHz, CDCl3) δ 7.33 (t, J = 10.5 Hz, 1H), 6.86 (qd, J = 10.5, 7.8 Hz, 1H), 6.77 (t, J = 7.8 Hz, 1H), 6.06 (t, J = 15.3 Hz, 1H), 1.51 (s, 9H).

38 – tert-butyl (2E,4Z)-5-(4,4,5,5-tetramethyl-1,3,2-dioxaborolan-2-yl)penta-2,4-dienoate

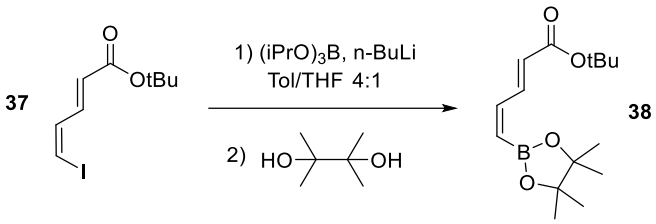

440 mg (1,57 mmol) of **37** were dissolved in dry toluene (11,2 ml) /THF (2,8 ml) and pinacol triisopropylborate (400 ul, 1,89 mmol) was added. Then, the temperature was lowered to -78 °C. It follows the addition of nBuLi 1,60 M (982 ul, 1,57 mmol) and the reaction is left to go for 30 minutes. Then, pinacol (222 mg, 1,73 mmol) was added and the reaction is left to go to room temperature, covered with aluminium foil and left to go overnight. The solution was then diluted with Et2O, washed with NH4Cl and brine and extracted with Et2O. The organic phase is then dried over MgSO4, filtered and the solvent is removed under reduced pressure. TLC check 4:1 Hex:AcOEt. The product was isolated by column chromatography. 191 mg of **38** were recovered (43% yield).

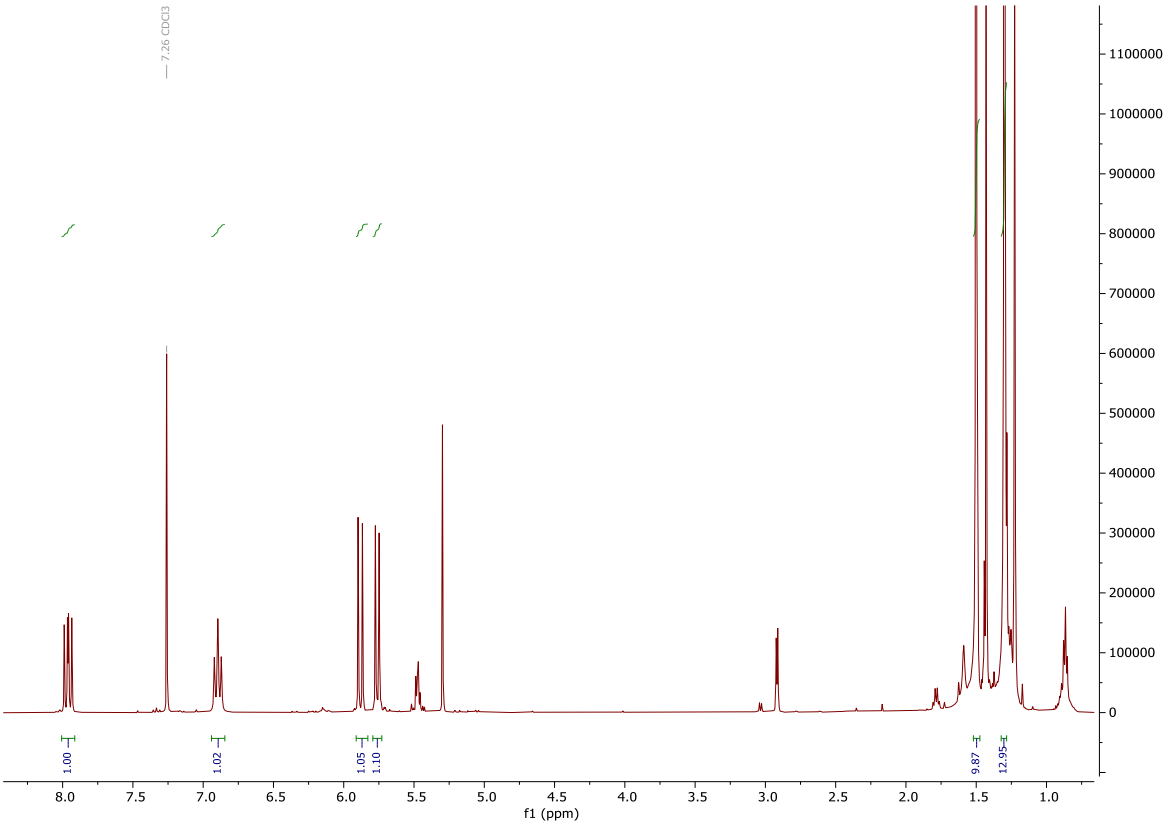

38 - 1H NMR (500 MHz, CDCl3) δ 7.96 (dd, J = 15.4, 11.5 Hz, 1H), 6.90 (t, J = 12.4 Hz, 1H), 5.88 (d, J = 15.4 Hz, 1H), 5.76 (d, J = 13.2 Hz, 1H), 1.50 (s, 9H), 1.30 (s, 12H).

39 – (2E,4Z)-5-(4,4,5,5-tetramethyl-1,3,2-dioxaborolan-2-yl)penta-2,4-dien-1-ol

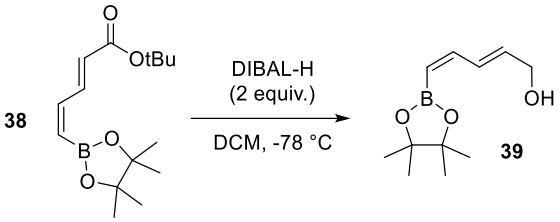

38 (115 mg, 0.41 mmol) was dissolved in dry DCM (10.25 ml), then the solution was brought down to -78 C. Then, DIBAL-H in heptane (820 ul, 0.82 mmol) was added slowly and the reaction is left to go at the same temperature for 2 h. After TLC check confirming full conversion. The reaction was quenched with 1,8 ml of MeOH, followed by 12 ml of Rocher salt saturated solution. The reaction was allowed to go to room temperature, then 18 ml of Et2O were added and the reaction allowed to stir at the same temperature for 1 hour at 1000 rpm. Then, the layers were allowed to separate, discarding the aqueous layer. The organic phase was then allowed to separate, dried over MgSO4, filtered and the solvent removed under reduced pressure. The product was purified by column chromatography (1:1 Hex:Et_2O), yielding 30 mg of **39** (40% yield).

NB using oven-dried silica the isolated yield raises to 55-60%.

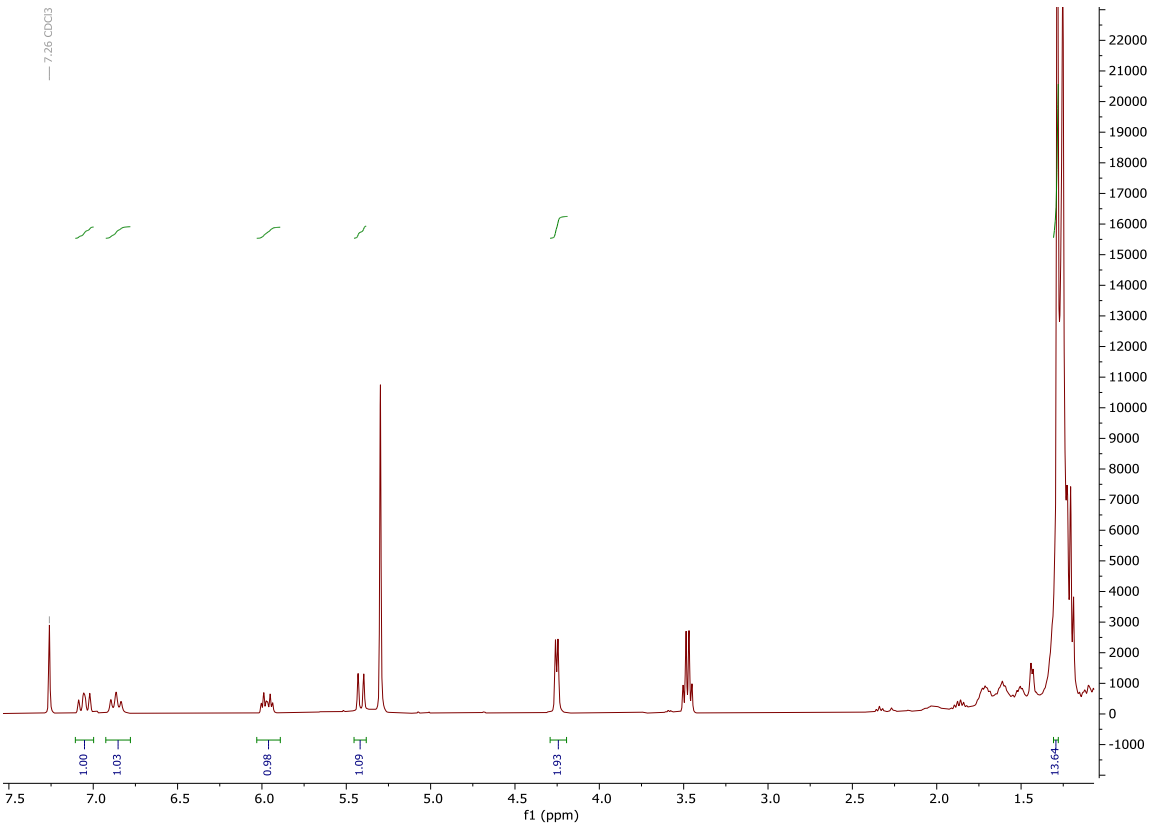

39 - 1H NMR (400 MHz, CDCl3) δ 7.05 (dd, J = 15.2, 11.1 Hz, 1H), 6.87 (t, J = 12.2 Hz, 1H), 5.97 (dt, J = 15.1, 5.8 Hz, 1H), 5.41 (d, J = 13.3 Hz, 1H), 4.25 (d, J = 5.9 Hz, 2H), 1.28 (s, 12H). Spectrum contains still some diethyl ether and hexane.

42 – (E)-dimethyl(phenyl)(2-(tributylstannyl)vinyl)silane

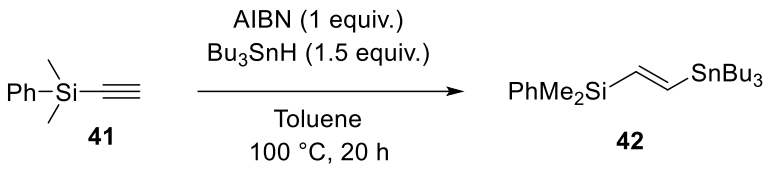

Into an oven dried round bottom flask 2 g (12.5 mmol) of alkyne 41 and set under inert atmosphere. Then, 20 ml of dry toluene under inert atmosphere were added to dissolve it. It follows the addition of AIBN (2,05 g, 12.5 mmol) and Bu3SnH (5 ml, 18.7 mmol). The reaction is refluxed 20 h (100 °C). After this time the toluene was removed under reduced pressure and the product was purified by column chromatography in pure hexane. 4.63 g of 42 were recovered (82% yield).

45 - tert-butyl(((2E,4E)-5-(dimethyl(phenyl)silyl)penta-2,4-dien-1-yl)oxy)dimethylsilane

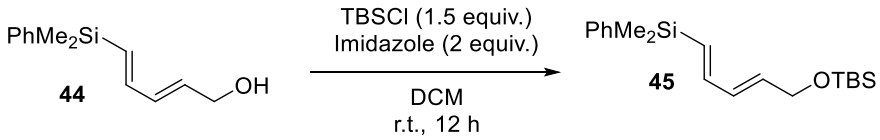

97,5 mg (0.45 mmol) of 44 were weighted into a vial and put under inert atmosphere. The material was dissolved into 1 ml of dry DCM. Then, imidazole (30,4 mg, 0.45 mmol) and TBSCl (74 mg, 0.49 mmol) were added at 0 °C. After 24 hours the reaction was quenched with water and extracted with DCM. The organic phase was dried over MgSO4, filtered and the solvent removed under reduced pressure. Product **45** was purified by column chromatography (Hex:AcOEt 4:1), isolating 110 mg (74% yield).

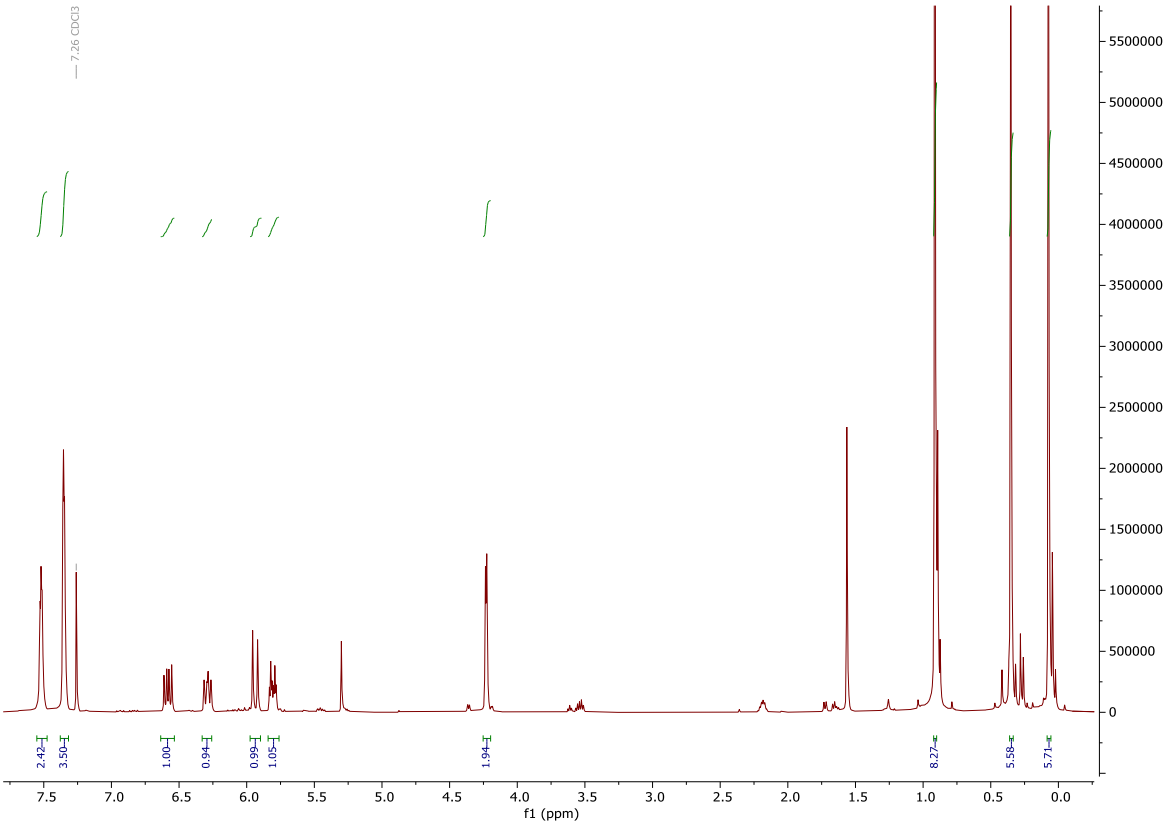

45 - 1H NMR (500 MHz, CDCl3) δ 7.54 – 7.48 (m, 2H), 7.37 – 7.31 (m, 3H), 6.58 (dd, J = 18.3, 10.1 Hz, 1H), 6.29 (dd, J = 15.3, 10.2 Hz, 1H), 5.94 (d, J = 18.3 Hz, 1H), 5.81 (dt, J = 15.2, 5.0 Hz, 1H), 4.23 (d, J = 5.0 Hz, 2H), 0.91 (s, 9H), 0.35 (s, 6H), 0.07 (s, 6H).

46 - (1S,4R)-4-((tert-butyldimethylsilyl)oxy)-4-methylcyclopent-2-en-1-yl (2E,4E)-5-(dimethyl(phenyl)silyl)penta-2,4-dienoate

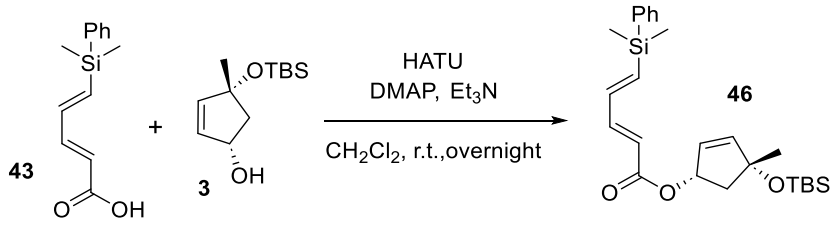

122 mg of the acid (0.52 mmol) were weighted into a 50 ml 2 neck RBF and put under N2. Into a separated vial, 100 mg of the alcohol 3 (0.44 mmol) were weighted and put under inert atmosphere. Then, 3,9 ml of dry DCM were used to dissolve the alcohol and are transferred to the acid. Then, TEA (119 ul, 0.88 mmol) is injected, followed by DMAP (10,7 mg, 0.09mmol). Finally 333 mg of HATU (0.88 mmol) were added. The reaction is left to stirr at room temperature overnight. The reaction is then quenched with water and extracted with DCM. Then, the organic phase is dried over $MgSO_4$, filtered and the solvent is removed under reduced

pressure. The crude undergoes chromatographic purification (4:1 Hex:AcoEt), recovering 81.6 mg of compound 46 (44% yield).

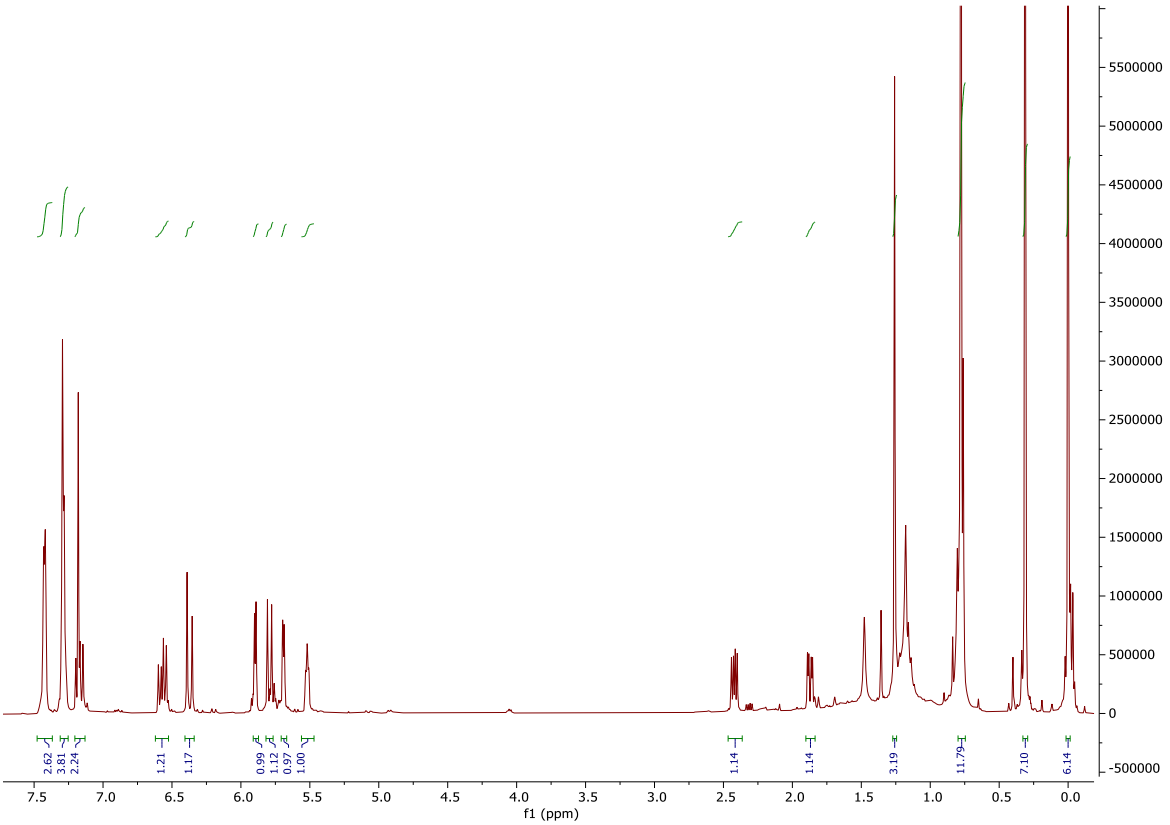

46 - 1H NMR (500 MHz, CDCl3) δ 7.41 – 7.39 (m, 3H), 7.27 (m, 2H), 7.18 – 7.11 (m, 1H), 6.55 (dd, J = 18.3, 10.4 Hz, 1H), 6.35 (d, J = 18.3 Hz, 1H), 5.87 (d, J = 5.6 Hz, 1H), 5.77 (d, J = 15.3 Hz, 0H), 5.68 – 5.65 (m, 1H), 5.50 (t, J = 6.2 Hz, 1H), 2.40 (dd, J = 13.7, 7.4 Hz, 1H), 1.85 (dd, J = 13.7, 4.8 Hz, 1H), 1.24 (s, 3H), 0.75 (s, 12H), 0.29 (s, 6H), -0.02 (s, 6H). Traces of an isomerized product and/or rotamers are clearly visible.

48 – tert-butyl(((2Z,4E)-5-ethoxypenta-2,4-dien-1-yl)oxy)dimethylsilane

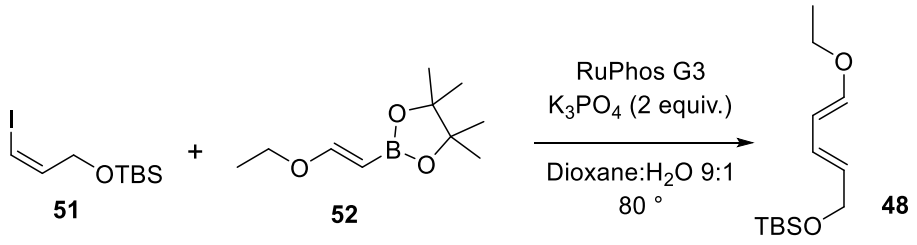

Vinyl iodide 51 (100 mg, 0.33 mmol) was weighted into a vial, followed by boronate 52 (60 mg, 0.30 mmol). Then, 1,7 ml of THF:H2O 9:1 were added, followed by K3PO4 (129 mg, 0.61 mmol). Finally, Pd complex RuG3 was added

(12.7 mg, 0.015 mmol). The system is degassed and the reaction is allowed to go at 80 °C for 16 h.

Reaction is quenched with water and extracted with DCM. The organic phase is dried over MgSO4, filtered and the solvent is removed under reduced pressure. The product was purified by column chromatography (Hex:Et2O 99:1 to 80:20 in slow gradient). 18.5 mg of compound 56 were recovered (25% yield).

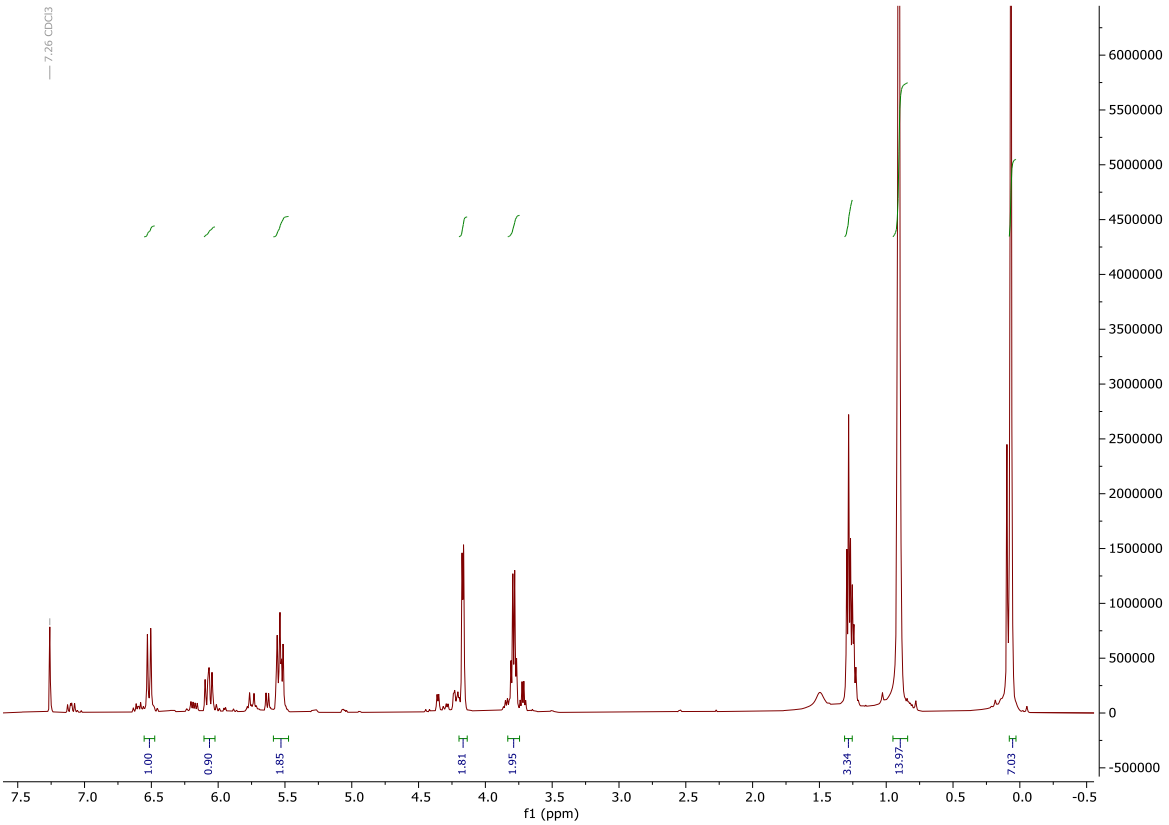

48 - 1H NMR (500 MHz, CDCl3) δ 6.52 (d, J = 12.6 Hz, 1H), 6.07 (dd, J = 15.1, 10.8 Hz, 1H), 5.53 (m, 2H), 4.17 (d, J = 5.7 Hz, 2H), 3.79 (q, J = 7.0 Hz, 2H), 1.28 (q, J = 7.1 Hz, 3H), 0.90 (m, 14H), 0.07 (m, 9H).

49^{I} – (3R,3aR,6aS)-5'-methoxy-3a,4,6,6a-tetrahydro-2H,5H,5'H-spiro[cyclopenta[b]furan-3,2'-furan]-5-one

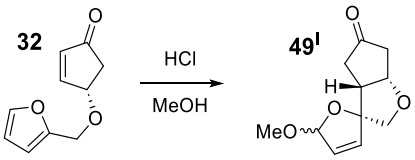

Procedure: 191 mg (1.07 mmol) of the substrate are dissolved in 21 ml of MeOH. Then, 92 ul of HCl 36% (1.07 mmol) in water are added and the reaction is monitored by TLC. In a few minutes the reaction is complete. Reaction was quenched with water and extracted with DCM. The organic solvent was removed

under reduced pressure, isolating two spot (which actually contain more than one product). One still has the furane moiety, but the alkene is gone. Probably is some sort of methanol addition. The other has an alkene, but many methoxide peaks, so probably it's a Michael adduct. The structure is very complicated, so no assignments were really done, as we were not interested in byproducts.

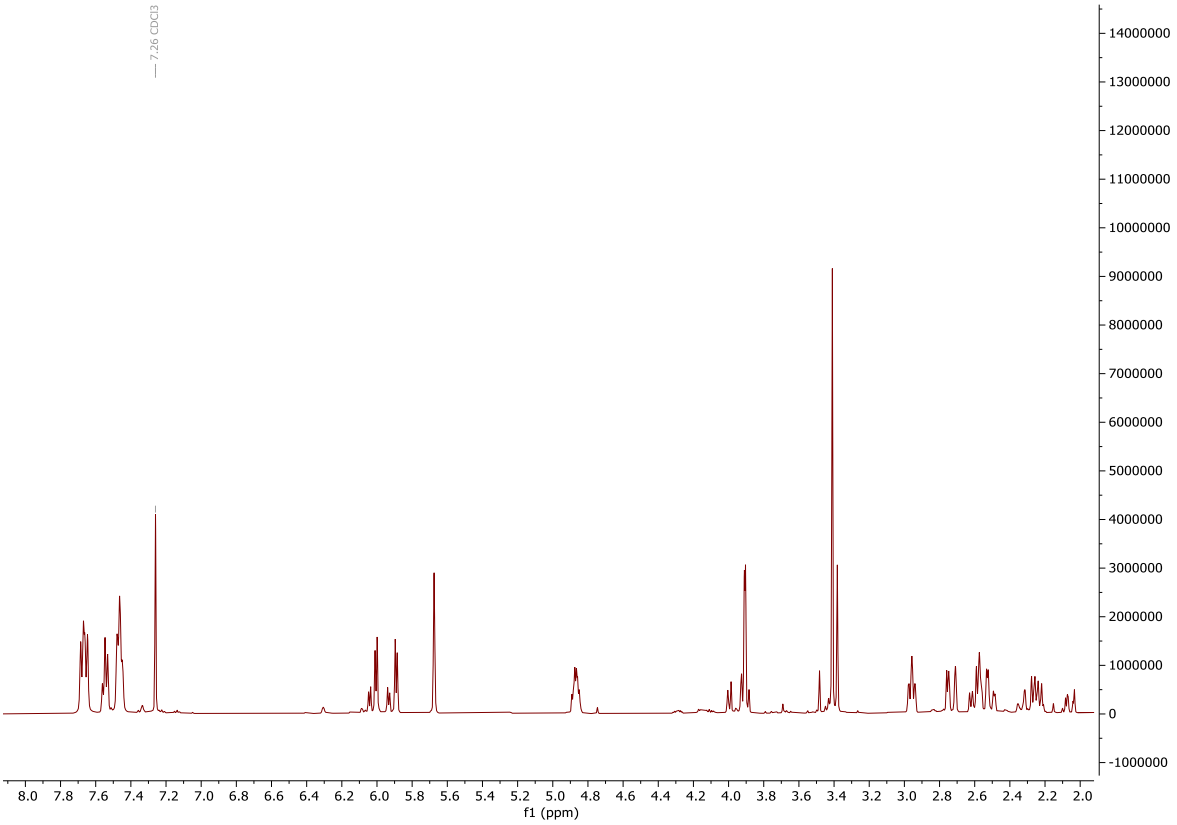

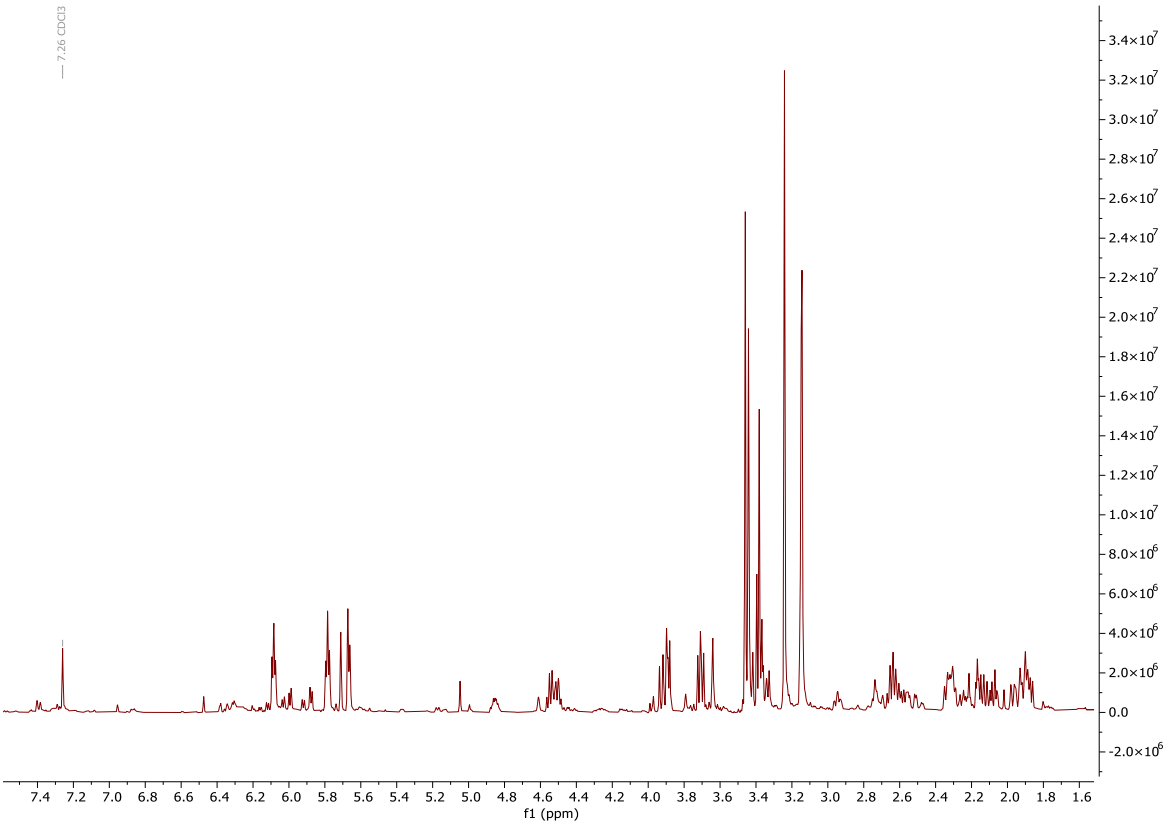

49^{II} - 2-(methoxymethyl)furan

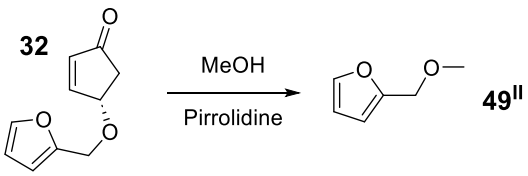

32 (30 mg, 0.17 mmol) is dissolved in MeOH (1,5 ml), then pyrrolidine is added (14 ul, 0.17 mmol). In a few minutes the conversion is total, as confirmed by TLC analysis (a pink spot appears). The solvent is removed under reduced pressure, and the pink spot was isolated via column chromatography.

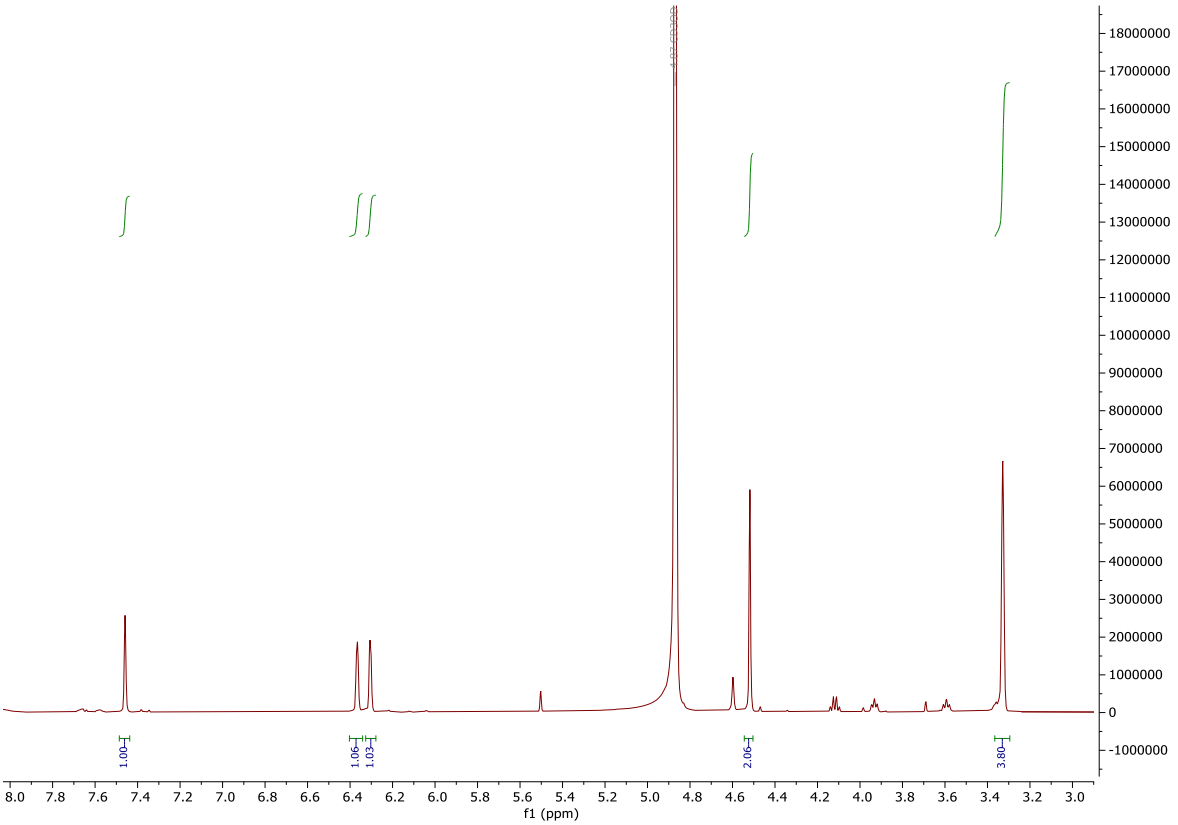

49[II] - 1H NMR (500 MHz, MeOD) δ 7.46 (d, J = 2.5 Hz, 1H), 6.37 (d, J = 2.7 Hz, 1H), 6.30 (d, J = 3.2 Hz, 1H), 4.52 (s, 2H), 3.33 (bs, 3H). Traces of other byproducts detected in the background.

50 - (Z)-3-iodoprop-2-en-1-ol

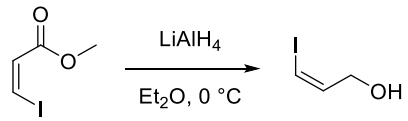

35[II] **50**

1 g of **35** was dissolved in 5 ml of dry Et2O under inert atmosphere. Then, 200 mg of LiAlH4 are put under inert atmosphere and 50 ml of dry Et2O are added to do a slurry, which is then submerged into an ice bath. The substrate dissolved in Et_2O in then added dropwise and the reaction is left to go until disappears on TLC (30 minutes). Quench: 1 M NaOH (30 ml), dilution with Rocher salts saturated solution, extraction with Et2O. The organic layer is dried over MgSO4, filtered and the solvent is slowly removed under reduced pressure. 784 mg of 50 (90 % yield) were isolated and used immediately as it is volatile.

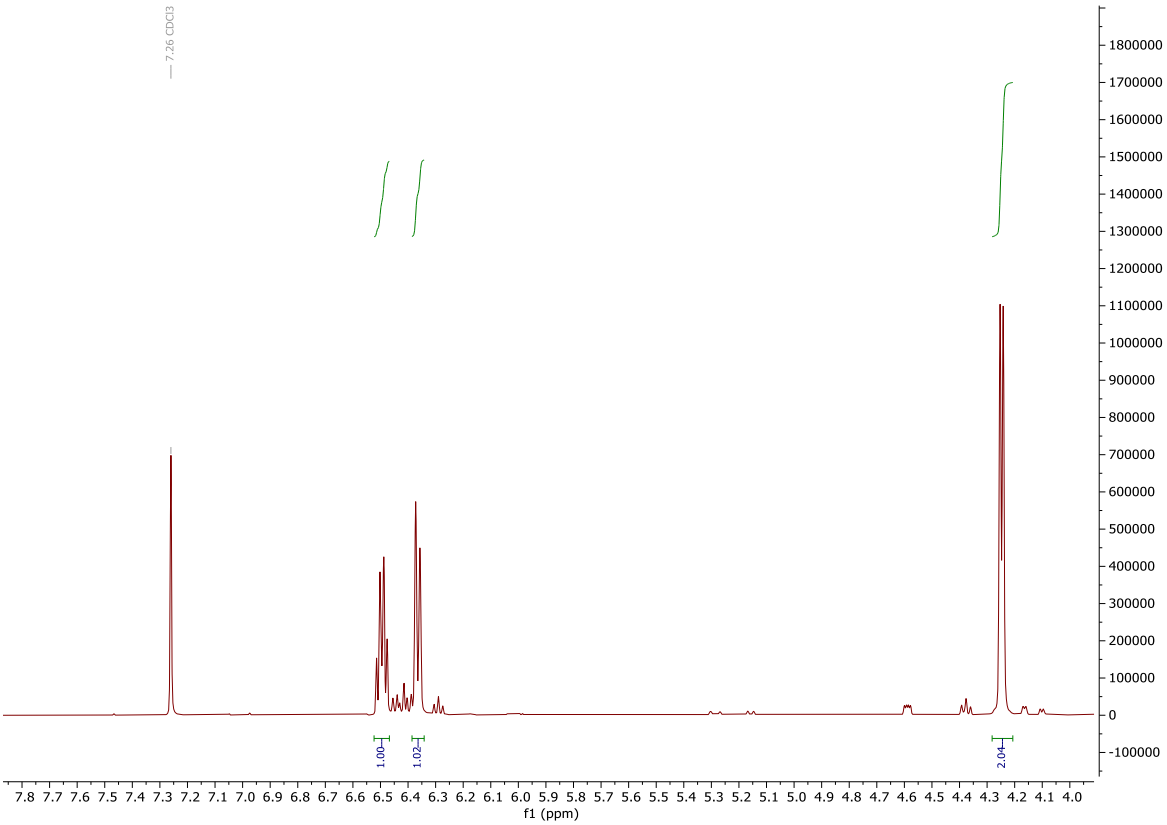

1H NMR (500 MHz, CDCl3) δ 6.49 (t, J = 6.0 Hz, 1H), 6.36 (tq, J = 7.7, 1.4 Hz, 1H), 4.25 (t, J = 5.7 Hz, 2H). Some diethyl ether still present, as it was not possible to completely remove it without losing product. Some isomerization product present as well in small quantities.

51 - (E)-tert-butyl((3-iodoallyl)oxy)dimethylsilane

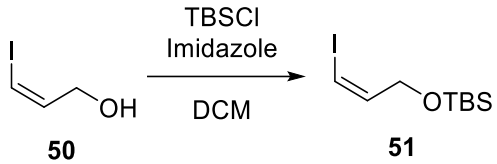

Cp_2ZrClH (3,63 g, 14.1 mmol) was weighted in the glovebox into a round bottom flask. Then, the organometallic reagent was suspended in dry THF (41,5 ml) at 0 °C. It follows the addition of starting material (2,00 g, 11.74 mmol) and the reaction let stirring in the dark for 2 hours. Then, the system was cooled down to -78 °C and a solution of I2 (3,58 g, 14.1 mmol) in dry THF (9,4 ml) was added and the reaction was allowed to stir for 30 minutes. It followed the quench with saturated ammonium chloride at -78 °C and extraction with Et2O. The organic phase was then dried over MgSO4, filtered and the solvent was removed under reduced pressure.

The crude undergoes chromatographic purification (99:1 Hex:AcOEt, dry loading to collect also the insoluble zirconium salts).

1,36 g of **51** were obtained (39% yield).

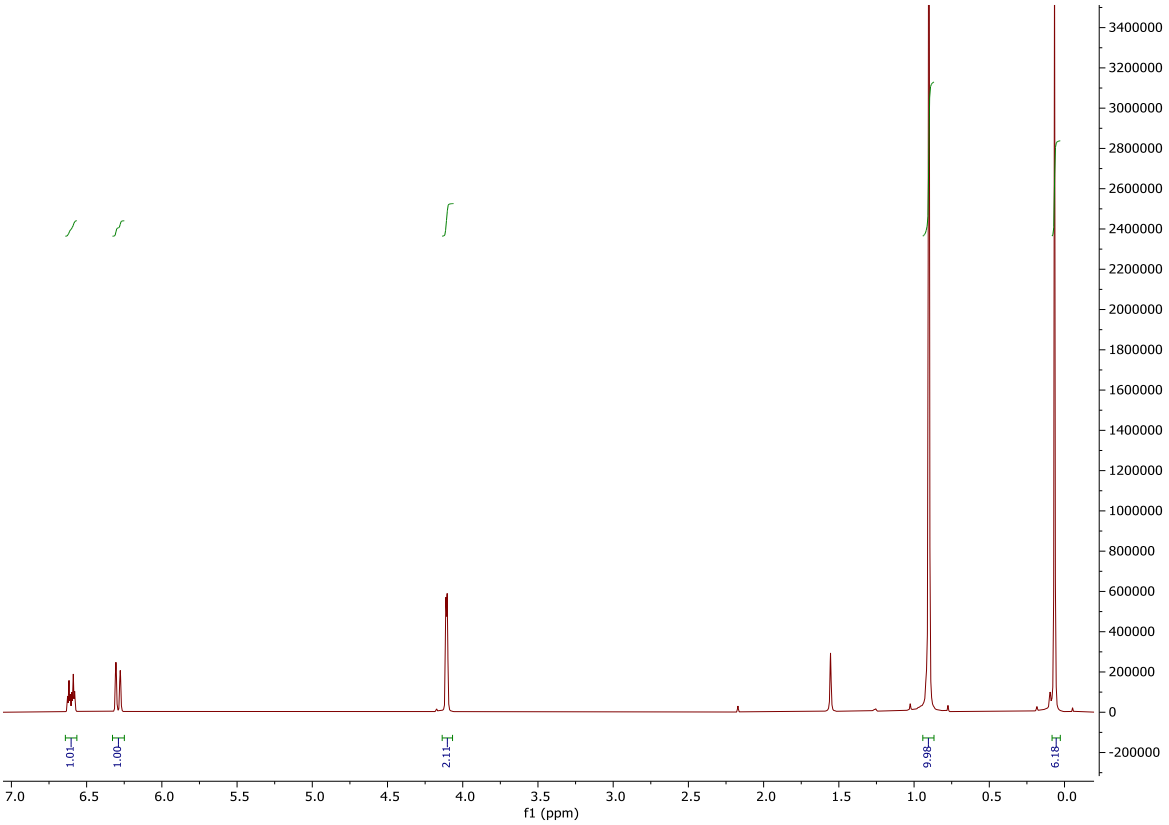

51 - 1H NMR (500 MHz, CDCl3) δ 6.60 (dt, J = 14.4, 4.6 Hz, 1H), 6.29 (d, J = 13.3 Hz, 1H), 4.11 (d, J = 4.6 Hz, 2H), 0.90 (s, 9H), 0.07 (t, J = 1.0 Hz, 6H).

52 – (E)-2-(2-ethoxyvinyl)-4,4,5,5-tetramethyl-1,3,2-dioxaborolane

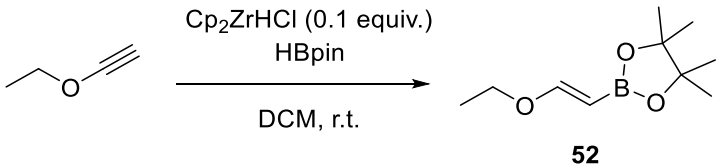

52

Schwartz catalyst (735 mg, 2.85 mmol) was weighted into a flame-dried round bottom flask. A solution of ethyloxiacetylene (6.83 ml, 28.5 mmol) is diluted in dry DCM (14 ml). This solution is then transferred over the Cp2ZrHCl catalyst. It follows the addition of pinacol borane (4,55 ml, 31.4 mmol) stirring at r.t. for 1 h. The reaction was quenched with NaHCO3, extraction with DCM. The organic phase was then dried over MgSO4, filtered, and the solvent removed unde reduced pressure. Product 52 was then purified by column chromatography (Hex:AcOEt

9:1), recovering 880 mg of product (16% yield). The low yield is due to accidental spill of solution.

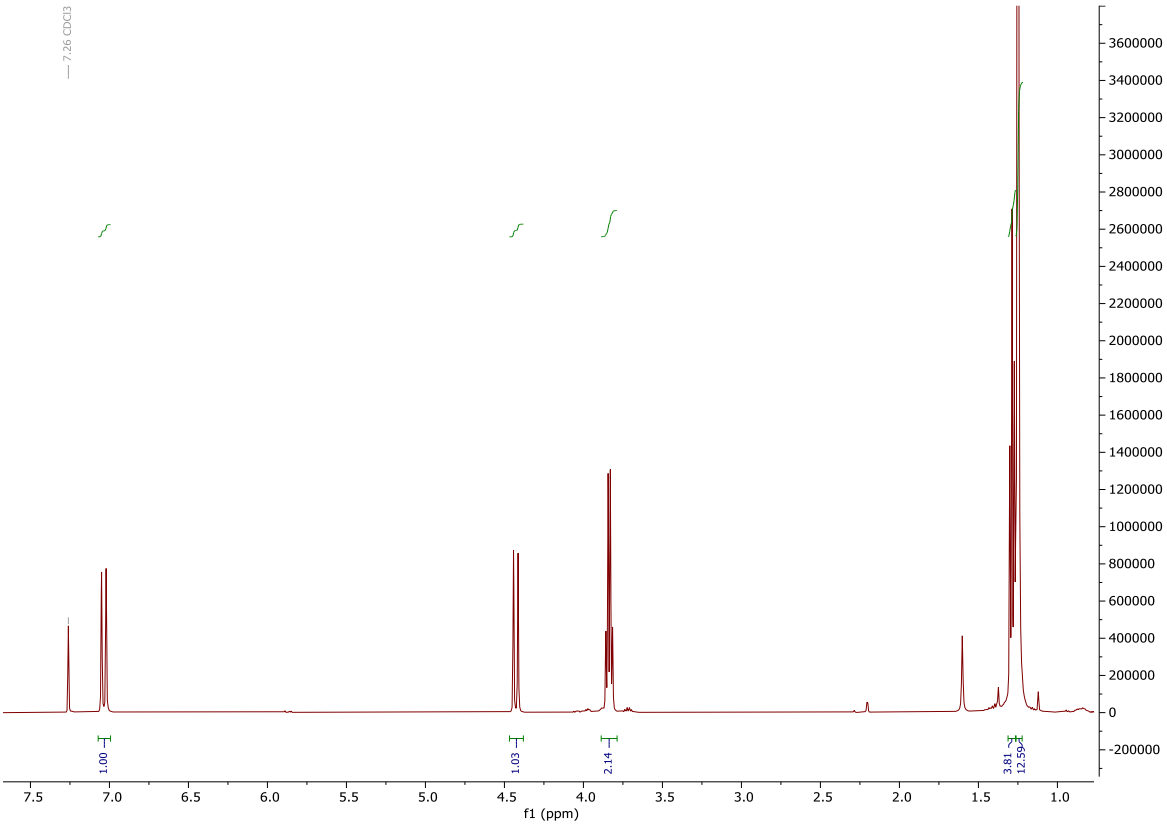

52 - NMR (500 MHz, CDCl3) δ 7.04 (d, J = 14.4 Hz, 1H), 4.43 (d, J = 14.4 Hz, 1H), 3.84 (q, J = 7.1 Hz, 2H), 1.29 (t, J = 7.1 Hz, 4H), 1.25 (d, J = 1.5 Hz, 13H).

54 – dimethyl (S)-1-oxo-1,2,3,3a,5,6-hexahydro-4H-indene-4,4-dicarboxylate

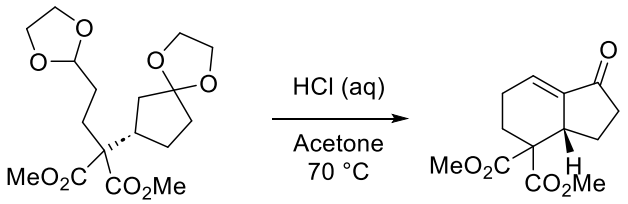

57 **54**

310 mg (0.86 mmol) of **57** were dissolved in 3 ml of acetone in a pressure vial. Then, 865 ul of 2 M HCl in water (1.73 mmol) were added. The vial was then sealed and heated to 70 °C for 16 h.

h. The reaction was cooled to room temperature and quenched with sat. NaHCO3 (300 mL) and partially concentrated in vacuo to remove acetone. The resulting

mixture was extracted with CH2Cl2 (3 x 450 mL), and the combined organic extracts were dried over Na2SO4, filtered, and concentrated in vacuo.

The crude was then purified by column chromatography (9:1 to 6:4 Hex:AcOEt), yielding 70 mg of **54** (32% yield).

55 - dimethyl (R)-2-(3-oxocyclopentyl)malonate

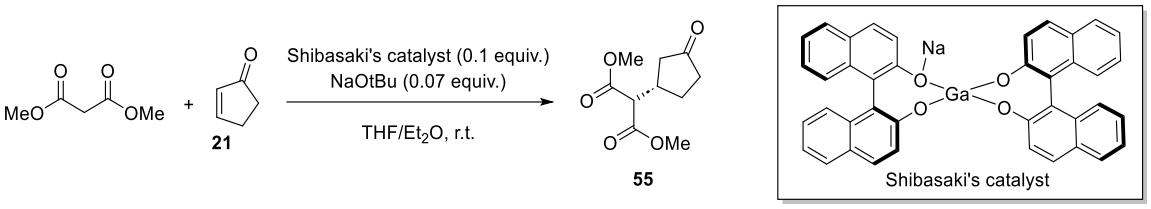

Catalyst preparation: NaOtBu (6,71 g, 70 mmol) was weighted into a flame-dried round bottom flask inside the glove box and dissolved in 122 ml of dry THF. R-BINOL was weighted into a 3-neck flame-dried round bottom flask, then dissolving it with 106 ml of dry THF. The tBuONa was solution was cannulated over the BINOL solution and in 10 minutes and let rest for 20 minutes.

GaCl3 (3,07 g, 17.5 mmol) was weighed into a flame dried round bottom flask in the glovebox and dissolved into 125 ml of 2,5:1 THF:Et2O dry mixture. The solution of BINOL-Na was transferred over the GaCl3 solution over 20 minutes and let to stir for 1 h at r..t. After that time the stirring is switched-off and the solution is let to rest overnight to allow NaCl to settle. The day later the surnattant solution was used as it is.

NaOtBu (967 mg, 10.6 mmol) was weighted into a 3-neck flame-dried rbf (into the glovebox) and dissolved in 22,5 ml of dry THF. It follows the cannulation of the upper part of the of the catalyst via addition funnel (288 ml). It follows the addition of dimethyl malonate (19 g, 144 mmol) and cyclopentenone (11,8 g, 144 mmol). The solution is stirred at r.t. for 40 h.

Quench: slow addition of 900 ml of HCl, extraction with AcOEt (400 ml x 3). Some of the solvent was evaporated for convenince. Than the solven was washed with NaHCO3, the latter was back-extracted with AcOEt. The combined organic phases were washed with brine, dried over MgSO4, filtered and the solvent was removed under reduced pressure.

Purification by hig-vacuum distillation. 27,43 g recovered (89 % yield).

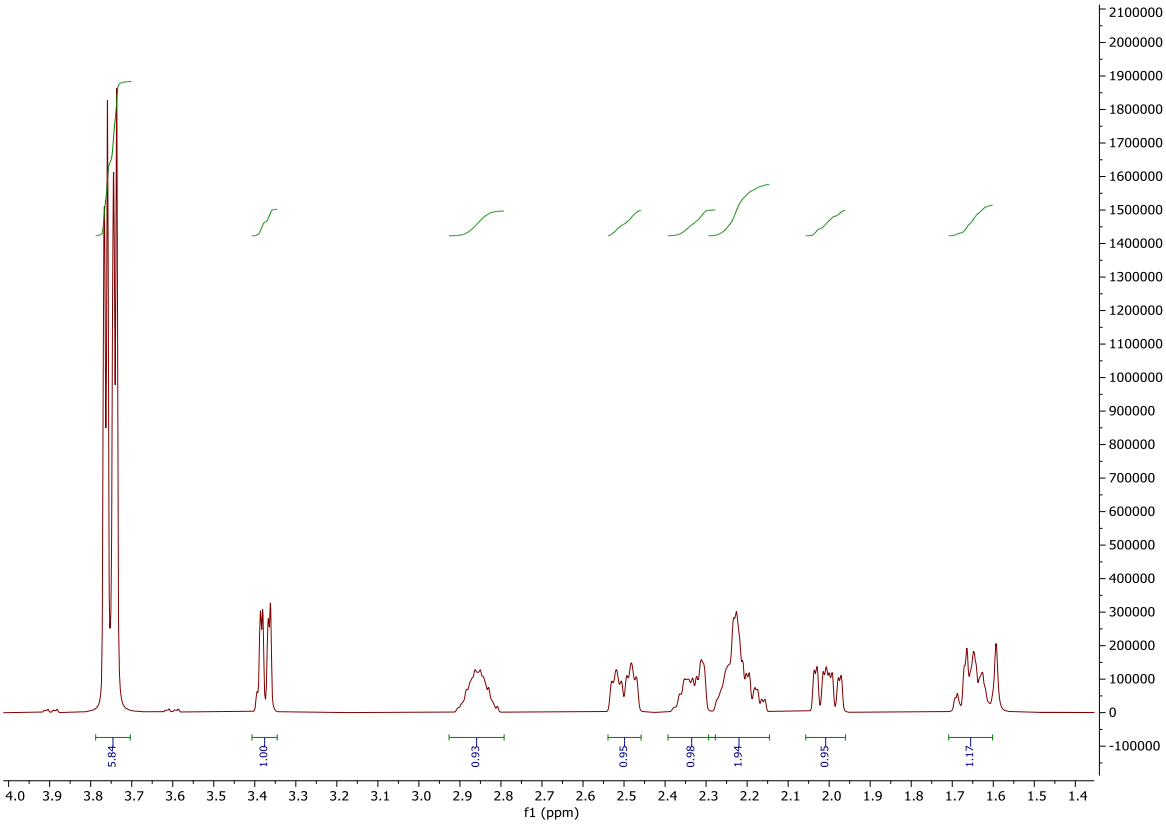

55 - 1H NMR (500 MHz, CDCl3) δ 3.76 (t, J = 3.9 Hz, 3H), 3.74 (d, J = 3.6 Hz, 3H), 3.37 (dd, J = 9.6, 2.9 Hz, 1H), 2.92 – 2.79 (m, 1H), 2.50 (dt, J = 18.6, 6.0 Hz, 1H), 2.34 (ddd, J = 18.7, 8.9, 4.4 Hz, 1H), 2.22 (dddd, J = 18.2, 13.9, 9.8, 3.7 Hz, 2H), 2.00 (ddd, J = 18.2, 10.9, 3.6 Hz, 1H), 1.70 – 1.61 (m, 1H).

56 - dimethyl (S)-2-(1,4-dioxaspiro[4.4]nonan-7-yl)malonate

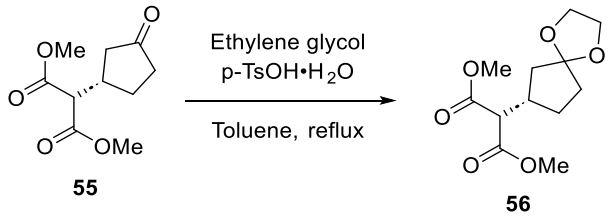

Into a single neck round bottom flask 6,44 g (30.1 mmol) of 55 were dissolved in 100 ml of toluene. Then, 3,36 ml (60.1 mmol) of ethyl glycol were added, followed by 572 mg (3.01 mmol) of p-TSA. The system was then reflux overnight, usign a dean-stark system to remove water.

The solution was then allowed to go to room temperature, diluted with diethyl ether, and aqueous NaHCO3 was then added to quench the acid. The organi phase was separated and the aqueous phase was then extracted several times. The organic phases were merged, washed with brine, dried over MgSO4, filtered and the organic solvents removed under reduced pressure. **56** was then isolated by

column chromatography (4:1 Hex:AcOEt + 2% TEA). 6,12 g were finally isolated (79% yield).

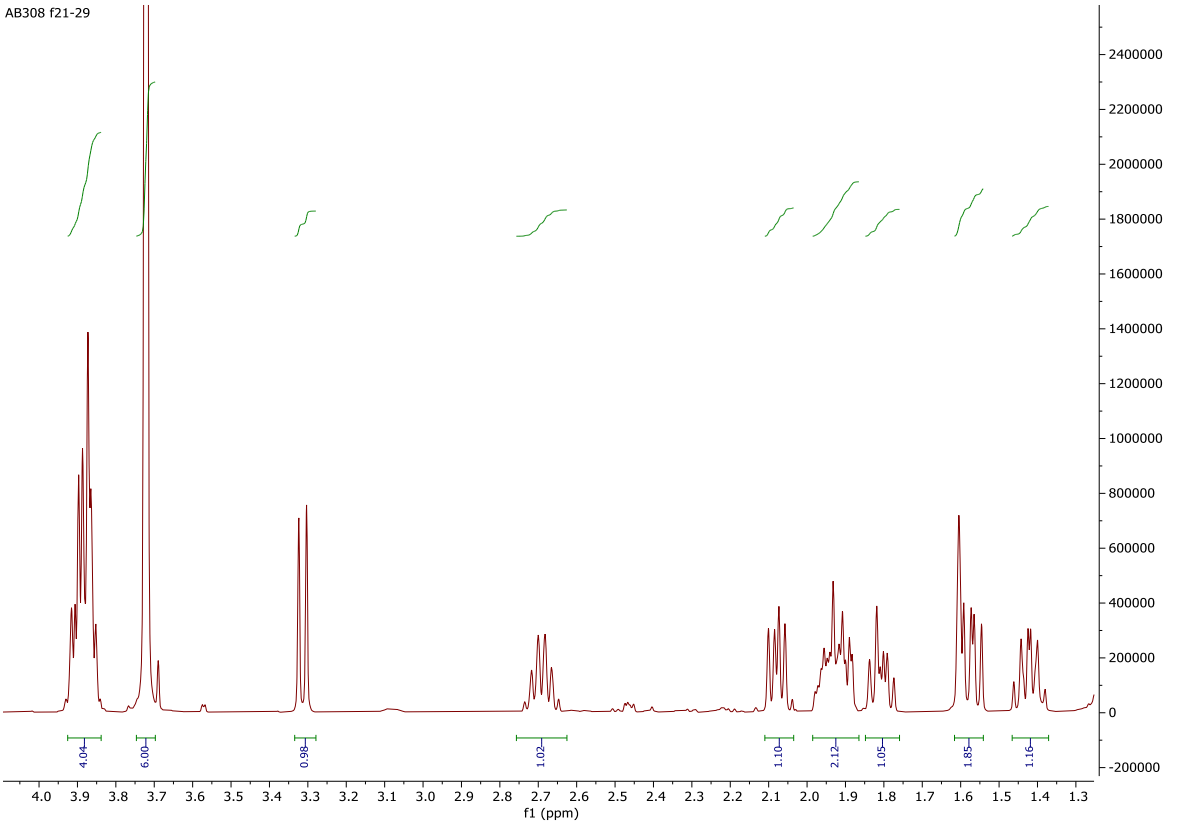

56 - 1H NMR (500 MHz, CDCl3) δ 3.94 – 3.83 (m, 4H), 3.72 (d, J = 3.5 Hz, 6H), 3.31 (d, J = 10.1 Hz, 1H), 2.69 (hept, J = 7.9 Hz, 1H), 2.08 (dd, J = 13.7, 8.0 Hz, 1H), 1.98-1.88 (m, 2H), 1.81 (m, 1H), 1.57 (dd, J = 13.6, 9.5 Hz, 1H), 1.42 (dq, J = 12.8, 9.6 Hz, 1H).

57 - dimethyl (S)-2-(2-(1,3-dioxolan-2-yl)ethyl)-2-(1,4-dioxaspiro[4.4]nonan-7-yl)malonate

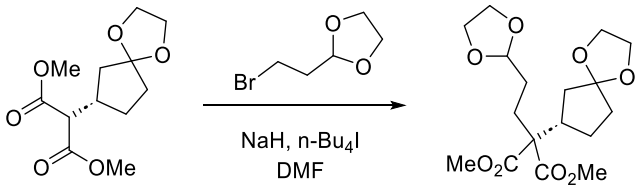

56 **57**

56 (570 mg, 2.21 mmol) is set under inert atmosphere, then dissolved in dry DMF (5,5 ml) and transferred to a flame-dried 3-neck round bottom flask. The temperature is lowered to 0 °C, then NaH (106 mg, 2.65 mmol) is added portion wise. Then, nBu4NI (163 mg, 0.44 mmol) was added, followed by the alkylating agent (390 ul, 3.31 mmol). The reaction was left to go to r.t. and stirred for 72 h.

The reaction wa then quenched with water to dilute DMF, extracted the aqueous phase with ethyl acetate multiple times. The organic phase is then washed several times with water to remove the residual DMF. The organic solvent was removed under reduced pressure and the product purified by column chromatography. 310 mg of **57** were isolated (40% yield).

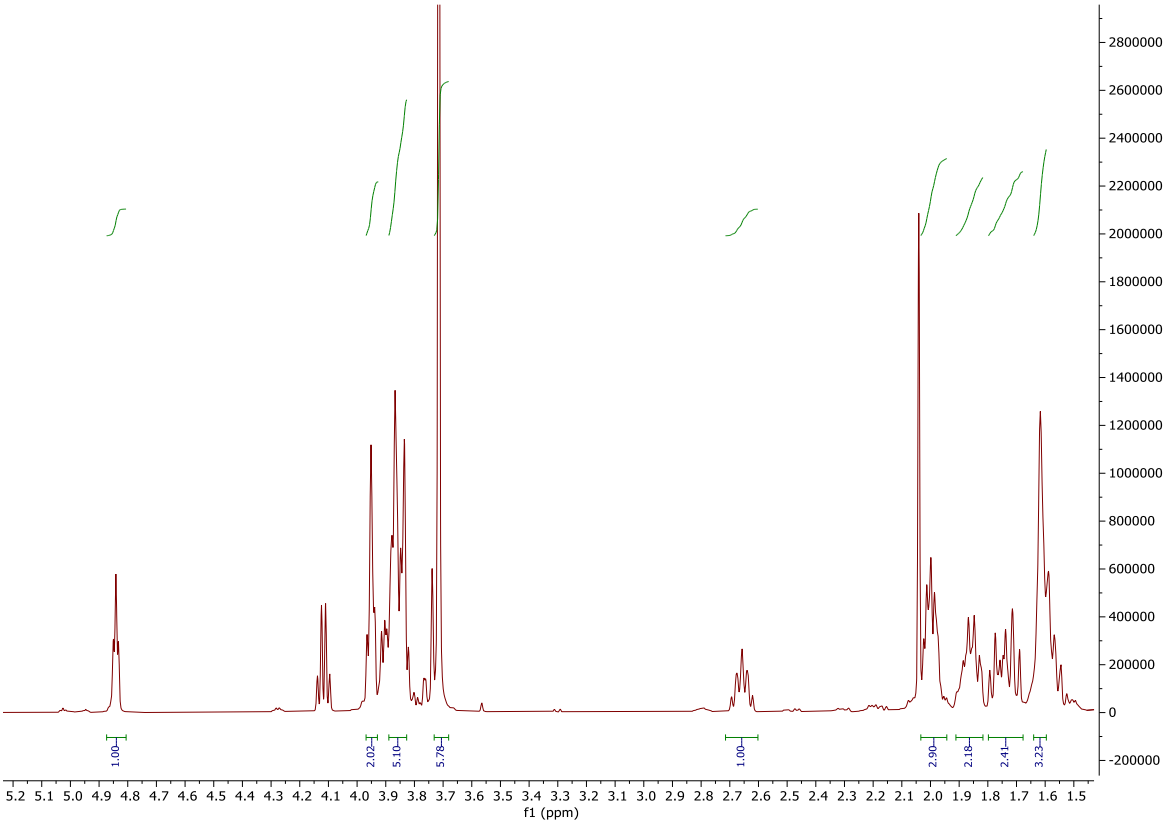

57 - 1H NMR (500 MHz, CDCl3) δ 4.84 (t, J = 4.6 Hz, 1H), 3.94 (m, 2H), 3.92 – 3.81 (m, 5H), 3.72 (s, 6H), 2.71 – 2.59 (m, 1H), 1.99 (m, 3H), 1.86 (m, 2H), 1.80 – 1.68 (m, 2H), 1.62 (m, 3H).

Some traces of ethyl acetate present.

58 - dimethyl (3aS,7R,7aS)-1-oxo-7-(4,4,5,5-tetramethyl-1,3,2-dioxaborolan-2-yl)octahydro-4H-indene-4,4-dicarboxylate

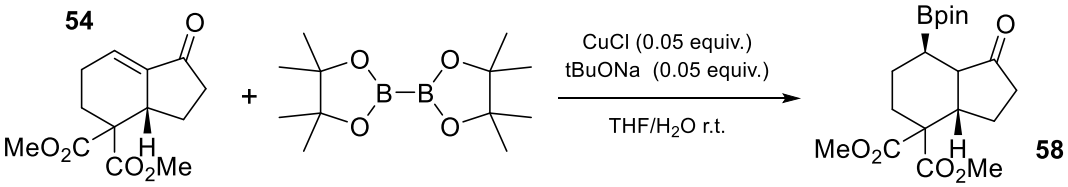

Procedure: CuCl (a spatula tip) and tBuONa (a spatula tip) were weighted into a vial in the glovebox. B2pin2 (53 mg) was weighted into a separated vial. The solution with the catalyst was dissolved in dry THF (145 ul) under inert

atmosphere and let to stir for 10 minutes. B2pin2 is dissolved in dry THF (115 ul) and then injected into the catalyst suspension, stirring for 10 minutes. The susbtrate (50 mg) was dissolved in dry THF (115 ul) under inert atmosphere and it follows the addition to the catalyst solution. The reaction was left to stir for 40 h. Then, brine was added and extract with AcOEt multiple times. The organic phase is then dried over MgSO4, filtered and the solvent is removed under reduced pressure. The crude in analyzed by HNMR to check the product formation. It seems the alkene is gone, so the reaction was purified by column chromatography (9:1 Hex:AcOEt). 41,2 mg of **58** were recovered (55% yield).

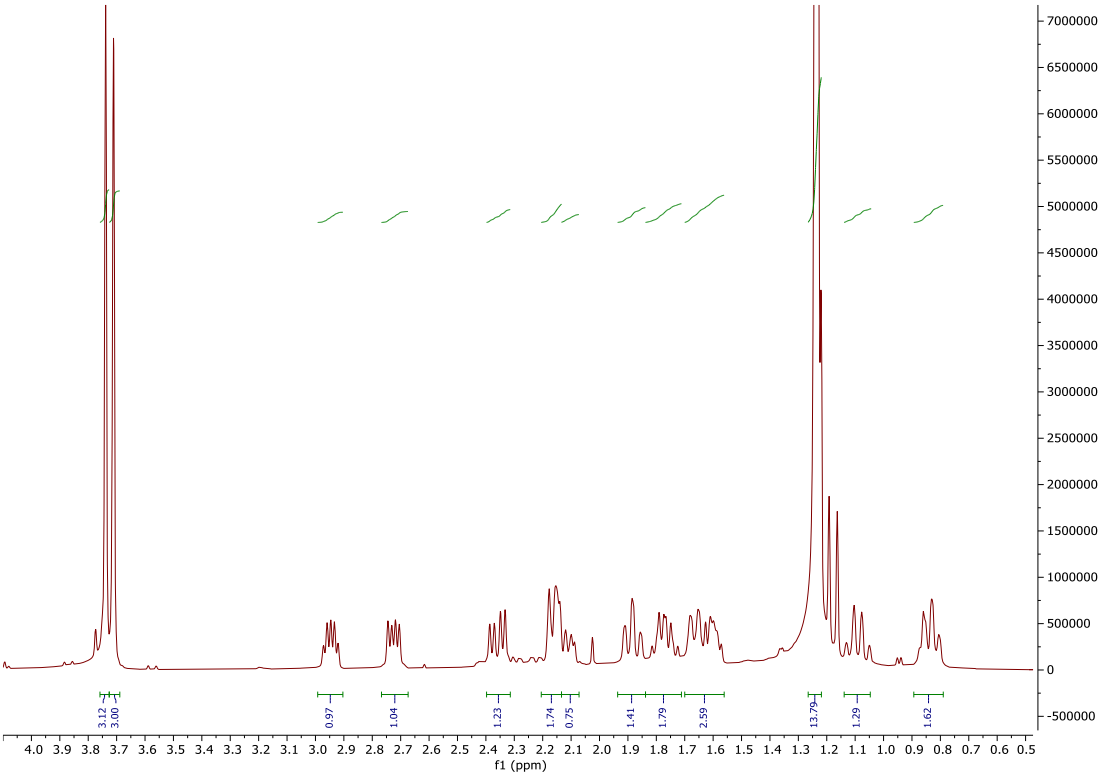

58 - 1H NMR (500 MHz, CDCl3) δ 3.74 (s, 3H), 3.71 (s, 3H), 2.95 (dt, J = 13.0, 6.5 Hz, 1H), 2.72 (dd, J = 13.3, 6.8 Hz, 1H), 2.36 (dd, J = 18.9, 8.3 Hz, 1H), 2.19 – 2.07 (m, 2H), 1.88 (m, 1H), 1.77 (m, 2H), 1.63 (m, 2H), 1.24 (s, 6H), 1.23 (s, 6H), 1.09 (t, *J* = 14.2 Hz, 1H), 0.90 – 0.77 (m, 2H). Traces of the minor diastereoisomer are detectable, as confirmed by 13CNM (areas are somehow unbalanced for this reason).

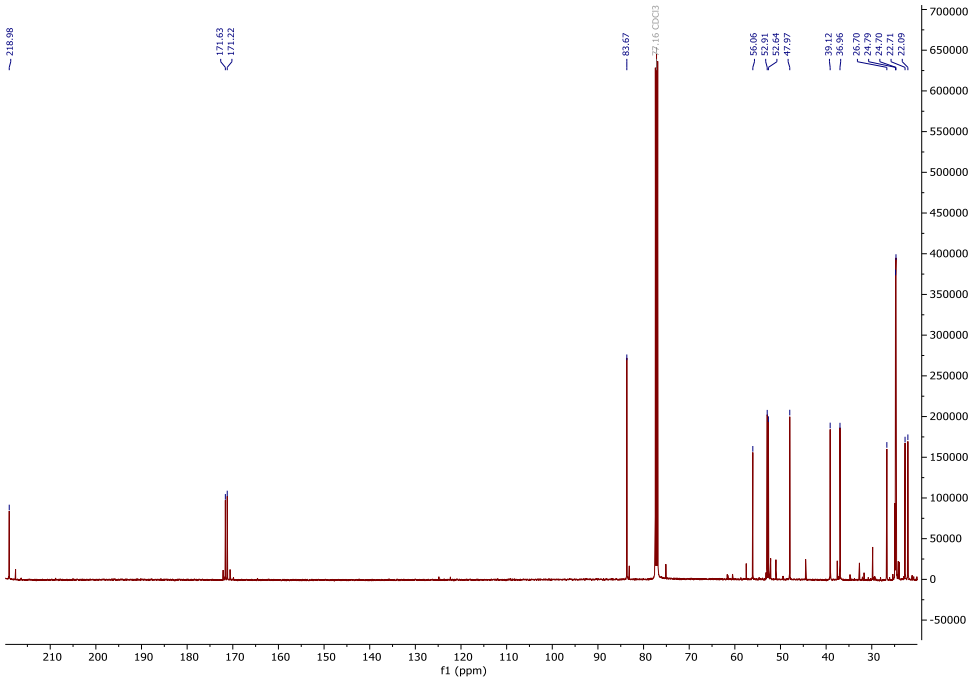

58 - 13C NMR (126 MHz, CDCl3) δ 218.98, 171.63, 171.22, 83.67, 56.06, 52.91, 52.64, 47.97, 39.12, 36.96, 26.70, 24.79, 24.70, 22.71, 22.09. All peaks have a similar-shifted peak with a much lower intensity, presumably due to the minor diastereoisomer. The stereochemical attribution was not done as the preparation of this compound proved to be somehow irreproducible.

59 - dimethyl (3aS,7R,7aR)-7-hydroxy-1-oxooctahydro-4H-indene-4,4-dicarboxylate

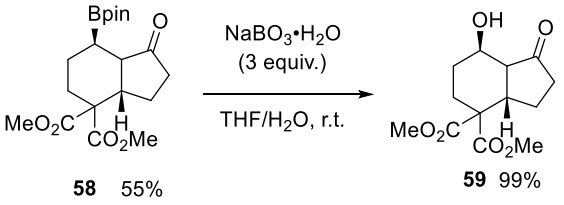

58 55% **59** 99%

58 (25 mg, 0.065 mmol) was dissolved in 1,8 ml of THF/H2O 1:1. Then, 30 mg (0.20 mmol) of $NaBO_3 \bullet 4H_2O$. After 3 hours 1,8 ml of H_2O are added (1:3 THF:H_2O created). The reaction was left to stir overnight. The morning after the reaction is quenched with aqueous Na2S2O3 and extracted with DCM. Solvent was removed under reduced pressure. Chromatographic purification is attempted (3:1 Hex:AcOEt). The main spot is isolated (some fraction mixed). 20.3 mg of 59 were isolated (>100%, probably some left hexane raises the weight). Considering that crude HNMR showed full conversion, a 99% yield is stated for this procedure. Importantly, in the isolated fraction contains mainly the same compound and another similar one (in a different proportion), presumably the isomeric aldol

product, possibly coming from retro-aldol/aldol equilibration processes. **59** was fully characterized.

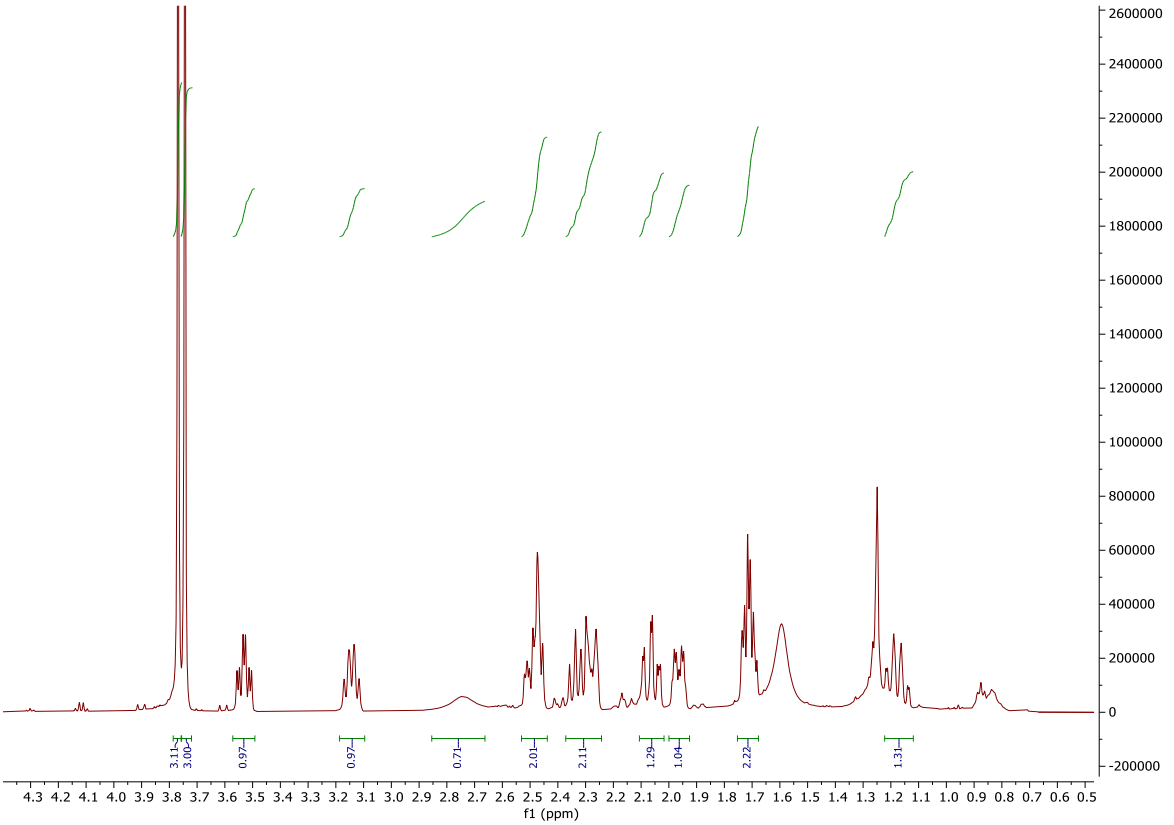

59 - 1H NMR (500 MHz, CDCl3) δ 3.77 (s, 3H), 3.74 (s, 3H), 3.53 (td, J = 10.9, 4.5 Hz, 1H), 3.14 (q, J = 9.2 Hz, 1H), 2.74 (bs, 1H), 2.49 (m, 2H), 2.38 – 2.23 (m, 2H), 2.06 (td, J = 14.5, 3.0 Hz, 1H), 1.96 (dq, J = 12.4, 4.0 Hz, 1H), 1.71 (m, 2H), 1.18 (tdd, J = 13.9, 11.4, 2.9 Hz, 1H). There are visible traces of hexane. Moreover, it seems that there are traces of the other aldol and/or slow ring flipping process generating a population of sub-peaks. These are not visible anymore in the 13CNMR spectrum shown below.

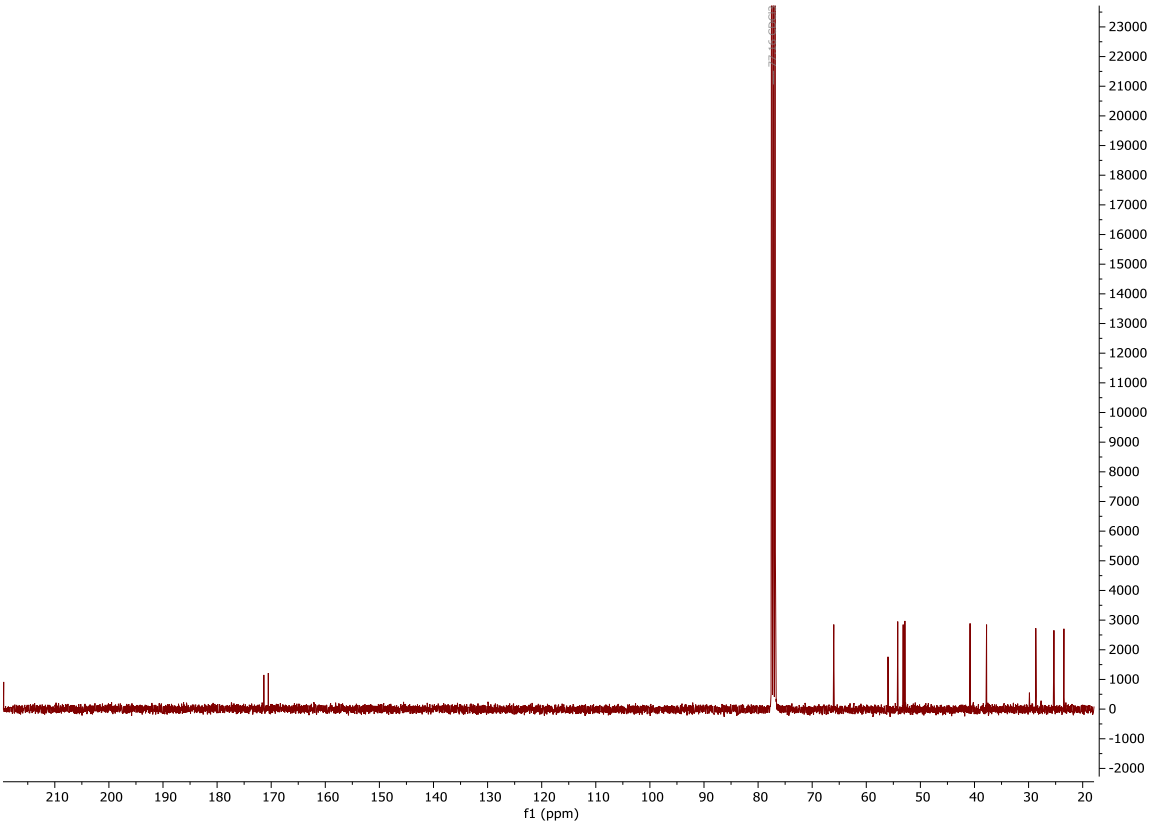

13C NMR (101 MHz, CDCl3) δ 219.45, 171.36, 170.53, 66.01, 55.98, 54.19, 53.18, 52.86, 40.82, 37.76, 28.67, 25.31, 23.47.

It can be observed that beside a small trace of an unidentified impurity, the spectrum looks clean, without any trace of the other diastereomeric aldol. Maybe conformers were observed, or the long acquisition time allowed for complete equilibration. It is difficult to be more precise than this in my opinion.

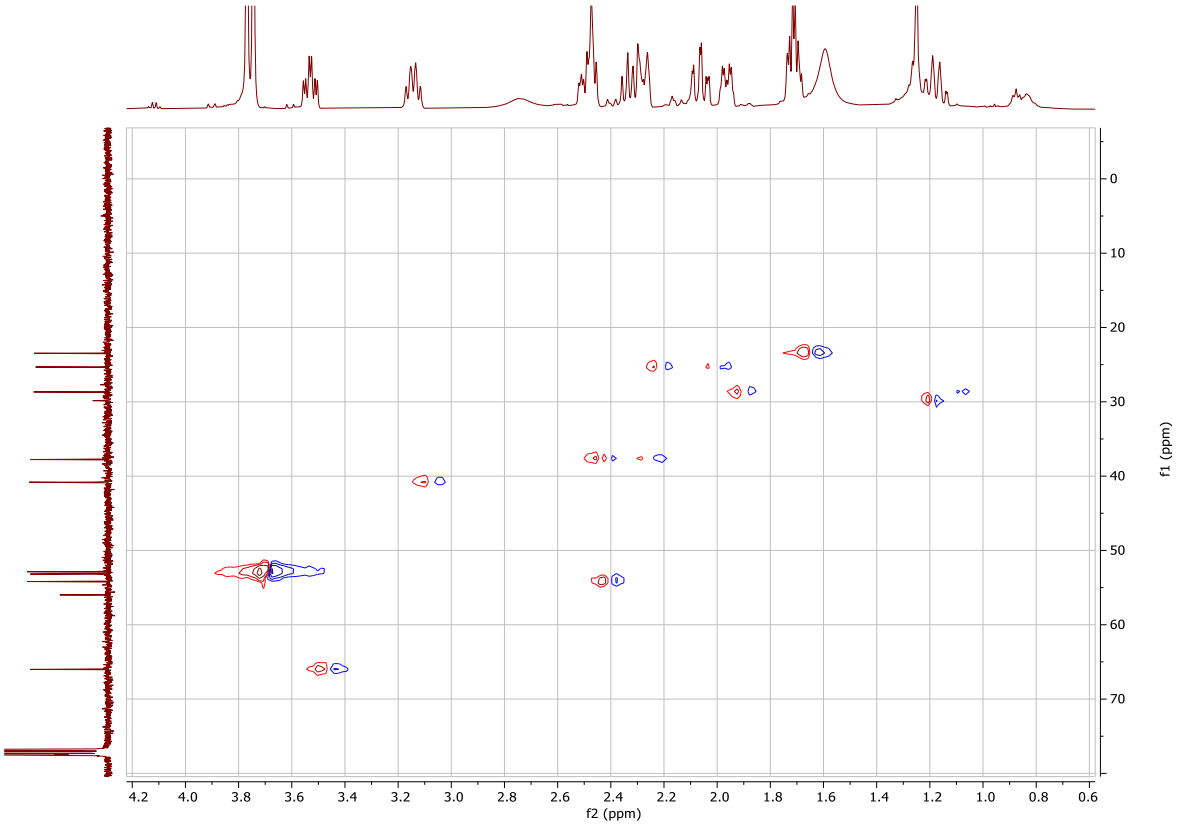

HSQC

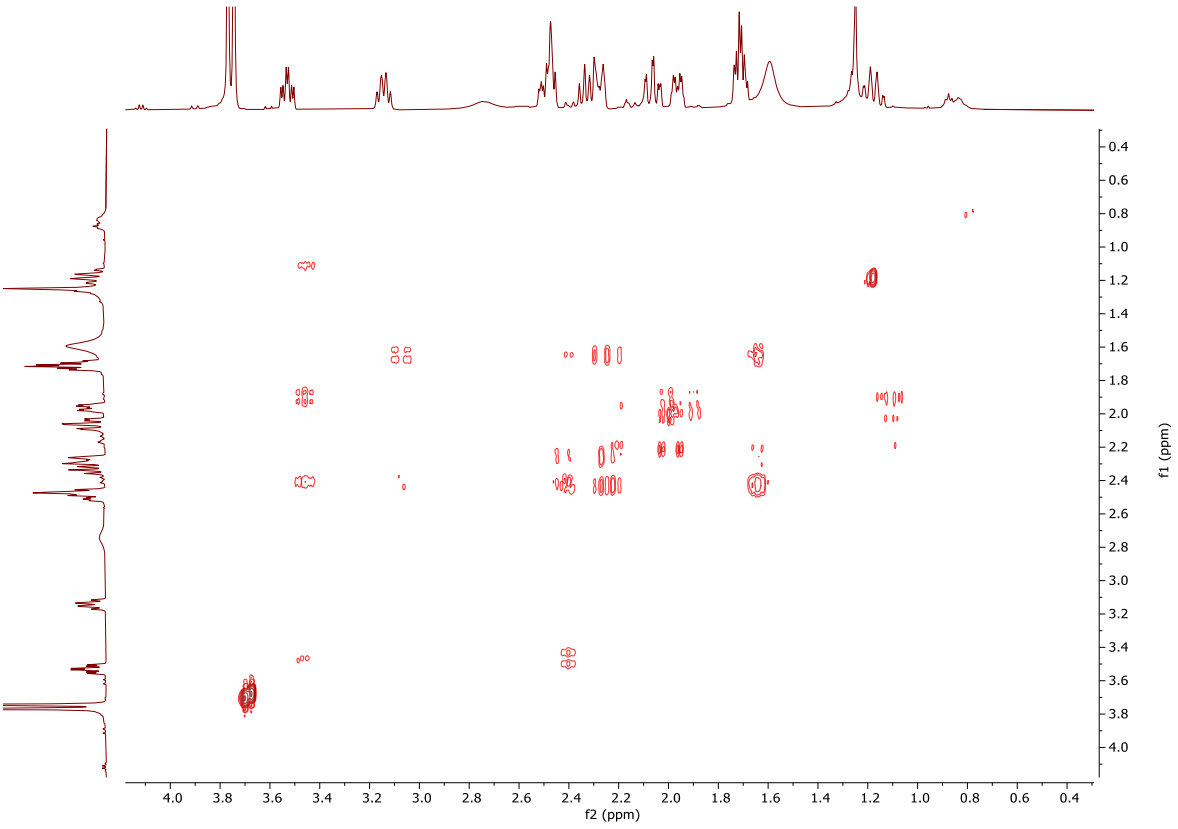

COSY

60 - dimethyl (3aS,7R,7aR)-7-((tert-butyldimethylsilyl)oxy)-1-oxooctahydro-4H-indene-4,4-dicarboxylate

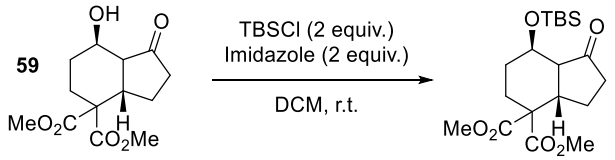

60 34%

59 (19 mg, 0.07 mmol) was put under inert atmosphere and dissolved in 700 ul of dry DCM. Then, 9.6 mg of imidazole (0.14 mmol), was added and the temperature lowered to 0 °C. It followed the addition of TBSCl (21 mg, 0.14 mmol). The reaction was allowed to reach room temperature. After 2 h the reaction is quenched (see below) and checked by HNMR, but no reaction occurred. Thus, the material was recovered and the procedure repeated using two equivalents of silylation agents and imidazole, overnight. After this time the reaction was quenched with water and extracted with DCM. The organic phase was dried over MgSO4, filtered and the solvent removed under reduced pressure. Starting material was not fully converted.

The product was separated via column chromatography (95:5 to 80:20 Hex:AcOEt). The 9.1 mg of product recovered (34% yield).

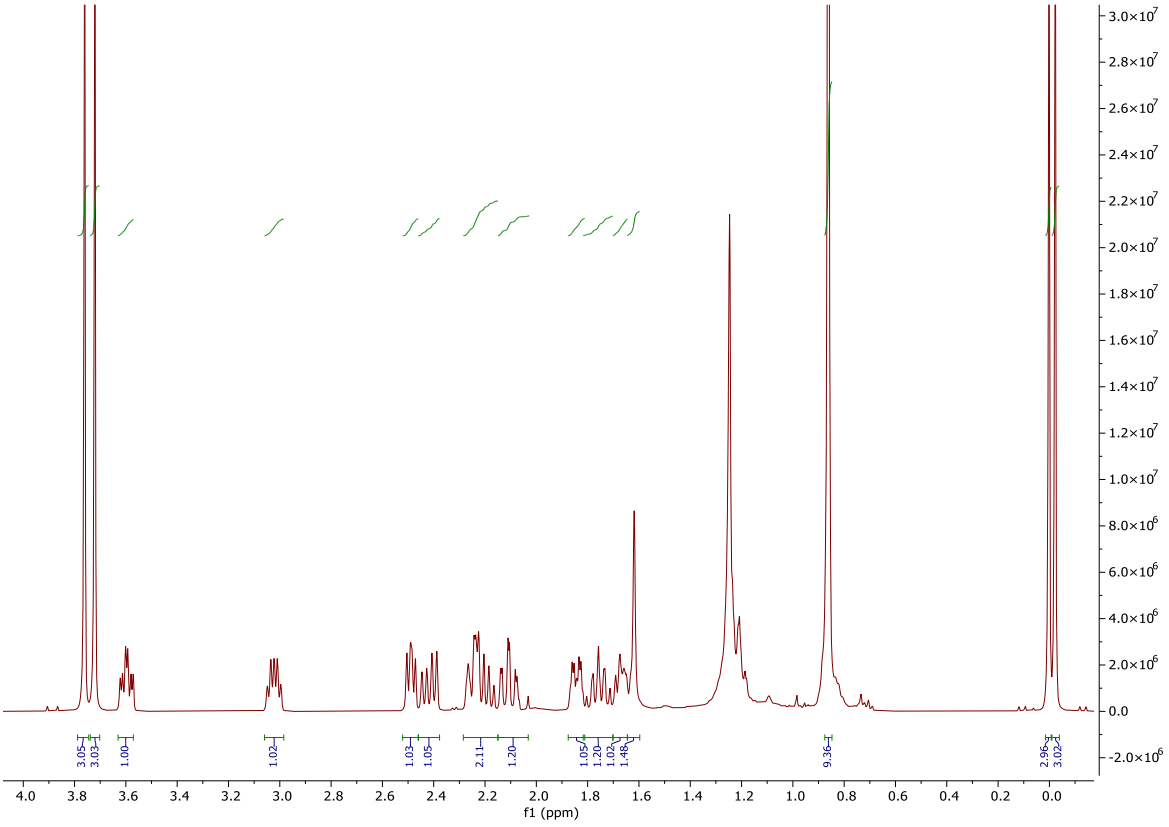

1H NMR (500 MHz, CDCl3) δ 3.76 (s, 3H), 3.72 (s, 3H), 3.60 (td, J = 10.5, 4.4 Hz, 1H), 3.02 (dt, J = 13.3, 6.8 Hz, 1H), 2.49 (dd, J = 9.9, 6.8 Hz, 1H), 2.42 (dd, J = 19.5, 9.4 Hz, 1H), 2.28 – 2.16 (m, 2H), 2.15 – 2.02 (m, 1H), 1.84 (m, 1H), 1.76 (ddd, J = 22.7, 12.7, 10.0 Hz, 1H), 1.67 (m, 1H), 1.62 (bs, 1H), 0.86 (s, 9H), 0.00 (s, 3H), -0.02 (s, 3H).

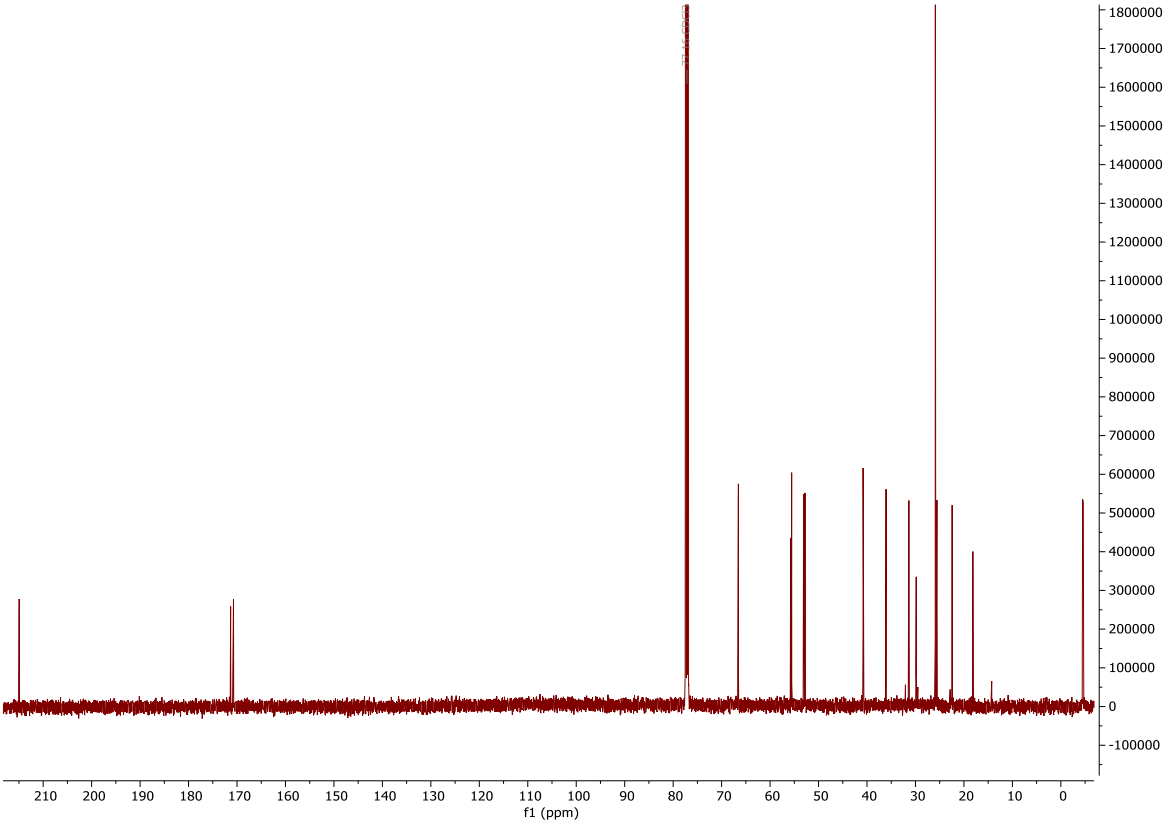

60 - 13C NMR (126 MHz, CDCl3) δ 214.95, 171.31, 170.73, 66.54, 55.75, 55.55, 53.08, 52.80, 40.81, 36.07, 31.36, 29.84, 25.90, 25.57, 22.44, 18.16, -4.48, -4.63.

62 - dimethyl (1R,3aS)-1-hydroxy-1-methyl-1,2,3,3a,5,6-hexahydro-4H-indene-4,4-dicarboxylate *(supposed to be)*

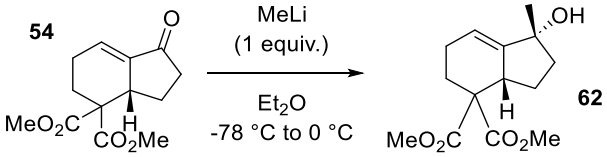

A stock solution of 0,16 M of MeLi in Et2O was prepared diluting a 1,6 M commercial solution, concentration in the calculation. 58 (15 mg, 0.06 mmol) was weighted into a vial and put under inert atmosphere. Then, 400 ul of dry Et2O are added and the solution was brought to - 0 °C. Then, 400 ul of MeLi stock solution (0.06 mmol of MeLi) were added. After 1 ht TLC check (Hex:AcOEt 1:1) confirms the formation of new products (similar Rf). The reaction is quenched with NH4Cl

and extracted multiple times with DCM. The organic phase is then dried over MgSO4, filtered and the solvent is removed under reduced pressure.

The HNMR analysis of the crude shows the formation of 2 new alkenes, probably the 2 diastereoisomers. The purification of the crude is attempted, but new peaks are seen in the alkere region, probably by dehydration (compound **63**). A clear characterization of **62** was thus not possible.

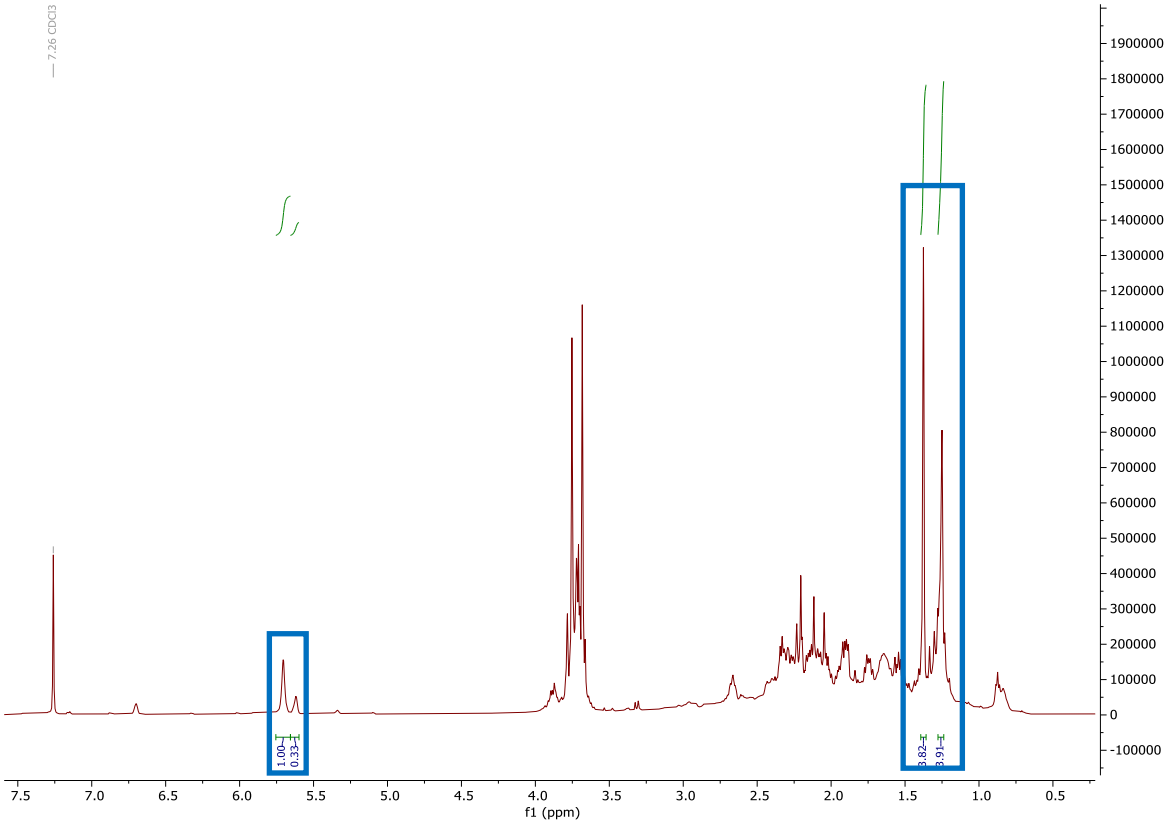

Alkenes and methyl groups are clearly visible by HNMR spectrum. Probably both diastereoisomers are formed in this reaction. Purification was not possible as decomposition over silica was observed, also with protected hydroxyl group.

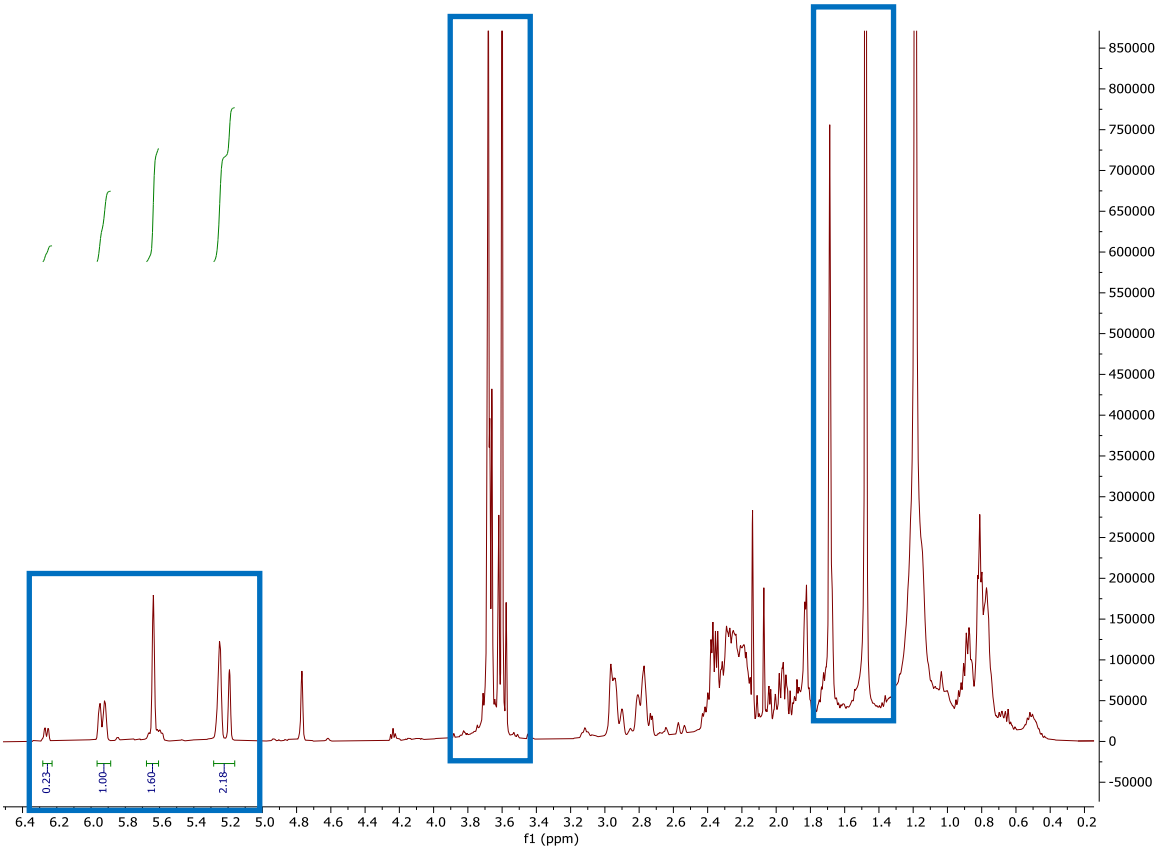

As it can be observed by this *single spot* 1HNMR spectrum, more alkene functionalities are detected, probably derived by more dehydration pathways. The added methyl groups are still visible, as well as the malonate groups. The mixture of compounds was not characterized better as we were interested only in the synthetic target.

64 - dimethyl (1R,3aS)-1-methyl-1-((triethylsilyl)oxy)-1,2,3,3a,5,6-hexahydro-4H-indene-4,4-dicarboxylate

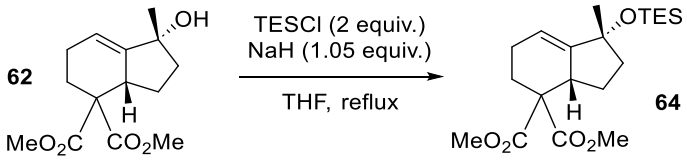

NaH (37,6 mg, 1.57 mmol) is weighted into a flame dried 2 neck round bottom flask in the glovebox. 62 (140 mg, 0.52 mmol) is put under inert atmosphere, then dissolved in 1,8 ml of dry THF. It follows the addition of this solution over the NaH in ice bath. After 10 mintues TESCl (130 ul, 0.78 mmol) was added and the reaction refluxed. After 1,5 h a TLC check (Hex:AcOEt 1:1) shows elimination product 63. The reaction is so quenched with NaHCO3, extracted with DCM, washed with

brine, dried over MgSO4, filtered and the solvent is removed under reduced pressure. A HNMR of the crude is taken, showing actually a single alkene peak and what seems a decently clean product 64 as diastereomeric mixture (starting material 62 is a diastereomeric mixture itself). Given the sensibility of the substrate that eliminates over TLC silica, this mixture was used as it is for the next epoxidation step.

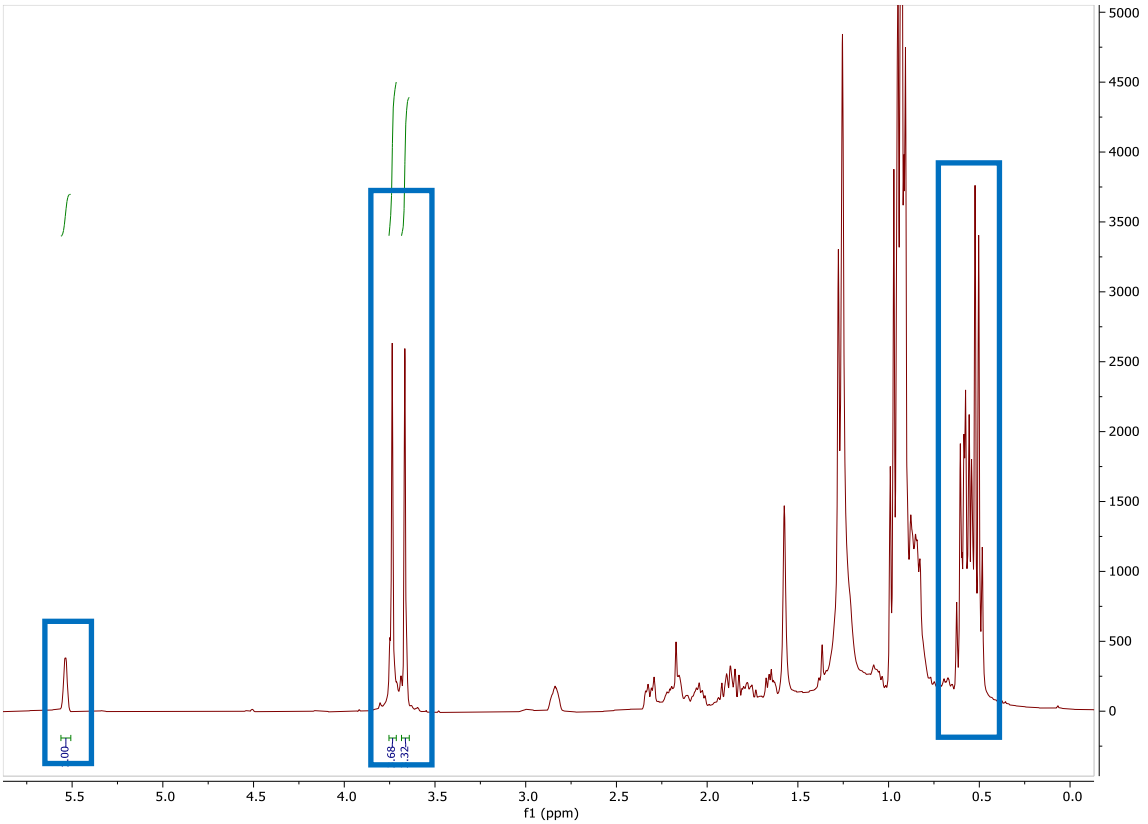

The 1HNMR was tentatively assigned to a diastereomeric mixture of substrate **64** as alkene, malonate methyl groups and silicon-attached ethyl groups are clearly visible. However, given the sensibility of the substrate it was not possible to attempt chromatographic purification.

65 – dimethyl (1aR,4aR,7R,7aS)-7-methyl-7-((triethylsilyl)oxy)hexahydroindeno[3a,4-b]oxirene-4,4(1aH)-dicarboxylate

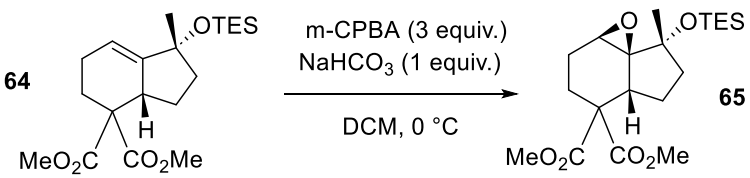

64 (21.1 mg, 0.05 mmol) was dissolved into 0,5 ml of DCM, then NaHCO3 was added (46.3 mg, 0.055 mmol). The temperature was lowered to 0 °C using an ice batch, then m-CPBA (28.6 mg, 0.165 mmol) was added. After around 1 hours the reaction was quenched with aqueous Na2S2O3, the oraganic phase separated and the aqueous phase extracted with DCM. The organic phases were merged, washed with aqueous NaHCO3, brine and dry over MgSO4. The organic phase was then filtered and the solvent removed the solvent under reduced pressure. HNMR shows the formation of a product, but given the sensibility of this substrate class separation over silica was not attempted, and other separation methods were not tried for time reasons.

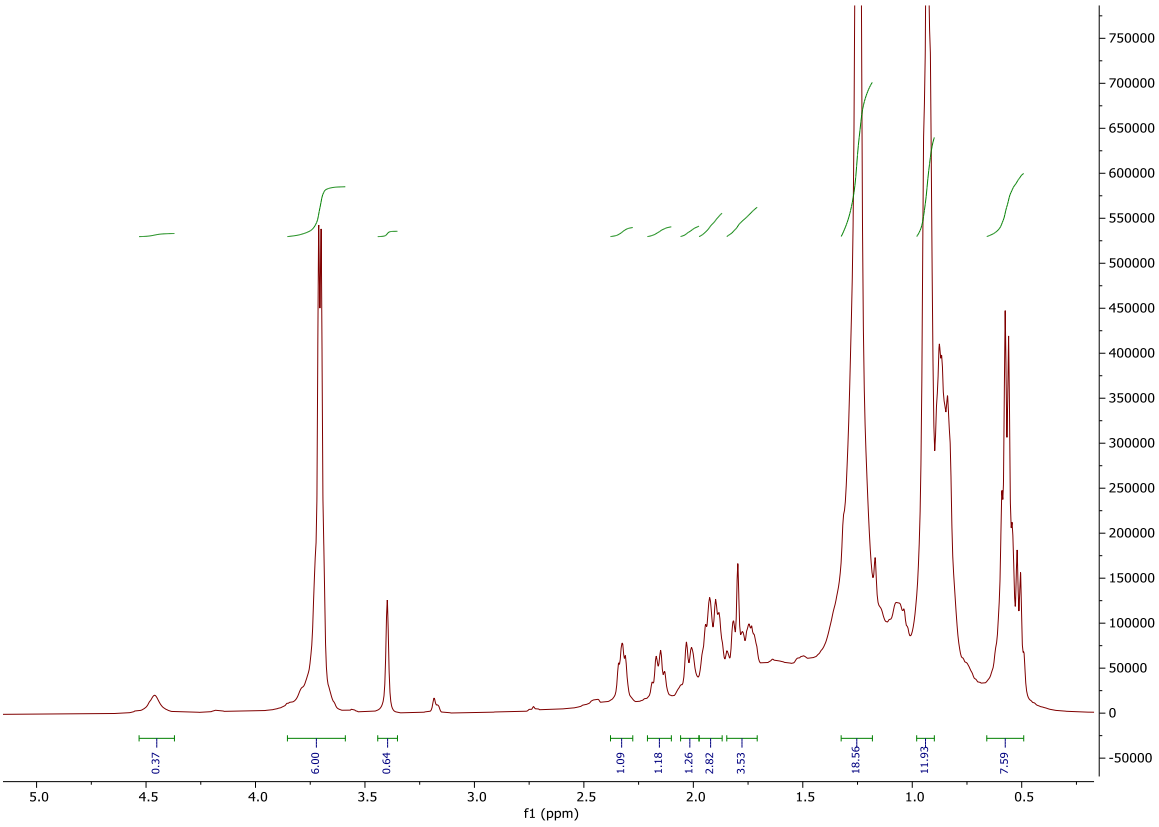

As can be observed by HNMR, there is clear formation of product, presumably a diastereomeric mixture. A proper characterization was not possible as the product was not purified for time reasons.

66 – dimethyl (1aR,7R,7aS)-7-hydroxy-7-methylhexahydroindeno[3a,4-b]oxirene-4,4(1aH)-dicarboxylate

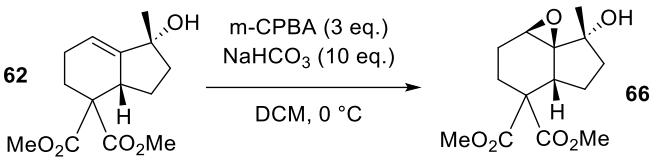

200 mg (0.79 mmol) of 54 were dissolved in 8 ml of dry THF under inert atmosphere. The temperature was set to - 78 °C, then 1.6 MeLi (520 ul, 0.82 mmol) wa added dropwise at the same temperature. The reaction is monitored by TLC. When the SM goes the reaction is quenched with MeOH and NH4Cl, extracted with DCM, dried over MgSO4, filtered and the solvent is removed under reduced pressure. The reaction is checked by HNMR to verify the formation of a diastereomeric mixture of products as already observed. It followed dissolution in DCM (4 ml) and addition of 666 mg of NaHCO3 (7.9 mmol), followed by m-CPBA (533 mg, 2.38 mmol), at 0 °C, then let go to room temperature. The reaction is monitored again by TLC. After 4 hours the reaction was quenched Na2S2O3 + NaHCO3 in acqueous solution (to buffer the mCPBA). The acqueous pahse is separated from the DCM and extracted again twice with the same solvent. Then, the organic phase is dried over MgSO4, filtered and the solvent is removed unde reduced pressure. HNMR shows the disappearance of the alkene peaks, so the compound is purified by flash chromatography. Both dehydration and fragmentation to yield **54** are observed.

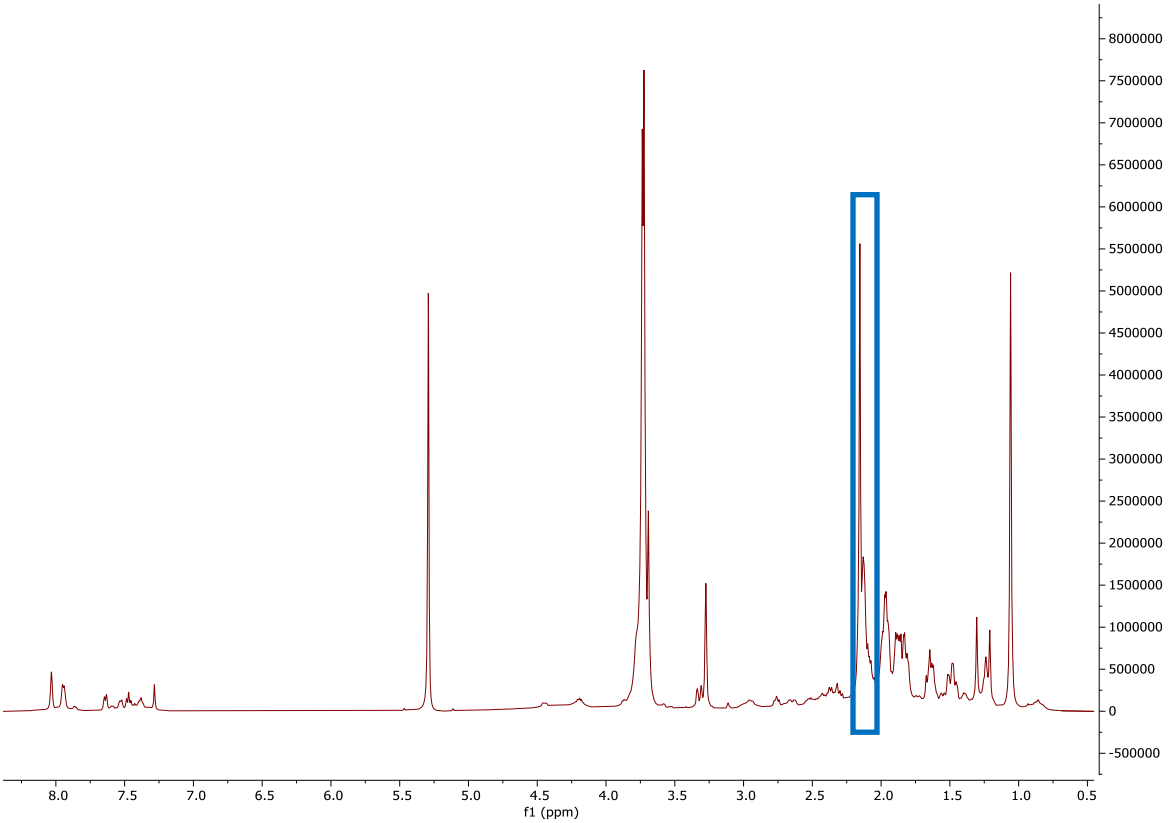

The 1HNMR of the crude before column chromatography is shown. Presumably, more diastereoisomers are formed, as the methyl addition to the ketone is not selective. However, here the alkenes are not visible anymore, so the reaction was concluded for sure. However, proper characterization was not possible, as substrate decomposed over silica yielding a dehydration product of type **63** and curiously **54**, the starting material.

67 – dimethyl (7S,7aS)-7a-bromo-7-hydroxy-1-oxooctahydro-4H-indene-4,4-dicarboxylate

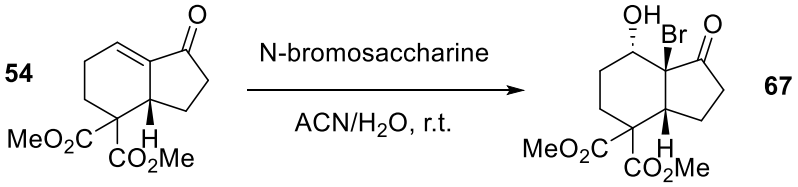

482 mg of **54** were weighted into a round bottom flask and dissolved in 8,5 ml of ACN. Then, 1,5 ml of water were added. The system was put at 0 °C. Finally N-bromosaccarine (700 mg) was added in small portions over 30 minutes. The reaction was left to go to room temperature and let to stir for 6 hours. The reaction was then quenched by the addition of a saturated Na2S2O3. The mixture was then extracted with Et2O (x3), and the combined organic extracts were washed with saturated NaHCO3 (x2), brine, dried over MgSO4, filtered, and concentrated in vacuo to afford a crude white solid. This was re-dissolved in Et2O (75 mL) at 35 °C. The solution was concentrated until ca. 30 mL of solvent remained, and then hexanes (30 mL) was added. The solution was concentrated until ca. 60 mL of solvent remained, with white solids suspended within. The solvent was filtered and washed carefully with hexane. 415 mg of **67** were recovered (62 % yield).

68 – dimethyl (1aS,4aR,7aR)-7-oxohexahydroindeno[3a,4-b]oxirene-4,4(1aH)-dicarboxylate

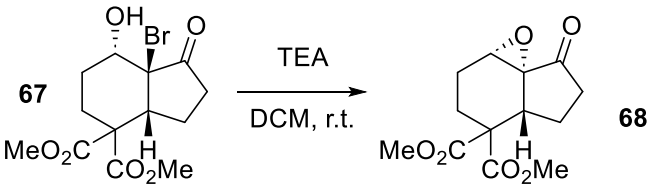

In a 50 mL, round-bottom flask, bromohydrin **67** (415 m g, 1.91 mmol, 1.0 equiv.) was dissolved in DCM (12 mL). Et_3N (318 ul, 2.29 mmol, 1.2 equiv.) was added, and the reaction was stirred at 20 °C for 18 h. After this time around 2/3 of the solvent were removed under reduced pressure. The mixture purified directly via flash chromatography (100% Hex, then 60:40 Hex:EtOAc in hexanes) affording compound **68** (455 mg, 1.7 mmol, 75% yield) as a white solid. The resulting solid was not recrystallized as reported but used as it was.

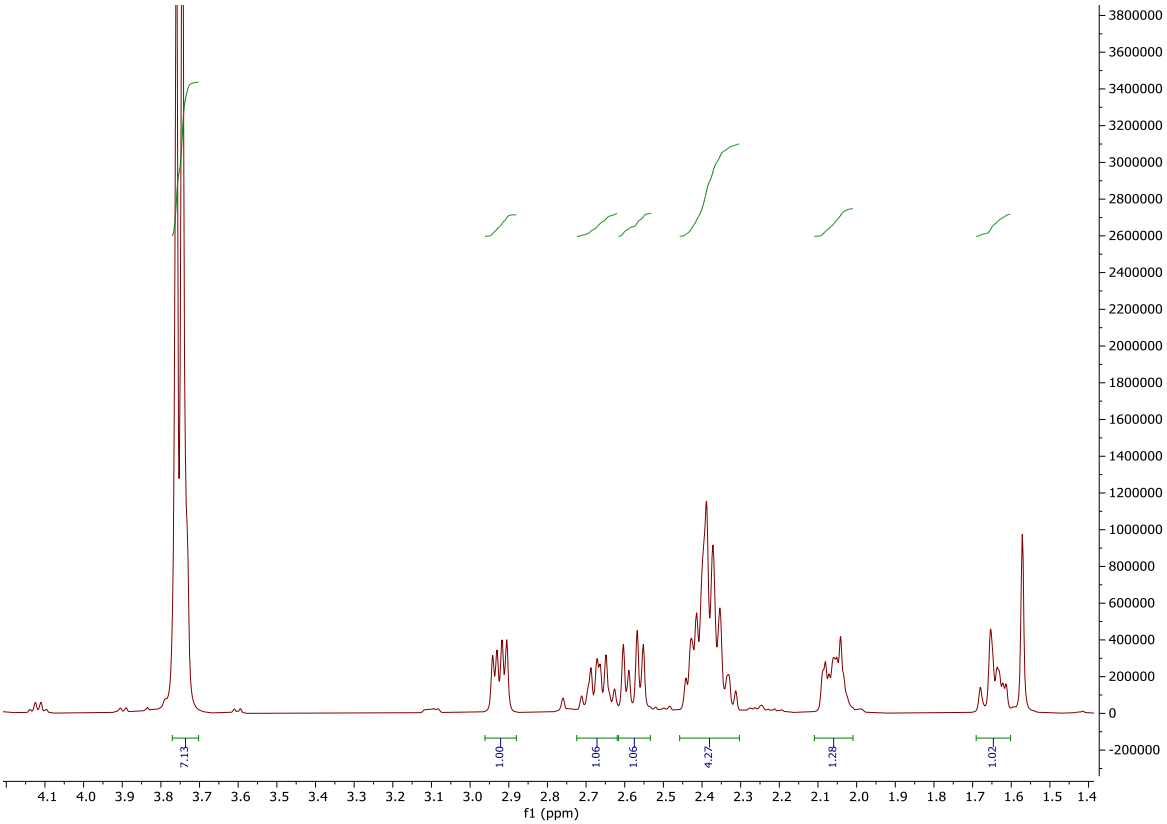

68 - 1H NMR (500 MHz, CDCl3) δ 3.75 (d, J = 7.8 Hz, 7H*), 2.92 (dd, J = 12.5, 5.9 Hz, 1H), 2.67 (qd, J = 11.5, 7.4 Hz, 1H), 2.58 (dd, J = 18.2, 7.6 Hz, 1H), 2.45 – 2.30 (m, 4H), 2.10 – 2.03 (m, 1H), 1.69 – 1.60 (m, 1H).

*One of the hydrogens signals is under the methyl signal

69 - dimethyl (1aS,4aR,7R,7aR)-7-hydroxy-7-methylhexahydroindeno[3a,4-b]oxirene-4,4(1aH)-dicarboxylate

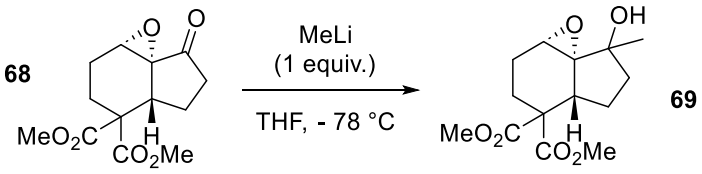

50 mg of epoxide **68** (0.18 mmol) were put under inert atmosphere dissolved in 1,86 ml of dry THF, helping with sonication. Then, temperature was lowered to -78 °C. 1.86 ml (0.186 mmol) od 0,1 M solution of MeLi in THF was also put at - 78 °C, then injected dropwise over the substrate.containing solution, monitoring conversion by TLC. After the reaction is finished 47.3 ul of TMSCl (0.37 mmol) were added and the system allowed to go to room temperature overnight. It seems by TLC that no silylation occurred. The reaction was then quenched with aqueous NaHCO3 and extracted with DCM.

HNMR shows the formation of two compounds. Half of the crude was separated by column chromatography (from 4:1 to 1:1 Hex:AcOEt)

The other half of the crude was kept for different silylation conditions

First spot was spilled by mistake (7 mg). Second spot (5 mg) was fully characterized. Mass ration between the two fraction matches the d.r. measure by HNMR. HPLC/MS shows actually two compounds with isomass, despite the product is clean. Probably it undergoes acid-catalyzed Payne rearrangement.

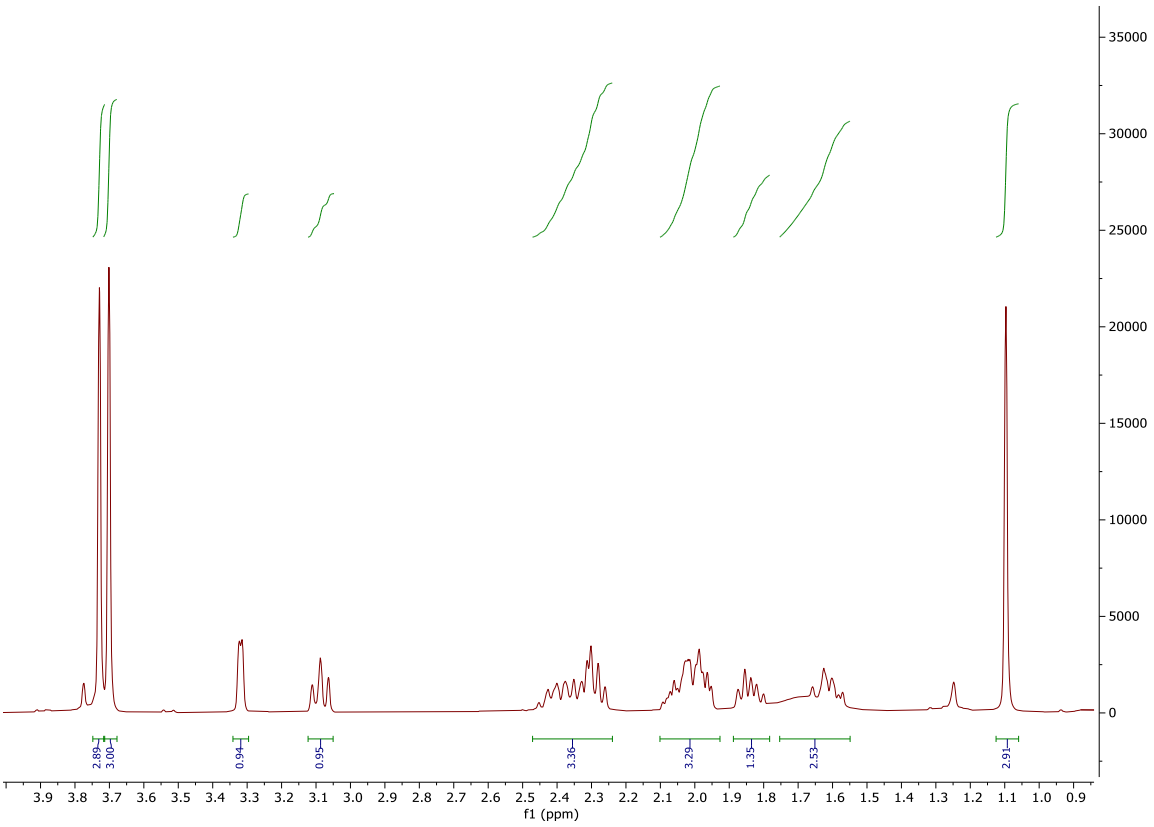

69 - 1H NMR (400 MHz, CDCl3) δ 3.73 (s, 3H), 3.70 (s, 3H), 3.32 (d, J = 3.7 Hz, 1H), 3.09 (dd, J = 10.4, 8.5 Hz, 1H), 2.47 – 2.24 (m, 3H), 2.02 (m, 3H), 1.84 (m, 1H), 1.78 – 1.55 (m, 2H), 1.10 (s, 3H).

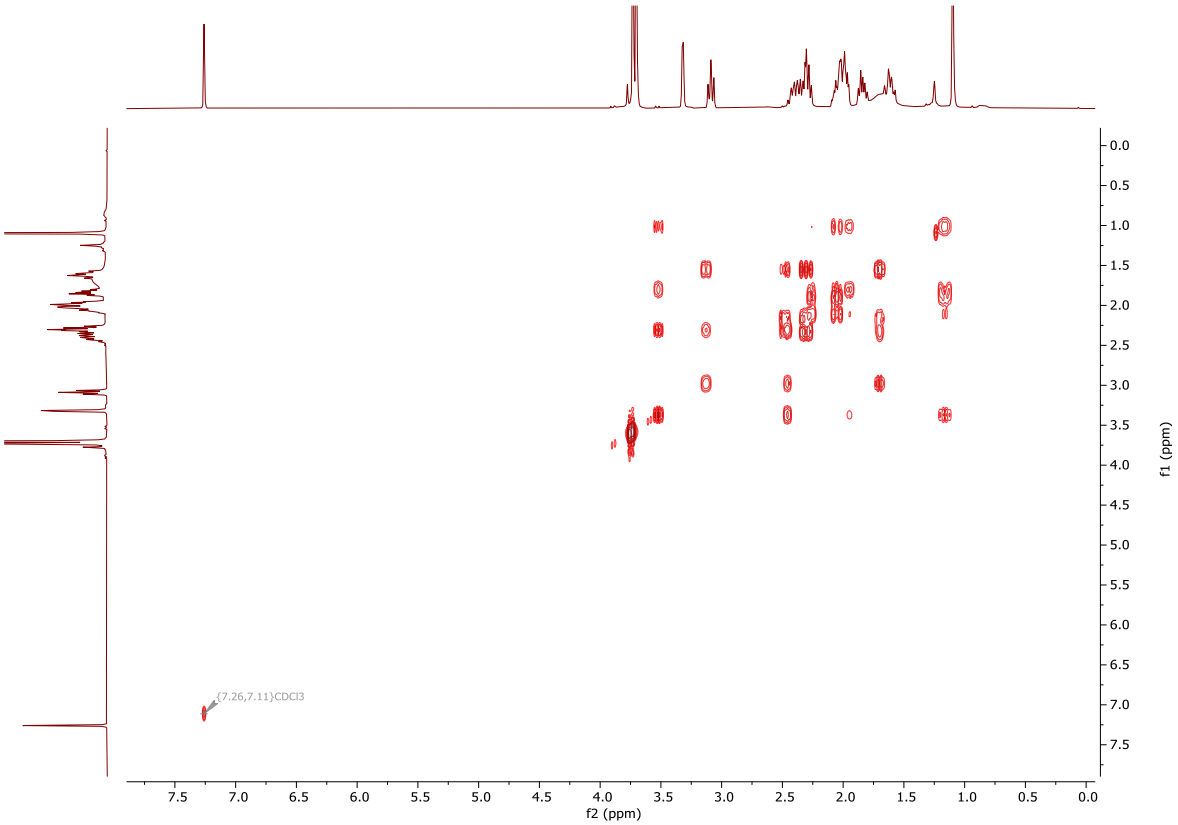

COSY

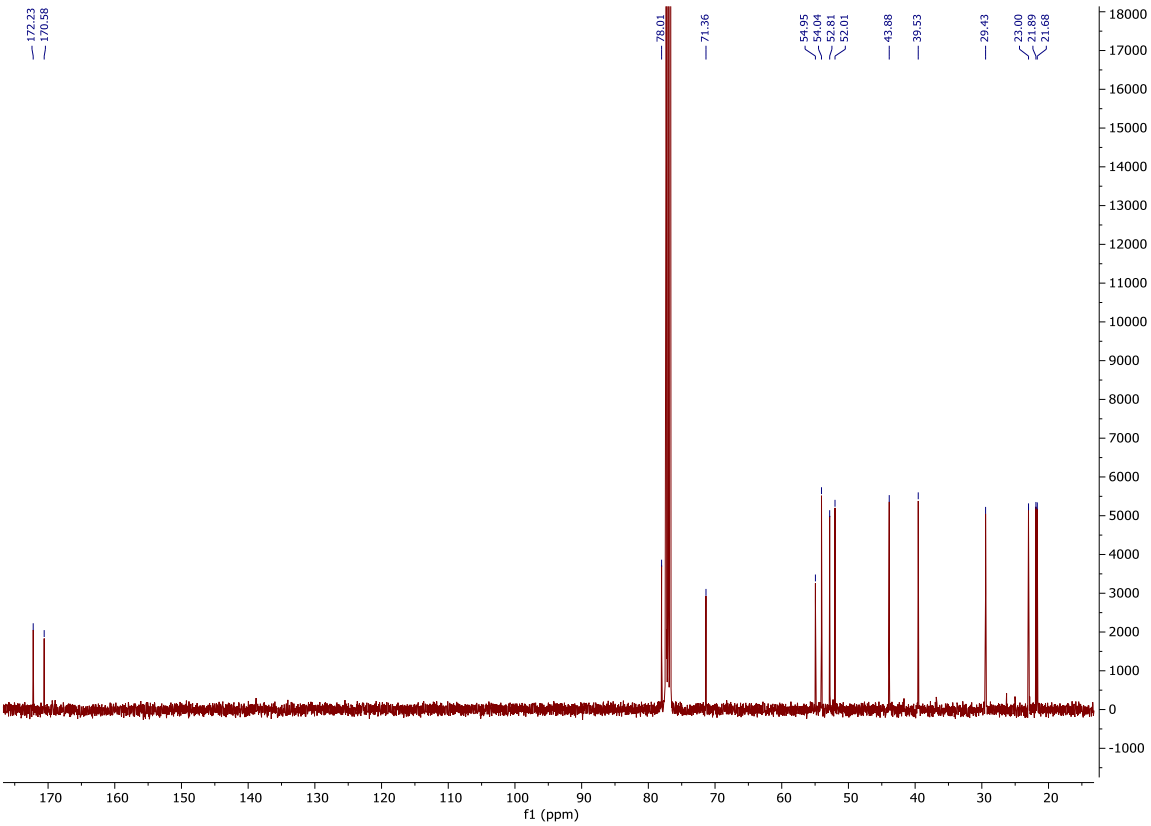

69 - 13C NMR (101 MHz, CDCl3) δ 172.23, 170.58, 78.01, 71.36, 54.95, 54.04, 52.81, 52.01, 43.88, 39.53, 29.43, 23.00, 21.89, 21.68.

70 - dimethyl (1aS,4aR,7R,7aR)-7-methyl-7-((trimethylsilyl)oxy)hexahydroindeno[3a,4-b]oxirene-4,4(1aH)-dicarboxylate

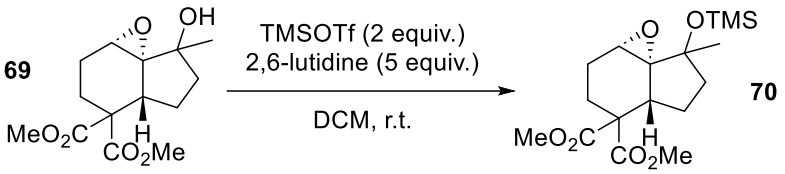

68 (40 mg, 0.15 mmol) set-up under under inert atmosphere and dissolved into 1,5 ml of dry THF. Then, temperature was lowered down to - 78 °C and 149 ul of a 0.1 M MeLi (0.15 mmol) pre-cooled to the same temperature was added dropwise and the reaction stirred at the same temperature for 2 hours. Then, the reaction was set-up at 0 °C to allow full conversion of the starting material (traces still present). After 15 more minutes the reaction wa quenched with aqueous NH4Cl and extracted with DCM. The organic phase was dried over MgSO4, filtered and the solvent was removed under reduced pressure. The crude was then put under inert atmosphere and dissolved in 1,5 of dry DCM. Temperature was lowered to 0 °C. 94 ul (0.81 mmol) of 2,6-lutidine are injected, followed by 60 ul (0.33 mmol) of TMSOTf. The reaction was allowed to reach room temperature and allowed to stir overnight. TLC check (1:1 Hex:AcOEt) shows full conversion.

The reaction was then quenched with aqueous NaHCO3, the organic phase was separated, and the aqueous phase is then extracted with DCM. The organic phases are then merged, dried over MgSO4, filtered and the solvent removed under reduced pressure. HNMR analysis shows multiple product formed. 70 was isolated via column chromatography (95:5 to 80:20 Hex:AcOEt as eluent). 11 mg of 70-type product was isolated as diastereomeric mixture (21% yield).

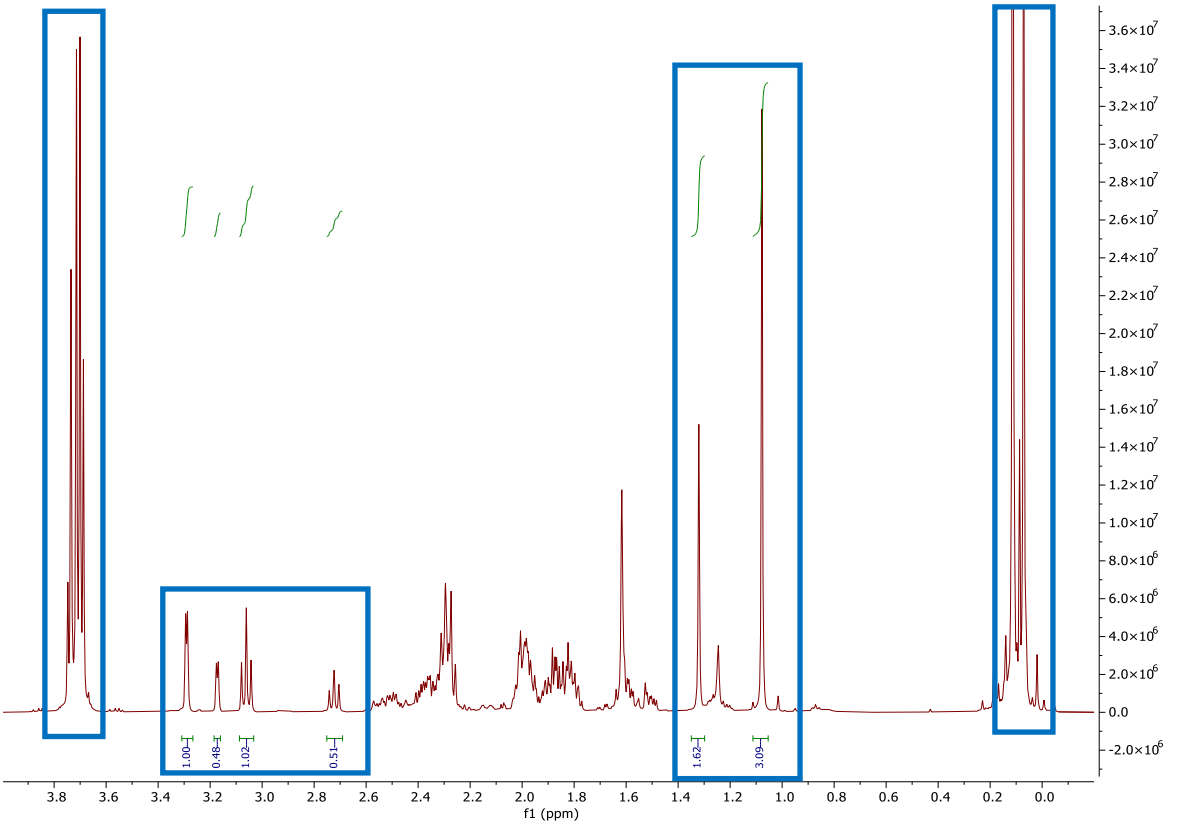

It is clear that two diastereoisomers are present from the methyl peaks typical of that structure and the “twin peaks” between 3.4 and 2.7 ppm and between 1.4 and 1.0 ppm in the same ratio. d.r. = 2:1

Bibliography

(1) Craig, R. A.; Stoltz, B. M. Polycyclic Furanobutenolide-Derived Cembranoid and Norcembranoid Natural Products: Biosynthetic Connections and Synthetic Efforts. *Chemical Reviews*. American Chemical Society June 28, 2017, pp 7878–7909. https://doi.org/10.1021/acs.chemrev.7b00083.

(2) Chen, P.; Li, R.; Zou, M.; Jia, Z. Recent Advances in Synthesis of the Polycyclic Norcembranoid and Cembranoid Diterpenoids. *Chemistry – A European Journal* 2025, *31* (32). https://doi.org/10.1002/chem.202500936.

(3) Marrero, J.; Rodríguez, A. D.; Baran, P.; Raptis, R. G.; Sánchez, J. A.; Ortega-Barria, E.; Capson, T. L. Bielschowskysin, a Gorgonian-Derived Biologically Active Diterpene with an Unprecedented Carbon Skeleton. *Org Lett* 2004, *6* (10), 1661–1664. https://doi.org/10.1021/ol049495d.

(4) Marrero, J.; Rodríguez, A. D.; Barnes, C. L. Intricarene, an Unprecedented Trispiropentacyclic Diterpene from the Caribbean Sea Plume *Pseudopterogorgia k Allos*. *Org Lett* 2005, *7* (9), 1877–1880. https://doi.org/10.1021/ol0505961.

(5) Ramesh, P.; Reddy, N. S.; Venlmteswarlu, Y.; Venkata, M.; Reddy, R.; Fauikner, D. J.; Oh, O. ~ ~; Ho, C.; Oh, _ J; Ome, C. *Rameswaralide, A Novel Diterpenoid from the Soft Coral Sinularia Dissecta*; 1998; Vol. 39.

(6) Anjaneyulu, A. S. R.; Sagar, K. S.; Venugopal, M. J. R. V. Terpenoid and Steroid Constituents of the Indian Soft Coral Sinularia Maxima. *Tetrahedron* 1995, *51*, 10997–11010.

(7) Iguchi, K.; Kajiyama, K.; Yamada, Y. Yonarolide: A New Marine Norditerpenoid Possessing a Novel Tricyclic Skeleton, from the Okinawan Soft Coral of the Genus, Sinularia. *Tetrahedron Lett* 1995, *36* (48), 8807–8808. https://doi.org/10.1016/0040-4039(95)01867-H.

(8) Duh, C.-Y.; Wang, S.-K.; Chia, M.-C.; Chiang, M. Y. *A Novel Cytotoxic Norditerpenoid from the Formosan Soft Coral Sinularia Inelegans*; 1999.

(9) Sheu, J. H.; Ahmed, A. F.; Shiue, R. T.; Dai, C. F.; Kuo, Y. H. Scabrolides A-D, Four New Norditerpenoids Isolated from the Soft Coral Sinularia Scabra. *J Nat Prod* 2002, *65* (12), 1904–1908. https://doi.org/10.1021/np020280r.

(10) Tseng, Y. J.; Ahmed, A. F.; Dai, C. F.; Chiang, M. Y.; Sheu, J. H. Sinulochmodins A-C, Three Novel Terpenoids from the Soft Coral Sinularia Lochmodes. *Org Lett* 2005, *7* (17), 3813–3816. https://doi.org/10.1021/ol051513j.

(11) Tang, B.; Bray, C. D.; Pattenden, G. A Biomimetic Total Synthesis of (+)-Intricarene. *Tetrahedron Lett* 2006, *47* (36), 6401–6404. https://doi.org/10.1016/j.tetlet.2006.06.150.

(12) Roethle, P. A.; Hernandez, P. T.; Trauner, D. Exploring Biosynthetic Relationships among Furanocembranoids: Synthesis of (–)-Bipinnatin J, (+)-Intricarene, (+)-Rubifolide, and (+)-Isoepilophodione B. *Org Lett* 2006, *8* (25), 5901–5904. https://doi.org/10.1021/ol062581o.

(13) Hafeman, N. J.; Loskot, S. A.; Reimann, C. E.; Pritchett, B. P.; Virgil, S. C.; Stoltz, B. M. The Total Synthesis of (–)-Scabrolide A. *J Am Chem Soc* 2020, *142* (19), 8585–8590. https://doi.org/10.1021/jacs.0c02513.

(14) Tuccinardi, J. P.; Wood, J. L. Total Syntheses of (+)-Ineleganolide and (-)-Sinulochmodin C. *J Am Chem Soc* 2022, *144* (44), 20539–20547. https://doi.org/10.1021/jacs.2c09826.

(15) Meng, Z.; Fürstner, A. Total Syntheses of Scabrolide A and Nominal Scabrolide B. *J Am Chem Soc* 2022, *144* (4), 1528–1533. https://doi.org/10.1021/jacs.1c12401.

(16) Gross, B. M.; Han, S.-J.; Virgil, S. C.; Stoltz, B. M. A Convergent Total Synthesis of (+)-Ineleganolide. *J Am Chem Soc* 2023, *145* (14), 7763–7767. https://doi.org/10.1021/jacs.3c02142.

(17) Serrano, R.; Boyko, Y. D.; Hernandez, L. W.; Lotuzas, A.; Sarlah, D. Total Syntheses of Scabrolide A and Yonarolide. *J Am Chem Soc* 2023, *145* (16), 8805–8809. https://doi.org/10.1021/jacs.3c02317.

(18) Simmons, E. J.; Ryffel, D. B.; Lopez, D. A.; Boyko, Y. D.; Sarlah, D. Total Syntheses of Scabrolide B, Ineleganolide, and Related Norcembranoids. *J Am Chem Soc* 2025, *147* (1), 130–135. https://doi.org/10.1021/jacs.4c16629.

(19) Lin, D. S.; Späth, G.; Meng, Z.; Wieske, L. H. E.; Farès, C.; Fürstner, A. Total Synthesis of the Norcembranoid Scabrolide B and Its Transformation into Sinuscalide C, Ineleganolide, and Horiolide. *J Am Chem Soc* 2024, *146* (35), 24250–24256. https://doi.org/10.1021/jacs.4c09467.

(20) Peng, C.; Guo, Q.; Xu, G.-X.; Huo, L.; Wu, W.; Chen, T.-Y.; Hong, X.; Hu, P. Divergent Synthesis of Scabrolide A and Havellockate via an *Exo - Exo - Endo* Radical Cascade. *J Am Chem Soc* 2024, *146* (21), 14422–14426. https://doi.org/10.1021/jacs.4c03995.

(21) Zhang, Y. P.; Du, S.; Ma, Y.; Zhan, W.; Chen, W.; Yang, X.; Zhang, H. Structure-Unit-Based Total Synthesis of (–)-Sinulochmodin C. *Angewandte Chemie - International Edition* 2024, *63* (2). https://doi.org/10.1002/anie.202315481.

(22) Truax, N. J.; Ayinde, S.; Liu, J. O.; Romo, D. Total Synthesis of Rameswaralide Utilizing a Pharmacophore-Directed Retrosynthetic Strategy. *J Am Chem Soc* 2022, *144* (40), 18575–18585. https://doi.org/10.1021/jacs.2c08245.

(23) Brill, Z. G.; Grover, H. K.; Maimone, T. J. Enantioselective Synthesis of an Ophiobolin Sesterterpene via a Programmed Radical Cascade. *Science (1979)* 2016, *352* (6289), 1078–1082. https://doi.org/10.1126/science.aaf6742.

(24) Du, Y.; Yao, L.; Li, X.; Guo, Y. Yonarolide A, an Unprecedented Furanobutenolide-Containing Norcembranoid Derivative Formed by Photoinduced Intramolecular [2+2] Cycloaddition. *Chinese Chemical Letters* 2023, *34* (2), 107512. https://doi.org/10.1016/j.cclet.2022.05.026.

(25) Wong, A. R.; Fastuca, N. J.; Mak, V. W.; Kerkovius, J. K.; Stevenson, S. M.; Reisman, S. E. Total Syntheses of the C 19 Diterpenoid Alkaloids (–)-Talatisamine, (–)-Liljestrandisine, and (–)-Liljestrandinine by a Fragment Coupling Approach. *ACS Cent Sci* 2021, *7* (8), 1311–1316. https://doi.org/10.1021/acscentsci.1c00540.

(26) Kerkovius, J. K.; Wong, A. R.; Mak, V. W.; Reisman, S. E. A Convergent Fragment Coupling Strategy to Access Quaternary Stereogenic Centers. *Chem Sci* 2023, *14* (16), 4397–4400. https://doi.org/10.1039/d2sc07023e.

(27) Luche, J. L. Lanthanides in Organic Chemistry. 1. Selective 1,2 Reductions of Conjugated Ketones. *J Am Chem Soc* 1978, *100* (7), 2226–2227. https://doi.org/10.1021/ja00475a040.

(28) Mori, Y.; Kuhara, M.; Takeuchi, A.; Suzuki, M. Stereoselective Reduction of β-Alkoxy Ketones: A Synthesis of Syn-1,3-Diols. *Tetrahedron Lett* 1988, *29* (42), 5419–5422. https://doi.org/10.1016/S0040-4039(00)82884-1.

(29) Curran, T. T.; Hay, D. A.; Koegel, C. P.; Evans, J. C. The Preparation of Optically Active 2-Cyclopenten-1,4-Diol Derivatives from Furfuryl Alcohol. *Tetrahedron* 1997, *53* (6), 1983–2004. https://doi.org/10.1016/S0040-4020(96)01169-6.

(30) Sun, K.; Lv, Q. Y.; Lin, Y. W.; Yu, B.; He, W. M. Nitriles as Radical Acceptors in Radical Cascade Reactions. *Organic Chemistry Frontiers*. Royal Society of Chemistry February 7, 2021, pp 445–465. https://doi.org/10.1039/d0qo01058h.

(31) Daiger, M. T.; Giofré, S.; Berthold, D.; Breit, B. Rhodium-Catalyzed Enantioselective Intramolecular Hydroalkoxylation of Allenes and Application in the Total Synthesis of (*R,R,R*)- α -Tocopherol. *Chemistry – A European Journal* 2024, *30* (46). https://doi.org/10.1002/chem.202402010.

(32) Dombroski, M. A.; Kates, S. A.; Snider, B. B. *Manganese(III)-Based Oxidative Free-Radical Tandem and Triple Cyclizations*; UTC, 1990; Vol. 112. https://pubs.acs.org/sharingguidelines.

(33) Ueno-Stork Cyclization. In *Comprehensive Organic Name Reactions and Reagents*; Wiley, 2010; pp 2826–2829. https://doi.org/10.1002/9780470638859.conrr633.

(34) Chatgilialoglu, C.; Griller, D.; Lesage, M. Tris(Trimethylsilyl)Silane. A New Reducing Agent. *J Org Chem* 1988, *53* (15), 3641–3642. https://doi.org/10.1021/jo00250a051.

(35) Danishefsky, S.; Kitahara, T.; Schuda, P. F. Preparation and <scp>D</Scp> Iels–<scp>A</Scp> Lder Reaction of a Highly Nucleophilic Diene: *Trans* -1-Methoxy-3-Trimethylsiloxy-1,3-Butadiene and 5β-Methoxycyclohexan-1-One-3β,4β-Dicarboxylic Acid Anhydride. In *Organic Syntheses*; Wiley, 2003; pp 147–147. https://doi.org/10.1002/0471264180.os061.30.

(36) Kozmin, S. A.; Rawal, V. H. Preparation and Diels–Alder Reactivity of 1-Amino-3-Siloxy-1,3-Butadienes. *J Org Chem* 1997, *62* (16), 5252–5253. https://doi.org/10.1021/jo970438q.

(37) K. Gurjar, M.; S. Chorghade, M.; Nageswar Reddy, C.; R. Kalkote, U. Studies toward the Total Synthesis of Carba Analogue of Motif C of M. TB Cell Wall AG Complex. *Heterocycles* 2009, *77* (2), 909. https://doi.org/10.3987/COM-08-S(F)59.

(38) Tietze, L.; Stadler, C.; Böhnke, N.; Brasche, G.; Grube, A. Synthesis of Enantiomerically Pure Cyclopentene Building Blocks. *Synlett* 2007, *2007* (3), 0485–0487. https://doi.org/10.1055/s-2007-967937.

(39) Le Liepvre, M.; Ollivier, J.; Aitken, D. J. Synthesis of Functionalized Bicyclo[3.2.0]Heptanes – a Study of the [2+2] Photocycloaddition Reactions of 4-Hydroxycyclopent-2-enone Derivatives. *European J Org Chem* 2009, *2009* (34), 5953–5962. https://doi.org/10.1002/ejoc.200900749.

(40) Le Liepvre, M.; Ollivier, J.; Aitken, D. J. Synthesis of Functionalized Bicyclo[3.2.0]Heptanes – a Study of the [2+2] Photocycloaddition Reactions of 4-Hydroxycyclopent-2-enone Derivatives. *European J Org Chem* 2009, *2009* (34), 5953–5962. https://doi.org/10.1002/ejoc.200900749.

(41) Nicolaou, K. C.; Liu, J. J.; Hwang, C.-K.; Dai, W.-M.; Guy, R. K. Synthesis of a Fully Functionalized CD Ring System of Taxol. *J Chem Soc Chem Commun* 1992, No. 16, 1118. https://doi.org/10.1039/c39920001118.

(42) Dai, Y.; Wang, F.; Zhu, S.; Chu, L. Selective Ni-Catalyzed Cross-Electrophile Coupling of Alkynes, Fluoroalkyl Halides, and Vinyl Halides. *Chinese Chemical Letters* 2022, *33* (8), 4074–4078. https://doi.org/10.1016/j.cclet.2021.12.050.

(43) Takeuchi, R.; Tanabe, K.; Tanaka, S. Stereodivergent Synthesis of (*E*)- and (*Z*)-2-Alken-4-Yn-1-Ols from 2-Propynoic Acid: A Practical Route via 2-Alken-4-Ynoates. *J Org Chem* 2000, *65* (5), 1558–1561. https://doi.org/10.1021/jo991350a.

(44) Tseng, N.-W.; Lautens, M. Rhodium-Catalyzed Vinylcyclopropanation/Cyclopentenation of Strained Alkenes via a Sequential Carborhodation Process. *J Org Chem* 2009, *74* (6), 2521–2526. https://doi.org/10.1021/jo900039g.

(45) Denmark, S. E.; Habermas, K. L.; Hite, G. A.; Jones, T. K. Silicon-Directed Nazarov Cyclizations-IV. *Tetrahedron* 1986, *42* (11), 2821–2829. https://doi.org/10.1016/S0040-4020(01)90571-X.

(46) Abarbri, M.; Parrain, J.-L.; Duchêne, A.; Thibonnet, J. Stereoselective Synthesis of Trienoic Acids: Synthesis of Retinoic Acids and Analogues. *Synthesis (Stuttg)* 2006, *2006* (17), 2951–2970. https://doi.org/10.1055/s-2006-950201.

(47) Craig, D.; Reader, J. C. A Novel Strategy for Regio- and Stereocontrol in [4 + 2] Cycloadditions. Intramolecular Diels-Alder Reaction of a Sllyl Acetal Triene.

Tetrahedron Lett 1990, *31* (45), 6585–6588. https://doi.org/10.1016/S0040-4039(00)97123-5.

(48) Chabuka, B. K.; Alabugin, I. V. Hole Catalysis of Cycloaddition Reactions: How to Activate and Control Oxidant Upconversion in Radical-Cationic Diels–Alder Reactions. *J Am Chem Soc* 2023, *145* (35), 19354–19367. https://doi.org/10.1021/jacs.3c06106.

(49) Bellville, D. J.; Wirth, D. W.; Bauld, N. L. Cation-Radical Catalyzed Diels-Alder Reaction. *J Am Chem Soc* 1981, *103* (3), 718–720. https://doi.org/10.1021/ja00393a061.

(50) Ozaki, A.; Yamaguchi, Y.; Okada, Y.; Chiba, K. Radical Cation Diels-Alder Reactions of Non-Conjugated Alkenes as Dienophiles by Electrocatalysis. *Chin J Chem* 2019, *37* (6), 561–564. https://doi.org/10.1002/cjoc.201900054.

(51) Cieplak, A. S. Stereochemistry of Nucleophilic Addition to Cyclohexanone. The Importance of Two-Electron Stabilizing Interactions. *J Am Chem Soc* 1981, *103* (15), 4540–4552. https://doi.org/10.1021/ja00405a041.

(52) Gouse, S.; Reddy, N. R.; Baskaran, S. A Domino Aza-Piancatelli Rearrangement/Intramolecular Diels-Alder Reaction: Stereoselective Synthesis of Octahydro-1 H-Cyclopenta[Cd]Isoindole. *Org Lett* 2019, *21* (10), 3822–3827. https://doi.org/10.1021/acs.orglett.9b01267.

(53) Kramer, C. S.; Bräse, S. Thiourea-Catalyzed Diels-Alder Reaction of a Naphthoquinone Monoketal Dienophile. *Beilstein Journal of Organic Chemistry* 2013, *9*, 1414–1418. https://doi.org/10.3762/bjoc.9.158.

(54) Ma, W.; Montinho-Inacio, E.; Iorga, B. I.; Retailleau, P.; Moreau, X.; Neuville, L.; Masson, G. Chiral Phosphoric Acid-Catalyzed Enantioselective Formal [4+2] Cycloaddition Between Dienecarbamates and 2-Benzothioazolimines. *Adv Synth Catal* 2022, *364* (10), 1708–1715. https://doi.org/10.1002/adsc.202200161.

(55) Ahrendt, K. A.; Borths, C. J.; MacMillan, D. W. C. New Strategies for Organic Catalysis: The First Highly Enantioselective Organocatalytic Diels - Alder Reaction [16]. *Journal of the American Chemical Society*. May 3, 2000, pp 4243–4244. https://doi.org/10.1021/ja000092s.

(56) Araki, Y.; Konoike, T. Enantioselective Total Synthesis of (+)-6- *Epi* -Mevinolin and Its Analogs. Efficient Construction of the Hexahydronaphthalene Moiety by High Pressure-Promoted Intramolecular Diels–Alder Reaction of (*R* ,2 *Z* ,8 *E* ,10 *E*)-1-[(*Tert* -Butyldimethylsilyl)Oxy]-6-Methyl-2,8,10-Dodecatrien-4-One. *J Org Chem* 1997, *62* (16), 5299–5309. https://doi.org/10.1021/jo970444m.

(57) Crestey, F.; Hooyberghs, G.; Kristensen, J. L. Concise Synthesis of New Bridged-Nicotine Analogues. *Tetrahedron* 2012, *68* (5), 1417–1421. https://doi.org/10.1016/j.tet.2011.12.029.

(58) Wang, B.; Lu, C.; Zhang, S.-Y.; He, G.; Nack, W. A.; Chen, G. Palladium-Catalyzed Stereoretentive Olefination of Unactivated C(Sp 3)–H Bonds with Vinyl Iodides at Room Temperature: Synthesis of β-Vinyl α-Amino Acids. *Org Lett* 2014, *16* (23), 6260–6263. https://doi.org/10.1021/ol503248f.

(59) Ingoglia, B. T.; Wagen, C. C.; Buchwald, S. L. Biaryl Monophosphine Ligands in Palladium-Catalyzed C–N Coupling: An Updated User's Guide. *Tetrahedron* 2019, *75* (32), 4199–4211. https://doi.org/10.1016/j.tet.2019.05.003.

(60) Northrup, A. B.; MacMillan, D. W. C. The First General Enantioselective Catalytic Diels-Alder Reaction with Simple (α,β-Unsaturated Ketones. *J Am Chem Soc* 2002, *124* (11), 2458–2460. https://doi.org/10.1021/ja017641u.

(61) Singh, R. P.; Bartelson, K.; Wang, Y.; Su, H.; Lu, X.; Deng, L. Enantioselective Diels–Alder Reaction of Simple α,β-Unsaturated Ketones with a Cinchona Alkaloid Catalyst. *J Am Chem Soc* 2008, *130* (8), 2422–2423. https://doi.org/10.1021/ja078251w.

(62) Corey, E. J. Enantioselective Catalysis Based on Cationic Oxazaborolidines. *Angewandte Chemie International Edition* 2009, *48* (12), 2100–2117. https://doi.org/10.1002/anie.200805374.

(63) Liu, D.; Canales, E.; Corey, E. J. Chiral Oxazaborolidine–Aluminum Bromide Complexes Are Unusually Powerful and Effective Catalysts for Enantioselective Diels–Alder Reactions. *J Am Chem Soc* 2007, *129* (6), 1498–1499. https://doi.org/10.1021/ja068637r.

(64) Mahender Reddy, K.; Bhimireddy, E.; Thirupathi, B.; Breitler, S.; Yu, S.; Corey, E. J. Cationic Chiral Fluorinated Oxazaborolidines. More Potent, Second-Generation Catalysts for Highly Enantioselective Cycloaddition Reactions. *J Am Chem Soc* 2016, *138* (7), 2443–2453. https://doi.org/10.1021/jacs.6b00100.

(65) Corey, E. J.; Shibata, T.; Lee, T. W. Asymmetric Diels–Alder Reactions Catalyzed by a Triflic Acid Activated Chiral Oxazaborolidine. *J Am Chem Soc* 2002, *124* (15), 3808–3809. https://doi.org/10.1021/ja025848x.

(66) Sakata, K.; Fujimoto, H. Quantum Chemical Study of Diels–Alder Reactions Catalyzed by Lewis Acid Activated Oxazaborolidines. *J Org Chem* 2013, *78* (7), 3095–3103. https://doi.org/10.1021/jo400066h.

(67) Paddon-Row, M. N.; Kwan, L. C. H.; Willis, A. C.; Sherburn, M. S. Enantioselective Oxazaborolidinium-Catalyzed Diels–Alder Reactions without CH···O Hydrogen Bonding. *Angewandte Chemie International Edition* 2008, *47* (37), 7013–7017. https://doi.org/10.1002/anie.200802002.

(68) Paddon-Row, M. N.; Anderson, C. D.; Houk, K. N. Computational Evaluation of Enantioselective Diels–Alder Reactions Mediated by Corey's Cationic Oxazaborolidine Catalysts. *J Org Chem* 2009, *74* (2), 861–868. https://doi.org/10.1021/jo802323p.

(69) Pham, H. V.; Paton, R. S.; Ross, A. G.; Danishefsky, S. J.; Houk, K. N. Intramolecular Diels–Alder Reactions of Cycloalkenones: Stereoselectivity, Lewis Acid Acceleration, and Halogen Substituent Effects. *J Am Chem Soc* 2014, *136* (6), 2397–2403. https://doi.org/10.1021/ja410220w.

(70) Blom, C. E.; Günthard, Hs. H. Rotational Isomerism in Methyl Formate and Methyl Acetate; a Low-Temperature Matrix Infrared Study Using Thermal Molecular Beams. *Chem Phys Lett* 1981, *84* (2), 267–271. https://doi.org/10.1016/0009-2614(81)80342-9.

(71) Gouse, S.; Reddy, N. R.; Baskaran, S. A Domino Aza-Piancatelli Rearrangement/Intramolecular Diels-Alder Reaction: Stereoselective Synthesis of Octahydro-1 H-Cyclopenta[Cd]Isoindole. *Org Lett* 2019, *21* (10), 3822–3827. https://doi.org/10.1021/acs.orglett.9b01267.

(72) Trembleau, L.; Patiny, L.; On Ghosez, L. *Diels±Alder Reactions of Activated Furans to Cyclopentenone Derivatives: A Regiodivergent Diels±Alder Approach towards Polyfunctionalised Cis-Hydrindanones*.

(73) Rulíšek, L.; Šebek, P.; Havlas, Z.; Hrabal, R.; Čapek, P.; Svatoš, A. An Experimental and Theoretical Study of Stereoselectivity of Furan–Maleic Anhydride and Furan–Maleimide Diels–Alder Reactions. *J Org Chem* 2005, *70* (16), 6295–6302. https://doi.org/10.1021/jo050759z.

(74) MAO FEI; XIN XING; LEUNG WAI-YEE. US_9222127_B2. 2013.

(75) Medrán, N. S.; Dezotti, F.; Pellegrinet, S. C. Remarkable Reactivity of Boron-Substituted Furans in the Diels–Alder Reactions with Maleic Anhydride. *Org Lett* 2019, *21* (13), 5068–5072. https://doi.org/10.1021/acs.orglett.9b01662.

(76) Arai, T.; Yamada, Y. M. A.; Yamamoto, N.; Sasai, H.; Shibasaki, M. Self-Assembly of Heterobimetallic Complexes and Reactive Nucleophiles: A General Strategy for the Activation of Asymmetric Reactions Promoted by Heterobimetallic Catalysts. *Chemistry – A European Journal* 1996, *2* (11), 1368–1372. https://doi.org/10.1002/chem.19960021107.

(77) Crump, R. A. N. C.; Fleming, I.; Urch, C. J. Conjugate Addition of the Phenyldimethylsilyl Group to Aβ-Unsaturated Carbonyl Compounds Using a Silylzincate in Place of the Silylcuprate. *J. Chem. Soc., Perkin Trans. 1* 1994, No. 6, 701–706. https://doi.org/10.1039/P19940000701.

(78) Ager, D. J.; Fleming, I.; Patel, S. K. The Conjugate Addition of a Silyl Group to Enones and Its Removal with Copper(<scp>II</Scp>) Bromide: A Protecting Group for the Aβ-Unsaturation of Aβ-Unsaturated Ketones. *J. Chem. Soc., Perkin Trans. 1* 1981, No. 0, 2520–2526. https://doi.org/10.1039/P19810002520.

(79) Lee, K.; Zhugralin, A. R.; Hoveyda, A. H. Efficient C–B Bond Formation Promoted by N-Heterocyclic Carbenes: Synthesis of Tertiary and Quaternary B-Substituted Carbons through Metal-Free Catalytic Boron Conjugate Additions to Cyclic and Acyclic α,β-Unsaturated Carbonyls. *J Am Chem Soc* 2009, *131* (21), 7253–7255. https://doi.org/10.1021/ja902889s.

(80) Diao, T.; Wadzinski, T. J.; Stahl, S. S. Direct Aerobic α,β-Dehydrogenation of Aldehydes and Ketones with a Pd(TFA) 2 /4,5-Diazafluorenone Catalyst. *Chem. Sci.* 2012, *3* (3), 887–891. https://doi.org/10.1039/C1SC00724F.

(81) Lebold, T. P.; Wood, J. L.; Deitch, J.; Lodewyk, M. W.; Tantillo, D. J.; Sarpong, R. A Divergent Approach to the Synthesis of the Yohimbinoid Alkaloids Venenatine and Alstovenine. *Nat Chem* 2013, *5* (2), 126–131. https://doi.org/10.1038/nchem.1528.

(82) Larock, R. C.; Hightower, T. R.; Kraus, G. A.; Hahn, P.; Zheng, D. A Simple, Effective, New, Palladium-Catalyzed Conversion of Enol Silanes to Enones and Enals. *Tetrahedron Lett* 1995, *36* (14), 2423–2426. https://doi.org/10.1016/0040-4039(95)00306-W.

(83) Chen, P. H.; Billett, B. A.; Tsukamoto, T.; Dong, G. Cut and Sew Transformations via Transition-Metal-Catalyzed Carbon-Carbon Bond Activation. *ACS Catalysis*. American Chemical Society February 3, 2017, pp 1340–1360. https://doi.org/10.1021/acscatal.6b03210.

(84) Ko, H. M.; Dong, G. Cooperative Activation of Cyclobutanones and Olefins Leads to Bridged Ring Systems by a Catalytic [4 + 2] Coupling. *Nat Chem* 2014, *6* (8), 739–744. https://doi.org/10.1038/nchem.1989.

Chapter 6 - Scalable, enantioselective total synthesis of (S)-autumnaline

Collaboration with Industry

Indena Spa is an Italian company, global leader in the identification, development, marketing and production of extracts and pure active ingredients, mainly derived from medicinal plants, for the pharmaceutical (APIs - Active Pharmaceutical Ingredients, by conventional chemical synthesis or semi-synthesis), food supplement, cosmetic and veterinary industries. The name Indena (*Figure 188*) stands for Industria Derivati Naturali - which means “industry of natural derivatives” in Italian. [1]

Figure 188 - Indena logo

Nowadays, thanks also to the know-how in botanic sciences, Indena still produces APIs (Active Pharmaceutical Ingredients) from plants, and it is also very active in the nutraceutical field. Moreover, this company produces some APIs by conventional chemical synthesis or semi-synthesis.

Indena also promotes the cooperation between academia and industry, and our group had the opportunity to work with Indena in several projects. One of them is the scalable, enantioselective total synthesis of (S)-autumnaline, an alkaloid. This work was done in cooperation with the group of Professor M. L. Gelmi from the University of Milan, Professor M. Aschi from the University of L’Aquila for the circular dichroism (CD) spectra simulation, Professor A. Mazzanti from the University of Bologna for CD acquisition.

Scope of the work

(S)-autumnaline (Figure 189) is an isoquinoline alkaloid found in plants of *Colchicum* genus. Its natural role is thought to be a biosynthetic intermediate of other secondary metabolites,[2] such as colchicine, which are well studied for their pharmaceutical activity.

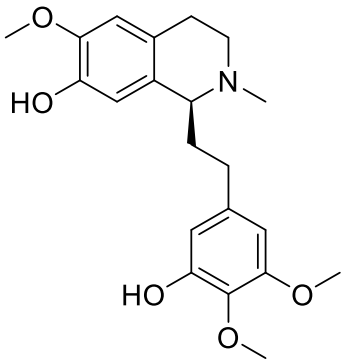

Figure 189 - (S)-autumnaline

Indena was interested in the synthesis of this compound in both its enantiomers, possibly developing a scalable and cheap process to have an enantiopure product.

Autumnaline synthesis to date

(S)-autumnaline was extracted and isolated for the first time in 1969 by F. Šantavý and co-workers.[3] The chiral center of the natural molecule was determined to be S by Backer and co-workers, via Cotton effect[4,5] measured on the autumnaline O-dibenzyl tartrate salt.[6] Until recently, autumnaline was prepared in racemic form and mainly for academic purposes – in particular for radiolabeling studies about plants metabolism. [2,6–8] Although the synthetic sequences used were inspiring, they are not described in detail for industrial purposes and provide only racemic material.[2,6,9] To the best of our knowledge, there is only one synthesis, patented and reported by Rao and co-workers, able to produce appreciable amounts of enantiopure (S)-autumnaline.[10,11] The authors engineered a strain of E. coli, importing the genes to perform the whole biosynthesis; the starting materials, phenyl propionic acid and dopamine, are readily available and cheap.[12] The synthetic process is represented in Figure 190.

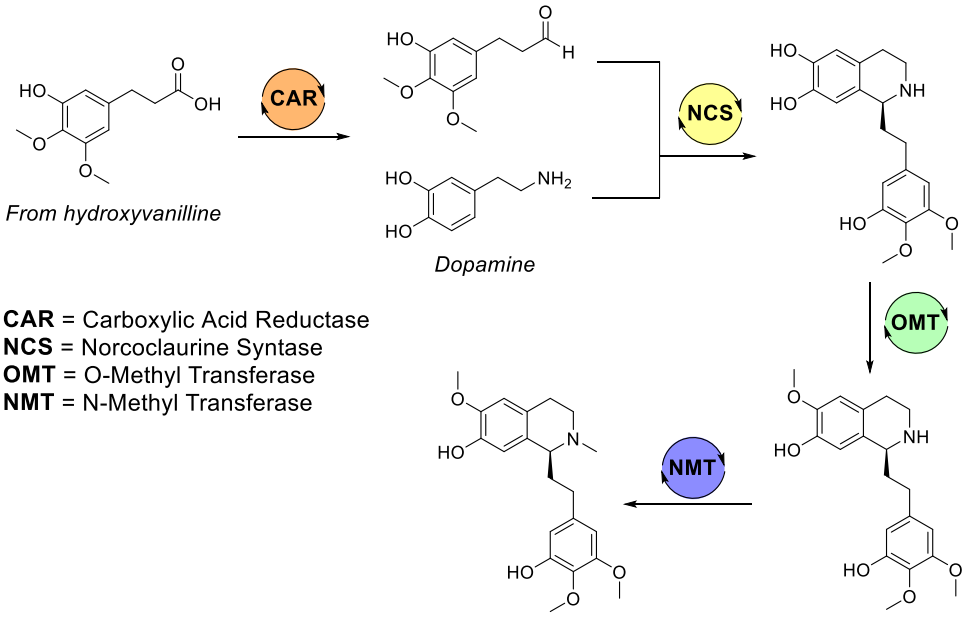

Figure 190 - Enzymatic multistep synthesis patented by Rao and co-workers

However, this process is patented in the Chinese market. If the patent is extended outside China, there will be no freedom to operate in the future. Moreover, the industrial production of (S)-autumnaline with this method has some issues. Indena wants a process that can be carried out on a standard multipurpose plant. Using fermentative technologies the production volume required would be excessive, so a synthesis that can be carried out on a multipurpose plant would be highly desirable. Second, the isolation of the final product by the Chinese teams was carried out via preparative HLPC – prohibitively expensive for a large-scale production.

Synthetic strategy evaluation

Our synthetic strategy for autumnaline is based on common disconnections that would lead to simple starting materials and, in principle, reasonably straightforward-to-develop industrially applicable reactions. Tetrahydroisoquinoline are well-known synthetic targets most commonly prepared *via* Bischler-Napieralski reaction, followed by asymmetric reduction of the corresponding imine, or asymmetric Pictet-Spengler reaction and asymmetric Pomeranz-Fritsch-Bobbitt reaction, followed by alkene hydrogenation (Figure 191).

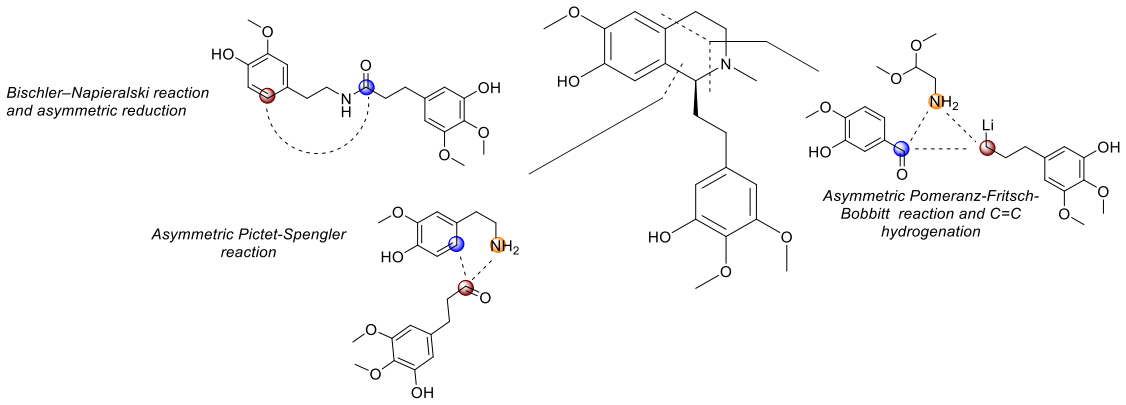

Figure 191 - Tetraisoquinoline core synthetic approaches

One of pivotal point of the strategy is to exploit the Bischler–Napieralski – asymmetric imine reduction, reactions that are generally reported to proceed with high conversion.[13] Furthermore, the asymmetric hydrogenation of imines to afford tetrahydroisoquinolines is well established, and reported with different catalytic platforms, providing the opportunity to fast explore the available chemical space.[14,15] The asymmetric Pictet-Spengler reaction on similar substrates was reported using chiral phosphoric acids, which we evaluated to be too expensive and difficult to tune for our purposes.[16,17] Finally, the Pomeranz-Fritsch-Bobbitt[18] reaction was not appealing to our goals, because the optimization of the enantioselective organolithium addition to the imine generally was reported to not perform well.[19]

The Bischler–Napieralski reaction leads the choice for the starting material needed for the core and, therefore, sets the stage for the rest of the disconnections, that are straightforward (Figure 192).

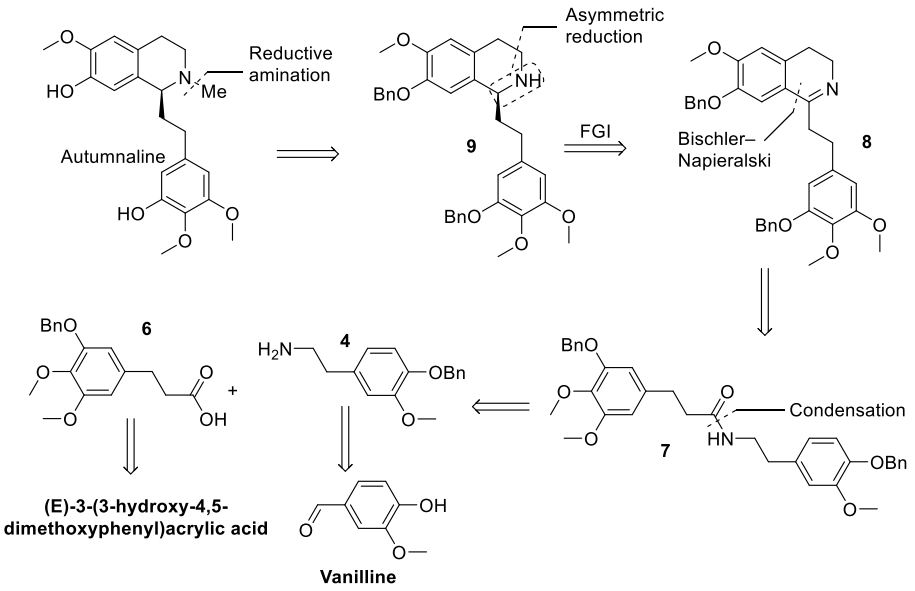

Figure 192 - Retrosynthesis of (S)-autumnaline

The first disconnection is simply the removal of the N-methyl group to obtain intermediate **9**. This would correspond to a simple reductive amination in the forward sense. Then, through functional group interconversion (FGI) of amine to imine the structure **8** is obtained. The conversion of **8** into **9** via asymmetric reduction sets the stereogenic center. The dihydroisoquinoline ring can be closed via a Bischler-Napieralski reaction as anticipated to give **7**. Finally, the amide bond disconnection yields **4** and **6**. **6** can be easily traced back to **(E)-3-(3-hydroxy-4,5-dimethoxyphenyl)acrylic acid**. **4** can be derived from **vanilline** through a homologation/amination sequence. In general, all the methodologies were chosen to have an easy set-up and straightforward purification, to be easily scalable and as cheap as possible.

It follows the detailed strategy and the experimental results for every step. The optimization process is discussed only for the steps I actively worked-on. Moreover, the work-up and purification procedures are briefly described – they are important aspects too for industrial-oriented projects.

Results

Intermediate 4

Intermediate **4** is very similar to dopamine, as shown in Figure 193. Dopamine is a bulk chemical itself, so the simplest thing to do would be the *direct functionalization* of the hydroxy group of dopamine directly. However, to the best of our knowledge there are only biocatalysis methods reported for doing this, and they're not selective.[20–23]

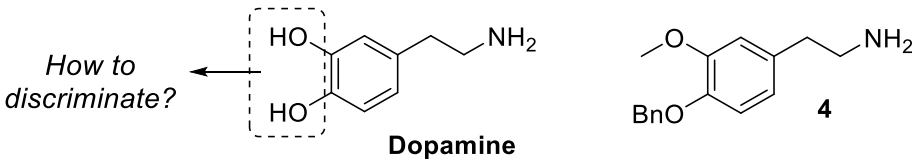

Figure 193 - Similarity between 4 and dopamine

So, we opted to buy the pre-functionalized aromatic ring and then work on the lateral chain. Among the starting materials available on the market, vanillin represents the best option for our purposes: cheap, available, safe, and with an aldehyde functionality already present. It follows the evaluation of the different strategies used for one carbon – one nitrogen homologation.

Strategies evaluated for homologation

We evaluated three strategies for the homologation sequence: Henry reaction followed by reduction, Wittig reaction followed by reductive amination, and Darzens reaction followed by glicidic acid rearrangement with oxime formation, followed by reduction (Figure 194).

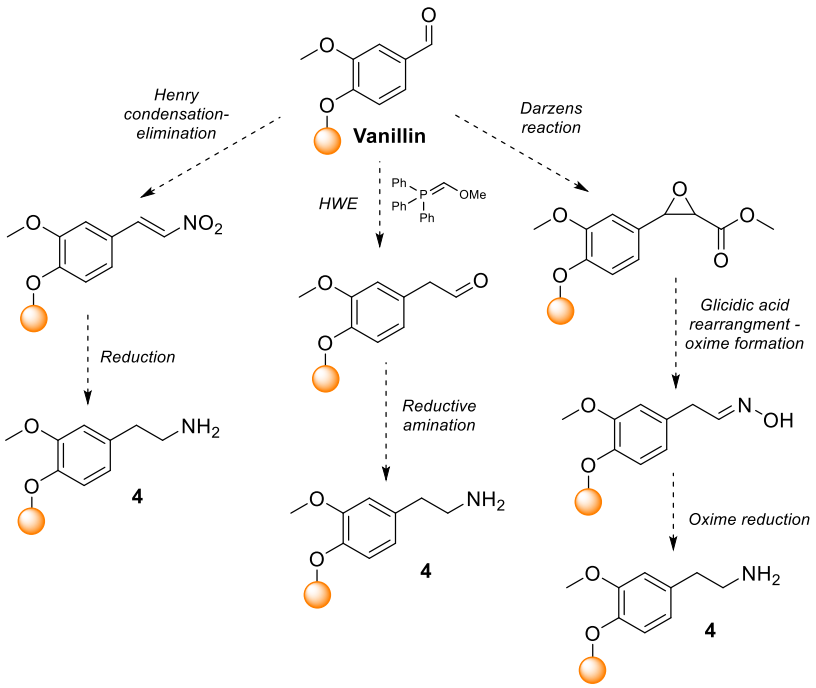

Figure 194 - One carbon - one nitrogen homologation strategies

The Henry reaction sequence is problematic on industrial scale when conducted under basic conditions, as the nitromethanoate ion tends to go out of solution and it's potentially explosive. However, if the reaction is conducted in acidic environment, the explosion risk is significantly lowered, and the process becomes appealing. This strategy has been experimentally evaluated – the details are in the next paragraph. The HWE reaction sequence looks appealing, but the olefination reagent is expensive. At the time, it was decided to give priority to other strategies, so it was not investigated. Finally, the glycidic acid rearrangement sequence is one step longer, but the reagents are all cheap. This strategy was experimentally investigated too, and it was the final choice. It follows a more detailed discussion about the synthesis of intermediate **4**.

Experimental results - Homologation

The final synthetic sequence of intermediate **4**, is shown in *Scheme 2*.

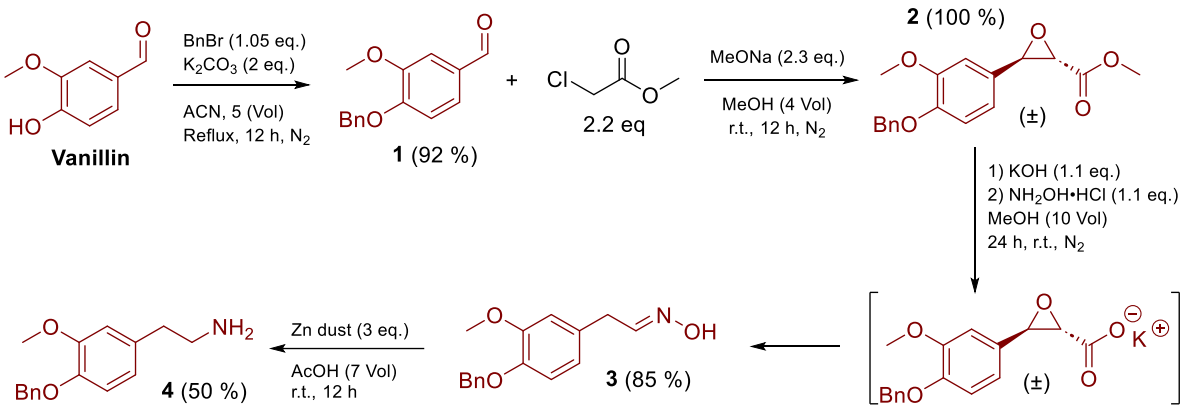

Scheme 2 - Synthesis of fragment 4

The sequence starts protecting vanillin as benzyl ether, because it could interfere with the reactivity of the next steps – particularly in the Darzens reaction, the asymmetric hydrogen atom transfer (HAT) reaction, and amide coupling (see later). The benzylation step is easy: 5% excess of benzyl bromide was used as benzylation agent, together with potassium carbonate as base in acetonitrile at reflux. **1** is finally isolated in 92 % yield after crystallization in isopropanol.

It follows a Darzens reaction with α-chloro-methyl acetate and sodium methoxide as base. The reaction reaches total conversion and quantitative yield, and the product is used directly for the next reaction. The mechanism is shown in Figure 195.

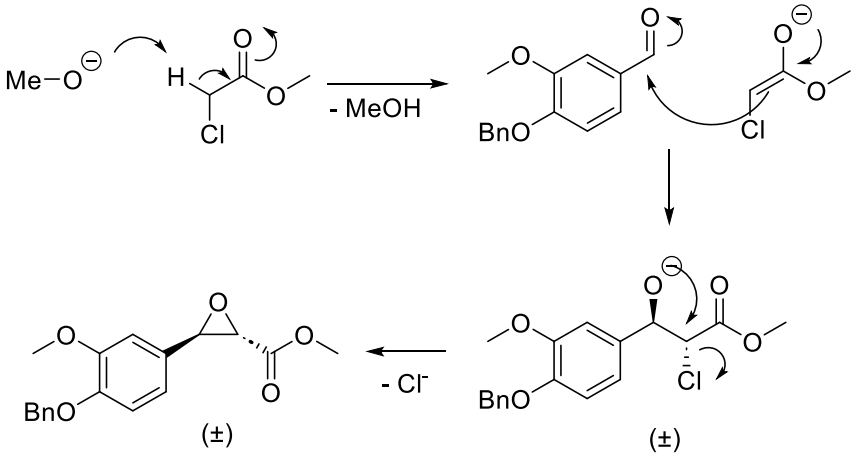

Figure 195 - Darzens reaction mechansim

It follows the saponification of **2** with potassium hydroxide (1,1 equivalent) in methanol. As expected, the conversion is total, and the crude undergoes directly the next step. 1,1 equivalents of hydroxylamine hydrochloride ($NH_2OH•HCl$) were used. This is a multistep reaction, and the mechanism reported in Figure 196.

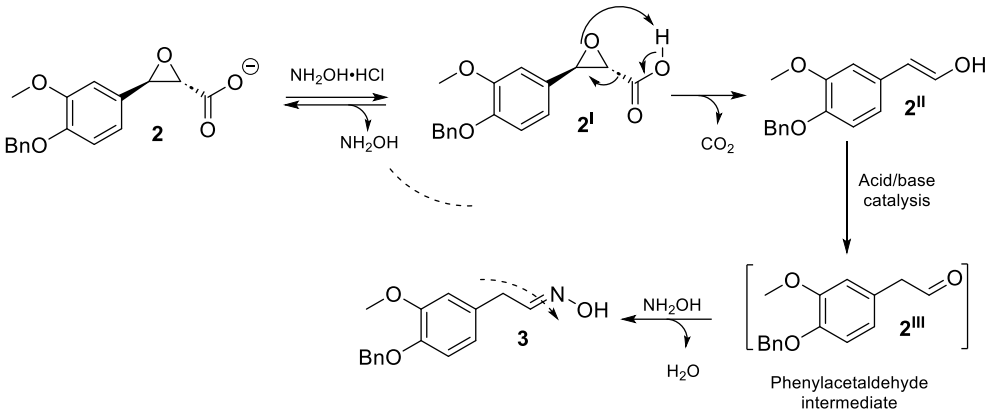

Figure 196 - Glycidic acid rearrangement

First, the excess of potassium hydroxide deprotonates immediately the hydroxylamine hydrochloride, freeing hydroxylamine. Then, the salt at equilibrium re-protonates the carboxylate, generating **2**^{I}. **2**^{I} undergoes the glycidic acid rearrangement:[24] the carboxylic acid protonates intramolecularly the epoxide, trigging a contemporary irreversible decarboxylation and ring opening, generating enol **2**^{II}. **2**^{II} is rapidly converted to **2**^{III} via keto-enol tautomerism. Hydroxylamine then captures **2**^{III} generating the aldoxime **3**. This sequence has several advantages: first, **3** was easily purified by crystallization in methanol. Second, phenylacetaldehydes usually tend to undergo self-aldol reaction fast with a significant yield drop, but oxime formation is faster and prevents any aldol event. Third, the nitrogen atom is already embedded in the structure - to obtain **4** only a reduction step is necessary.

As anticipated before, the synthesis of **4** was attempted also using the Henry condensation-dehydration sequence. Luckily, the reaction is already reported for this substrate,[25] so we just repeated the procedure to verify the reproducibility (Figure 197).

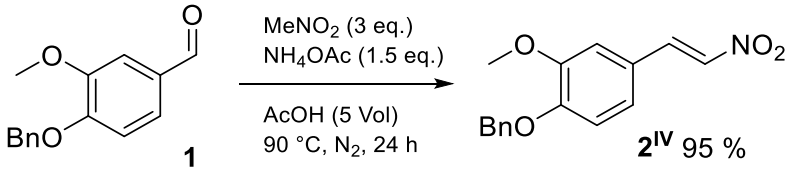

Figure 197 - Henry reaction in acidic conditions

The β-nitrostyrene **2**^{IV} is obtained in 95% yield by simple filtration as it precipitates out of solution. However, this synthetic route was abandoned as there was no possibility to cleanly obtain **4** by reduction.

Experimental results – Reduction

After the one carbon – one nitrogen homologation two different reducing agents were tested for the reduction to access intermediate **4**: lithium aluminum hydride[26] and elemental zinc.[27] Other methodologies found in literature were not tested for time reasons or because they are or not convenient.[28–30]

The reduction of both **3** and **2^{IV}** were attempted. The results are resumed in Table 22.

Substrate	Reducing agent	Conditions	Results
3	Zn	$HCOONH_4$, MeOH, reflux	Dimer and trimer, no product
3	Zn (2 eq.)	AcOH, r.t.	Byproduct + product
3	Zn (6 eq.)	AcOH (15 vol), r.t.	Product, total conversion
3	$LiAlH_4$	THF, reflux	Dimer and trimer + product
2^{IV}	$LiAlH_4$	2-Me-THF, reflux	Dimer and trimer + product

Table 22 - Reduction optimization

Surprisingly, most of the reactions performed yielded a lot of dimer and trimer of **4**. Only elemental Zn in 15 volumes acetic acid was able to yield a clean product. The use of acetic acid as solvent is not ideal at large scales, but it was preferred to obtain a clean product and avoid tedious chromatographic purification. The acetic acid was removed via simple evaporation, then toluene and 10 M sodium hydroxide were added to extract the product and solubilize Zn^{2+} as $Zn(OH)_4^{2-}$. After aqueous washing, toluene was removed under reduced pressure yielding the product in 50 % yield. This was attributed to the low yield to the low extraction efficiency of the product from the particles of $Zn(OH)_2$.[XXIV]

The formation of dimers and trimers using basic conditions can be rationalized with the presence of imines during the reduction process – these are able to undergo nucleophilic attack by the primary amines present, activated by the presence of Lewis acids such as Al^{3+} and Zn^{2+}. The corresponding mechanism is shown in Figure 198.

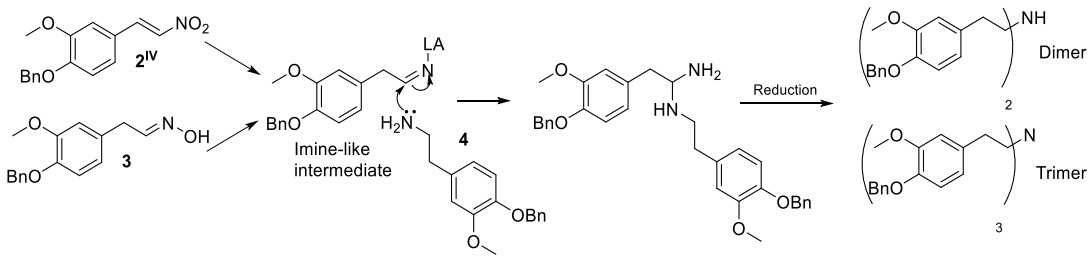

Figure 198 - Formation of dimer and trimer under basic reducing conditions

The presence of a net acidic environment protonates immediately the primary amines formed, hampering any further reactivity. Moreover, lowering the amount

[XXIV] Probably a longer extraction time would be beneficial.

of acetic acid is detrimental: with less solvent everything goes out of phase and the formation of byproducts was observed again.

Intermediate 6

As anticipated in the introduction, intermediate **6** was traced back to **(E)-3-(3-hydroxy-4,5-dimethoxyphenyl)acrylic acid**, a cinnamic acid. Indeed, the strategy followed for this fragment is like the strategy followed for intermediate **4**. It is convenient to buy directly the completely oxygenated and methylated substrate and work on the lateral chain. Luckily, the cinnamic acid is commercially available, or can be produced by Knoevenagel condensation on the corresponding aldehyde with malonic acid.[10]

Experimental results

The synthetic sequence is reported in Figure 199.

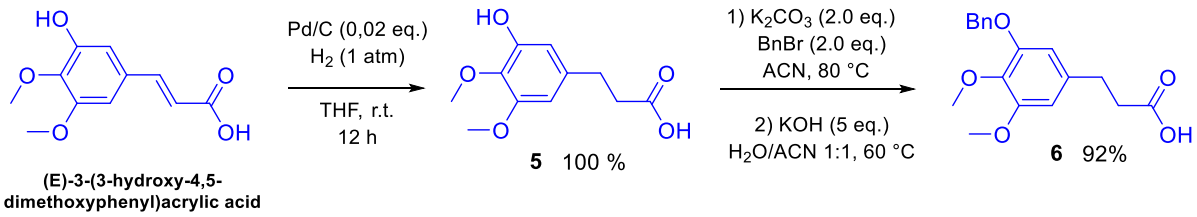

Figure 199 - Synthetic sequence of intermediate 6

The cinnamic acid was hydrogenated using 2% palladium on carbon, with hydrogen at 1 atmosphere in THF. The catalyst was removed by simple filtration over celite and the THF removed under reduced pressure to quantitatively yield **5**. Then, the phenol was protected as benzyl ether to avoid any possible interreference with the amide coupling and HAT transfer reaction that followed (see later). The same protocol for benzylation previously discussed was used, followed by a solvent change in H_2O/ACN 1:1 to do a saponification, as the carboxylic acid was benzylated too. After acidification with hydrogen chloride the product was isolated by simple filtration in 92% yield.

Intermediate 8 – experimental results

Intermediate **4** and intermediate **6** are coupled together to form amide **7**. The combination of 2 equivalent of 1-Ethyl-3-(3-dimethylaminopropyl)carbodiimide hydrochloride salt (EDC•HCl) as coupling agent and 10 % dimethyl-aminopyridine

(DMAP) as nucleophilic catalyst worked well. The conditions are reported in Figure 200.

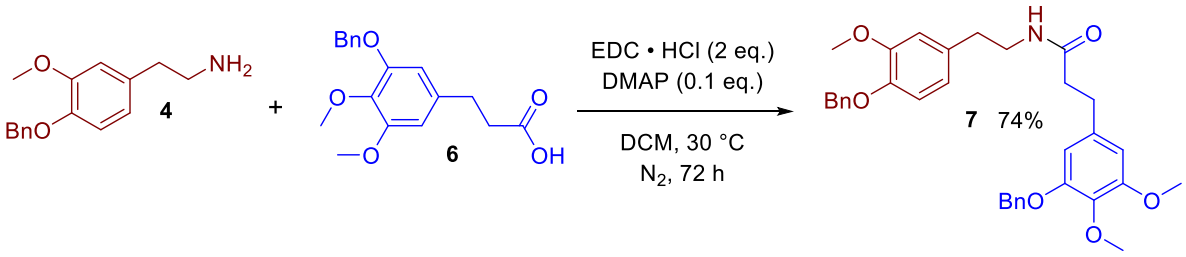

Figure 200 - Amide coupling

After reaction completion the organic phase was washed with 1 M aqueous HCl to remove the urea coproduct and DMAP. After further washings to remove the excess acid and water, the DCM was removed under reduced pressure and **7** was isolated by crystallization in isopropanol in 74 % yield.

After, the dihydroisoquinoline core was obtained by Bischler–Napieralski reaction[31], using toluene as solvent and phosphoryl trichloride as dehydrating agent (Figure 201).

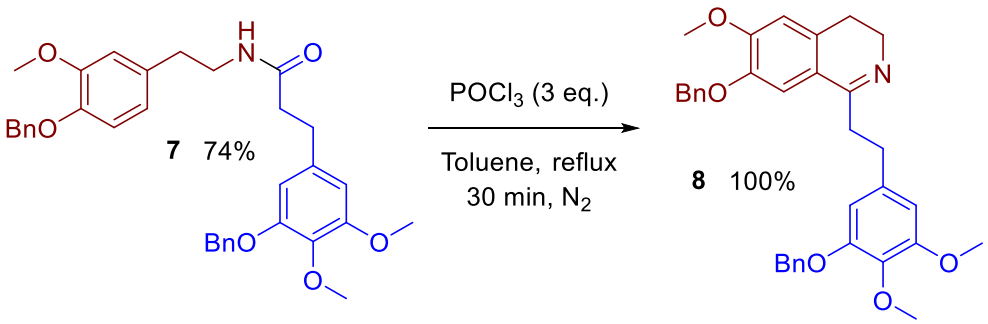

Figure 201 - Bischler-Napieralski ring reaction

The reaction takes only 30 minutes (or less) to finish once the system is in reflux conditions. After the solution cooled down it is injected into a cold Na_2CO_3 solution to quench the residual $POCl_3$ and the developed HCl. The organic phase is separated and the solvent removed under reduced pressure, yielding **8** quantitatively. Despite being an imine, **8** is stable for weeks in environmental conditions, both in its neutral form and salt. Probably this is due both to the intramolecular imine formation, and to the electron donating effect of the bis-oxygenated ring. The product is used as it is in the next step.

Intermediate 9 – strategy and asymmetric HAT optimization

The chiral center of the molecule is then introduced by asymmetric HAT on intermediate **8**. The asymmetric reduction of dihydroisoquinolines to obtain

tetrahydroisoquinolines is a widely explored reaction, also with ruthenium homogenous catalysis.[32] However, given the time available for the project, we choose to use reported conditions by Kouznestov and co-workers for the synthesis of Dysoxykum alkaloids, which are molecules similar to autumnaline.[13] Moreover, there were already encouraging results obtained from the University of Milan, so we went further with the optimization process.

The catalyst is a Noyori-type ruthenium complex, shown in Figure 202.

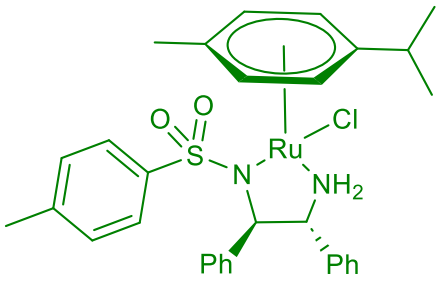

RuCl(p-cymene)[(R,R)-Ts-DPEN]

Figure 202 - Ruthenium catalyst used for imine reduction

The asymmetric ligand is derived from 1,2-diphenyl-diamminoethane, a cheap and available substance. It was decided to use only this ligand and perform a chiral resolution to raise the enantiomeric excess, instead of changing the ligand as it would have probably been extremely time consuming.

The conditions for the HAT process were screened, changing solvent, catalyst loading, reducing agent and temperature. The results obtained are shown in Table 23.

Entry	Catalyst loading	Solvent	Reducing agent	HNMR conversion[a]	Enantiomeric ratio	Scale	Notes
1	2 %	H_2O/MeOH 1:1 (100 vol)	HCOOH/TEA[b] 5:2 (10 eq.)	40 %	34:66	100 mg	Replica of Milan results
2	2 %	H_2O/DMF 1:1 (24 vol)	HCOOH/TEA 5:2 (10 eq.)	88%	16:84	85 mg	Change solvent
3	2 %	H_2O/DMF 1:1 (11 vol)	HCOONa (5 eq.)	30 %	13:87	100 mg	Alternative reducing agent
4	2 %	H_2O/DME[c] 1:1 (20 vol)	HCOOH/TEA 5:2 (10 eq.)	50 %	38:62	53 mg	Change solvent
5	2 %	H_2O/NMP[d] 1:1 (20 vol)	HCOOH/TEA 5:2 (10 eq.)	20-25 %	47:53	56 mg	Change solvent

6	0 %	H_2O/MeOH 1:1 (100 vol)	HCOOH/TEA 5:2 (10 eq.)	0 %	\	50 mg	Blank test
7	0 %	H_2O/DMF 1:1 (20 vol)	HCOOH/TEA 5:2 (10 eq.)	30 %	\	50 mg	Blank test
8	2 %	H_2O/DMF 1:1 (100 vol)	HCOOH/TEA 5:2 (10 eq.)	> 95%	35:66 + byproduct	50 mg	Dilution effect
9	5 %	H_2O/DMF 1:1 (10 vol)	HCOOH/TEA 5:2 (10 eq.)	\	Byproduct	200 mg	Concentration effect
10	5 %	H_2O (20 vol)	HCOOH/TEA 5:2 (10 eq.)	\	Byproduct	200 mg	Solvent change
11	5 %	H_2O (24 vol)	HCOONa (5 eq.)	0 %	0 %	200 mg	Solvent + reducing agent change
12	5 %	H_2O/DMF 1:1 (20 vol)	HCOOH/TEA 5:2 (1 eq.)	Low	Product + byproduct	185 mg	Stoichiometric amount of reducing agent
13	5 %	H_2O/DMF 1:1 (20 vol)	HCOOH/TEA 5:2 (10 eq.)	> 95 %	16:84	2 g	Acceptable result
14	5 %	H_2O/DMF 1:1 (20 vol)	HCOOH/TEA 5:2 (10 eq.)	> 95 %	\	15 g	Final scale-up + crystallization process

Table 23 - Asymmetric HAT condition screening

**All reactions were performed at a temperature between 50 °C and 55 °C.*

[a]Conversion estimated by HNMR as there was no calibration of the response factor for HPLC. [b]TEA = triethylamine, 5:2 is the ratio of azeotropic mixture used. [c]DME = dimethoxyethane. [d] NMP = N-methylpyrrolidone.

First, the reaction conditions developed by the group of Professor Gelmi at the university of Milan on 10 mg scale were tested on 100 mg (entry 1), but the results were worst in our hands. Thus, inspired by the work of Kouznestov[13], we started to test H_2O/DMF 1:1 as alternative solvent. The first results (entry 2) were encouraging. Then, sodium formate as a more benign and cheaper reducing agent was tested with poor results both in pure H_2O (entry 11) and H_2O/DMF 1:1 (entry 3). Inspired by other literature reports, other solvents such as H_2O/DME 1:1 (entry 4), H_2O/NMP 1:1 (entry 5) and pure H_2O (entry 10) were tested trying to replace DMF, again with poor results. Raising the catalyst loading from 2% to 5% (entry 13) improved the conversion in the reaction time given, but the enantiomeric excess was the same. Dilution (entry 8) or concentration (entry 9) had a negative effect on the reaction. In the first case the enantiomeric excess was lower with the formation

of a byproduct. In the second case there were solubility issues, as the imine precipitates out of the solution and again a byproduct formation was observed. Using only 1 equivalent of reducing agent (entry 12), as the stoichiometry requires in theory, again led to a bad rheology of the reaction, with formation of byproducts. The excess amount of reducing agent not only has the effect of speeding up the reaction, but it also acts as a cosolvent. It was observed in general that a real homogenous solution was difficult to obtain with this imine, and that any precipitate yields copious amount of un unidentified byproduct and low conversion.

At this point our best result was entry 13 and it was considered satisfactory enough: >95 % conversion in 16 h between 50 °C and 55 °C and with 10 equivalent of HCOOH/TEA 5:2 led to the formation of the asymmetric amine in 16:84 enantiomeric ratio. The scale-up of this reaction up to 15 g (entry 14) performed well and was directly coupled with the enantiomeric enrichment process (see later).

Moreover, during the optimization campaign, some blank tests were performed. In H_2O:MeOH 1:1 there is no appreciable background reactivity (entry 6), while in H_2O:DMF 1:1 a 30% conversion by HNMR in the same conditions (entry 7). The overall effect of the background reaction will be analyzed in the next paragraph.

The work-up procedure is simple: aqueous sodium hydroxide is added to quench formic acid. The solution is further diluted with water and extracted with ethyl acetate. The organic phase is then washed with water multiple times to remove all the DMF. Last washing was performed with brine to remove as much water as possible, as it could interfere with the following crystallization step. Finally, the solvent is removed by evaporation under reduced pressure with full recovery.

Mechanism and kinetic phenomena

Comparing the results obtained by Kouznestov and co-workers[13], the enantioselectivity of the HAT reaction is much lower – more than 90 % ee on average, against 68 % ee on our substrate. The mechanism of dihydroisoquinoline reduction has already been previously investigated[33], and a plausible transition state based on experimental observations is shown in Figure 203. It is supposed that the enantioselectivity of the process is induced by the π-π aromatic interaction between the substrate and the catalyst aromatic moieties, despite there is no DFT calculation supporting this hypothesis. In our case the presence of extra aromatic

rings due to the benzyl ethers could lower the ΔΔG between the two diastereomeric $TS^{(S)}$ and $TS^{(R)}$, lowering the overall enantioselectivity.[XXV]

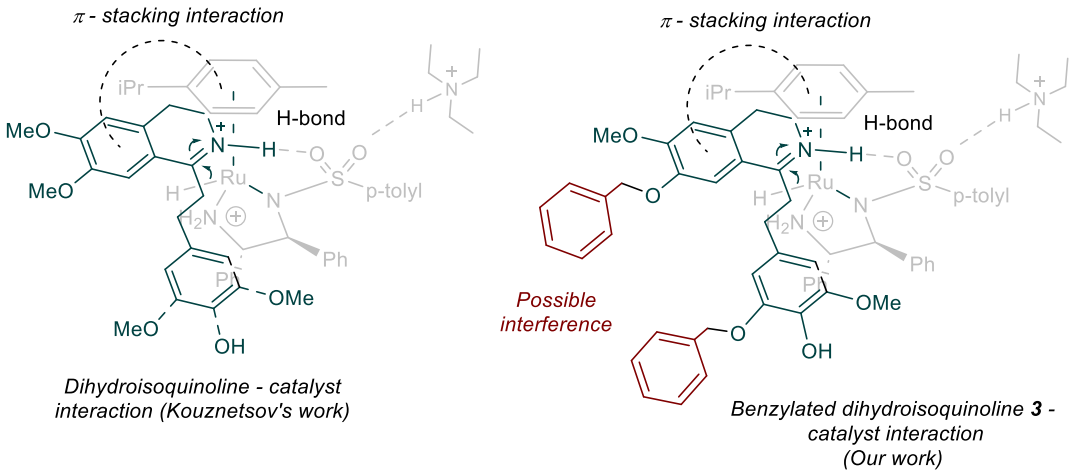

Figure 203 - Possible TS for asymmetric HAT

Some further experiments were done to better understand the sequence of events in our system. First, the ruthenium complex was put in the reaction environment without the presence of the substrate, to check how long it takes for the ruthenium hydride (Ru-H) to form the starting complex. After 22 minutes the signal of the hydride is observed at -7 ppm, reaching the maximum intensity at 28 minutes and getting stabilized (Figure 204). The experiment was performed at 30 °C.

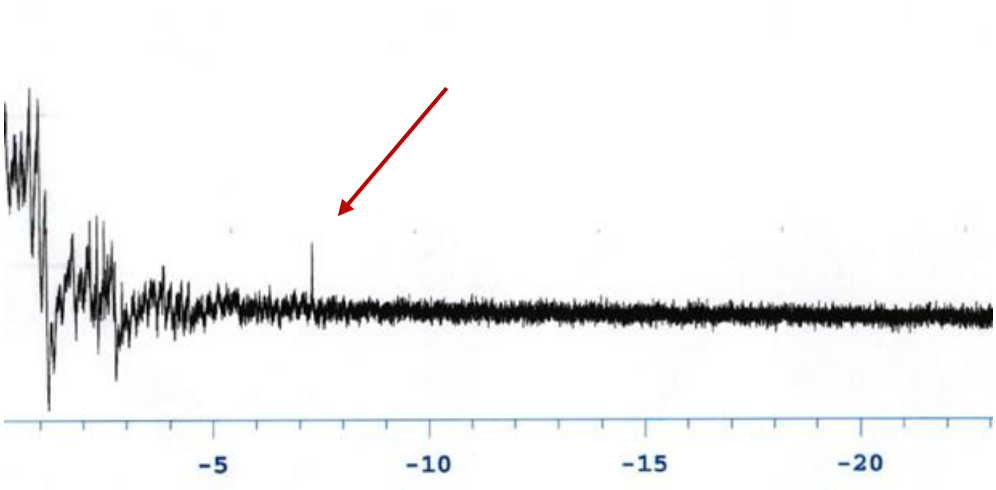

Figure 204 - HNMR spectra of the in-situ formed Ru-H complex

Then, the Ru-H hydride formation was also monitored overtime at 50 °C in the presence of the substrate. As soon as the spectra starts to be recorded (t_0, no imine) the formation of three different hydride species is observed. It follows the substrate

[XXV] Less than 1 kcal/mol is enough to disturb the process.

addition. After 1 hour the central peak has disappeared, while the other peaks get more intense, until after 3 hours the system enters a stationary state (Figure 205).

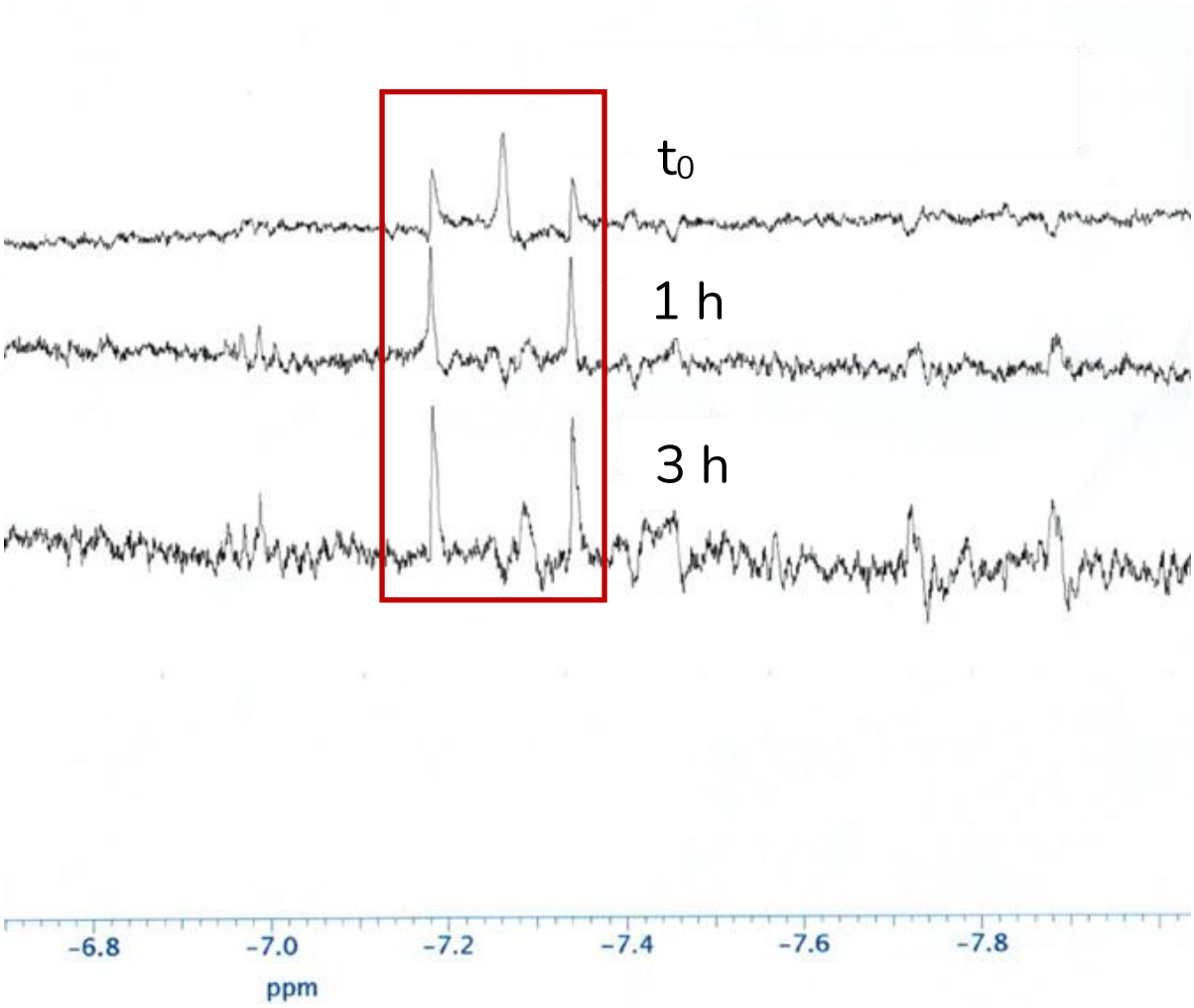

Figure 205 - Monitoring of Ru-H species over time in the presence of the substrate

We can conclude that a stationary state in which the rate of hydride formation equals the rate of imine reduction is reached after around 3 hours. The two side peaks should correspond to two different diastereomeric Ru-H complexes, as reported in literature.[34,35] Probably, at 50 °C it is possible to have both the complexes at the equilibrium, while at 30 °C one is prevalent (Figure 204). I could not assign any structure to the other Ru-H observed at t_0, but it's probably a transient species, as it is observed *before* the imine addition.

To summarize, it was observed that there is a substantial background reactivity, as the imine is reduced even *without* the presence of the catalyst in the reaction conditions. Thus, the ruthenium catalyzed and the background reaction must compete, with the latter lowering the overall enantioselectivity. With a higher catalyst loading (from 2 % to 5 %) the catalyzed process should have been faster

of 2,5 times, suppressing the racemic background process. However, it was observed only a higher conversion, but the enantiomeric excess was identical. It is difficult to rationalize this result, and further investigation is needed to support any hypothesis.

At the time, with these results in our hands and the crystallization process developed, we were satisfied with these conditions: the rheology and chemoselectivity issues were solved, the process is reproducible, scalable, and the intermediate was easily purified (see next paragraph). However, something more can be done to further optimize this reaction in the future. First, lowering the amount of catalyst - with the same reaction time, probably 3% is enough. And given the high cost of ruthenium, lower the catalyst loading would be a significant improvement. Second, the temperature could be optimized as well to improve the enantioselectivity. Finally, different solvents and/or a more selective ligand could further improve the process, but this would require a new optimization campaign.

Crystallization

To obtain an optical pure product, we decided to isolate the desired enantiomer via crystallization with an acid. I followed two different strategies: first, knowing that there is a good enantiomeric ratio (84:16), it is possible to induce the major enantiomer to crystallize using an achiral acid. Second, using a chiral acid it is possible that one diastereomeric salt is much *less soluble* than the other. Acetic acid and tartaric acid were investigated for the scope. The choice of the acids was based both on internal know-how, preliminary results obtained by Dr. D. Lanaro, cost and availability of the reagents and literature.[32] The results are resumed in Table 24.

Entry	Acid	Solvent	Temperature ramp	Result	Comment
1	AcOH (1 eq.)	AcOEt	Reflux to 0 °C	No precipitate	\
2	AcOH (1 eq.)	MeOH	Reflux to 0 °C	No precipitate	\
3	L-tartaric (1 eq.)	EtOH	50 °C to 0 °C	Partial precipitation, sluggish	Not investigated anymore
4	L-tartaric (1 eq.)	MeOH	70 °C to 0 °C, or 20 °C	>99,5 % ee, 60 % yield	Ok- Hemi-tartrate salt.
5	L-tartaric (2 eq.)	MeOH	70 °C to 0 °C	>99,5 % ee, 60 % yield	No change
6	L-tartaric (0,5 eq.)	MeOH	70 °C to 0 °C	>99,5 % ee, 50 % yield	Worst

Table 24 - Crystallization tests

First, I tried to crystallize the major enantiomer using acetic acid both in ethyl acetate (entry 1) and methanol (entry 2), but nothing was observed. Then, I tried to use L-tartaric acid in ethanol (entry 3), but the crystallization was slow compared to methanol (entry 4). So, entry 3 was discarded. The crystals obtained in methanol showed to belong to only one enantiomer. The crystallization procedure is very fast, reproducible and selective. This is useful for the purification of the intermediate in general: the catalyst, DMF and triethylamine traces all go in the mother liquor.

The salt was characterized by NMR and stoichiometric tests, and it's *hemi-tartrate* compound (Figure 206). It was then tested if 2 equivalents (entry 5) or 0,5 equivalents (entry 6) of L-tartaric acid could raise the yield, but no improvement was observed.

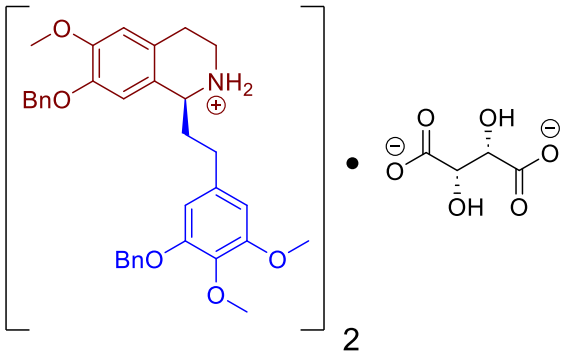

Figure 206 - Hemitartrate salt

The salt can be stored as it is, and "unlocked" with aqueous sodium hydroxide and DCM when needed, yielding intermediate **9** in 60 % yield over 2 steps.

Moreover, the mother liquor was analyzed by HPLC, to check the enantiomeric excess. It was measured an enantiomeric ratio compatible with a racemic mixture.[XXVI] This data, together with the observation that more L-tartaric acid does not produce more precipitate, led us to think that the *racemic mixture* (L)-tartaric acid salt is very soluble in methanol and behaves as a different chemical species. With an enantiomeric ratio of 16:84, the 16 % of undesired enantiomer binds 16 % of desired enantiomer, for a total of 32 % of product that goes in the mother liquor. So, the maximum theoretical yield would be 68 %. Isolated yields range from 60% to 65 %, accounting for some matter lost in the whole process. For this reason, we evaluated that the recovery process could not be significantly improved.

[XXVI] The overall area of the major peaks is probably "contaminated" with something else, as already observed studying the HAT step

Intermediate 10

The secondary amine of intermediate **9** was methylated to obtain intermediate **10**. As anticipated, reductive amination is the reaction of choice, as simple methylation with methyl iodide could lead to quaternary salt formation. Luckily, the same reaction on a similar substrate[13] was already reported and we used the same methodology, shown in Figure 207.

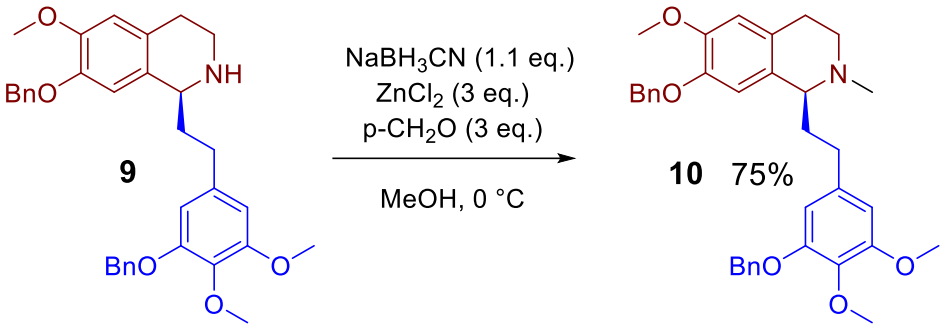

Figure 207 - Reductive amination

The work-up procedure developed consists only in basic washings to destroy the excess reagents, followed by a controlled acidification to avoid amine protonation, and extraction with organic solvent. **10** is recovered in 75% yield or more, keeping an enantiomeric excess >99,5 %. During the para-formaldehyde addition the formation of a chewy solid is observed. The solid re-dissolves during the reaction time with strong stirring. Small-scale operations are more difficult for this reason: in bigger reactors the solid can be smashed more efficiently and the reaction is faster. The recovered yield in these cases goes up to 95 %. The crude is used as it is for the final step.

Usually, the methylation via reductive amination is performed at room temperature using only paraformaldehyde and sodium cyanoborohydride. The presence of a plus-stoichiometric amount of zinc chloride and the low temperature is justified by the iminium ion isomerization phenomenon reported in these systems (Figure 208).[13,36,37]

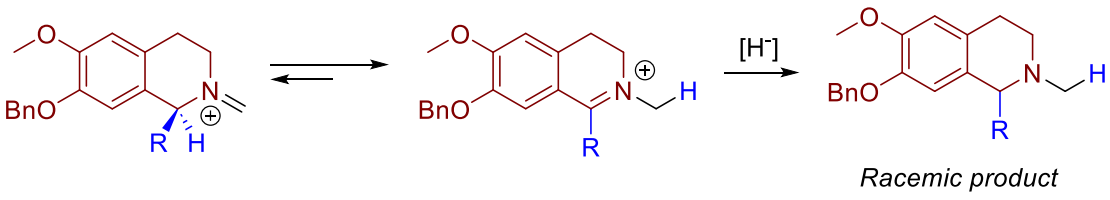

Figure 208 - Iminium ion isomerization

Indeed, it is observed that the presence of the zinc chloride seems to suppress the isomerization reaction, despite there is no explanation for this. The isomerization of

the iminium ion to the *benzylic* position deletes the chiral center. The mechanism of isomerization was not investigated as well.

I tried also to perform a simple Eschweiler–Clarke reaction, but the formation of multiple products was observed.[38]

Autumnaline

The final step consists in the simple hydrogenolysis of the benzyl ether to free the phenolic groups. Hydrogen at 1 atmosphere is enough to do the job, and the catalyst is simple palladium on carbon. The reaction is shown in Figure 209.

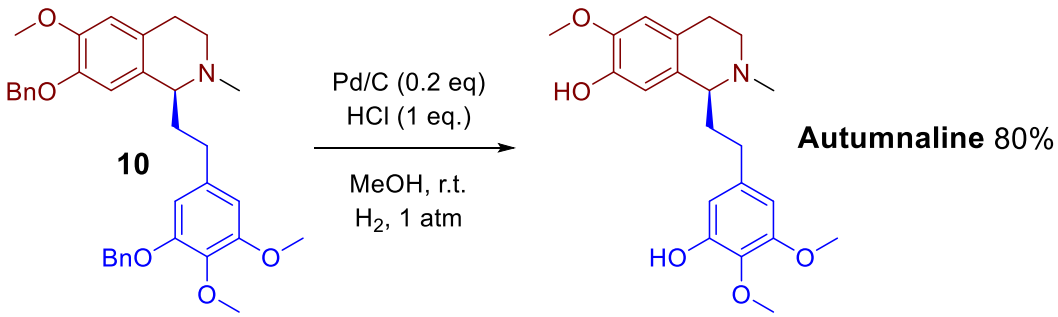

Figure 209 - Hydrogenolysis of benzyl ethers

Hydrogen chloride is used to keep the amine protonated, helping the desorption from the catalyst. During the work-up the catalyst is removed under a pad of celite, then the solvent is removed under reduced pressure. The crude is re-dissolved in organic solvent and washed with aqueous ammonia to deprotonate the amine but not the phenolic groups. The solvent is removed under reduced pressure and then under high vacuum for 24 hours to remove the last traces of solvents. The final product is in the form of thin,white crystals (Figure 210).[XXVII] The recovered yield is 80 %, with >99,5% ee. The product was fully characterized.

[XXVII] Autumnaline shows some solvatochromic effect in the solid state. Depending on the extraction solvent used and the amount of solvent left different light colors are observed.

Figure 210 - Autumnaline crystals

Circular dichroism analysis

Finally, we had to make sure that we made (S)-autumnaline for real. A sample of natural alkaloid was not available, and a single crystal X-ray analysis was not possible. Initially, the absolute optical rotation was measured, finding $[\alpha]^D = 21.7$ °. The only reported optical rotation value[39] is $[\alpha]^D = -5 \pm 3$ °, an absolute value not comparable. We reasoned that this discrepancy may be due to both the better measuring capacity available in our laboratories and the fact that the reference value comes from a natural sample, and some impurities can alter the measurement. Thus, it was decided to record the circular dichroism (CD) spectrum of our autumnaline sample and assign the chiral center with CD computation. The experimental (black) and simulated (red) spectra of (S)-autumnaline are shown overlapped in Figure 211.

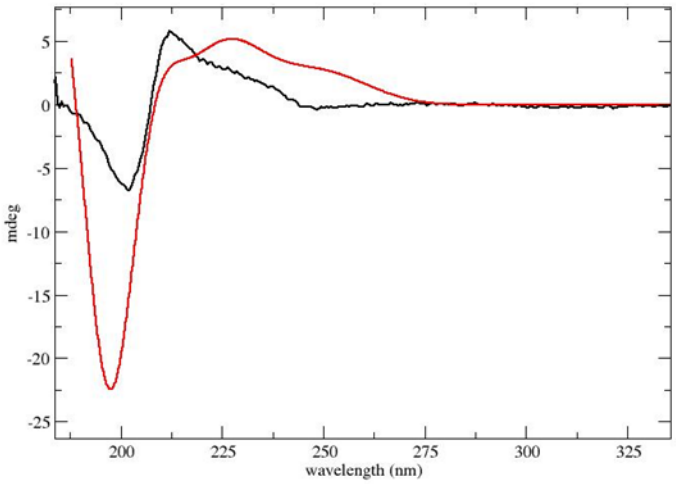

Figure 211 - Experimental and simulated CD spectra of autumnaline – experimental is black, simulated is red

The simulated spectrum is compatible with the experimental spectrum, especially in the polarity inversion region above 200 nm – our sample is actually (S)-autumnaline. The catalyst used for this batch has the (R,R)-configuration. The chiral information relationship between the catalyst and the product is same observed by Kouznetsov and co-workers,[13] despite the presence of benzyl ethers.

Conclusions

An easy, scalable and enantioselective total synthesis of (S) - autumnaline from affordable and commercially available compounds, industrially applicable and of commercial interest, has been reported. The synthesis of the homo-benzylamine **4** was accomplished from vanilline via the Darzens reaction – glycidic acid rearrangement sequence with oxime-trapping and subsequent reduction to amine. The tri-oxygenated fragment **6** was synthesized by simple hydrogenation of a commercially available cinnamic acid derivative, followed by benzylation. The desired amide **7** was obtained via carbodiimide coupling and the dihydroisoquinoline **8** ring was forged with a Bischeler-Napieralsky reaction. The chiral center was introduced via ruthenium catalyzed asymmetric hydrogen transfer of the imine. It was essential to crystalize the desired enantiomer using D-tartaric acid to have a good optical purity. Then, the amine was methylated via reductive amination and the benzyl groups were removed via hydrogenolysis. The development of the process focused on simple purification steps; indeed, no chromatographic purification was eventually necessary. In summary, (S)-autumnaline was synthesized in 11 steps, 9 steps as the longest linear sequence, with a total 13,5% yield, and in enantiopure form.

Supporting information

All the experiments were carried out using chemical purchased from Merk and BLDpharm. The chemicals were used as delivered or purified by distillation or crystallization. The NMR spectroscopy was done using different spectrometers: Agilent MR400 DD2 VNMRJ, Bruker Ascend Evo 600 and Varian MERCURY 300 MHz. Chemical shifts (δ) are given in ppm relative to the $CHCl_3$ internal standard, and the coupling constants J are reported in Hertz (Hz). The ESI spectra were recorded using a quadrupole for ions separation with the following operative conditions: positive ionization mode, mass range = 100-900 Da, data continuum, cone voltage = 2 V, sampling rate 2 point/sec, ion source voltage = 0.8 kV and probe temperature = 300 °C. The HPLC analysis ware carried out using a JASCO and Agilent 1220 Infinity liquid chromatographers, using Daicel Chiralcel OD-H

250*4.6 mm, 5µm, p/n 14325 as chiral column. Circular dichroism spectrum was recorded with a JASCO J-810 spectropolarimeter.

Synthetic procedures

It follows the synthetic procedure for every step in the synthesis of **(S)-autumnaline**, the ECD experimental data by Professor Mazzanti and the ECD computational simulation parameters by Professor Achi, without coordinates data. These will be available in the published paper.

4-(benzyloxy)-3-methoxybenzaldehyde (1)

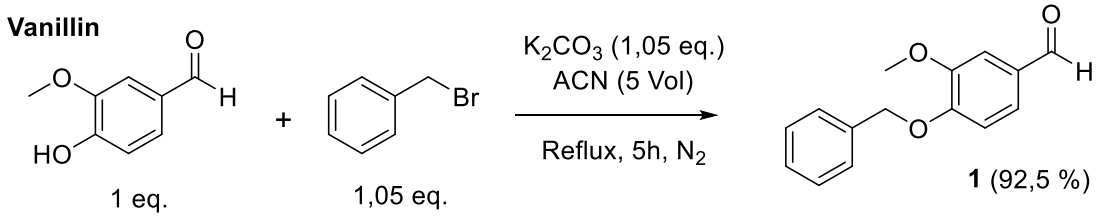

38,2 g (276 mmol, 1,05 eq.) of anhydrous K_2CO_3 were put into a 3 neck round bottom flask (500 ml) and put under N2 with vacuum-nitrogen cycles. Then, 200 ml (5 volumes) of acetonitrile were added, followed by 40 g (263 mmol, 1 eq.) of **vanillin**. The solution was stirred for a few minutes to dissolve **vanillin**. Then, 32.8 ml (276 mmol, 1,05 eq.) of benzyl bromide were added and the reaction was set-up to reflux. Ater 5 h the reaction is complete by TLC (Hex:AcOEt 1:1). The system was allowed to go between 20°C and 25°C and then the suspension was filtered through a büchner filter using filter paper. The solid cake washed with 25 ml of acetonitrile for 4 times. The solvent is then evaporated under reduced pressure, leaving around 100-150 ml of acetonitrile in the flask. Then, 250 ml of toluene are added, followed by 200 ml of water, stirring for 15 minutes. The organic phase is separated. The operation is repeated, extracting again with 150 ml and 100 ml of toluene. Toluene was then removed under reduced pressure. 100 ml of iPrOH were added and evaporated to strip the residual toluene (procedure repeated 3 times or less). 175 ml of IPA (4,4 volumes taking vanillin as reference) were then added and the system was set-up to reflux. Once all the solid was dissolved, the solution was allowed to go between 20°C and 25°C and then put at 0 °C overnight. Alternatively, a programmed temperature ramp can be done, going from 80 °C to 0 °C over the course of 6 hours, keeping the system at 0 °C overnight. The precipitated crystals are then filtered and washed with ice-cold isopropanol (100 ml), then dried under vacuum at 40 °C. 57,14 g of **9** were recovered. The mother liquor was then evaporated and 3 g of solid are still there. Thus, the crystallization procedure was repeated using 9 ml (3 volumes) of isopropanol, recovering 1,8 g more of product. The total mass was 58,9 g, for a total yield of 92,5 %.

NB: the kinetic of the crystallization process is slightly different from batch to batch. If there is no solid, there are two separated phases. In that case the system can be mechanically stimulated or set-up again to reflux, repeating the temperature ramp.

The product was analyzed by HNMR and the spectrum matches the literature data.[40]

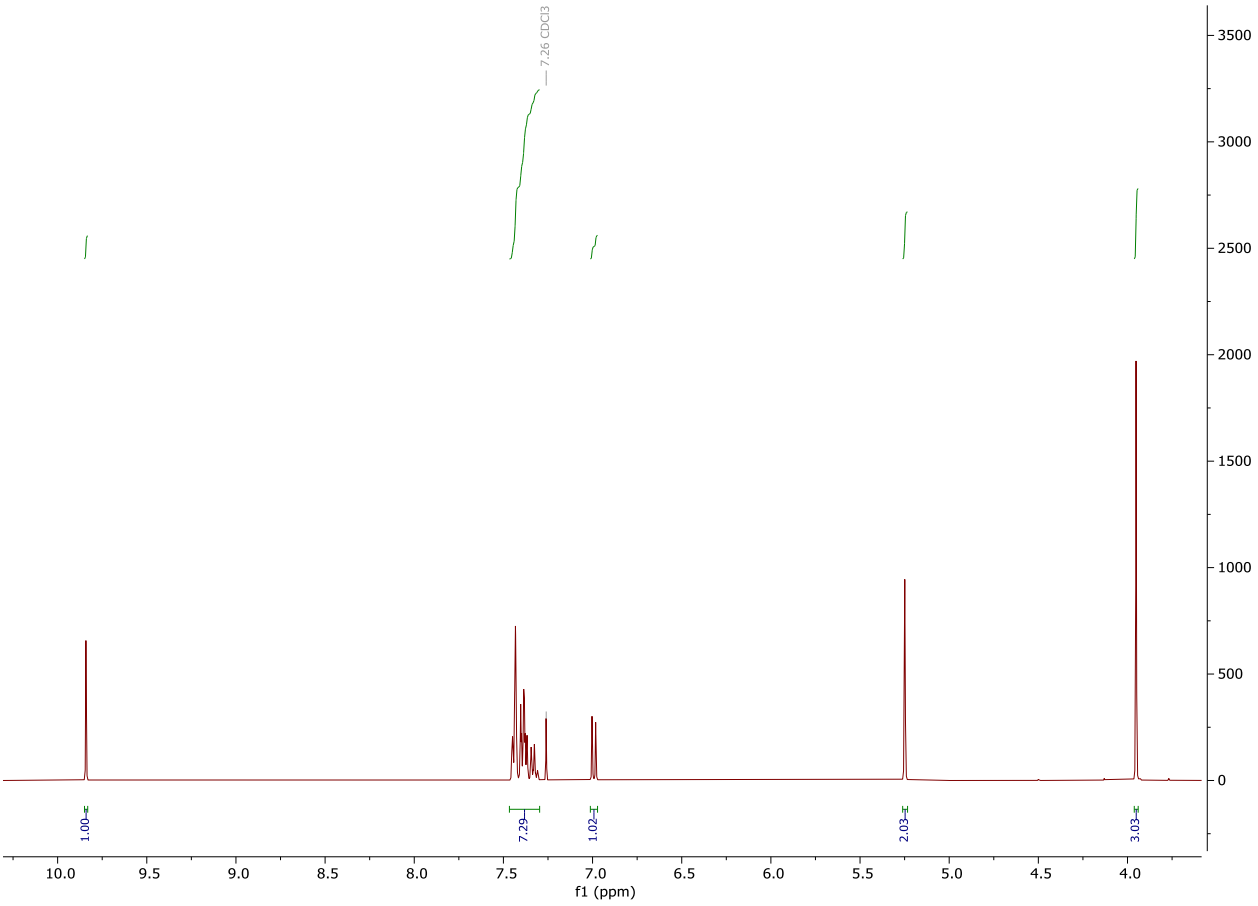

1 1H NMR (300 MHz, CDCl3) δ 9.83 (s, 1H), 7.52 – 7.29 (m, 7H), 6.98 (d, J = 8.2 Hz, 1H), 5.25 (s, 2H), 3.95 (s, 3H).

4-(benzyloxy)-3-methoxybenzaldehyde (2)

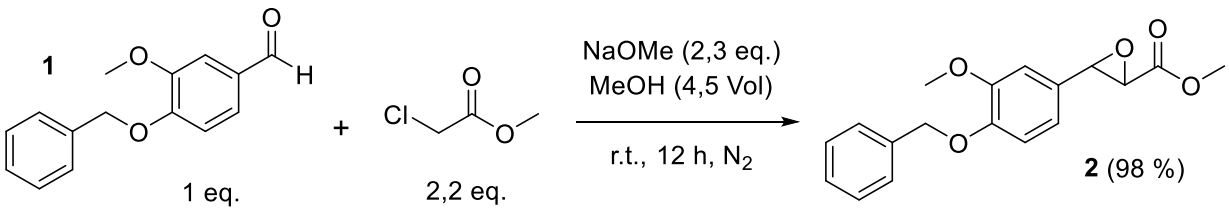

In a 250mL reactor with dropping funnel, thermometer, condenser, and mechanical stirrer, operating under N2 atmosphere, 20g (82,6 mmol, 1 eq.) of **1** and 80 mL (4 volumes) of methanol were added. The suspension was stirred and cooled to a temperature between -12 and -7°C. 54,3 ml (190 mmol, 2,3 eq.) of sodium

methoxide in methanol (25% *w/w*) was added dropwise to the suspension over the course of 15 minutes. The suspension was stirred for at least 15 minutes and 20 ml (182 mmol, 2,2 eq.) of methyl chloroacetate were added dropwise to the suspension at a temperature between – 12 °C and -7° C. The suspension was then stirred at a temperature between -12 and -7°C for 30 minutes and then heated to 0°C in 10 minutes and stirred at this temperature for 1 hour. The suspension is then heated to 25°C and let under stirring for at least 12 hours. The reaction is checked by HNMR.[XXVIII] If it's not complete, some more sodium methoxide and methyl chloroacetate are added, following the same procedure. Once the reaction is completed, 6,2 ml (107 mmol, 1,3 eq.) of glacial acetic acid is added dropwise to the suspension to neutralize the solution, adding AcOH dropwise until pH = 5. The suspension is left to stir between 20°C and 25°C for 1 hour. The suspension is then filtered, and the cake washed twice with 20mL of methanol. The wet product was collected and dried under vacuum between 20 and 25 °C for 24 hours, to yield 24.1 g of **2** (98 % yield) as a single diastereoisomer.

NB there could be some coprecipitation of NaCl, but it does not really matter, since it can be filtered out in the next step. Methanol was difficult to remove from the crude product, since the material was not warmed to avoid decomposition.

2 was characterized by HNMR, CNMR and ESI mass spectrometry.

[XXVIII] A sample is taken ad the solvent removed under reduced pressure. The crude is dissolved in DMSO-d_6. The reaction is considered concluded when the **A**-benzyl signal (5.2 ppm) is less then 5 % compared to the **B**-benzyl signal (5.06 ppm). The aldehyde signal can also be monitored.

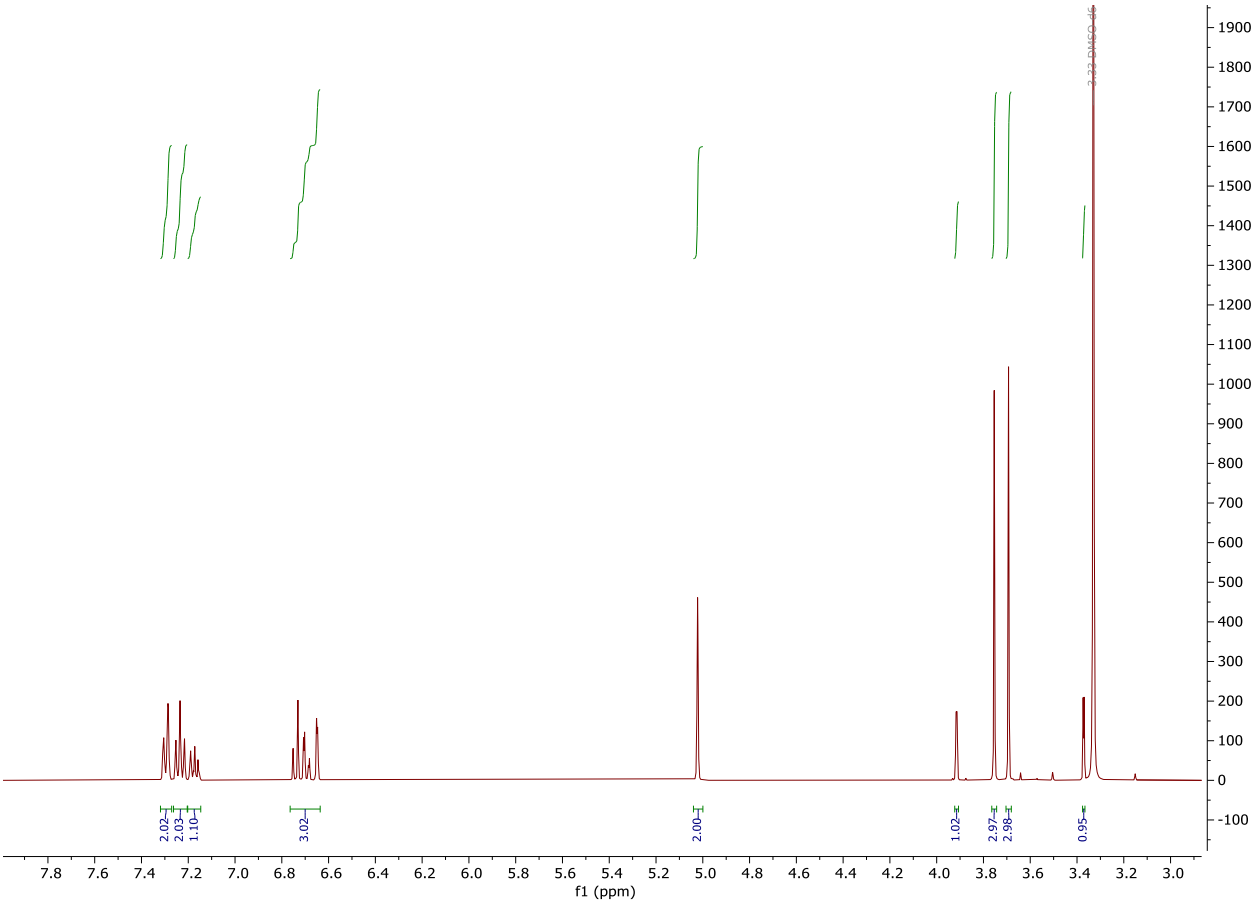

2 1H NMR (400 MHz, DMSO-d6) δ 7.45 – 7.27 (m, 5H), 7.01 (d, *J* = 8.1 Hz, 1H), 6.94 – 6.86 (m, 2H), 5.07 (s, 2H), 4.07 (d, *J* = 1.8 Hz, 1H), 3.84 (dd, *J* = 1.8, 0.7 Hz, 1H), 3.75 (s, 3H), 3.72 (s, 3H).

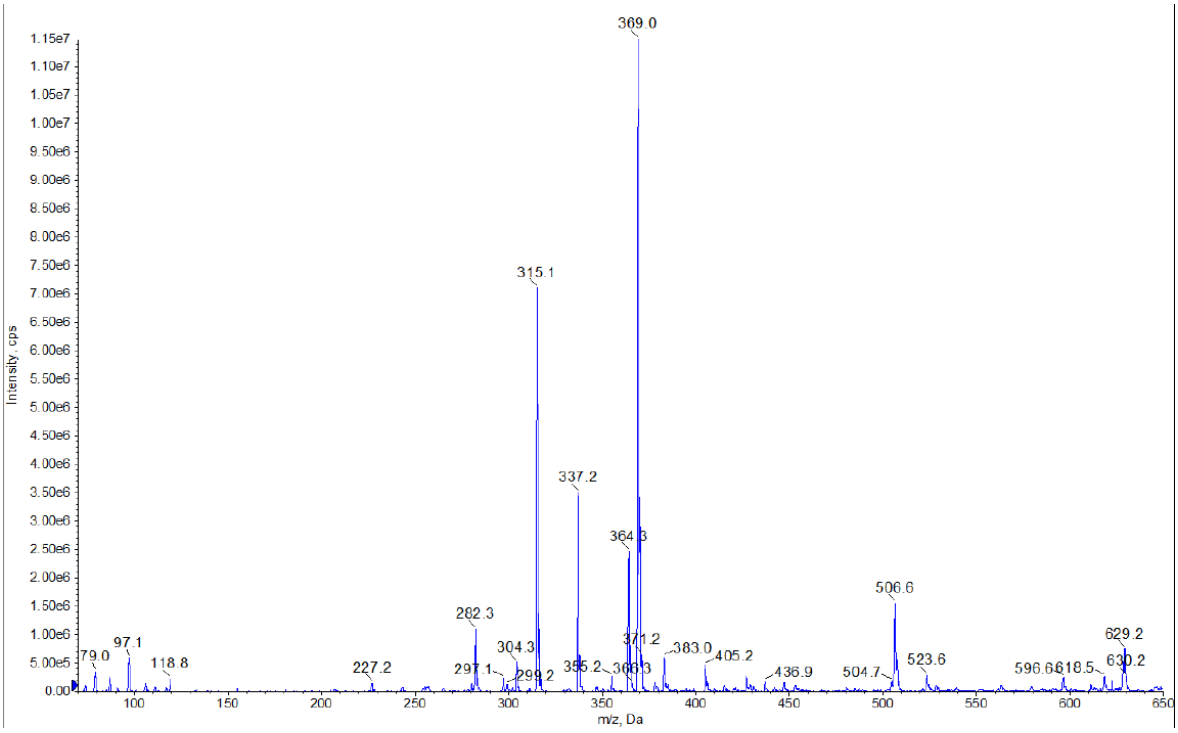

MS identification:

m/z	Identification
282,2	M + MeOH + H^+
315,0	M + H^+
337,1	M + Na^+
364,3	M + MeOH + H_2O+
368,9	M + Na + $MeOH^+$

(E)-2-(4-(benzyloxy)-3-methoxyphenyl)acetaldehyde oxime (3)

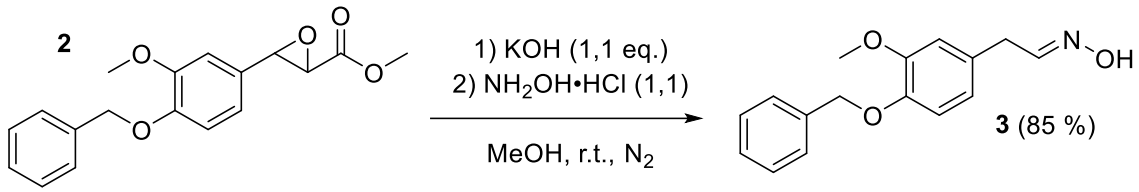

In a 2L reactor equipped with refrigerator, thermometer and dropping funnel, operating under N2 atmosphere, 65 g (207 mmol, 1 eq.) of epoxide **2** and 650 mL (10 volumes) of methanol were added. 12.8 g (227 mmol, 1,1 eq.) of potassium hydroxide were dissolved in 65 mL (5 volumes) of methanol and the solution was added dropwise to the suspension at a temperature between 20°C and 25°C. The mixture was stirred for at least 24 hours. The saponification was monitored via HNMR.[xxix] The solution gets a "sorbetto like" consistency and the diffusion can be slowed down, hampering the completation of the hydrolysis. Some more KOH solution and/or methanol can be added to help. If KOH is added the same equivalents of NH_2OH•HCl must be added as well in the next step to compensate the basicity. After the completion of the hydrolysis 15.8 g (227 mmol, 1,1 eq.) of hydroxylamine hydrochloride were added at a temperature between 20 and 25 °C and the mixture was stirred for at least 24 hours. The reaction is monitored by HNMR.[xxx] When the reaction was completed, the suspension was heated to 40°C and stirred for at least 1 hour. The suspension was filtered, and the cake was washed 2 times with 60mL of methanol. The solvent was removed under vacuum.

Crude was suspended in 600 mL (9,2 volumes) of methanol and the suspension was stirred and heated to 40°C until a solution was obtained. Oxime **3** was

[xxix] A sample was taken and the solvent removed under vacuum. The crude was dissolved in DMSO-d6. The reaction is finished when the singlet at 3,74 ppm is disappeared. TLC monitoring can give false results for spot dragging.

[xxx] A sample was taken and the solvent removed under vacuum. The crude was dissolved in DMSO-d6. The reaction is finished when the singlet at 3,66 ppm is disappeared.

crystallized cooling the solution to 0°C in 6 hours, washing with cold methanol. If a proper cooling system is not available, the crystallization can be performed by just putting the room temperature solution at 0 °C overnight.[XXXI] 48,7 g were recovered, yield= 87%

3 was then characterized with HNMR, CNMR and ESI mass spectrometry.

The reported HNMR spectrum matches literature data[41].

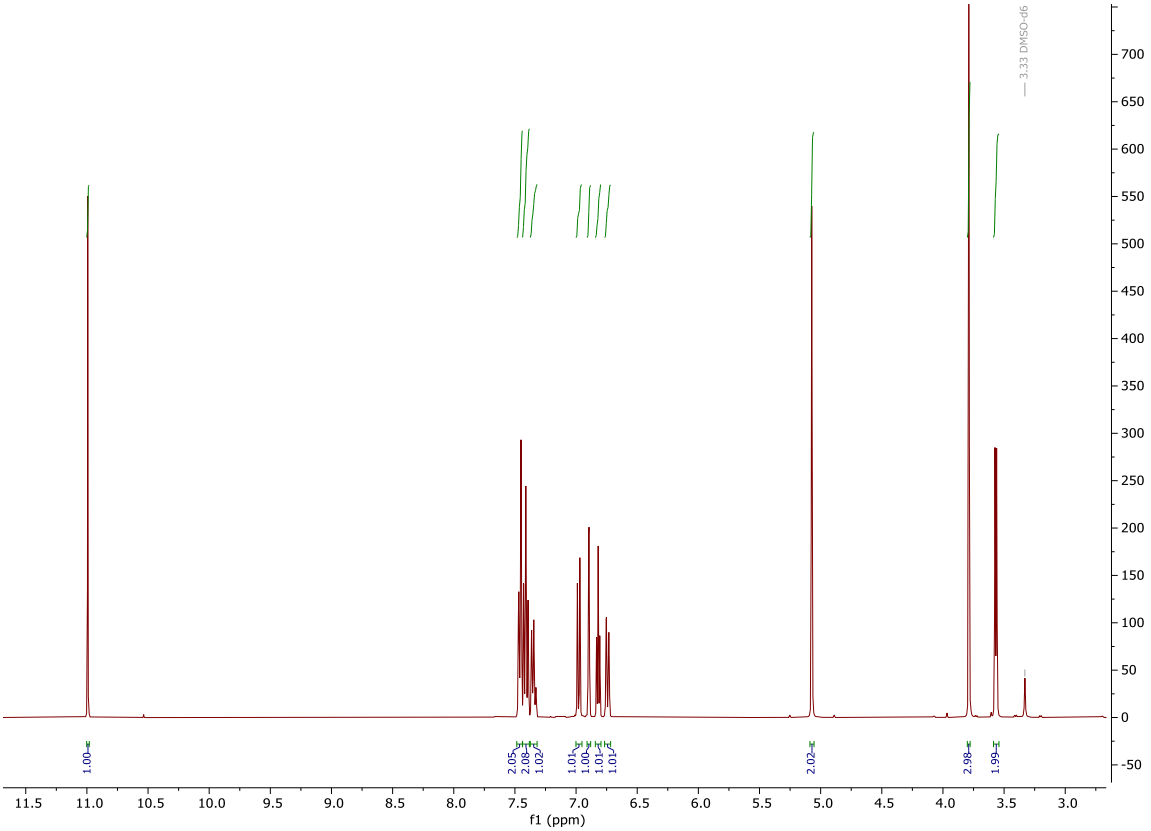

3 1H NMR (400 MHz, DMSO-d6) δ 10.97 (d, J = 2.1 Hz, 1H), 7.46 – 7.33 (m, 5H), 7.33 – 7.26 (m,

1H), 6.97 – 6.91 (m, 1H), 6.85 (d, J = 2.0 Hz, 1H), 6.77 (td, J = 5.3, 0.9 Hz, 1H), 6.72 – 6.68 (m, 1H), 5.03 (s, 2H), 3.74 (d, J = 0.8 Hz, 3H), 3.52 (d, J = 5.3 Hz, 2H).

[XXXI] A fast cooling induced the crystallization of both E and Z isomers. A slow cooling gives only one isomer.

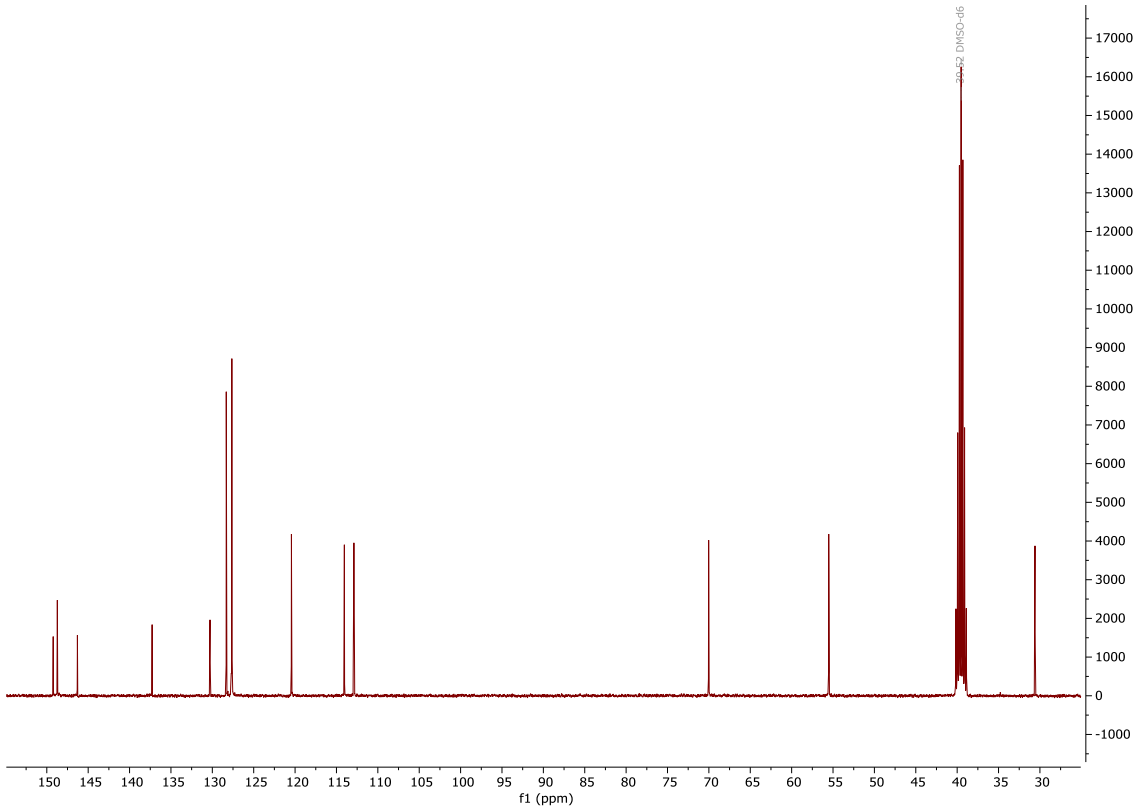

11 - 13C NMR (101 MHz, DMSO) δ 149.23, 148.73, 146.30, 137.27, 130.28, 128.31, 127.70, 127.64, 120.44, 114.05, 112.89, 70.03, 55.52, 30.59

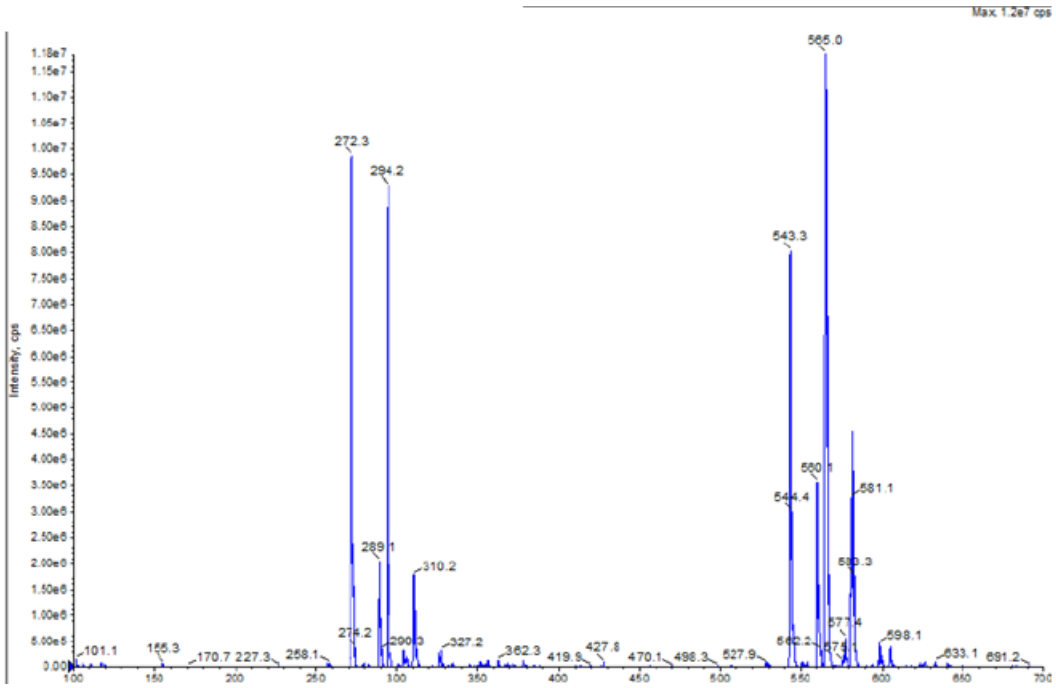

MS identification:

m/z	Identification
272.3	$M + H^+$

289.1	M + NH_4^+
294.2	M + Na^+
310.2	M + K^+
543.3	2M + H^+
560.1	2M + NH_4^+
565.0	2M + Na^+
581.1	2M + K^+

2-(4-(benzyloxy)-3-methoxyphenyl)ethan-1-amine (4)

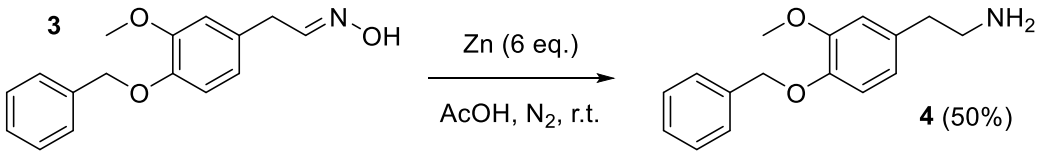

4 g (14.7 mmol, 1 eq.) of **3** are put into a 250 ml 2 neck RBF and put under N2 using N2/vacuum cycles. Then, 60 ml (15 volumes) of glacial acetic acid were added. It follows the addition of 5,78 g (88,5 mmol, 6 eq.) of zinc dust. The reaction was left to stir 16 h at room temperature and the conversion checked.[XXXII] If full conversion is reached, the solvent is directly evaporated under reduced pressure. Then 40 ml (10 volumes) of NaOH 10 M and 40 ml (10 volumes) of toluene are added to the crude, stirring vigorously for 30 minutes.[XXXIII] Then, the bifasic solution is filtered through celite under vacuum to remove the particles of metallic zinc and zinc hydroxide left. The filtrate is recovered collecting also celite and is re-extracting again using the reaction vessel with 40 ml (10 volumes of toluene) for a few minutes, filtering again the suspension using some more fresh celite. The procedure is repeated one more time. In the meantime, the aqueous and organic phase were separated using a separatory funnel. The aqueous phase is then re-extracted with the toluene obtained from the filtrate washing. The organic phases are then merged together and washed with 50 ml (11 volumes) of water for 3 times to remove the residual sodium hydroxide. The toluene is then removed under reduced pressure and the oil obtained is then put under high vacuum for 1 h to remove the residual toluene. 1,90 g of **4** were obtained (50% yield).

[XXXII] . A sample of the suspension was collected under nitrogen and the acetic acid is removed under reduced pressure. It follows the addition of some NaOH 10 M, extracting with DCM. The extracted sample can be checked by TLC (9:1 DCM:MeOH), should be just one spot. The solvent was removed unde reduced pressure and the crude dissolved in DMSO-d_6 and the HNMR spectrum was recorded. The oxime peak at 11 ppm has to disappear when full conversion is reached.

[XXXIII] Make sure to wash properly all the surface of the reaction vessel.

NB: the procedure is optimized to avoid the formation of unfilterable particles of zinc hydroxide and to properly wash the left metallic zinc. Zinc hydroxide seems to retain the product.

4 was characterized by HNMR and ESI mass spectrometry. HNMR spectrum matches the reported spectrum in literature.[42]

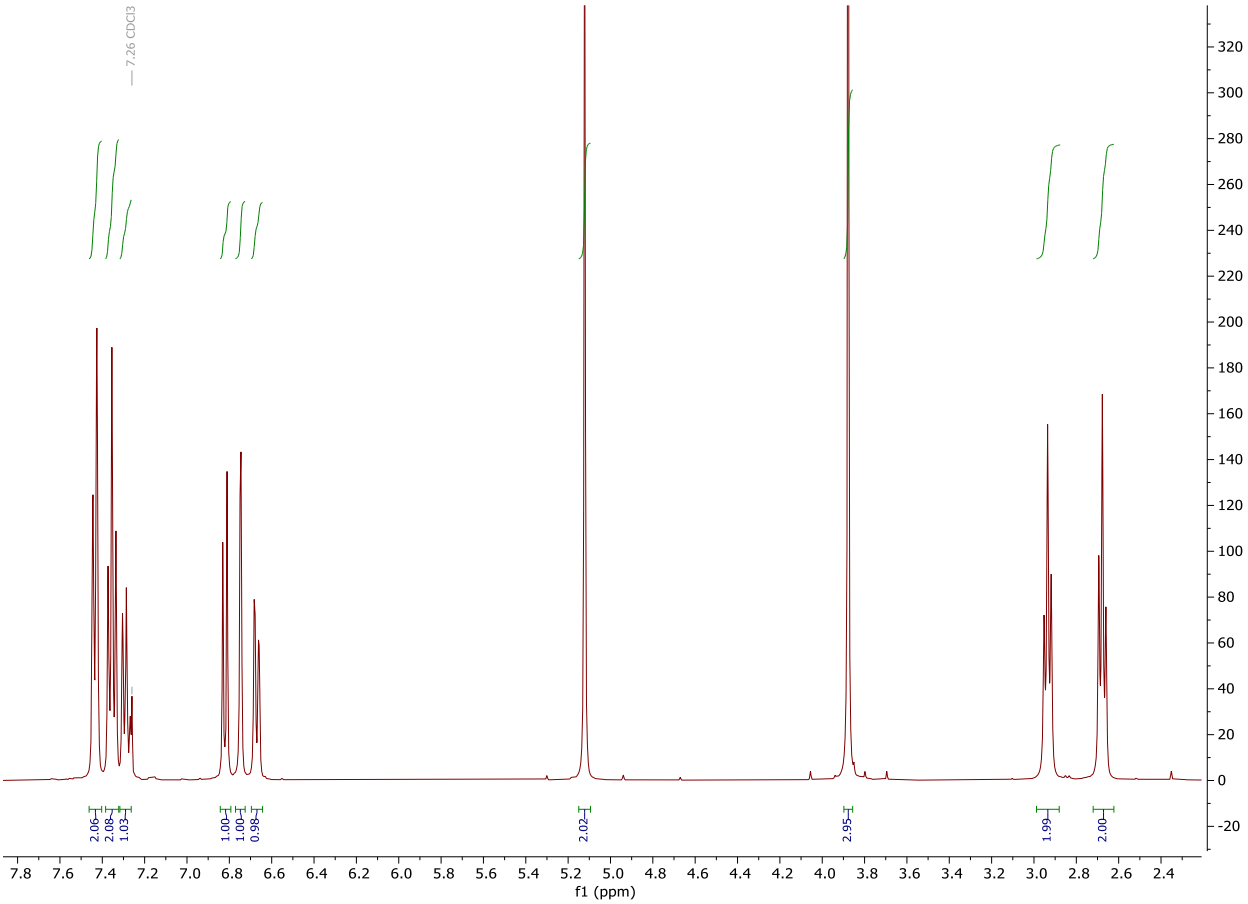

4 1H NMR (300 MHz, CDCl3) δ 7.47 – 7.27 (m, 5H), 6.81 (d, J = 8.1 Hz, 1H), 6.74 (d, J = 1.9 Hz,

1H), 6.67 (dd, J = 8.1, 2.0 Hz, 1H), 5.13 (s, 2H), 3.89 (s, 3H), 2.93 (t, J = 6.8 Hz, 2H), 2.68 (t, J

= 6.8 Hz, 2H).

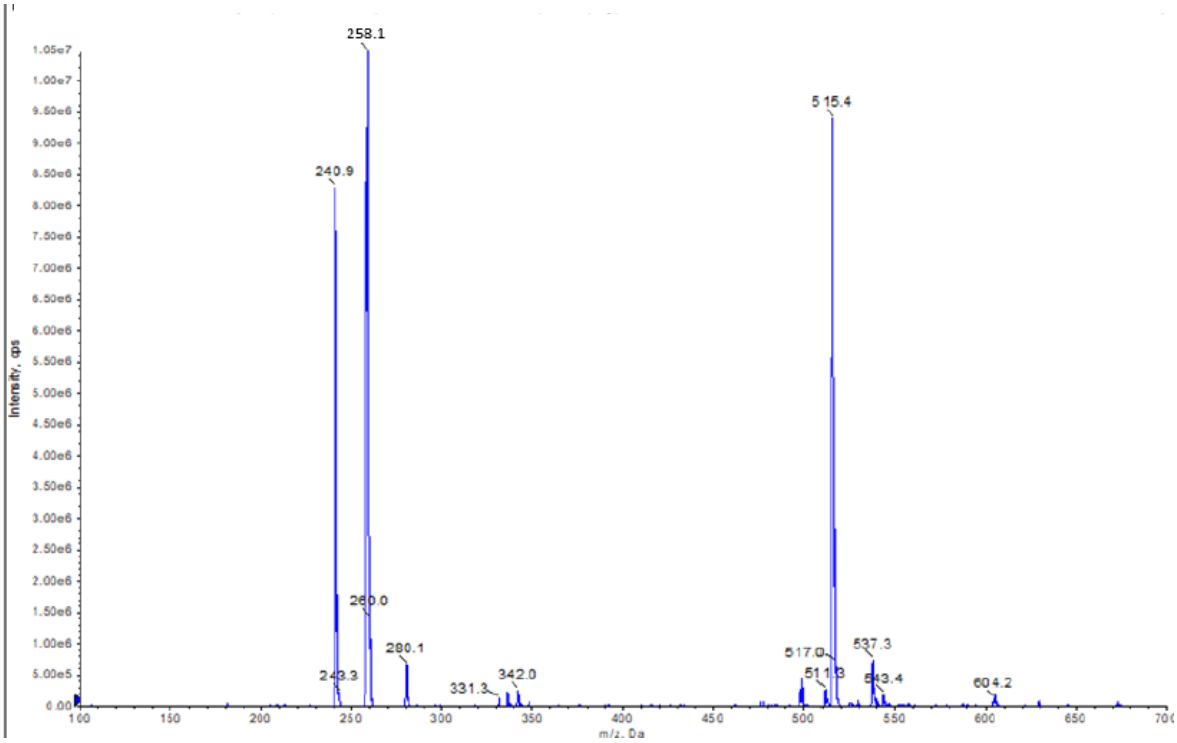

m/z	Identification
240.9	M-NH2 + H^+
258.1	M + H^+
280.1	M + Na^+
515.4	2M + H^+
537.3	2M + Na^+

3-(3-hydroxy-4,5-dimethoxyphenyl)propanoic acid (5)

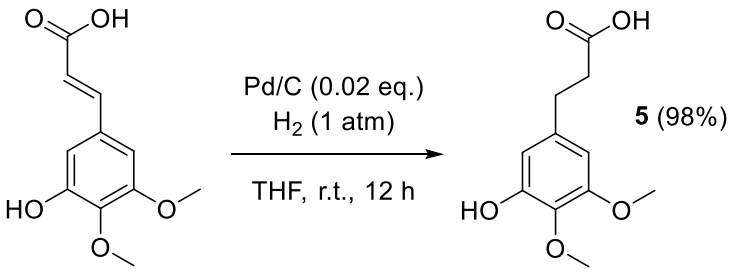

(*E*)-3-(3-hydroxy-4,5-dimethoxyphenyl)acrylic acid

In a 1L three necked round bottom flask equipped with magnetic stirrer, thermometer and (later) H_2 balloon, 30g (133,8 mmol, 1 eq.) of **3-(3-hydroxy-4,5-dimethoxyphenyl)propanoic acid** and 10g (2,676 mmol, 0,02 eq.) of palladium on carbon (5% loading, 50% w/w wet with water) and 600 mL (20 volumes) of THF

were added at a temperature of 20-25°C. The suspension is stirred, and 3 vacuum/N_2 cycles were performed to operate under inert atmosphere. Then the atmosphere was changed to H^2 with three cycles of vacuum/H_2. The suspension was stirred in H_2 atmosphere for at least 12 hours at 20-25°C. After this time, the conversion can be checked by HNMR.[XXXIV] At the completion of the reaction the suspension was filtered over celite pad, and the cake was washed 2 times with 30mL (2 volumes) of THF. The solvent was evaporated under reduced pressure and 29.8g of **5** were collected as a light orange solid, with 98% yield.

5 was characterized by HNMR. The spectrum matches literature data.[43]

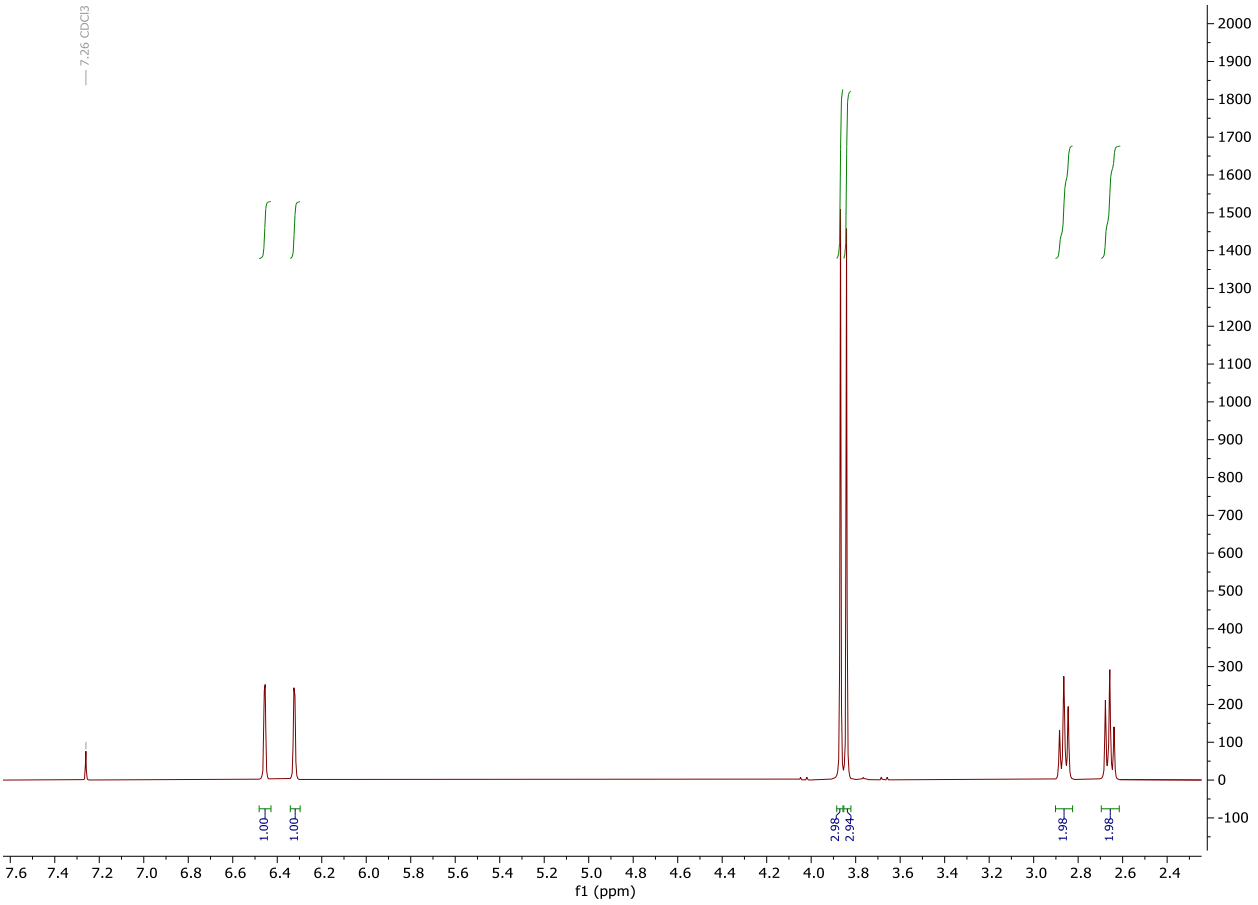

5 1H NMR (300 MHz, CDCl3) δ 6.44 (d, J = 1.9 Hz, 1H), 6.31 (d, J = 1.9 Hz, 1H), 3.85 (s, 3H), 3.83

(s, 3H), 2.85 (t, J = 7.7 Hz, 2H), 2.64 (t, J = 7.9 Hz, 2H).

[XXXIV] A sample of suspension was filtered on a PTFE filter or celite and the solvent evaporated under reduced pressure. The oily residue was dissolved in $CDCl_3$ and then analyzed by HNMR. The reaction is
considered complete when the alkene signals at 6.83 ppm and 6.66 ppm are not observed anymore.

3-(3-(benzyloxy)-4,5-dimethoxyphenyl)propanoic acid (6)

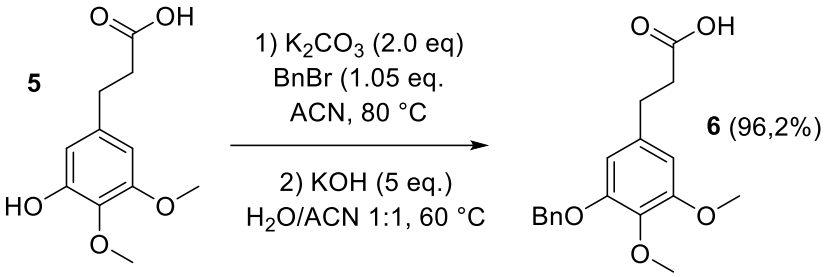

30,9 g of **5** (132,6 mmol, 1 eq.) was added to a 1 L round bottom flask and 300 ml (10 volumes) of acetonitrile were added to dissolve the solid. Then, the system is put under nitrogen using N_2/vacuum cycles. It follows the addition 47,2 g (2,5 eq.) of K_2CO_3. The system was set-up to reflux for 1 h. Then, after cooling down to around 40 °C, 32,5 ml (2 eq.) of benzyl bromide were added. The system was set-up to reflux for 12 h. After this time the system is allowed to go back to room temperature and IPC confirmed the complete conversion[xxxv]. The suspension was then directly filtered under reduced pressure, washing the cake with around 100 ml of acetonitrile (3,3 volumes). Then, the volume of the filtered solution was reduced to around 250 ml under reduced pressure. It follows the addition of 37,5 g of KOH (5 eq.), dissolved in 250 ml of water. The reaction stirred at 60 °C for 1 h, then allowed to reach room temperature. IPC[xxxvi] was done, showing full conversion. The acetonitrile was then removed under reduced pressure at 60 °C, adding 250 ml of water since the system becomes jelly. The aqueous solution is then extracted with 250 ml of toluene twice to remove benzylic alcohol. The aqueous solution was then acidified using 37 % aqueous HCl until pH = 1 (50 ml of acid were used). A precipitate starts to form, and the system is allowed to stir for 16 hours at room temperature. The suspension was then filtered, and the cake was washed with 30 ml of HCl 1 M. After as much liquid as possible was removed via filtration, the cake was dried at 50 °C under vacuum for 48 h, to yield 40,0 g of **6** (92, 6 % yield).

6 was then characterized by HNMR. The data matches the reported spectrum.[44]

[xxxv] TLC Hex:AcOEt 7:3.
[xxxvi] TLC Hex:AcOEt 7:3.

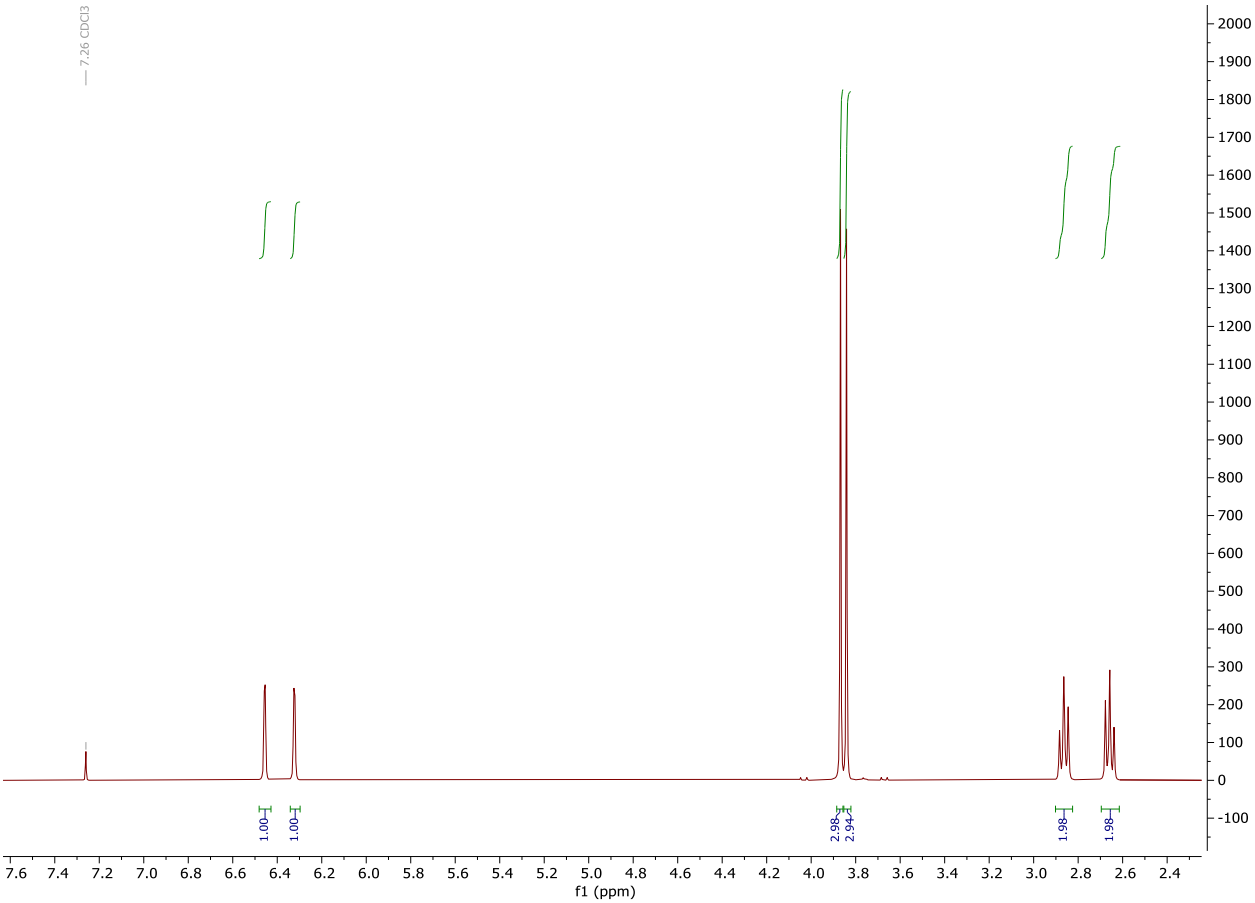

6 1H NMR (400 MHz, CDCl3) δ 7.39 – 7.28 (m, 5H), 6.44 (d, J = 1.9 Hz, 1H), 6.29 (d, J = 1.9 Hz,

1H), 5.12 (s, 2H), 3.86 (s, 3H), 3.80 (s, 3H), 2.87 (t, J = 7.7 Hz, 2H), 2.65 (t, J = 7.8 Hz, 2H).

N-(4-(benzyloxy)-3-methoxyphenethyl)-3-(3-(benzyloxy)-4,5-dimethoxyphenyl)propanamide (7)

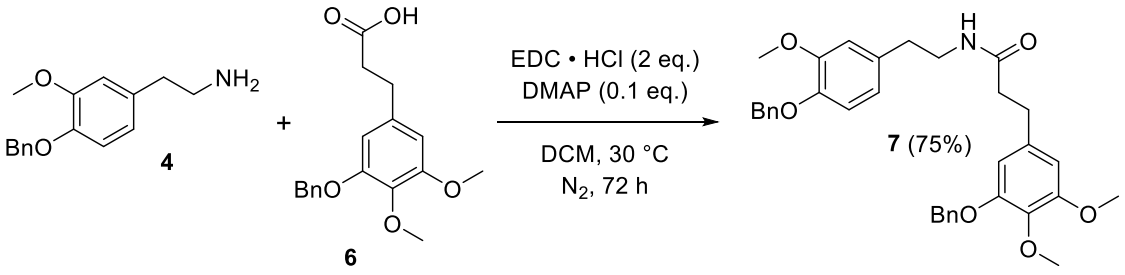

2,3 g (8,9 mmol, 1 eq.) of **4** were put under inert atmosphere and then dissolved in 23 ml (10 volumes) of DCM. 2,83 g (8,9 mmol, 1 eq.) of **6** are weighed into a 2 neck RBF and put under N_2 with vacuum/nitrogen cycles. It follows the addition of the

amine solution over the solid. Then, 3,43 g (2 eq.) of EDC•HCl and 109 mg (0.1 eq.) of N,N-dimethylamminopyridine (DMAP) were put under inert atmosphere and then suspended into 23 ml (10 volumes compared to the limiting reagent) of DCM. The main solution is put at 0 °C, then the suspension was added and the reaction left to go to r.t. After 72 hours IPC[XXXVII] was done, confirming the full conversion. Then, 46 ml of HCl 1 M (same volume of DCM) were added, stirring for 1,5 h. The emulsion is put into a separatory funnel, allowed to separate and the aqueous phase is discarded. Then, the organic phase was washed with 50 ml of $NaHCO_3$. Then, the organic phase was washed with 50 ml of brine and the solvent removed under reduced pressure. The amide **7** was purified by crystallization: 20 ml of isopropanol (4 volumes) were added to the crude and heated-up to reflux, until the whole crude is dissolved. Then, the solution was slowly allowed to cool down (0,5 °C/min). At around 40 °C the precipitation of the amide is observed. The round bottom flask was then left at 0 °C for 18 hours and filtered, washing the precipitate with cold isopropanol. The solid was then put at 80 °C under vacuum for 48 h to remove the residual isopropanol. 3,66 g of **7** were recovered (74 % yield).

7 was characterized by HNMR and ESI mass spectrometry.

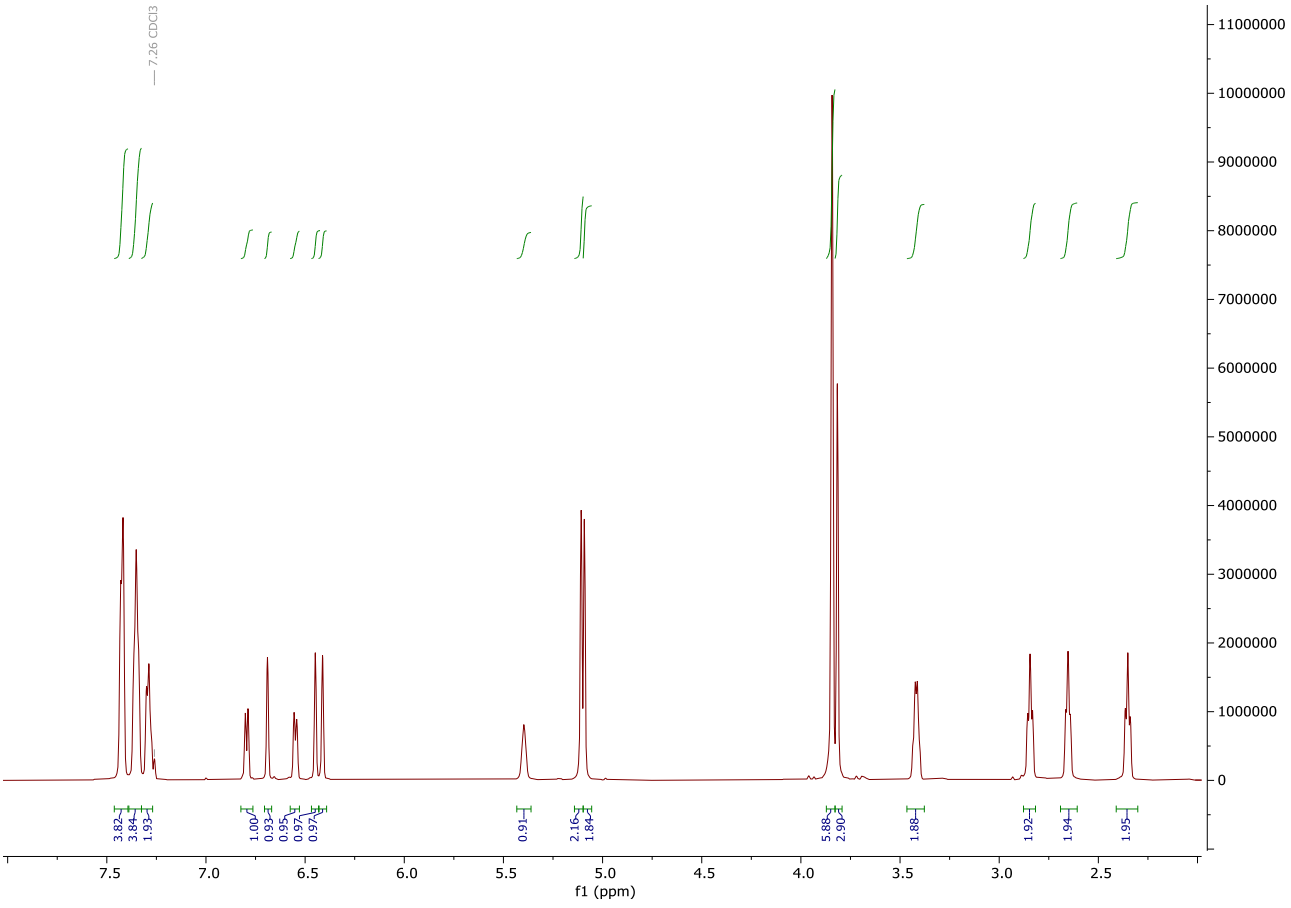

[XXXVII] TLC Hex:AcOEt 1:1

7 1H NMR (600 MHz, $CDCl_3$) δ 7.42 (m, 4H), 7.37 – 7.33 (m, 4H), 7.29 (m, 2H), 6.79 (dt, *J* = 8.1, 2.1 Hz, 1H), 6.69 (bs, 1H), 6.45 (bs, 1H), 6.41 (d, *J* = 2.8 Hz, 1H), 5.40 (bs, 1H), 5.11 (bs, 2H), 5.09 (bs, 2H), 3.84 (bs, 6H), 3.82 (s, 3H), 3.42 (q, *J* = 7.2 Hz, 2H), 2.84 (t, *J* = 7.3 Hz, 2H), 2.65 (t, *J* = 6.4 Hz, 2H), 2.35 (t, *J* = 7.1 Hz, 2H).

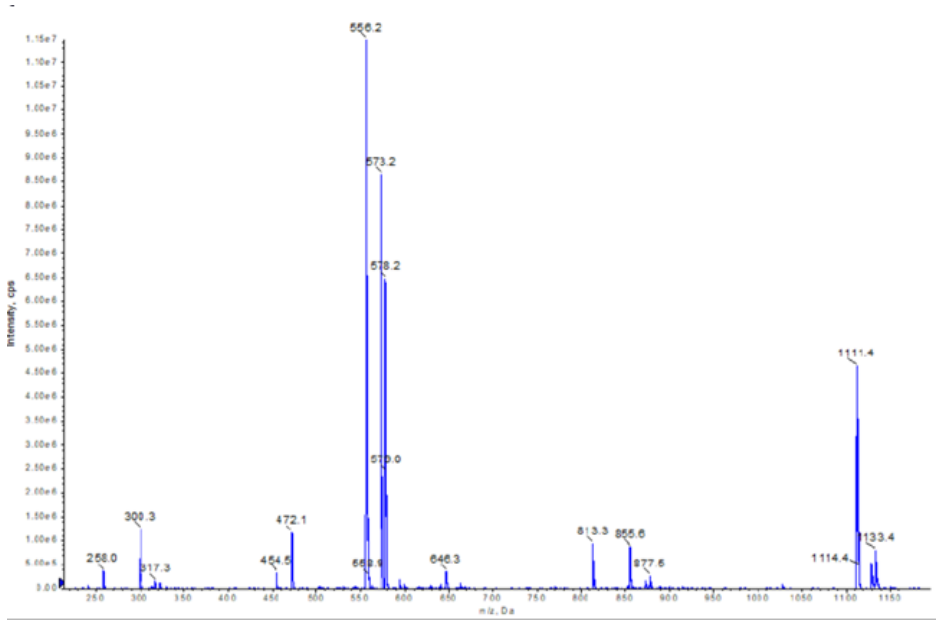

m/z	Identification
556.2	$M+H^+$
573.2	$M+NH_4^+$
578.2	$M+Na^+$
1111.4	$2M+H^+$
1133.4	$2M+Na^+$

7-(benzyloxy)-1-(3-(benzyloxy)-4,5-dimethoxyphenethyl)-6-methoxy-3,4-dihydroisoquinoline (8)

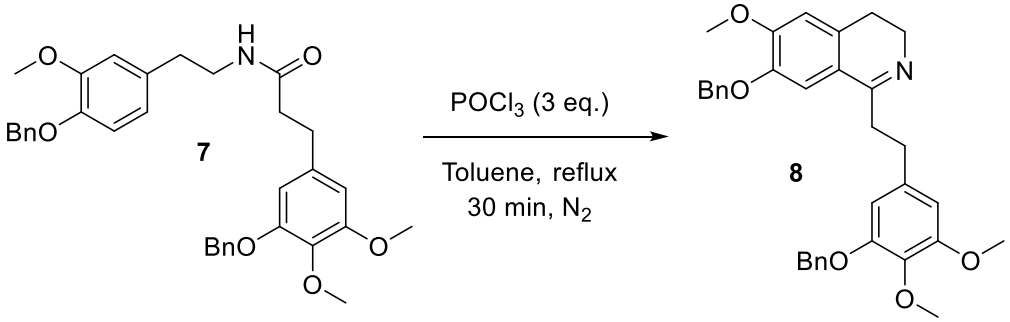

25 g (50 mmol, 1 eq.) of **7** was put into a 3 neck round bottom flask with a refrigerating system. Then, the solid is put under an inert atmosphere with vacuum/N_2 cycles. It follows the addition of 175 ml (7 volumes) of toluene. The suspension was put at 0 °C, then 12,6 ml of $POCl_3$ (3 eq.) were added slowly. After the addition the system was set-up to reflux. During the heating time at around 90 °C complete dissolution of the solid is observed. After 30 minutes IPC[XXXVIII] showed complete conversion and we can go on with the quench procedure. 2 quench procedures were developed.

Quench procedure 1: in the direct evaporation of the solvent, removing the excess $POCl_3$ (a proper trap for the acids should be installed). The crude was the re-dissolved in 150 ml (6 volumes) of DCM. 150 ml of saturated aqueous $NaHCO_3$ (6 volumes) were then added, stirring for 30 minutes, in order to neutralize the excess HCl. The organic phases were then separated, and the aqueous phase was washed with 75 ml (3 volumes) of DCM. The organic phases were merged and washed with 100 ml of brine and the solvent was evaporated under reduced pressure, leading to 20,2 g of crude.

Quench procedure 2: this procedure was applied to other batches, but the results were always a quantitative recover. After the solution was left to cool down, it was slowly cannulated directly into 10 volumes of a Na_2CO_3 saturated aqueous solution at 0 °C, to quench the acid. After the cannulation the emulsion was left to stir for 30 minutes and allowed to go to room temperature, to ensure complete quench. The organic phase and aqueous phase were then separated and the aqueous phase was washed with 3 volumes of toluene to ensure complete recover. Then, the organic phases were merged and the toluene was removed under reduced pressure (the residual water is removed in the same unitary operation via azeotropic distillation).

In general it was observed that variable amount of residual solvents do not interfere in the next step (the crude was used as it is). The imine is bench-stable for weeks.

8 was isolated for characterization with HNMR and CNMR.

[XXXVIII] TLC AcOEt:MeOH 9:1

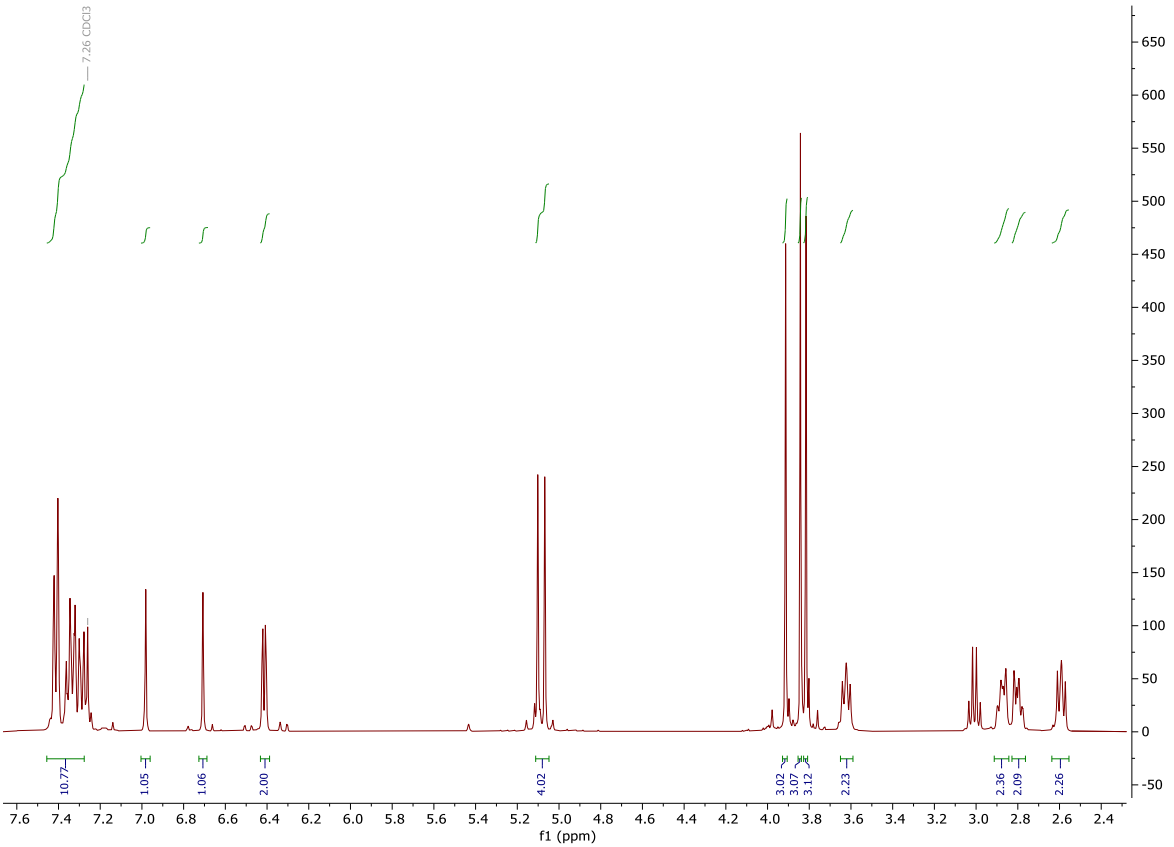

8 1H NMR (300 MHz, CDCl3) δ 7.47 – 7.26 (m, 10H), 6.98 (s, 1H), 6.71 (s, 1H), 6.42 (dd, J = 5.3, 1.8 Hz, 2H), 5.11 (s, 2H), 5.08 (s, 2H), 3.92 (s, 3H), 3.85 (s, 3H), 3.82 (s, 3H), 3.68 – 3.56 (t, J = 7.3, 2H), 2.95 – 2.74 (m, 4H), 2.64 – 2.51 (t, J = 7.62, 2H).

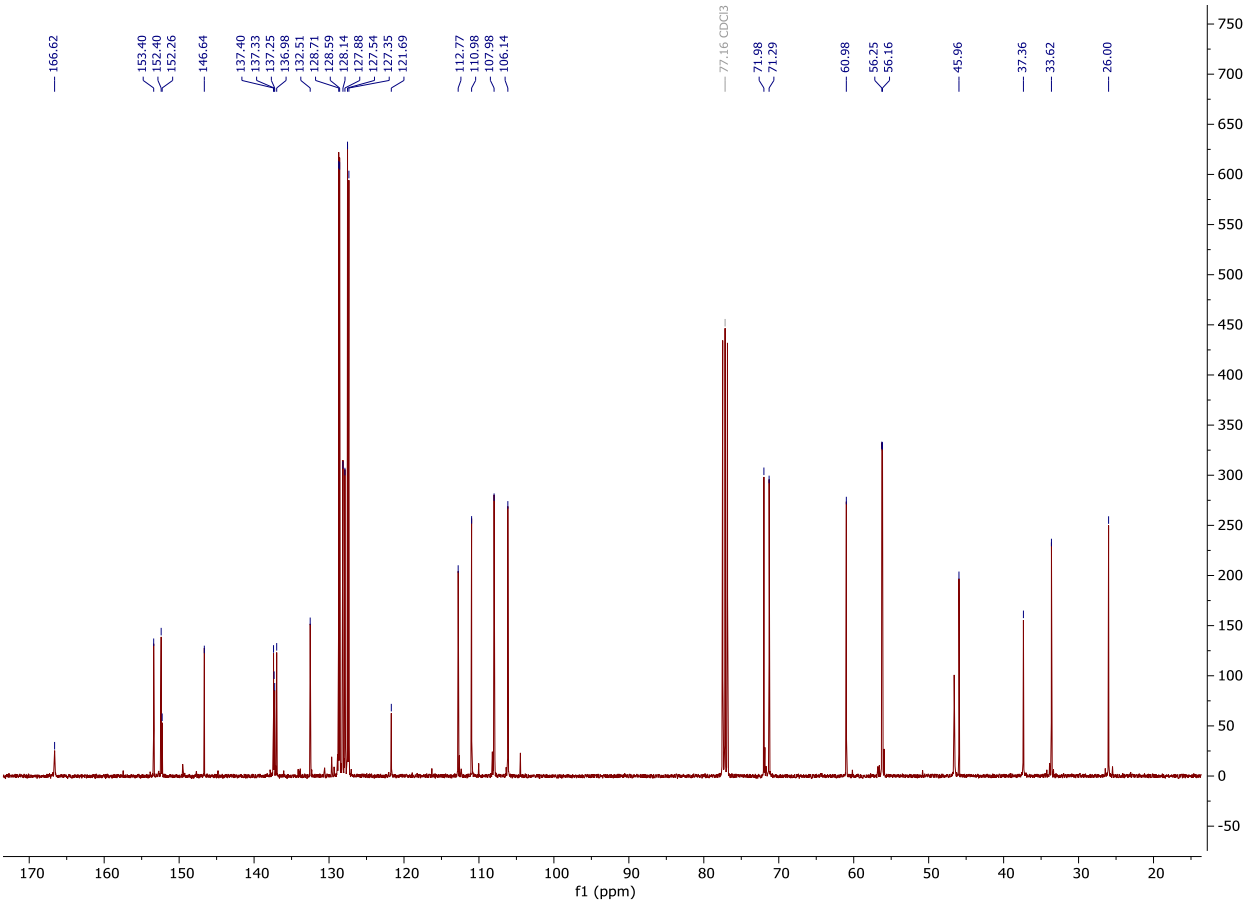

13C NMR (400 MHz, cdcl3) δ 166.62, 153.40, 152.40, 152.26, 146.64, 137.40, 137.33, 137.25, 136.98, 132.51, 128.71, 128.59, 128.14, 127.88, 127.54, 127.35, 121.69, 112.77, 110.98, 107.98, 106.14, 71.98, 71.29, 60.98, 56.25, 56.16, 45.96, 37.36, 33.62, 26.00. (triethylamine peaks and traces of impurities not considered)

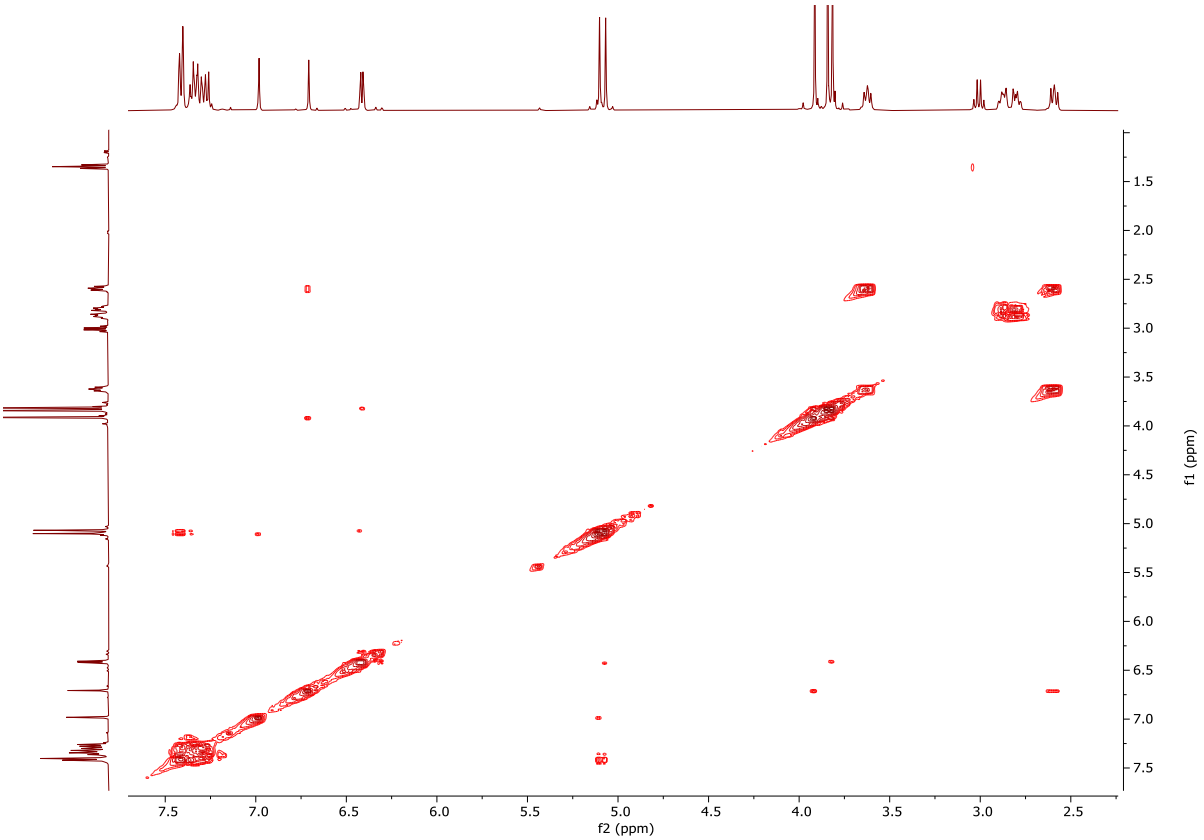

COSY (triethylamine signal suppressed for clarity)

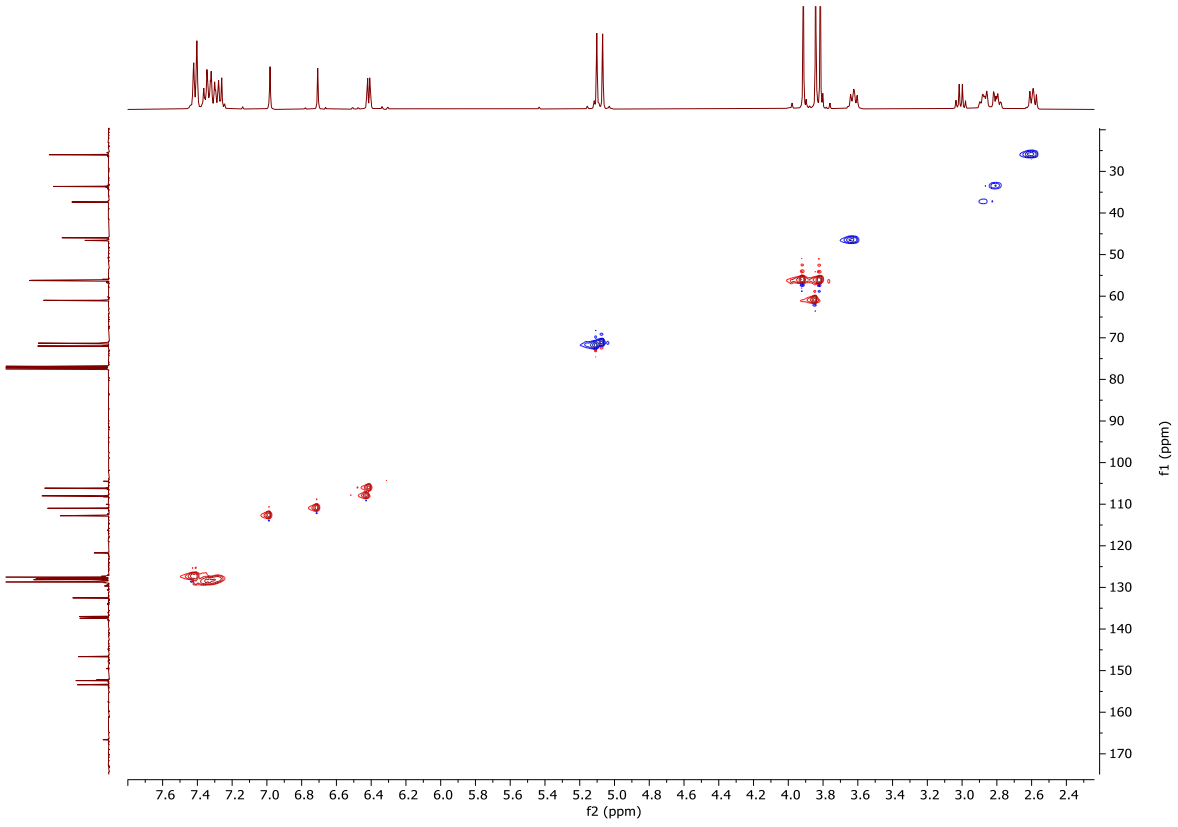

HSQC (triethylamine signal suppressed for clarity)

(S)-7-(benzyloxy)-1-(3-(benzyloxy)-4,5-dimethoxyphenethyl)-6-methoxy-1,2,3,4-tetrahydroisoquinoline (9)

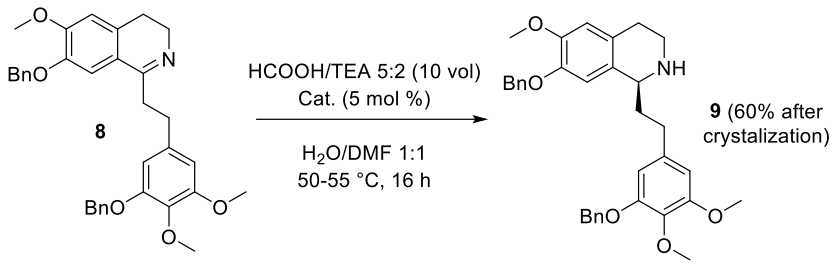

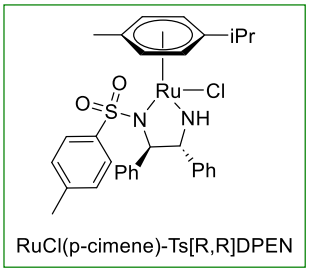

Catalyst

15 g of **8** (27,9 mmol, 1 eq.) in a 1 l round bottom flask were dissolved in 150 ml of DMF. The stirring rate was 250 rpm during the whole process, to avoid splashes of insoluble material. Then, 150 ml of water was added slowly to avoid splashes. The imine goes out of phase after the addition of water. 900 mg (0.05 eq.) of RuCl(p-cimene)-Ts[R,R]DPEN were dissolved into 31 ml of DMSO (32 volumes, compared to the catalyst) and slowly injected into the emulsion. The system was brought to 53 °C (between 50 °C and 55 °C considering the temperature fluctuation during the reaction time) and then 45,2 ml (10 volumes) of HCOOH:TEA[XXXIX] 5:2 azeotropic mixture were added. After the addition everything goes into solution and the reaction was stirred at 250 rpm at 53 °C for 15 hours. During this time a lot of carbon dioxide was liberated. The system must be able to resist the pressure. At this scale we just used a simple plastic cap and waited 1 hour before leaving the lab. In case the cap jumps out it is not a problem, there is no need for an inert atmosphere, and the solvents are not volatile. After this time IPC[XL] showed complete conversion and the reaction can be quenched. 150 ml (10 volumes) of 5 M NaOH were added to neutralize the residual formic acid.[XLI] Then, 750 ml (50 volumes) of water were added to help dissolve DMF. The amine is in the form of suspended droplets. The aqueous phase was extracted twice with 250 ml (16,7 volumes) of AcOEt. Then, the organic phases were merged and washed with twice 350 ml (23,3 volumes) of water to remove any residual salt and DMF, then washed with 300 ml of brine (20 volumes) to remove the residual water.[XLII] The solvent was

[XXXIX] Formic acid:triethylamine

[XL] TLC DCM:MeOH 9:1

[XLI] The pH of the solution should be 13 or more.

[XLII] Probably the last washings could be reduced in volume, but we wanted to make sure there was no interference with the following crystallization step.

then removed under reduced pressure, leading to a viscous oil. At this stage the enantiomeric excess was 67,7%.

The mixture was then enantioenriched via crystallization with D-tartaric acid. The crude was dissolved into 73 ml (4,87 volumes) of methanol. Then, 4,23 g (1 eq.) of tartaric acid were dissolved into 32,5 ml (2,16 volumes) of methanol. The tartaric acid solution was added dropwise to the amine solution and a white precipitate starts to form. The suspension was allowed to reflux for 2 h, to allow the impurities in the crystal to migrate back into solution. The system was cooled down to 0 °C in 2 h.[XLIII] The mother liquor was then filtered out and the with solid washed with cold methanol until the crystals are perfectly white as shown in the picture below. The crystals were characterized via HNMR and CNMR.

[XLIII] A similar result in terms of purity and yield can be obtained also without the thermal treatment. Going up to a higher scale it is expected than the thermal treatment gives more reproducible results.

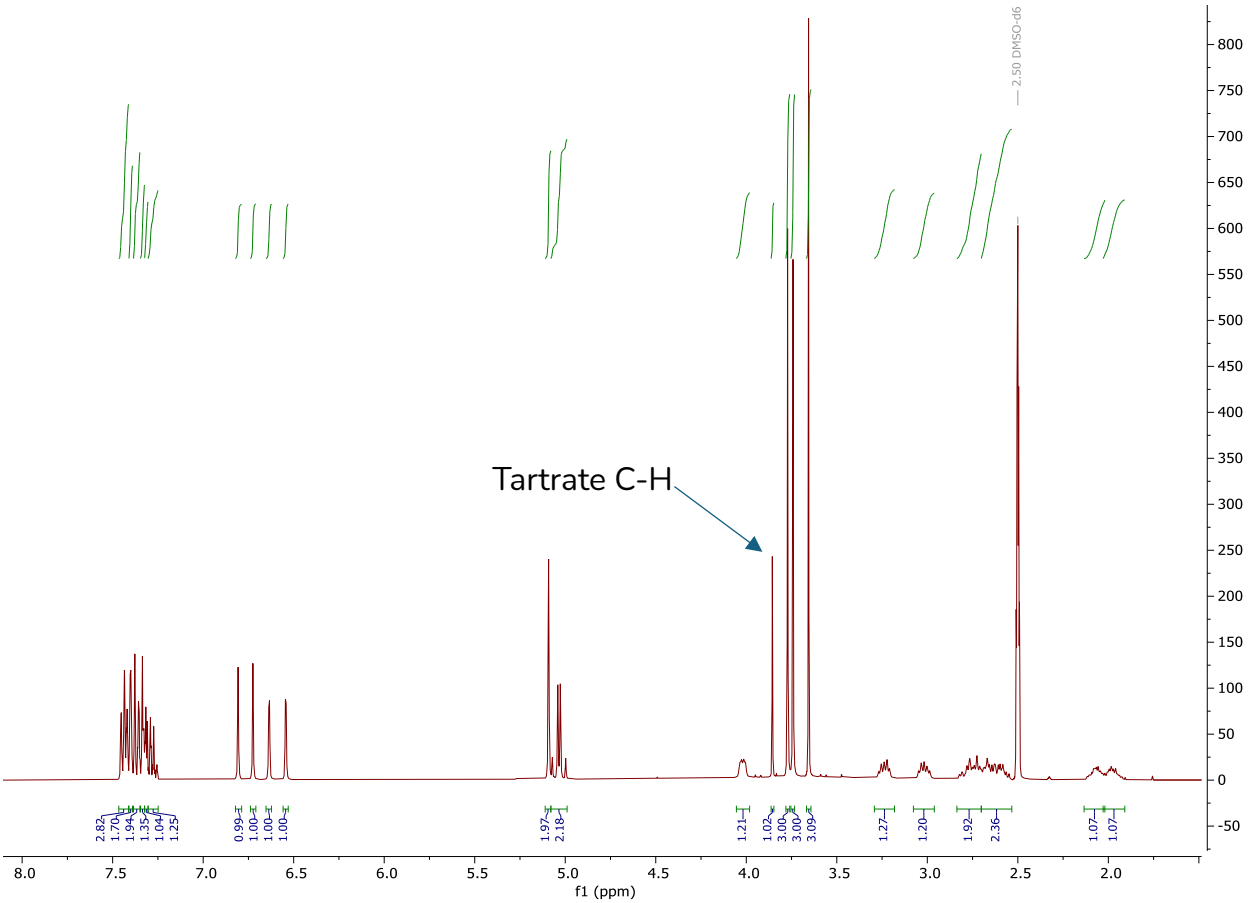

^{1}H NMR (400 MHz, dmso) δ 7.46 – 7.41 (m, 3H), 7.41 – 7.39 (m, 2H), 7.38 (m, 2H), 7.37 – 7.35 (m, 1H), 7.34 – 7.30 (m, 1H), 7.30 – 7.25 (m, 1H), 6.81 (s, 1H), 6.73 (s, 1H), 6.64 (d, *J* = 1.8 Hz, 1H), 6.54 (d, *J* = 1.7 Hz, 1H), 5.09 (s, 2H), 5.08 – 4.99 (m, 2H), 4.02 (m, 1H), 3.86 (s, 1H), 3.77 (s,3H), 3.74 (s, 3H), 3.66 (s, 3H), 3.24 (dt, *J* = 11.9, 5.8 Hz, 1H), 3.02 (dt, *J* = 12.5, 6.3 Hz, 1H), 2.82 – 2.69 (m, 2H), 2.69 – 2.55 (m, 2H), 2.06 (m, 1H), 2.02 – 1.91 (m, 1H).

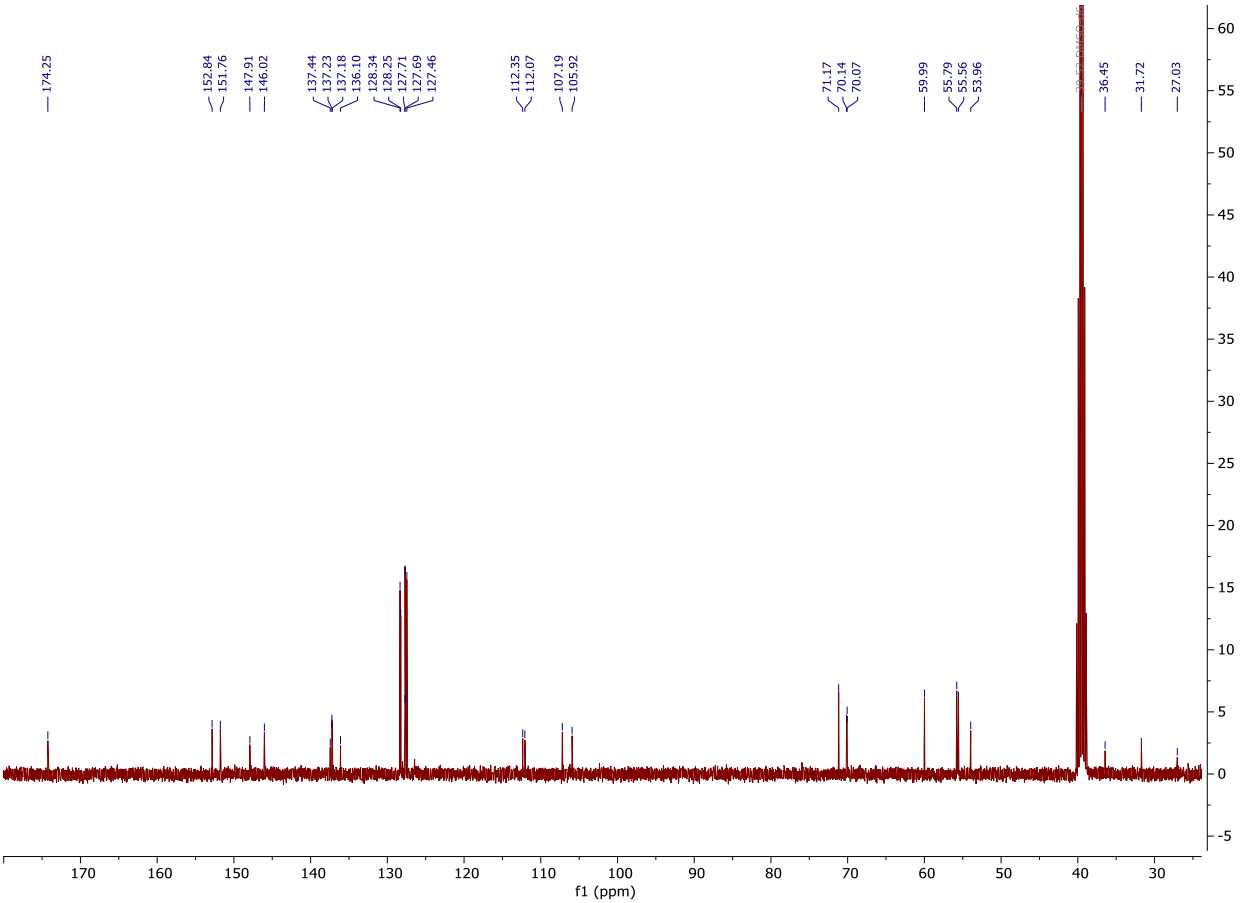

^{13}C NMR (400 MHz, dmso) δ 174.25, 152.84, 151.76, 147.91, 146.02, 137.44, 137.23, 137.18, 136.10, 128.34, 128.25, 127.71, 127.69, 127.46, 112.35, 112.07, 107.19, 105.92, 71.17, 70.14, 70.07, 59.99, 55.79, 55.56, 53.96, 36.45, 31.72, 27.03. Quaternary carbon atoms of isoquinoline systems seem not visible. Probably one aliphatic signal is under the solvent signal.

Integrating the HNMR spectrum it was observed a 2:1 ratio amine:tartaric acid. So, the hemitartrate salt was obtained. The salt was then allowed to dry under vacuum for 18 hours and the recovered mass is 10,2 g (60 % yield). Considering that the racemic mixture is purged in the mother liquor, this is almost a quantitative recovery of enantioenriched amine.

The desired amine can be recovered dissolving the salt in 50 ml of DCM (5 volumes) and washing with 50 ml of NaOH 1 M (5 volumes).[XLIV] The organic phase was washed twice with 25 ml (2,5 volumes) of water to remove the residual NaOH and with 25 ml (2,5 volumes) of brine to remove the residual water. The solvent was removed under reduced pressure to give the amine quantitatively recovered

[XLIV] pH should be 13 or more.

from the hemi tartrate salt. The amount of recovered **2** confirms the stoichiometry of the salt.

The chromatographic method for the analysis of both conversion and enantiomeric excess is the following:

Column: Daicel Chiralcel OD-H 250*4.6 mm, 5µm, p/n 14325

Eluent: n-hexane/absolute ethanol 70/30 + 0.05 % Diethylamine (v/v)

λ = 285 nm; Column T = 35°C; Autosampler T = 10 °C; Injection volume = 5µl; Flow = 1.0 ml/min; Sample diluted into absolute ethanol

However, ethanol for HPLC is quite expensive, so n-hexane:isopropanol, 70/30 as eluent with the same column and conditions can be used instead.

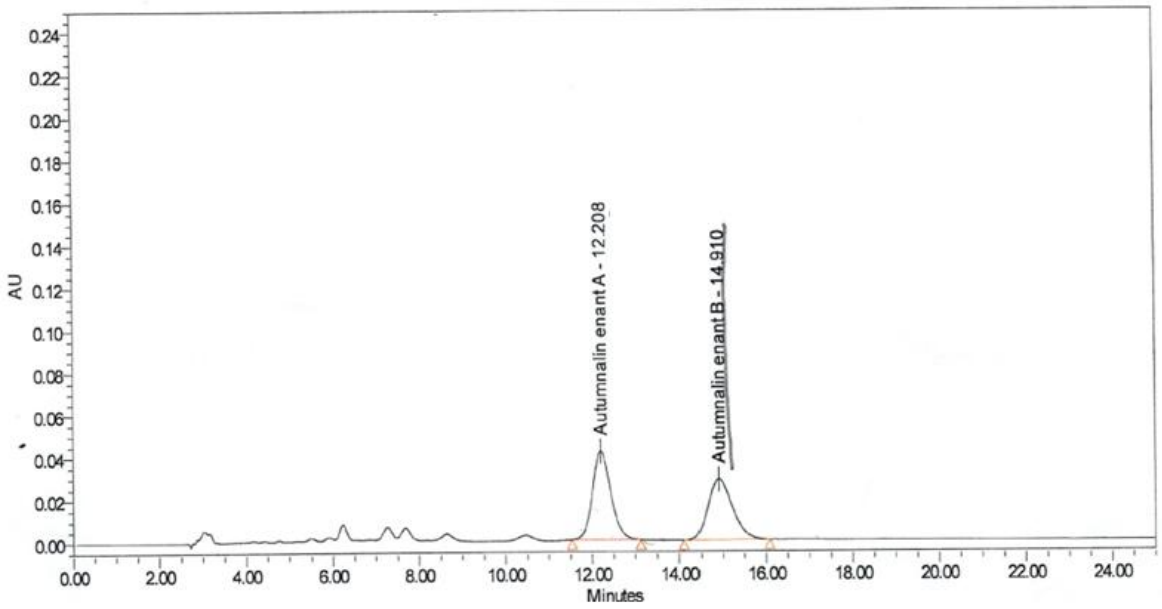

Racemic **9** – normal method

Analyte	RT (min)	Area (uV*sec)	%Area[XLV]
(S)-9	12.208	1244922.45	52.40
(R)-9	14.910	1131078.60	47.60

[XLV] Area is not perfect, as an impurity runs together with (S)-2 analyte. The chromatogram was considered ok for *non-GMP* enantiomers retention identification. Longer analysis time allow to separate this impurity, confirming the good balance between enantiomers within the experimental error.

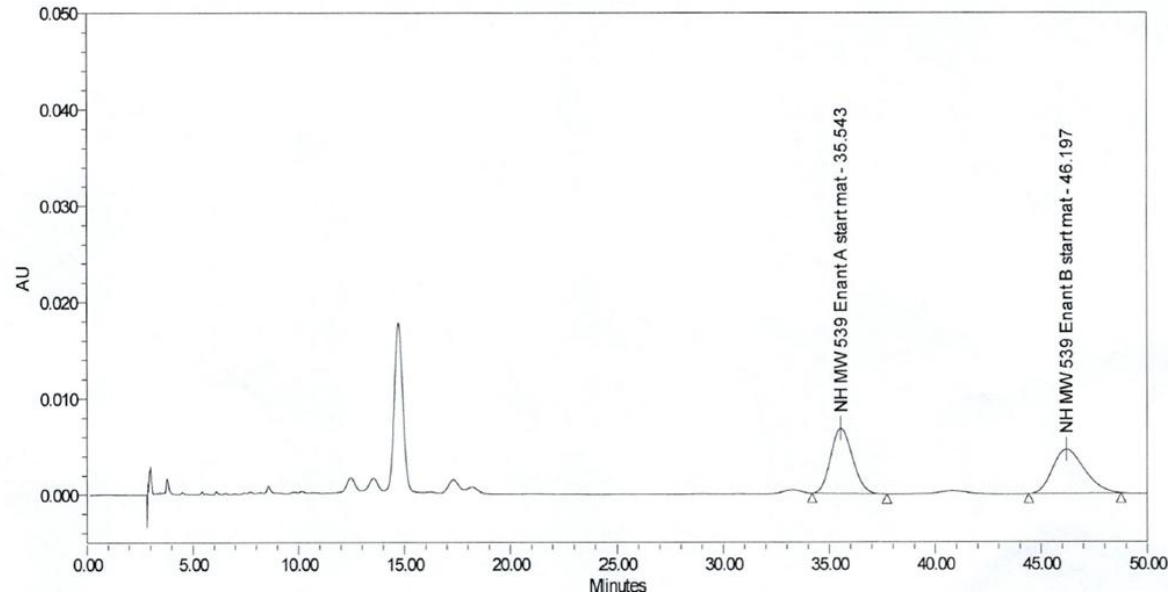

Racemic **9** – longer method. Area balance check.

Analyte	RT (min)	Area (uV*sec)	%Area
(S)-9	35.543	483283.36	49.97
(R)-9	46.197	483837.60	50.03

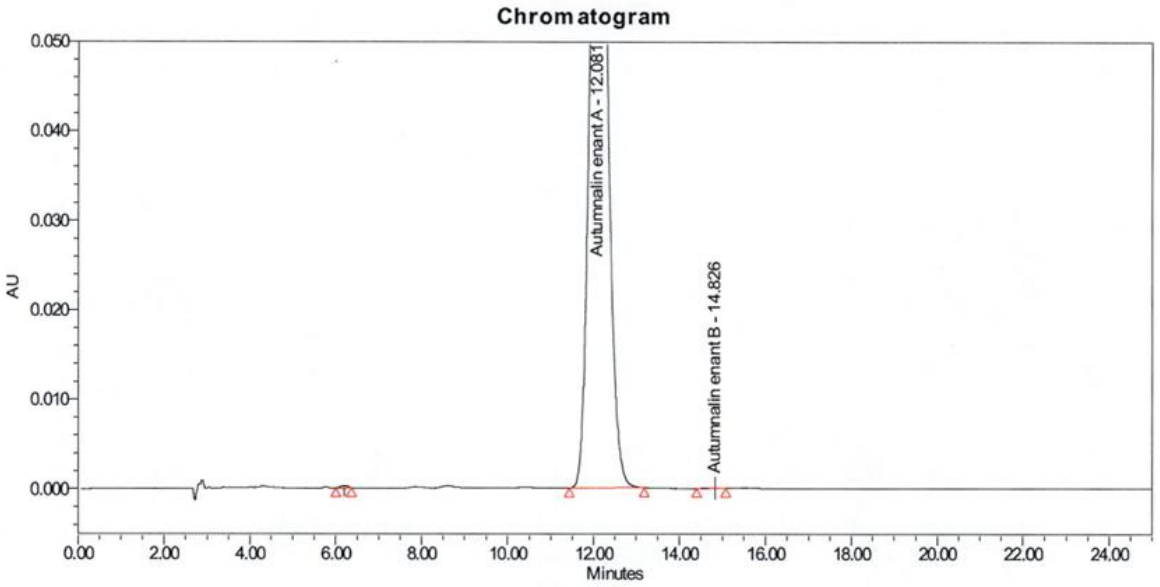

Enantioenriched **9**

Analyte	RT (min)	Area (uV*sec)	%Area
(S)-9	12.081	2465974.85	99.86
(R)-9	14.826	602.85	0.002

Racemic 7-(benzyloxy)-1-(3-(benzyloxy)-4,5-dimethoxyphenethyl)-6-methoxy-1,2,3,4-tetrahydroisoquinoline (Racemic 9)

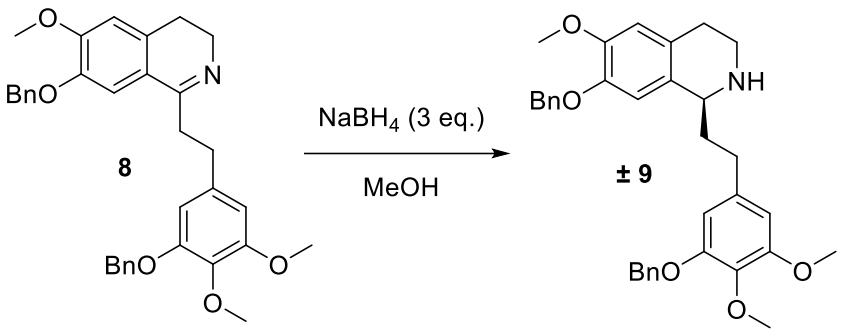

It follows the procedure for the preparation of the racemic **9**:

The crude **8** (122 mg) was dissolved in 2 ml of MeOH. Then, 30 mg of NaBH4 were added at room temperature, stirring. After a few minutes IPC[XLVI] was done, showing full conversion.

The methanol was evaporated, then a saturated solution of NH_4Cl was added, extracting with DCM. The solvent was removed under reduced pressure and the crude was purified directly via column chromatography (gradient elution, from AcOEt:MeOH 9:1 to more polar eluent mixtures). Once the compound is isolated it was used as it is for HPLC analysis.

(S)-7-(benzyloxy)-1-(3-(benzyloxy)-4,5-dimethoxyphenethyl)-6-methoxy-2-methyl-1,2,3,4-tetrahydroisoquinoline (10)

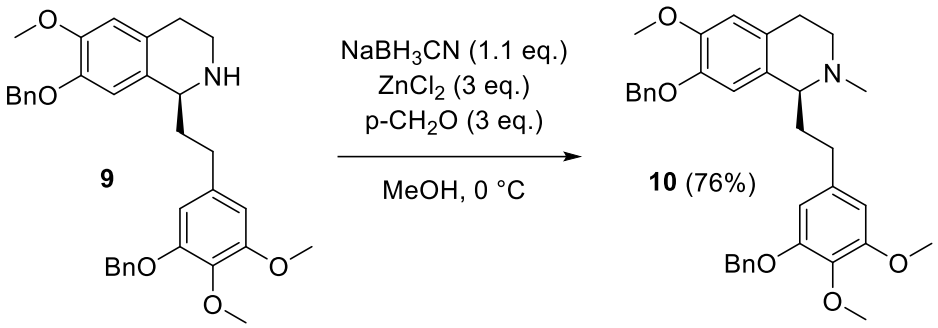

7,32 g (3 eq.) of $ZnCl_2$ were put into a reactor, followed by 1,24 g (1,1 eq.) of $NaBH_3CN$. It follows the addition of 30 ml of MeOH (3,3 volumes compared to the main substrate). 8,95 g of freshly prepared **9** (16,6 mmol, 1 eq.) were dissolved into 30 ml (10 volumes) of methanol and 0,552 g (3 eq.) of para-formaldehyde were added. The suspension was slowly injected into the reactor using a dropping funnel under strong stirring. The flasks containing the amine residues was washed

[XLVI] TLC 9:1 AcOEt:MeOH. We have 3 spots, 2 after work-up. The main spot is the product.

with further 30 ml of methanol and the solution put in the reactor. As soon as the amine is added, a gummy solid appears. The reaction is stirred at 350 rpm for 18 hours and after that time the solid was fragmented. IPC[XLVII] shows full conversion. The system was allowed to go to 25 °C, then the suspension was transferred to a round bottom flask, washing with further 50 ml of methanol. Then, 60 ml of 1 M NaOH were added, followed by 130 ml of aqueous NH_4Cl 30%, having a partial clarification. 100 ml of DCM were then added to extract, continuing the extraction until there is no organic compound anymore in the aqueous phase (TLC check). The organic phases were then washed with 200 ml of brine and the DCM removed under reduced pressure, yielding 7,02 g of crude which is used as it is for the next step (76,5 % yield). The chiral chromatographic analysis shows some traces of other compounds and e.e. = 99,7 %. Thus, despite the procedure used, a slight racemization process is still observed.

The racemic version of autumnaline can be prepared following the same procedure, starting from racemic **9**.

10 was then characterized by HNMR

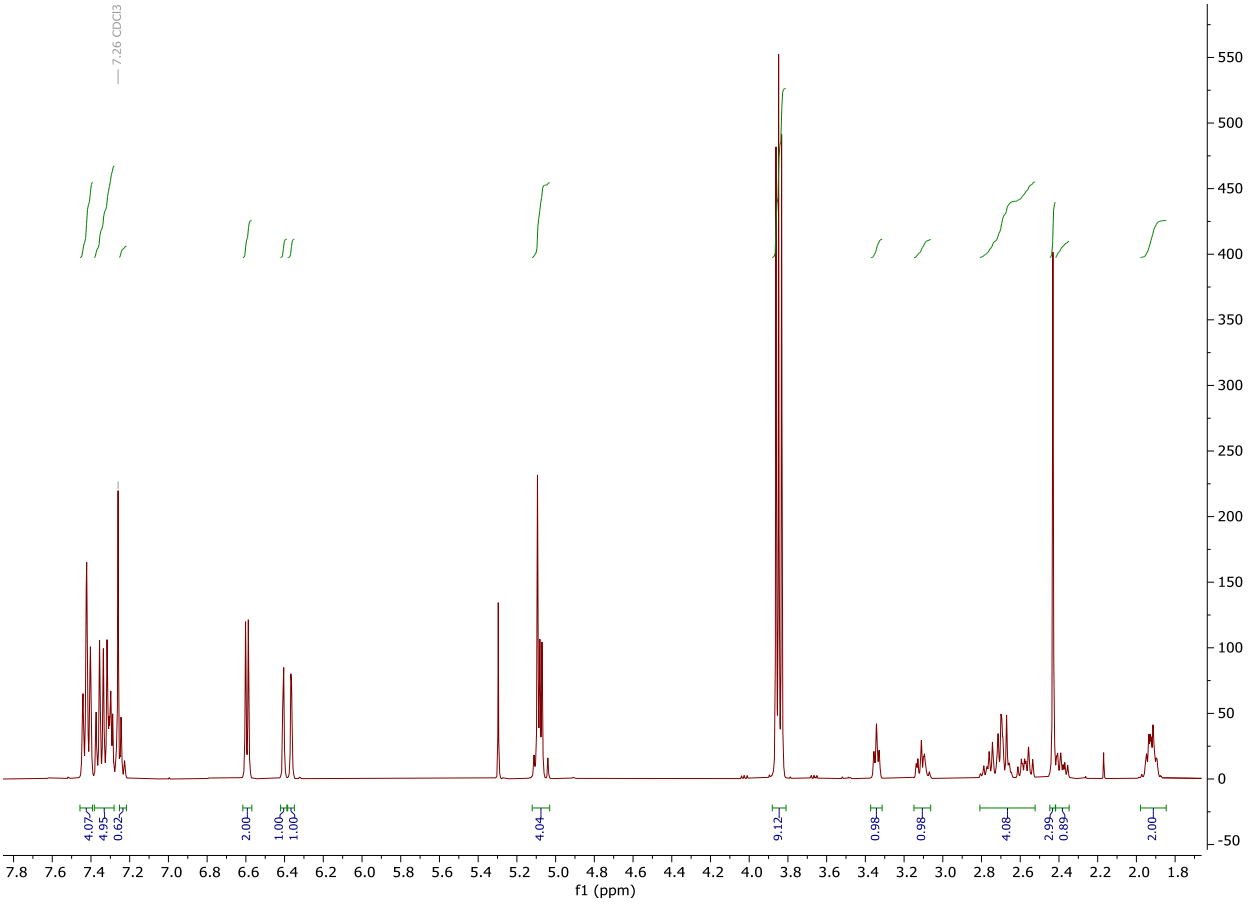

[XLVII] TLC AcOEt:MeOH 9:1

15 1H NMR (300 MHz, CDCl3) δ 7.47 – 7.23 (m, 10H), 6.59 (d, J = 8.7 Hz, 2H), 6.39 (dd, J = 12.1, 1.7 Hz, 2H), 5.10 (s, 2H), 5.08 (s, 2H), 3.86 (s, 3H), 3.85 (s, 3H), 3.83 (s, 3H), 3.37 (t, J = 5.4 Hz, 1H), 3.19 – 3.07 (m, 1H), 2.85 – 2.51 (m, 5H), 2.44 (s, 3H), 2.09 – 1.79 (m, 2H). Some DCM present in the sample.

The chromatographic method for the analysis of enantiomeric excess is the following:

Column: Daicel Chiralcel OD-H 250*4.6 mm, 5µm, p/n 14325

Eluent: n-hexane/absolute ethanol 90/10 + 0.05 % Diethylamine (v/v)

λ = 285 nm; Column T = 35°C; Autosampler T = 10 °C; Injection volume = 5µl; Flow = 1.0 ml/min; Sample diluted into absolute ethanol.

However, ethanol for HPLC is quite expensive, so n-hexane:isopropanol, 70/30 as eluent using the same column and conditions can be used.

r

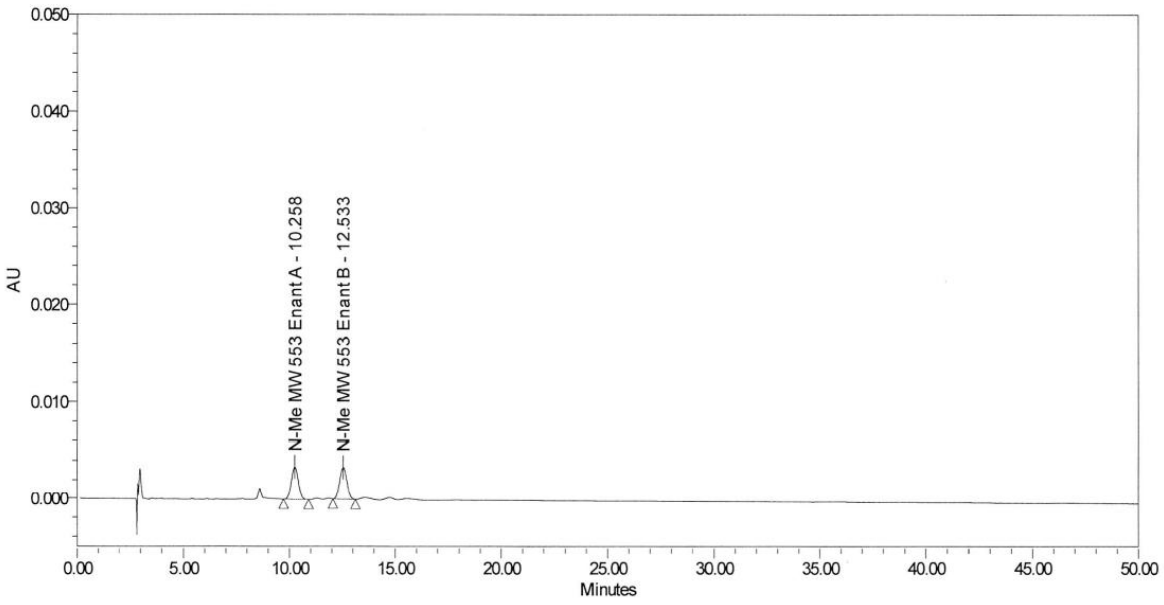

Racemic **10**

Analyte	RT (min)	Area (uV*sec)	%Area
(S)-10	10.258	79225.18	49.38
(R)-10	12.533	81202.38	50.62

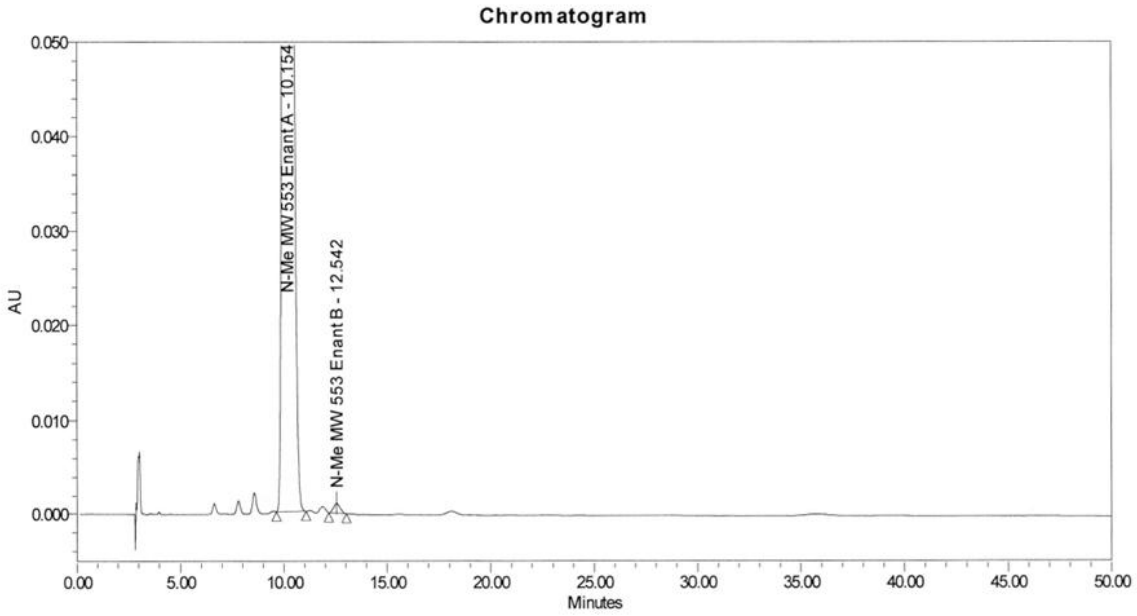

Enantioenriched **10**

Analyte	RT (min)	Area (uV*sec)	%Area
(S)-10	10.154	8769747.58	99.71
(R)-10	12.542	25404.60	0.29

[(S)-autumnaline] (S)-1-(3-hydroxy-4,5-dimethoxyphenethyl)-6-methoxy-2-methyl-1,2,3,4-tetrahydroisoquinolin-7-ol

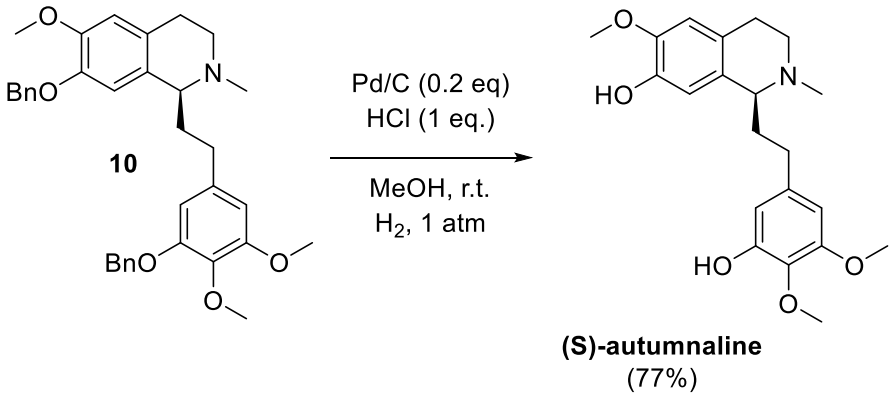

In a 250 ml single-neck round bottom flask 1,65 g (0.2 eq.) of Pd/C 10% were loaded. Then, the system was put under nitrogen with vacuum/N_2 cycles using a septum. Then, 2,88 of **10** (5,2 mmol, 1 eq.) was put under inert atmosphere with the same method and dissolved into 50 ml (17,3 volumes) of methanol.[XLVIII] Then, 440 ul (1 eq.) of aqueous 37% HCl were added to the amine solution. The solution is then injected into the round bottom flask containing the catalyst. The amine flask

[XLVIII] The dissolution is very slow

was washed with 20 ml (7 volumes) of methanol and the solution added to the reaction mixture with the same procedure. Then, the gas contained in the reaction was evacuated, filling the head space with H_2 at 1 atmosphere, using balloons. The reaction was stirred at room temperature for 18 h. After this time the H_2 was evacuated, filling the system with N_2 and a sample undergoes IPC.[XLIX] The reaction showed complete conversion. The suspension was then filtered over celite, washing with MeOH to recover as much product as possible. Then, the methanol was evaporated and the crude was dissolved back using 60 ml of DCM (21 volumes) and washed with 60 ml of 8 % aqueous NH_4OH to neutralize the acid. The aqueous phase was extracted again with DCM until no product was visible via TLC of the aqueous phase. The organic phases were merged and washed with 15 ml (5 volumes) of brine to remove the residual water. DCM was evaporated under reduced pressure, yielding 1,5 g of **(S)-autumnaline** (77 %).

The racemic version of autumnaline can be prepared following the same procedure, starting from racemic **10**.

DCM is difficult to remove completely from the product. A high residence time into a vacuum system is needed. The product appears as a fluffy solid as shown in the picture below.

The chiral chromatographic analysis showed a clean product with e.e. ranging from 99,4 % to 99,6 % for different batches. Thus, the last step should not induce any racemization. The main impurity found, as anticipated, was the residual DCM, ranging from 0,9 % to 2,3 % w/w. The drying procedure should be optimized to remove the last traces of DCM in GMP batches.

[XLIX] TLC AcOEt:MeOH:Triethylamine 36:4:1. Autumnaline has a distinctive shape.

The chromatographic method for the analysis of enantiomeric excess is the following:

Column: Daicel Chiralcel OD-H 250*4.6 mm, 5µm, p/n 14325

Eluent: n-hexane/absolute ethanol 90/10 + 0.05 % Diethylamine (v/v)

λ = 285 nm; Column T = 35°C; Autosampler T = 10 °C; Injection volume = 5µl; Flow = 1.0 ml/min; Sample diluted into absolute ethanol.

The product was fully characterized:

$[\alpha]^{D}$ = 21,7 ° (T = 20 °C)

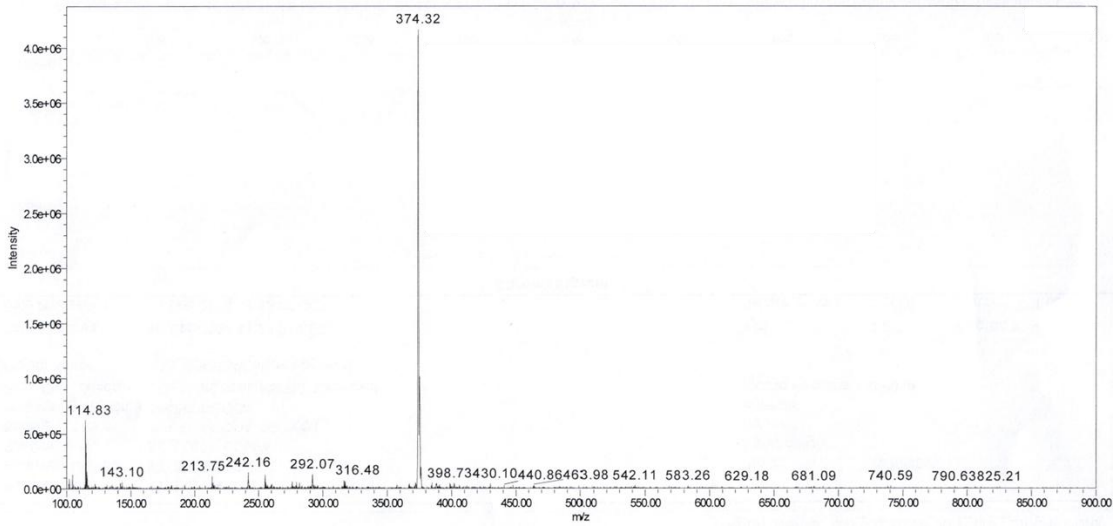

ESI spectrum $[M+H^{+}]$

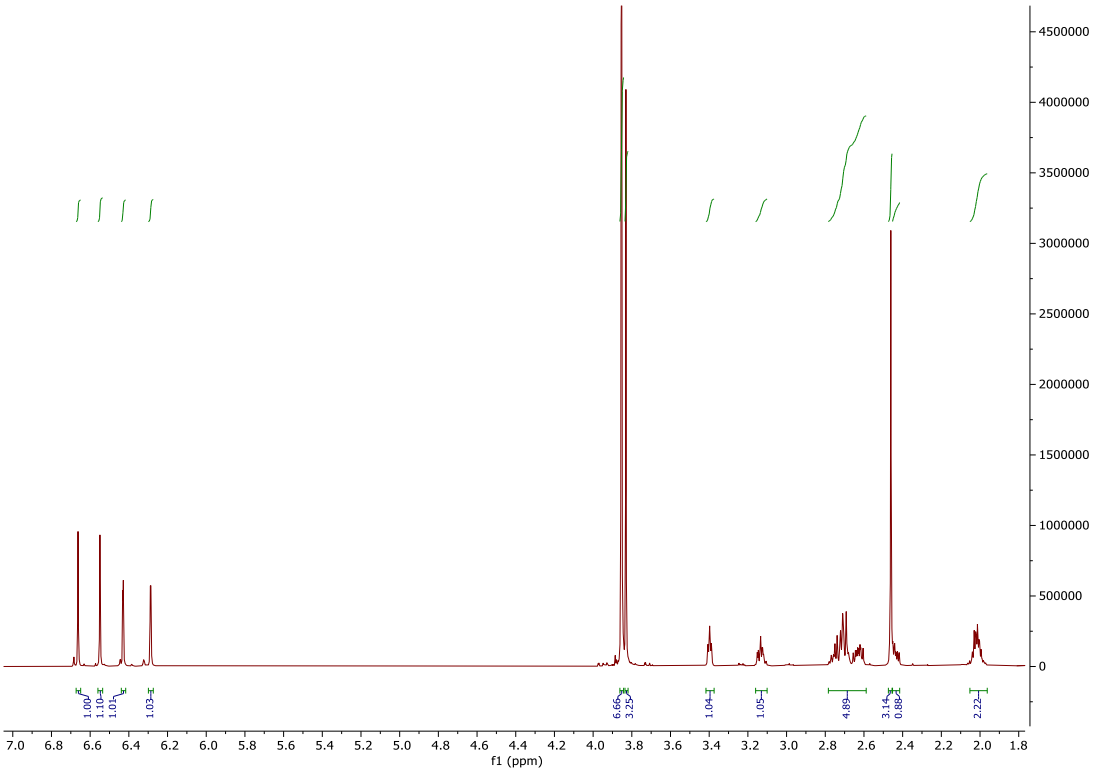

HNMR - **1** 1H NMR (600 MHz, CDCl3) δ 6.66 (s, 1H), 6.55 (s, 1H), 6.43 (d, J = 1.9 Hz, 1H), 6.29 (d, J = 1.9 Hz, 1H), 3.855 (s, 3H), 3.852 (s, 3H), 3.83 (s, 3H), 3.39 (t, J = 5.4 HZf, 1H), 3.13 (m, 1H), 2.79 – 2.59 (m, 5H), 2.46 (s, 3H), 2.46 – 2.41 (m, 1H), 2.07 – 1.97 (m, 2H).

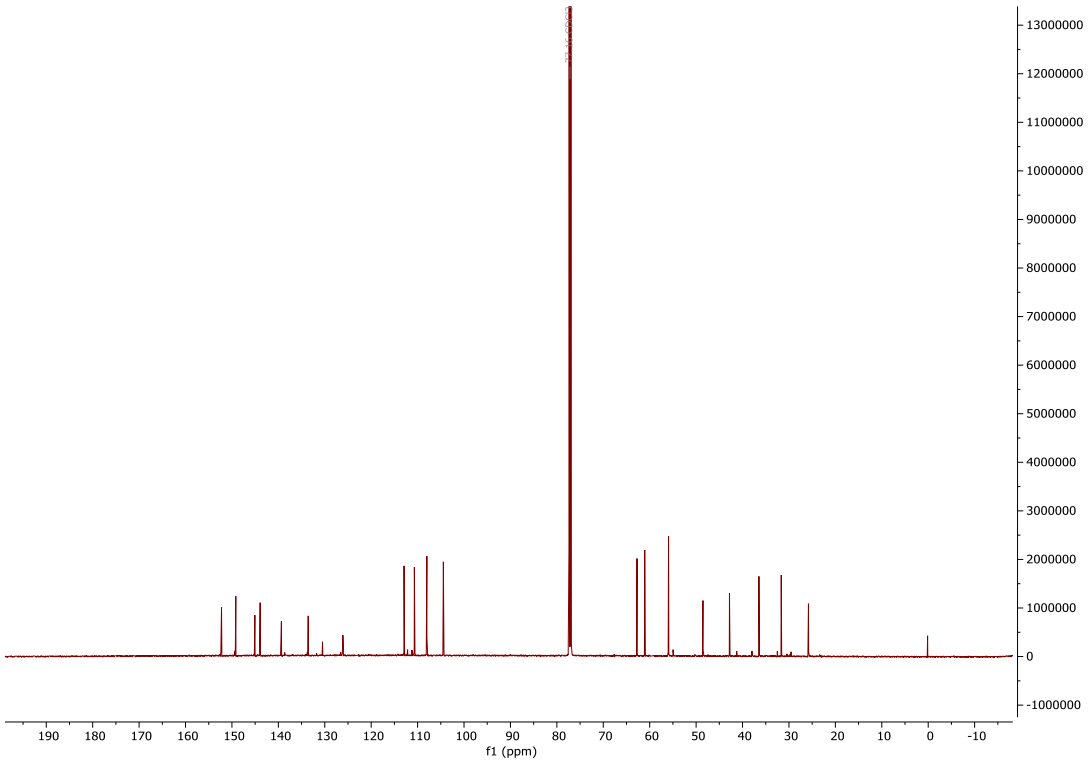

1 - 13C NMR (151 MHz, CDCl3) δ 152.24, 145.06, 143.92, 139.34, 133.57, 130.49, 126.10, 112.92, 110.70, 108.00, 104.45, 62.73, 61.07, 55.99, 55.94, 48.52, 42.81, 36.47, 31.66, 25.80.

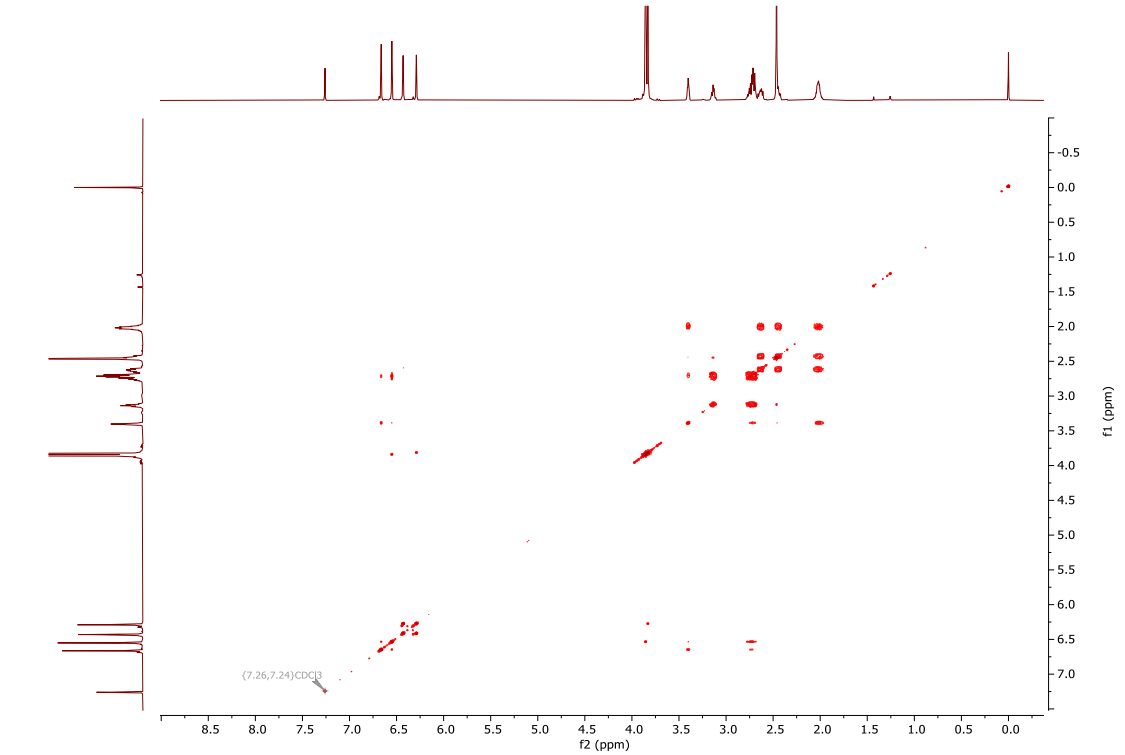

COSY

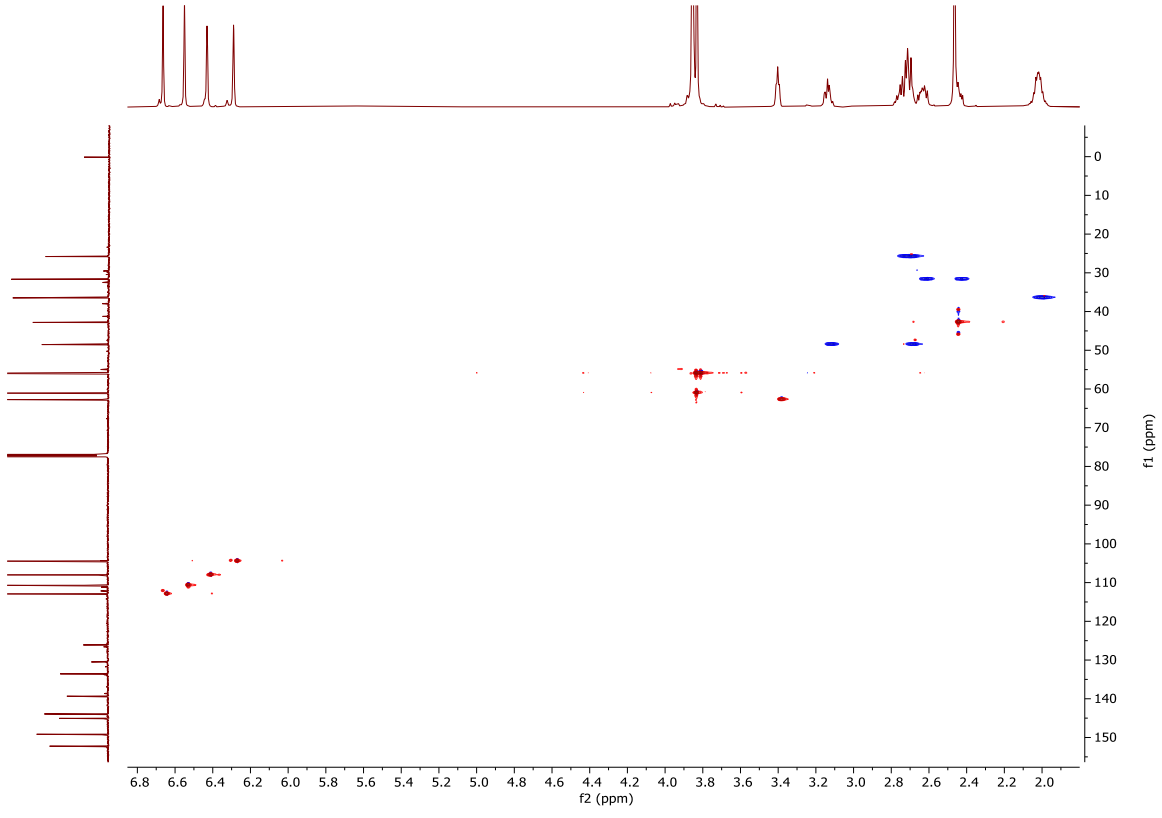

HSQC

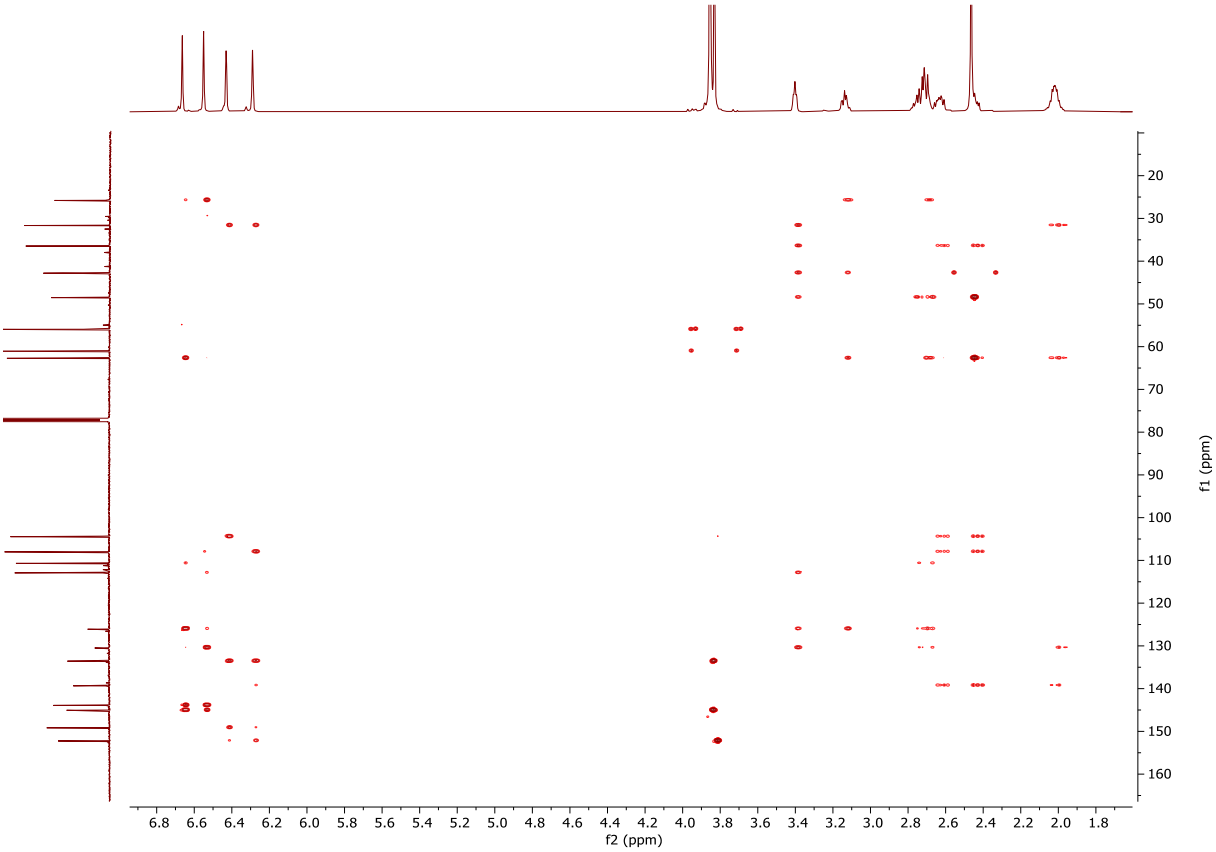

HMBC

Electronic Circular Dichroism

Experimental procedure for ECD spectrum recording

The ECD spectrum of **(S)-autumnaline** was acquired on a JASCO J-810 spectropolarimeter in LC-MS grade acetonitrile solution (about $1 \cdot 10^{-4}$ M) with a cell path of 0.1 cm in the 190-400 nm region by the sum of 16 scans at 50 nm/min scan rate (Figure 212). The ECD spectrum showed two main Cotton effects at 201 (negative) and 215nm (positive), and a broad positive band centred at 226nm.

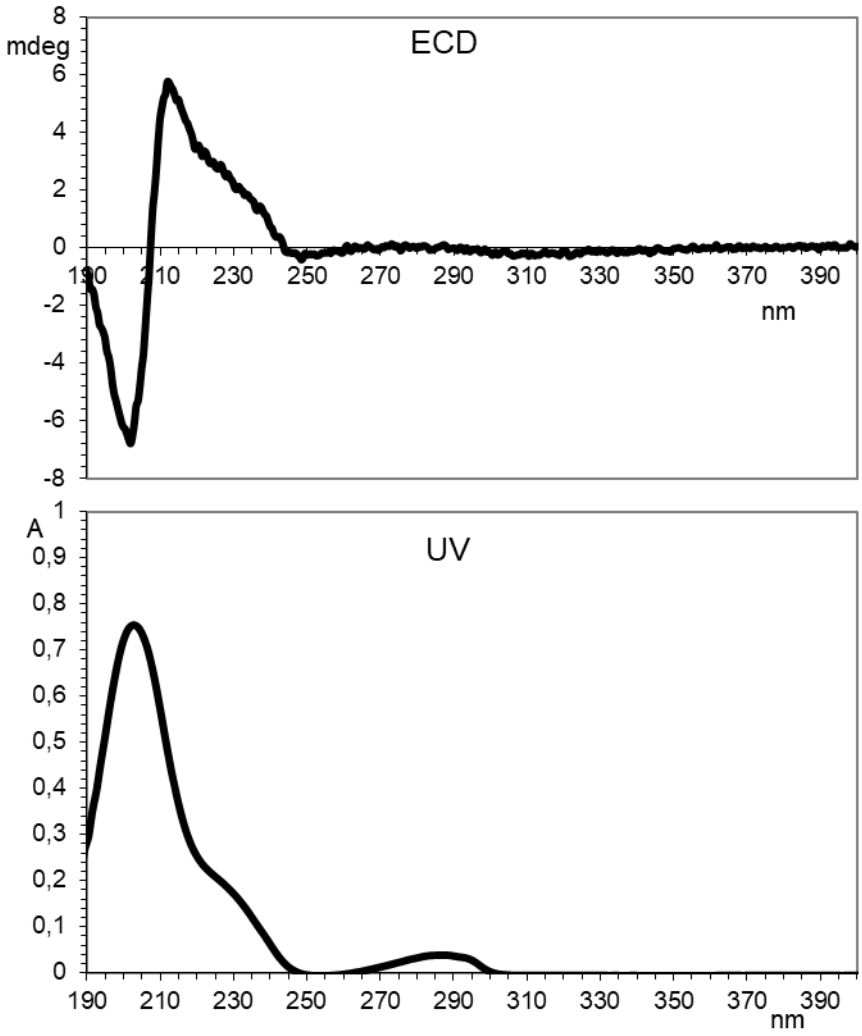

Figure 212 - Top: ECD spectrum of compound 1. Bottom: UV spectrum (10-4 M in acetonitrile)

Computational procedure for the calculation of the ECD spectrum

Step 1. Conformational sampling.

(S)-autumnaline was simulated through Molecular Dynamics (MD) simulation in acetonitrile (453 molecules) at the temperature of 25°C and at the pressure of 1.0 bar. The simulation box is pictorially represented in Figure 213.

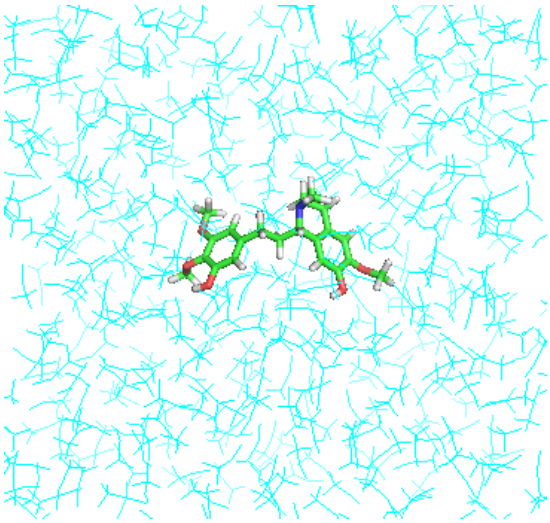

Figure 213 - Simulation box of 1 in acetonitrile (blue).

The simulation was propagated for 60 ns. At the end, the conformational space of **(S)-autumnaline** was analyzed through Essential Dynamics.

Briefly: the all-atom covariance matrix of the **1** was constructed, after removing the corresponding roto-translational degrees of freedom, and diagonalized. This operation produces a set of eigenvectors and associated eigenvalues whose spectrum is represented in Figure 214.

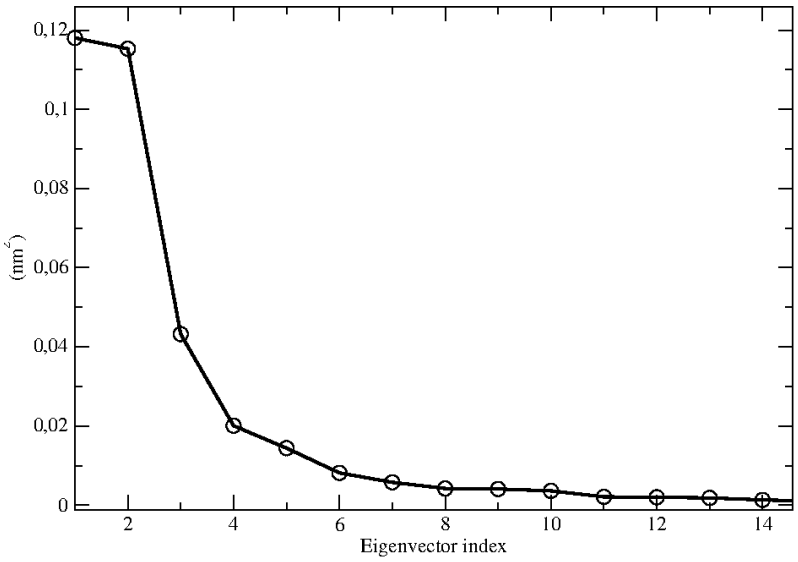

Figure 214 - Spectrum of the eigenvalues of the all-atom covariance matrix of 1 in acetonitrile (blue) evaluated from a MD simulation of 60 ns.

As usual the eigenvectors showing higher eigenvalues describe the internal (generalized) coordinate of **1** responsible of the corresponding large amplitude fluctuations. On the other hand, the eigenvectors characterized by low eigenvalues

describe quasi-harmonic, and hence conformationally irrelevant, eigendirections. The spectrum clearly shows that the first two eigenvalues are much higher than the others accounting for more than 50% of the whole fluctuations. This means that the conformational repertoire of **(S)-autumnaline** can be safely and exhaustively determined by using these two eigenvectors ($\mathbf{v}_1$ and $\mathbf{v}_2$).

The projection of the MD simulation, i.e. the sequence of **(S)-autumnaline** cartesian coordinate onto $\mathbf{v}_1$ and $\mathbf{v}_2$. produces the free-energy landscape (virtually coincident with probability landscape) reported in Figure 215.

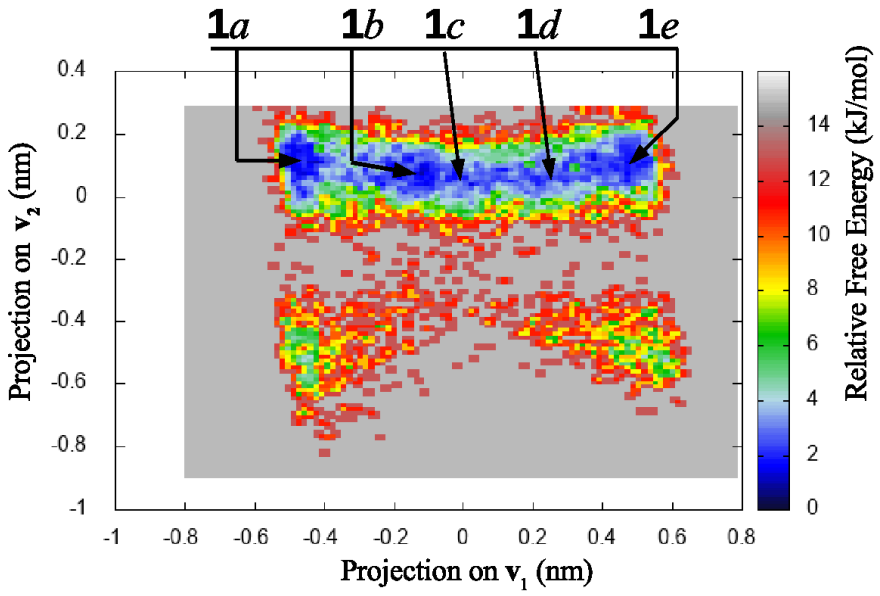

Figure 215 - Free energy landscape of 1 in the space formed by the first two eigenvectors of all-atom covariance matrix.

In this Figure we observe a conformational region (in blue) much more stable than the rest of the conformational space, from which we extracted 5 representative structures (**1***a*-*e*).

These structures are reported in Figure 216.

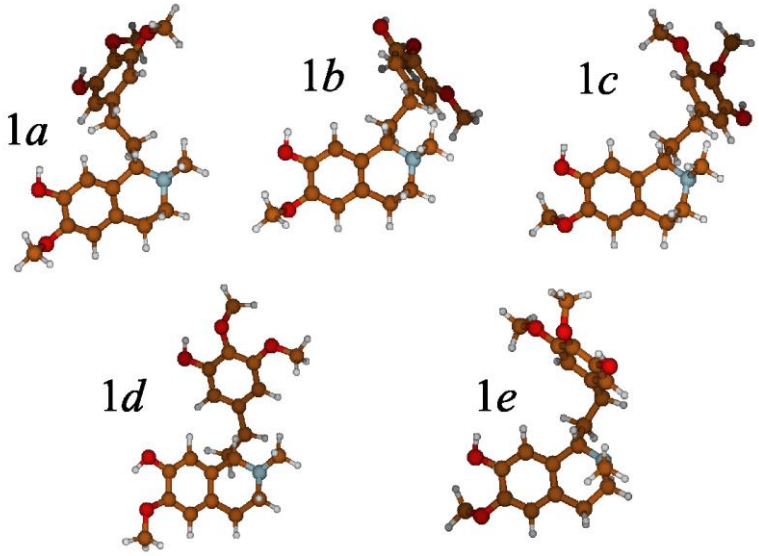

Figure 216 - Schematic view of the 5 structures representing the most stable sub-region of the conformational space (Fig S3).

Step 2. Quantum-chemical calculations.

Each of the above five structures were used for calculating the corresponding spectrum of 1 in acetonitrile.

For this purpose we adopted, for each of the five structures, the following protocol.

2a) *Constrained minimization*: the geometry was optimized at the B3LYP/6-311+G** level of theory in the set of quasi-harmonic internal coordinates excluded by the previous conformational analysis. In other words, we blocked the torsion angles (proper dihedrals) of **(S)-autumnaline** relaxing the bond distances, bond angles and improper dihedrals. The atomic coordinates of the structures 1a-e are not reported here but are available in the supporting information of the currently under revision manuscript.

Bibliography

(1) *https://www.indena.com/about-us/our-story/*.

(2) Nasreen, A.; Gundlach, H.; Zenkt, M. H. Incorporation of Phenethylisoquinolines into Colchicine in Isolated Seeds of Colchicum Autumnale. *Phytochemistry* 1997, *46* (1), 107–115. https://doi.org/https://doi.org/10.1016/S0031-9422(97)00242-2.

(3) Potěšilová, H.; Šantavý, J.; El-Hamidi, A.; Šantavý, F. Substances from the Plants of the Subfamily Wurmbaeoideae and Their Derivatives. LXXII. Further Chemical

Investigation of the Plant Colchicum Cornigerum. *Collect Czechoslov Chem Commun* 1969, *34* (11), 3540–3552. https://doi.org/10.1135/cccc19693540.

(4) Ernest L. Eliel; Samuel H. Wilen. *Stereochemistry of Organic Compounds*, 1st ed.; 1994.

(5) Snatzke, G.; Ho, P. C. Circular Dichroism—XLVI - Rules for Benzene Cotton-Effect. *Tetrahedron* 1971, *27* (15), 3645–3653. https://doi.org/10.1016/S0040-4020(01)97775-0.

(6) Barker, A. C.; Battersby, A. R.; Mcdonald, E.; Ramage, R.; Clements, J. H. Biosynthesis of Colchicine: Ring Expansion and Later Stages. Structure of Speciosine. *Chemical Communications (London)* 1967, No. 8. https://doi.org/10.1039/C1967000390B.

(7) Nasreen, A.; Rueffer, M.; Zenk, M. H. Cytochrome P-450-Dependent Formation of Isoandrocymbine from Autumnaline in Colchicine Biosynthesis. *Tetrahedron Lett* 1996, *37* (45), 8161–8164. https://doi.org/https://doi.org/10.1016/0040-4039(96)01852-7.

(8) Maier, U. H.; Zenk, M. H. Colchicine Is Formed by Para-Para Phenol Coupling from Autumnaline. *Tetrahedron Lett* 1997, *38* (42), 7357–7360. https://doi.org/https://doi.org/10.1016/S0040-4039(97)10011-9.

(9) Kametani, B. T.; Yagi, H.; Satoh, F.; Fukumoto, K.; Kametani, T.; Battersby, A. R.; Herbert, R. B.; Pijewska, L.; Santavf, F. The Synthesis of Homoproaporphine-Type Compounds by Phenolic Coupling. *CoZZ. Czech. Chem. Comtn* 1968, *78* (0), 546. https://doi.org/https://doi.org/10.1039/J39680000271.

(10) Gao, Y.; Li, F.; Luo, Z.; Deng, Z.; Zhang, Y.; Yuan, Z.; Liu, C.; Rao, Y. Modular Assembly of an Artificially Concise Biocatalytic Cascade for the Manufacture of Phenethylisoquinoline Alkaloids. *Nat Commun* 2024, *15* (1). https://doi.org/10.1038/s41467-023-44420-7.

(11) Rao Yijian; Gao Yue; Li Fei; Na Jeong-San. CN117660386A.

(12) Rao Yijian; Gao Yue; Li Fei; Na Jeong-San. Method for Synthesizing (S)-Autumnaline and Derivatives Thereof and Construction of Whole-Cell Catalytic System. *CN117660386* 2023.

(13) Puerto Galvis, C. E.; Kouznetsov, V. V. Biomimetic Total Synthesis of Dysoxylum Alkaloids. *Journal of Organic Chemistry* 2019, *84* (23), 15294–15308. https://doi.org/10.1021/acs.joc.9b02093.

(14) Lu, S. M.; Wang, Y. Q.; Han, X. W.; Zhou, Y. G. Asymmetric Hydrogenation of Quinolines and Isoquinolines Activated by Chloroformates. *Angewandte Chemie* -

International Edition 2006, *45* (14), 2260–2263. https://doi.org/10.1002/anie.200503073.

(15) Barrios-Rivera, J.; Xu, Y.; Wills, M.; Vyas, V. K. A Diversity of Recently Reported Methodology for Asymmetric Imine Reduction. *Organic Chemistry Frontiers* 2020, *7* (20), 3312–3342. https://doi.org/10.1039/d0qo00794c.

(16) Scharf, M. J.; List, B. A Catalytic Asymmetric Pictet-Spengler Platform as a Biomimetic Diversification Strategy toward Naturally Occurring Alkaloids. *J Am Chem Soc* 2022, *144* (34), 15451–15456. https://doi.org/10.1021/jacs.2c06664.

(17) Mons, E.; Wanner, M. J.; Ingemann, S.; Van Maarseveen, J. H.; Hiemstra, H. Organocatalytic Enantioselective Pictet-Spengler Reactions for the Syntheses of 1-Substituted 1,2,3,4-Tetrahydroisoquinolines. *Journal of Organic Chemistry* 2014, *79* (16), 7380–7390. https://doi.org/10.1021/jo501099h.

(18) Bobbitt, J. M.; Roy, D. N.; Marchand, A.; Allen, C. W. Synthesis of Isoquinolines. VI. N-Alkyl-1,2,4-Tetrahydroisoquinolines. *J Org Chem* 1967, *32* (7), 2225–2227. https://doi.org/10.1021/jo01282a030.

(19) Głuszynâ Ska, A.; Rozwadowska, M. D. Enantioselective Modi®cation of the Pomeranz-Fritsch- Bobbitt Synthesis of Tetrahydroisoquinoline Alkaloids: Synthesis of (-)-Salsolidine and (-)-Carnegine. *Tetrahedron Asymmetry* 2000, *11* (11). https://doi.org/https://doi.org/10.1016/S0957-4166(00)00196-8.

(20) Salinger, M. T.; Castellano Garrido, D.; Lamming, E. D.; Ward, J. M.; Moody, T. S.; Jeffries, J. W. E.; Hailes, H. C. An Alternative Cascade for the Selective Methylation of Catechols and Tetrahydroisoquinolines by *O* -Methyltransferases. *ChemCatChem* 2024, *16* (17). https://doi.org/10.1002/cctc.202400492.

(21) Su, Y.; Li, H.; Zhang, M.; Ding, X.; Xu, J.; Chen, Q.; Zheng, G. Regioselectivity Inversion of an *O* -Methyltransferase via Semi-rational Mutagenesis Combined with Metal Ion Substitution. *ChemCatChem* 2022, *14* (23). https://doi.org/10.1002/cctc.202200844.

(22) Wen, X.; Leisinger, F.; Leopold, V.; Seebeck, F. P. Synthetic Reagents for Enzyme-Catalyzed Methylation. *Angewandte Chemie International Edition* 2022, *61* (41). https://doi.org/10.1002/anie.202208746.

(23) Shoup, R. E.; Davis, G. C.; Kissinger, P. T. Determination of Catechol-O-Methyltransferase Activity in Various Tissues by Liquid Chromatography. *Anal Chem* 1980, *52* (3), 483–487. https://doi.org/10.1021/ac50053a024.

(24) Shiner, V. J.; Martin, Brian. The Mechanism of Decarboxylation of Glycidic Acids. *J Am Chem Soc* 1962, *84* (24), 4824–4827. https://doi.org/10.1021/ja00883a038.

(25) Ronson, T. O.; Kitsiou, C.; Unsworth, W. P.; Taylor, R. J. K. Synthetic Approaches to Pallimamine and Analogues Using Direct Imine Acylation. *Tetrahedron* 2016, *72* (40), 6099–6106. https://doi.org/10.1016/j.tet.2016.05.009.

(26) Robert Walter C. Jr. Preparation of Primary Amines by Reduction of Oximes with Lithium Aluminum Hydride and by the Leuckart Reaction. *J Am Chem Soc* 1952, *5* (2), 328. https://doi.org/https://doi.org/10.1021/ja01140a060.

(27) Abiraj, K.; Gowda, D. C. Zinc/Ammonium Formate: A New Facile System for the rapid and Selective Reduction of Oximes to Amines. *J. Chem. Research (S)* 2003, 332–334. https://doi.org/https://doi.org/10.3184/030823403103174281.

(28) Leeds, J. P.; Kirst, H. A. A Mild Single-Step Reduction of Oximes to Amines. *Synth Commun* 1988, *18* (8), 777–782. https://doi.org/10.1080/00397918808057845.

(29) D'Andrea, L.; Jademyr, S. Facile One-Pot Reduction of β-Nitrostyrenes to Phenethylamines Using Sodium Borohydride and Copper(II) Chloride. *Beilstein Journal of Organic Chemistry* 2025, *21*, 39–46. https://doi.org/10.3762/bjoc.21.4.

(30) Taylor, K. E. Reduction of Ketoximes to Amines by Catalytic Transfer Hydrogenation Using Raney Nickel and 2-Propanol as Hydrogen Donor, University of Tennessee at Chattanooga, 2014. https://scholar.utc.edu/honors-theses.

(31) Bischler, Aug.; Napieralski, B. Zur Kenntniss Einer Neuen Isochinolinsynthese. *Berichte der deutschen chemischen Gesellschaft* 1893, *26* (2), 1903–1908. https://doi.org/10.1002/cber.189302602143.

(32) Ji, Y.; Gao, Q.; Han, W.; Fang, B. Recent Advances in the Synthesis of Chiral Tetrahydroisoquinolines via Asymmetric Reduction. *Catalysts* 2024, *14* (12), 884. https://doi.org/10.3390/catal14120884.

(33) Kuzma, M.; Václavík, J.; Novák, P.; Přech, J.; Januščák, J.; Červený, J.; Pecháček, J.; Šot, P.; Vilhanová, B.; Matoušek, V.; Goncharova, I. I.; Urbanová, M.; Kačer, P. New Insight into the Role of a Base in the Mechanism of Imine Transfer Hydrogenation on a Ru(Ii) Half-Sandwich Complex. *Dalton Transactions* 2013, *42* (14), 5174. https://doi.org/10.1039/c3dt32733g.

(34) Cheung, F. K.; Clarke, A. J.; Clarkson, G. J.; Fox, D. J.; Graham, M. A.; Lin, C.; Crivillé, A. L.; Wills, M. Kinetic and Structural Studies on "tethered" Ru(Ii) Arene Ketone Reduction Catalysts. *Dalton Transactions* 2010, *39* (5), 1395–1402. https://doi.org/10.1039/b915932k.

(35) Hayes, A. M.; Morris, D. J.; Clarkson, G. J.; Wills, M. A Class of Ruthenium(II) Catalyst for Asymmetric Transfer Hydrogenations of Ketones. *J Am Chem Soc* 2005, *127* (20), 7318–7319. https://doi.org/10.1021/ja051486s.

(36) Lin, W.; Ma, S. Highly Efficient and General Enantioselective Synthesis of Naturally Occurring Isoquinoline Alkaloids. *Organic Chemistry Frontiers* 2014, *1* (4), 338–346. https://doi.org/10.1039/c4qo00058g.

(37) Lin, W.; Cao, T.; Fan, W.; Han, Y.; Kuang, J.; Luo, H.; Miao, B.; Tang, X.; Yu, Q.; Yuan, W.; Zhang, J.; Zhu, C.; Ma, S. Enantioselective Double Manipulation of Tetrahydroisoquinolines with Terminal Alkynes and Aldehydes under Copper(I) Catalysis. *Angewandte Chemie* 2014, *126* (1), 281–285. https://doi.org/10.1002/ange.201308699.

(38) Pine, S. H.; Sanchez, B. L. Formic Acid-Formaldehyde Methylation of Amines. *J Org Chem* 1971, *36* (6), 829–832. https://doi.org/10.1021/jo00805a022.

(39) Battersby, A. R.; Ramage, R.; Cameron, A. F.; Hannaway, C.; Šantavý, F. 1-Phenethylisoquinoline Alkaloids. Part II. The Structures of Alkaloids from Colchicum Cornigerum(Sweinf.) Tackh. et Drar. *J. Chem. Soc. C* 1971, *0* (0), 3514–3518. https://doi.org/10.1039/J39710003514.

(40) Lai, W.; Zhao, S.; Lai, Q.; Zhou, W.; Wu, M.; Jiang, X.; Wang, X.; Peng, Y.; Wei, X.; Ouyang, L.; Gou, L.; Chen, H.; Wang, Y.; Yang, J. Design, Synthesis, and Bioevaluation of a Novel Hybrid Molecular Pyrrolobenzodiazepine–Anthracenecarboxyimide as a Payload for Antibody–Drug Conjugate. *J Med Chem* 2022, *65* (17), 11679–11702. https://doi.org/10.1021/acs.jmedchem.2c00471.

(41) Barton, D. H.; Fernandez, I.; Richard, C. S. *A Mild Procedure for the Reduction of Aliphatic Nitro Compounds to Oxime*; 1987; Vol. 43.

(42) Gilmartin, P. H.; Kozlowski, M. C. Vanadium-Catalyzed Oxidative Intramolecular Coupling of Tethered Phenols: Formation of Phenol-Dienone Products. *Org Lett* 2020, *22* (8), 2914–2919. https://doi.org/10.1021/acs.orglett.0c00577.

(43) Kametani, B. T.; Yagi, H.; Satoh, F.; Fukumoto, K.; Kametani, T.; Battersby, A. R.; Herbert, R. B.; Pijewska, L.; Santavf, F. *Kametani and I. Noguchi*; 1967; Vol. 78.

(44) Nimgirawath, S. ChemInform Abstract: Synthesis of (.+-.)-Isoautumnaline and (.+-.)-Dysoxyline. *ChemInform* 1994, *25* (36). https://doi.org/10.1002/chin.199436253.

Chapter 7 – Synthonpedia

Introduction

As anticipated in the introduction, total synthesis of organic molecules is the final technological application of the catalytic methodologies: once the tool set is created, you can build your object. However, to make an efficient total synthesis of a target molecule, catalysis itself is not enough; strategy is essential. A significant example of this concept is represented by the synthesis of tetrodotoxin (TTX), the molecule responsible for the poisoning effect of pufferfish, which is also used in biological research as sodium channel blockage agent.[1,2] Different synthetic approaches have been reported, and here the synthesis by Isobe and co-workers (2004)[3] and by Trauner and co-workers (2022)[4] are compared (Figure 217).

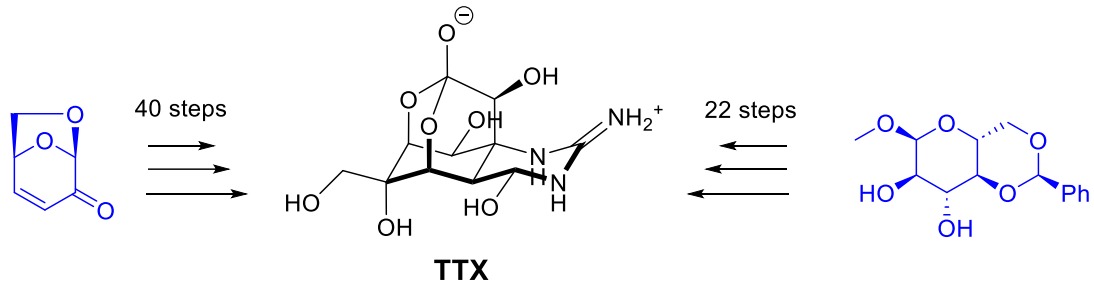

Figure 217 - Importance of strategy in total synthesis - the TTX case

Both strategies started with a chiral, oxygenated 6-membebered cycle, which undergoes further oxygenation and the introduction of the guanidinium ring to create a complex polycyclic scaffold. In the Isobe synthesis much of the synthetic elaboration is employed to introduce oxygenated functionalities, while Trauner starts from a glucose derivative with many of the functionalities already there. Using ruthenium catalysis and other catalytic strategies they were able to save 18 steps!

This example shows that to create a good synthetic strategy, and efficiently make the target molecule, the recognition of patterns, substructures, a deep retrosynthetic analysis, and the use of innovative methodologies is of primary importance.

Experienced chemists know a lot about methodologies and organic chemistry strategy, so they can create synthetic plans for complex molecules. Unluckily, not everyone has years of experience in the field of total synthesis, and clever ideas to make molecules are rare.

These are the reason that pushed me and Mr. S. Zanella, an extremely talented informatic engineer, to create “Synthonpedia”, a free software tool to help chemists

in finding new ideas to make molecules. Thanks to the expertise of S. Zanella, it was possible to create the necessary informatic architecture (relational database, website, integration of chemical libraries, and so on).

It follows an introduction on retrosynthetic analysis and computer-driven retrosynthesis and the workflow of Synthonpedia. As the topic of this thesis is chemistry, the description of the software does not go into detail in the informatic part.

Retrosynthetic analysis

Retrosynthetic analysis is a well-established problem-solving technique employed in organic synthesis to devise plausible synthetic plans. The core concept is easy: starting with a target structure, one imagines breaking a bond within the molecule (a *disconnection*), resulting in two fragments termed synthons.[5] Typically, during retrosynthetic analysis, a charge is assigned to these synthons to define their nucleophilic or electrophilic character. Subsequently, a reliable chemical reaction *corresponding* to the disconnection envisioned has to be identified. This process is shown in Figure 218.

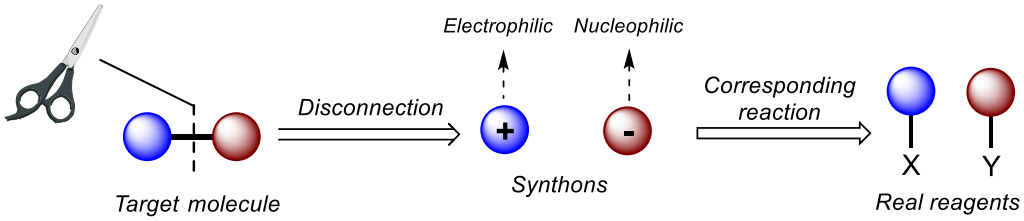

Figure 218 - General retrosynthetic analysis

Iterating this process for all compounds generated through retrosynthesis eventually leads back to simple and readily available starting materials, thus defining a synthetic pathway. Consequently, retrosynthesis would be a perfect approach to virtually solve *every* synthesis problem. However, identifying the "corresponding reaction" for the desired synthons is often not straightforward. In practice, when performing disconnections, organic chemists tend to generate fragments that can be easily traced-back to familiar reactions. This inevitably introduces a bias that favors reactions known to the chemist, thereby limiting the exploration of alternative synthetic strategies.

Computer-driven retrosynthesis

Computer-driven retrosynthesis (CDR) has been under investigation since the late 1960s, leading to the development of several computer programs based on

traditional algorithms.[5–9] This introduced significant of innovation in the field, including new data format and a general framework to address this problem.[10] Despite these promising advancements, such software has not gained widespread popularity within the organic chemistry community.

Recent years have seen an unprecedented development in AI, which has found applications in diverse scientific and technological fields. A prominent illustration in chemistry is the 2024 Nobel Prize recognizing the work of Demis Hassabis, David Baker, and John M. Jumper for their application of AI in protein structure prediction and computational protein design. AI has also been successfully employed in computer-aided retrosynthesis, encompassing both reaction prediction and retrosynthetic planning.[11] Notably, *Synthia*, a program by B. A. Grzybowski and coworkers, reportedly achieved a level of sophistication sufficient to pass the Turing test five years ago.[12] Nevertheless, despite these impressive advancements, several challenges persist for AI-based retrosynthesis algorithms. Current algorithms are typically trained to favor reactions with a high likelihood of success, relying exclusively on literature-derived datasets. However, access to *negative* results would be beneficial for improving their accuracy. Additionally, the tendency of AI models to follow existing publication trends can lead to inherent biases. Furthermore, computer programs often aim to identify the shortest synthetic routes, potentially neglecting simpler, albeit longer, strategies that commonly involve protecting groups.[13]

Filling the gap

Given this scenario, we questioned whether it is possible to develop a *complementary* tool that integrates the qualities of both chemists and computers: the former's creativity, experience, and understanding of chemical principles, with the latter's virtually unlimited memory and unbiased knowledge. Indeed, the synergy between machines and humans has already proven fruitful, particularly in the domain of AI-driven retrosynthesis.[12,14,15]

The basic idea behind Synthonpedia is to fill the gap between an arbitrary-designed synthon and a reliable corresponding transformation, as shown in Figure 219.

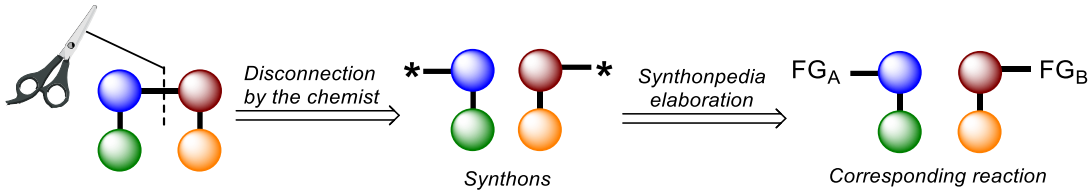

Figure 219 - Synthonpedia – chemist cooperation – filling the gap

For a target molecular structure, represented by the four-ball chain, the chemist chooses a disconnection, leading to synthons. The Synthonpedia algorithm then identifies the matching reaction(s). Importantly, we are not aiming to replace AI or other tools; our goal is to *enhance* chemists' creative input.

Synthonpedia operates on principles akin to Wikipedia, with the primary difference being its repository of reactions rather than articles. This freely accessible web server is available for use by all chemists, whether in academic or industrial settings. Mirroring Wikipedia, users can both access existing information and contribute their own knowledge. As a community-driven, open-source platform, Synthonpedia value and capability grow with increasing user contributions of reaction data.

Software workflow

It follows a scheme of software workflow – the different parts are briefly discussed below (Figure 220).

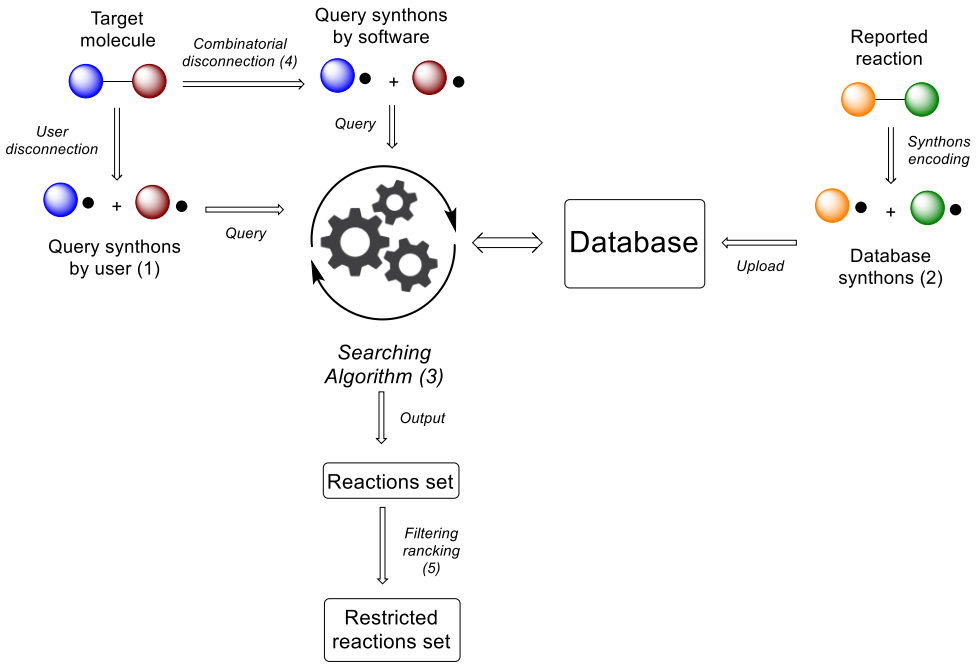

Figure 220 - Synthonpedia workflow

The Synthonpedia workflow is split into four different parts:

- Reaction upload: users can load their favorite reactions and the corresponding synthons, termed “database synthons” (DSs). These data build the database for matching research.
- Query: user can make a *query* to the database. It works starting from a molecule of interest and cutting the desired bond(s), making the so called “query synthons” (QSs). If desired, the software can automatically cut the bonds, making a list of QSs as query.
- Matching: the Synthonpedia core algorithm compares the QSs with DSs, looking for a match. Every reaction that matches the query is a potential methodology to realize that disconnection.
- Output: the results are then listed in the output. It is possible to filter the results using different attributes. We created also a ranking function to rank the different disconnections in case of a combinatorial query. The idea is to quantify *how much* a disconnection is efficient for a given target.

It follows a more detailed description of the software parts. The number of paragraphs refers to different parts in Figure 220.

1 – Synthons as query elements

Synthons are defined as fragments derived from molecular structures carrying a formal electric charge, which indicates their reactivity, as depicted in Figure 221. However, in our re-interpretation, synthons represent only molecular *connectivity*, without any inherent reactivity or stereochemistry.[5] Any unfulfilled valence from the disconnection is “capped” with a radical. Indeed, “radical synthons” in this context does not mean “radical reactivity”.

This slightly changed synthons definition provides some key benefits: the conversion of a reaction into general synthons is straightforward and unambiguous, and it makes it easy for the user to disconnect the target molecule. When building the query, the user just needs to “cut the bond”, without any bias given by the charge assignment. An example of this concept with a simple aldol reaction is represented in Figure 221.

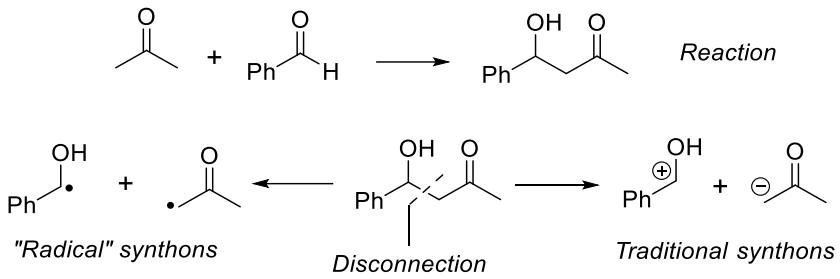

Figure 221 - Radical synthons

If a reaction combines several fragments, then multiple synthons will be associated with it. In case a multiple bond is disconnected the corresponding diradical or triradical synthons are generated. The synthons generated by disconnection (QSs) are coded as a SMILES[16] string. Thus, the query is simply composed of one or more distinguished strings.

2 – Synthons as database elements and encoding rules

Following the same concepts, the reactions and methodologies reported in literature can be uploaded in the database in the form of synthons. To each uploaded reaction is associated *a list* made by at least one synthon which univocally corresponds to that specific reaction – DSs. While QSs can simply be generated by cutting bonds in the desired synthetic target, DSs must be as general as possible, as they are intended to represent all the possible structures of the substrate. General structures are represented using R-groups or other notations available with Indigo, a chemoinformatic library available for free.[17]

To standardize reaction-synthon association, some *encoding rules* were established: following these rules, every reaction gives only one set of DSs. There is no room for personal interpretation of reactivity. The encoding rules are fully explained in the supporting information session. An example of DSs generation is the shown in Figure 222, with the ene-reaction between alkenes.

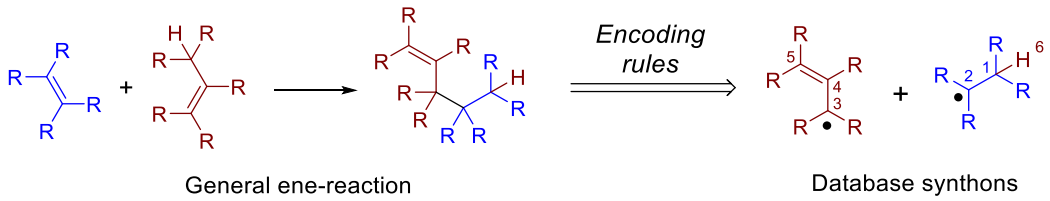

Figure 222 - Example of ene-reaction DSs generation

One advantageous feature of this data format is the user's ability to encode multiple sequential reactions as a single transformation, as illustrated in Figure 223.

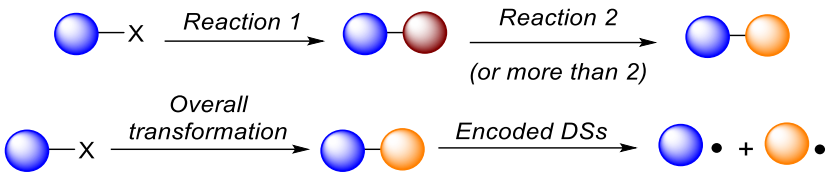

Figure 223 - Encoding more than one reaction in just one synthon

The encoding of a reaction sequence is recommended if that sequence is very well established in organic synthesis or deemed relevant by the user. An example to clarify this concept is provided by the alkylation-decarboxylation of a malonate Figure 224.

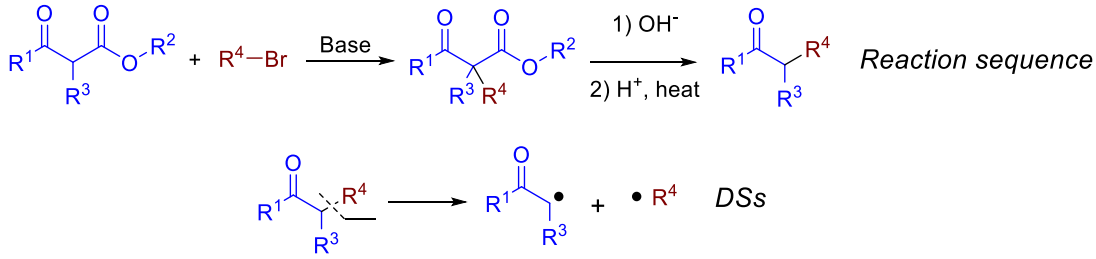

Figure 224 - Malonate alkylation-decarboxylation as example of encoded reaction sequence

All these additional features do not exclude the "original reaction" from the game: a reaction can be uploaded in different versions (corresponding to a different DSs set). For instance, the malonate synthesis can be uploaded without the decarboxylation sequence. In the latter case, the reaction will only be matched if the malonate group is present in the QS(s).

To summarize, the univocal representation of a reaction as a set of synthons is an easy and computationally cheap method to *express the connectivity transformation* that a chemical reaction makes. The match between QSs and DSs means that the user request on making that bond(s) is possible, as the same connectivity transformation is reported. It follows the basics principles of the searching algorithm.

3 – Searching algorithm

The core function of the search algorithm is based on recognition of *subgraphs*, already encoded in common chemoinformatic libraries. It is just the comparison between DSs and QSs to check if the former is a *substructure* of the latter. If yes, there is a match, as the general structure of DSs represents also the QSs case (Figure 225).

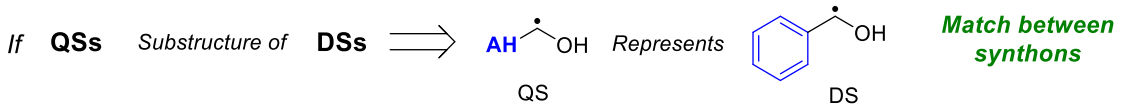

Figure 225 - General matching problem

The matching algorithm compares the QSs set with all the available DSs set in the database. The matching algorithm is designed to look only at the connectivity of the structures: the stereogenic centers and the double bonds configuration are not considered. A list of all the matched reactions constitutes the *raw output*. Data filtration and/or ranking can be done on user request later (see subparagraph 5). The filtering/ranking parts help in choosing methodologies with different descriptors.

4 – Combinatorial disconnection

After the first tests with Synthonpedia, we questioned whether it was possible to help the user also in the disconnection step. With this design the user can only perform one disconnection at the time and evaluate the results. Peculiar disconnections are less spontaneous, as the user would probably avoid them for its biases. The main problem associated with retrosynthesis could still affect the creation of new ideas! So, we decided to include an automatic *combinatorial disconnection* function: the molecule is disconnected in every possible bond (excluding C-H or X-H bond, as these are not included in the rules), chopping the molecule in 2, 3 or 4 pieces, to include also multicomponent reactions. Every QSs set is then processed separately, returning *all* the possible disconnection approaches with the available data.

It was calculated how many QSs are generated using the combinatorial approach (Equation 1), to estimate if this approach is computationally feasible. For *every* set of generated QSs, there is one interaction of these with the database.

$$\text{N° QSs} = \sum_{k=1}^{k=i} \frac{n!}{(n-k)!\,k!}$$

Equation 1 - Number of QSs generated by combinatorial disconnection
n = Number of bonds in the molecule
k = number of disconnection (1, 2 or 3 for this example)

The trend of Equation 1 is shown in Figure 226.

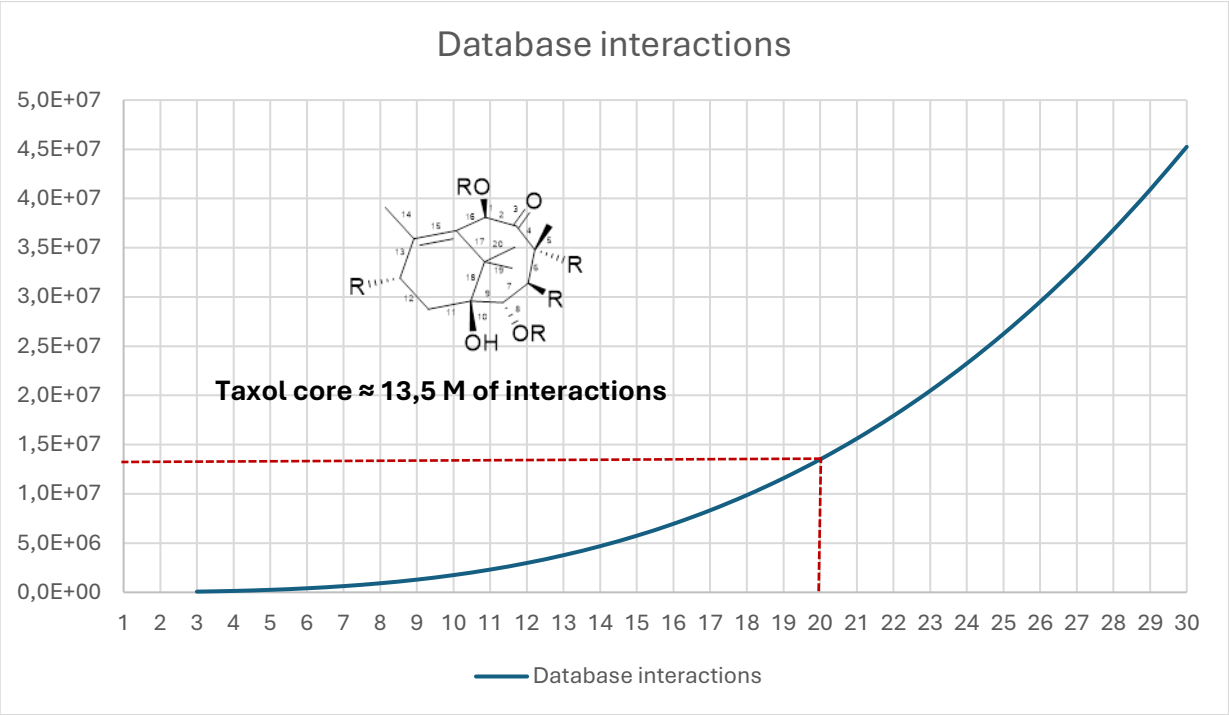

Figure 226 - Database interactions trend

For a molecule of considerable complexity, such as a portion of the core system of Taxol, which has n = 20, the number of interactions is about 13,5 million. This number of interactions was tested in the Synthonpedia database, taking around 3 minutes[L] – a short time considering that it was explored *all the possible ways* of disconnecting a system of such complexity. This is due to the inherent speed of relational database algorithms,[18,19] a great advantage for software aiming to be used by many people every day at the same time. Indeed, the hardware required to run Synthonpedia web server at the moment is a 20 $ physical server (Figure 227).

Figure 227 - Physical web server

[L] The test was done using a database of 50 reactions. Given the intrinsic speed of relational databases, the total time required time should not raise significantly.

5^{I} – Filtering

The raw output of the server is just the list of the matched reactions, which are then evaluated by the user. However, in case of many results, it would be convenient to filter and/or rank the results obtained. Filtering is a straightforward task: during the upload procedure it is required to fill out some general information about the methodology – the so-called *reaction attributes*. The reaction attributes are stereoselectivity, fundamental reactivity, chemistry-type classification, year of first publication and greenness. The user can filter the results using these attributes. More details about this are provided in the supporting information.

5^{II} – Ranking

The ranking function was designed to handle massive outputs, as would be expected in case of *combinatorial disconnections*. The idea is to highlight the reactions which forge the molecular skeleton in the most efficient way possible when many disconnections are made. Guided by literature reports about this topic[5,6] we designed a simple scoring function which uses the following descriptors:

- Number of reaction components, to privilege multicomponent reaction.
- Number of forged bond bonds in the transformation, both σ and π – the formation of more bonds in a row is advantageous.
- Dimension of disconnected fragments – disconnecting two fragments of similar dimension simplifies the problem, favoring divergent approaches.
- Number of cycles forged in the transformation. Cyclic structures are usually the most difficult to obtain.[5]

All these parameters are then evaluated by *ad hoc* function and properly weighted using a coefficient in the scoring function (*Equation 2*).

$$Score = \sum_{i=0}^{n} a_i * x_i$$

Equation 2 - Scoring function for reaction ranking
a_i = weighting coefficient of i-th descriptor
x_i = function of the i-th descriptor

The details about the scoring function are described in the next subparagraph.

Scoring function and a_i evaluation

It follows a description of the various *ad hoc* descriptors used and the coefficients evaluation method.

The number of reaction components is simply evaluated as it was named "$\mathbf{x_1}$". For example, for a three-component reaction, $x_1 = 3$.

The number of forged bonds is counted following the already mentioned rules for bond formation: every *new* bond formed between two atoms different from hydrogen is counted as 1. The broken bonds are just ignored – what matters is new connectivity. This function is named "$\mathbf{x_2}$". For example, the simple alkylation of a malonate has $x_2 = 1$, as a simple σ bond is created.

The evaluation of fragment dimensions similarity was the most difficult descriptor to evaluate, as similarity is a broad-meaning term. To simplify the problem, we accounted for similarity as the weight of the disconnected fragment. Indeed, since the atoms contained in organic molecules are roughly always the same and have similar weight, the overall weight of a certain molecular portion is considered to be a good indicator of the "complexity" of a fragment. With this point, it was then selected a similarity function to numerically evaluate this parameter. First, not only the net difference of molecular weight between fragments is important, but also the *comparison* of this difference with the molecular weight itself. For example, if two fragments weigh 500 u and 505 u and two other fragments weigh 50 u and 55 u, the difference is 5 u in both cases, but it is evident that in the former example there is much more similarity. Intuitively, a ratio between the weight of the two fragments and their difference must be somehow expressed. Considering that having up to four fragments is possible for the software design, the comparison must work for N-fragments. Thus, average and standard deviation can be used to describe the dimension of fragments and their difference in similarity comparison. Moreover, considering the potential wide range of molecular weight, from around 30 u of a carbonyl fragment to around 1000 u of a complex fragment, it was chosen to use data in logarithmic form for similarity evaluation. The following, easy math was used; for a disconnection generating N-fragments with MW molecular weight, MW is converted to its logarithmic form $\mu_i = \ln(MW_i)$. Then, the simple standard deviation (σ) is calculated. Finally, σ is converted back to normal form with the exponential function, scaling the result. A parameter K is included in the equation, arbitrary equal to 2 to have and easy to read result.[LI] The final form of the function thus gives the score for the similarity of fragments and is named "$\mathbf{x_3}$" (Equation 3).

[LI] An arbitrary K value can be used, it is just a re-scaling of x_3.

$$X3 = \exp(-K\sigma),\ K = 2$$

Equation 3 - X_3 function

Another advantage of this function form comes directly from its math: the x_3 value is "well distributed" for all its application field. This means that σ values are equally reworded: the most similar things are well distinguished from "average similar" things. Non-logarithmic functions tend to squeeze the results to the same value when σ approaches zero. In case we are dealing with an intramolecular reaction x_3 is formally set to be zero, despite theoretically being one, as the similarity of an object with itself is maximum. However, the similarity evaluation was made for two or more components reactions, so it makes no sense to use it for mono-component reactions.

The last parameter is just number of *new* cycles formed, so again a very simple function, named "x_4". For example, a [4+2] cycloaddition of a simple diene and alkene has $x_4 = 1$.

As an example, the x_n values of a disconnection taken from the dataset we used are calculated (Figure 228).

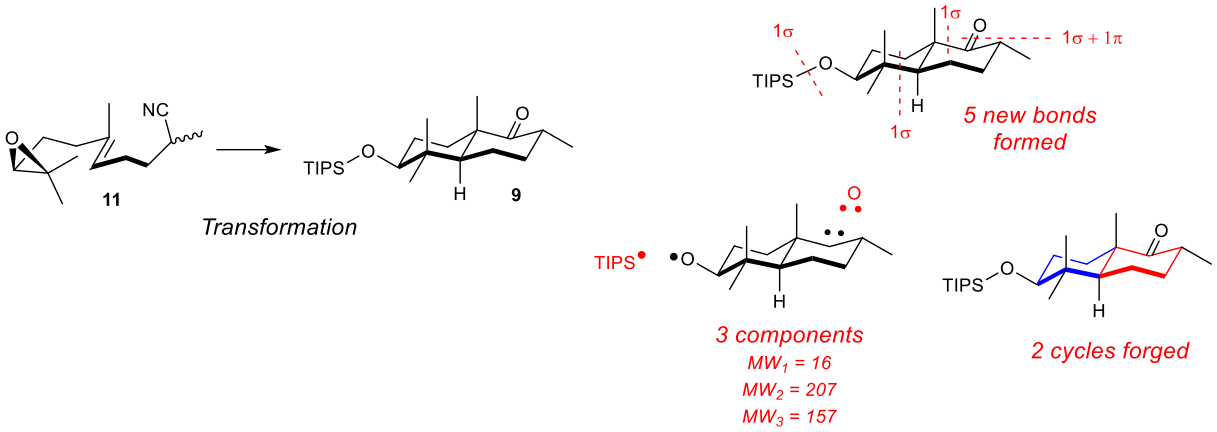

Figure 228 - 11 to 9 x_n calculation

The conversion of **11** to **9** in the total synthesis of Isomalabaricane triterpenoids[20] is analyzed. First, applying the Synthonpedia retrosynthetic logic, the new bonds and atoms of **9** are highlighted. 3 σ bonds (O-Si and C-C twice) are immediately visible. The newly formed C=O bond, originated from nitrile group, counts as $1\sigma + 1\pi$ bond, for a total of 5 new bonds (x_1 = 5). The reaction is mainly intramolecularly, but there are new fragments introduced from the outside: the TIPS group and the oxygen atom. In total, three components are formally merged in this reaction (x_2 = 3). The weights of the reaction components are then easily calculated (MW_1 = 16, MW_2 = 207 and MW_3 = 157). Following the previously

introduced logarithmic function, x_3 = 0.07692. Finally, it is clearly visible that two new cycles have been forged, so x_4 = 2.

Once the indicators calculation rules have been defined, the weighting coefficients a, b, c and d of the scoring function have to be extrapolated. To do this, some conditions must be formulated to have an analytically solvable problem. After extensive discussion, it was decided to try to *mimic* a selected set of "smart" reactions reported for the total synthesis of complex molecules. The core idea is very simple: once a set of reactions is selected, it is postulated that all these have the same arbitrary-defined score. In other words, we're postulating that these "very good reactions" all equally represent the best of the art. Once this has been defined, it follows naturally that the weighting coefficients must be regulated trying to force the scoring function to be as close to the top score as possible. This idea is exemplified below in Figure 229.

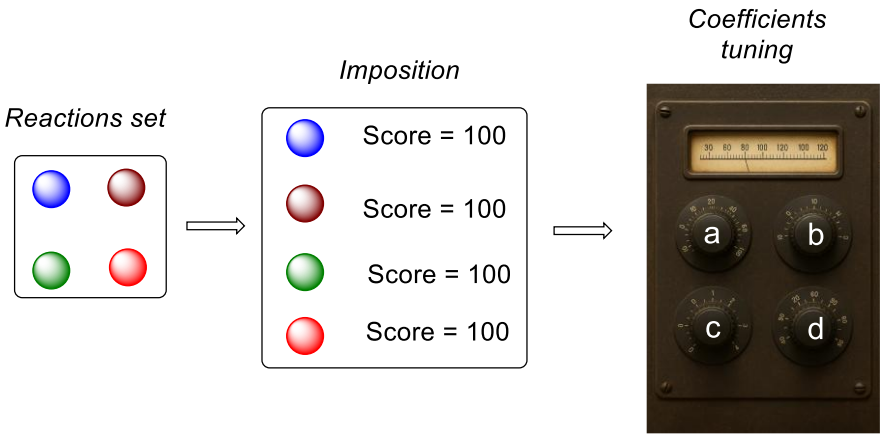

Figure 229 - Coefficient tuning for a simple set of four reactions

Taking as example a simple set of four reactions, represented with colored spheres, a score of 100 (arbitrary chosen) is imposed for the scoring function of every reaction in the selected set. To make this assumption *as true as possible*, the coefficients have to be finely regulated. Mathematically, this is simply translated into minimizing the standard deviation of the scoring function for the whole dataset, which is a 4 variables equation (a, b, c and d). Minimizing every variable produces a 4 equations system, fully solvable. The final equations set is shown in *Equation 4*.

$$\frac{\partial \sigma}{\partial a} = 0, \frac{\partial \sigma}{\partial b} = 0, \frac{\partial \sigma}{\partial c} = 0, \frac{\partial \sigma}{\partial d} = 0$$

$$\sigma = \sqrt{\frac{\sum_{i=1}^{n} (Yi - z)^2}{n}}$$

Equation 4 - Final equation set

Every partial derivative is imposed to be 0, and the standard deviation σ is reminded to be sum of the squared difference of the scoring result $\mathbf{y_i}$ (the result of the scoring function for the reaction i-th) and the imposed maximum score **z**, all divided by n - the number of reactions in the set. The problem is now easily solvable.

A small dataset of 43 reactions was then provided, choosing reactions reported for the total synthesis of complex molecules raging from 2007 to 2025. Importantly, only what we considered *not obvious and skeletal forging* reactions were selected, as we are interested mimicking "original disconnections". The calculated coefficients are reported in Table 25.

Weighting coefficient	Value	Associated function	Meaning
a	16.05233213	x_1	Reaction components number
b	13.04533849	x_2	New bonds
c	3.070200894	x_3	Fragments similarity
d	18.65139366	x_4	Forged cycles

Table 25 - Weighting coefficients outcome

With the coefficients calculated, it is now possible to rank the disconnections found by the deep-research function. The calculation of functions x_1, x_2, x_3 and x_4 was easily implemented in the software. Indeed, without going into coding details, all the parameters can be easily extrapolated from the matching query synthons sets.

Finally, we were curious about *how much* every of the four x_n functions is important in the scoring function. So, we compared the score done by every one of the four functions taken as an average for the whole dataset. The data are represented in Figure 230.

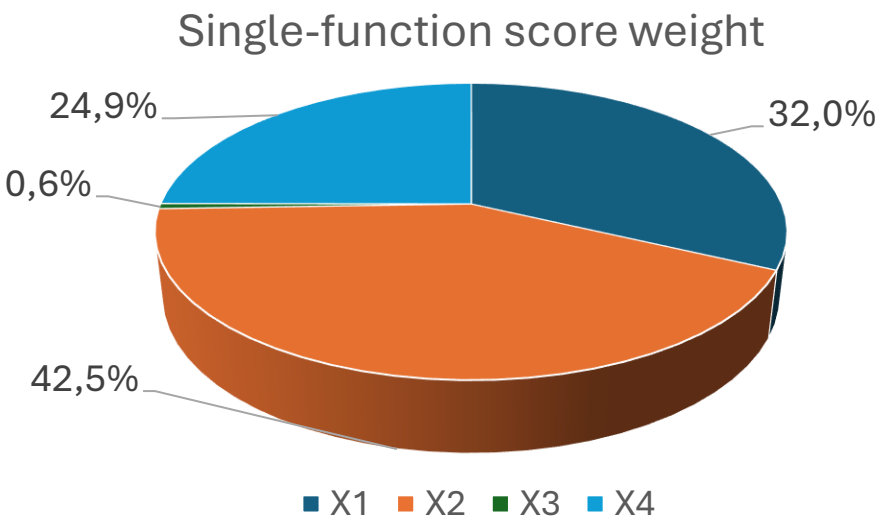

Figure 230 - Single-function score weight

The weight of x_1, x_2 and x_3 is somehow expected: the number of reaction components, bond made and cycle forged are all important if you want a disconnection that mimics the top players in total synthesis. However, at least in my opinion, the fact that the similarity of the molecular fragments is insignificant (0,6 %) is kind of surprising. Evidently, key disconnections tend to focus more on singular functionalization than putting together molecular fragments of similar complexity, at least for the dataset we chose.

Of course, a bigger dataset would be more meaningful in the weighting coefficient calculation. It was not possible to expand the current dataset for time reasons, but this can be done more easily the future now that the calculation architecture is there. It was decided to keep the dataset out of user's manipulation, preferring a direct reactions choice, in cooperation with Professor F. Romiti, who selected part of the literature used.

Finally, the same descriptors calculation system can be potentially used to rank results with different standards: entire synthetic reactions sequences from academic literature can be used to search for "efficient disconnections" in general. We can also turn our attention to industrial synthesis of complex APIs, to give weighting coefficients that favor disconnections typical of industrial practice. Thus, we believe that this method in general can be applied to generate a sort of "fingerprint" of different synthesis styles, and exploit this to privilege some strategies in deep research ranking. Moreover, if desired, more parameters can be included in the description, for example disconnection between heteroatoms.

Synthetic tree problem

We questioned whether it is possible to create a tool to automatically perform functional group interconversion (FGI) or functional group addition (FGA).[6] By doing so, every functional group in a molecular structure can be converted into another, creating different "starting points" for disconnections. If *every one* of these starting points undergoes combinatorial disconnection, the chemical space would be fully explored. But all the combinations would be too much to be handled, with computation time raising to unpractical levels. A graphical representation of the problem is shown in Figure 231.

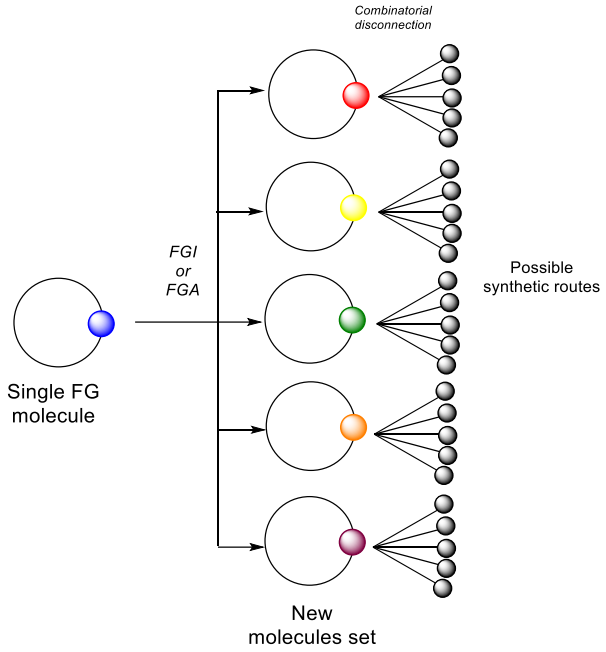

Figure 231 - Synthetic tree problem – one FG converted to another (colored ball)

This problem is known in literature as “synthetic tree”[6,9,14] and it is one of the main limitations in the field of CDR. Until now, the only rational way found to prune the tree is to simply privilege some FGI or FGA which are known to easily give access to synthetic possibilities. One example could be the introduction of multiple bonds around the molecule, or the introduction of specific groups such as carbonyls. However, the effective advantage of this approach, the computational feasibility, both in terms of time and coding issues, still have to be evaluated. Possibly, in the future this feature will be implemented as well in Synthonpedia.

Conclusions

A novel informatic retrosynthesis tool is introduced to offer an alternative to the well-established, yet still somehow limited, artificial intelligence approach. This new tool is called “Synthonpedia”, and it is a database of synthons. Synthonpedia takes inspiration from Wikipedia, being a community-driven software: every user can both upload new reactions and request to associate disconnection fragments with the stored reactions. This functionality is enabled by arbitrarily defined codification rules, the relational database used for data storage, and the free public license. The overarching concept is that the chemist disconnects the molecule fully leveraging its creativity, while the software bridges the gap between synthons and *associated* reactions. Alternatively, the disconnections can be directly proposed by the software, unbiasing completely the disconnection research. The outcome reactions can be rated using a proper scoring function and subsequently evaluated

by the user. Moreover, for time reasons, the integration of a FGI and FGA tool is still under design and evaluation, and it will possibly be implemented in the future.

We hope that this alternative tool will help the synthetic community to develop innovative approaches towards complex molecules. The web app for Synthonpedia is available at https://synthonpedia.org/.

Supporting information

Further details about Synthonpedia, resources used, and a use example are included in the supporting information.

Resources

All the reactions loaded in the database come from Wikipedia pages, organic chemistry portal pages (https://www.organic-chemistry.org/) and general literature known by the authors. All the non-peer-reviewed resources were used only as inspiration, uploading data extracted from paper(s) published. All the reactions used to create a starting database for Synthonpedia were chosen randomly, aiming to test different cases (multicomponent, redox, rearrangements, ...).

The web application has been developed using different available software: Next.js[21], Ketcher by Epam[22], PostgreSQL[23], Bingo PostgreSQL by Epam[24] and Indigo Toolkit by Epam[25].

Part of the code used is available at https://github.com/Simone99/sintopedia_reborn. The web application is available at https://synthonpedia.org/

The logo (Figure 232) was designed by Angelica Di Lorenzo and Alessia Bianchini, who we greatly thank.

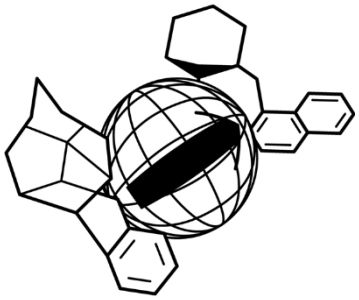

Figure 232 - Synthonpedia logo

Synthonpedia – client usage

To show into detail how to use Synthonpedia a usage example from the “client” point of view is reported, step by step.

Building the query

The molecule to disconnect can be represented using the drawing tool or imported as string form with different formats, for example SMILES or directly as a file. An example of molecule is represented in Figure 233.

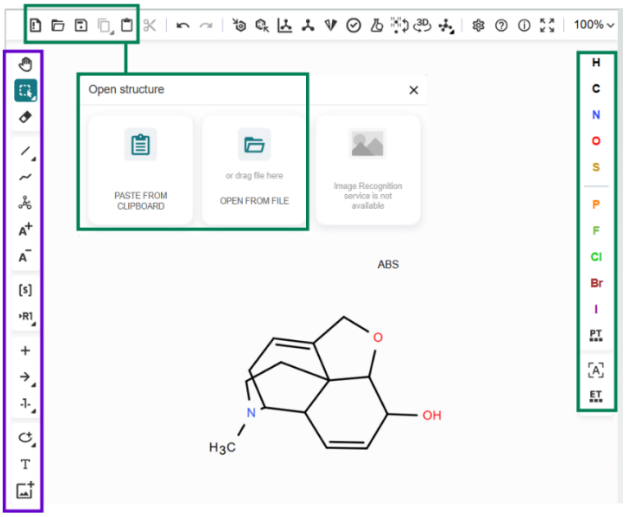

Figure 233 - Loading the molecule the molecule - Drawing toolbar and string or file loading tool highlighted

Then, to make a disconnection is sufficient to erase the corresponding bond(s) and give a radical character to the disconnected atoms (right click and set the atom properties - Figure 234).

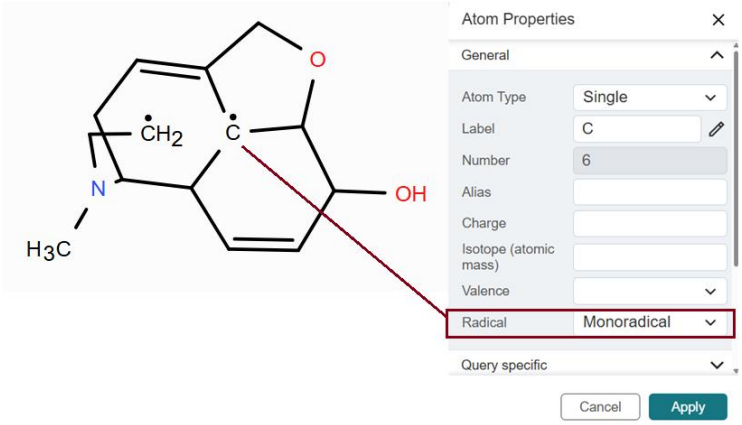

Figure 234 - Example of user’s disconnection

Clicking the button “Search!” the query synthons will be matched with the corresponding database synthons. The results will be shown on a list. The “deep

research tool" (combinatorial disconnection) is also available. For this test molecule and with the current dataset (48 reactions), the deep research tool furnished two results when disconnecting alkenes: Heck reaction and Peterson olefination, while no results are found for the user disconnection in Figure 234.

Filtering the results

The output list looks like this (*Figure 235*):

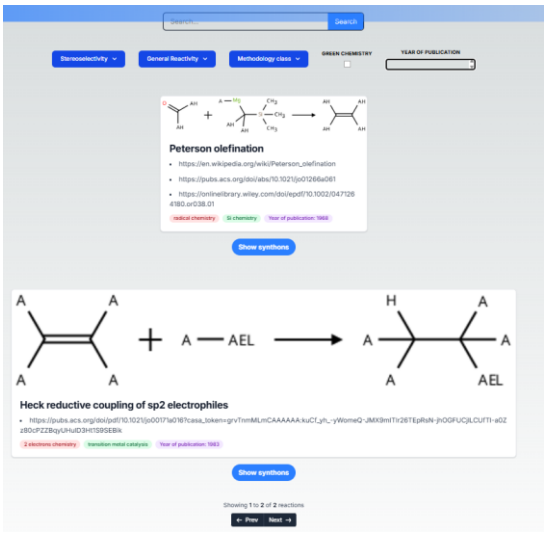

Figure 235 - Output after deep research function

For all reactions the associated general database synthons are shown, together with the reaction and the associated attributes (link(s), name, configurational selectivity, general reactivity, methodology class, green chemistry and year of publication). The attributes can be used also as tags to filter the results, selecting one or more options from the top toolbar, as shown in Figure 236.

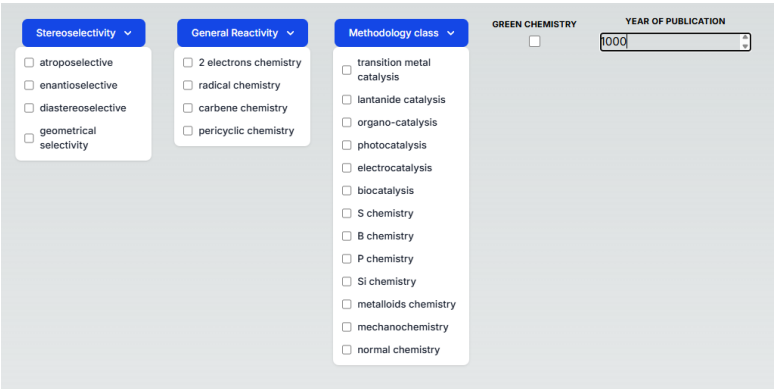

Figure 236 - results filtration toolbar

Attributes

Attributes deserve a brief explanation to use correctly Synthonpedia.

- Configurational selectivity: the formation of stereoisomers is not considered by the software – only the connectivity is important. The formation of one specific stereoisomer is evaluated by the user. Nevertheless, many methodologies are reported to be stereoselective, so the choice of the user can already target toward these.
- General reactivity: this attribute ranks the reactions on their mechanism or activation mode (polar chemistry, radical chemistry, and so on). This helps the chemist to discriminate against reaction in very general sense. For example, one could desire to have no radicals around because its product polymerizes easily. Eliminate directly the radical chemistry as a bulk.
- Methodology class: this attribute focuses on the type of methodology used, looking at the catalyst or very specific groups, and not to the reaction mechanism. This again helps to discriminate against undesired methodologies, for one reason or another. An example is to not use transition metal catalysis in the last step of an API synthesis.
- Green chemistry: this a yes or no attribute. Its use is straightforward: choosing a green methodology for an environmentally sustainable process.
- Year of publication: the year of publication of the cited methodology can be used to select only very-well established chemistry, or to chose something new to use in your synthetic process, to make it more appealing for a good publication.

Synthonpedia – database upload usage

The user, if registered, can upload reactions to the database. To show into detail how to upload reactions into Synthonpedia the codification rules and a usage example step by step are reported. To do the reaction interpretation rules must be used. These rules are designed to always generate a group of two or more synthons for a given reaction unambiguously. An exception to this is the possibility of neglecting a redox transformation inherent in a rearrangement, to make that reaction easier to match. In that case two groups of synthons can be created for a reaction, it's the user's choice.

Synthon codification rules

The codification rules are explained here, using examples to make things easier.

- Every disconnection made regards only the *forming* bond(s) and is represented by radical synthons. Don't have to worry about the polar nature of the synthon. A simple general example is shown in Figure 237:

Figure 237 - General disconnection

- Atoms can be connected via single, double and triple bonds. To disconnect a single bond use the radical symbol, to disconnect a double bond use the *singlet carbene* symbol and to disconnect a triple bond use the *triplet carbene* symbol (Figure 238). Singlet and triplet carbene are just a convention to account for double and triple radical, respectively. Triple radicals are not encoded by Ketcher.

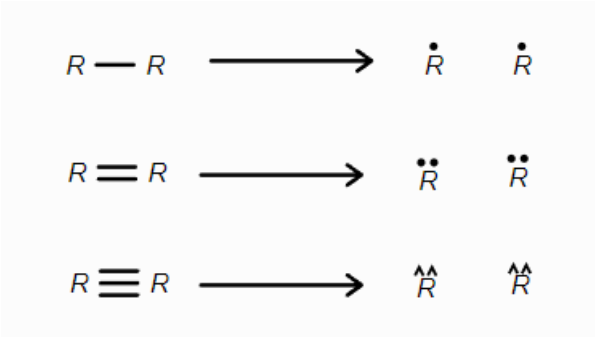

Figure 238 - Multiple bond disconnections

- Multiple synthons disconnections are allowed and encouraged. The same rule described for simple disconnections apply. Thanks to this feature, multicomponent reactions and/or synthetic sequences can be coded. A general scheme is shown in (Figure 239):

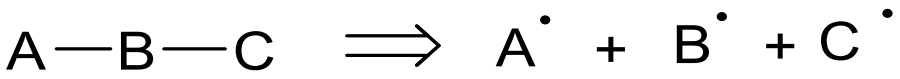

Figure 239 - Multiple synthons disconnection

- Reactions can be both *intermolecular* and *intramolecular*. Always write a reaction as *intermolecular*, to be as general as possible, unless a reaction can only occur as *intermolecular*. The software is able to consider *intramolecular* cases of disconnections reported as *intermolecular*, but not the opposite.

- As already stated above, Synthonpedia does not consider the stereochemistry of sp^3 atoms in the structural match or any other chiral element of molecules. Just don't care about this. The structure with the

correct stereochemistry *can* be upload, the software just does not consider that. The concept is resumed in Figure 240.

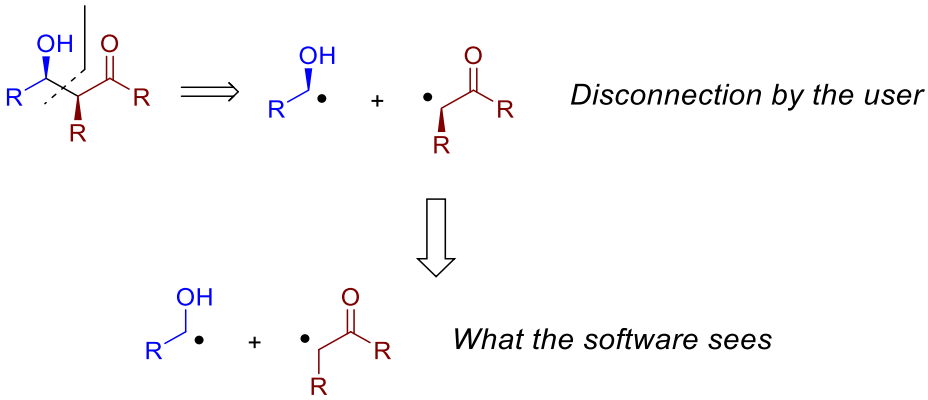

Figure 240 - Flow sheet for stereoselective disconnections

- The disconnections to be represented are *only* about the fundamental connectivity of the molecule: reagents are not considered. One representative example is reported in Figure 241:

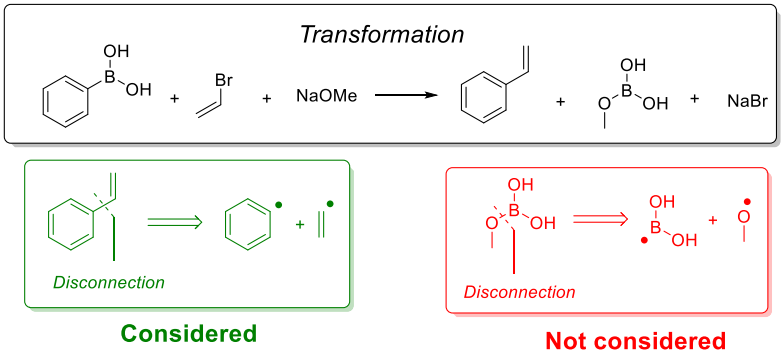

Figure 241 - Disconnection - considering only the main substrate, not auxiliary reagents and co-products

- *Desaturation reactions* are not part of the Synthonpedia project. Indeed, those transformations can be represented *directly* as reaction and other sources are available for this type of research. In other words, if you represent a hydrogen addition (saturation) or removal (desaturation), you already know which FGs are involved, and the disconnection logic of this software does not make any sense. Oxidations and reductions can be represented if they are not saturation/desaturation, because in that case *there is* a new connectivity (Figure 242).

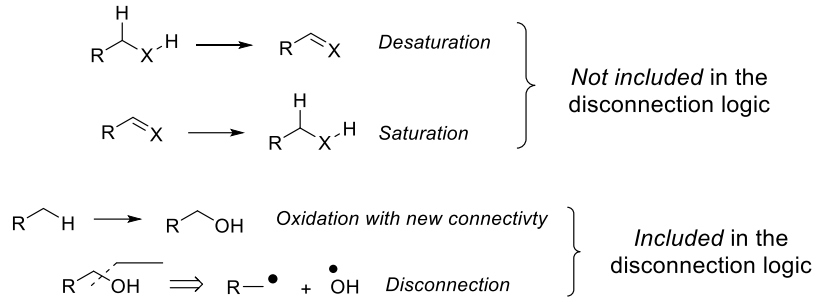

Figure 242 - Saturation-desaturation scheme

- Disconnection of pure H atoms are *not encoded*. No user will disconnect in the forward sense – the Hs re-organize automatically the organic reactions. The following example will clarify the concept (Figure 243):

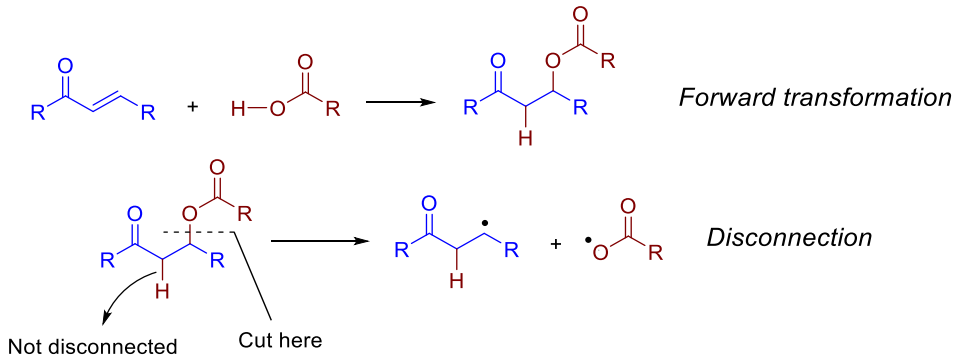

Figure 243 - Hs disconnection neglected

- You must be as general as you can in coding the disconnections associated with the reactions. The library used by Synthonpedia allows to encode a broad range of substructures. The more general is the structure of the synthons, the higher the possibility of having the associated reaction as outcome. The user has also to be realistic in "expanding" the scope of the reaction: as a rule of thumb, *not reported substrate cannot be included* in the disconnection. For example, if a reaction is reported to work with primary and secondary alcohols, but not on tertiary alcohols, the disconnection will *not* include tertiary alcohols, even if they could work in theory.

- Multiple bond migrations are ignored. With "multiple bonds migration" we mean some π-electrons shifting and creating a new π-bond, thus changing the bond order instead of creating a new connectivity. Again, this is done to make things simpler and to obtain easy synthons. An illustrative example is shown in (Figure 244) with the ene-reaction.

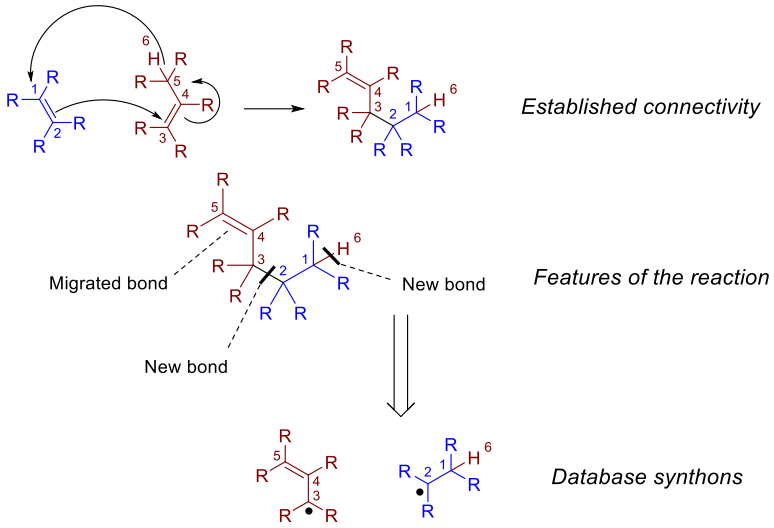

Figure 244 - π -electrons migration neglected - ene reaction

- Rearrangement reactions are coded following the same rules described above. The outcome looks non-intuitive, but this approach will to spot the rearrangement possibility with simple disconnections. The following example with the Overmann rearrangement will clarify the concept (Figure 245):

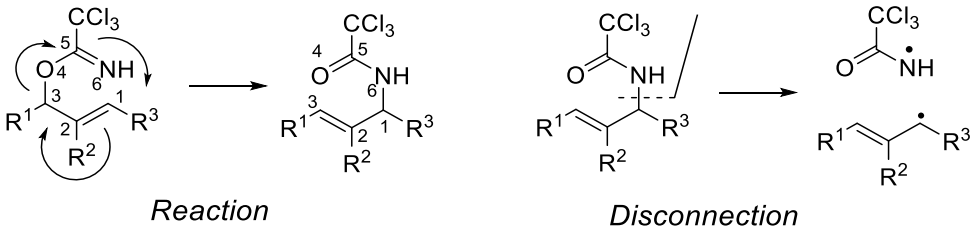

Figure 245 – Overmann rearrangement disconnection

- Depending on the case, the redox-derived connectivity can be neglected in a transformation, focusing only on the main connectivity. Indeed, it is more productive to show the *fundamental connection(s)* between the fragments in order to maximize the probability for the user to find that reaction while disconnecting. One example of this situation is the Favorskii rearrangement, represented in Figure 245.

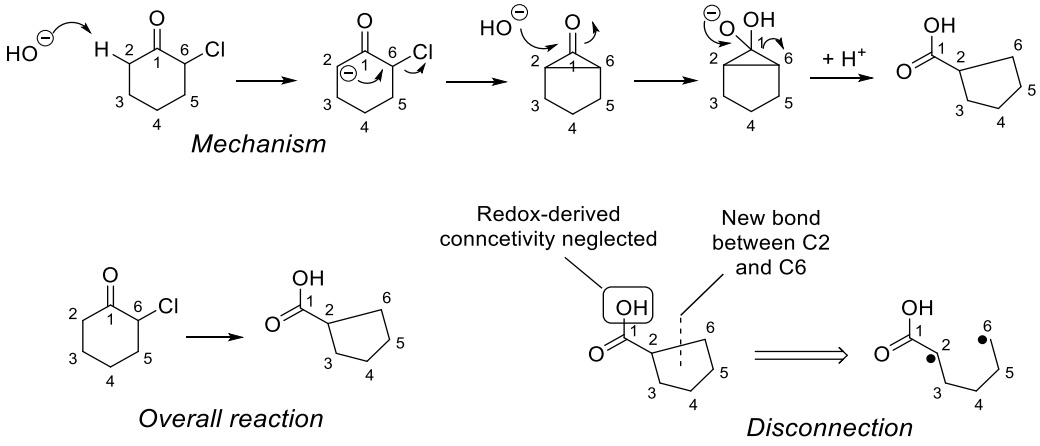

Figure 246 – Neglet the redox connectivity – Favorskii rearrangement

In this example the mechanism is shown just for clarity. The final synthon has not been generalized for the same reason. As you can see, the disconnection represented in this fashion is easy to find out following the common course of disconnecting around the molecule.

- It is possible, and encouraged, to upload entire n-steps synthetic sequences as a single transformation. Doing so, multi-step methodologies are encoded as a simple disconnection. The following scheme (Figure 247) will give you an example of a multistep sequence encoded as single transformation.

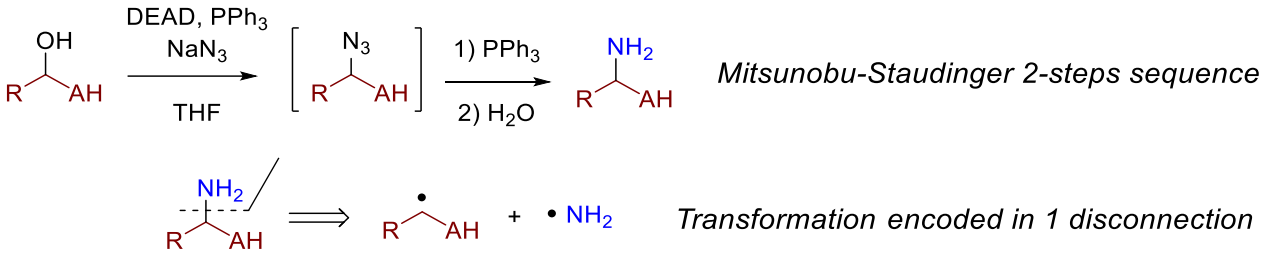

Figure 247 - Multi-step sequence encoded

Synthons uploading

After the target reaction has been encoded into synthons following the rules, the structures can be easily updated. The database synthons are uploaded as general structures. The general substituent, usually indicated as "R" in organic chemistry, are introduced in this library as *pseudoatoms* – something that is counted as an atom but is an object which represents a larger structure. Thus, the most important pseudoatoms to encode structure are introduced here:

- G → general group, which means everything but hydrogen atom.
- GH → general group *or* hydrogen atom

- A → any atom, but not hydrogen
- AH → any atom *or* hydrogen
- X → any halogen
- XH → any halogen *or* hydrogen

We're currently work to implement a "CH" pseudoatom, which would be very useful. An illustrative example of reaction with the ene-reaction follows.

To upload a new reaction the user can click on "Add new reaction!" on the top right corner (Figure 248).

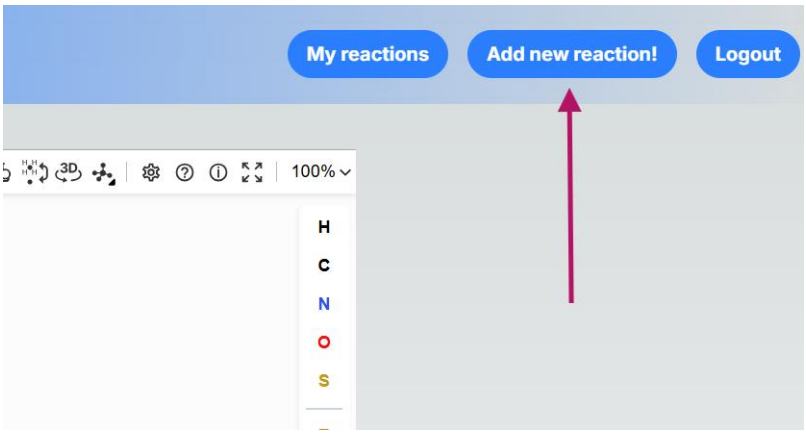

Figure 248 - Add new reaction

There are three windows for the reaction uploading: "reaction" (Figure 249), in which the user writes the reaction in the general form. It is actually not necessary but helps the user visually. Then, in the "synthons" window (Figure 249) the user uploads the database synthons. Finally, in the "search query example" window (Figure 250) the user uploads a *representative* example of that reaction, which will be visualized by the client.

About the attributes, the reaction name window is on the top of the page (Figure 249). The other attributes are in the middle (Figure 251).

Clicking on the button "Add!" at the bottom the reaction will be included in the database.

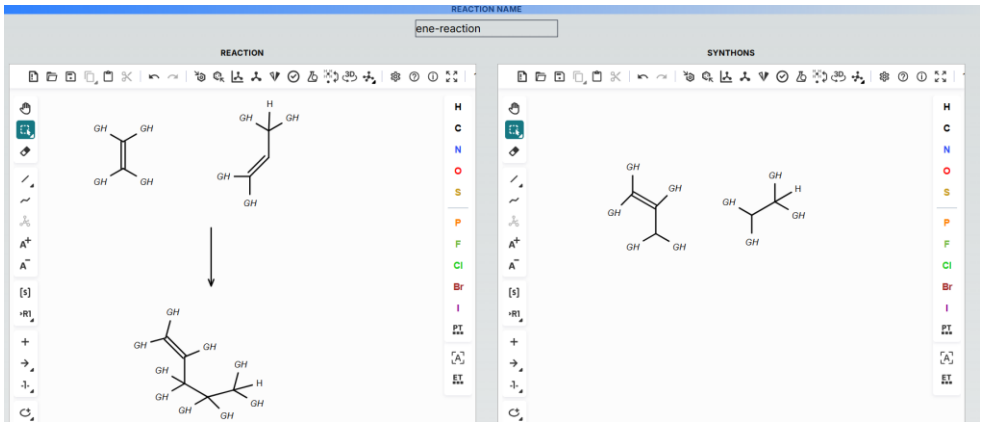

Figure 249 - Reaction window and synthons window - example with ene-reaction

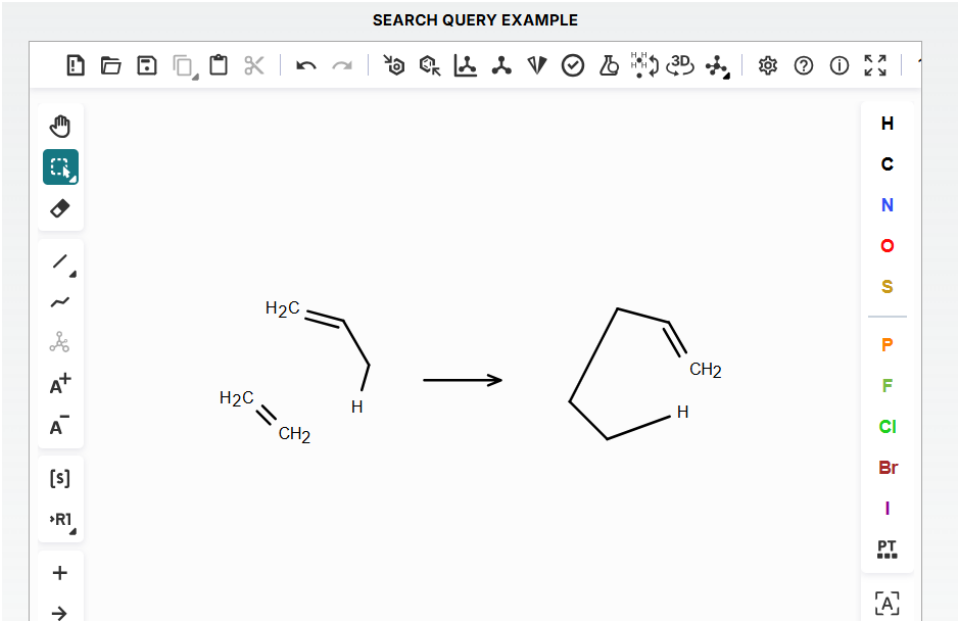

Figure 250 - Search query example window - example with ene reaction

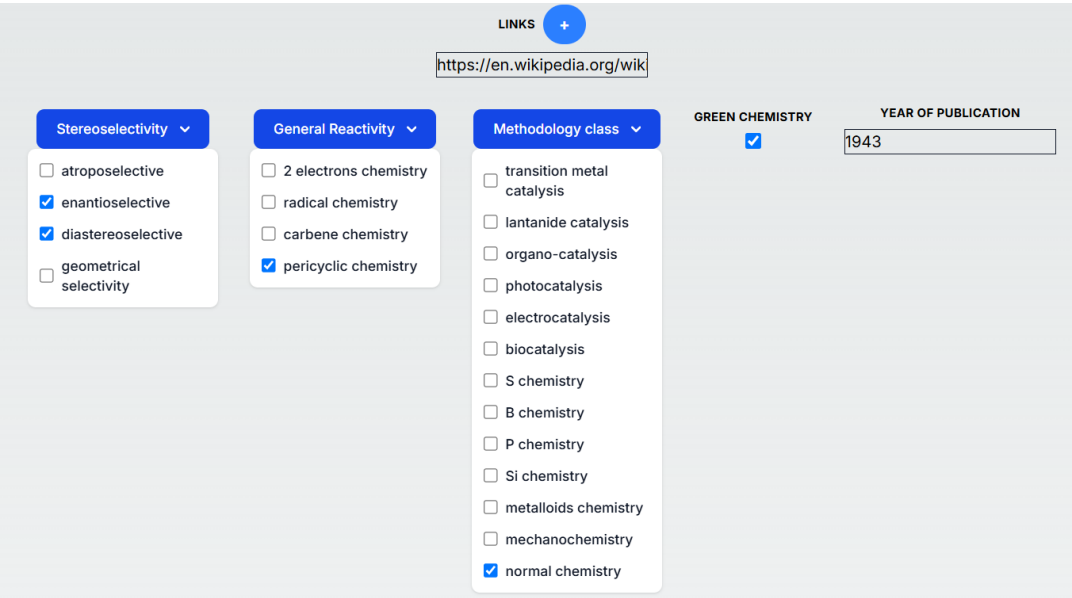

Figure 251 – Attributes – example with ene-reaction

Bibliography and sitography

(1) Hucho, F. Toxins as Tools in Neurochemistry. *Angewandte Chemie International Edition in English* 1995, *34* (1), 39–50. https://doi.org/10.1002/anie.199500391.

(2) Narahashi, T.; Moore, J. W.; Scott, W. R. Tetrodotoxin Blockage of Sodium Conductance Increase in Lobster Giant Axons. *J Gen Physiol* 1964, *47* (5), 965–974. https://doi.org/10.1085/jgp.47.5.965.

(3) Nishikawa, T.; Urabe, D.; Isobe, M. An Efficient Total Synthesis of Optically Active Tetrodotoxin. *Angewandte Chemie - International Edition* 2004, *43* (36), 4782–4785. https://doi.org/10.1002/anie.200460293.

(4) Konrad, D. B.; Rühmann, K.-P.; Ando, H.; Hetzler, B. E.; Strassner, N.; Houk, K. N.; Matsuura, B. S.; Trauner, D. *A Concise Synthesis of Tetrodotoxin*; 2022.

(5) Corey, E. J. General Methods for the Construction of Complex Molecules. *Pure and Applied Chemistry* 1967, *14* (1), 19–38. https://doi.org/10.1351/pac196714010019.

(6) David A. Pensak; Elias. J. Corey. LHASA—Logic and Heuristics Applied to Synthetic Analysis. In *Computer-Assisted Organic Synthesis*; 1977; pp 1–32. https://doi.org/10.1021/bk-1977-0061.ch001.

(7) Hanessian, S.; Franco, J.; Larouche, B. The Psychobiological Basis of Heuristic Synthesis Planning - Man, Machine and the Chiron Approach. *Pure and Applied Chemistry* 1990, *62* (10), 1887–1910. https://doi.org/10.1351/pac199062101887.

(8) Johnson, P. Y.; Burnstein, I.; Crary, J.; Evans, M.; Wang, T. Designing an Expert System for Organic Synthesis; Hohne, B. A., Pierce, T. H., Eds.; 1989; pp 102–123. https://doi.org/10.1021/bk-1989-0408.ch009.

(9) Gasteiger, J.; Pförtner, M.; Sitzmann, M.; Höllering, R.; Sacher, O.; Kostka, T.; Karg, N. *Computer-Assisted Synthesis and Reaction Planning in Combinatorial Chemistry*; KLUWER/ESCOM, 2000; Vol. 20.

(10) Szymkuć, S.; Gajewska, E. P.; Klucznik, T.; Molga, K.; Dittwald, P.; Startek, M.; Bajczyk, M.; Grzybowski, B. A. Computergestützte Syntheseplanung: Das Ende Vom Anfang. *Angewandte Chemie* 2016, *128* (20), 6004–6040. https://doi.org/10.1002/ange.201506101.

(11) Zhong, Z.; Song, J.; Feng, Z.; Liu, T.; Jia, L.; Yao, S.; Hou, T.; Song, M. Recent Advances in Artificial Intelligence for Retrosynthesis. *Cornell University* 2023.

(12) Mikulak-Klucznik, B.; Gołębiowska, P.; Bayly, A. A.; Popik, O.; Klucznik, T.; Szymkuć, S.; Gajewska, E. P.; Dittwald, P.; Staszewska-Krajewska, O.; Beker, W.; Badowski, T.; Scheidt, K. A.; Molga, K.; Mlynarski, J.; Mrksich, M.; Grzybowski, B. A. Computational Planning of the Synthesis of Complex Natural Products. *Nature* 2020, *588* (7836), 83–88. https://doi.org/10.1038/s41586-020-2855-y.

(13) Beker, W.; Roszak, R.; Wolos, A.; Angello, N. H.; Rathore, V.; Burke, M. D.; Grzybowski, B. A. Machine Learning May Sometimes Simply Capture Literature Popularity Trends: A Case Study of Heterocyclic Suzuki-Miyaura Coupling. *J Am Chem Soc* 2022, *144* (11), 4819–4827. https://doi.org/10.1021/jacs.1c12005.

(14) Badowski, T.; Gajewska, E. P.; Molga, K.; Grzybowski, B. A. Synergy Between Expert and Machine-Learning Approaches Allows for Improved Retrosynthetic Planning. *Angewandte Chemie International Edition* 2020, *59* (2), 725–730. https://doi.org/10.1002/anie.201912083.

(15) Grzybowski, B. A.; Szymkuć, S.; Gajewska, E. P.; Molga, K.; Dittwald, P.; Wołos, A.; Klucznik, T. Chematica: A Story of Computer Code That Started to Think like a Chemist. *Chem*. Elsevier Inc March 8, 2018, pp 390–398. https://doi.org/10.1016/j.chempr.2018.02.024.

(16) SMILES. In *The IUPAC Compendium of Chemical Terminology*; International Union of Pure and Applied Chemistry (IUPAC): Research Triangle Park, NC, 2014. https://doi.org/10.1351/goldbook.ST06980.

(17) *https://lifescience.opensource.epam.com/indigo/index.html,*.

(18) Chaudhuri, S. An Overview of Query Optimization in Relational Systems. In *Proceedings of the seventeenth ACM SIGACT-SIGMOD-SIGART symposium on*

Principles of database systems; ACM: New York, NY, USA, 1998; pp 34–43. https://doi.org/10.1145/275487.275492.

(19) Neumann, T. Query Optimization (in Relational Databases). In *Encyclopedia of Database Systems*; Springer New York: New York, NY, 2018; pp 3009–3015. https://doi.org/10.1007/978-1-4614-8265-9_293.

(20) Boyko, Y. D.; Huck, C. J.; Sarlah, D. Total Synthesis of Isomalabaricane Triterpenoids. *J Am Chem Soc* 2019, *141* (36), 14131–14135. https://doi.org/10.1021/jacs.9b08487.

(21) *https://nextjs.org/*.

(22) *https://lifescience.opensource.epam.com/ketcher/*.

(23) *https://www.postgresql.org/*.

(24) *https://lifescience.opensource.epam.com/bingo/bingo-postgres.html*.

(25) *https://lifescience.opensource.epam.com/indigo/index.html*.

Final remarks

To summarize, during my PhD I had the opportunity to work on different topics: organocatalyzed Enders' cascade using acetaldehyde dimethyl acetal, Organo-photocatalyzed α -functionalization of carbonyl compounds with aryl-diazo compounds, asymmetric photo-organocatalyzed Danheiser cyclopentane annulation, asymmetric photo-organocatalyzed reductive homocoupling of cinnamaldehyde with oxalic acid as reducing agent, divergent total synthesis of polycyclic norcembranoid diterpenes, a scalable, enantioselective total synthesis of (S)-autumnaline and the Synthonpedia project. These thematics captured my attention for the reasons exposed in the introduction: development of new methodologies as chemical tools for the synthesis of complex molecules, and synthesis of family of complex molecules themselves, including all the different strategies and approaches, which is the part of this work I love the most.

Moreover, thanks to the cooperation with Industry, I had the opportunity to work to different projects with a *commercial* aim. Besides the chemistry explored thanks to this cooperation, that work also though me how to communicate with people of a different working environment. I appreciated their pragmatic approach, which is essential if you want to use the means of organic chemistry to really make an API. The choice of chemical reactions to use, the purification methodologies and the constant fight with intellectual property is something that usually is not really encountered in academia.

I would like to thank Professor Armando Carlone, my supervisor, and Dr. Fabio Pesciaioli, my co-supervisor, for having driven me across the word of chemistry in these years. Moreover, I want to thank Professor Filippo Romiti to have host me in its lab and giving me the opportunity to work on a total synthesis project, Professor Stefano Protti for the cooperation with Pavia university, and Mr. Pietro Allegrini, Dr. Andrea Bonetti and Dr. Andrea Gambini from Indena S.p.A. for the cooperation and their precious help. I also thank Vitality for the generous fundings and all the opportunities offered.

Finally, I want to thank my family and friends and all the people who have always supported me, in particular my parents – their help is important as scientific mentoring. A special thanks goes also to Mr. Simone Zanella and Dr. Niccolò Tampellini, both for their scientific help and for being good friends too.

I hope that all the chemistry and new concepts developed during these three years will be some day useful for someone in the scientific community and/or in industry. At the end organic chemistry is making molecules!

Finanziato dall'Unione europea-*NextGeneration EU*
Missione 4, Componente 1 – CUP E13C22001060006